Synthesis and Conformational Analysis of Fluorinated Pyrrolidines

Lorraine E. A. Combettes

A thesis submitted to the Board of the Faculty of Physical Sciences in partial fulfillment of the requirements for the degree of Doctor of Philosophy at the University of Oxford.

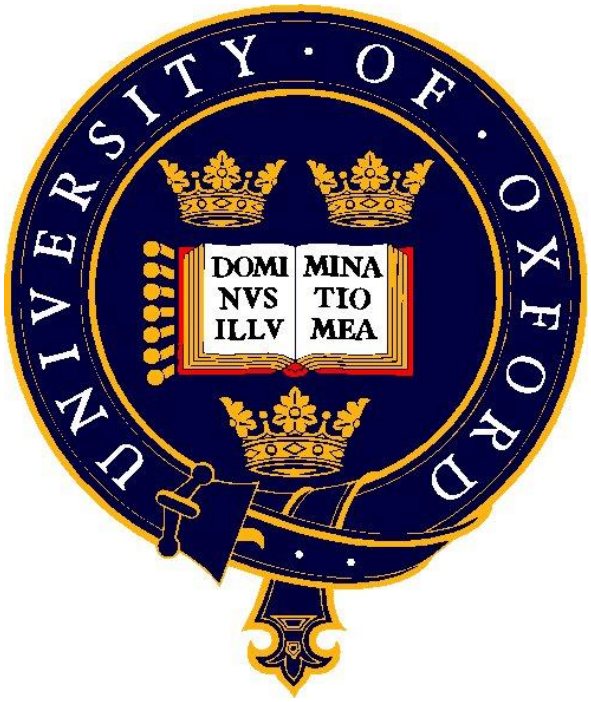

St Hilda's College

Trinity Term 2012

The work presented in this thesis was conducted at the Chemistry Research Laboratory at the University of Oxford between Michaelmas Term 2007 and Trinity 2012 under the supervision of Prof. Véronique Gouverneur.The work described in this thesis is entirely my own, except where I have *either* acknowledged help from a named person *or* given a reference to a published source or a thesis. Text taken from another source will be enclosed in quotation marks and a reference given.

Lorraine Combettes

August 2012

Synthesis and Conformational Analysis of Fluorinated Pyrrolidines

The aim of this thesis was to investigate the synthesis and the conformational analysis of fluorinated pyrrolidines. We focused on two strategies namely, the iodoamination and fluoroamination of fluorinated precursors.

Iodoamination

Our first approach for the synthesis of fluorinated pyrrolidines relied on the iodocyclisation of allylic fluorides bearing pendant nitrogen nucleophiles. These allylic fluorides were obtained by fluorodesilylation of suitably functionalised allylsilanes. After validation of this methodology, the scope and limitations of the iodoamination were investigated. Furthermore, we were able to probe the influence of the fluorine moiety on the level of diastereocontrol of the cyclisation.[1]

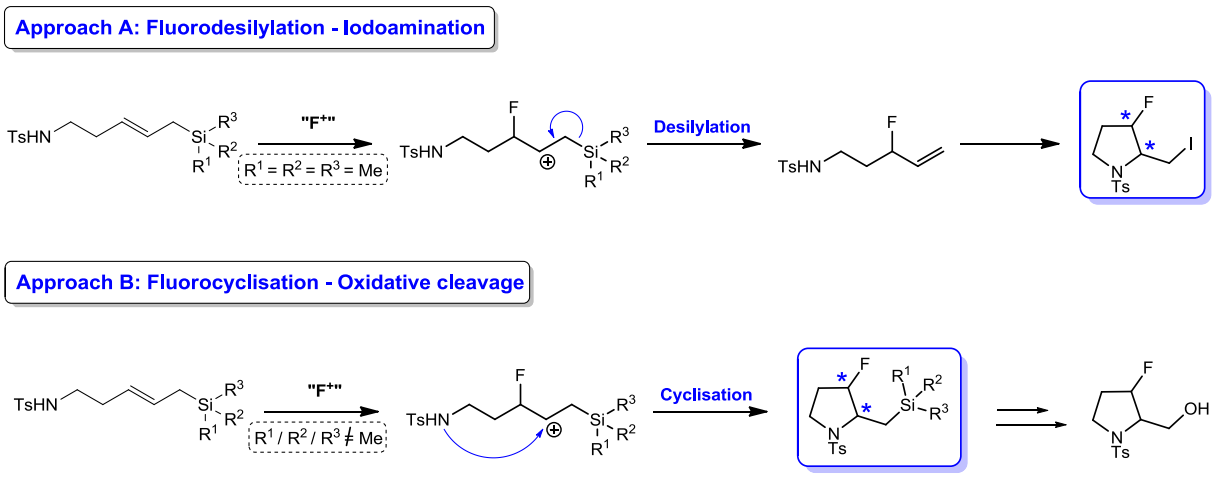

Scheme 1.12: Synthesis of fluorinated pyrrolidines. Approach A: fluorodesilylation/iodoamination; Approach B: fluorocyclisation.

Fluoroamination

The second route focused on a key reaction: an unprecedented electrophilic fluoroamination of an aminated allylsilane. From a mechanistic point of view, the presence of the silyl group act as a 1,2-dipole and activate the double bond towards electrophilic fluorination. This methodology required the initial screening of a silyl directing group that would promote electrophilic addition, without subsequent desilylation. Finally, we investigated the level of diastereocontrol displayed by these cyclisations as a function of the E/Z geometry of the starting aminated allylsilane.[2]

Conformational analysis

Moreover the 3-fluoropyrrolidines obtained via iodoamination served to investigate the stereoelectronic influence of the fluorine gauche effect on ring conformations. Solid state single crystal X-ray analysis and solution phase NMR spectroscopy were used for this purpose. Due to complicated conformational analysis of saturated five-membered rings in solution, 1D ^{19}F-^{1}H heteronuclear nOe (HOESY) experiments have been optimised for applications to this type of small molecules. These have been employed to estimate ^{19}F-^{1}H internuclear distances and were combined with vicinal $^{3}J_{FH}$ and $^{3}J_{HH}$ scalar coupling constants in order to analyse the ring conformations.[3]

[1] L. E. Combettes, M. Schuler, R. Patel, B. Bonillo, B. Odell, A. L. Thompson, T. D. W. Claridge, V. Gouverneur, *Chem. Eur. J.* **2012**,*18*, 13126-13132.
[2] L. E. Combettes, O. Lozano, V. Gouverneur, *J. Fluorine Chem.* **2012**, *143*, 167-176.
[3] L. E. Combettes, P. Clausen-Thue, M. King, B. Odell, A. L. Thompson, V. Gouverneur, T. D. W. Claridge, *Chem. Eur. J.* **2012**,*18*, 13133-13141.

Acknowledgments:

I would like to thank Professor Véronique Gouverneur for giving me the opportunity to carry out my DPhil at the University of Oxford and work on an exciting and challenging project. I am also greatly indebted to the EPSRC for funding my DPhil.

My warmest thanks must go to the people who have directly contributed in some way to the work presented in this thesis. Dr. Marie Schuler deserves a big thank you for starting off the preliminary results on iodocyclisation and fluoroamination. She provided me with a working project to begin my PhD and gave me her expert advice on how to deal with fluorine chemistry and the lab in general.
I must also thank Dr. Tim Claridge and Dr. Barbara Odell for spending many long hours with me next to an NMR machine. They have been the core of the NMR project and I would like to express here my gratitude for the pleasure to work with so enthusiastic and skilled persons. I would also like to thank Dr. Amber Thompson and Dr. David Watkin for training me to run and analyse my own crystals. I have been particularly impressed by their breadth of knowledge in their field, the desire to share their passion for crystallography and their availability whenever I was calling for help.
Thank you to the mass spectrometry services for their assistance with characterisation. A big thank you to Levi and all the staff members of the stores for being so helpful whenever I was looking for a special piece of equipment, a lost chemical or moving boxes.
I would also like to thank Dr. Matthew Tredwell for proof reading this thesis in such a very short time.

I would like to express my sincere thanks to several members of St Hilda's College, namely Mr. Richard Berry, the college bursar, Mrs Suzie Hancock, the academic registrar and Mrs Chris Cowley, the tutorial officer, for their constant support throughout my PhD. My deep thanks go as well to Dr. Paul Roberts and Dr. Lorna Smith for giving me the opportunity to take an active part in the college life and their support regarding my academic progression.

I have been privileged to meet Elena Benedetto and Oscar "Chicha" Galicia and I wish to express here my profound respect and gratitude for their deep and enduring friendship. They always successfully managed to cope with my grumpiness with a smile. They also helped me to get through tough times (many times) and I feel greatly indebted to them. I wish also to thank my dear friends Justyna Walkowiak and Stan Kulikowsky for all the good time spent in their company. Their strength of character and their determination were inspirational. A big thank you goes to John Ilupeju and "le Président" Rodrigue Leuma-Yona for trying to teach me the true meaning of optimism and how to enjoy the simple things of life. I would also like to wish good luck to Jamie Wolstenhulme (I am deeply sorry if there is a mistake in your name, I never knew how to spell it properly) with the carbocyclisation project.

Many thanks to my colleagues from F9/F12 for all the good time in the lab (disco Friday, watching the football world cup… while working hard!). I would like to thank all the past and present members of Gouverneur group. A special mention must go to the football team for many enjoyable moments. I am also particularly grateful to have found so many great friends in Oxford: Nathalie, Christian, Cédric, Akshat, Massaba, Manuel, Ali, Radek, Johannes, Guiseppe, Charlotte, Dr. Victor Lee, Giulia, Filippo, Mei Ling and many others.

Many thanks also to Nicolas and Christine for their support and their lasting friendship over the years. We all started our PhD at the same time and I am the last to finish… I should have known better.

"Scientiae prosum, quod gaudio mihi est…" …it depends on the day

Abbreviations and symbols:

Å	Angström
Ab initio	Quantum chemistry method
Ac	Acetyl
AcOH	Acetic acid
AIBN	2,2'-Azobisisobutyronitrile
AIM	Atom-in-molecule quantum theory
app.	apparent
B_0	External magnetic field
Boc	*tert*-Butyloxycarbonyl
Bn	Benzyl
br	broad
^{t}Bu	*tert*-butyl (-C(CH_3)$_3$
Bz	Benzoyl
Cbz	Carbobenzyloxy
CCDC	Cambridge Crystallographic Structural Database
1,1'CDI	1,1'-Carbonyldiimidazole
CI	Chemical Ionisation
d	Doublet
d_{X-X}	Distance between the atoms X and X
1D	One dimension
2D	Two dimensions
3D	Three dimensions
D	Debye
DAST	(diethylamino)sulfur trifluoride
DIBAL-H	Di*iso*butylaluminium hydride
dig	Digonal
DCC	*N*,*N*-dicyclohexylcarbodiimide
DCM	Dichloromethane
Deoxofluor®	Bis(2-methoxyethyl) aminosulfur trifluoride
DFT	Density functional theory
$(DHQ)_2PYR$	Hydroquinine 2,5-diphenyl-4,6-pyrimidinediyl diether
DMAP	4-Dimethylaminopyridine
DMF	Dimethylformamide
DMSO	Dimethyl sulfoxide
DNA	Deoxyribonucleic acid
DPP-IV	Dipeptidyl peptidase IV
d.r.	Diastereomeric ratio
ee	Enantiomeric excess
e.g.	For example
Eq.	Equivalent
ESI	Electrospray ionisation
et al.	and others
FABS	Fluorine Atoms for Biochemical Screening
FAXS	Fluorine chemical shift Anisotropy and eXchange for Screening
FI	Field ionisation
FID	Free induction decay
Flp	(2*S*,4*R*)-4-fluoroproline
GABA	γ-aminobutyric acid
GC	Gas Chromatography
Gly	Glycine
h	Hour(s)
h	Planck's constant
ħ	Reduced Planck's constant
HFIP	Hexafluoroisopropanol
HOESY	Heteronuclear Overhauser Effect SpectroscopY
HOMO	Highest occupied molecular orbital
HPLC	High-performance liquid chromatography
HRMS	High Resolution Mass Spectrometry
HSAB	Hard and soft acids and bases
Hyp	(2*S*,4*R*)-4-hydroxyproline
Hz	Hertz
I	Ionization energy
I	Nuclear spin quantum number
^{i}Pr	Isopropyl (-CH(CH_3)$_2$)
^{i}PrLi	Isopropyl Lithium
IRC	Intrinsic reaction coordinate
IR	Infrared
IUPAC	International Union of Pure and Applied Chemistry
J	Scalar coupling constant
kcal	Kilocalorie
$K_{trans/cis}$	Rate constant of trans/cis isomerisation
LCD	Liquid crystal display
LDA	Lithium diisopropylamide
LiHMDS	Lithium bis(trimethylsilyl) amide
LUMO	Lowest unoccupied molecular orbital
mg	Milligram
m.p.	Melting point
M	mol.dm^{-3}
m	Multiplet
Me	Methyl
MeCN	Acetonitrile
MeOH	Methanol
MHz	Megahertz
mol	Mole(s)
MRI	Magnetic Resonance Imaging
MRS	Magnetic Resonance Spectroscopy
MRSI	Magnetic Resonance Spectroscopy Imaging
Ms	Methanesulfonyl. Mesyl
MsCl	Methanesulfonyl chloride
NBS	*N*-Bromosuccinimide
NEt_3	Triethylamine
NFSI	*N*-fluorobenzenesulfonimide
NIS	*N*-Iodosuccinimide

NMR	Nuclear Magnetic Resonance
nOe	nuclear Overhauser effect
NOESY	Nuclear Overhauser Effect SpectroscopY
p-	Para
P	Angular momentum
PET	Positron emission tomography
Ph	Phenyl
ppm	Parts per million
Pro	(2*S*)-proline
q	Quadruplet
R	Alkyl group
rad	Radian
R_f	Retention factor
RNA	Ribonucleic acid
r.t.	Room temperature
s	Singlet
Selectfluor®	1-Chloromethyl-4-fluoro-1,4diazoniabicyclo[2.2.2]octane bis(tetrafluoroborate)
SI	International System of Units
SNR	Signal-to-noise ratio
t	Triplet
T	Tesla
TBAF	Tetrabutylammonium fluoride
TBCO	2,4,4,6-tetrabromo-2,5-cyclohexadienone
TBME	*tert*-butyl methyl ether
tert	Tertiary
THF	Tetrahydrofuran
TLC	Thin layer chromatography
Tol	Tolyl
TMS	Trimethylsilyl
TMSCl	Chlorotrimethylsilane
trig	trigonal
Ts	*p*-Toluenesulfonyl. Tosyl
TsCl	*p*-Toluenesulfonyl chloride
Xaa	Any amino acid
Yaa	Any amino acid
γ	Magnetogyric ratio
δ	Chemical shift
δ^+	Partial positive electric charge
δ^-	Partial negative electric charge
μ	Dipole/magnetic moment
ν	Wavenumber
ν	Resonance frequency
σ	Bonding molecular orbital
σ^*	Antibonding molecular orbital
σ	Shielding parameter
σ_d	Diamagnetic shielding term
σ_p	Paramagnetic shielding term
σ_i	Environmental shielding term
τ_{BD}	Bürgi-Dunitz trajectory
τ_m	Mixing time
Φ	Dihedral angle
χ	Electronegativity
°	degree
°C	Degree Celsius

Contents:

CHAPTER 1:

Introduction – Properties of the C-F bond and its use as a conformational tool 1

1.1 General aspects of the C-F bond: 2

1.1.1 Electronegativity, orbitals and bond strength

1.1.3 Size of the fluorine atom and isosteric replacement 3

1.1.3 Inductive and mesomeric effects 4

1.1.4 Fluorine-hydrogen bonding 5

1.2 Conformational effects associated with the C-F bond 6

1.2.1 Dipole/dipole interactions 6

1.2.2 Charge/dipole interactions 7

1.2.3 Hyperconjugation effects 9

1.2.3.1 The σ^*_{C-F} antibonding orbital 9

1.2.3.2 *Gauche* effect or 1,2-F bond attraction 10

1.2.3.3 The 1,3-F bond repulsion 12

1.3 Understanding the implications of conformational effects of the C-F bond 14

1.4 Selective synthesis of mono fluorinated pyrrolidines 20

1.5 Aim of the thesis 27

CHAPTER 2:

Stereoselective synthesis of fluorinated pyrrolidines – The fluorine as stereo-directing group 31

2.1 Use of allylsilanes as activators for the electrophilic addition of fluorine to olefins 31

2.1.1 Generalities about the electrophilic addition of halogens to alkenes 31

2.1.2 The singularity of the electrophilic addition of fluorine to olefins 32

2.1.3 Use of silanes as olefins activator 35

2.1.4 Fluorodesilylation of allylsilanes 37

2.2 Methodological concept: towards the stereoselective synthesis of fluorinated pyrrolidines 44

2.3 Stereoselective synthesis of fluorinated pyrrolidines via iodocyclisation 45

2.3.1 Iodocyclisation 45

2.3.1.1 General aspect of iodocyclisation reactions 45

2.3.1.2 Stereoselectivity of intramolecular iodocyclisation 45

2.3.2 Preliminary results and optimisation 48

2.3.2.1 Synthesis of allylic fluorides and feasibility of the reaction 48

2.3.2.2 Optimisation 50

2.3.3 Scope and limitations: 51

2.3.3.1 Design of substrates and synthesis 51

2.3.3.2 Iodocylisation 57

2.3.3.3 Further functionalisation: synthesis of fluorinated indolizidines derivatives 63

2.3.4 Rationalisation of the diastereoselectivity 64

2.3.4.1 Comparison with previous study 64

2.3.4.2 Theoretical calculations 68

2.4 Fluoroamination 72

2.4.1 Concept 72

2.4.2 Initial investigation 73
2.4.3 Validation of the cyclisation 76
2.4.4 Scope and limitations 79
2.4.4.1 Design of substrates and synthesis 79
2.4.3.2 Fluoroamination cyclisation 83
2.4.4.2 Assignment of the relative stereochemistry 85
2.4.4.3 Comparison with previous study 88
2.4.5 Rationalisation of the diastereoselectivity 90
2.5 Conclusion 98

CHAPTER 3:
Design of a new 1D 19F HOESY NMR experiment and its application to the structural and conformational elucidation of mono-fluorinated pyrrolidines 101

3.1 Generalities on ^{19}F NMR 101
3.1.1 Properties of the ^{19}F nucleus 101
3.1.2 Principal applications of ^{19}F NMR 105
3.2 Analytical tools for the structural and conformational study of fluorinated 5-membered rings 112
3.2.1 General aspects on the conformation of 5-membered rings 112
3.2.2 Previous structural and conformational analysis of fluorinated 5-membered rings 114
3.3 Conformational analysis of fluorinated pyrrolidines using ^{19}F-^{1}H scalar couplings and heteronuclear nOes (HOESY) 119
3.3.1 A practical NMR technique for structural and conformational elucidations: the nOe 119
3.3.2 Outline of the project 121
3.3.3. ^{19}F NMR HOESY methodology - Description of the new technique 122
3.3.4 Solid-state crystallographic analysis 129
3.3.5 Solution phase NMR analysis 134
3.4 Conclusion 149

CHAPTER 4:
Experimental section 151

4.1 General information 151
4.2 General procedures 152
4.3 Synthesis of organotrimethylsilanes and allylic fluorides 153
4.4 Synthesis of 3-fluoro-2-iodomethylpyrrolidines and 4-fluoro-5-iodomethyl pyrrolidin-2-ones 188
4.5 Synthesis of indolizidines 201
4.6 Synthesis of organosilanes 205
4.7 Fluorocyclisation of organosilanes 222

REFERENCES 231
APPENDIX 241

Chapter 1:

INTRODUCTION – PROPERTIES OF THE C-F BOND AND ITS USE AS A CONFORMATIONAL TOOL

The aim of many chemists in industry and academia is the discovery of new chemicals displaying advantageous properties which could be exploited in a wide range of fields. Efforts in this direction have been pursued in many ways but to date, the introduction of carbon-fluorine bonds into organic compounds represents a spectacular progress in the quest for innovation. Theoretical, synthetic, biomedical chemistry and material sciences have contributed to the development of this fascinating area of research which has been widely reported.[1] The incorporation of fluorine confers unique properties to polymers, advanced materials as well as pharmaceutical and agrochemical molecules that cannot be attained using other elements. Fluorine occurs abundantly in natural mineral sources such as fluorspar (CaF_2), cryolite (Na_3AlF_6), fluoroapatite ($Ca_5(PO_4)_3F$). Surprisingly, only six different natural fluorinated products have been so far identified.[2] Despite the rarity of fluorine-containing compounds, fluoroorganic chemistry has met an exponential development. This success story is striking because it spans a broad variety of chemical and life-science industries. Since the pioneering work of H. Moissan[3] and F. Swarts in the late 19th century, industrial applications of fluorinated compounds have ranged from fluorinated pharmaceuticals and agrochemicals to fluoropolymers and surfactants. Today, organofluorine chemistry and organofluorine compounds find applications in advanced state-of-the-art technologies using fluorinated liquid crystals for LCD systems or fluorinated resistors for microelectronics and the fabrication of integrated circuits. The incorporation of fluorine into organic molecules impacts on many properties, including their conformation. As a consequence, the properties and functions of organofluorine compounds can be dramatically influenced. The stereoselective introduction of fluorine atom can therefore be exploited as a conformational tool for the synthesis of shape-controlled functional molecules in a predictable

manner. This type of strategic fluorination has been exploited only recently but finds applications in a variety of fields[4] as demonstrated through some selected examples.

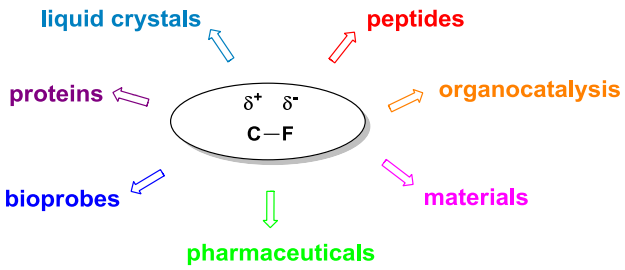

Figure 1.1: The C-F bond as a conformational tool in a variety of fields.

There are two known isotopes of fluorine: fluorine-19 the natural occurring isotope, and fluorine-18, an artificial radionuclide. Fluorine-19 is an essential probe nucleus for NMR spectroscopy because of a nuclear spin of ½, a natural abundance of 100%, high NMR sensitivity, and pronounced long-range effects.[5] Consequently ^{19}F NMR data provide a wealth of information about structural and conformational changes within a molecule, its orientation in a larger framework or the kinetics of reactions. With the increasing popularity of fluorinated compounds in pharmaceutical research, *in vivo* ^{19}F MR spectroscopy or its medical adaptation, magnetic resonance imaging (MRI), has become a valuable tool for identifying and monitoring fluorinated compounds and metabolites. On the other hand, fluorine-18 has particularly appealing properties as positron-emitting radioisotope for positron emission tomography (PET), an imaging technique used in diagnostic medicine and pharmacological testing.[6] ^{18}F has a relatively long half-life of 109.77 minutes, which accounts for radiotracers multistep radiolabeling procedures.

The usefulness of organofluorine chemistry lies in the understanding of some key aspects of its fundamental subunit, the C-F bond itself.[7]

1.1 General aspects of the C-F bond:

1.1.1 Electronegativity, orbitals and bond strength:

Fluorine is the most electronegative element of the periodic table with a value of $\chi = 3.98$ according to the Pauling scale.[8] This high electronegativity has important consequences on the nature and the

properties of the C-F bond. The ionisation energy helps to portray the electronegative behaviour of the fluorine. The removal of one electron from the 2p orbital to generate F^+ is very difficult (I = 401. kcal.mol^{-1}) compared to oxygen (e.g. for the oxygen I = 312.9 kcal.mol^{-1}).[9] Fluorine possesses the smallest atomic radius[10] of the second period elements (after neon) due to the contraction of its high nuclear charge (nine protons). This means that the three lone pairs of fluorine are tightly held by the nucleus and unlikely to participate in resonance or hydrogen bonding. As fluorine is the most electronegative element, the C-F bond is polarised with the electron density oriented towards the fluorine atom. This effect imparts to the fluorine a partial negative charge while the carbon atom bears a partial positive charge. This electrostatic attraction between $F^{\delta-}$ and $C^{\delta+}$ gives to C-F bond a significant ionic character[11] and an increased strength, 108.3 kcal.mol^{-1}, which is the strongest dissociation energy for a single bond in organic chemistry.[12] The nature of the bond directly influence its length, the C-F bond being shorter (1.38 Å) compared to other carbon-heteroatom bonds (see Table 1.1).

	Element (X)					
	H	C	O	**F**	Cl	Br
Pauling's electronegativity χp	2.20	2.55	3.44	**3.98**	3.16	2.96
Van der Waals radius (Å)	1.20	1.70	1.52	**1.47**	1.75	1.85
Atom polarisability (Å^3)	0.67	1.76	0.82	**0.56**	2.18	3.05
Ionisation energy (kcal.mol^{-1})	313.6	240.5	312.9	**401.8**	299.0	272.4
Electron affinity (kcal.mol^{-1})	17.4	29.2	3.7	**78.5**	83.4	77.6
H_3C-X bond length (Å)	1.087	1.535	1.425	**1.382**	1.785	1.933
H_3C-X dissociation energy (kcal.mol^{-1})	103.1	88.0	90.2	**108.3**	81.1	67.9

Table 1.1: Representative physical data of selected elements.

1.1.2 Size of the fluorine atom and isosteric replacement:

With a Van der Waals radius of 1.47 Å, its size is roughly 20% larger than hydrogen but its volume is actually closer to that of oxygen. This intrinsic property allows the convenient replacement of hydrogen or hydroxyl group by fluorine on isosteric grounds. That means that fluorine can be introduced into organic molecules without dramatically altering their overall molecular size. The

specific replacement of a hydrogen with a fluorine can effectively block metabolic processes which normally occurs via hydroxylation of the C-H bond. However such replacement will also have a significant impact on the electronic properties of the molecule. Due to the electron-withdrawing nature of the fluorine, neighbouring substituents and functional group will experience a change of their electron density. This electronic effect decreases the pK_a values and Lewis basicity of these functional groups and retards their oxidation. The replacement of oxygen for fluorine is less electronically disturbing as one electronegative atom replaces another but it involves the loss of the acidic hydrogen and its ability to make hydrogen bond. The substitution of a hydroxyl group by fluorine has been developed as a good tool in probing the role of C-OH hydrogen bonding in biological systems.[13]

1.1.3 Inductive and mesomeric effects:

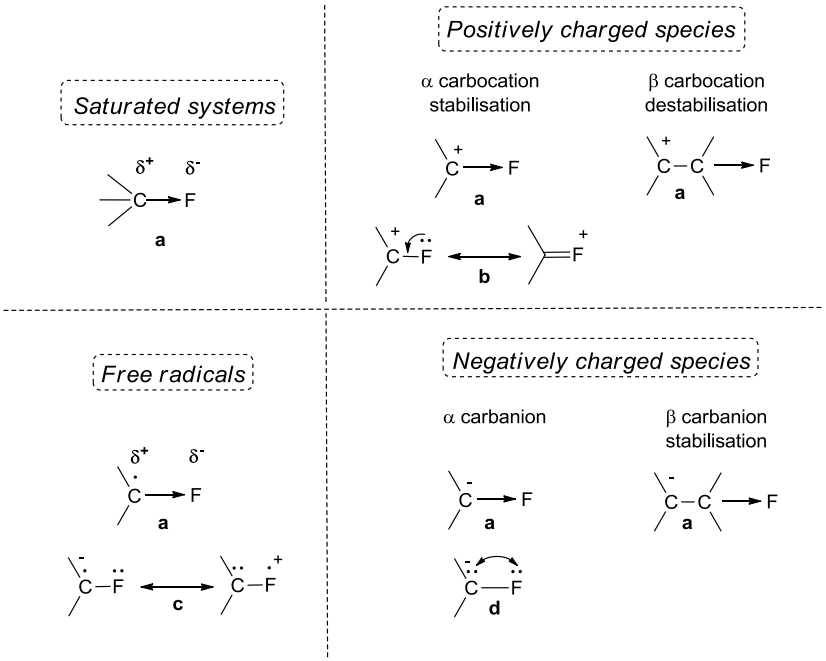

Figure 1.2: Summary of the inductive and mesomeric interactions of the C-F bond: **a** = inductive electron withdrawal; **b** = mesomeric π-donor; **c** = resonance stabilisation; **d** = repulsive interaction.

In saturated systems, the C-F substituent acts as a strong electron-withdrawing group due to the high polarity of the bond. The presence of such substituent will greatly increase the acidity of neighboring hydrogens atoms while they largely reduce the basicity of amines.[14] On the other hand, the presence of fluorine affects the stability of carbocations differently depending on their position. In case of α-

carbocation, it is admitted that fluorine can act as a weak donor, thus stabilising the carbocation through a mesomeric interaction.[15] However when fluorine is placed β to the carbocation, it has a strong destabilising negative inductive effect.[16] In the case of negatively charged species, fluorine can either have a moderate stabilising or destabilising effect on α-carbanions. Conversely, the presence of the fluorine in the β position strongly stabilises the anion by inductive effect. For free radicals, an inductive electron withdrawal will affect the polar characteristics of the fluorinated radical species but this effect is also balanced by resonance stabilisation.[17]

1.1.4 Fluorine-hydrogen bonding:

Fluoride anion can be considered as an excellent hydrogen bond acceptor ($[F\cdots H\cdots F]^-$ = 40 kcal.mol^{-1})[18], in contrast the C-F bond acts as a poor acceptor of hydrogen bond (X-H···F-C = 2-3 kcal.mol^{-1}). Despite the strong electonegativity of fluorine, its lone pairs of electrons are not able to readily engage in H bonding due to the low polarisability of the s and p electrons.[19] Different surveys of the Cambridge Crystallographic Structural Database (CCSD) were carried out to evaluate the occurrence of fluorine hydrogen bonds in small molecular crystals. At this point, it is important to recall that crystallographic techniques are able to locate accurately all atoms except hydrogens. The position of the protons is determined later during the refinement of the data by specialised algorithms based on geometrical considerations. Therefore the interpretation of hydrogen bonding in crystallography might be misleading. The general criterion determining the existence of a hydrogen bond to fluorine is an interatomic distance equal to or below the sum of the combined Van der Waals radii (~ 2.65 Å). In their study, O'Hagan *et al.* searched for crystal structures with CF···HX bond distance of 2.35 Å or less and found 38 matches out of 5947.[20] Independently Dunitz and Taylor performed the same search with using criteria such as CF···HX distance less than 2.30 Å and C-F-···H-X bond angle greater than 90 °.[21] Only 37 structures were found fulfilling these conditions out of 5947. However the average values observed in crystallographic structures for the distance between two X-H and F-C bonds are about 2.5-3.0 Å. This leads to confusion and ambiguities between interactions which should simply be qualified as "short-contact" and genuine hydrogen bonds. Most of the examples of H···F bonds listed in the literature report intramolecular hydrogen

bonds in fluoroalcohols, fluorophenols and fluoroanilines. The calculation of the strength of the hydrogen bond C-F···H-O shows that it is approximately two times weaker than the typical hydrogen bond C=O···H-OR (~ 2.4 kcal.mol^{-1}, ~ 1.9 Å).[22] Hydrogen bonds between fluorinated substrates and biological macromolecules have been postulated in some enzyme-substrate complexes. However, it is rather difficult to determine if these hydrogen bonds are really genuine: other factors may stabilise the conformation corresponding to the short H···F interatomic distance observed. This conformation can be favoured by other factors (e.g., other stronger hydrogen bonds present in the molecule, *gauche* effect), without the participation of an H···F interaction to stabilise the molecular architecture.[23] The existence and possible role of H···F bonds in the interactions between fluorinated substrates and biological macromolecules should be subjected to careful interpretation of the data.

1.2 Conformational effects associated with the C-F bond:

As previously described the C-F bond is a highly polarised unit in which the fluorine atom bears a non-negligible negative charge. Consequently it is suggested that this bond will interact with its surrounding primarily through a combination of electrostatic interactions and hyperconjugative delocalisations.

1.2.1 Dipole/dipole interactions:

The dipole formed by the partial ionic character of the C-F bond ($C^{\delta+}$-$F^{\delta-}$) plays an important role in orienting the conformational preference of organofluorine compounds. The polarisation of the C-F bond induces large dipole moment (μ). This value is 1.85 D in fluoromethane and 1.97 D in difluoromethane.[7] In α-fluoroamide compounds for example, the C-F will prefer to align antiparallel to the amide carbonyl group, a conformation which opposes both dipoles. For this substrate the *anti* conformation is preferred by 7.5 kcal.mol^{-1} to the *syn*.[24] A similar effect exists for analogous α-fluorocarbonyl compounds, but the conformational preference decreases as the dipole moment of the carbonyl group becomes weaker (Figure 1.3).[25]

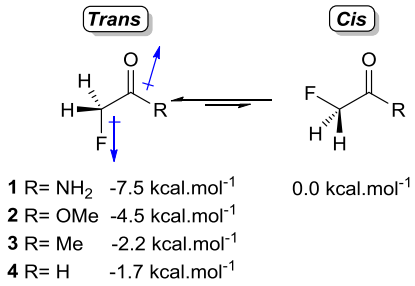

Figure 1.3: Calculated energy difference between the *trans* and *cis* conformers of some α-fluorocarbonyl compounds.

1.2.2 Charge/dipole interactions:

The stabilisation of certain conformations can also occur through charge/dipole electrostatic interaction. This type of interaction involving the C-F bond and a formal charge is larger in term of energy than the dipole/dipole interaction. The influence of the C-F bond on the conformation was first observed in 3-fluoropiperidinium ring system **5** where the fluorine atom preferentially adopts an axial position (favoured by 5.4 kcal.mol^{-1} compared to the fluorine in an equatorial position see Figure 1.4).[26] Similarly conformational study of 2-fluoroethylammonium ion **7** and protonated 2-fluoroethanol **8** shows a clear preference for the *gauche* conformers.[27]

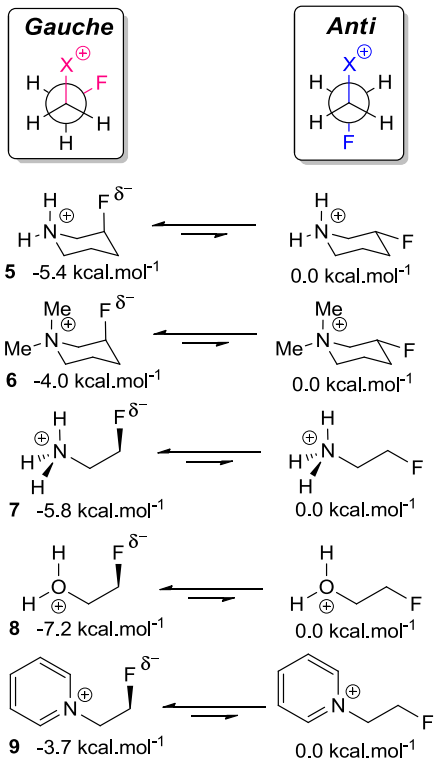

Figure 1.4: The charge/dipole interactions between the C-F bond and a positively charged heteroatom lead to a *gauche* conformational preference.

As a result of such conformations, the CF···HN^+ distance is short (~ 2.4-2.5 Å). It would be possible to explain this preference by the presence of an intramolecular hydrogen bond but it is worth noticing that the *gauche* preference is also maintained for the fluoroethylpyridinium cation **9** (favoured by ~ 3.8 $kcal.mol^{-1}$), where no intramolecular hydrogen bond can be formed (Figure 1.4).[20] In these cases the *gauche* conformers are strongly preferred because they bring the partially negatively charged fluorine close to the formally positively charged nitrogen or oxygen. It is therefore reasonable to describe this interaction in these systems as charge-dipole rather than any weak hydrogen bond. Another example of the four-membered ring 3-fluoroazetidinium cation **10** shows that the charge/dipole interaction can directly influence the ring puckering of the system.[28]

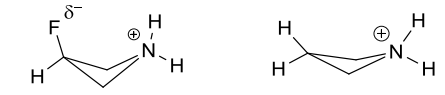

10 **11**

Figure 1.5: The charge/dipole interactions between the C-F bond and a positively charged heteroatom lead to an increased puckering of 4-membered ring.

The presence of the C-F bond bending towards the ammonium cation favours a more puckered structure compared to the almost planar azetidinium cation **11**. This dipole/dipole or charge/dipole interaction induced by the C-F bond with its environment has the potential to be used to probe the conformation of protonated substrates with their target proteins.

Indeed this type of interaction has been recently exploited to uncover the binding mode of γ-aminobutyric acid (GABA) to its receptors. The γ-aminobutyric acid **12** (GABA) is one of the major inhibitory neurotransmitters in the central nervous system. Its conformational flexibility is particularly important for its biological function, as GABA (**12**) adopts different conformations to bind specifically to its different receptors: $GABA_{A, B, C}$ and to $GABA_{AT}$ transaminase.[29]

Studying the relative activities of fluorinated GABA analogues helped to define the binding conformations required for each receptor.[30] For instance, 3(*S*)-F-GABA enantiomer (*S*)-**13** was found to be a more potent inhibitor for GABA transaminase than its 3(*R*)-F-GABA (*R*)-**13** counterpart.

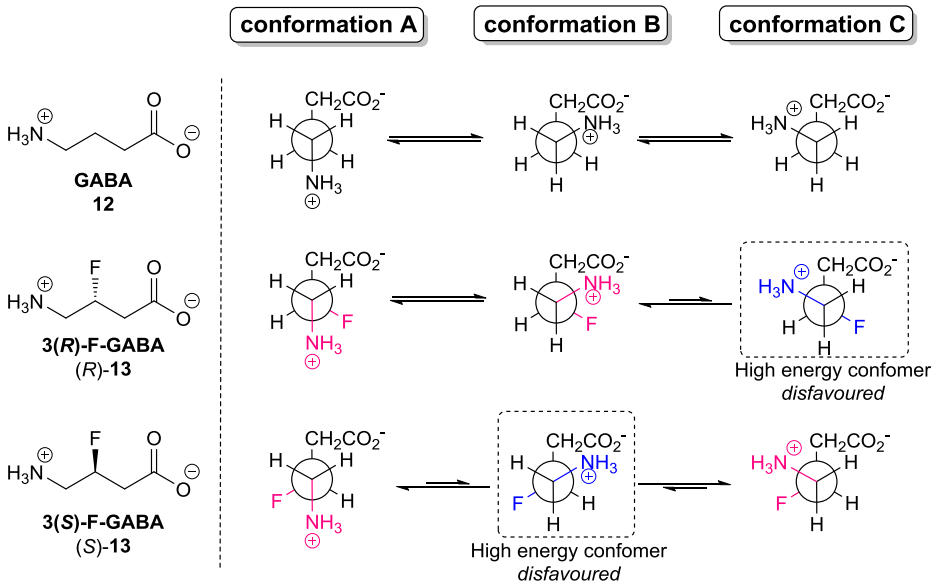

Figure 1.6: The Newman projections of GABA **12**, (*R*)-**13** and (*S*)-**13** along the C3-C4 bond describe the three possible staggered binding conformations.

The preferential conformation adopted by (*S*)-**13** seems to be the reason for the difference in metabolic rate between the two substrates. Each enantiomer can adopt three different conformations. However conformations featuring the fluorine and the amine gauche are favoured by 5 kcal.mol^{-1}. Since (*S*)-**13** is more active, conformation **C** is likely to play an important factor in its inhibition of GABA transaminase. The *gauche* conformation **C** of (*S*)-**13** is the result of the electrostatic charge/dipole interaction between the C-F bond and the positive ammonium ion in addition to a *gauche* effect. In contrast, the conformation **C** of (*R*)-**13** is disfavoured by an anti configuration. Similarly, a study revealed that each enantiomers bind with the same affinity to the receptor GABA $_A$. This suggests in this case that (*S*)-**13** and (*R*)-**13** adopt preferentially a conformation that is easily accessible for both of them, the conformation **A**.

1.2.3 Hyperconjugation effects:

Along with dipole/dipole and charge/dipole interactions, hyperconjugation effects play a more subtle but essential role in the conformational influence of compounds.

1.2.3.1 The σ* $_{C-F}$ antibonding orbital:

The strong electronegativity of fluorine renders its molecular orbitals low lying. As a consequence its vacant σ*$_{C-F}$ antibonding orbital can readily accept electron from a vicinal electron-donating

orbital such as C-H, C-C, π bonds and lone pairs, while the electron-occupied $\sigma_{C\text{-}F}$ orbital is reluctant to donate electrons. This type of hyperconjugation leads to a C-F bond which becomes longer and less covalent in character. But it remains strong because of the coulombic interactions taking place, this balances the decrease in covalent character of the bond. Overall, the conformers allowing hyperconjugation are stabilised and their energy is lowered. This effect can be exemplified by the study of the anomeric effect in 2-fluoropyran **14** (Figure 1.7).[31]

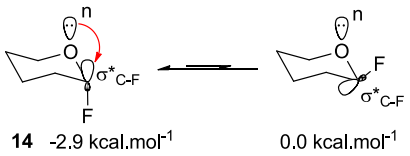

Figure 1.7: The anomeric effect in 2-fluoropyran **14**. The n- $\sigma^*_{C\text{-}F}$ hyperconjugative donation favours the conformation featuring the fluorine in an axial position.

Indeed the conformation featuring the fluorine in an axial position is preferred by 2.8-2.9 kcal.mol^{-1} to the one featuring fluorine equatorial. This can be explained by the donation of electron density from the lone pair of the oxygen into the $\sigma^*_{C\text{-}F}$ antibonding orbital. As a result the electron-donating group is aligned with the $\sigma^*_{C\text{-}F}$ orbital through a n- σ* overlap, favouring the conformation with fluorine axial.

1.2.3.2 *Gauche* effect or 1,2-F bond attraction

The so called "*gauche* effect" is characterised by a preferential *gauche* (synperiplanar) conformation in an X-C-C-Y moiety (Figure 1.8), where X and Y are two electron-withdrawing elements. It is generally caused by the donation of electron density from the neighboring electron-releasing $\sigma_{C\text{-}H}$ molecular orbital to the low-lying electron-accepting $\sigma^*_{C\text{-}F}$ molecular orbital through an antiperiplanar relationship that serves to maximize the stabilization of this geometry.[32] The well studied molecule 1,2-difluoroethane **15** can be used as example to understand this phenomenon (Figure 1.8). This molecule can adopt two conformations, *gauche* and *anti*. From a steric and electrostatic point of view, one would expect that the *anti* conformer would be more stable by minimising the repulsion between the two electronegative elements. However it has been

demonstrated by infrared and Raman spectroscopy,[33] NMR,[34] electron diffraction[35] and *ab initio* calculations[36] that the *gauche* conformation is preferred by 1.0 kcal.mol^{-1}.

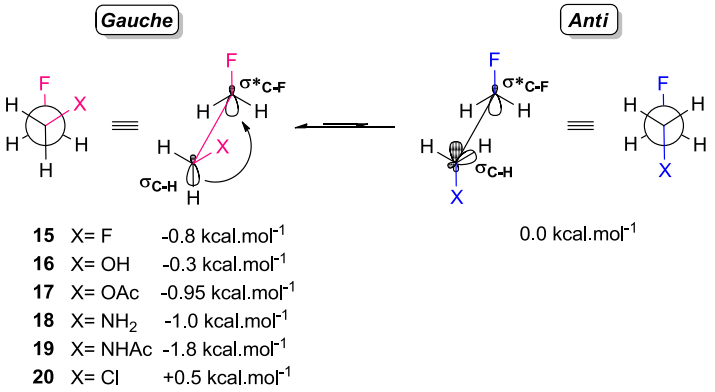

15 X= F -0.8 kcal.mol^{-1}
16 X= OH -0.3 kcal.mol^{-1}
17 X= OAc -0.95 kcal.mol^{-1}
18 X= NH_2 -1.0 kcal.mol^{-1}
19 X= NHAc -1.8 kcal.mol^{-1}
20 X= Cl +0.5 kcal.mol^{-1}

Figure 1.8: Hyperconjugative delocalisation of the σ_{C-H} into the σ^*_{C-F} favours the *gauche* conformer.

In the series of 1,2-dihaloethanes presented in Figure 1.8, this preference for the *gauche* conformation is observed in the case of 1,2-difluoroethanes **15-20**.[7] In the case of 2-fluoroethanol **16**,[37] this preference was initially attributed to the formation of an intramolecular F···H-O hydrogen bond. However it has been found later that the 1-fluoro-2-methoxyethane also adopts a similar *gauche* conformation as predominant structure despite its inability to form hydrogen bonding.[38] Therefore **16** adopts such a *gauche* orientation where the hydrogen atom faces fluorine in order to minimise the electrostatic lone/lone pair repulsion between the two electronegative elements (Figure 1.9).

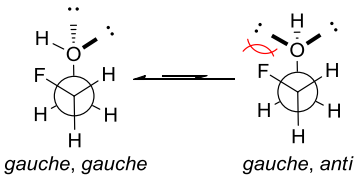

16

Figure 1.9: Conformational preference of 2-fluoroethanol **16**.

However, when the atom X is a chlorine atom (i.e. 1-fluoro-2-chloroethane **20**), this change induces an *anti*-conformation because the hyperconjugation is now counterbalanced by the steric hindrance caused by the interaction the bulkier halogen.[39] The *gauche* effect is very general and applies to other systems such as compounds containing F-C-C-O[40] and F-C-C-N[41] bonds (Figure 1.8).

An alternative explanation has been given to rationalise the *gauche* effect conjointly to the hyperconjugation. According to the "bent bond theory", the polarity of the C-F bond would be responsible for the geometric changes of the σ-bonds (C-C and C-H) on the carbon.[42] However, the argument in favour of the hyperconjugation being responsible for the *gauche* preference has become more popular.[43]

1.2.3.3 The 1,3-F bond repulsion:

This type of interaction varies slightly from the typical case of 1,3-difluoropropane **21**. In such substrate, the two fluorine atoms tend to repel each other. Four staggered conformers exist, ranked according to their relative stability as GG < GA < AA < GG' (Figure 1.10).[44]

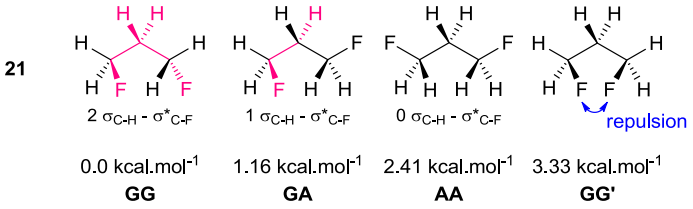

Figure 1.10: Rationalisation of the 1,3C-F bond repulsion in 1,3-difluoropropane **21**.

Hyperconjugation can be invoked to rationalise this order (assuming that C-H bond is a better donor than C-CF). Conformer GG induces two $\sigma_{C-H} \rightarrow \sigma^*_{C-F}$ interactions, GA only one and AA none. However the conformer of highest energy GG' presents an electronic repulsion between the two fluorines held on the same side. This destabilising interaction is superior to the stabilising effect of the two hyperconjugative σ_{C-H} - σ^*_{C-F} interactions which explains why the conformer GG' is 3.33 kcal.mol^{-1} higher in energy than the conformer GG. The parallel alignment of two C-F bonds in a 1,3-position results in an electrostatic repulsion which destabilises such conformation.

To exemplify this concept, O'Hagan and Kirsch investigated an under-explored class of compounds named "multi-vicinal fluoroalkanes" (Figure 1.11).[45]

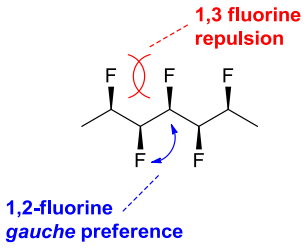

Figure 1.11: Conformational effect in multi-vicinal fluoroalkane: avoidance of 1,3 fluorine repulsion and preference of 1,2-*gauche* arrangement.

These molecules are made of an aliphatic alkane chain in which each adjacent carbon bears an atom of fluorine. The construction of molecules containing vicinal fluorines allows studying the cumulative effects of each additional C-F bond depending on the chain length and its impact on the conformation. It emerges from this detailed study that the chain featuring an all-*syn* configuration adopts preferentially a "bent" conformation. In such a case, the linear or zigzag conformation would force one every two C-F bonds to align parallel to one another, inducing 1,3-repulsions between each pair of dipoles. In order to avoid such destabilising interactions, the chain adopts a more favourable conformation (favoured by 8.4 kcal.mol^{-1}) by rotating slightly every C-C bonds so as to avoid 1,3-F-F repulsion but still retains a *gauche*-relationship between every vicinal fluorines. As a consequence the general conformation of the molecule will appear "bent" or helical depending on the chain length. This helical orientation of the C-F bonds along the carbon backbone can be visualised by looking at the arrangement of the C-F dipoles along the molecular axis in **22** (Figure 1.12).[46]

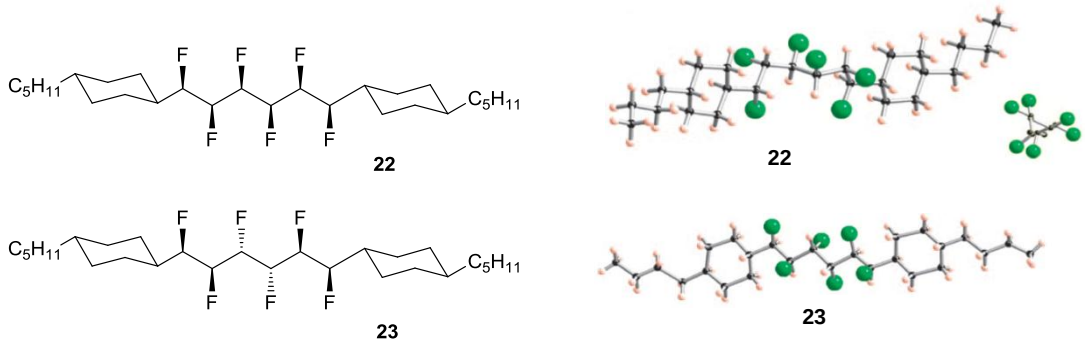

Figure 1.12: X-ray of the helical structure of the all-*syn* hexafluoroalkane **22** with a side-view along the molecular axis and the zig-zag structure of its *syn-anti-syn-anti-syn* diastereoisomer **23**.

It also clearly appears that the avoidance of 1,3 C-F repulsions dominates the forces governing the preferred conformation in multi-vicinal fluoroalkanes. *Gauche* interactions have a relatively subtle influence and exert their full potential only in the absence of repulsive 1,3 interactions.

The knowledge of stereolectronic effects associated with the C-F bond such as the dipole/dipole interactions, the charge/dipole interactions and the hyperconjugation gives a good overview of the useful potential of the C-F bond as conformational tool. Such conformational influence that fluorine exerts on the properties of functional molecules has been exploited in a wide range of field including

material science, biotechnology, medicinal chemistry and organocatalysis. This concept of tunable molecular design is guaranteed to play an increasing role in the future.

1.3 Understanding the implications of conformational effects of the C-F bond:

Fluoroproline in collagen:

As already described, the introduction of fluorine into organic compounds plays a very important role in the conformational control of molecules. Fluorine can become a conformational directing element when incorporated in a ring system. The intrinsic properties of fluorine have been exploited to fine-tune the ring puckering of the cyclic amino acid proline. It was demonstrated that the additional constraints imposed on the ring by the presence of the fluorine has direct consequences on the peptide backbone conformation, which can critically affect the biological activity. Most relevant examples of the use of fluoroproline are found in the assessment of collagen stability.

Collagen is the most abundant protein in animals[47] and constitutes three quarter of human connective tissues (skin, bone, tendon, cartilage, ligament, blood vessels and teeth).[48] This protein is made of three parallel polyprolines strands twisted so as to form a triple helix structure which exhibits great tensile strength. The cohesiveness of this structure is maintained by a network of interlaced hydrogen bonds running through the different strands.

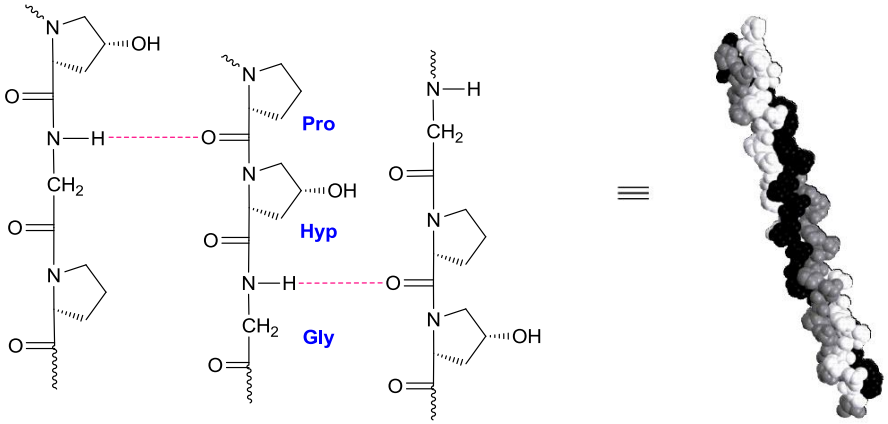

Figure 1.13: Hydrogen bonding in triple-helical collagen. The ladder of interstrand ProC=O···HNGly hydrogen bonds insures the cohesiveness of the structure.

Each individual strand is composed of a repeat sequence of amino acids XaaYaaGly. In natural occurring collagen, Xaa is mostly (2*S*)-proline **26** (Pro) whilst Yaa is mainly (2*S*-4*R*)-4-

hydroxyproline **25** (Hyp). The origin of collagen's high stability has been intensely debated. According to many, the hydroxyproline sub-motif **25** would play a significant role in maintaining the cohesiveness of the structure. A first theory suggests that the Hyp **25** hydroxyl group would be involved in a lace of hydrogen bonds promoting the stabilisation of the whole structure.[49] On the other hand, a second model explains the stability of the protein by the preorganisation of each single strands. By inducing a constrained ring puckering, the electron-withdrawing effect of the hydroxyl group would stabilise the *trans*-conformation of the proline amide bond which is essential for the protein folding.[50] In order to test the stereoelectronic influence of Hyp on the collagen stability, the hydroxyproline was replaced by (2*S*-4*R*)-4-fluoroproline **24** (Flp). The incorporation of Flp **24** in the collagen mimic resulted in an increase of the thermal and structural stability.[51] The conformational changes imparted by the fluorine on the proline ring are similar to those observed in Hyp **25**. Noteworthy, the pyrrolidine ring of proline can adopt generally two different puckerings or ring conformations in which the C^{β} and C^{γ} atoms are displaced from the mean plane of the ring.[52] The two extreme puckered forms are usually referred as C^{γ}-exo or C^{γ}-endo (Figure 1.14).

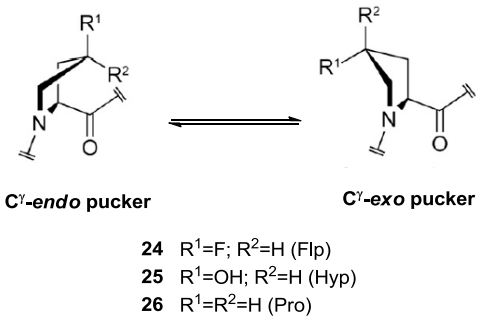

Figure 1.14: Equilibrium of ring conformations of 4-substituted prolines. The C^{γ}-exo conformation is favoured for Flp **24** and Hyp **25**.

Both Hyp **25** and Flp **24** favour a C^{γ}-exo ring pucker both in the solid state and in solution. However, it seems that the higher electronegativity of fluorine imparts stronger constraints on the ring conformation. In order to get a better understanding of the fluorine influence on conformation, a simplified model was investigated. The crystallographic, NMR and computational data of *N*-acetyl-4(*R*)-fluoroproline methylester **27** (Ac-4*R*-Flp-OMe) were found to be consistent with the manifestation of a *gauche* arrangement between the fluorine substituent and the nitrogen, as illustrated by the value of the N-C^{δ}-C^{γ}-F dihedral angle (-85 °).[53] According to energy calculations,

the C^{γ} exo-form is 0.85 kcal.mol^{-1} more stable than the C^{γ} endo-conformation. The origins of such preference can be rationalised by the analysis of the hyperconjugative delocalisation.

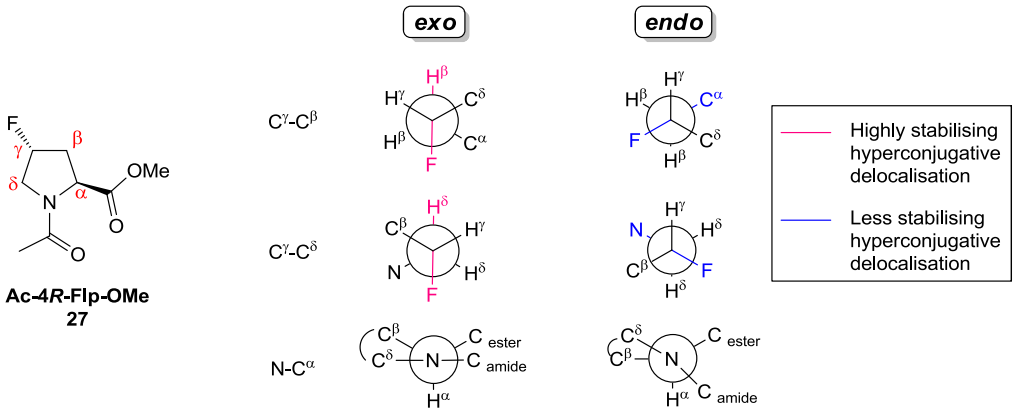

Figure 1.15: Newman projections about three bond axes illustrating the stereochemistry of the Ac-4*R*-Flp-OMe **27** model compound in its *exo* and *endo* conformations. For simplicity, each dihedral angle is shown in its fully staggered conformation rather than its optimised geometry.

The C^{γ}-exo ring pucker enables the alignment of the pseudo-axial C-F bond with two anti-parallel C-H bonds thus maximising the number of *gauche* interactions. The σ*(C^{γ}-F) anti-bonding orbital is better able to accept electron density from the C-H bonds than from the C-C or C-N bonds. Calculations estimate that the stabilisation energy provided by hyperconjugative delocalisation of the σ(C^{β}-H^{β}) and the σ(C^{δ}-H^{δ}) into the σ*(C^{γ}-F) is respectively 4.53 and 4.08 kcal.mol^{-1}. In comparison with the endo pucker, the anti-parallel σ(C^{β}-C^{α}) and σ(C^{δ}-N) provides only 2.89 and 1.52 kcal.mol^{-1} stabilisation energy into the σ*(C^{γ}-F) (Figure 1.15). As a result, the C^{γ}-exo conformation is preferred. Such conformational preference of the proline residue induces profound changes in the geometry and the nature of the surrounding bonds and has significant implications on the overall orientation of the peptide bond. Indeed the fluorine being held in a pseudo-axial position in the C^{γ}-exo pucker, exerts a stronger electron-withdrawing effect on the nitrogen than if it would be held in a pseudo-equatorial position (Figure 1.15). This has the consequence of lowering the amide C(O)-N bond order. This bond being weaker, the energy barrier to the amide-bond *trans/cis* isomerisation is reduced in favour of the *trans* conformation. It was calculated that rate constant of isomerisation for **24** in C^{γ} exo-conformation was $K_{trans/cis}$ = 4.0 in favour of the *trans* form of the amide bond. This preferred *trans*-amide conformation also promotes the stabilising hyperconjugative n → π* interaction between the two carbonyl groups along a close to optimal

Bürgi-Dunitz trajectory (τ_{BD}). The τ_{BD} value arises from maximising the overlap between the lone pair (n) of the amide oxygen and the π^* antibonding orbital of the ester carbonyl group (Figure 1.16).[54]

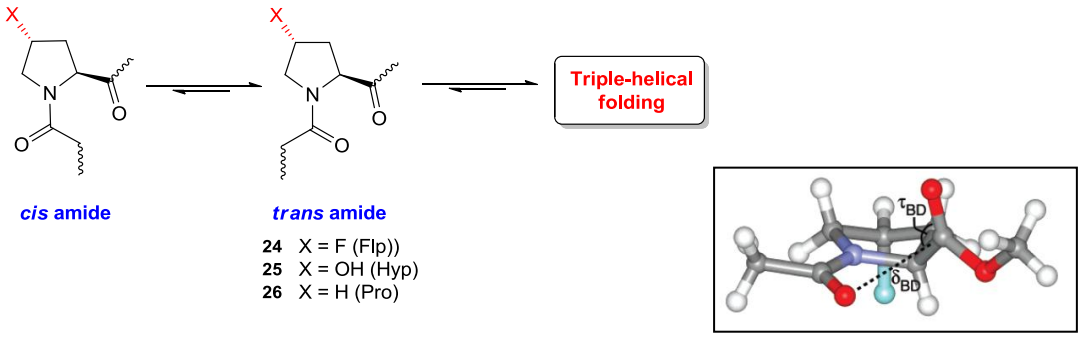

Figure 1.16: Relationship between *cis-trans* prolyl peptide bond isomerisation and the formation of collagen triple helix, which contains only *trans* peptide bonds. Inset: Crystalline structure of Ac-4*R*-Flp-OMe **27** illustrating the Bürgi-Dunitz trajectory, which is the preferred angle (τ_{BD}) of approach of a nucleophile to a distance (δ_{BD}) from a carbonyl group for an acyl transfer reaction.

Globally the introduction of Flp **24** with its distinctive C^{γ}-exo ring pucker into collagen mimic favors the all-*trans* conformation of the peptide bonds which is a prerequisite to the folding of the native collagen triple helix. Moreover the C^{γ}-exo pucker orients the C-F dipole towards an anti-parallel alignment to the proximal C=O dipoles and thus helps to maximise long-range dipole/dipole interactions.[55] Thereby the structural preorganisation of a collagen single strand is improved which results in the three helices being tighter together due to the optimal geometry of the connective hydrogen bonds network (Figure 1.13). In summary the subtle fluorine "*gauche* effect" imparts a crucial conformation to the pyrrolidine ring pucker which triggers a series of preorganisational mechanisms leading to the hyperstability of the fluorinated collagen analogue.

Overall the conformational directing power of the C-F bond could be developed to modulate the design of proteins and regulate their interactions. But beyond this example, the importance of the fluorinated pyrrolidine core reveals itself as a powerful synthon for the pharmaceutical and chemical industry. Therefore the selective synthesis of this specific motif has attracted a large interest. More examples of fluorinated pyrrolidines containing biologically active compounds can be found in more

detail in the book chapter *Fluorinated Five-Membered Nitrogen-Containing Heterocycles*, in *Fluorinated Heterocyclic Compounds: Synthesis, Chemistry, and Applications*, Wiley, **2009**.[56]

Fluorinated pyrrolidines in organocatalysis:

The potential of the C-F bond as a conformational directing group also finds application in the field of organocatalysis.[57] The understanding of the interactions governing the asymmetric amplification mediated by small organic molecules has become crucial.[58] The purpose of the introduction of C-F moiety into an organocatalyst structure is primarily to impose a conformational rigidness to the complex that will be translated by a noticeable difference in energy between the possible conformers. Five-membered heterocyles such as pyrrolidines have become increasingly popular as a platform for organocatalysts design. Enantiomerically pure analogues can be easily accessed using proline as building block and their conformational preferences can be finely-tuned according to requirements of the catalytic reaction.

This concept was exemplified in iminium catalysis (Scheme 1.1), where the introduction of fluorine positioned β to the iminium imposes a *gauche* arrangement[59] to the catalyst side chain.

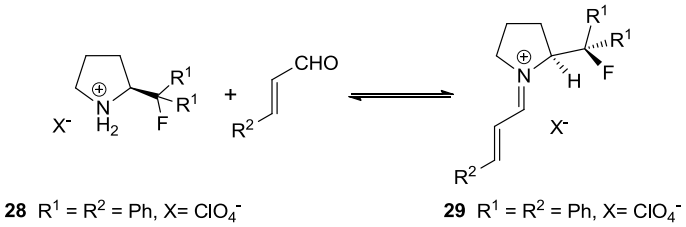

28 $R^1 = R^2 = Ph$, $X = ClO_4^-$ **29** $R^1 = R^2 = Ph$, $X = ClO_4^-$

Scheme 1.1: Schematic principle of the fluorine-iminium ion *gauche* effect.

In fluorinated pyrrolidine **28**, X-rays have confirmed the *gauche* conformation of the C-F bond with a dihedral angle N^+-C-C-F of 57° (Figure 1.17). Further DFT calculations demonstrated that the *gauche* conformation for the *E* and *Z* iminium ions were 3.9 kcal.mol^{-1} and 4.3 kcal.mol^{-1} respectively more stable than the *anti* conformation. Moreover the *gauche* conformation in the non-fluorinated catalyst analogue is only favoured by 1.2-1.4 kcal.mol^{-1}. This orientation arises from a combination of stabilising hyperconjugative $\sigma_{CH} \rightarrow \sigma^*_{CF}$ donations and dipole/charge electrostatic interaction $N^+ \cdots F^{\delta-}$. This special N^+-C-C-F arrangement imparts an extra degree of torsional rigidity to the molecular topology of the catalyst that will have consequences on the level of enantio-

induction of the reactive π systems. Moreover the presence of fluorine does not disrupt the overall steric volume of the molecule, whilst its electronegativity contributes to lower the LUMO of the catalyst. The control of the spatial interaction between the β-fluoro-iminium ion in diphenylmethylpyrrolidine and approaching nucleophiles has been the focus of a recent study.[60]

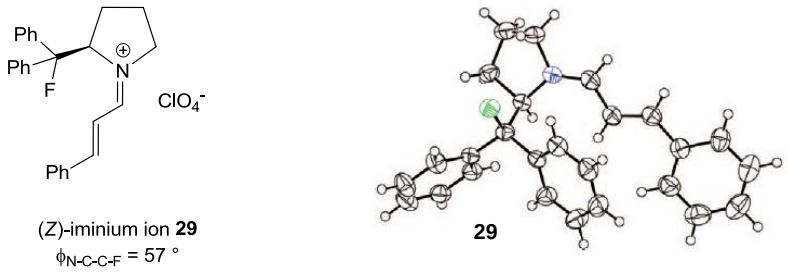

Figure 1.17: β-fluoro-iminium ion of (*R*)-2-(fluorodiphenylmethyl)pyrrolidine perchlorate **29** and its crystal structure.

The potential for enantio-induction of this novel catalyst was tested on the stereoselective epoxidation of α, β-unsaturated aldehydes with hydrogen peroxide.

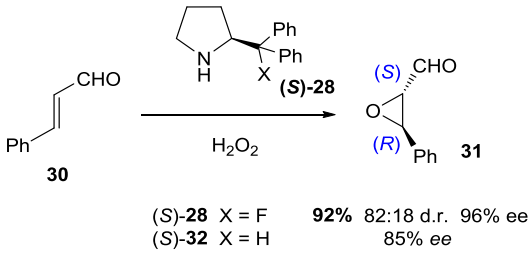

Scheme 1.2: Asymmetric epoxidation of α, β unsaturated aldehydes using (*S*)-**28** and hydrogen peroxide. Reactions performed in $CHCl_3$ with aldehyde (500 μmol), (*S*)-**28** (10 mol%), and H_2O_2 (1.3 eq.) for 3 hours at r.t. Optical purity of (*S*)-**28** of 98% ee, determined by HPLC.

The results gave a good level of both diastereo- and enantioselectivity (Scheme 1.2). Throughout the screening of various aldehydes, the diastereoselectivity remains constant around 4:1 and the level of enantio-enrichment reaches up to 96% ee with a catalyst loading ranging from 5 mol% up to 10 mol%. Comparatively the same reaction carried out using the non-fluorinated catalyst provided a lower ee of 85%. This experiment shows that the C-F bond and the *gauche* conformation that it induces, plays a significant role in the efficient transfer of chirality in amine-catalysed reactions. A mechanistic reasoning suggests that the fluorine *gauche* arrangement imparts a new orientation to the geminal phenyl rings which is now located in a parallel plane above the π system and thus acts as a steric shield (Figure 1.18).

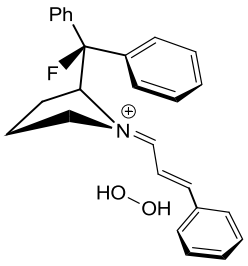

Figure 1.18: Conformation of the activated iminium ion **29** in a *gauche* arrangement with the fluorine. The top face of the π-system is shielded by one of the phenyl rings.

As a result, the nucleophile approaches the alkene on the least hindered face. The peroxide is delivered to the *Si* face of the *E* iminium ion with a high level of enantio-control. This example demonstrates that the fluorine *gauche* effect can be utilised as a conformational tool to preorganise the reactive form of the intermediate in the catalytic cycle. This new concept will be highly valuable for the design of novel organocatalysts.

1.4 Selective synthesis of mono fluorinated pyrrolidines:

Some recent important applications of fluorinated pyrrolidines in drug design have sustained interest in their development. Indeed the pyrrolidine ring is interesting in its own right, as it is found abundantly in both naturally occurring and synthetic biological active compounds. Pyrrolidines are also attractive because they hold a prominent position as a key submotif in many alkaloids such as indolozidines and pyrrolozidines. In order to develop bioactive substances containing pyrrolidine analogues with enhanced properties, researchers have focused on selective fluorination of this motif. Indeed a series of fluorinated pyrrolidines has been identified as important lead candidates to the development of dipeptidyl peptidase IV enzyme (DPP-IV) inhibitors.[61] An inhibitor of the DPP-IV enzyme prolongs and enhances the activity of incretins that play an important role in insulin secretion and blood glucose control regulation.[62] Inhibitors of the DPP-IV are a potent treatment for type-2 diabetes, which is one of the fastest growing health concerns in the world. The DPP-IV is a dipeptidase that selectively binds substrates that contain proline. This explains why inhibitors featuring a 5-membered heterocyclic ring that mimics proline have been the main focus of research. Pharmaceutical companies have explored the potency of fluorinated pyrrolidines as DPP-IV inhibitors.[63] These analogues include the α-amino amide **33**,[64] oxadiazole **34**,[65] amide **35**, **36** and

37 developed by Merck & Co.,[66] the amide **38** and **39** developed by Pfizer[67] and cyano-pyrrolidines **40**[68] and **41** developed by GSK which was the only one to reach phase III of development (Figure 1.19).[69]

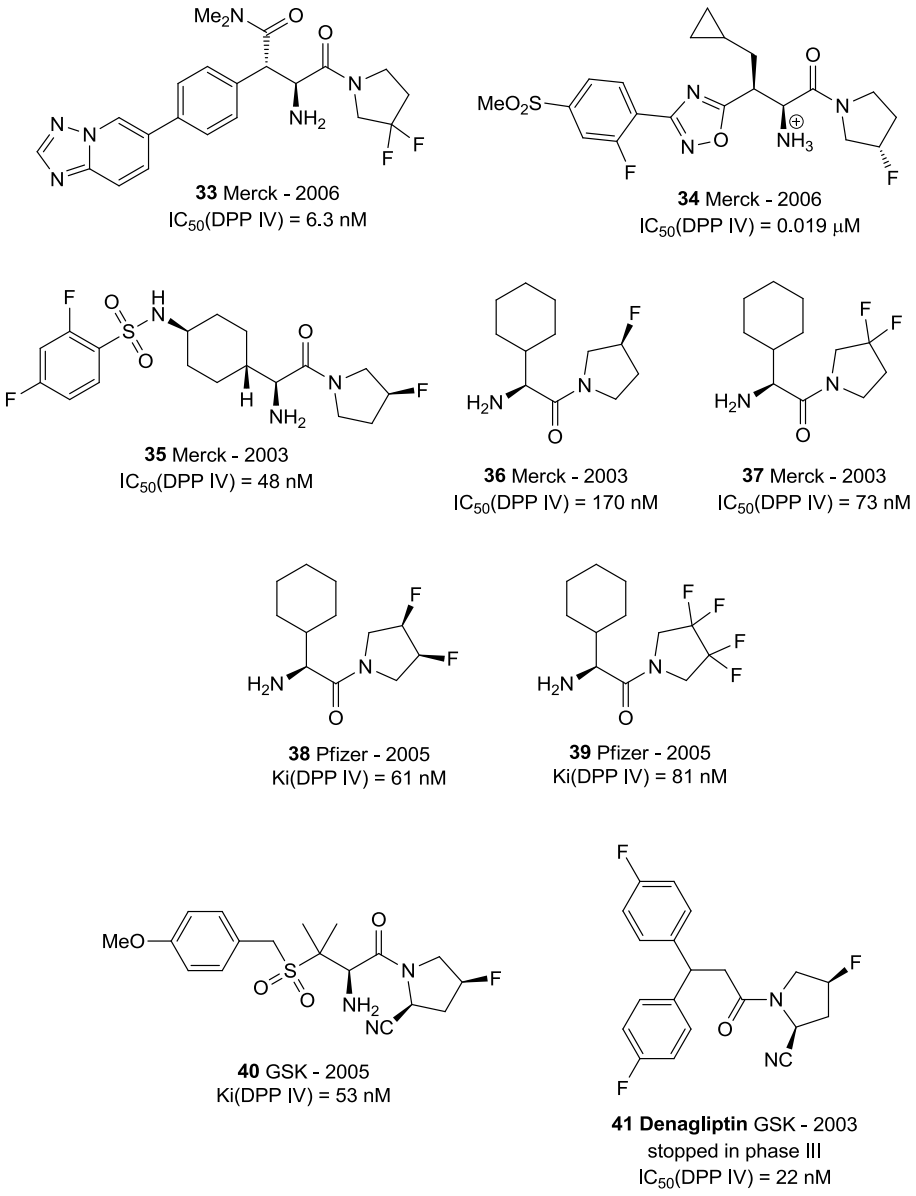

Figure 1.19: Fluoropyrrolidine based inhibitors of dipeptidyl peptidase IV.

The development of efficient synthetic methods for preparing fluorine-containing analogues of these compounds has received increasing attention in recent years. We will focus mainly on the synthesis of mono 3- and 4-fluoropyrrolidines and prolines.

Nucleophilic fluorination:

In the majority of cases, fluorinated pyrrolidines have been synthesised by nucleophilic fluorination, especially fluorination of alcohols and ketones. Initially, the *R*- and *S*-3-fluoropyrrolidine **43** were prepared by nucleophilic displacement of the optically pure *N*-carbobenzyloxy-3-tosyloxypyrrolidine with potassium fluoride (KF) (Scheme 1.3).[70]

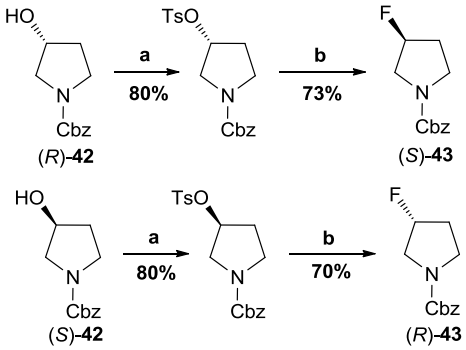

Scheme 1.3: Synthesis of 3-fluoropyrrolidine by tosylation and displacement with fluoride. **a**) TsCl, pyridine, -5 °C, 24 h; **b**) spray-dried KF, ethylene glycol, 85 °C, 18 h.

The synthesis of mono fluorinated pyrrolidine was later improved using a variation of the previous procedure. 3-Hydroxypyrrolidines can undergo a fluorodeoxygenation with diethylaminosulfur trifluoride **44** (DAST)[22] or bis(2-methoxyethyl)aminosulfur trifluoride **45** (Deoxofluor) as the nucleophilic source of fluorine (Scheme 1.4).[71]

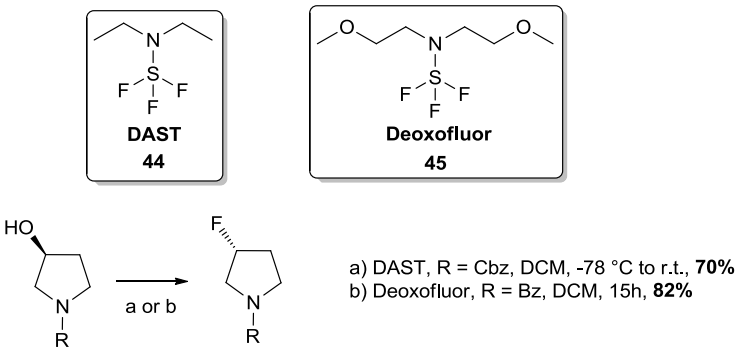

Scheme 1.4: Fluorodeoxygenation of 3-hydroxypyrrolidine with diethylaminosulfurtrifluoride **44** (DAST) and bis(2-methoxyethyl)aminosulfur trifluoride **45** (Deoxofluor).

The use of such reagents allows for the convenient introduction of fluorine into target molecules by converting alcohols into monofluorides. Young *et al.* demonstrated that fluorination with DAST occurs with complete inversion of configuration via a S_N2 process.[72] However upon heating, DAST converts to SF_4 and $(NEt_2)_2SF_2$, a high-boiling and explosive compound. Deoxofluor gave a slightly

improved yield relative to DAST, its higher thermal stability especially makes its applicability much wider ranging.[73] This strategy has also been used for the fluorination of 3-hydroxyproline (Scheme 1.5).[74]

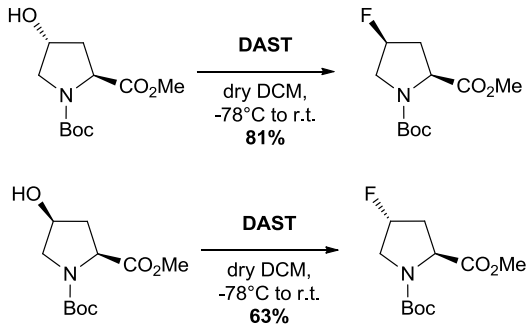

Scheme 1.5: Fluorination of hydroxyproline with DAST.

A second approach relies on the nucleophilic opening of suitably functionalised 3,4-epoxy pyrrolidines by fluoride anion displacement, affording fluorohydrin pyrrolidines (Scheme 1.6). In the first example **A** [67], a Boc-protected dihydropyrrole, obtained by ring-closing metathesis with Grubbs 2nd generation catalyst was converted into the corresponding epoxide using potassium peroxymonosulfate (Oxone). Opening of the epoxide with triethylamine hydrogen fluoride afforded the resulting fluorohydrin in a moderate yield of 45%. In the second example **B**,[75] the preparation of the chiral epoxyamine relied on the enantioselective epoxidation of an allylic alcohol followed by an intramolecular displacement of the alcohol by the pending benzylamine under Appel's conditions.[76] The regioselective nucleophilic attack of the epoxide was optimised using a solution of HF·pyridine complex at 60 °C for 24 h. Other nucleophilic source of fluoride such as TBAF and *i*Pr_2NH·3HF failed to deliver the desired product. The corresponding flurorinated pyrrolidine was obtained in 86% yield with a regioselectivity of 92:8 in favour of the introduction of the fluorine at the C-2 position (Scheme 1.6).

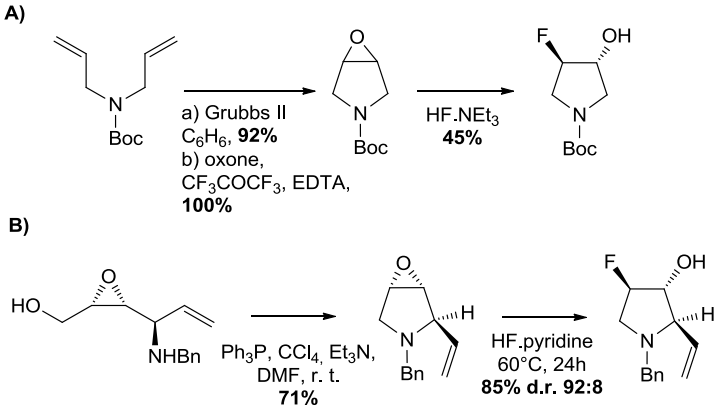

Scheme 1.6: Nucleophilic ring-opening of epoxy pyrrolidines using fluoride anion

This methodology was further refined by developing an enantioselective ring opening of epoxides using stoichiometric chiral reagents.[77] The first results reported moderate conversion with relatively low to good level of enantioinduction (up to 90% ee), using various source of fluorides with a chiral Lewis acid. Recent work from Doyle *et al.* culminated in the first example of catalytic enantioselective opening of epoxides by fluoride in good yield and good level of enantio-induction.[78] Using a dual catalyst system of a chiral amine and a chiral Lewis acid, fluoride was catalytically generated from benzoyl fluoride and an alcohol (HFIP). Following this new method, the 4-fluoropyrrolidin-3-ol was successfully obtained in 84% yield and 80% ee (Scheme 1.7).

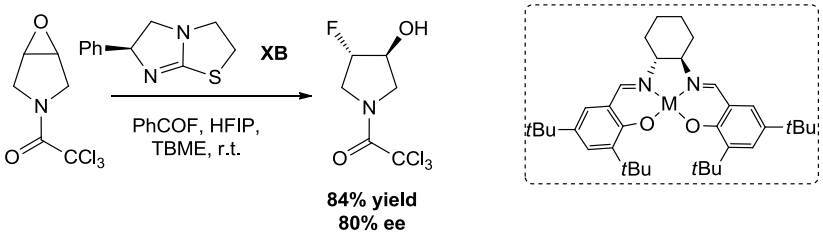

Scheme 1.7: Enantioselective ring-opening of epoxy pyrrolidines using fluoride anion.

A different methodology was also exploited for the synthesis of 3-fluoropyrrolidine. It relies on the reactivity of functionalised azetidines and the ring strain associated with such heterocycles. Therefore the stereospecific rearrangement of optically pure 2-hydroxyalkylazetidines has been investigated in presence of a nucleophilic source of fluorine (DAST or Deoxofluor).[79] The stereodefined synthesis of fluorinated pyrrolidines derived from primary or secondary azetidinols

proceeded in fair to good yield (from 45% up to 81%) while tertiary alcohols failed to rearrange (Scheme 1.8).

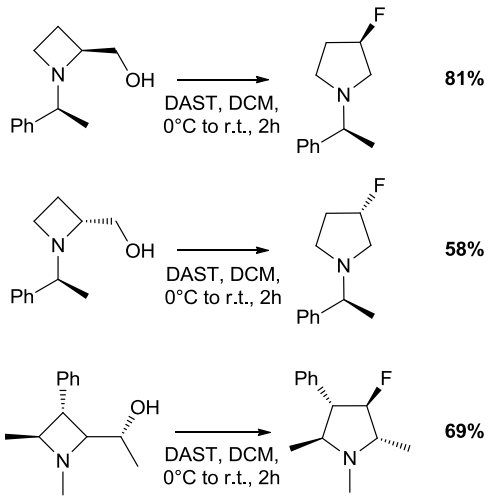

Scheme 1.8: Nucleophilic fluorination of functionalised 2-hydroxyalkylazetidines

In all the examples described, only one diastereoisomer was produced. The desired products present a 2,3-*trans* arrangement between the fluorine and the adjacent phenyl substituent. The reaction is believed to proceed *via* the regioselective attack of the fluoride on the azetidinium intermediate (Scheme 1.9).

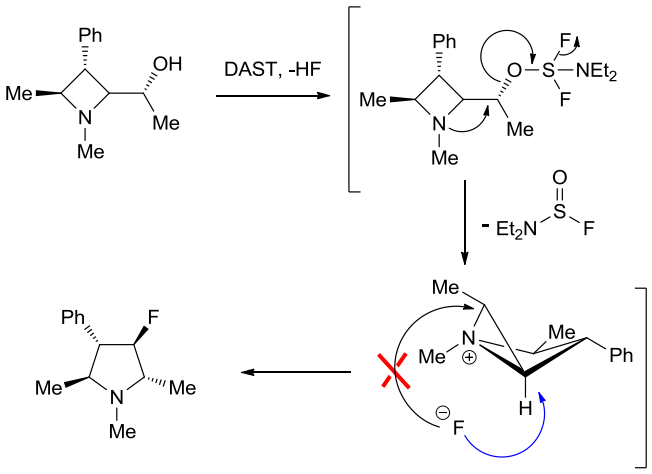

Scheme 1.9: Mechanism of the regioselective attack of the azetidium intermediate by fluoride.

This result contrasts with previous studies carried out on the similar ring expansion of prolinols which unselectively provided a mixture of 3-fluoropiperidine and 2-fluoromethylpyrrolidine.[80] The strained nature of the azetidinium intermediate seems to account for the high level of stereospecificity of the reaction.

Use of fluorinated building blocks:

Simultaneously alternative research direction based on the use of fluorinated building block was investigated. This new approach offers some advantages over the direct nucleophilic fluorination of alcohols. In the case of displacement of hydroxyl groups by fluoride, problems of chemoselectivity with the formation of side products are often observed. Moreover the presence of several hydroxyl functionalities requires additional steps of protection-deprotection. Above all, the use of nucleophilic fluorinating reagents such as DAST is strongly hampered by the handling difficulties and toxicity problems associated with such substances. Fluorinated building blocks represent an alternative to these drawbacks. At first, the 1,3-dipolar cycloaddition of azomethine ylides to electron-deficient olefins was considered.[81] Applying this approach to (*E*)-ethyl-3-fluoroacrylates using L-menthol as chiral auxiliary led the stereoselective and regioselective synthesis of enantiopure fluorinated pyrrolidines. Careful removal of the chiral auxiliary gave the corresponding fluorinated proline derivatives.

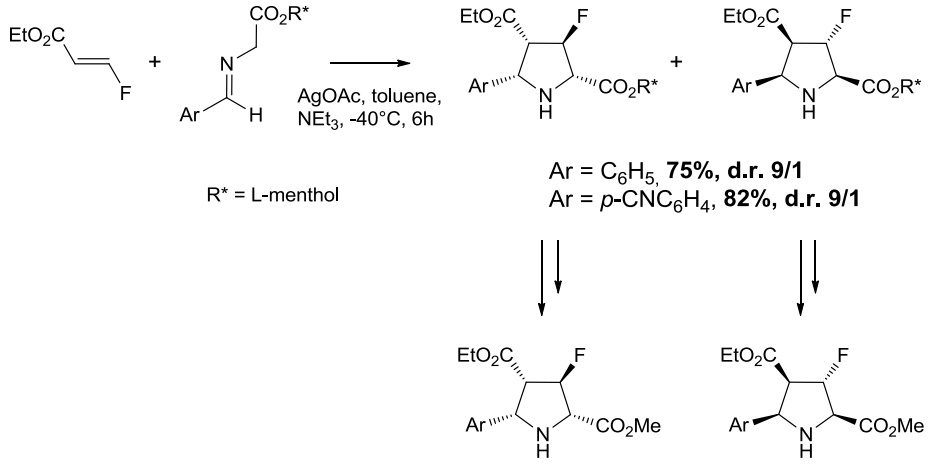

Scheme 1.10: 1,3-dipolar cycloaddition with 3-fluoroacrylates.

Electrophilic fluorination:

The syntheses of simple fluorinated pyrrolidines are based mainly on the introduction of the C-F bond through nucleophilic fluorination, however one example of electrophilic fluorination has been found in the literature.[82] In the synthesis of a new fluoroquinolone antibiotic, the intermediate lactam was fluorinated with the electrophilic fluorinating agent N-fluorobenzenesulfonimide **46** (NFSI) to give a single diastereoisomer. Treatment of this monofluoropyrrolidinone with base

followed by quenching with 2,6-di-tert-butylphenol gave access to the other diastereoisomer. Further manipulations including deoxygenation produced the desired fluoropyrrolidine intermediate used for the preparation of **47-49**.

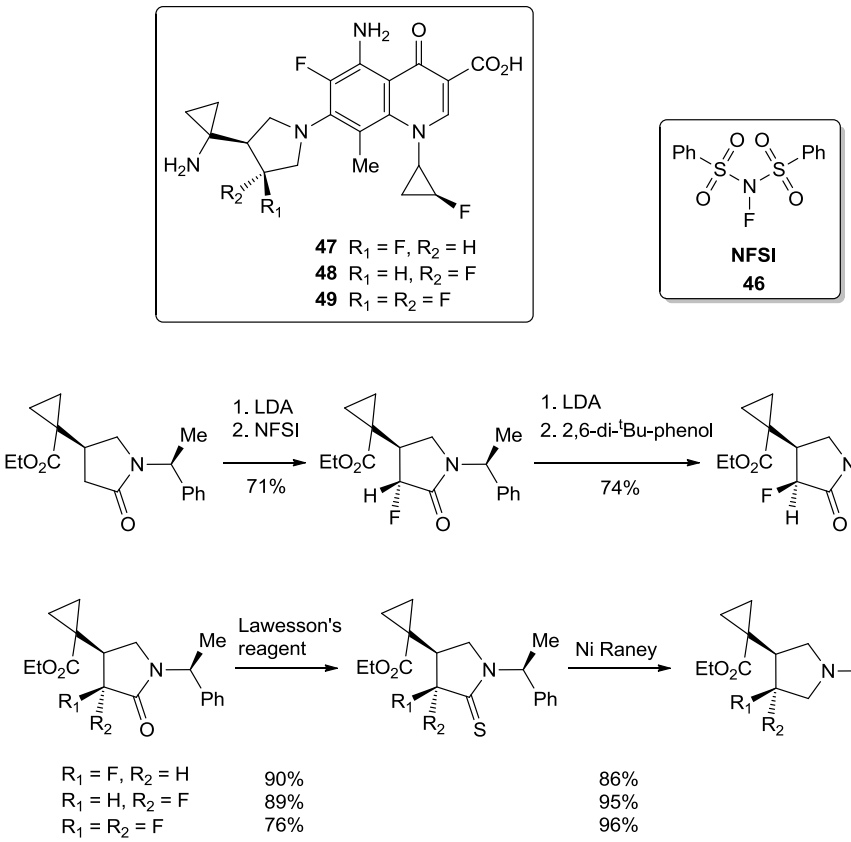

Scheme 1.11: Electrophilic fluorination of an intermediate for the synthesis of a new fluoroquinolone antibiotics.

1.5 Aim of this thesis:

The aim of this thesis is to investigate the synthesis and the conformational analysis of fluorinated pyrrolidines. We will focus on two strategies namely, iodoamination of fluorinated precursors and fluoroamination.

Iodoamination

Our first approach for the synthesis of fluorinated pyrrolidines will examine the iodocyclisation of allylic fluorides bearing pendant nitrogen nucleophiles. A series of factors will be examined, such as appropriate N-protecting groups, if required, in order to promote cyclisation. Furthermore, we will

probe the influence of the fluorine moiety on the level of diastereocontrol of the cyclisation. Once the iodoamination has been validated, the scope and limitations of this methodology will be investigated upon varying the substitution pattern of the starting material.

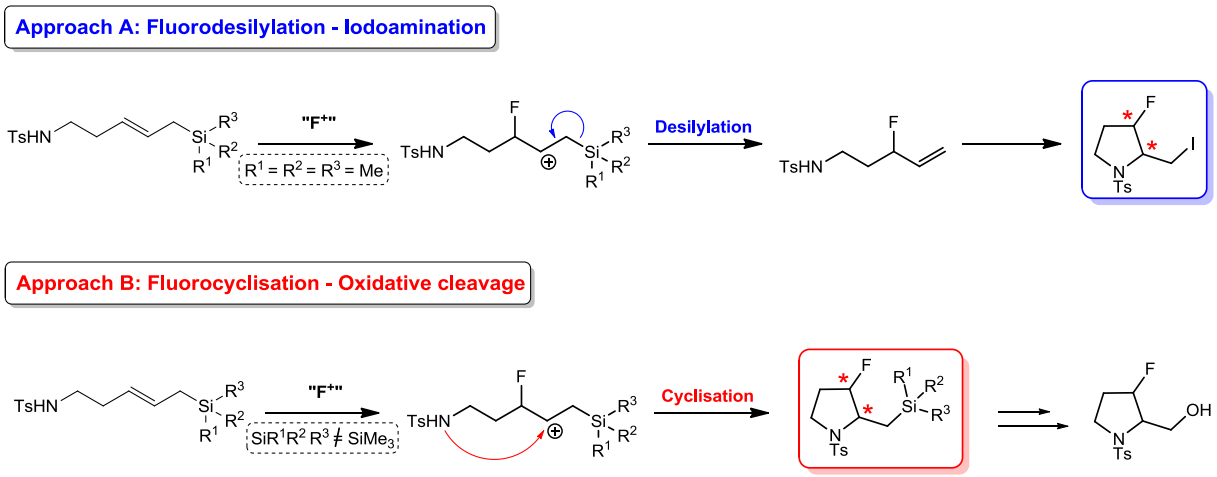

Scheme 1.12: Synthesis of fluorinated pyrrolidines. Approach A: fluorodesilylation/iodoamination; Approach B: fluorocyclisation.

Fluoroamination

The second route will focus on a key reaction: an unprecedented electrophilic fluoroamination of the aminated allylsilane. From a mechanistic point of view, the presence of the silyl group will act as a 1,2-dipole and activate the double bond towards electrophilic fluorination. The newly formed β carbocation could be intramolecularly trapped by the strategically positioned nucleophilic amine. This methodology will require a silyl directing group that will promote electrophilic addition, without subsequent desilylation. Ideally the identity of the silyl group will also be amenable to further functionalisation, for example oxidative cleavage. Finally, we would like to investigate the level of diastereocontrol that these cyclisations display as a function of the *E*/*Z* geometry of the starting aminated allylsilane. As for the previous strategy, we plan to explore more elaborate targets upon validation of this chemistry.

Moreover the 3-fluoropyrrolidines obtained via iodoamination will serve to investigate the influence of the stereoelectronic fluorine *gauche* effect on ring conformations in the solid state by single crystal X-ray analysis and in solution phase by NMR spectroscopy. It is well known that the conformational analysis of saturated five-membered rings in solution is complicated by their

inherent flexibility, and the interpretation of proton-proton scalar coupling constants (J_{HH}) and nuclear Overhauser effects (nOes) is often challenging in such systems. Therefore 1D ^{19}F-^{1}H heteronuclear nOe (HOESY) experiments have been optimised for applications to small molecules. These have been employed to estimate ^{19}F-^{1}H internuclear distances and were combined with vicinal $^{3}J_{FH}$ and $^{3}J_{HH}$ scalar coupling constants in order to analyse the ring conformations.

Chapter 2:

STEREOSELECTIVE SYNTHESIS OF FLUORINATED PYRROLIDINES – THE FLUORINE AS A STEREO-DIRECTING GROUP

2.1 Use of allylsilanes as activators for the electrophilic addition of fluorine to olefins:

The products of electrophilic addition of halogens to olefins are among the most versatile building blocks in synthesis. This reaction promotes the insertion of an internal or external nucleophile upon treatment of an alkene with an electrophilic species. In order to achieve the synthesis of fluorinated pyrrolidines, we would like to exploit the reactivity of alkenes towards electrophilic sources of fluorine. To that end, several parameters need to be investigated.

2.1.1 Generalities about the electrophilic addition of halogens to alkenes:

The generally accepted order of reactivity of halogens to olefins is as follow F_2>Cl_2>Br_2>I_2.[83] The addition of iodine is reversible (even in the presence of an excess of alkene). The overall mechanism involves three steps. The initial step relies on the formation of a π-complex between the alkene and the halogen. The existence of such complexes has been observed spectroscopically (with bromine and iodine).[84] The second step promotes the transformation of the neutral complex into an ionic intermediate. This intermediate can be of two sorts: a bridged halonium ion or a β-halocarbocation. The last step consists in the trapping of the β-halocarbocation or the ring opening of the bridged halonium ion by an internal or external nucleophilic species.

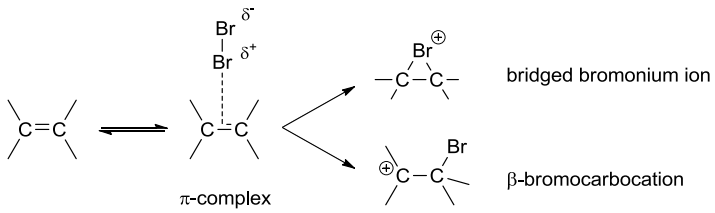

Scheme 2.1: Schematic representation of the mechanism of electrophilic addition to olefins.

The stereospecificity and selectivity of the reaction is directly dependent on the nature of the ionic intermediate. Aliphatic alkenes, lacking susbtituents which could stabilise a carbocation or possessing an electron withdrawing group would tend to favour the formation of a bridged halonium ion. In contrast olefins substituted with aromatic rings or any other electron releasing groups would provide enough stabilisation to a carbocation to promote the formation of a β-halocarbocation.[85] The trend is also influenced by the nature of the halogen. Although fewer details are available regarding the mechanism of fluorination and iodination of alkenes, the mechanism for the addition of bromine and chlorine is well documented. The π-complex formed upon addition of bromine usually collapses into a bridging bromonium ion. Stable examples of bromo-, chloro-, iodonium ion have been isolated and characterised.[86] Opening of the halonium occurs with an overall stereospecific *anti* addition.[87] However in some borderline cases such as the addition of bromine to styrene, a non negligible proportion of the *syn* product is observed.[88] The formation of a β-bromocarbocation accounts for this stereochemical outcome. If the nucleophilic attack occurs faster than the free rotation of the β-bromocarbocation around the C-C bond, the product will result in a non stereospecific addition. Addition of chlorine follows somehow the same pattern although with less stereospecific control.[89] Indeed chlorine is less polarisable than bromine and less eager to bear a positive charge, thus its ability to form a bridged cation is diminished.

2.1.2 The singularity of the electrophilic addition of fluorine to olefins:

Several computational studies have been carried out in order to compare the stabilisation energy of the two types of positive intermediate for fluorine, chlorine and bromine.[90] It was found that the formation of a β-fluorocarbocation is highly favoured compared to the bridged fluoronium ion. The contrast is less significant for chlorine and on the contrary the bromonium ion is found to be more stable than the corresponding open carbocationic species.

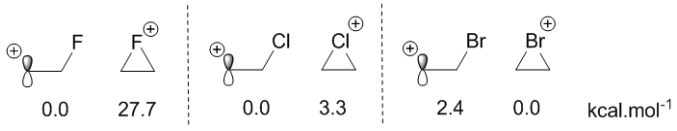

Scheme 2.2: Relative energy of the open and bridged halonium ions.

AIM charges (atom-in-molecule quantum theory) have been calculated for the different bridged halonium ions with ethene. The fluorine atom is shown to carry a negative relative charge which does not favour the formation of the cyclic intermediate. Noteworthy the computational results agree with the F<Cl<Br order in term of bridging ability but they tend to underestimate the stability of the bridge ions such as bromine at least as compared to solution behaviour.

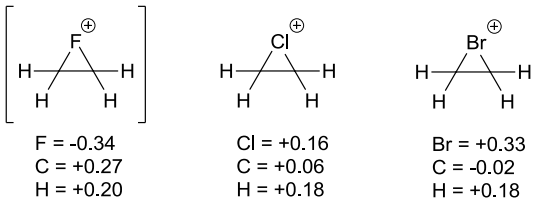

Scheme 2.3: Estimation of the atomic net charges for the bridged ions.

These results demonstrate that the formation of bridging fluoronium ion is highly improbable. The whole process of addition of elemental fluorine to ethane was analysed by *ab initio* MP2/6-31 +G level method and IRC (intrinsic reaction coordinate) algorithm.[91] The reaction path was found to involve first the approach of the fluorine vertically to the middle of the C=C, leading to the formation of a perpendicular complex. This intermediate further evolves to a deformed rhombic-type complex as the transition state, not as a square-type complex as previously considered. From there, the C-C and F-F bonds lengthen as the reaction progresses and a net negative charge develops on the proximal fluorine owing to the shift of electrons from ethane to the fluorine atom. The rapid recombination of the distal fluoride counterion to the electropositive species gives the final product of *syn* addition.

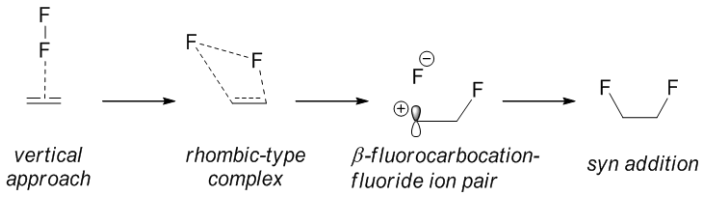

Scheme 2.4: Reaction pathway for addition of F_2 to olefins.

Experimental data corroborates this mechanism relying on the formation of a β-fluorocarbocation-fluoride ion pair. Upon addition of dilute F_2 to alkenes, the *syn* stereochemistry is observed as the major product.[92] The reaction of acetyl hypofluoride proceeds similarly.[93]

When electrophilic fluorinating agents such as N-F reagents are used for this type of addition, the reaction becomes more challenging due to their lower reactivity.[94] Fluorination of alkenes has been confirmed mainly in the case of activated substrates using the most powerful N-F reagents such as 1-chloromethyl-4-fluoro-1,4-diazoniabicyclo[2.2.2]octane bis(tetrafluoroborate) (Selectfluor® **50**),[95] DesMarteau reagent (**52**)[96] and N-fluoropentachloropyridinium triflate (**51**).[97]

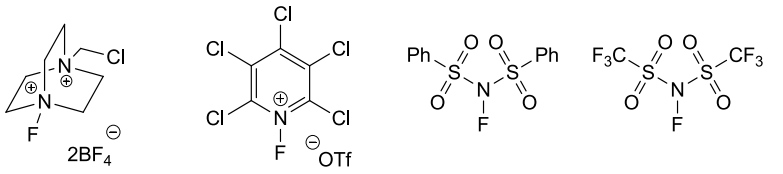

50 **Selectfluor** | **51** **N-fluoropentachloro-pyridinium triflate** | **46** **N-fluorobenzene-sulfonimide** | **52** **DesMarteau reagent**

Scheme 2.5: Most commonly used electrophilic fluorinating reagents.

Unactivated alkenes such as cyclohexene, 1-octene, did not afford fluorinated products under various conditions with the aforementioned electrophilic sources of fluorine. With N-F reagents, the use of an external weak nucleophile such as H_2O, AcOH, MeOH, HF.pyridine, is usually necessary to prevent the formation of complex product mixtures. The β-fluorocarbocation intermediate is quenched with a nucleophilic species from the reaction media or by proton elimination. The reaction very often leads to the product of Markovnikov-type regioselective addition. The reactivity of the alkenes can be significantly enhanced by adding substituents to the olefin; phenyl groups have been widely used for this purpose. It appeared from the study of the electrophilic fluorination of styrene derivatives that the nature of the substituents or the configuration of the alkene affects only moderately the stereochemical outcome (*syn* vs. *anti*) of the reaction, however the products are formed in good yields.

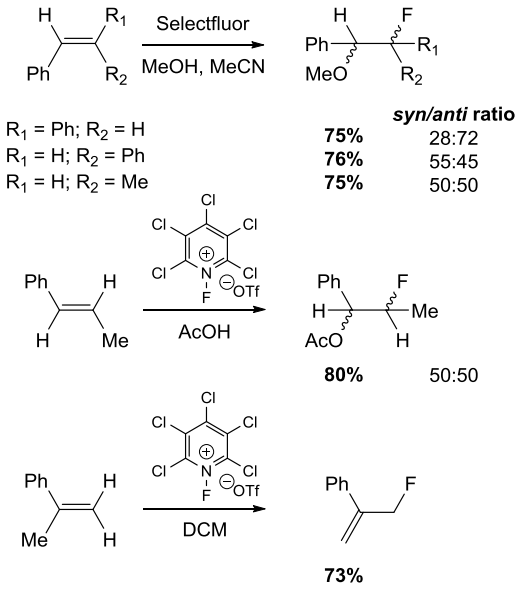

Scheme 2.6: Examples of fluorination of styrene derivatives with various sources of electrophilic fluorine.

This approach was successfully applied to the formation of 1,2-fluoroethers,[98] 1,2-fluoroamides[99] and fluorinated carbo- and heterocycles such as phenyl substituted cyclohexenes, indenes and benzocyclene.[100] Although highly regioselective, activation of olefins by the stabilisation of benzylic carbocation results in low stereoselectivity and does not afford a large structural variety.

2.1.3 Use of silanes as olefins activator:

Abundant literature has demonstrated that allylsilanes react readily with a wide variety of electrophiles. The substitution of a double bond with a silyl moiety has emerged as a powerful and more versatile alternative to activate the olefins towards electrophilic addition of fluorine. Depending on the nature of the process they are undergoing, allylsilanes are considered as useful synthetic equivalent of either allyl anions or 1,2-dipoles.

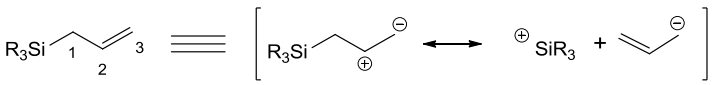

Scheme 2.7: Allylsilanes as synthetic equivalent of dipoles.

They can undergo two types of reactions:[101] an S_E2' addition followed by the loss of the silyl group, or a nucleophilic attack on the carbocationic intermediate subsequent to the electrophilic addition.

The high regioselectivity of the electrophilic reactions with allylsilanes is determined by the β-effect. Silicon is more electropositive (χ = 1.8) in nature than carbon (χ = 2.5) or hydrogen (χ = 2.1),

therefore the $\sigma_{C\text{-}Si}$ orbital is more polarisable and can more efficiently donate electron density than the $\sigma_{C\text{-}C}$ or $\sigma_{C\text{-}H}$ orbitals.[102] The presence of the silicon group can facilitate the electrophilic addition to olefins in two different ways.

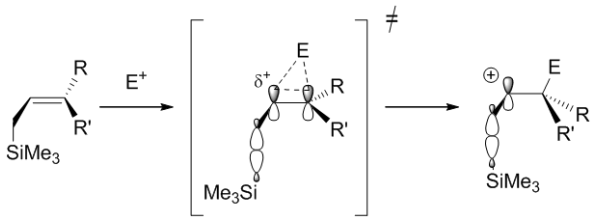

Scheme 2.8: Addition of electrophile on allylsilanes - the silicon β-effect.

Firstly, in term of reactivity, the $\sigma_{C\text{-}Si}$ orbital aligns parallel to the π orbital of the double bond with a maximum overlap. Thus the energy of the HOMO raises and the nucleophilicity of the alkene is enhanced.[103] To draw a parallel between the reactivity of propene (**11**) and allyltrimethylsilane (**12**), their respective nucleophilicity towards diarylcarbocations was probed. The allylsilane had an activation energy 18 kcal.mol^{-1} lower than propene.[104] Secondly, the β-silylcarbocation formed upon electrophilic attack is strongly stabilised by hyperconjugative donation of electron density from the $\sigma_{C\text{-}Si}$ orbital to the empty p_z orbital of the carbocation.

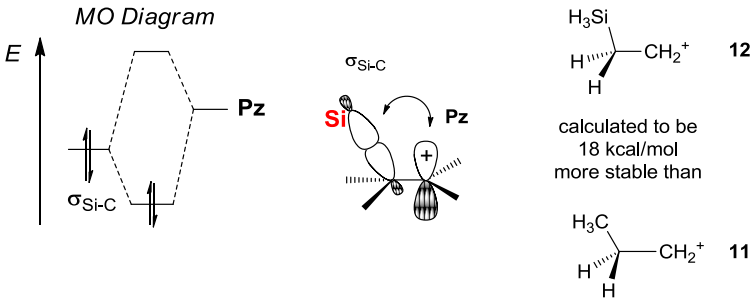

Scheme 2.9: Stabilisation of the carbocationic intermediate by hyperconjugation.

A non coplanar stabilisation in the form of a silacyclopropenium cation has also been suggested to challenge the idea of an open silyl carbocation.

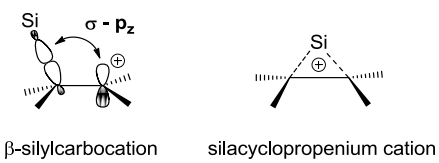

Scheme 2.10: Two possible forms of stabilisation of carbocations: open form and bridged form.

While *ab initio* and gas phase calculations tend to claim that both forms are isoenergetic,[105] investigations using secondary deuterium isotope effect demonstrates that the silicon β-effect is consistent only with an open, unbridged species.[102] *Ab initio* molecular orbital calculations have demonstrated that the β stabilisation due to the silyl group is significantly larger by 25 kcal.mol^{-1} than the β stabilisation arising from a methyl group. The strongest component of the energy of stabilisation results from hyperconjugation (29 kcal.mol^{-1}) and a more modest participation of induction and polarisation (9 kcal.mol^{-1}).[106] Therefore the reactivity of organosilanes is strongly influenced by electronic factors, but it is very often difficult to distinguish them from steric effects which may contribute to the same results.

2.1.4 Fluorodesilylation of allylsilanes:

The reactivity of the allylsilanes towards electrophiles therefore represents an attractive approach for the preparation of fluorinated substrates, in particular for allylic fluorides. Indeed the scope and limitations of the fluorodesilylation reaction has been extensively investigated by the Gouveneur group. This novel methodology provides access to a wide variety of allylic fluorides using a mild and regiospecific route. The overall reaction leads to the complete regioselective addition of the fluorine to the alkene with subsequent full transposition of the double bond. This methodology is very versatile and offers great functional group tolerance.[107] Only α–fluorinated carbonyl groups cannot be obtained since the β-stabilisation provided by the silicon is not sufficient to overcome the electron withdrawing effect of the carbonyl group (Table 2.1, entry 7).

Entry	Allyl silane	Allylic fluoride[a]	Yield (%)
1	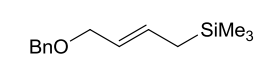	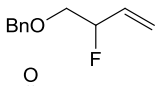	71
2	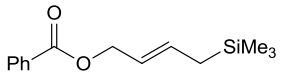	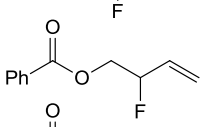	74
3	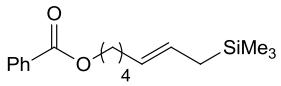	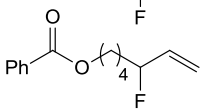	33
4	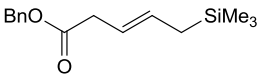	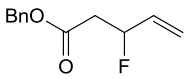	69
5	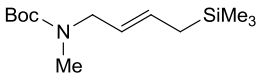	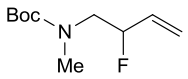	52
6	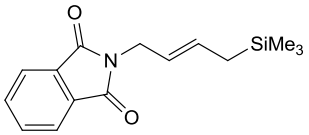	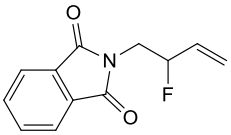	82
7	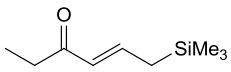	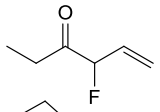	0
8	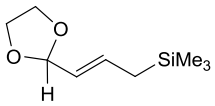	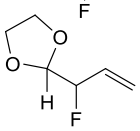	100[b]
9	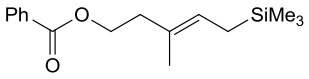	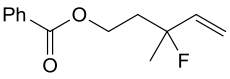	79

Table 2.1: Scope and limitations of the electrophilic fluorodesilylation reaction; [a] Selectfluor, MeCN, r.t. 48 h; [b] Conversion. (Table reproduced from S. Thibaudeau, V. Gouverneur**,** *Org. Lett.* **2003,** *5*, 4891-4893).[107]

The potential role of the silicon as a stereo-directing element was further probed and the diastereoselectivity of the fluorodesilylation reaction was investigated. According to the study conducted by Tredwell *et al.*, the electrophilic fluorination of enantiopure allylsilanes featuring a chiral centre remote from the silyl moiety, produced the corresponding β-fluoro carboxylic acid derivatives in good yield but with low diastereocontrol (Scheme 2.11).[108] It was then concluded that the presence of a stereogenic centre remote from the silicon group had no effect on the sense of selectivity of the reaction. A later investigation led by Sawicki *et al.* on the stereoselective fluorination of branched (*E*) allylsilanes possessing a silylated stereocentre demonstrated the important role of the silicon as a stereo-directing group.[109] When subjected to the reaction, the various *anti* and *syn* (*E*) allylsilanes delivered the corresponding fluorinated products in high yield

but also with accurate transfer of chirality from the silylated to the fluorinated stereocentre (Scheme 2.11).

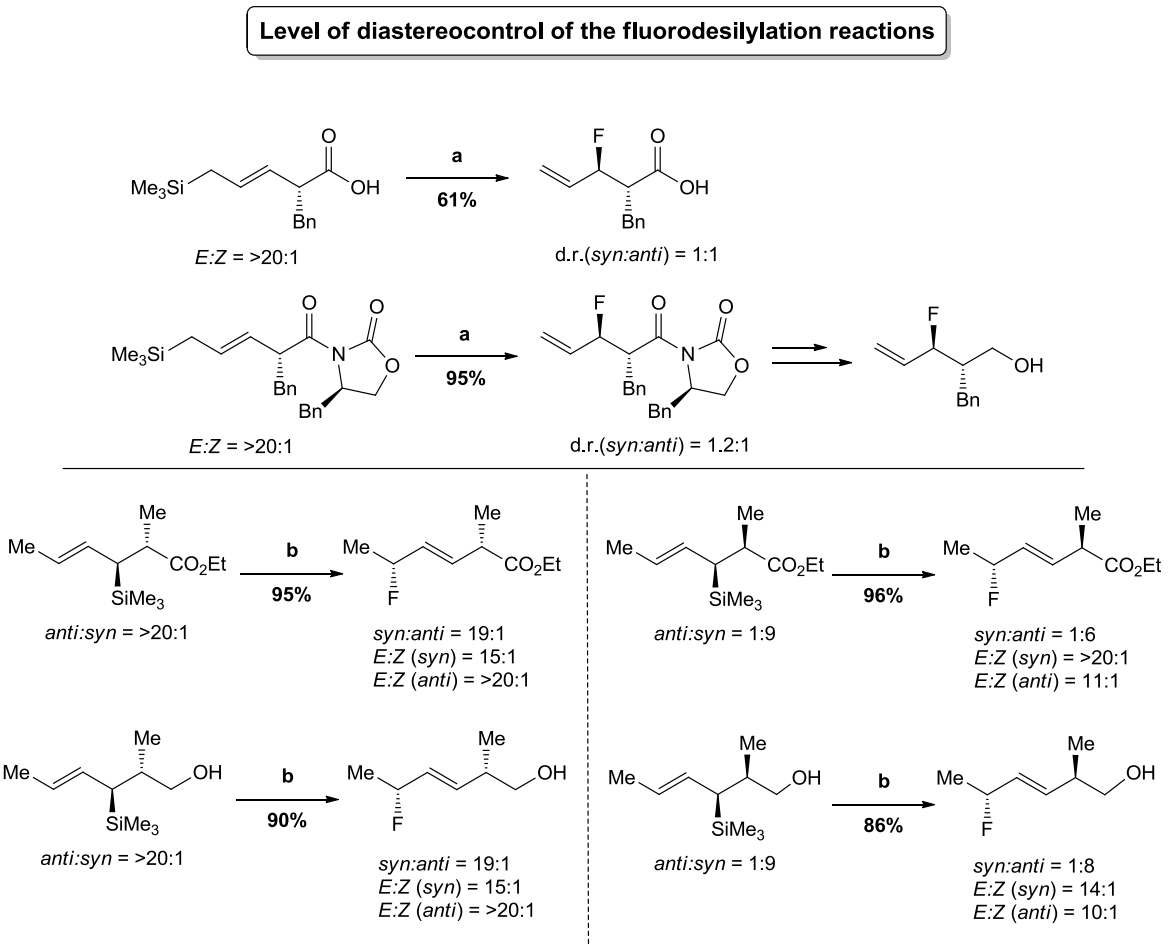

Scheme 2.11: Comparison of the level of diastereocontrol between the fluorodesilylation of enantiopure *E*-allylsilanes and chiral *E*-crotylsilanes. **a**) Selectfluor, MeCN, r.t., 48 h (reproduced from M. Tredwell, K.Tenza, M. C. Pacheco, V. Gouverneur, *Org. Lett.* **2005,** *7*, 4495-4497)[108]; **b**) Selectfluor, $NaHCO_3$, MeCN, r.t., 48 h (reproduced from M. Sawicki, A. Kwok, M. Tredwell, V. Gouverneur, *Beil. J. Org. Chem.* **2007**, *3*, 34-38)[109].

Identical results were observed in the asymmetric *de novo* synthesis of fluorinated derivatives of L-glucitol and L-mannitol (Scheme 2.12).[110] These results indicate the predominance of *anti* addition of fluorine with respect to the silyl group, which is consistent with the *anti* stereospecificity of electrophilic addition on allylsilanes. This sense of selectivity can be understood by considering the ground state conformation of the allylsilane where the smallest subsitutent α to the silicon (hydrogen) adopts an inside position, eclipsing the double bond, in order to decrease allylic $A^{1,3}$ strain with the vinylic hydrogen. The silyl substituent obstructs the upper face of the alkene, forcing the fluorine electrophile to approach from the opposite face. The Si-C bond is positioned perpendicularly to the olefin so as to stabilise the developing β-silylcarbocation intermediate, which

tends to retain its configuration due to hyperconjugation. The loss of the silyl group generates afterwards the stereoselective formation of the *E* allylic fluoride.

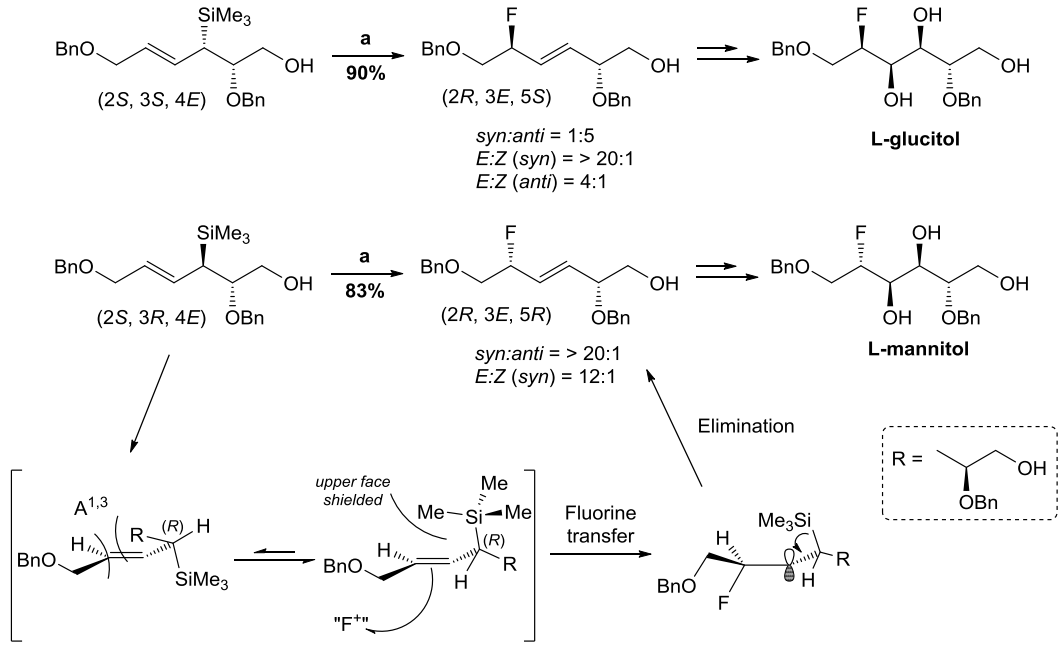

Scheme 2.12: Diastereocontrol through the anti-S_E2' mechanism illustrated by the electrophilic fluorodesilylation of a enantioeneriched acyclic allylsilane in the synthesis of L-glucitol and L-mannitol. (Reproduced from G. T. Giuffredi, S. Purser, M. Sawicki, A. L. Thompson, V. Gouverneur, *Tetrahedron: Asymmetry* **2009**, *20*, 910-920) [110]

High levels of diastereocontrol could also be obtained in the fluorination of selected cyclic allylsilanes (Scheme 2.13).[111,112]

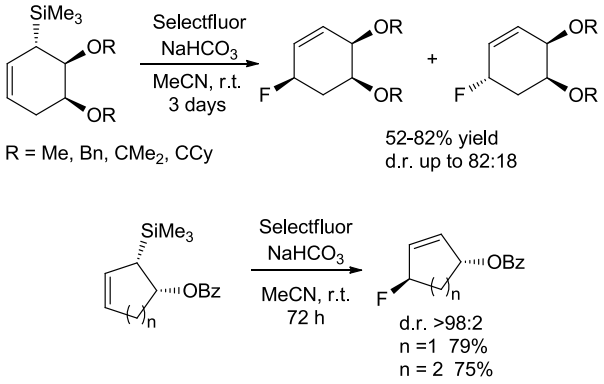

Scheme 2.13: Fluorination of cyclic allylsilanes. (Reproduced from S. Purser, C. Wilson, P. R. Moore, V. Gouverneur, *Synlett* **2007**, *7*, 1166-1168 [111] and S. Purser, B. Odell, T. D. W. Claridge, P. R. Moore, V. Gouverneur, *Chem. Eur. J.* **2006**, *12*, 9176-9185 [112]).

This methodology was extended to a Diels-Alder reaction followed by electrophilic fluorodesilylation which provided a route to both fluorinated carbo- and heterocycles in good yields and diastereoselectivity (Scheme 2.14).[113,114]

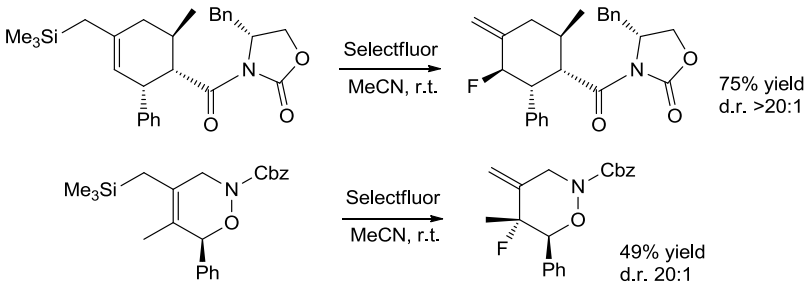

Scheme 2.14: Fluorination of allylsilanes obtained by Diels-Alder reaction. (Reproduced from Y.-h. Lam, C. Bobbio, I. R. Cooper, V. Gouverneur, *Angew. Chem. Int. Ed.* **2007**, *46*, 5106-5110 [113] and Y.-h. Lam, M. N. Hopkinson, S. J. Stanway, V. Gouverneur, *Synlett* **2007**, *19*, 3022-3027 [114]).

The scope of the electrophilic fluorodesilylation reaction of allylsilanes was further extended to an enantioselective variant.[115] The asymmetric fluorodesilylation was carried out using chiral N-F reagent prepared *in situ* by mixing various cinchona alkaloids with Selectfluor. The allylsilanes underwent full conversion smoothly after 24 hours at -20 °C to deliver the corresponding chiral allylic fluorides in up to 96% ee (Table 2.2, entries 1-3). Futhermore, an asymmetric catalytic alternative of the preceding method was later developed by Shibata *et al.*[116] By replacing Selectfluor by NFSI, a less powerful fluorinating agent; the reaction could be performed with a sub-stoichiometric amount of alkaloid. The outcome of the reaction was equally successful in delivering the chiral allylic fluorides in up to 95% ee using NFSI, 10 mol% of alkaloid and 6 equivalent of K_2CO_3 (Table 2.2, entries 4-7).

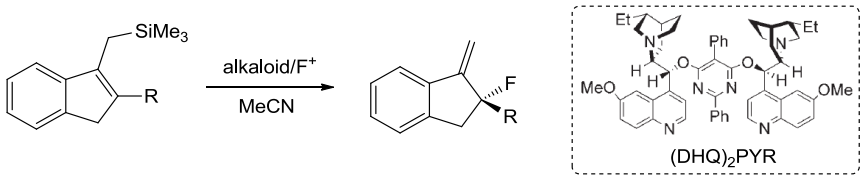

Entry	F^+	R	Alkaloid	Yield [%]	*ee* [%]
1	Selectfluor	$CH_2C_6H_5$	$(DHQ)_2PYR$	>95 [a]	96
2	Selectfluor	H	$(DHQ)_2PYR$	>95[a]	22
3	Selectfluor	Me	$(DHQ)_2PYR$	>95[a]	45
4	NFSI	$CH_2C_6H_5$	$(DHQ)_2PYR$	75	94
5	NFSI	$CH_2C_6H_4$-p-Me	$(DHQ)_2PYR$	75	95
6	NFSI	$CH_2C_6H_4$-p-Cl	$(DHQ)_2PYR$	81	94
7	NFSI	Me	$(DHQ)_2PYR$	73	72

Table 2.2: Enantioselective fluorodesilylation of allylsilanes catalised by cinchona alkaloid. [a] Conversion. **Entries 1-3** reproduced from B. Greedy, J.-M. Paris, T. Vidal, V. Gouverneur, *Angew. Chem. Int. Ed.* **2003**, *42*, 3291-3294.[115] **Entries 4-7** reproduced from T. Ishimaru, N. Shibata, T. Horikawa, N.Yasuda, S. Nakamura,T. Toru, M. Shiro, *Angew. Chem. Int. Ed.* **2008**, *47*, 4157-4161.[116]

The electrophilic fluorodesilylation provides a general and mild technique for the selective introduction of fluorine into an organic compound. This is a useful transformation as allylic fluorides are considered key building blocks. Electrophilic fluorodesilylation has been successfully applied to the synthesis of fluorinated natural product analogues such as monofluorinated sphingosine[117] and vitamin D_3.[118] The convergent synthesis of the fluorinated sphingosine relies on a sequential cross-metathesis-fluorodesilylation-cross-metathesis process (Scheme 2.15). Unfortunately due to the remote position of the chiral centre, the fluorinating step did not afford a good level of stereocontrol delivering the allylic fluoride as an equal mixture of separable *syn* and *anti* isomers.

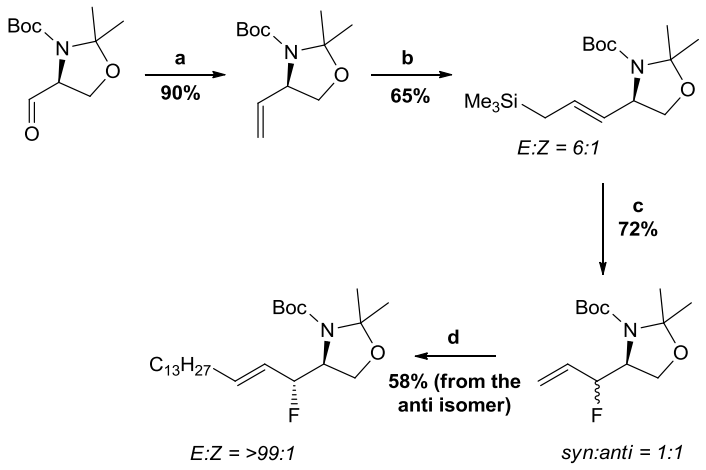

Scheme 2.15: Synthesis of the monofluorinated sphingosine analogue. **a**) Ph_3PMeBr, KHMDS; **b**) trimethylallylsilane, 0.3 eq. $Ti(O^iPr)_4$, 0.1 eq. Grubbs 2nd generation catalyst; **c**) 2.2 eq. Selectfluor, MeCN; **d**) 1-pentadecene, 0.1 eq. Hoveyda-Grubbs catalyst. (Reproduced from H. Teare, F. Huguet, M. Tredwell, S. Thibaudeau, S. Luthra, V. Gouverneur, *Arkivoc*, **2007**, 232-244 [117]).

Similarly the synthesis of the fluorinated analogue of the key "A-ring" intermediate for the preparation of the vitamin D_3 was achieved using an electrophilic fluorodesilylation reaction (Scheme 2.16). The major *trans* product results from the preferential axial attack of the electrophile *anti* to the silyl group in the least hindered half-chair conformation.

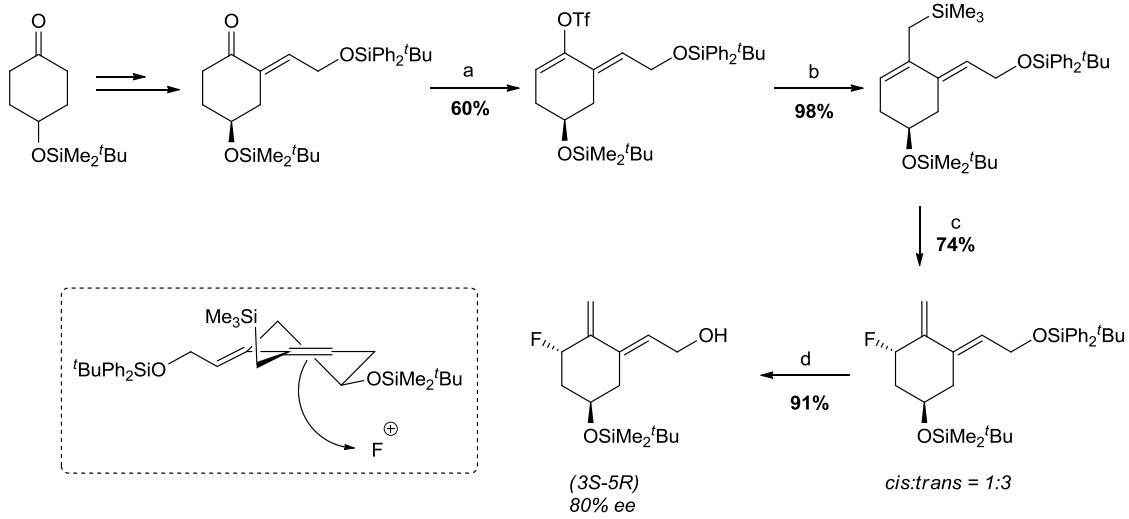

Scheme 2.16: Enantioselective synthesis of a fluorinated analogue of the "A-ring" intermediate for the preparation of vitamin D_3; **a**) LDA, $(CF_3SO_2)_2NPh$; **b**) Me_3SiCH_2MgCl, LiCl, 0.1 eq. $Pd(PPh_3)_4$; **c**) Selectfluor, $NaHCO_3$, MeCN; **d**) KOH. (Reproduced from G. Giuffredi, C. Bobbio, V. Gouverneur, *J. Org. Chem.* **2006**, *71*, 5361-5364 [118]).

2.2 Methodological concept: towards the stereoselective synthesis of fluorinated pyrrolidines

The synthesis of 3-fluoropyrrolidines using the versatility of allylsilanes is the objective of the present work. We would like to use the silicon moiety as a means to enhance the reactivity of the alkenes towards the regio- and diastereocontrol of the electrophilic addition of fluorine. We would also like to probe the stereodirecting effect of fluorine. Therefore we considered two approaches to solve this research problem. In the first instance, **approach A** will investigate the conversion of an allylic fluoride derived from the electrophilic fluorodesilylation of an allylsilane, into a fluorinated pyrrolidine *via* iodocyclisation in a two-step procedure. **Approach B** will focus on a concerted fluorination-cyclisation process to deliver the desired fluorinated heterocycles. Depending on the nature of the allylsilane, the reaction could be rerouted so that the carbocationic intermediate formed upon electrophilic fluorination could be intramolecularly trapped by a strategically positioned amine nucleophile.

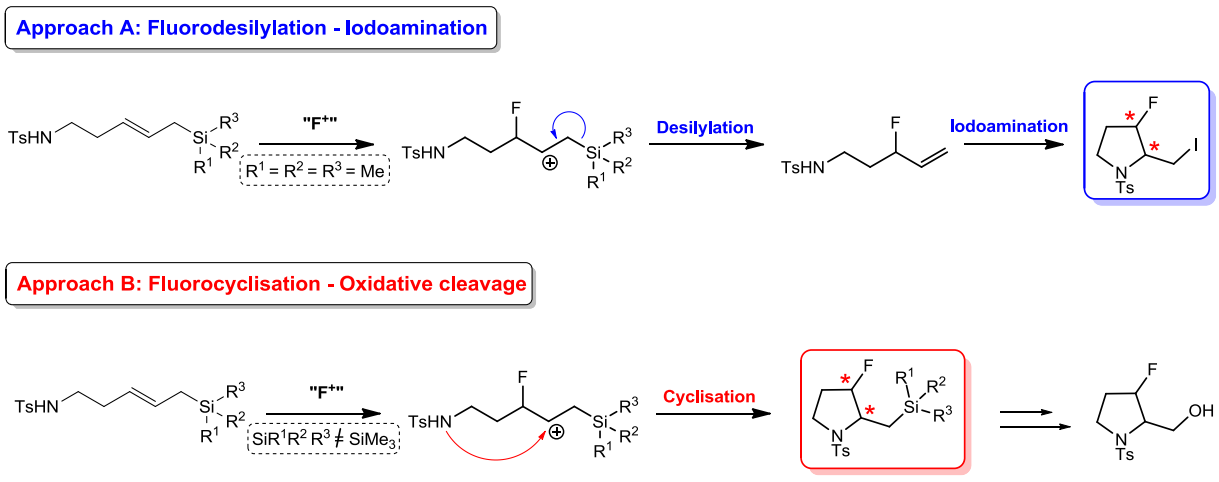

Scheme 2.17: Methodological concept.

2.3 Stereoselective synthesis of fluorinated pyrrolidines via iodocyclisation:

2.3.1 Iodocyclisation:

2.3.1.1 General aspect of iodocyclisation reactions:

Electrophilic halocyclisations of olefins are generally very versatile transformations and a wide range of nucleophiles such as OH, COOH, NHR and SR can be successfully used to generate a variety of different heterocycles. [119] Reactions carried out using iodine as an electrophile have been known for more than a century, and have emerged as a general method for the preparation of heterocyclic compounds. The possibility of regio- and stereocontrolled functionalisation of the double bonds by iodine is also considered as crucial in synthesis.

The reaction is expected to proceed *via* the activation of the double bond by the electrophile, leading to the intramolecular addition of the pending internal nucleophile. Depending on the stereochemistry and the ring size, this process can occur either in an *exo* or *endo* fashion.[120] The first step is the reaction between the electrophile and the π system of the alkene. Theoretical calculations demonstrated that there is almost no charge transfer involved and moreover kinetic investigations suggested an iodine-π complex as intermediate rather than iodonium ion.[86, 121] The regioselectivity of simple iodocyclisation is controlled by electronic factors (Markovnikov rule) and steric factors. There is a general preference for *exo* cyclisation over *endo* cyclisation.[119] The stereochemistry can also be influenced by additional conformational and entropic factors. As the addition steps may be reversible, kinetic or thermodynamic control will account for the observed stereochemistry.[122]

2.3.1.2 Stereoselectivity of intramolecular iodocyclisation:

Many efforts have been devoted to the investigation of the stereochemical preference during the synthesis of 5-membered ring *via* iodocyclisation.[123] Asymmetric induction has been granted special attention because it affords the possibility to control the stereochemistry of the halomethyl moiety which constitutes the basis for further functionalisation. For this purpose the influence of the substituent at the allylic position was probed. A systematic investigation into iodoetherification and iodoamination of allylic alcohol derivatives was carried out by Yoshida and co-workers.[124,125] These two complementary studies reported respectively the stereoselective synthesis of 2-iodomethyl-3-

hydroxytetrahydrofurans[124] and 2-iodomethyl-3-hydroxypyrrolidines (Table 2.3).[125] The use of kinetic conditions (I_2, $NaHCO_3$, Et_2O-H_2O) led to the formation of the desired cyclised heterocycles in good yield with a very high level of diastereoselectivity in favour of the *syn* products.

Entry	Substrate	Product	d.r. (*syn:anti*) yield (%)[a]	Substrate	Product	d.r. (*syn:anti*) yield (%)[a]
1	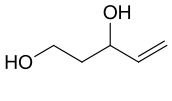	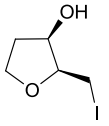	19:1 87	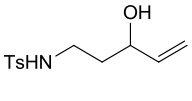	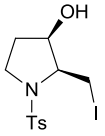	>20:1 86
2	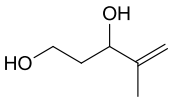	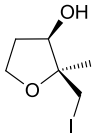	10:1 94	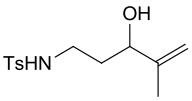	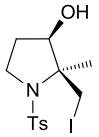	13:1 99
3	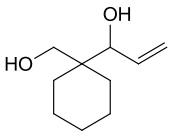	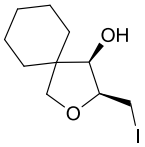	>20:1 98	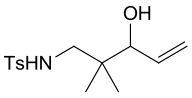	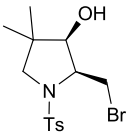	19:1[b] 88
4	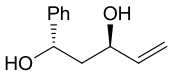	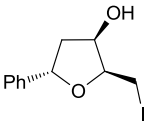	>20:1 98	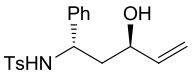	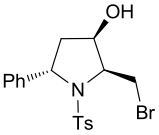	19:1[b] 80

Table 2.3: Representative examples of iodoetherification and iodoamination of allylic alcohols. [a] Condition: I_2, $NaHCO_3$, Et_2O-H_2O, 0 °C; isolated yields; d.r. determined by ^1H, ^{13}C NMR and HPLC analysis; [b] Condition: NBS, DME-H_2O. Reproduced from Y. Tamaru, M. Hojo, S. Kawamura, S. Sawada, Z. Yoshida, *J. Org. Chem.* **1987**, *52*, 4062-4072 (left)[124] and Y. Tamaru, S. Kawamura, T. Bando, K. Tanaka, M. Hojo, Z. Yoshida, *J. Org. Chem.* **1988**, *53*, 5491-501 (right)[125].

This pronounced stereochemical preference occurring during the ring closure is in agreement with the reactivity model proposed by Chamberlin and Hehre on structurally related lactones.[126] This model rationalises the effect of an allylic hydroxyl substituent as a diastereodirecting group. The electrophilic attack is preferred on the conformer featuring the hydroxyl group on the "inside position", meaning eclipsing the alkene. In such a conformation, the internal nucleophile is ideally positioned to attack *anti* to the iodine-π complex, giving rise to the experimentally observed major *syn* product (Scheme 2.18).

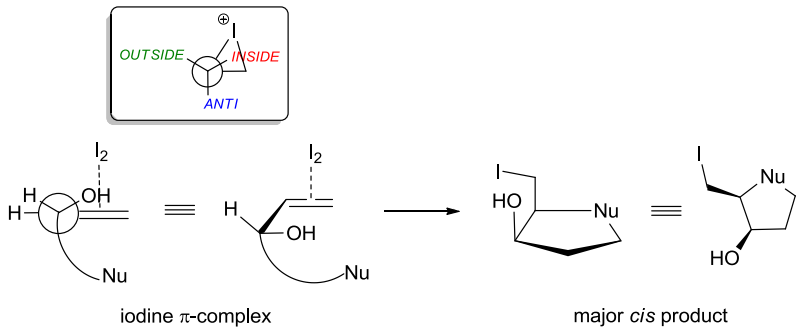

Scheme 2.18: Reactivity model rationalising the influence of the hydroxyl group at the allylic position on the diastereoselectivity.

Labelle *et al.* reported the iodoetherification of 4,6-dihydroxy-2-hexenoate with the successive replacement of the hydroxyl group by a methyl, methyloxy and fluorine substituent (Table 2.4).[127] It appeared that all of the substituents led to the formation of the major *syn* cyclised product. Furthermore the allylic fluoride was converted into the corresponding *syn* fluorinated furan with the highest level of diastereoselectivity.

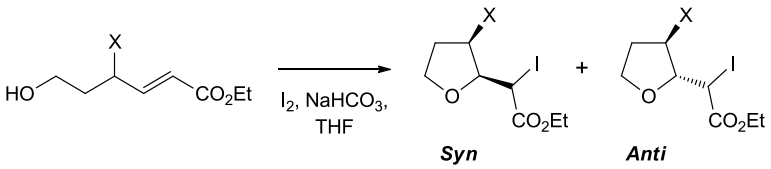

X	*d.r. (syn:anti)*	Yield (%)
OH	7.2:1	76
F	9.3:1	89
OMe	6.6:1	72
Me	2.3:1	97

Table 2.4: Effect of the allylic substituent on the diastereoselectivity. (Table reproduced from M. Labelle, Y. Guindon, *J. Am. Chem. Soc.* **1989**, *111*, 2204-2210 [127]).

This study is in accordance with earlier work in our group which has shown that an allylic fluoride bearing a strategically positioned nucleophile (alcohol or carboxylic acid) could be transformed into the corresponding fluorinated tetrahydrofuran or lactone *via* iodocyclisation (Table 2.5).[128] Moreover it has been found that the fluorine substituent also acts as a highly efficient *syn*-diastereodirecting group during the ring closure.

Entry	Substrate	Product	d.r. (syn:anti) yield (%)[a]
1	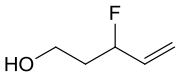	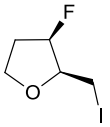	12:1 52
2	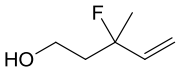	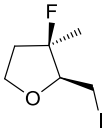	9:1 88
3	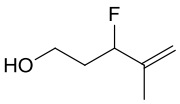	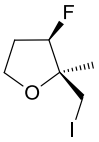	9:1 69
4	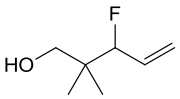	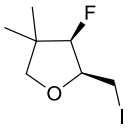	>20:1 92
5	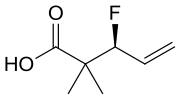	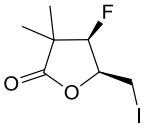	>20:1 48

Table 2.5: Stereoselective iodolactonisation and iodoetherification of allylic fluorides. [a] Condition: I_2, DCM/$NaHCO_3$ $_{(aq)}$; isolated yields; d.r. determined by ^{19}F NMR analysis; (Table reproduced from M. Tredwell, J. A. R. Luft, M. Schuler, K. Tenza, K. N. Houk, V. Gouverneur, *Angew. Chem. Int. Ed.* **2008**, *47*, 357-360 [128]).

Encouraged by these results, we hypothesised that the same methodology could be expanded to allylic fluorides bearing a pending nucleophilic amine. This novel approach would allow us to access a wide range of fluorinated pyrrolidines and their derivatives.

2.3.2 Preliminary results and optimisation:

The first approach of our present work consists of the activation of the homoallylic amine using the β-effect of the silicon to promote the fluorodesilylation process. The resulting allylic fluoride will be then converted into pyrrolidines *via* iodocyclisation.

2.3.2.1 Synthesis of allylic fluorides and feasibility of the reaction:

We first looked at the choice of the amine protecting group as it is indeed critical to comply with several requirements for the synthesis of allylic fluorides. The protecting group should be able to lower the nucleophilicity of the amine to avoid *N*-fluorination whilst not suppressing reactivity for

iodocyclisation. The use of a tosyl as protecting group was chosen in the first instance as it has been previously employed in the iodocyclisation of non-fluorinated substrates.[125] Accordingly, preliminary experiments were carried out using this group.

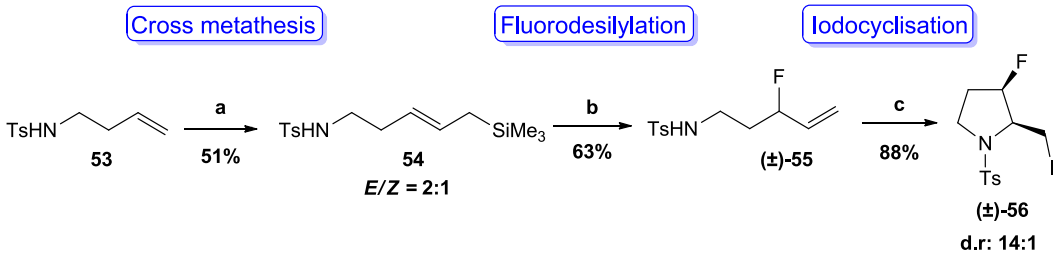

Scheme 2.19: Sequential cross-metathesis/fluorodesilylation/iodocyclisation. **a**) allyltrimethylsilane, Grubbs 2nd (5 mol%), 1,4-benzoquinone, DCM, reflux, 3 days; **b**) Selectfluor, $NaHCO_3$, MeCN, 48 h. **c**) I_2, DCM/$NaHCO_{3\,(aq)}$ (1/1), 16 h., r.t.

The allylsilane **54** was accessed through cross-metathesis of the tosyl-protected homoallylic amine **53** with allyltrimethylsilane in the presence of the 2nd generation Grubbs catalyst, affording an inseparable mixture of *E/Z* isomers (2:1 ratio). During the reaction we observed the formation of a truncated side product **60**, shorter by one methylene group, occurring from an isomerisation process of the desired product, followed by a reversible cross-metathesis (Scheme 2.20).

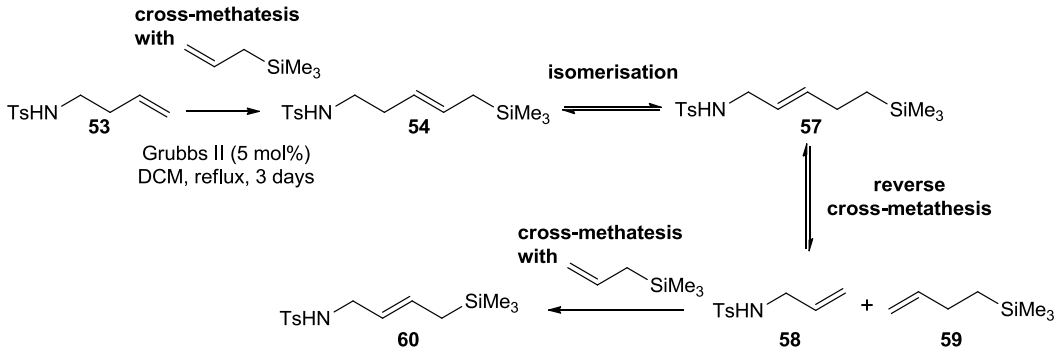

Scheme 2.20: Isomerisation and reversed cross-metathesis

The isomerisation of the double bond during the cross-metathesis reaction could occur *via* the formation of a π-allyl complex, as previously reported by Nolan *et al.*[129] However, following the recommendations of Grubbs, this competitive side reaction was suppressed using 1,4-benzoquinone.[130]

The resulting silane **54** was subsequently converted into the corresponding allylic fluoride **55** in 63% yield upon treatment with Selectfluor in the presence of $NaHCO_3$, a process occurring presumably *via* a S_E2'mechanism.

2.3.2.2 Optimisation:

With the allylic fluoride precursor in hand, we attempted the key iodoamination reaction using iodine in the first instance under a variety of conditions. The choice of the solvent was crucial as it has been previously reported by Bartlett *at al*. that for iodolactonisation, a mixture of DCM/$NaHCO_{3\,(aq)}$ promoted kinetic control whereas MeCN involved thermodynamic control.[122] The optimisation study showed that the highest yield (88%) and d.r. (14:1) were obtained when the reaction was performed in DCM/$NaHCO_{3\,(aq)}$ (Table 2.6, entry 1).

Entry	Solvent	Reaction time	Yield (%)[a]	d.r. (*syn/anti*)[b]
1	**DCM/$NaHCO_{3\,(aq)}$ (1:1)**	**16h**	**88**	**14:1**
2	MeCN	16h	50	10:1
3	Et_2O	16h	51	10:1
4	Acetone	16h	39	8:1

Table 2.6: Optimisation of the reaction conditions using iodine as nucleophile. [a] Isolated yields; [b]Determined by ^{19}F NMR analysis of the crude reaction mixture.

We also studied the effect of different electrophiles, both NIS and NBS delivered the corresponding fluorinated pyrrolidine in moderate yields (56% and 61% under condition **A**, 82% and 71% conversion under condition **B**) with similar or slightly reduced diastereoselectivity in comparison with iodine (Table 2.7, entries 3-6).

Entry	Electrophiles	Conditions[a]	Yield (%)[b]	d.r. (*syn/anti*)[c]
1	I_2	A	50	10:1
2	**I_2**	**B**	**88**	**14:1**
3	NIS	A	56	12:1
4	NIS	B	82	12:1
5	NBS	A	61	11:1
6	NBS	B	71[d]	8:1

Table 2.7: Screening of electrophiles. [a] Condition **A**: MeCN, 16 h., r.t; Condition **B**: DCM/$NaHCO_{3\ (aq)}$ (1/1), 16 h., r.t. [b] Isolated yield; [c] Determined by ^{19}F NMR analysis of the crude reaction mixture; [d] Conversion determined by ^{19}F NMR analysis of the crude reaction mixture.

The optimised conditions were therefore iodine in DCM/$NaHCO_{3\ (aq)}$, at r.t overnight in the absence of light.

The stereochemistry of the major product was assigned through NOE/HOESY experiments suggesting a *syn*-relationship between the fluorine atom and the substituent bearing the iodine. In addition X-ray analysis provided unequivocal evidence of the *syn* pyrrolidine as the major diastereoisomer. Details of the stereochemical assignment and conformational analysis of this newly formed fluorinated pyrrolidine will be given in Chapter 3.

2.3.3 Scope and limitations:

2.3.3.1 Design of substrates and synthesis:

Design of the substrates:

In order to assess the scope of the reaction, a range of substrates were designed. The influence of the nitrogen protecting group was explored by replacing the tosyl group by a *tert*-butyloxy carbonyl (Boc) group (**61**). Substrates featuring substituents at the allylic position (**62**) as well as on the double bond (**63**) were chosen to probe the influence of steric hindrance on the selectivity. To probe the use of other nucleophiles, allylic fluorides derived from amides were chosen (**65** and **66**), which upon cyclisation may lead to the formation of lactams.

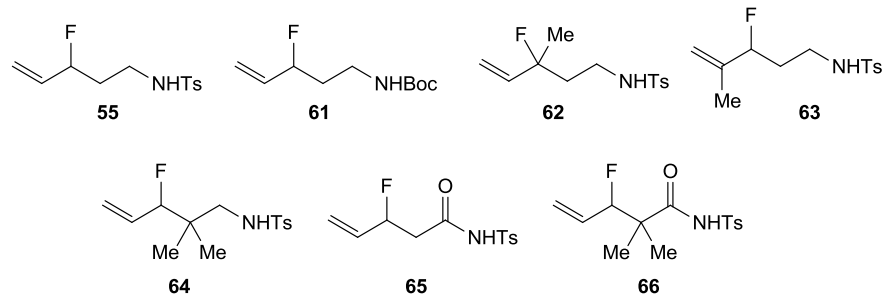

Figure 2.1: Selected substrates

To further probe the scope of this reaction, substrates containing a benzyl ether functionality were investigated (*syn*-**67** and *anti*-**67**). A series of allylic fluorides of varying chain length were selected to probe the feasibility of 5-*endo*-trig and 6-*exo*-trig cyclisation (**68** and **69**). Finally non terminal allylic fluorides were also designed (**70** and **71**).

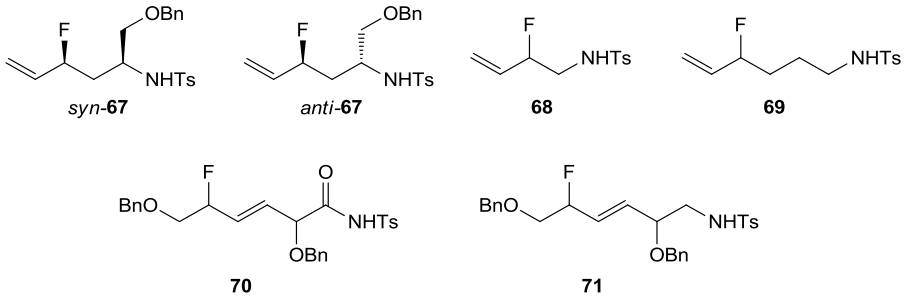

Figure 2.2: Selected substrates.

Synthesis of the substrates:

Following the synthetic routes already developed within the group for similar substrates, the introduction of methyl group in **62** and **63** proved not to be trivial. Although cross-metathesis to access tri-substituted alkenes has been already reported in the literature,[131] previous attempts to react allyltrimethylsilane with 3-methyl-3-buten-1-ol were unsuccessful.[132] We therefore chose to follow a multi-step sequence to access the allylsilanes required for subsequent electrophilic fluorination: ring-closing/ring-opening metathesis (Scheme 2.21 and scheme 2.22).

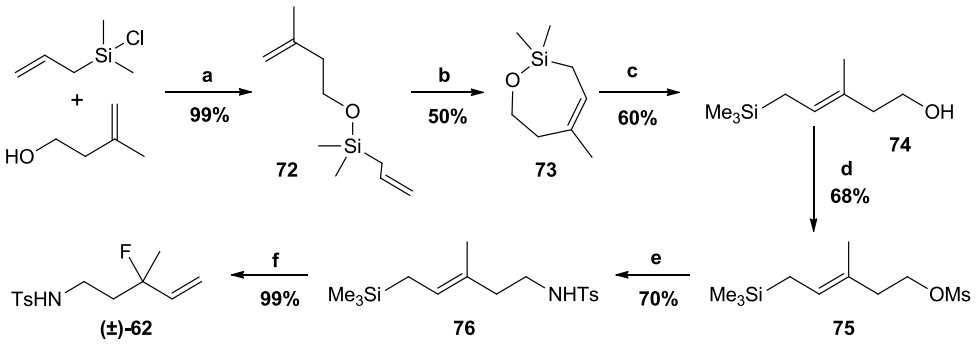

Scheme 2.21: Synthesis of the quaternary allylic fluoride **62**; **a**) NEt_3, DCM, 0 °C, 19 h; **b**) Hoveyda-Grubbs 2nd (2 mol%), DCM, reflux, 2 h; **c**) MeLi, THF, -78 °C, 3 h; **d**) MsCl, NEt_3, DCM, 0 °C, 2 h; **e**) NH_2Ts, KOH, DMF, 120 °C, 3 h; **f**) Selectfluor, MeCN, $NaHCO_3$, r.t., 24 h.

The allyl(chloro)dimethyl silane was treated with 3-methyl-buten-1-ol in presence of NEt_3 affording the corresponding protected alcohol **72** in 99%. This compound was submitted to a ring-closing metathesis with Hoveyda-Grubbs 2nd generation catalyst, which gave **73** in 50% yield. **73** was subsequently ring opened with MeLi affording **74** in 60% yield. The methylated homoallylic alcohol **74** thus generated, was transformed into the corresponding mesylate **75** (68%) and then substituted by tosylamine (70%). The desired homoallylic tosyl amine **76** underwent fluorodesilylation with Selectfluor and $NaHCO_3$ to afford the corresponding quaternary allylic fluoride **62** in 99% yield.[i] An analogous route was used for the preparation of **63**.

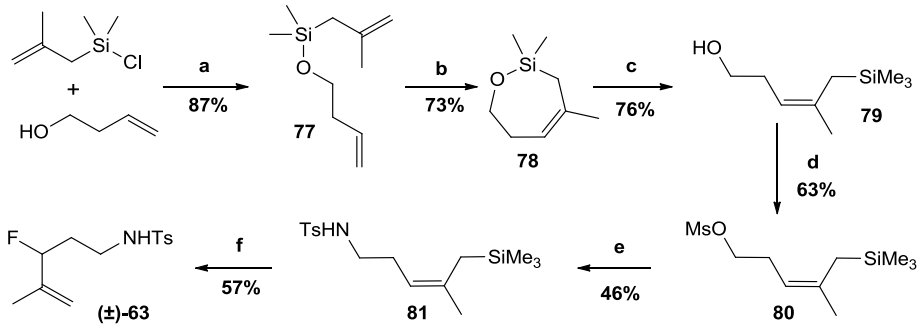

Scheme 2.22: Synthesis of disubstituted allylic fluoride **63**; **a**) NEt_3, DCM, 0 °C, 15 h; **b**) Hoveyda-Grubbs 2nd (2 mol%), DCM, reflux, 90 min; **c**) MeLi, THF, -78 °C, 4 h; **d**) MsCl, NEt_3, DCM, 0 °C, 2h 30 min; **e**) NH_2Ts, KOH, DMF, 120 °C, 3 h; **f**) Selectfluor, MeCN, $NaHCO_3$, r.t., 24 h.

For the synthesis of substrate **63**, 3-buten-1-ol was added to chloro-2-methylallyldimethylsilane to afford the diene **77** in 87% yield. Ring-closing metathesis using Hoveyda-Grubbs' 2nd generation

[i] The synthesis of the allylic fluoride **62** and the corresponding fluorinated pyrrolidine **102** was carried out by Rakesh Patel and Baltasar Bonillo.

catalyst (2 mol%) in dichloromethane at reflux gave the 7-membered ring in **78** in 73% yield. Ring opening of the trisubstituted alkene led to the desired allylsilane **79** in 76% yield. Subsequent mesylation and displacement with tosylamine provided the homoallylic amine **81** which was then converted to allylic fluoride **63** in moderate 57% yield.

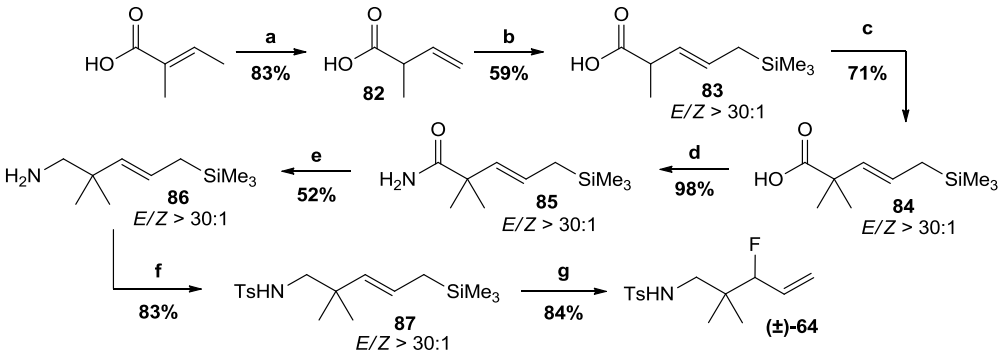

Scheme 2.23: Synthesis of gem-dimethyl substituted allylic fluoride **64**; **a**) LDA, THF, -78 °C, 1 h; **b**) allyltrimethylsilane, Hoveyda-Grubbs 2nd (3 mol%), DCM, reflux, 24 h; **c**) LDA, MeI, THF, -78 °C, 1 h; **d**) 1,1'-CDI, NH_4OH, DMF, 80 °C, 1 h; **e**) $LiAlH_4$, THF, r.t, 16 h; **f**) TsCl, NEt_3, DMAP, DCM, r.t, 3 h; **g**) Selectfluor, $NaHCO_3$, r.t, 48 h.

The synthesis of **64** started with the isomerisation of tiglic acid with LDA, affording **82** in 83% yield which underwent subsequently a cross metathesis with allyltrimethylsilane in presence of Hoveyda-Grubbs 2nd generation catalyst to give **83** in 59% yield. The resulting acid **83** was converted to the corresponding *gem*-dimethyl substrate **84** by addition of MeI (71%). Previous attempts within the group to access this product directly by cross-metathesis were unsuccessful.[132] No reaction occurred when the *gem*-dimethyl acid was employed, presumably due to the formation of an unproductive chelate, as suggested to account for other unsuccessful ring-closing metathesis reactions.[133] The acid **84** was then transformed into the amide **85** using 1,1'CDI and NH_4OH, followed by reduction of the carbonyl group by $LiAlH_4$ (52%). The primary amine **86** was protected with tosyl chloride (83%) and finally underwent fluorodesilylation to deliver the desired allylic fluoride **64** (84%).

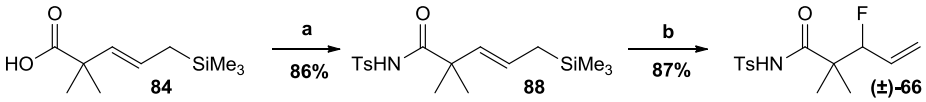

Scheme 2.24: Synthesis of gem-dimethyl allylicfluoroamide **66**; **a**) Tosylisocyanate, NEt_3, THF, 1 h; **b**) Selectfluor, MeCN, 48 h.

The same route was used to obtain the *gem*-dimethyl substituted fluorinated amide **66** by reacting the *gem*-dimethyl acid **84** with tosyl-isocyanate (86%) following by fluorodesilylation (87%).

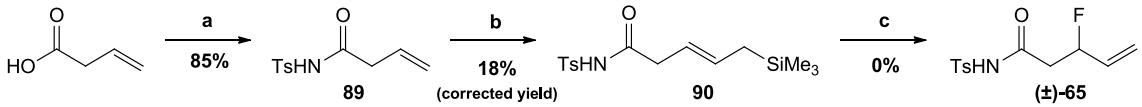

Scheme 2.25: Synthesis of allylic fluoroamide **65**; **a**) tosylisocyanate, NEt_3, THF, 1 h; **b**) allyltrimethylsilane, Grubbs 2nd (5 mol%), 1,4-benzoquinone, DCM, reflux, 4 days; **c**) Selectfluor, $NaHCO_3$, MeCN, r.t., 6 days.

Similarly, 3-butenoic acid was converted to tosylamide upon addition of tosylisocyanate in 85% yield. Despite the use of 1,4-benzoquinone, cross-metathesis of **89** with (trimethyl)allylsilane provided a complex inseparable mixture containing mainly 4-(trimethylsilyl)but-2-en-tosylamide which is the product of isomerisation of the double bond and only 18% (corrected yield) of the desired allylsilane **90**. When the mixture was submitted to the fluorination conditions, only the product of isomerisation was recovered unreacted. Indeed allylsilanes derived from α,β-unsaturated carbonyl compounds are too electron deficient to react with Selectfluor. This synthesis was not pursued any further.

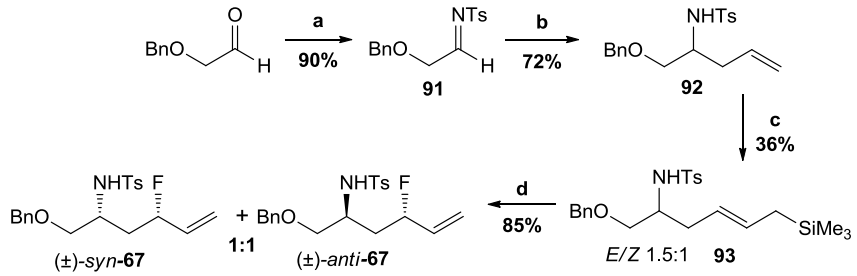

Scheme 2.26: Synthesis of the couple of diastereoisomers *syn*-**67** and *anti*-**67**. **a**) tosyl amine, sodium toluene sulfimide, formic acid, H_2O, 24 h. r.t.; **b**) allylmagnesium bromide ([1M] in Et_2O), DCM, -78 °C, 5 h.; **c**) allyltrimethylsilane, Grubbs 2nd (5 mol%), 1,4-benzoquinone, DCM, reflux, 3 days; **d**) Selectfluor, $NaHCO_3$, MeCN, 48 h, r.t.

Compound *syn*-**67** and *anti*-**67** were synthesised by addition of allylmagnesium bromide to *N*-(2-(benzyloxyethylidene)-tosylamide **92** (72%), followed by cross metathesis with allyltrimethylsilane in presence of the 2nd generation Grubbs catalyst and benzoquinone (36%). Fluorodesilylation of **93** afforded two diastereoisomers *syn*-**67** and *anti*-**67** which were separable by column chromatography on silica gel (85%, mixture 1:1).

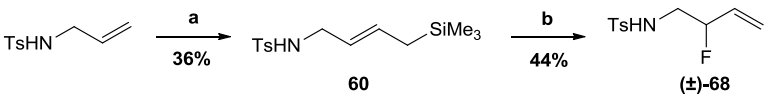

Scheme 2.27: Synthesis of allylic fluoride **68**; **a**) allyltrimethylsilane, Hoveyda-Grubbs 2nd (5 mol%), 1,4-benzoquinone, DCM, reflux, 3 days; **b**) Selectfluor, $NaHCO_3$, MeCN, r.t. 2 days.

The allylic fluoride **68** was synthesised using a 2-propen-tosylamine as starting material for the cross metathesis (36%) and subsequently submitted to fluorodesilylation to yield the product **68** in 44% yield.

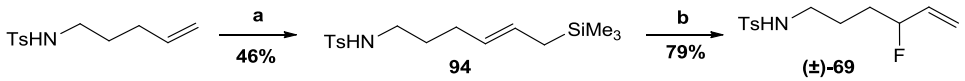

Scheme 2.28: Synthesis of allylic fluoride **69**; **a**) allyltrimethylsilane, Hoveyda-Grubbs 2nd (5 mol%), 1,4-benzoquinone, DCM, reflux, 3 days; **b**) Selectfluor, $NaHCO_3$, MeCN, r.t., 6 days.

After mesylation of pent-4-en-1-ol and displacement with tosylamine, pent-4-en-1-tosylamine was converted to the corresponding allylsilane by cross-metathesis with Hoveyda-Grubbs' 2nd generation catalyst to afford **94** in 46% yield which was then transformed into the allylic fluoride **69** in 79% yield.

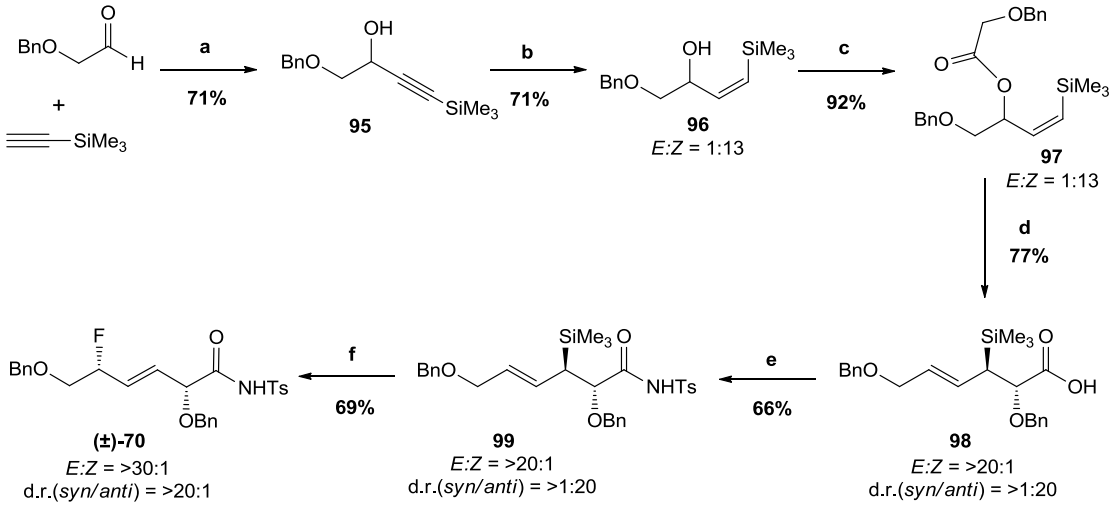

Scheme 2.29: Synthesis of compound **70**; **a**) n-BuLi, THF, 78 °C, 35 min then 0 °C 2 h; **b**) BH_3, THF, cyclohexene, 15 h; **c**) 2-benzyloxy acetic acid, DMAP, DCC, DCM, 0 °C, 15 h; **d**) LiHMDS, TMSCl, THF, -78 °C, 1 h then r.t. 13 h; **e**) $TsNH_2$, DCC, DMAP, DCM, r.t., overnight; **f**) Selectfluor, $NaHCO_3$, MeCN, 48 h.

The synthesis of the silylated propargylic alcohol **95** was achieved by deprotonation of trimethylsilyl acetylene with *n*-BuLi in THF followed by addition of 2-(benzyloxy)acetaldehyde in 71% yield. **96** was prepared in 71% yield by reduction with BH_3.THF and freshly distilled cyclohexene in THF. Subsequent esterification with 2-benzyloxy acetic acid using DCC and DMAP delivered **97** in 92%.

Treatment of this ester with LiHMDS and TMSCl provided the *Z*-*O*-silylketene acetal intermediate, which underwent a [3,3]-sigmatropic rearrangement affording the hexenoic acid **98** in 77% isolated yield. The acid was then reacted with DCC and DMAP to produce the corresponding tosylamide **99** (66%) which was then mixed with Selectfluor to deliver the product of fluorodesilylation **70** in 69% yield.[ii]

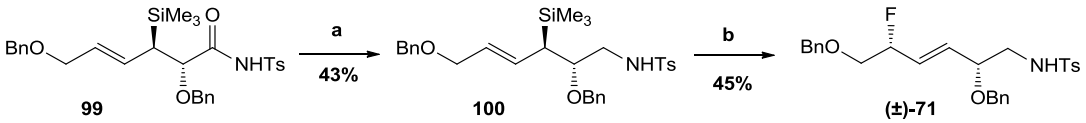

Scheme 2.30: Synthesis of **71**; **a**) $LiAlH_4$, THF, r.t., overnight; **b**) Selectfluor, $NaHCO_3$, MeCN, r.t., 3 days.

In a similar fashion, compound **99** was reduced using $LiAlH_4$ and subjected to fluorodesilylation to access the allylic fluoride precursor **71** in 45% yield.

2.3.3.2 Iodocylisation:

With substrates in hand, the scope and limitations of the iodocyclisation of allylic fluoride could be assessed. Using the optimised conditions, the prepared precursors were subjected to iodocyclisation. Two different conditions were investigated: r.t. in the absence of light using iodine in MeCN (**A**) or DCM/$NaHCO_{3\ (aq)}$ (**B**) to define whether the reaction would be under thermodynamic or kinetic control. The reactivity of unsaturated amines towards halocyclisation is strongly influenced by the nature of the protecting group.[125] In order to assess the impact of the protecting group on the reaction, we replaced the tosyl group by a *tert*-butyloxy carbonyl (Boc) in **61**. The new substrate (Table 2.8, entry 1) was submitted to the optimised conditions of iodocyclisation to afford the corresponding pyrrolidine in a reduced yield (42%) and much lower d.r. (4:1) confirming our initial choice of tosyl group as the most suitable. Moreover this compound was found to be very unstable and had to be stored at -20 °C in absence of light. This result shows that the relative reactivity of the carbamate group towards iodocyclisation agrees with a general tendency: the more acidic the NH, the higher the nucleophilic reactivity.[125,134,135]

[ii] The synthesis of the allylic fluoride **70** was carried out by Dr. Marie Schuler.

The iodocyclisation of allylic fluorides **62**, **63**, **64** (Table 2.8, entries 3-5) led to the corresponding fluorinated substituted pyrrolidines in moderate to high yields. The d.r. observed for the two products **102** and **103** possessing a quaternary centre, were equal or superior to 8:1 (Table 2.8, entries 3 and 4). The addition of base (conditions **B**) led to increased yields in comparison to conditions **A**, and the level of diastereocontrol remained similar for both sets of conditions.

The pyrrolidine **104** featuring a *gem*-dimethyl substituent was formed as a single isomer in quantitative amount (d.r. > 20:1, Table 2.8, entry 5). The iodolactamisation of the structurally related amide **66** using condition **B** was equally successful, delivering the fluorinated lactam **105** in good yield (62 %) with a very high level of stereocontrol (>20:1). However the reaction delivered a second product, a furan with an exocyclic imine functionality **107** in 24% yield and d.r. >20:1. The formation of this product arises from the donation of the nitrogen lone pair to the carbonyl group leading to the competitive attack of the iodonium ion by the negatively charged oxygen. Structural elucidation of these two products was achieved by comparison of carbon NMR and IR data. Chemical shifts of the amide and imine carbons were very similar, as were the carbons bearing the gem-dimethyl substituent in both products. However in compound **107**, the chemical shift of the carbon bearing the methyliodide moiety was higher (85.2 ppm) than its counterpart in the lactam **105** (61.9 ppm). Moreover, the frequency of vibration in IR of the imine **107** was recorded at 1650 cm^{-1} which corresponds to the standard value. The frequency of vibration of the amide **105** was recorded at 1738 cm^{-1} which is slightly higher than expected for five-ring lactams. It is known that the usual value of 1700 cm^{-1} can be shifted to higher frequency when the nitrogen atom is in a bridged system in which overlap of the nitrogen lone pair with the C=O π bond is diminished. The structure of both isomers was unambiguously confirmed based on single crystal X-ray analysis. When the reaction was carried out under conditions **A**, analysis of the reaction mixture after 16 h revealed the presence of the same compound **107** along with its product of hydrolysis, the corresponding lactone **108** in a 1:1 ratio. The reaction finally reached completion after 7 days, affording the lactone **108** as the sole product in 84% and >20:1 d.r. These results are in agreement with previous studies detailing the preference for *O*-cyclisation versus *N*-cyclisation. This can be interpreted based on the HSAB (hard

and soft acids and bases) theory, where the oxygen atom being more electronegative than its nitrogen counterpart, will preferentially attacks the iodine-π complex due to its hard electrophilic character. Selective lactamisations have been performed using *N*,*O*-bissilylation,[136] strong bases,[137] or thioimidate derivatives.[138]

The method was extended to the preparation of fluorinated pyrrolidines *syn*,*syn*-**106** and *syn*,*anti*-**106** bearing a benzyloxy group. In both cases the observed d.r. was found to be good (13:1 and 17:1) with high yields (95% and 78%, Table 2.8, entries 7 and 8). The presence of an existing stereogenic centre has no influence on the stereochemical outcome of the reaction.

Entry	Substrate	Product	Conditions[a]	Yield (%)[b]	d.r. (*syn*/*anti*)[c]
1	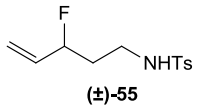 **(±)-55**	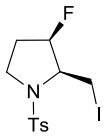 **(±)-56**	B	88	14:1
2	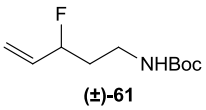 **(±)-61**	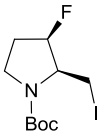 **(±)-101**	B	42	4:1
3	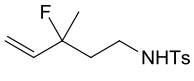 **(±)-62**	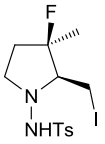 **(±)-102**	A B	42 85	12:1 8:1
4	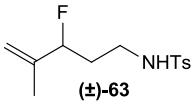 **(±)-63**	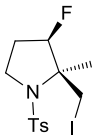 **(±)-103**	A	65	10:1
5	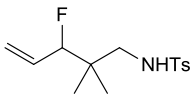 **(±)-64**	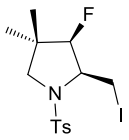 **(±)-104**	B	97	>20:1
6	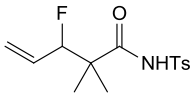 **(±)-66**	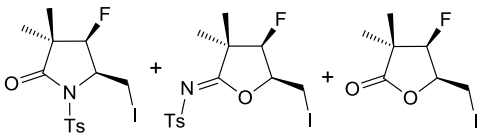 **(±)-105** **(±)-107** **(±)-108**	A B	0; 0; 84 62; 24; 0	>20:1 >20:1[d]
7	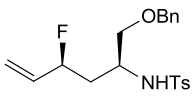 **(±)** *syn*-**67**	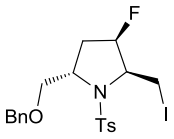 **(±)** *syn,anti*-**106**	B	78	17:1
8	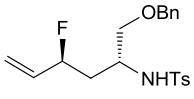 **(±)** *anti*-**67**	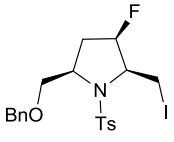 **(±)** *syn,syn*-**106**	B	95	13:1

Table 2.8: Iodocyclisation of allylic fluorides; [a] condition **A**: I_2, MeCN, 16 h, r.t.; condition **B**: I_2, DCM/$NaHCO_{3\ (aq)}$ (1:1), 16 h, r.t.; [b] isolated yields; [c] determined by ^{19}F NMR analysis of the crude reaction mixture; [d] d.r. for each isolated products.

To further investigate the synthetic value of the iodocyclisation procedure, we prepared additional substrates. The potential for the 5-*endo*-trig cyclisation was investigated in the case of *N*-(2-fluorobut-3-en-yl)tosylamine **68**. We found that the allylic fluoride **68** did not react under either conditions **A** or **B** at r.t. but could undergo the reaction at 75 °C affording the corresponding fluorinated pyrrolidine **109** in low yield (29%) as the predominant *syn*-product (d.r. 10:1, Table 2.9, entry 1). This experiment clearly reveals that the 5-*endo*-trig cyclisation is less favoured than the 5-*exo*-trig cyclisation.

In general 5-*endo*-trig cyclisations are unfavoured according to Baldwin's rules.[120] However, extended studies carried out by Knight and co-workers on the 5-*endo*-trig iodocyclisation of homoallylic sulfonamides, demonstrated that this type of reactions delivered smoothly the corresponding pyrrolidines in moderate to high yields.[139,140] In the case of non substituted terminal alkene, a lack of diastereoselectivity was observed. Yet, some examples of iodine induced *syn*-selective 5-*endo*-trig cyclisations featuring an allylic alkoxy group, were reported by Park[141] and Knight[142] in two different studies. In each example, the *syn* relationship was established between the iodine and the substituent occupying the homoallylic position. It did not appear that the allylic alcohol moiety had any influence on the sense of stereoselectivity. This observation is in contrast to our experimental results for the related 5-*exo*-trig cyclisation. It is possible that the reaction mechanisms differ in these cases.

We also considered the reaction of **69** which would afford the corresponding fluorinated piperidine **110** using condition **B** (Table 2.9, entry 2). Unfortunately, GC analysis suggested that during the reaction the substrate either did not react or decomposed *via* elimination of HF to the corresponding diene. This result suggests that the rate of cyclisation is slower than elimination and therefore the 6-*exo*-trig cyclisation is not observed. However the failure of this cyclisation is not surprising in the light of literature precedent. Yoshida *et al.* reported unsuccessful attempts to cyclise *N*-tosyl-4-hydroxy-5-hexenylamines under various halogenation conditions.[125] Compound **111** was delivered in an excellent d.r. (>20:1) and moderate yield (49 %) using condition **B**. The concomitant diastereo-directing effect of the allylic fluorine atom and the allyl benzyloxy substituent delivered exclusively

the all *syn* diastereosisomer. However the reaction did not proceed when carried out using condition **A**. Product **111** was assigned as a lactam by analogy with the previous analytic data of **105** by comparing IR and ^{13}C chemical shifts. Unfortunately the compound was not suitable for X-ray crystallography to confirm the structure. The iodocylisation was also attempted with the structural related amine **71**, yet the reaction failed to deliver the cyclised product using various conditions.

Entry	Substrate	Product	Conditions[a]	Yield (%)[b]	d.r. (*syn*/*anti*)[c]
1	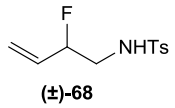 **(±)-68**	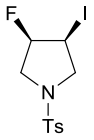 **(±)-109**	C	29	10:1
2	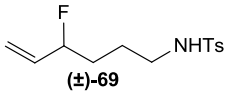 **(±)-69**	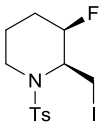 **(±)-110**	B	0	-
3	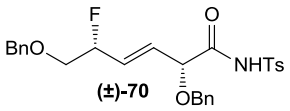 **(±)-70**	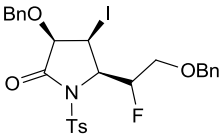 **(±)-111**	A B	0 49	- >20:1
4	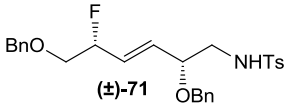 **(±)-71**	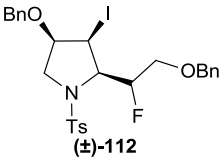 **(±)-112**	A, B or C	0	-

Table 2.9: Iodocyclisation of various allylic fluorides; [a] Condition **A**: I_2, MeCN, 16 h, r.t.; Condition **B**: I_2, DCM/$NaHCO_{3\ (aq)}$ (1:1), 16 h, r.t.; Condition **C**: I_2, MeCN, 16 h, 75 °C; [b] isolated yields; [c]determined by ^{19}F NMR analysis of the crude reaction mixture.

The relative stereochemistry of the major diastereoisomers were assigned by NOE/HOESY experiments on all substrates and X-ray diffraction analysis on suitable samples. All the compounds featured a *syn*-relationship between the fluorinated substituent and the newly formed stereogenic center.

2.3.3.3 Further functionalisation: synthesis of fluorinated indolizidines derivatives

The *trans* configuration of the C-2 hydrogen substituent with respect to C-3 hydroxyl group in the pyrrolidine ring is abundant in many alkaloids.[143] Since our methodology results in the same stereochemical relationship between, C-2 and C-3, we applied this route for the preparation of a model indolizidine derivative. This methodology could lead to the synthesis of a variety of natural product analogues. Fortunately the presence of the iodo-methyl substituent provides a readily reactive functionality for further modification of the molecule. In order to validate the conversion of our pyrrolidines into indolizidine derivatives, we selected **56** and **106** as starting materials.

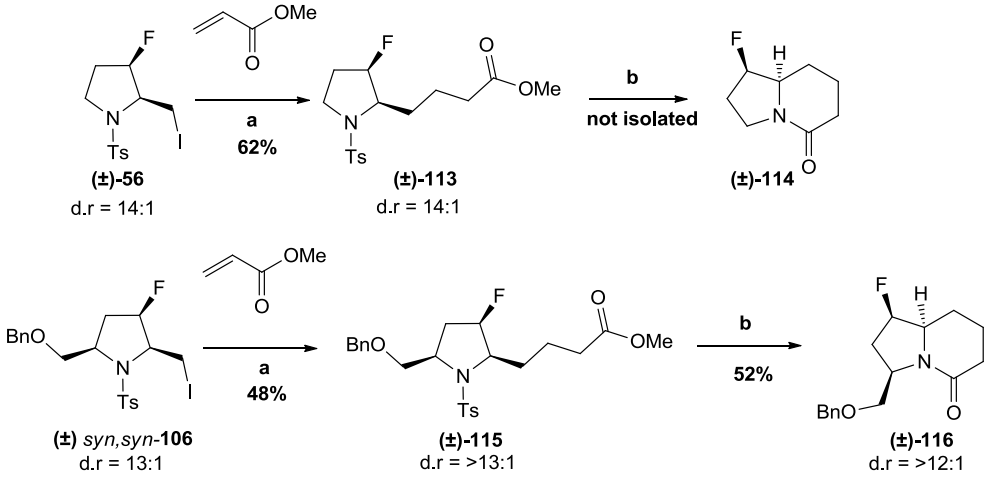

Scheme 2.31: Synthesis of fluorinated indolizidines **114** and **116**; **a**) CuI, Zn, H_2O/MeOH, sonication, 45 min.**; b**) NaHg (5%), Na_2HPO_4, MeOH, 4 h, r.t.

In our first attempt to further functionalise the iodine substituent, we performed a radical reaction involving iodide **56** with methyl acrylate in presence of AIBN and $HSnBu_3$ which afforded the ester **113** in 27% yield and a slightly eroded d.r. of 10:1 along with the corresponding deiodinated derivative of **56** in 13% yield.[144] An alternative procedure using a sonicated mixture of CuI and Zn provided the ester **113** in a much improved yield of 62% whilst also conserving the d.r. of 14:1, along with the allylic fluoride **55** in 20% yield.[145] The next step, which did provide the desired product **114**, was a *N*-detosylation/cyclisation using sodium amalgam. The presence of the bicyclic product in the crude mixture was diagnosed by ^{1}H NMR spectroscopy by the disappearance of the tosyl peaks and confirmed by mass spectrometry ESI. Unfortunately, **114** could not be isolated.

The same procedure was applied to the pyrrolidine **106** bearing a benzyloxymethyl group in the C-5 position. The first step provided the desired ester **115** in only 48% yield along with the allylic fluoride *anti*-**67** in 30% yield, without any erosion of diastereoselectivity. Subsequent *N*-detosylation/cyclisation afforded the final fluorinated indolizidine **116** in moderate yield (52%) whilst conserving a good d.r., superior to 12:1.

2.3.4 Rationalisation of the diastereoselectivity:

2.3.4.1 Comparison with previous study:

The high level of diastereoselectivity observed experimentally in our present study is very similar to the results obtained in the iodoetherification of allylic fluorides previously reported by our group.[128] Moreover a survey of the past literature reveals a similar trend for iodocyclisations of structurally related derivatives benefiting from the stereo-directing influence of an allylic hydroxyl group. Indeed the reported iodocyclisation of *N*-(tosyl)pent-4-enylamines[125] and 4-penten-1-ols[124] featuring an hydroxy group at the allylic position appears to be highly stereoselective and provides the corresponding *syn*-heterocycles as the major product. Such cyclisations exhibit comparatively the same level of diastereoselectivity in the *O*-series and the *N*-series in good to excellent yield as demonstrated in Table 2.10. We can notice a striking similarity between the iodoetherification and the iodoamination of allylic fluorides (Table 2.11).

Entry	Substrate	Product	d.r. (*syn:anti*) yield (%)[a]	Substrate	Product	d.r. (*syn:anti*) yield (%)[a]
1	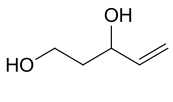	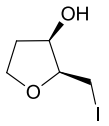	19:1 87	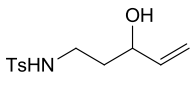	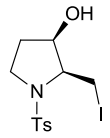	>20:1 86
2	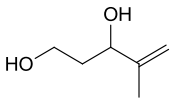	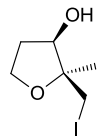	10:1 94	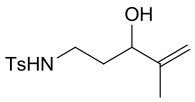	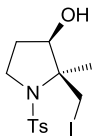	13:1 99
3	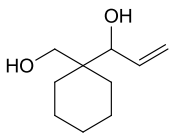	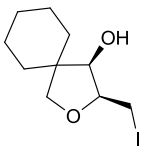	>20:1 98	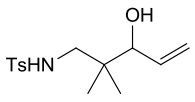	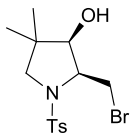	19:1[b] 88
4	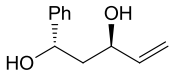	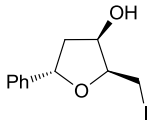	>20:1 98	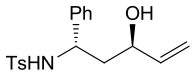	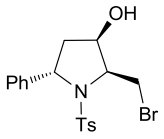	19:1[b] 80

Table 2.10: Comparison between the electrophilic induced-etherification and –amination directed by an allylic hydroxyl group. [a] Condition: I_2, $NaHCO_3$, Et_2O-H_2O, 0 °C; isolated yields; d.r. determined by ^1H, ^{13}C NMR and HPLC analysis; [b] Condition: NBS, DME-H_2O. Reproduced from Y. Tamaru, M. Hojo, S. Kawamura, S. Sawada, Z. Yoshida, *J. Org. Chem.* **1987**, *52*, 4062-4072 (left)[124] and Y. Tamaru, S. Kawamura, T. Bando, K. Tanaka, M. Hojo, Z. Yoshida, *J. Org. Chem.* **1988**, *53*, 5491-501 (right)[125].

Entry	Substrate	Product	d.r. (*syn:anti*) yield (%)[a]	Substrate	Product	d.r. (*syn:anti*) yield (%)[a]
1	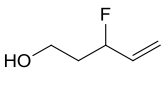	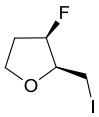	12:1 52	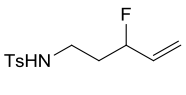	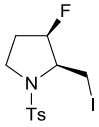	14:1 88
2	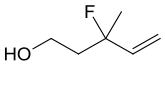	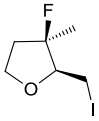	9:1 88	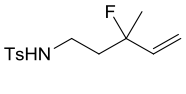	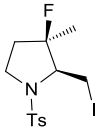	8:1 85
3	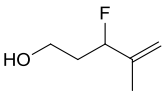	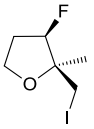	9:1 69	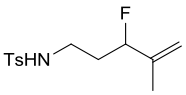	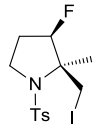	10:1[b] 65
4	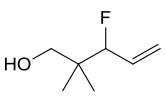	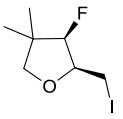	>20:1 92	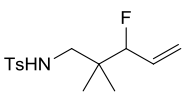	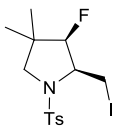	>20:1 97
5	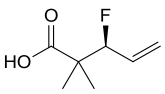	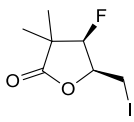	>20:1 48	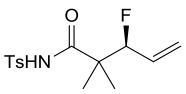	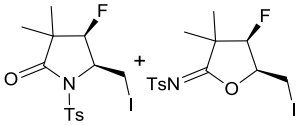	>20:1[c] 62;24

Table 2.11: Comparison between the iodoetherification and -amination directed by an allylic fluoride group. [a] Condition: I_2, DCM/$NaHCO_{3\,(aq)}$; isolated yields; d.r. determined by ^{19}F NMR analysis; [b] Condition: I_2, MeCN; [c] identical d.r. for both products. Reproduced from M. Tredwell, J. A. R. Luft, M. Schuler, K. Tenza, K. N. Houk, V. Gouverneur, *Angew. Chem. Int. Ed.* **2008**, *47*, 357-360 (left)[128], present work (right).

We can notice a strong correlation between the yield and the level of asymmetric induction for each structurally related substrate whether in the oxygen series or the nitrogen series.

In this context several factors could influence of the reaction.

- *Internal nucleophile: acidity/nucleophilicity vs steric flexibility nature*

Despite the fact that no significant differences were found in the reaction outcome in the *O*-series and the *N*-series of iodocyclisation described above, the nature of the internal nucleophile could explain the feasibility of the cyclisation. It was shown in the case of iodoamination that the reactivity of the homoallylic amine largely depends on the type of amine protecting group. Yoshida and co-workers tested in this study[125] the influence of sulphonamides, carbamates, urea and acid amide as *N*-protecting group. In an analogous fashion we observed that all amines equipped with a tosyl group underwent iodoamination while the replacement by a carbamate group resulted in a loss of selectivity and a reduced yield (Table 2.12).

Entry	Substrate	Product	d.r. (*syn:anti*) yield (%)[a]	Substrate	Product	d.r. (*syn:anti*) yield (%)[b]
1	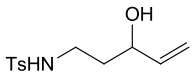	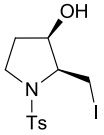	>20:1 86	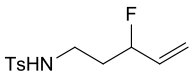	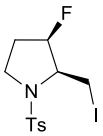	14:1 88
2	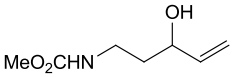	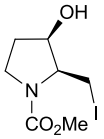	13:1 83	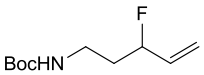	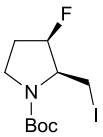	4:1 42

Table 2.12: Comparative reactivity of *N*-protecting group. [a] Condition: I_2, $NaHCO_3$, Et_2O-H_2O, 0 °C; isolated yields; d.r. determined by ^1H, ^{13}C NMR and HPLC analysis; [b] Condition: I_2, DCM/$NaHCO_{3\,(aq)}$; isolated yields; d.r. determined by ^{19}F NMR analysis. Reproduced from Y. Tamaru, S. Kawamura, T. Bando, K. Tanaka, M. Hojo, Z. Yoshida, *J. Org. Chem.* **1988**, *53*, 5491-501 (left)[125], present work (right).

Yoshida found that carbamate derivatives were unreactive and recovered unchanged for some substrates. Furthermore, ureas were described as even less reactive, providing a complex mixture of products under standard conditions. These observations suggest that the feasibility of the reaction is directly linked to the nature of the internal nucleophile. Interestingly, all the acyl groups tested ($COCF_3$, COMe, COPh), failed to cyclise, providing at best the corresponding halohydrins under aqueous conditions. Only NHTos (pK_a (DMSO) ~ 16)[134] and NHBoc (pK_a (DMSO) ~ 25)[146] provided the desired cyclised compound. The different rotational barrier between the acid amide,

carbamate and arylsulfonamide could explain this specific unreactivity.[147] The increase of $A^{1,3}$ strain between the "developing" iodomethyl substituent and the acid amide group in the product or the transition state would prevent the reaction. Therefore the feasibility of the iodoamination cyclisation depends more on the structural flexibility of the protecting group than on the acidity or the nucleophilicity of the internal amine. However both could have an impact on the defined steric and electronic environment of the transition state.

- *Allylic groups: H bonding; steric hindrance*

Other factors were believed to be responsible for the stereochemical outcome of the reaction. In early work, Yoshida hypothesised that the presence of an intramolecular hydrogen-bonding in the transition state between the directing allylic substituent and the internal nucleophile would affect the selectivity (Figure 2.3).[124]

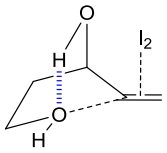

Figure 2.3: Possible asymmetric induction by H-bonding.

This hypothesis was soon invalidated by the fact that other allylic subsituents not amenable to H-bond formation such as OMe, OAc, $OSiR_3$ and OBn provided also good level of stereocontrol.[126,127] In the event that a F-H bond existed, it is highly probable that this type of intramolecular H-bonding would deactivate or lower the reactivity of the pending nucleophile. Therefore the pre-organisation of the transition state by an internal H-bond seems unlikely to be responsible for the rationalisation of the diastereoselectivity.

Similarly it has been noticed that the size of the allylic substituent used as stereo-directing group was not a distinguishing element to explain the level of stereocontrol. Substituents such as H or Me do not give rise to any selectivity, while F, OH and OMe are highly stereoselective. Fluorine is comparable to hydrogen in size but slightly smaller than oxygen. The electronegativity of the substituents seems therefore a more important factor than their steric hindrance.

- *Reaction conditions: kinetic vs thermodynamic*

Very often the sense of diastereoselectivity is imposed by the reaction conditions i.e. whether the reaction is under kinetic or thermodynamic control. According to the literature, the presence of a base in an aqueous media results generally in a kinetic control of the iodocyclisation process. Meanwhile the use of iodine in acetonitrile tends to favour a reversible process yielding the most stable product.[122] In our present study, the difference in reaction conditions seems to affect principally the yield of the reaction but the level of stereo-induction remains similar. In order to probe whether the iodoamination of allylic fluorides is under kinetic or thermodynamic conditions, we proceeded to perform control experiments. These experiments indicated that neither a prolonged or heated reaction, nor an exposure of the isolated product mixture to the halogenation conditions altered the observed ratio. Such results are in good agreement with literature precedents claiming to have been carried out under kinetic control.[124,125] This implies that the ratio between the *syn* and *trans* isomers will be decided upon the relative energy of the cyclisation transition state structures.

2.3.4.2 Theoretical calculations:

In order to rationalise the origin of this diastereoselectivity, Houk and Gouverneur carried out theoretical studies on related iodolactonisation and etherification of allylic fluorides which demonstrated a similar high level of stereocontrol.[128] The comparison between previous studies shows that the results produced in either iodoetherification or iodoamination are very similar in yield and diastereoisomeric ratio. In regard to these similarities, it is therefore reasonable to think that the same effects are responsible for the observed sense of stereocontrol. The results observed in the *N*-series could be rationalised by analogy to the theoretical studies carried out for the iodocyclisation of allylic fluorides in the *O*- series. The starting point of this latter investigation was to probe the relative stability of the substrates. In the first instance the conformational properties of allylic fluorides were analysed[148] and the 3-fluoro-1-butene was chosen as a simplified model. From optimised theoretical calculations that the allylic fluoride adopts preferentially a conformation in which the fluorine is eclipsed with the double bond. In the two other possible conformers, the fluorine is skew to the double bond with either H or Me eclipsed (Figure 2.4).

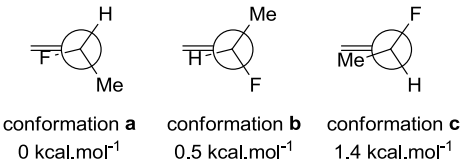

Figure 2.4: Optimised conformers of 3-fluoro-1-butene.

Conformation **a** is favoured by 0.5 kcal.mol^{-1} relative to conformation **b** (H eclipsed) and 1.4 kcal.mol^{-1} relative to conformation **c** (Figure 2.4).

Since investigations on the energy difference between the various conformers of the allylic fluorides do not provide a satisfying answer which would account for the stereoselectivity observed, studies of models for the transition state were undertaken. Similarly to the reactivity model developed for the iodolactonisation of allylic alcohol proposed by Chamberlin and Hehre,[126] the nucleophilic trapping of the iodonium complex is believed to be the rate-limiting step of the reaction. In the first instance geometrical optimisations of an unsubstituted iodonium ion revealed that the iodonium complex lies between an iodonium ion and an iodonium-π complex. Calculations based on a formally unsubstituted ethylene iodonium ion demonstrate that the length of the carbon-carbon bond (1.44 Å) lies between the length of a single and a double bond (1.54 Å and 1.34 Å respectively). The carbon-iodine bonds are longer (2.29 Å) than a conventional sp^3 C-I bond (2.20 Å) agreeing with previous experimental results (Figure 2.5).[149]

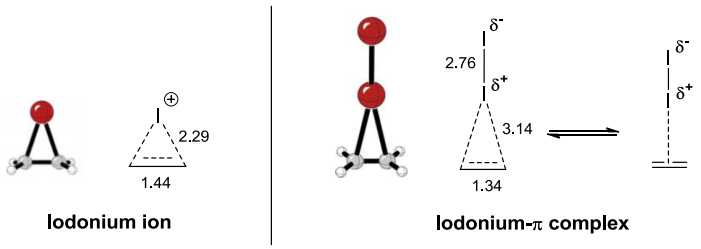

Figure 2.5: Structure comparison between the calculated iodonium ion and the iodonium-π complex.

The iodonium-π complex is loosely associated. The length of the C-C bond correspond to the one of a standard double bond (1.34 Å) and the C-I bond are much longer (3.14 Å) than in the iodonium ion, which is the marked difference between the two structures. The formation of the iodine-π complex from separate I_2 and ethylene is endergonic by 3.1 kcal.mol^{-1}.

The second step was to determine the relative energy of rotamers of substituted iodonium ions. Iodonium ions derived from the addition of iodine to 1-butene, 3-fluoro-1-propene and 3-fluoro-1-butene were selected for this study and theirs different staggered rotamers were computed. Each staggered iodonium ions will present an individual rotational preference, where the C3-substituents can occupy either the *inside*, *outside* or *anti* position (Figure 2.6).

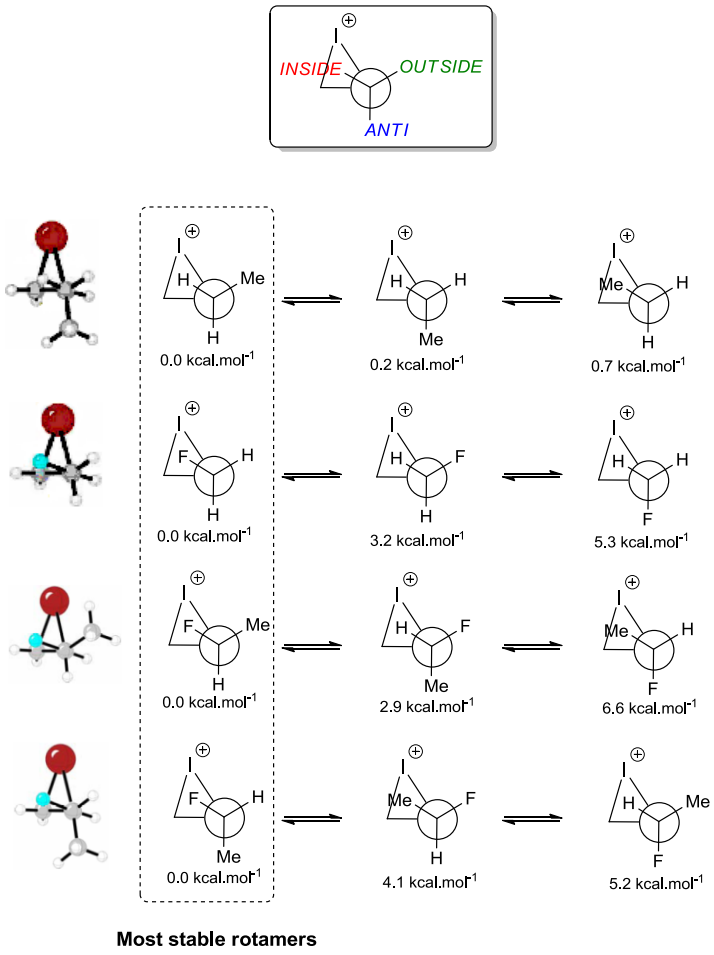

Figure 2.6: Relative energies of substituted iodonium ions rotamers. (Reproduced from M. Tredwell, J. A. R. Luft, M. Schuler, K. Tenza, K. N. Houk, V. Gouverneur, *Angew. Chem. Int. Ed.* **2008**, *47*, 357-360 [128]).

In the case of a methyl moiety, little conformational preference is observed between the different rotamers. Structures placing the methyl group *outside* or *anti* are equally stable (0.0 and 0.2 kcal.mol^{-1} respectively) whereas the rotamer featuring the methyl *inside* is slightly higher in energy (0.7 kcal.mol^{-1}) due to $A^{1,3}$ strain. In clear contrast, the fluorine prefers to reside *inside* by 3.2 kcal.mol^{-1} compared to *outside* and 5.3 kcal.mol^{-1} to *anti*. When both fluorine and methyl are borne by the carbon at the position 3, rotamers that place the fluorine *inside* are equal in energy (0.0 kcal.mol^{-1}), since the methyl does not present a conformation preference for *outside* versus *anti*.

Finally, the transition structures for the iodo-etherification reaction were also located. However, the transition structures could not be found without incorporating a second iodine atom for stabilisation. Consequently, in addition to the calculations based on the formation of an iodonium ion already described, the attack of an *O*-anion on a substituted I_2-π complex was then investigated as model. As predicted, the most stable transition state features the fluorine on the *inside* position and is preferred by 2.4 kcal.mol^{-1} to its *outside* counterpart (Figure 2.7). In the light of the experimental results and the close similarities with literature precedents, the origin of the diastereoselectivity observed with the *N*-nucleophiles seems to be the same.

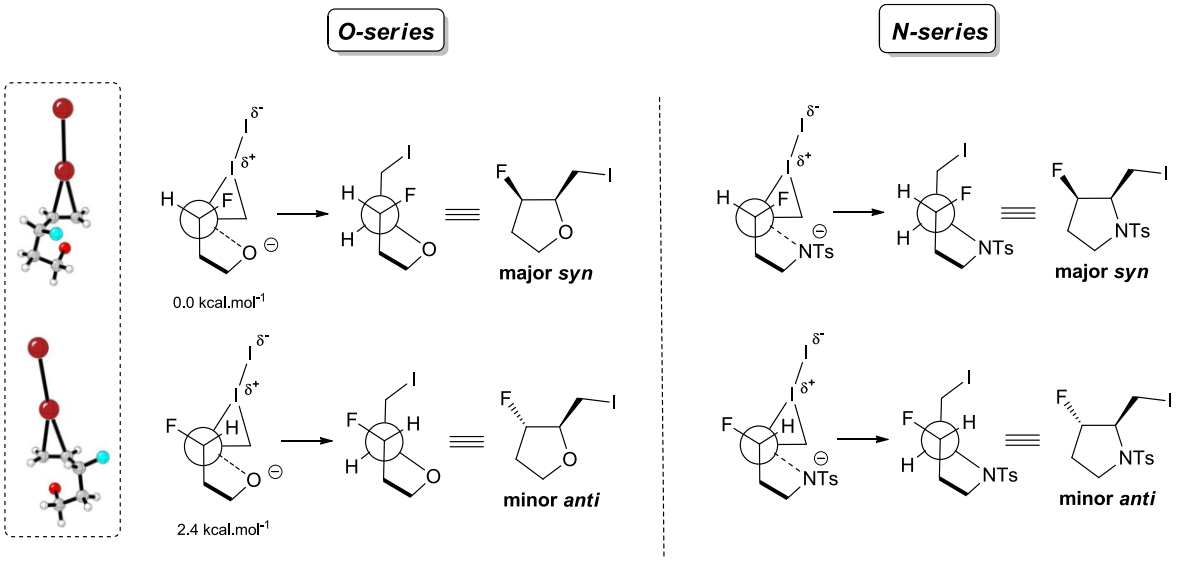

Figure 2.7: Transition state rotamers of I_2-π complex and how they account for the observed diastereoselectivity in iodo-cyclisation of allylic fluorides.

This "*inside*-fluoro effect" seems to be responsible for the conformational preference of the transition structures which in turn accounts for the experimental stereochemical outcome of the reactions. To explain the origin of this effect, it was proposed that at the transition state, the fluorine being placed at the *inside* position minimises the unfavourable interaction of the electron withdrawing $\sigma^*_{C\text{-}F}$ orbital with one of the electron deficient C-I bonds. In the fluoro-*anti* rotamer such interaction would be maximised thus destabilising the iodonium ion or the I_2-π complex. Fluoro-*inside* also enables the fluorine lone pairs to stabilise the partially positive iodine atom. Preference for fluoro-*inside* is less marked in the I_2-π complex since it is neutral compared to the formally charged iodonium ion. It is assumed that additional stabilisation of the *inside* position

would also arise from favourable electrostatic interactions similar to the charge/dipole or dipole/dipole interactions described in Chapter 1. Moreover the most stable rotamers have the fluorine on the *inside* position with the bulky alkyl group in the least sterically demanding *anti* position. Thus the internal nucleophile in the *O*- and *N*-series is ideally positioned to attack on the back-side of the $\sigma^*_{C\text{-}I.}$ In the absence of fluorine, none of the rotamers is predicted to be favoured since methyl substituent has little conformational preference. This would results in a poor stereoselectivity in agreement with previous experiments.

Although theoretical studies were not conducted on the *N*-series, we can hypothesise that the model of "*inside*-fluoro effect" could account for the high diastereoselectivity observed for fluorinated pyrrolidines. The preferential *syn* selectivity of the cyclisations would arise from the formation of a loosely associated I_2-π complex adopting the preferential *inside* fluoro conformation. The proximally oriented tosylated amino group would be ideally positioned to attack from the backside of the iodonium ion. In this favoured conformation, the transition state would lead to the major *syn* product as seen experimentally. By analogy to the "*inside*-alkoxy effect" described by Chamberlin *et al.* for lactones[150] and explained by Houk,[151] the "*inside*-fluoro effect" could be used to predict with accuracy the stereochemical outcome of electrophilic addition to allylic fluorides leading preferentially to the formation of the *syn* adduct with a wide range of internal nucleophiles.

2.4 Fluoroamination:

2.4.1 Concept:

Despite the great utility of fluorinated hetero- and carbocycles as pharmaceutical and agrochemicals [1e,56], fluorocyclisations have been slow to develop and only have been applied to a limited range of alkenes.[152] The fundamental problems of reactivity and selectivity must be addressed by the implementation of novel strategies allowing for fluorocyclisations to become a more general and powerful transformation. Therefore we hypothesised that alkenes temporarily activated by a silyl group other than trimethylsilyl would display the reactivity profile necessary for the fluorocyclisation to occur, thereby bypassing the competing fluorodesilylation process.

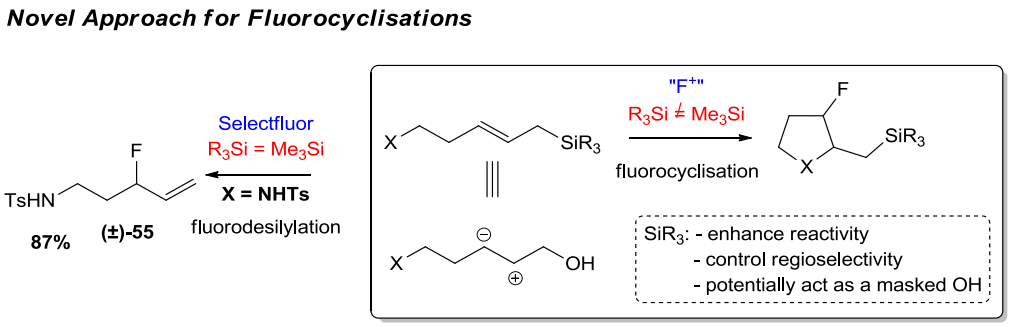

Scheme 2.32: Methodological concept: electrophilic fluorocyclisation versus fluorodesilylation.

In this approach, the allylsilane would function as a 1,2-dipole where the silyl group could potentially act as a masked hydroxyl group, being displaced by oxidative cleavage after the cyclisation event. The silicon would also serve to enhance the reactivity of the olefin towards electrophilic addition and control the regioselectivity of the attack.

2.4.2 Initial investigation:

Halocyclisations of allylsilanes have been reported. In the first instance, Ting and Bartlett investigated a cyclisation/ring-contraction strategy in order to synthesise trans-2,5-disubstituted tetrahydropyrans in a stereocontrolled manner.[153] For this purpose they examined the possibility for the silane moiety to increase the regioselectivity of the cyclisation step. Upon treatment of the suitably functionalised *Z*-allylsilane with the electrophilic brominating agent 2,4,4,6-tetrabromo-2,5-cyclohexadienone (TBCO), the desired bromotetrahydropyran was obtained in 55% yield (Scheme 2.33). The relative stereochemistry of the product was determined by ^{1}H, ^{13}C NMR and GC analysis and appeared to be *cis* with respect to the bromo and silyl group. On the other hand the same reaction conducted with the *E*-allylsilane afforded a mixture of corresponding cyclised *trans*-bromotetrahydropyran in 10-20% yield along with the bromotetrahydrofuran (Scheme 2.33).

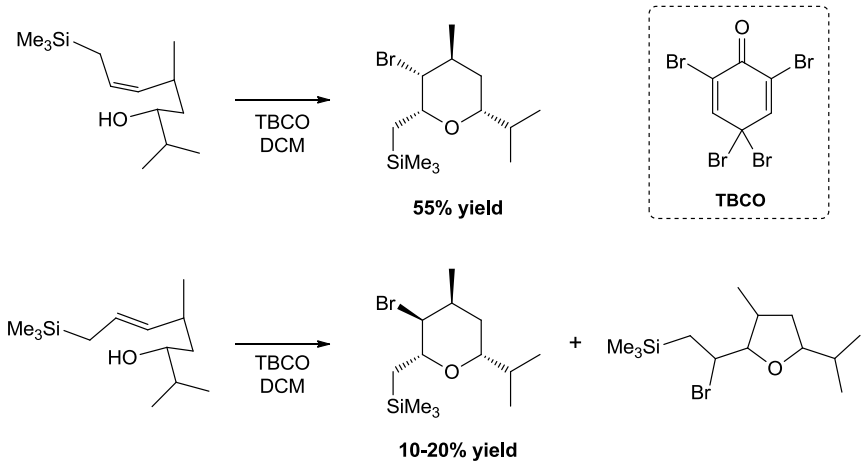

Scheme 2.33: Example of bromocyclisation of allylsilanes. (Reproduced from P. C. Ting, P. A. Bartlett, *J. Am. Chem. Soc.* **1984,** *106*, 2668-2671 [153]).

Another example involved the bromocyclisation of silylated 4-alken-1-ols.[154] A 2:1 diastereomeric mixture of allylsilanes was engaged to the reaction with NBS in DCM and delivered a 2:1 mixture of corresponding silylated tetrahydrofurans with a predominantly 2,3-*trans* stereochemistry in 71% yield (Scheme 2.34).

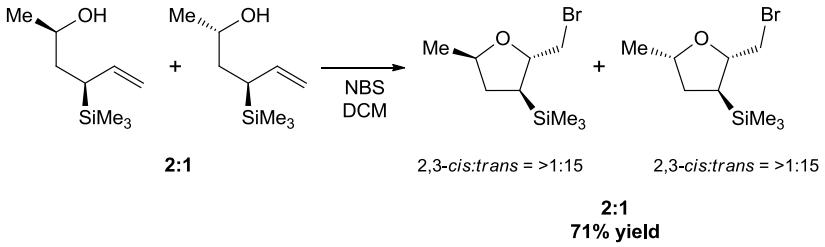

Scheme 2.34: Example of bromocyclisation of allylsilanes. (Reproduced from G. Adiwidjaja, H. Flörke, A. Kirshning, E. Schaumann, *Liebigs Ann.* **1995**, 501-507 [154]).

These two examples demonstrate that allylsilane derivatives are useful precursors for electrophilic induced cyclisation however, as we have observed earlier in this chapter, trimethyl-substituted allylsilanes underwent a complete fluorodesilylation process when exposed to Selectfluor. In order to suppress this competing reaction and promote the fluorocyclisation, we conducted a survey of the literature to determine the most suitable silyl substituents for this purpose. It appears that the size of the silyl moiety is critically important in the Lewis acid catalysed annulations of aldehydes and ketones. Indeed the cyclisation process is in competition with the undesired Sakurai allylation resulting from desilylation of the allylsilanes.[155] As illustrated by the annulations of

silylcyclopentanes arising from the reaction of allylsilanes with α,β-unsaturated ketones, the screening of various silyl groups proved that bulky substituents favour annulations versus allylations (Table 2.13).[156] Successful annulation was achieved in 86% and 92% yield with both a triisopropylsilyl or benzhydryldimethylsilyl groups respectively with a minimal amount of the allylation product.

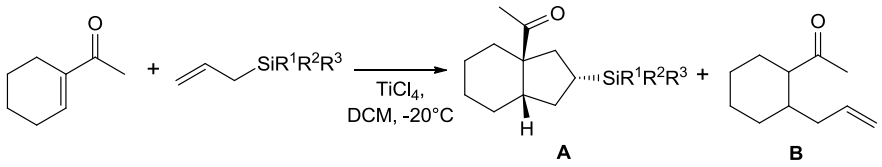

R^1	R^2	R^3	A	B
Me	Me	Me	18	76
Me	Me	Ph	19	76
Ph	Ph	Ph	51	39
^{i}Pr	^{i}Pr	Ph	**68**	**traces**
^{i}Pr	^{i}Pr	^{i}Pr	**86**	**2**
Me	Me	$CHPh_2$	**92**	**traces**

Table 2.13: Annulation of allylsislanes with enones. (Table reproduced from H.-J. Knölker, N. Foitzik, H. Goesmann, R. Graf, *Angew. Chem. Int. Ed.* **1993**, *32*, 1081-1083; M. D. Groaning, G. P. Brengel, A. I. Meyers, *J. Org. Chem.* **1998,** *63*, 5517-5522; Z.-H. Peng, K. A. Woerpel, *Org. Lett.* **2000**, *2*, 1379-1381 [156]).

This observation is in accordance with earlier work in our group detailing a conceptually novel process for stereocontrolled fluorocyclisation of tetrahydrofurans.[157] This study has shown that allylsilanes equipped with bulky substituents were amenable to promote the fluorocyclisation of a derivative bearing an internal nucleophilic alcohol while by-passing competing fluorodesilylation (Table 2.14).

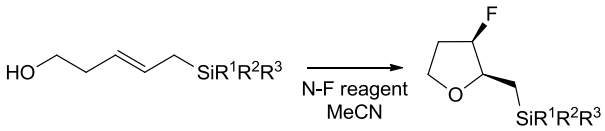

R^1	R^2	R^3	*E*:*Z*	Conditions	Yield (%)	d.r. (*syn*/*anti*)
^{i}Pr	^{i}Pr	^{i}Pr	2:1	Selectfluor, $NaHCO_3$, r.t. 6h	90	2.5:1
^{i}Pr	^{i}Pr	*p*-Tolyl	2:1	NFSI, $NaHCO_3$, reflux 15h	60	3:1
Me	Me	CH_2Ph	2:1	Selectfluor, $NaHCO_3$, r.t. 6h	41	3:1
Me	Me	Ph	4:1	Selectfluor, $NaHCO_3$, r.t. 6h	-	-

Table 2.14: Screening of silyl substituents for the fluorocyclisation of tetrahydrofurans. (Table reproduced from S. C. Wilkinson, O. Lozano, M. Schuler, M. Pacheco, R. Salmon, V. Gouverneur, *Angew. Chem. Int. Ed.* **2009**, *48*, 7083-7086 [157]).

Encouraged by these results, we hypothesised that the same methodology could be expanded to the electrophilic fluorination of allylsilanes bearing a pending nucleophilic amine. We would probe whether the relative stereochemistry of the products could be controlled by the alkene geometry and thus be predictable. This novel approach would allow us to access fluorinated pyrrolidines from allylsilanes in an *endo* fluorocyclisation process.

2.4.3 Validation of the cyclisation:

In the first instance the fluoroamination of simple linear homoallylic amines was selected as a model reaction. In order to assess the feasibility of the reaction, silyl substituents and *N*-protecting groups were examined. Guided in our choice by previous studies within our group, these substituents were selected according to their bulkiness.[157] Triisopropyl, *p*-tolyldimethylsilyl, triphenylsilyl, dimethylphenylsilyl and the benzhydryldimethylsilyl groups were chosen as a replacement to trimethylsilyl, in order to disfavour desilylation; all these groups with the exception of the triisopropyl group have been shown to undergo oxidative cleavage.[158] Tosyl and Boc groups were selected as protecting group of the pending amino nucleophile.[159] All the desired precursors, with the exception of **78**, were obtained by cross-metathesis of homoallylic tosylamine with various allylsilanes partners in presence of Grubbs's 2nd generation catalyst and 1,4-benzoquinone. For the synthesis of allysilane **78**, we noted that the direct cross-metathesis of the homoallylic tosylamine with allyl(diisopropyl)(4-methylphenyl)silane led to the synthesis of the truncated side-product. The cross-metathesis reaction was performed with but-3-enol then the primary alcohol group **77** converted into the tosylated amine. Starting allylsilanes other than commercially available triphenyl silyl and triisopropyl silyl were obtained by substitution of the corresponding chloroallylsilanes with the required aryl lithium according to procedures already established within the group.[160] All cross-metathesis reactions gave the corresponding allylsilanes as inseparable mixtures of *E* and *Z* geometrical isomers with low selectivity, the best *E/Z* ratio being 5/1 and isolated yields ranging from 54% to 89% (Scheme 2.35).

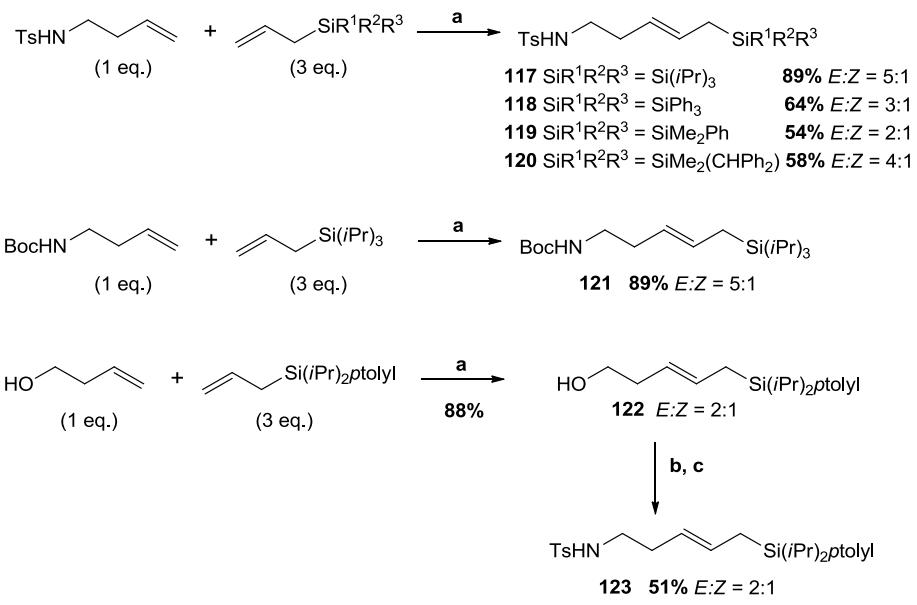

Scheme 2.35: Synthesis of amines **117-121** and **123**; **a**) Grubbs 2nd (5 mol%), 1,4-benzoquinone, DCM, reflux, 3 days; **b**) MsCl, NEt_3, DCM, 0 °C, 2 h 30min; **c**) NH_2Ts, KOH, DMF, 120 °C, 3 h.

The homoallylic amines bearing this selection of silyl substituents were then subjected to a variety of fluorination conditions using either Selectfluor (1.1 eq.) or NFSI (1.1 eq.) (Table 2.15). All reactions were performed in the presence of a base to minimize protodesilylation and to encourage cyclization by deprotonation of the protected nitrogen nucleophile. The desired cyclised products were formed when the silicon substituents were either diisopropyl tolyl or triisopropyl. The homoallylic amine **123** containing the pending diisopropyltolylsilyl group gave the cyclised product in 23% isolated yield, along with 50% of the undesired product of fluorodesilylation (entry 5). The triisosopropylsilyl group was found to be optimum, the precursor **117** giving the pyrrolidine **124** in isolated yields up to 58% (entries 1-4) despite the formation of the product of competitive fluorodesilylation (ranging from 17 to 34% yield). However the amines **118**, **119** and **120** did not undergo fluorination-cyclisation but led exclusively to the allylic fluoride **55**. In an attempt to verify the reactivity of the amine nucleophile with protecting group other than tosyl, the Boc homoallylic amine **121** was submitted to the reaction and also successfully underwent cyclisation.[iii] The change of protecting group affected the yield or the product ratio between **129** and **61** to a small extent.

[iii] The synthesis of the homoallylic amine **121** and its corresponding fluorinated pyrrolidine **129** was carried out by Dr. Oscar Lozano.

All the cyclised products were obtained as inseparable mixtures of *syn* and *anti* isomers, with respect to the fluorine and silylmethyl group. The diastereomeric ratio of the cyclised pyrrolidines was superior to the *E*/*Z* ratio of the starting allylsilanes; the *syn* isomer being consistently predominant as determined from the crude ^{1}H and ^{19}F NMR spectra. Overall the highest yields of the cyclised products were obtained when Selectfluor was used as the fluorinating agent in acetonitrile in presence of $NaHCO_3$ at room temperature. Treatment of **117** with NFSI in acetonitrile at reflux resulted in comparable yield and level of diastereoselectivity. When NFSI was used at r.t., the reaction time increased but did not lead to better results. Moreover the presence or the nature of basic additive did not seem to affect the outcome of the reaction nor shorten the reaction time (Table 2.15, conditions **B** and **C**). The use of Selectfluor in acetonitrile at room temperature was retained for further investigation.

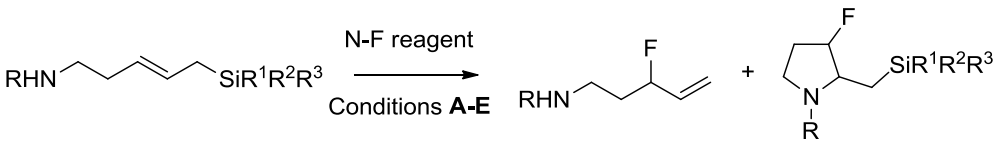

117 R = Ts; $SiR^1R^2R^3$ = Si(*i*Pr)$_3$
123 R = Ts; $SiR^1R^2R^3$ = Si(*i*Pr)$_2$-*p*-tolyl
118 R = Ts; $SiR^1R^2R^3$ = $SiPh_3$
119 R = Ts; $SiR^1R^2R^3$ = $SiMe_2Ph$
120 R = Ts; $SiR^1R^2R^3$ = $SiMe_2(CHPh_2)$
121 R = Boc; $SiR^1R^2R^3$ = Si(*i*Pr)$_3$

55 R = Ts
61 R = Boc

124 R = Ts; $SiR^1R^2R^3$ = Si(*i*Pr)$_3$
125 R = Ts; $SiR^1R^2R^3$ = Si(*i*Pr)$_2$-*p*-tolyl
126 R = Ts; $SiR^1R^2R^3$ = $SiPh_3$
127 R = Ts; $SiR^1R^2R^3$ = $SiMe_2Ph$
128 R = Ts; $SiR^1R^2R^3$ = $SiMe_2(CHPh_2)$
129 R = Boc; $SiR^1R^2R^3$ = Si(*i*Pr)$_3$

Entry	Allylsilanes (*E:Z*)	Condition (time)[a]	Yield [%] of **55** or **61**[b]	Yield [%] of **124-129** (*syn:anti*)[c]
1	**117** (5:1)	**A** (24 h)	**55**, 34	**124** 58 (9:1)
2	**117** (5:1)	**B** (48 h)	**55**, 17	**124** 55 (7:1)
3	**117** (5:1)	**C** (48 h)	**55**, 22	**124** 53 (7:1)
4	**117** (5:1)	**D** (24 h)	**55**, 18	**124** 50 (9:1)
5	**123 (**2:1)	**A** (24 h)	**55**, 50	**125** 23 (5:1)
6	**118 (**3:1)	**A** (16 h)	**55**, 44	-[e]
7	**118** (3:1)	**E** (72 h)	**55**, 56	-[e]
8	**119 (**2:1)	**A** (16 h)	**55**, 72	-[e]
9	**119** (2:1)	**E** (16 h)	**55**, 63	-[e]
10	**120** (4:1)	**A** (48 h)	**55**, 34	-[e]
11	**120** (4:1)	**E** (72 h)	**55**, 46	-[e]
12	**121** (5:1)	**A** (24 h)	**61**, 43	**129** 54 (5:1)

Table 2.15: Fluorocyclisation of **124-129;** [a] Conditions: **A** = Selectfluor (1.1 eq.), $NaHCO_3$ (1.1 eq.) CH_3CN, r.t.; **B** = Selectfluor (1.1eq.), K_2CO_3 (1.1 eq.), CH_3CN, r.t.; **C** = Selectfluor (1.1 eq.), CH_3CN, r.t.; **D** = NFSI (1.1 eq.), $NaHCO_3$ (1.1 eq.), CH_3CN, reflux; **E** = NFSI (1.1 eq.), $NaHCO_3$ (1.1 eq.), CH_3CN, r.t.; [b] Yield of the isolated product; [c] d.r. determined by ^{19}F NMR analysis on the crude product; [e] Fluorodesilylation only.

2.4.4 Scope and limitations:

To further assess the reactivity of silyl-activated homoallylic alcohols and amines, we investigated the influence of the double bond geometry of both (*E*)- and (*Z*)-allylsilanes on the cyclisation.

2.4.4.1 Design of substrates and synthesis:

To investigate the scope and limitations of this reaction we selected a range of architecturally diverse substrates featuring the appropriate silyl groups either triisopropyl or diisopropyltolyl. Following the same route as previously developed for the synthesis of allylic fluorides, the starting allylsilanes of

predominantly *E* geometry would be accessed through direct cross-metathesis reaction whereas the predominant *Z* isomers would be obtained *via* a ring-closing/ring-opening metathesis sequence. Substrates were chosen to probe how tolerant the reaction is of substituents on the double bond. The compatibility of the reaction with different functional groups was also further studied and a substrate containing an amide group as internal nucleophile was investigated.

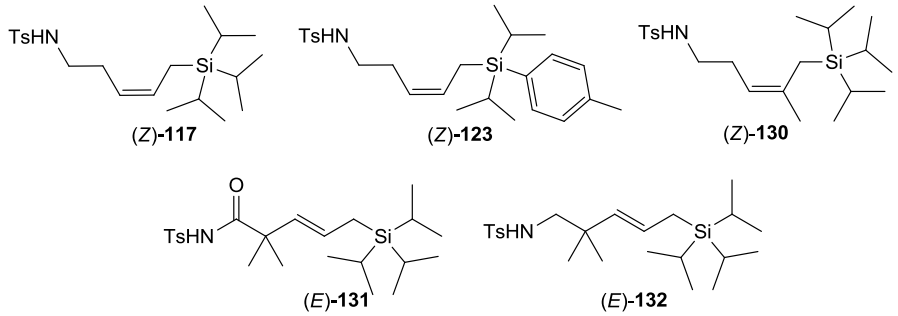

Figure 2.8: Substrates for fluorocylisation.

Synthesis of the substrates:

For the synthesis of substrates (*Z*)-**117** and (*Z*)-**123**, allylmagnesium chloride followed by 3-buten-1-ol were added to allyldichlorodiisopropylsilane to afford the diene **133** in 34% yield. Ring-closing metathesis using Grubbs' 2nd generation catalyst (3 mol%) in dichloromethane at reflux for 1 h gave the cyclised product in **134** in 70% yield. Ring opening with isopropyllithium led to the desired allylsilane **136** in 46% yield. Subsequent mesylation and displacement with tosylamine provided the homoallylic amine (*Z*)-**117** in moderate 54% yield with a *E/Z* ratio of 1:10. The corresponding tolyl derivative was obtained by treating the 7-membered ring product with tolyllithium prepared *in situ*. The resulting allylsilane **135** was then converted into the desired homoallylic amine (*Z*)-**123** in 58% and *E/Z* ratio of 1:12.

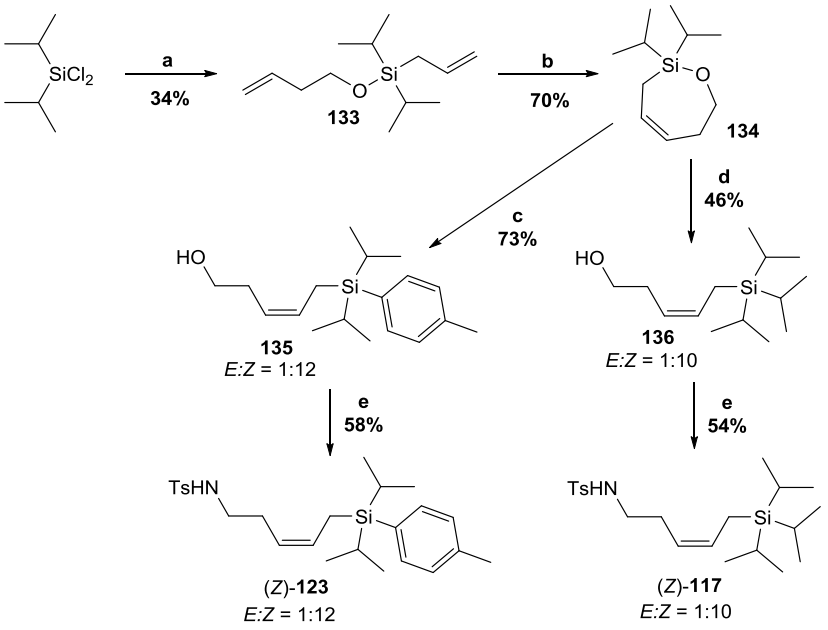

Scheme 2.36: Synthesis of *Z* allylsilanes (*Z*)-**117** and (*Z*)-**123**. **a**) Allylmagnesium chloride, THF, r.t., 2 h, then NEt_3, 3-buten-1-ol, DMAP, THF, r.t., 13 h, yield over two steps; **b**) Grubbs' 2nd (3 mol%), DCM, reflux, 1 h; **c**) tolyllithium Et_2O, -78 °C-r.t., overnight; **d**) isopropyllithium, Et_2O, -78 °C-r.t., overnight; **e**) $MeSO_2Cl$, NEt_3, DCM, r.t., 2 h, then KOH, $TsNH_2$, DMF, 120 °C, 3 h, yield over two steps.

Synthesis of the trisubstituted allylsilane (*Z*)-**130** began by protection of 3-buten-1-ol with allyldichlorodiisopropylsilane followed by the addition of the commercially available 2-methylallylmagnesium chloride Grignard to afford the precursor **137** for ring-closing metathesis in 50% yield over two steps. The diene was then subjected to a ring-closing metathesis reaction using Hoveyda-Grubbs' 2nd generation catalyst for 2 h and the product **138** was obtained in 90% yield. Subsequent ring-opening with isopropyllithium, gave the desired product **139** in a moderate 42% yield. Surprisingly, a loss in diastereomeric purity of the double bond occurred during the ring-opening and the product **139** was delivered with a much lower *E:Z* ratio of 1:2 than expected for this type of system. Formation of a mesylate followed by its displacement with tosylamine gave the corresponding trisubstituted allysilane (*Z*)-**130** in 47% over two steps.

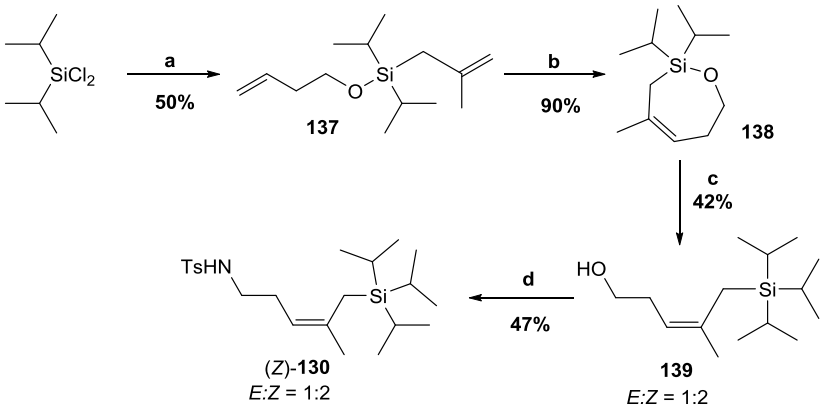

Scheme 2.37: Synthesis of trisubstitued allylsilane (*Z*)-**130**; **a**) 3-buten-1-ol, NEt_3, DCM, reflux, 48 h, then 2-methylallylmagnesium chloride, THF, r.t., 16 h, yield over two steps; **b**) Hoveya-Grubbs 2nd (2 mol%), DCM, reflux, 2 h; **c**) Isopropyllithium, THF, r.t., 23 h; **d**) $MeSO_2Cl$, NEt_3, DCM, r.t., 2 h, then KOH, $TsNH_2$, DMF, 120 °C, 3 h, yield over two steps.

In order to access the allylsilanes (*E*)-**131** and (*E*)-**132**, the synthesis was conducted using the corresponding carboxylic acid. Hoveyda-Grubbs' 2nd generation catalyst gave the desired product **140** in 47% yield as the sole *E* diastereoisomer by cross-metathesis. This high level of selectivity is in line with previous examples in the literature describing that the cross-metathesis of allylsilanes with alkenes bearing a substituent α to the double bond led preferentially to the formation of the product of *E* geometry.[161] A possible explanation could be that the introduction of steric hindrance close to the olefin group directs the cross-metathesis towards the *E* isomer which is less sterically hindered. Subsequent reduction of the amide (*E*)-**131** with lithium aluminium hydride gave the tosylamine (*E*)-**132** in 48% with an *E:Z* ratio = 16:1.

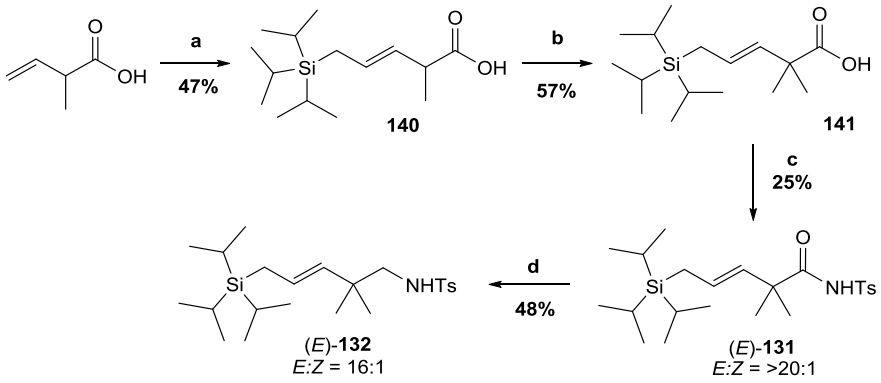

Scheme 2.38: Synthesis of gem-dimethyl substituted allylsilanes (*E*)-**131** and (*E*)-**132**; **a**) allyltriisopropylsilane, Hoveyda-Grubbs' 2nd (5 mol %) DCM, reflux, 3 days; **b**) LDA, MeI, THF, -78 °C, 1 h; **c**) tosylisocyanate, NEt_3, THF, r.t., overnight; **d**) $LiAlH_4$, THF, r.t, 16 h;

2.4.3.2 Fluoroamination cyclisation:

This series of precursors was then subjected to our general cyclisation condition using Selecfluor as the source of fluorine in MeCN, with $NaHCO_3$ at r.t. The reactions proceeded as expected, with all the precursors affording the desired fluorinated pyrrolidines with yields ranging from 14% to 58% (Table 2.16). In all cases the cyclised products were accompanied by a large amount of the fluorodesilylation product resulting from the competing side-reaction. As previously described for homoallylic alcohols, we observed that both the *E*- and *Z*- isomers of the substituted homoallylic amines could undergo the fluorocyclisation reaction.

Entry	Allylsilane	Product [a]	Yield (%) [b] (d.r. (*syn:anti*)) [c]	Product **55**, **63** or **64**	Yield (%) [b]
1	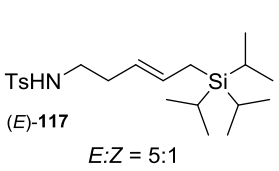 (*E*)-**117** *E*:*Z* = 5:1	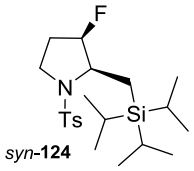 *syn*-**124**	58% (9:1)	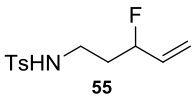 **55**	34%
2	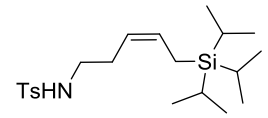 (*Z*)-**117** *E*:*Z* =1:10	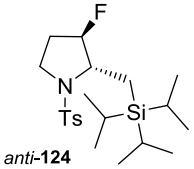 *anti*-**124**	34% (>1:20)	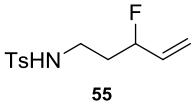 **55**	38%
3	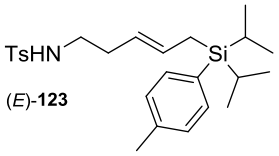 (*E*)-**123** *E*:*Z* = 2:1	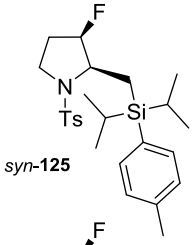 *syn*-**125**	23% (5:1)	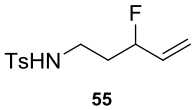 **55**	50%
4	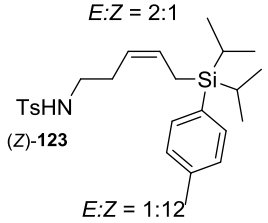 (*Z*)-**123** *E*:*Z* = 1:12	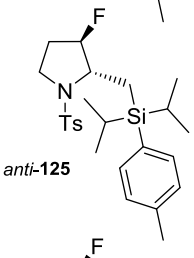 *anti*-**125**	14% (1:23)	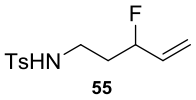 **55**	56%
5	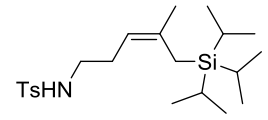 (*Z*)-**130** *E*:*Z* = 1:2	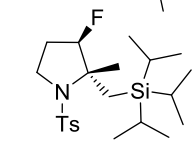 *anti*-**142**	61% (1:1.3)	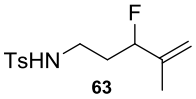 **63**	27%
6	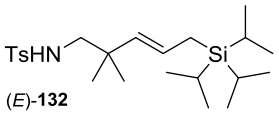 (*E*)-**132** *E*:*Z* = 16:1	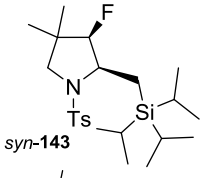 *syn*-**143**	36% (6:1)	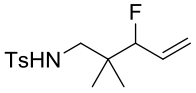 **64**	45%
7	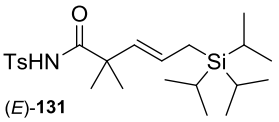 (*E*)-**131** *E*:*Z* = 16:1	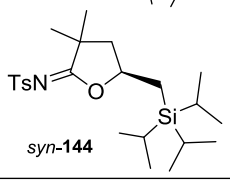 *syn*-**144**	31% (6.6:1)	_[d]	

[a] Major isomer shown; [b] Yield of the isolated product; [c] d.r. determined by ^{19}F NMR analysis on the crude product; [d] no product of desilylation was isolated.

Table 2.16: Scope of Electrophilic Fluorocyclisation.

Several trends emerge from this study. The cyclisation of triisopropylallylsilanes was more efficient than the corresponding precursors presenting with the diisopropyltolylsilyl group; this stands true both for the *E* and *Z* series (Table 2.16, entries 1 and 2 vs. entries 3 and 4). In the *Z* series, (*Z*)-allyltriisopropyl **117** and (*Z*)-allyldiisopropyltoyl **123** silanes delivered exclusively the *anti* cyclised

products **124** and **125** starting from a *E:Z* ratio of 1:10 and 1:12 respectively. The presence of an alkene methyl substituent proximal to the silyl group was beneficial in terms of product distribution. The branched amine (*Z*)-**130** gave the product of cyclisation **142** in 61% yield (entry 5) but the linear allylsilane (*Z*)-**123** gave **124** with a chemical yield of only 14% (entry 4). The d.r. of 1.3:1 observed for the cyclised pyrrolidine **142** possessing a quaternary centre was slightly eroded in comparison to the *E:Z* ratio of 1:2 in the starting *Z*-alkene **130**. The stereochemical transfer was less efficient upon cyclisation of the major *E*-allylsilanes. As seen previously in the optimisation study, the conversion of sample of (*E*)-**117** and (*E*)-**123** enriched in *E*-diastereoisomers into the *syn* products **124** and **125** was achieved in low to moderate yields of 58% and 23% respectively and slightly increased diastereomeric ratio. Precursor (*E*)-**117** which was engaged as a 5:1 *E/Z* mixture gave the corresponding *syn* fluorinated pyrrolidine **124** with a d.r. of 9:1. Similarly (*E*)-**123** engaged with a 2:1 *E/Z* mixture gave a 5:1 ratio in favour of the *syn* product **125**. For (*E*)-**132**, the allylic fluoride **64** was isolated as the major product (45%) and the 3-fluoropyrrolidine was obtained in 36%. These low yields were accompanied by a significant drop in the level of stereocontrol. The substrate (*E*)-**132** engaged as a sole *E*-isomer led upon fluorination to a *syn/anti* ratio of 6:1 of *syn*-**143**. The fluorocyclisation of the structurally related amide (*E*)-**131** did not afford the expected fluorinated lactam but a furan with an exocyclic imine *syn*-**144** functionality in a moderate yield of 31%. The diastereomeric ratio was also much reduced with the product *syn*-**144** being delivered in a d.r. of 6.6:1 starting from the single *E*-isomer of the allyl silane (d.r. > 20:1, Table 2.16, entry 7). The formation of the desired lactone was not observed.

2.4.4.2 Assignment of the relative stereochemistry:

Simple analysis of *J* coupling constants extracted from ^{1}H proton spectra and chemical shifts were not conclusive. The relationship between the fluorine, the proton H^2 and proton H^3 was particularly relevant. As exemplified for the isomers *syn*-**124** and *anti*-**124**, the key $^{3}J_{F\text{-}H2}$ and $^{3}J_{H2\text{-}H3}$ coupling constants would normally give an indication of the relative stereochemistry, in this case are very similar.

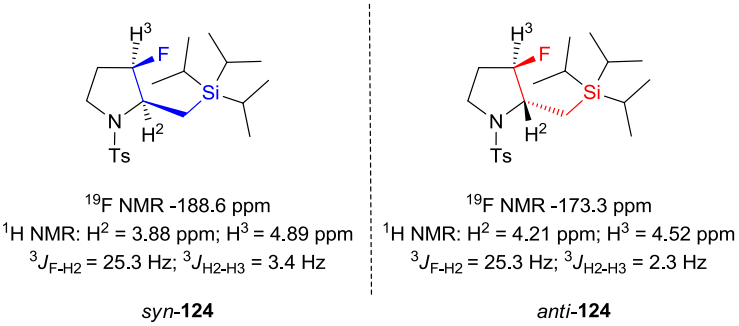

Figure 2.9: Comparison between the ^{1}H and ^{19}F chemical shifts and proton coupling constants.

In isomer *syn*-**124**, anticipated to be *syn*, $^{3}J_{F\text{-}H2}$ = 25.3 Hz and $^{3}J_{H2\text{-}H3}$ = 3.4 Hz which is comparable in order of magnitude to the $^{3}J_{F\text{-}H2}$ = 25.3 Hz and $^{3}J_{H2\text{-}H3}$ = 2.3 Hz found for the presumably *anti* isomer *anti*-**124**. The chemical shift of the H^2 and H^3 protons did not provide conclusive data. In isomer *syn*-**124** the chemical shifts of H^2 and H^3 were found at 3.9 ppm and 4.9 ppm (in deuterated benzene) respectively while *anti*-**124** exihibits chemical shifts for the same protons at 4.2 ppm and 4.5 ppm. The differences between the two sets of coupling constants and proton chemical shifts are not remarkable enough to give a conclusive answer regarding the geometry of the compounds. However the analysis of fluorine chemical shifts was more productive. It appeared as a general trend, that compounds assumed to be *anti* diastereoisomers have a more downfield ^{19}F chemical shift than their *syn* counterparts. At this stage an analogy can be drawn between the fluorinated pyrrolidines and the fluorinated tetrahydrofurans resulting from a previous study. A good agreement was found, based on the comparison of the fluorine chemical shift, between the stereochemistry of the nitrogen series compounds and their structurally related homologues from the oxygen series which had already been assigned (Table 2.17).

Entry	Pyrrolidines	^{19}F NMR δ (ppm)	Tetrahydrofurans	^{19}F NMR δ (ppm)
1	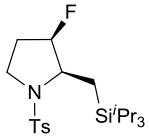	-188.6	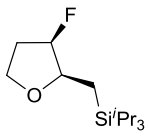	-189.4
2	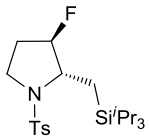	-173.3	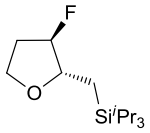	-172.8
3	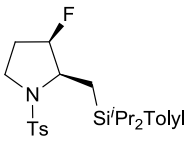	-188.7	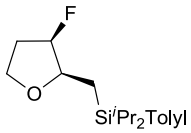	-189.3
4	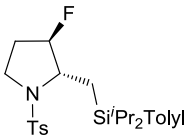	-174.1	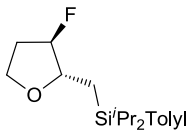	-173.0
5	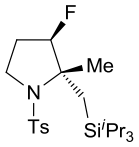	-182.0	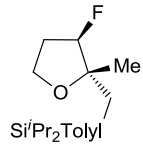	-180.8
6	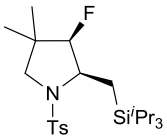	-192.6	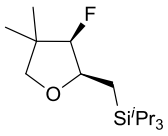	-197.7
7	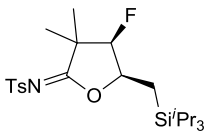	-197.3	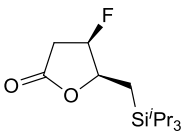	-192.5

Table 2.17: Comparative analysis of ^{19}F chemical shifts in the *N*- and *O*- series. Reproduced from S. C. Wilkinson, O. Lozano, M. Schuler, M. Pacheco, R. Salmon, V. Gouverneur, *Angew. Chem. Int. Ed.* **2009**, *48*, 7083-7086 (right)[157], present work (left).

Steady state NOE/HOESY experiments were conducted for each cyclised compound to confirm the stereochemistry of the products. Across the whole series of our fluorinated pyrrolidines, a strong NOE interaction was found between the H^3-H^2 protons for the *syn*-pyrrolidines. HOESY analysis confirmed also the presence of a strong interaction between the fluorine atom and one the isopropyl substituent of the adjacent silicon group. These combined observations strongly support the *syn* spatial arrangement of these two substituents. In contrast, the *anti*-pyrrolidines exhibited a strong HOESY interaction between the fluorine and H^2 proton, and a weak NOE interaction between H^3-H^2, which is diagnostic of an *anti* relationship (Figure 2.10).

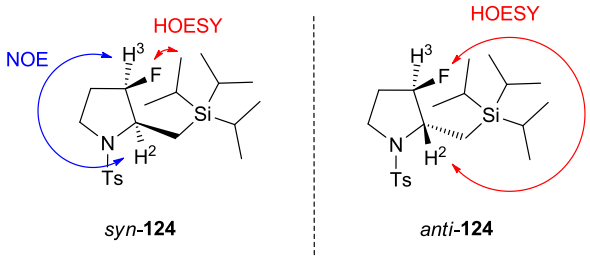

Figure 2.10: NOE and HOESY interactions observed for a pair of diastereoisomers.

The X-ray structure of compound *syn*-**124** was obtained, which was in agreement with the NMR observations and analysis, confirming the *syn* geometry of the heterocycle (Figure 2.11).

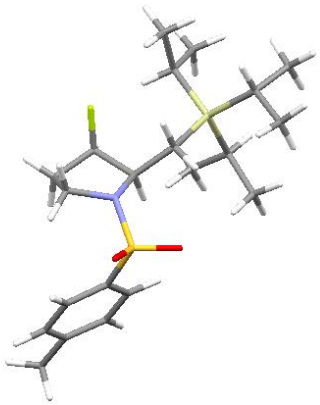

Figure 2.11: X-ray structure of compound *syn*-**124**.

2.4.4.3 Comparison with previous study:

The results obtained in this study are similar in term of sense of selectivity to the previously reported study on the fluorocyclisation of various silylpent-3-en-1-ols. However this study revealed that the pending nucleophile has a clear influence on the efficiency of the cyclisation process.

Entry	Allylsilane [a]	Product [b]	Yield (%) [c] d.r. (*syn*/*anti*) [d]	Allylsilane [a]	Product [b]	Yield (%) [c] d.r. (*syn*/*anti*) [d]
1	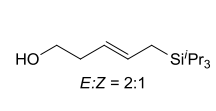 *E*:*Z* = 2:1	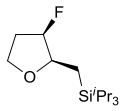	90% 2.5:1	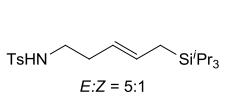 *E*:*Z* = 5:1	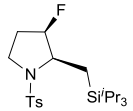	58% 9:1
2	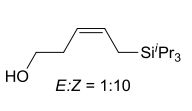 *E*:*Z* = 1:10	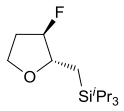	58% 1:8	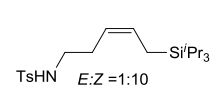 *E*:*Z* =1:10	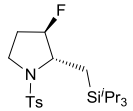	34% 1:>20
3	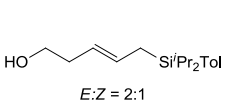 *E*:*Z* = 2:1	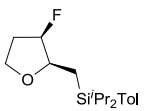	60% 3:1	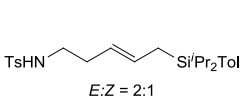 *E*:*Z* = 2:1	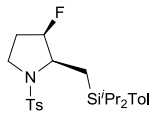	23% 5:1
4	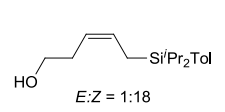 *E*:*Z* = 1:18	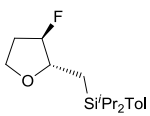	49% 1:6	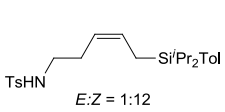 *E*:*Z* = 1:12	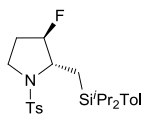	14% 1:23
5	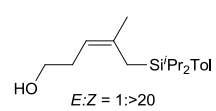 *E*:*Z* = 1:>20	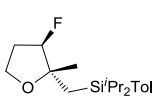	67% 1:16	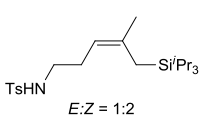 *E*:*Z* = 1:2	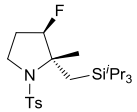	61% 1:1.3
6	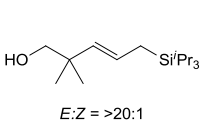 *E*:*Z* = >20:1	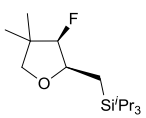	72% >20:1	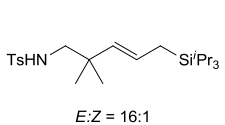 *E*:*Z* = 16:1	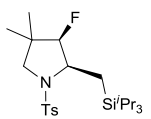	36% 6:1
7	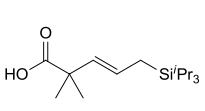 *E*:*Z* = 3:1	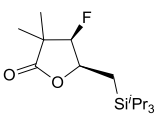	80% 3:1	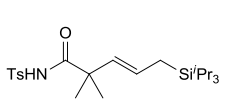 *E*:*Z* = >20:1	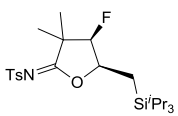	31% 6.6:1

Table 2.18: Scope of electrophilic fluorocyclisation of fluorinated tetrahydrofurans and pyrrolidines. [a] Selectfluor, $NaHCO_3$, MeCN, r.t. [b] Major isomer shown. [c] Yield of the isolated product. [d] *syn*/*anti* ratio determined by ^{19}F NMR of crude product. (Reproduced from S. C. Wilkinson, O. Lozano, M. Schuler, M. Pacheco, R. Salmon, V. Gouverneur, *Angew. Chem. Int. Ed.* **2009**, *48*, 7083-7086 (left)[157], present work (right).

In the *O*- series, in contrast to the *N*- series, no allylic fluorides were recovered at the end of the reaction. The products of electrophilic fluorodesilylation or protodesilylation may well have been formed but due to their high volatility they could not have been isolated. The overall yield of the cyclisation was significantly higher when oxygen was used as internal nucleophile as exemplified in the Table 2.18. In the case of *E* allylsilanes, the fluoroetherification delivered the major *syn* products with a high level of stereocontrol. The stereochemical information was accurately transferred to the product as shown in Table 2.18, entries 1 and 3. An enrichment in diastereoisomeric ratio could be observed in some cases in the favour of the major *syn* product compared to *E/Z* ratio of the starting material. For compounds engaged as pure *E* isomers, only the formation of the *syn* products could be identified by ^{1}H or ^{19}F NMR of the crude mixture. On the other hand, the diastereoselective transformation of *Z* allylsilanes into *anti* fluorinated tetrahydrofurans suffered from some stereochemical erosion. These observations seem to be in contrast to the nitrogen series where control over selectivity was typically superior, at least for the linear systems, especially for the conversion of *Z* alkenes. The branched precursors however led to significant erosion of d.r. upon cyclisation.

2.4.5 Rationalisation of the diastereoselectivity:

The stereochemical outcome of the reaction is consistent with a predominant overall *syn* addition to the double bond. As described in the introduction to this chapter, the addition of fluorine deriving from an electrophilic N-F reagent to allylsilanes is expected to take place *anti* to the silyl group in accord with our previous studies on fluorodesilylation. Calculations of the electrostatic potential of the diastereotopic faces have shown that the face opposite to the silyl group is the most reactive.[162] Upon electrophilic desilylation reactions, the model allylsilane adopts a conformation close to the most stable with the smallest substituent α to the silicon (usually H) on the inside position, meaning eclipsing or partially eclipsing the double bond (**conformation A**).

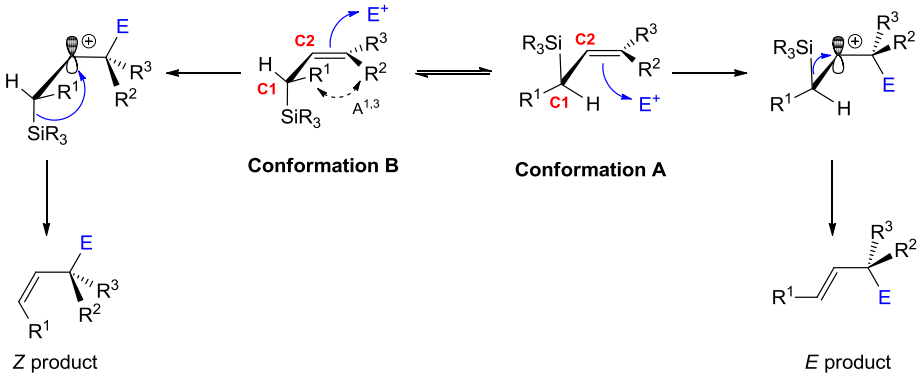

Scheme 2.39: *Anti* addition mechanism of allylsilanes leading to the formation of the *E* and *Z* products.

An alternative conformation is possible (**conformation B**), resulting from rotation of the silyl group around the C2-C3 bound). When the R^1 substituent is relatively small such as a methyl group, the $A^{1,3}$ strain between the inside methyl and the vinylic proton would be minimal thus the conformation would be only slightly higher in energy than **A**.[163] In the case of a bulkier R^1 substituent, Z allylsilane gives usually a better level of *E:Z* stereoselectivity due to the increase of the $A^{1,3}$ strain in the structure. However, independently of the conformation **A** or **B** adopted, or the geometry of the alkene, the products will result from the *anti* electrophilic attack to the silyl group (Scheme 2.39).

In the transition state of fluorocyclisation, the chain adopts very probably an envelope as the reactive conformation. Such conformation allows aligning the C-Si bond of the allylsilanes parallel to the empty p orbital of the resulting β-silylcarbocation. Thus a σ-p hyperconjugative stabilisation is achieved and the developing positive charge is stabilised by the β-effect of the silicon. Subsequent cyclisation occurs with the insertion of the internal nucleophilic nitrogen to the β-silyl cation, preferentially *anti* to the bulky silyl group. The whole process leads to an overall *syn* addition to the allylsilane. This proposed mechanism accounts for the potential high level of stereocontrol of this reaction. Despite the fact that the transfer of selectivity seems to be substrate dependent, the geometry of the alkene plays an important role in the sense of the diastereoselectivity. As demonstrated experimentally, the fluorocyclisation of samples enriched in *E* isomers lead preferentially to formation of the major *syn* pyrrolidines, while samples enriched in *Z* isomer produce the major *anti* pyrrolidines. The model for the proposed mechanism can exemplify the stereochemical outcome of these cyclisations (Scheme 2.40).

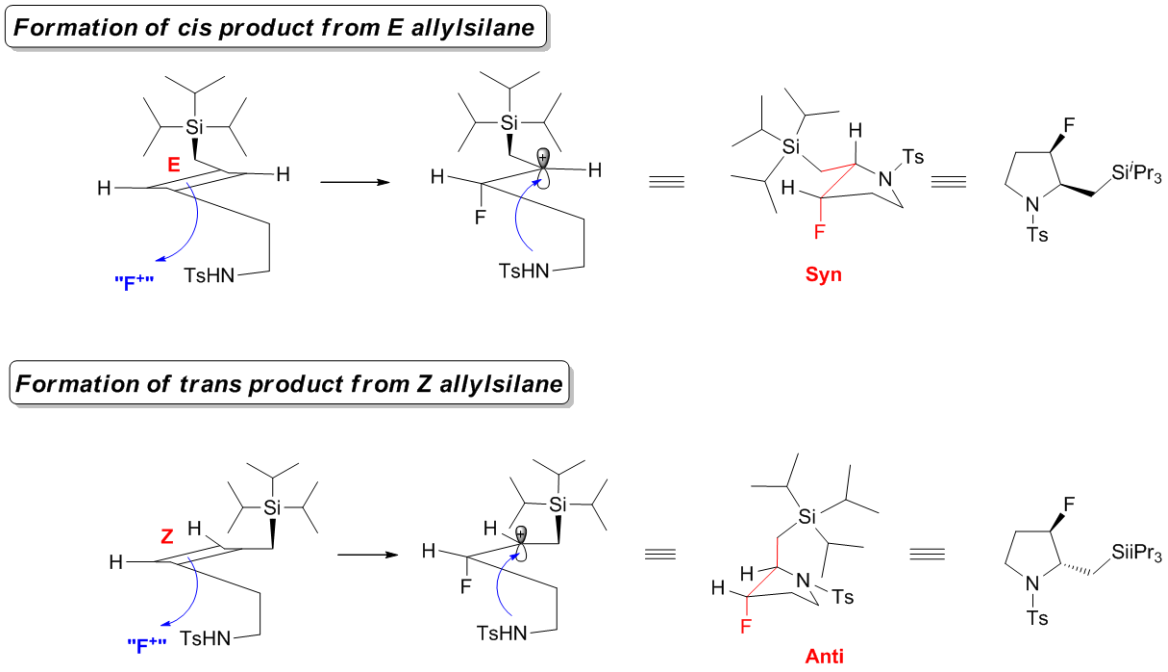

Scheme 2.40: Mechanistic models explaining the sense of diastereoselectivity.

The stereochemical outcome of these diastereospecific cyclisations contrasts with the known literature precedents of 5-*endo*-trig halocyclisation of non-silylated alkenes. Indeed accordingly to the work of D. Knight and F. Davis on the iodocyclisation of homoallylic sulfonamides, only the *E*-isomers are the active partners delivering in good yield the major *trans* products whilst the *Z*-isomers are either inert or afford a gross mixture of *syn/anti* cyclised pyrrolidines in much reduced yield (Scheme 2.41).[164]

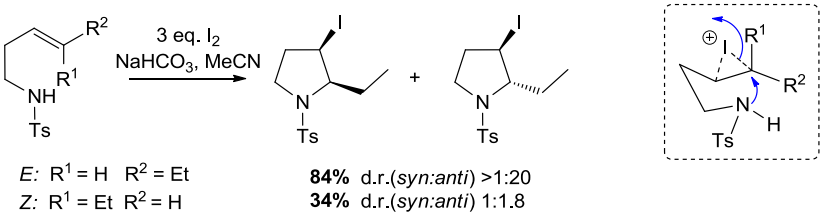

Scheme 2.41: 5-*endo*-trig iodocyclisation of homoallylic sulfonamides. (Reproduced from A. D. Jones, D. W. Knight, D. E. Hibbs, *J. Chem. Soc., Perkin Trans. 1*, **2001**, 1182-1203 [164]).

The level of stereocontrol can be understood by considering a chair-like conformation of the transition state arising from the addition of iodine across the double bond. The pseudo axial position of the subsitutent R^1 in such a conformation might be responsible for the low stereochemical outcome in *Z* series of alkenes. Noteworthy there are major differences between the mechanism of iodocylisation and the annulations of allylsilanes induced by electrophiles, namely the reactive

intermediate. The addition of iodine to the double bond usually leads to the formation of a bridged iodonium ion which is likely to be reversible.

In order to verify the stability of our fluoropyrrolidines, we performed a control experiment by resubmitting the *anti* product to the reaction conditions. Isomerisation to the *syn* product was not observed and the diastereomeric ratio was conserved which indicated that the reaction was likely under kinetic control. The stereochemical stability of the fluorinated pyrrolidines may be due to the difficulties of undergoing the cycloreversion process. Indeed the formation of a carbocation β to the fluorine would be a source of instability for the structure and therefore the isomerisation is not favoured.

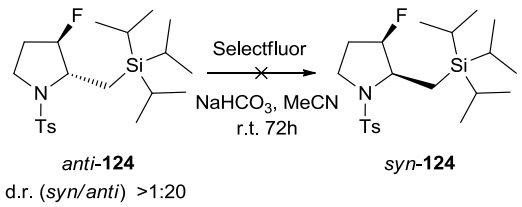

Scheme 2.43: Attempted isomerisation of the *anti* product to the *syn* product.

From the experimental results considered as a whole, erosion of the diastereomeric ratio was observed generally for the conversion of *E* allylsilanes. A representative example of such erosion was observed in the fluorocyclisation of *syn*-**143** (Scheme 2.44).

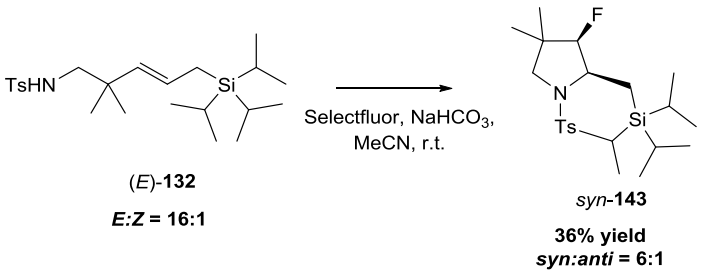

Scheme 2.44: Stereochemical erosion in the transfer of diastereoselectivity from *E*-allylsilane **132** to the *syn*-fluorinated pyrrolidine **143**.

A similar loss of stereospecifity was experienced in the reaction of the *E* allylsilane (trimethyl(pent-3-en-2-yl)silane) with adamantly chloride as a representative simple external electrophile and a catalytic amount of titanium tetrachloride.[165] Despite the *E*-allysilane being engaged as a pure enantiomer, a mixture of *Z* and *E* products was obtained in a 60:40 ratio. After separation, it was

found that the major *Z* product was essentially enantiomerically pure in a >99.5:0.5 e.r. However the minor *E* product suffered from a loss of enantioselectivity being isolated as a 90:10 mixture of enantiomers (Scheme 2.45).

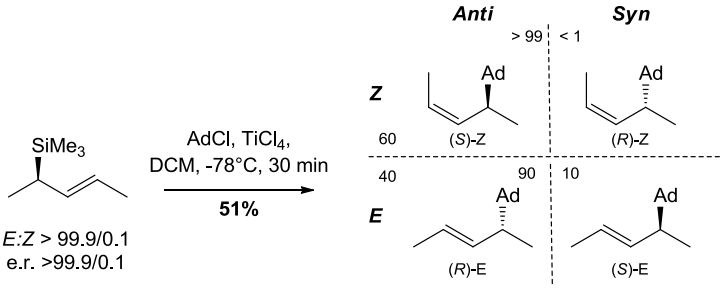

Scheme 2.45: Level of stereospecificity of the electrophilic *anti* addition on *E*-allylsilanes. (Reproduced from M. J. C. Buckle, I. Fleming and S. Gil, *Tetrahedron Lett.*, **1992**, *33*, 4479-4482 and M. J. C. Buckle, I. Fleming, S. Gil, K. L. C. Pang, *Org. Biomol. Chem.* **2004**, *2*, 749-769 [165]).

The degree of stereospecificity observed in this reaction is still very high and in order to explain the difference of enantiomeric induction between the *E* and the *Z* product, two hypotheses were suggested.

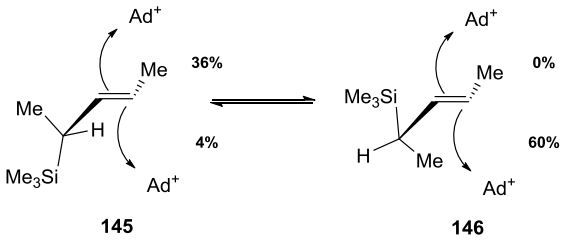

Figure 2.12: Possible conformations for the S_E2' reaction of *E*-allylsilanes.

The first explanation relies on the fact that in conformation **145**, the methyl substituent α to the silyl group may obstruct the upper face of the olefin thus disfavouring the electrophilic attack *anti* to the silicon. The *anti* attack is now competing with the more favourable *syn* attack. On the contrary in conformation **146**, the presence of a proton on the lower face does not hinder the approach of the electrophile. The attack on the lower face of **146** is more selective than the attack on the upper face of the alternative **145** conformation. This argument hypothesises that the entire *E* product is formed by attacking the conformation **145** and all the *Z*, the conformation **146**. Therefore no rotation around the C1-C2 is considered in the intermediate cationic species before the loss of the silyl group. However the second hypothesis explores the eventuality of this rotation. The cation **147** produced by

the attack on the lower face of **146** may alter its conformation to the cation **148** leading to the formation of the (*S*)-*E* product. The rotation of **147** may also occur to a greater extent than the rotation of **149** which would produce the (*R*)-*Z* product.

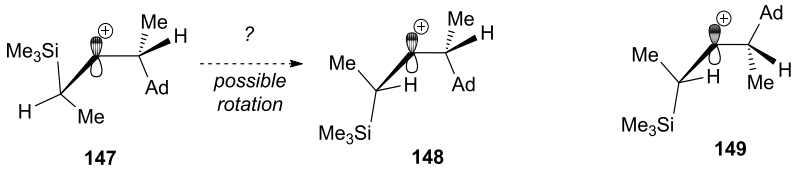

147 **148** **149**

Figure 2.13: Possible bound rotation in the cationic intermediate responsible for the loss of selectivity.

Assuming that the fluorocyclisations are kinetically controlled, we can draw an analogy with the previous example to explain the origin of such stereochemical leakage. The first possible explanation for the loss of stereocontrol could be the rotation of the β-silylcarbocation bond prior to the cyclisation, leading to an overall *anti* addition to the double bond.[163] Alternatively a second hypothesis would involve the lack of selectivity of the nitrogen nucleophilic addition *anti* to the silyl group leading to an overall *anti* addition too.[163] However considering the bulkiness of both the silyl substituents (triisopropyl or diisopropyltolyl) and the tosylamine, the *syn* addition of the nucleophile seems to be less favourable (Scheme 2.46).

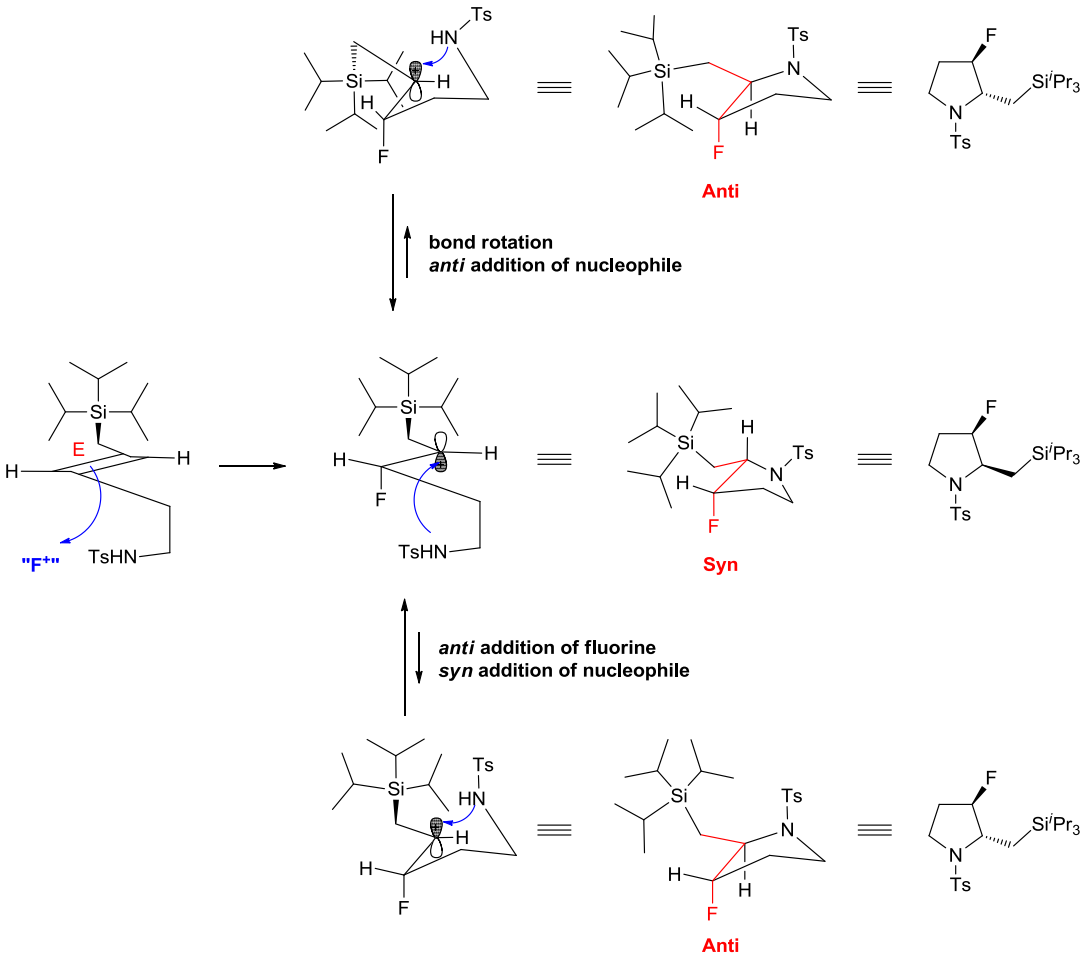

Scheme 2.46: Possible models explaining the loss of stereocontrol for the (*E*)-allylsilane.

On the other hand, the level of diastereocontrol in the fluorocyclisation was greatly enhanced in the case of *Z* allylsilanes as demonstrated by the example below.

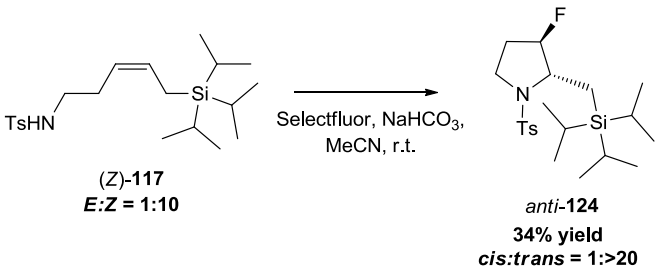

Scheme 2.47: Stereochemical enhancement in the transfer of diastereoselectivity from *Z*-allylsilane **117** to the t*rans*-fluorinated pyrrolidine **124**.

If we refer to the previously quoted example, the same experiment was conducted with the enantiomerically pure *Z* allylsilane. The higher level of $A^{1,3}$ strain in the starting material led to an improved diastereoselectivity, the *E* product being almost exclusively isolated as a 95:5 mixture of enantiomers. For the record, only 0.2% of the *Z* product was detected.

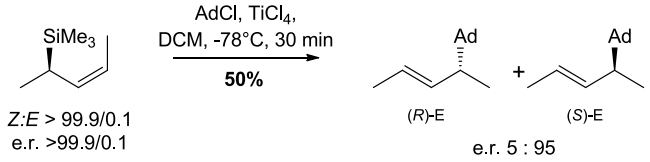

Scheme 2.48: Level of stereospecificity of the electrophilic anti addition on **Z**-allylsilanes.

Again the 5% formation of the (*R*)-*E* product can be explained by the two mechanisms seen previously. Either a small amount of *syn* addition occurs during the reaction of the most stable conformer **150** or a small quantity of conformer **151** undergoes an electrophilic *anti* addition followed by rotation of the carbocationic intermediate around the C1-C2 axis before the silyl group is removed.

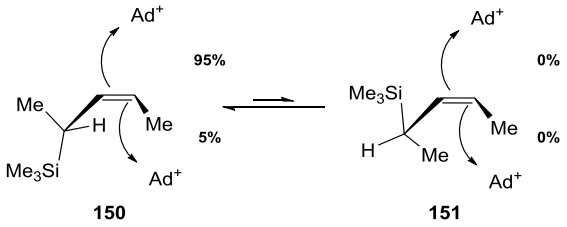

Figure 2.14: Possible conformations for the S_E2' reaction of *Z*-allylsilanes.

Both mechanisms would account for the formation of the minor (*R*)-*E* product. The similarity between the 95:5 ratio for the *Z* allyl product and the 90:10 for the *E* does not provide clear evidence in favour of one or other mechanism. It is very likely a combination of both.

As suggested by this reported example, the increase of the $A^{1,3}$ allylic strain in the *Z*-allylsilane could favour the *anti* stereoselective addition of the fluorine to the double bond. The nitrogen nucleophilic addition *anti* to the silyl group seems to be highly favoured compared to the *syn* addition due to the steric clash that such approach would generate. One should also not exclude the possibility for the minor *E*-allylsilane contained in the mixture to convert to the *trans*-fluoropyrrolidine by bond rotation once the carbocationic species is formed thus enriching the product in *anti* isomer. Overall this postulated mechanism for fluorocyclisation would account well for the stereochemical outcome observed experimentally.

2.5 Conclusion:

This study presents the first examples of iodocyclisation with functionalised allylic fluorides bearing nitrogen nucleophiles. The 5-*exo*-*trig* cyclisation of variously substituted *N*-tosylated 3-fluoro-4-pentenylamines is a suitable transformation to prepare 3-fluoropyrrolidines in high yields (up to 97%) and with good to excellent level of diastereocontrol (up to d.r. > 20:1). The striking similarities observed for allylic fluorides bearing *O*- and *N*-tosyl nucleophiles with respect to stereocontrol, suggest that the sense and level of diastereocontrol observed upon iodoamination is imposed by the fluorine substituent. The diastereselective formation of *syn*-3-fluoropyrrolidines studied herein is likely the result of an "*inside*-fluoro effect" which involves I_2-π complex with the fluorine adopting the *inside* position.

An alternative route was developed to access fluorinated pyrrolidines, relying on the fluorocyclisation of allylsilanes behaving as synthetic equivalent of 1,2-dipoles. This part of the work demonstrates that *N*-tosyl and *N*-Boc homoallylic amines activated by a triisopropylsilyl or *p*-tolyldiisopropylsilyl group are amenable to electrophilic fluorocyclisation. The silyl group controls the regioselectivity of addition of the fluorine, by the way of the β-effect, and could potentially act as a masked hydroxyl group.The *E* or *Z* geometry of the alkene functionality dictates the preferential *syn* or *anti* stereochemical outcome of these kinetically controlled reactions. Important differences have been noted between allylsilanes substituted with oxygen or nitrogen nucleophiles. Competitive fluorination leading to allylic fluorides could not be avoided with homoallylic amines but the level of stereocontrol achieved was superior at least for linear substrates.

Chapter 3:

DESIGN OF A NEW 1D ^{19}F HOESY NMR EXPERIMENT AND ITS APPLICATION TO THE STRUCTURAL AND CONFORMATIONAL ELUCIDATION OF MONO-FLUORINATED PYRROLIDINES

3.1 Generalities on ^{19}F NMR spectroscopy:

3.1.1 Properties of the ^{19}F nucleus:

Fluorine NMR spectroscopy has become an essential part of the tool-kit of any organic chemist wishing to elucidate the structure and conformation of complex molecules.[166] Indeed the ^{19}F nucleus is very similar to the ^{1}H nucleus (Table 3.1), one of its particularities is its spin of ½ which makes it well suited for straightforward structural investigation. It has also a high theoretical sensitivity (83% of the sensitivity of proton) and a natural abundance of 100%.[167] However, in practice the ^{19}F sensitivity can be found superior to the ^{1}H sensitivity due to the absence of problems originating from background signals encountered with ^{1}H detection experiments. In comparison to other isotopes the ^{19}F nucleus possesses the highest magnetogyric ratio γ of 25.181 .10^{-7} rad.s^{-1}.T^{-1} after ^{1}H.[167] This value is given by the ratio of the magnetic moment (μ) and the angular momentum (P).[168] The magnetogyric ratio γ has a characteristic value for each magnetically active nucleus.

$$\gamma = \frac{\mu}{P} = \frac{\mu}{I\hbar} = \frac{2\pi\mu}{Ih}$$

γ : magnetogyric ratio (rad.s^{-1}.T^{-1})

μ : magnetic moment (J.T^{-1})

P = $I\hbar$: angular momentum (J.s)

$\hbar = \frac{h}{2\pi}$: reduced Planck's constant (1.054. 10^{-34} J.s.rad^{-1})

h = Planck's constant (6.626.10^{-34} J.s)

I = nuclear spin quantum number (dimensionless)

Where the magnetic moment μ is expressed in J.T^{-1}, the nuclear spin quantum number I is a dimensionless number and the reduced Planck's constant ħ is1.054.10^{-34} J.s.rad^{-1} expressed in SI

units.[168] In addition to a high γ value, ^{19}F is able to establish strong dipolar couplings with other non-zero spins.[166] These effects make it possible to address relatively long-range distances between two spins. In other words, the coupling between the fluorine atom and a proton separated by four or more bonds can be observed.

Nucleus	NMR frequency (MHz) at 9.396 T	Natural abundance (%)	Gyromagnetic ratio ($rad.s^{-1}.T^{-1}$) x 10^{-7}	Relative sensitivity	Shift parameter range (ppm)
^{1}H	400.00	99.98	26.7519	1.00	15
^{19}F	**376.32**	**100**	**25.181**	**0.833**	**400**
^{31}P	161.92	100	10.841	0.0663	530
^{13}C	100.56	1.11	6.7283	0.0159	250
^{15}N	40.52	0.37	-2.712	0.00104	1700

Table 3.1: Properties of spin ½ nuclei.[167]

Another similarity with ^{1}H is the short spin-lattice relaxation time which can be quantified as a rate constant of a few seconds or less.[169] It refers to the mean time for the nucleus to return to its thermodynamic equilibrium state. In the case of small molecules, the spin-lattice relaxation time and the spin-spin relaxation time have the same order of magnitude which allows the recording of sharp signals in the spectra and provides reliable integration values. The intensities of individual signals in ^{19}F NMR spectra constitute an accurate measure of the relative number of fluorine atoms responsible for such signals.[166]

Despite these common properties, there are some important differences in the NMR parameters of the two nuclei. The range of usual chemical shift is much higher for ^{19}F (about 400 ppm) than for ^{1}H (about 15 ppm). The scope of observable resonance frequencies is dependent on the shielding parameter. This dimensionless constant defines how the magnetic environment impacts on the considered nucleus. In fluorine NMR spectroscopy the wide dispersion of chemical shift is controlled by the fluorine lone-pairs which provide a large paramagnetic term in the shielding

formula.[166,169] The chemical shielding parameter (σ) for a spin of a molecule in solution that tumbles rapidly is defined as follow:

$$\sigma = \sigma_d + \sigma_p + \sigma_i$$

σ : shielding parameter

σ_d : diamagnetic shielding term

σ_p : paramagnetic shielding term

σ_i : environmental shielding term

The diamagnetic term σ_d finds its origin in the response of the electron cloud surrounding the nucleus to an externally imposed magnetic field B_0. The *s* orbital has a spherical geometry and the electrons circulating in this orbital react to the applied field B_0 by producing a local magnetic field of opposite direction. This means that the effective field strength felt by the nucleus is lower than the strength of the external field.[166] For the proton which possesses only a *s* orbital, the diamagnetic term is entirely responsible for the shielding or screening effect on the nucleus. On the other hand the paramagnetic term σ_p derives from the excitation of *p* electrons upon the external field B_0. However electrons in *p* orbitals have no spherical symmetry. They produce comparatively large localised magnetic fields at the nucleus having the same direction as B_0 but of opposite sense to those generated by the *s* electrons. This results in a "deshielding"effect. σ_p is influenced by several factors including the electron density in the various *p* orbitals and the distance separating those orbitals to the nucleus.[169] The term σ_i results from the effect of neighboring groups, which can increase or decrease the field at the nucleus.[169]

In the case of fluorine, the magnitude of the paramagnetic term σ_p largely predominates the magnitude of the diamagnetic term σ_d. Different factors affect the chemical shielding parameter which is translated in difference in chemical shifts. They find their origin namely in local magnetic fields that result from electronically anisotropic groups, local hydrogen bonds formation, electronic fields from dipoles or formal charges or van der Waals interactions.[169]

For technical reasons it is not possible to determine directly the value of the shielding parameter σ for a spin due to the difficulty to measure accurately the absolute value of B_0. However, resonance frequencies ν can be determined with very high accuracy and measurement of these is used to define

values for shielding parameters relative to the shielding parameter of some reference compound. The resonance frequency of one nucleus is reported as the mathematically defined equation:[169]

$$\nu = \frac{\gamma B_0}{2\pi}(1 - \sigma)$$

ν : resonance frequency of the nucleus (Hz)

γ : magnetogyric ratio (rad.s^{-1}.T^{-1})

B_0: external magnetic field (T)

σ : shielding parameter (dimensionless)

Here ν is the resonance frequency of the fluorine spin, γ is its magnetogyric ratio, B_0 is the laboratory magnetic field used for the experiment. NMR instruments operate at different values of B_0 so the dimensionless (and magnetic field independent) parameter δ or chemical shift scale expressed in ppm is defined:[169]

$$\delta = \frac{\nu_{sample} - \nu_{reference}}{\nu_{reference}}$$

This represents the difference between the shielding parameter for the reference signal and that of the nucleus of interest. Fluorine chemical shifts span over a very wide range and there is no single fluorine-containing compound that is experimentally convenient to be used as a universal reference compound. Chemical shifts are often quoted relative to fluorotrichloromethane ($CFCl_3$), a reference compound with a small fluorine shielding parameter which is assigned the value of δ = 0 ppm.[166]

Local magnetic fields arising from aromatic rings, carbonyls, and other electronically anisotropic groups usually generate a chemical shift change of less than 2 ppm in magnitude in ^{19}F NMR spectroscopy, which is insufficient to explain the observed wide chemical shift range.[166] The two forces that dominate the ^{19}F chemical shifts therefore arise from its immediate environmental surrounding such as van der Waals and electrostatic field interactions.

A substantial advantage of fluorine NMR spectroscopy over proton is the ability to record spectra in non-deuterated solvent. This opportunity offers a clear window of analysis without solvent

interference, particularly for the studies of proteins in solution containing more than 90% of water. The measurement can be performed in a buffered solution most appropriate for protein's stability and solubility, avoiding the need of costly deuterated buffers.

3.1.2 Principal applications of ^{19}F NMR spectroscopy:

The potential applications of ^{19}F NMR have been investigated for more than 40 years. Combined with X-ray crystallography, the two modalities have proven to be splendidly complementary techniques. ^{19}F NMR spectroscopy became progressively popular in the fields of biochemistry and organometallic chemistry as a powerful tool for mechanistic investigation.

Chemistry:

Among all the techniques available to analyse and characterise organic compounds, the 2D homonuclear nOe techniques (^{1}H-^{1}H) hold a prominent position and have been used for many years. These techniques are well described for ^{1}H but heteronuclear techniques involving ^{1}H-^{13}C are rarer and suffer from many drawbacks. Principally due to the low abundance of the ^{13}C nucleus, these 2D nOe experiments are difficult to implement and very often do not provide good results. Moreover, little information regarding the structure of the molecule can be extracted from these experiments, rendering the technique with limited applications. However the structural and conformational analysis of organic molecules containing fluorine atoms is greatly facilitated by the useful properties of the ^{19}F nucleus previously described. One of the most powerful experiments using ^{19}F resonances is certainly the heteronuclear ^{1}H-^{19}F Overhauser spectroscopy (HOESY). The original heteronuclear NOESY experiment, applicable to a wide variety of heteroatom nuclei, was first described in 1983 by Rinaldi and Levy.[170] Since then the HOESY became a very popular experiment, mainly for conformational analysis of biomolecules containing ^{19}F labels or for probing the structure of metal-ligand complexes in inorganic chemistry.

However despite the high abundance of both nuclei, application of ^{19}F-^{1}H NMR methods to fluoro-chemicals is not as routine as those for proton.[171] Even though HOESY has great potential, there are

few ^{19}F experiments available for the organic chemists to allow for structure elucidation and to date, its application has been limited.

A privileged area of application of the HOESY technique remains inorganic chemistry. Indeed the introduction of fluorine labels on organic substituents such as aromatic rings can provide a wealth of information in inorganic or organometallic chemistry.[172] Applications include determination of dynamic metal catalysis processes in solution, unraveling the geometry of ligands and complexes, and detection of unusual coordination modes. The observation of the change in chemical shift is the most utilised technique. Indeed ^{19}F resonances are highly influenced by the electronegativity and oxidation state of neighboring groups and also the stereochemistry of complexes even if the fluorinated probes are remote. The use of fluoroaryl groups as reporter ligands allows the investigation of the different steps involved in catalytic cycles such as oxidative addition, reductive elimination or β-hydride elimination. The monitoring of the reaction pathway can also be achieved by labelling several reaction partners. Due to the large range of fluorine chemical shifts, ^{19}F resonances often appear distinctively for each label, giving information on the fate of each partner. This technique becomes very useful in competitive reactions, where the kinetics of a process is being monitored. The importance of ^{19}F NMR is obvious in reactions where a C-F activation process is involved. The oxidative addition of the C-F bond leads to the formation of a new metal-F bond. For a given metal the fluorinated resonances are very characteristic and can be easily distinguished from other fluorinated signals. Moreover, a similar technique to the 2D ^{19}F-^{1}H NOESY has been employed with ^{19}F nucleus to evaluate the level of contact between fluorinated ions and their counterparts in the course of catalytic reactions.[171,173]

The value of the ^{19}F NMR spectroscopy should not be limited to the study of fluorinated compounds. The nature of the ^{19}F nucleus makes it a powerful technique to be applied to many chemical problems when the familiar ^{1}H and ^{13}C NMR find limitations. This possibility should be taken into account when planning research, particularly in the fields of kinetics and reaction mechanism studies.

Drug discovery:

In recent years considerable effort has been devoted to increasing the success rate of the drug discovery process. Due to their ease of implementation and their robustness, NMR-based screening has emerged as a powerful and valuable tool in the identification of potential drug candidates.[174] Currently NMR-based screening is used mainly in hit finding, hit validation, and lead optimisation (see Scheme 3.1). Its greatest potential in drug discovery lies in the information that it can reveal about molecular interactions at the atomic level.

Most NMR based methodologies utilise experiments with proton detection whereas only a few utilise the favorable properties of the ^{19}F nucleus. However ^{19}F NMR spectroscopy has been able to demonstrate its versatile nature and has shown its full capability for identifying quality drug leads that have high potential for development into therapeutic agents.

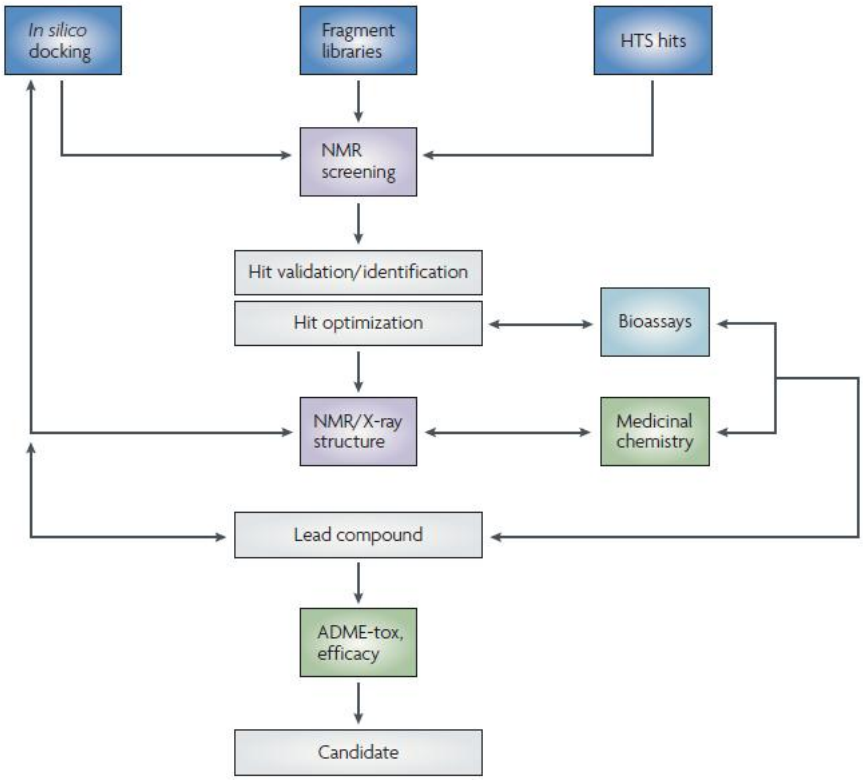

Scheme 3.1: Overview of application of NMR in drug design. ADME-tox: absorption, distribution, metabolism, excretion and toxicity. (Scheme reproduced from M. Pellecchia, I. Bertini, D. Cowburn, C. Dalvit, E. Giralt, W. Jahnke, T. L. James, S. W. Homans, H. Kessler, C. Luchinat, B. Meyer, H. Oschkinat, J. Peng, H. Schwalbe, G. Siegal, *Nature Rev. Drug Discov.* **2008**, *7*, 738-745).

For biochemists ^{19}F NMR is a powerful technique for the study of protein structures and their dynamic behavior during reactions.[175] Fluorine labels are often located in critical regions of the target protein. One or more fluorine labels can be easily incorporated, either biosynthetically or chemically, into specific sites on a protein, where they provide a relatively non-perturbing yet sensitive probe with no background signals. Thereby the use of ^{19}F NMR can provide a wealth of information about the chemical environment, the local geometry, the dynamic behavior, or the three-dimensional architecture of a specific molecular site. The analysis of ^{19}F NMR chemical shift has been mostly used to probe the geometry and the kinetics of conformational changes.[176] This approach maps out the regions involved by observing which ^{19}F NMR resonances undergo chemical shift changes. As noted earlier, fluorine chemical shifts are extremely sensitive to changes in the local van der Waals environment and local electrostatic fields. The observation of a chemical shift change indicates that the protein environmental structure has been altered in the vicinity of the probe. Therefore important information emerges from this observation: whether a small molecule binds to a target protein, what parts of the small molecule were interacting and to which part of the macromolecular target the small molecule is bound. In fact, the extreme sensitivity of the ^{19}F chemical shift to its environment provides what is perhaps the most sensitive physical method available for detection of local conformational changes.

Beyond the structure elucidation of potential target, a specific ^{19}F NMR experiment can determine the binding affinity of a ligand to a receptor.[177] The competition ligand-based NMR screening technique named FAXS (Fluorine chemical shift Anisotropy and eXchange for Screening)[173] allows the screening of different ligands against the biomolecular target of interest, thus increasing the throughput. It is performed in the presence of a weak- to medium affinity ligand of known binding constant referred as the “spy molecule” (S signal) and a control fluorinated molecule (C signal) serving as internal reference (Scheme 3.2).

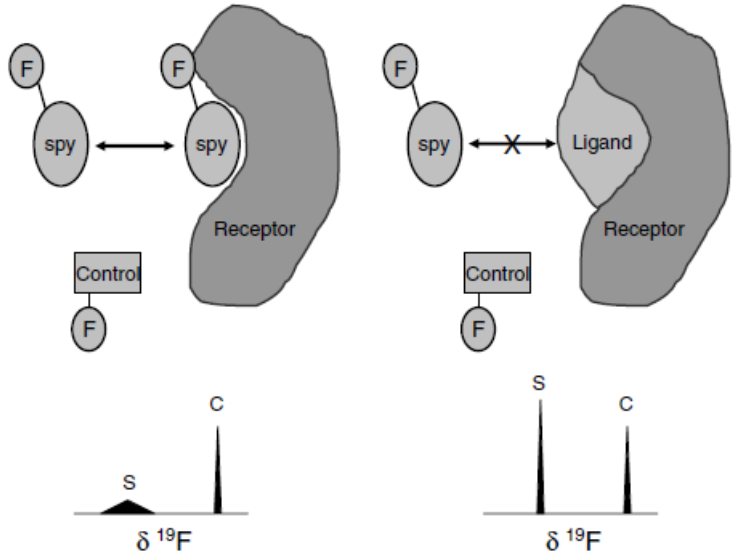

Scheme 3.2: Schematic diagram of the FAXS experiment. The broad signal of the spy molecule (S) becomes sharp in the presence of a competitive ligand due to the displacement from the receptor. The sharp signal of the control molecule (C) represents an internal reference. (Scheme reproduced from C. Dalvit, *Prog. Nucl. Magn. Reson. Spectrosc.* **2007**, *51*, 243-271).

Competition ligand-based NMR screening experiments are robust and result only in the identification of specific binding ligands. Non specific binders fail to displace the spy molecule and therefore are not detected. ^{19}F NMR can also be used in order to gain insights into the kinetics of the binding events in an enzymatic reaction. The FABS (Fluorine Atoms for Biochemical Screening)[173] experiment has been specifically designed for such a purpose (Scheme 3.3).

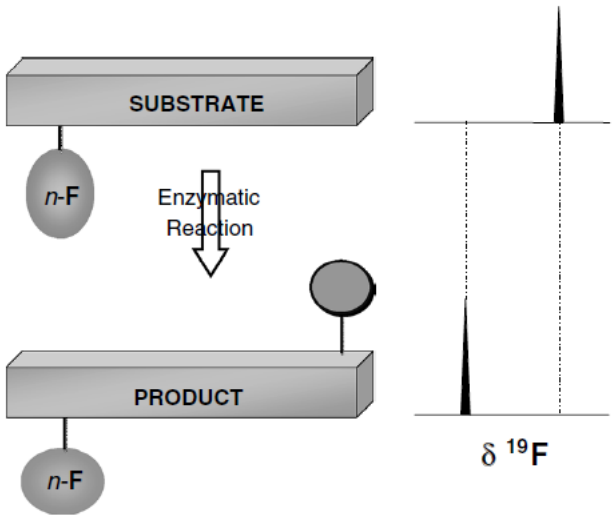

Scheme 3.3: The schematic principle of FABS experiment. n-F is the number of chemically equivalent fluorine labels used for the detection. (Scheme reproduced from C. Dalvit, *Prog. Nucl. Magn. Reson. Spectrosc.* **2007**, *51*, 243-271).

This approach requires the tagging of the substrate or cofactor with a fluorine moiety. Modification of the substrate through the enzymatic reaction changes the fluorine chemical shift even when the ^{19}F label is distant from the reaction site. Therefore distinct ^{19}F chemical shifts for the initial substrate and the product (or products) are observed. Analysis of the relative intensities of the ^{19}F resonances for the substrate and the different products allows the detection of inhibitors of the enzymatic cascade and the direct identification of the inhibited enzymes. Titration experiments on the individual products as a function of the substrate concentration provide a detailed insight into kinetics. The analysis of the data is straightforward since only the integrals of two signals have to be measured. Therefore FABS is used to determine the percentage of inhibition of the substrate with a given compound. For this purpose several experiments are recorded at different inhibitor concentration and the integral of the product or substrate ^{19}F resonance is measured.

The simplicity of the FABS experiment is particularly convenient in the hit to lead phase of a drug discovery project. The optimisation of potency, selectivity, metabolic stability and pharmacokinetic properties of compounds in development can be accurately evaluated. The challenge in these drug discovery approaches still remains the detection of the weakly active fragments. Both FAXS and FABS are particularly suited for fragment-based screening and dynamic library screening. In the fragment-based approach it is not the throughput that is most relevant but the possibility of detecting chemical scaffolds which in turn could be used for designing suitable pharmacophores.

Thanks to the reliability and reproducibility of these techniques, the fluorine NMR approach represents a powerful tool for performing screening against a biomolecular target. The precise quantification of the binding affinity and the percentage of inhibition for the different substrates allow the identification of meaningful structural motifs.

^{19}F MRS and MRI:

The advantageous properties of ^{19}F nucleus (high magnetogyric ratio, spin ½, 100% natural abundance) have encouraged the use of fluorine spectroscopy for applications in Magnetic Resonance Spectroscopy Imaging (usually denoted MRS, MRI or MRSI), a medical technique

which combines both spectroscopic and imaging methods.[178] This non-invasive technique produces spatially localised spectra within the sample or the patient, which can be later recombined to build a 3D model. The ^{19}F nucleus potentially represents an extremely interesting biomedical contrast agent and biomarker for *in vivo* MRSI. The use of fluorine as detectable MR tracer benefits from the lack of naturally occurring fluorinated background signals.

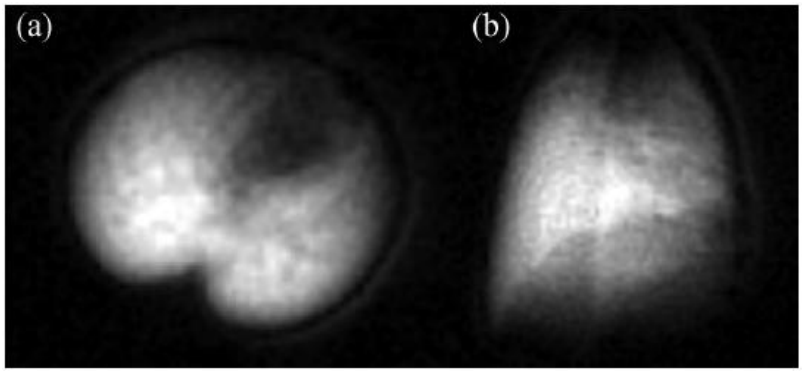

Figure 3.1: Post-mortem ^{19}F MRI of lung gas density using C_2F_6. Axial images (a) were acquired within 2 min and coronal images (b) were acquired within 3 min using a 4.7-T magnet. (Figure reproduced from J. Ruiz-Cabello, B. P. Barnett, P. A. Bottomley, J. W.M. Bulte, *NMR Biomed.* **2011**, *24*, 114-129).

MRI is mainly applied in drug design for preclinical or clinical research applications to monitor the local physiological environment of fluorinated drugs, their bio-distribution and pharmacokinetics *in vivo* and in excised tissues[179] (example of a 3D model in Figure 3.1). ^{19}F MRSI provides a highly specific tool for the investigation of metabolism by identifying and tracking the by-products that contain a fluorine atom. Under certain conditions, this technique is also potentially suitable for quantified analysis. However, as the detected signal obtained by this experiment is used to encode spatial and spectral information, the MRSI requires a high signal-to-noise ratio (SNR) to deliver an image of correct resolution. In ^{19}F MR, the limitations due to the relative low SNR remain a challenge. In order to obtain an acceptable resolution in imaging, the contrast agent needs to have a very high density of spectroscopically equivalent ^{19}F nuclei on the molecule and a highly localized concentration of the product. These findings promoted the use of perfluorinated molecules as biomarkers. The quantification is also complicated by technical difficulties associated with the use of fluorine. Even if a ^{1}H MRI scanner can be conveniently retuned to record ^{19}F data, the probe has a tendency to generate non-uniform excitation of fields. To remedy this inconvenience, adiabatic

frequency swept excitation pulses are used conjointly with the injection of a reference substrate of known concentration. Despite the difficulties currently encountered, ^{19}F MRSI still facilitates the understanding of the metabolic aspects and the cytotoxicity of fluorinated drugs.

3.2 Analytical tools for the structural and conformational study of fluorinated 5-membered rings:

As detailed in the previous sections, ^{19}F spectroscopy finds multiple applications in a wide range of fields. However conformational elucidation of small fluorinated molecules, particularly 5-membered rings, is rarely undertaken. For such analysis, researchers usually rely upon proton spectroscopy. The Karplus equation allows the determination of the dihedral angles through the measurement of the coupling constants. Internal distances can generally be evaluated using transient ^{1}H-^{1}H NOESY protocols. The analysis of these two parameters is often sufficient, under careful consideration, to build up a structural and conformational model of the molecule. As previously described in Chapter 1, the insertion of fluorine into 5-membered rings introduces a conformational bias which cannot be neglected. Yet it appears that the structural and conformational analysis of fluorinated heterocycles suffers from the absence of generalised methods relying on ^{19}F spectroscopy. The most important challenge at this stage would be to develop and combine different analytical tools to assess to which extent the fluorine can influence the ring puckering. In this context the potential for fluorine based NMR investigations is worthy consideration.

3.2.1 General aspects on the conformation of 5-membered rings:

The importance of the conformation of 5-membered ring puckers has been well established by the numerous examples reported in the literature regarding the folding of collagen[180] and DNA/RNA helices.[181] In both cases, the heterocyclic ring occupies a pivotal position as it is responsible for the backbone and the side chain strain. In order to identify or design new substrates featuring similar properties, it is essential to collect analytical data characterising the conformation of these 5-membered heterocycles. Therefore it is necessary to define an accurate description of the ring

conformation. Three characteristic parameters are of great importance: bond length, bond angle and most essentially the endocyclic torsion angles or dihedral angles. 5-Membered rings such as proline or ribose sugar very rarely exhibit a planar structure. For unsubstituted rings, a very large number of conformations are potentially available as the ring puckering can interconvert with low potential energy barriers. Broadly speaking, all these conformations can be depicted as belonging to two sub-categories: envelope (E) or twist (T).[182] Envelope conformations are characterised by the residency of four out five atoms in the same plane, while the fifth atom lying out of this plane by roughly ~0.5 Å. In twist conformations, two adjacent atoms are displayed on opposite sides of the plane defined by the three remaining atoms. As a whole, the different ring puckerings are distributed around the pseudorotational cycle as a function of the sum of all the endocyclic dihedral angles (Figure 3.2). This concept of pseudorotational cycle, originally developed to describe the nucleoside sugar ring, can be transposable to the study of other 5-membered heterocycles.

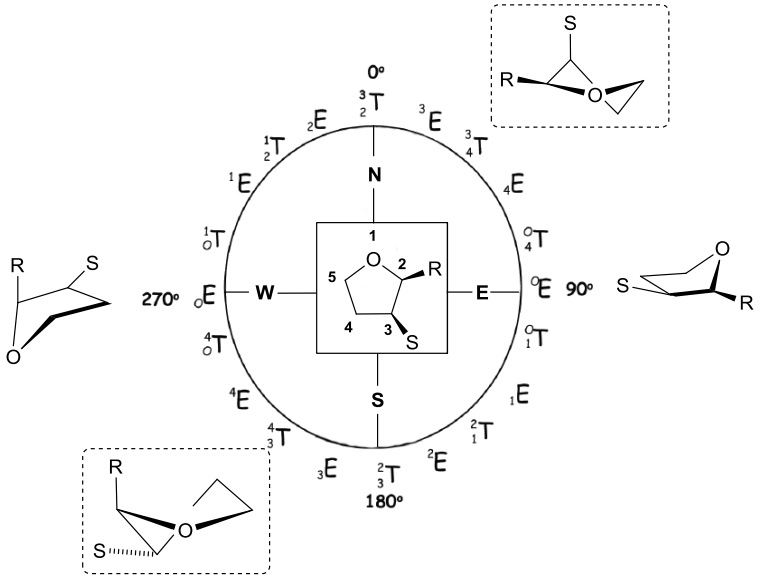

Figure 3.2: Pseudorotational cycle representative of the pseudorotational pathway of the substituted tetrahydrofurane ring. The cycle shows the relation between the sum of the endocyclic torsion angles and the conformation adopted (envelope (*E*) or twist (*T*)) by the ring puckering. Four poles (noth, east, south, and west) can be distinguished in the cycle, they mark to boundary of different sectors.

However in the case of rings, substituted by elements such as fluorine, which are capable of influencing on the ring conformation, one or two puckering modes are preferred.

Usually these modes are defined as N-type conformations, corresponding to the northern half (0±90°), and S-type corresponding to the southern half of the pseudorotational cycle (180±90°). Yet

a rapid survey of the literature reveals that several nomenclatures coexist. Indeed N-type and S-type conformations are sometimes referred as C$^{\gamma}$-exo and C$^{\gamma}$-endo respectively. These latter belong to a sub-group twisted conformation. This type of twisted ring possesses three adjacent atoms in a plane (C$^{\delta}$-N-C$^{\alpha}$ for the pyrrolidine, C$^{\delta}$-O-C$^{\alpha}$ for tetrahydrofuran) with one of the carbons above this plane and the other below it (referring as C$^{\gamma}$ and C$^{\beta}$). When C$^{\gamma}$ is placed above the plane, *syn* to the substituent borne by C$^{\alpha}$, the conformation is called C$^{\gamma}$-endo. Similarly the C$^{\gamma}$-exo conformation refers to C$^{\gamma}$ being placed below the ring mean plane.

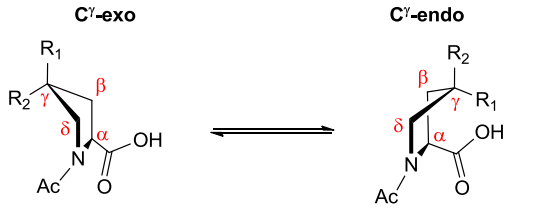

Figure 3.3: C$^{\gamma}$-exo/C$^{\gamma}$-endo conformation equilibrium exemplified with N-acetylproline substituted at the 4 position.

For more clarity, we will only refer to the C$^{\gamma}$-exo/C$^{\gamma}$-endo type of conformations for the rest of our analysis.

3.2.2 Previous structural and conformational analysis of fluorinated 5-membered rings:

Despite the presence of a fluorine atom as an analytical tool in 5-membered heterocycles, the conformational investigation of such structures has remained limited to a few examples. The aim of the comprehensive structural studies previously undertaken (discussed below) was to determine whether the fluorine input to the ring puckering was the result of *gauche* or other stereoelectronic interactions,[4,7,41] in addition to identifying the most stable conformation. For this purpose, a series of complementary experimental analyse were carried out on fluorinated prolines and nucleosides.

Analytical tools used for structural assignment:

Although these kinds of studies are relatively limited and scattered, they all rely on the same experimental techniques, namely: solid state analysis by the mean of crystallography, solution analysis involving various NMR experiments and computational methods. We do not intend here to

provide the reader with an exhaustive list of publications relating to the structural characterisation of 5-membered heterocycles. Only meaningful examples will be discussed.

As early as 1973, Gerig *et al.* reported one of the first studies devoted to the conformational analysis of *cis* and *trans*-4-fluoro-L-proline in aqueous solution.[183]

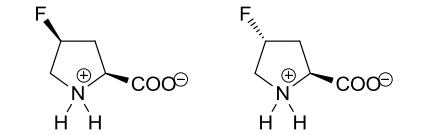

cis-4-fluoro-L-proline *trans*-4-fluoro-L-proline

Figure 3.4: Investigation of the conformation of *cis*- and *trans*-4-fluoro-L-proline in aqueous solution.

Although previous crystallographic determinations of analogous L-proline structures revealed the prevalence of a puckered ring,[184] it was not assumed that such a conformation would also prevail in the solution state. Special attention was drawn to the determination of vicinal $^{3}J_{\text{H-H}}$ and $^{3}J_{\text{F-H}}$ coupling constants which were extracted from computed theoretical spectra which best matched experimental spectra. The dependence of the dihedral angles on the vicinal coupling constant through the Karplus equation is a unique tool in conformational analysis.[185] However, the use of the Karplus equation requires the careful consideration of a number of parameters before applying it in a straightforward manner. It is very important to identify the parameters best adapted to the chemical structure and the type of vicinal coupling constants investigated. Indeed these coupling constants depend on several factors ranging from the dihedral angles between the coupled nuclei, their nature, the position of substituents and the changes in bond lengths and bond angles. In Gerig's study, Karplus coefficients were empirically determined to best fit the experimental data. Although the parameterisation may not be optimal to the substrate, the same equation has been applied to the two fluorinated prolines under consideration, the dihedral angles determined by this mean still have a semi-quantitative validity. Simultaneously computational analysis were carried out in which known parameters such as C-C bond length taken from the crystal structure were inputted to the calculations as constrains in order to generate a new conformational model. The process was iterated until it converged to one conformer whose computed coupling constants best fitted the experimental observations. In conclusion, the authors found that each compound existed as a single conformer

also in solution and that the dominant conformation favoured the pseudo axial positioning of the C-F bond. The *trans* isomer would therefore adopt a C$^{\gamma}$-exo envelope conformation while the *cis* isomer, a C$^{\gamma}$-endo. A similar study was conducted one year later on three different pyrimidine-2'-fluoro-2'-deoxyribonucleosides.[186]

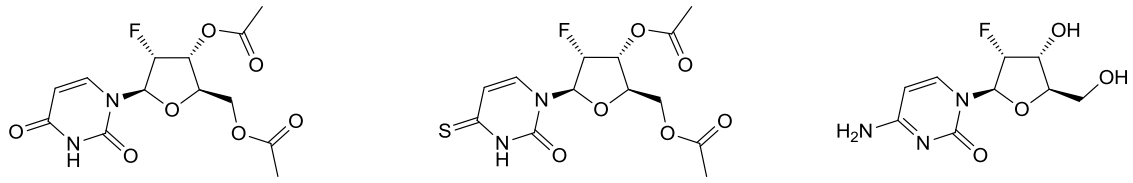

Figure 3.5: Investigation of the conformation of three different pyrimidine-2'-fluoro-2'-deoxyribonucleosides.

Analysis of the experimental NMR data (a study of vicinal coupling constants $^{3}J_{\text{H-H}}$ and $^{3}J_{\text{H-F}}$, followed by the deduction of the dihedral angles) came to the conclusion. Good agreement was found between the crystallographic data[187] and the solution state, thus strengthening the suggestion that the ring puckering might well be influenced by the nature of the substituent at the 2' position. More elaborated and refined conformational studies have emerged with the progress made in NMR apparatus and the steady development of more complex methods of calculation. Among those studies it is worth mentioning the work of Barchi on the conformational analysis of four different 2'- and 3'-monofluorinated dideoxyuridines.[188]

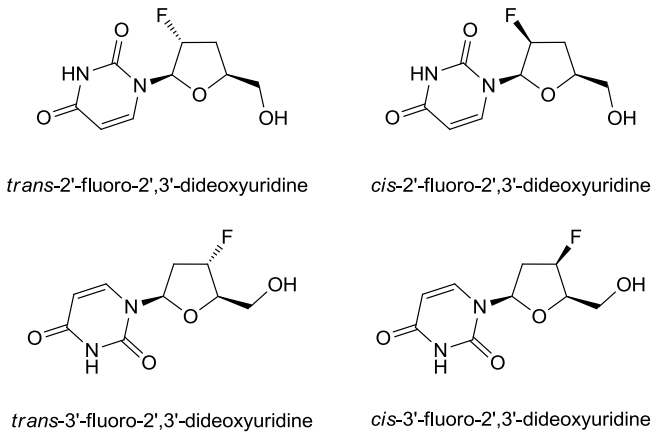

Figure 3.6: Investigation of the conformation of a series of four different 2'- and 3'- monofluorinated dideoxyuridines.

A series of NMR experiments were performed in combination molecular mechanics, *ab initio* calculations and pseudorotational analysis. The information generated by ^{1}H steady state nOes was

employed to confirm the assignment of ring protons resonances. Again, the study of vicinal coupling constants revealed itself critical. $^{3}J_{H\text{-}H}$ and $^{3}J_{H\text{-}F}$ were extracted from resolution enhanced 1D spectra and spectral simulations. These coupling constants were then converted to dihedral angles using an improved generalised Karplus-type equation. The modification of the electronegativity scale parameter within this type of equations usually ensures the adequacy of the results with the nature of coupled nuclei. It is important to mention at this stage that, the development of a new generalized Karplus-type equation relating vicinal $^{3}J_{H\text{-}F}$ coupling constants to H-C-C-F dihedral angles has become a topic in its own right. Noteworthy, San Fabian[189] and Chattopadhyaya[190] reported independently two similar articles in the space of few months on this subject. Both authors proposed a revised Karplus-type equation integrating correction terms for each substituent's electronegativity derived from an extended experimental data set. In agreement with the previous studies, the NMR data collected by Barchi *et al.* qualitatively determined that the fluorine atom governs the ring pucker conformation in order to adopt a pseudo-axial position. Molecular mechanics were then utilised to generate nucleosides conformer models which were in turn energy minimised using pre-defined ring torsion constraints. *Ab initio* calculations helped to measure the energy difference between the C^{γ}-exo/C^{γ}-endo local minima in order to assess the most stable conformation of each substrate. Computational calculations agreed with the experimental NMR data for three out of four nucleosides investigated. The authors invoked several reasons to justify the inadequacy between the computed results and the solution state analysis, among which an inappropriate choice of initial parameters was a factor. Overall this study revealed the effects of the fluorine on the ring conformation of nucleosides, particularly enlightening the dual forces being at stake in such molecules: the gauche interaction and the anomeric effect. Even if this study complements well the knowledge on conformational preference of fluorinated furanose-type substrates, the relationship between the fine tuning of the ring pucker and the presence of biological activity remains to be elucidated. It is in fact difficult to assess the quantitative effect of a fluorine substitution in a 5-membered heterocycles because of the absence of general libraries detailing the characteristic parameters for a representative series of analogous substrates. Further studies were undertaken on difluorinated nucleosides in attempt to rationalise how two fluorine atoms can affect nucleosides

conformation.[191] For this purpose X-ray crystallographic structures and solution state data were used together with theoretical calculations. Fluorinated prolines have also received significant interest. The work produced by Raines and co-workers, amongst other groups, on this topic came to the same conclusion.[50,51,53] The ring pucker of fluorinated 5-membered heterocycles is strongly influenced by the presence of the fluorine which imposes constraints on the endocyclic bond angles in order to maximise the number of *gauche* interactions.

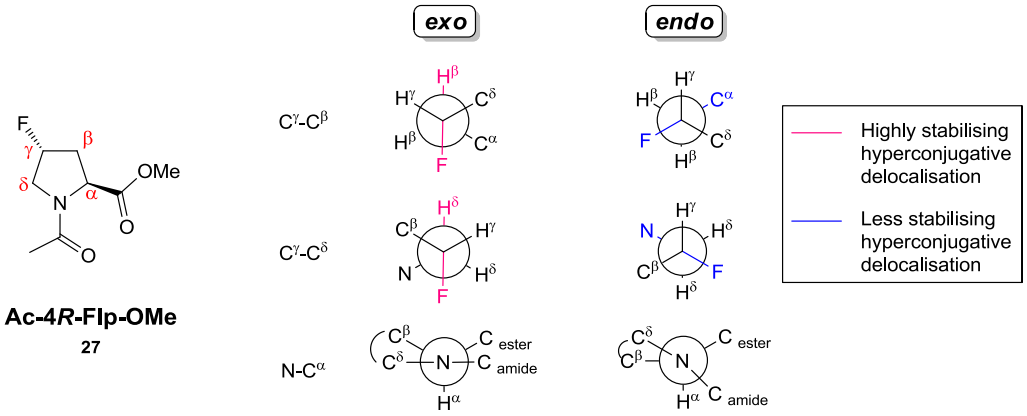

Figure 3.7: Newman projections about three bond axes illustrating the stereochemistry of the Ac-4*R*-Flp-OMe model compound in its *exo* and *endo* conformations. For simplicity, each dihedral angle is shown in its fully staggered conformation rather than its optimized geometry.

Potential drawbacks:

Despite the examples quoted above detailing the conformation of fluorinated 5-membered heterocycles, this topic remains very broad and therefore the information is scattered. Careful observations reveal that the analysis of NMR data does not provide extensive information regarding coupling constants. The major reason for this is that most of the studies undertaken rest on a limited set of molecules, reflecting a lack of representativeness for this class of compounds. In many cases, computer assisted conformational analysis and molecular modelling which have become extremely popular among synthetic chemists, have supplanted more traditional analytic investigation techniques. It is a fact that such computer assisted methods can yield qualitative and quantitative information such as the evaluation of the steric environment or the measurement of interatomic distances. However the sole creation of a model and its manipulation does not necessarily ensure the validity or the accuracy of the results. It is therefore imperative to find a good agreement with the acknowledged experimental data. This is why a greater importance should be given to NMR

spectroscopy techniques which would be more suitable for routine analysis. In this context, ^{19}F NMR seems to have been particularly under-estimated for its ability to provide information for such interesting topic. The development of a simpler method for data collection relying on ^{19}F NMR would be highly desirable. Such technique could potentially benefit synthetic chemists in a broad sense as the conformational analysis of a given class of substrates certainly will be of value for other classes as well.

3.3 Conformational analysis of fluorinated pyrrolidines using ^{19}F-^{1}H scalar couplings and heteronuclear nOes (HOESY):

3.3.1 A practical NMR technique for structural and conformational elucidations: the nOe

The Nuclear Overhauser Effect or nOe technique is an important tool in structural analysis where it plays a unique role.[192] It is mainly used to probe spatial geometry and distances, therefore it can reveal the 3D structure and conformation of molecules. NOes develop directly from through space magnetic interactions. Their origins come from the cross-relaxation of a spin I ("interesting") with a neighbouring saturated spin S ("source") via dipole-dipole coupling. The nOe interactions are characterised by the net change in signal intensities of the NMR resonances. NOe enhancements contain information on the distances between two spins. However their rates or efficiency depends on many factors, such as strength and frequency of the fluctuating fields, tumbling rate of the molecules, the viscosity of the solvent and the characteristics of the nuclei themselves. Only the internuclear separation of spins relatively "close" in space (up to 5 Å) can be evaluated as the effect of the nOe falls off rapidly as r^{-6} where r is the distance between the two nuclei. The ^{1}H-^{1}H nOe experiment is one of the most well-known techniques in structural elucidation, being used mainly qualitatively to determine the relative stereochemistry of molecules. However it can also be used quantitatively to enable the measurement of internuclear separations, although in this context the interpretation of nOe measurements requires great care.

The nOe technique itself can be divided in two types of experiments: those using the steady-state nOes such as the nOe difference technique and those using transient protocols such as the NOESY technique which can be either 2D or 1D.

The steady-state nOe:

In a two spin system I-S, I is the spin whose resonance is measured and S is the spin whose resonance is irradiated. The spin S is selectively saturated by a low power rf field that will not directly perturb the spin I. The irradiation is maintained for a time t that is much longer than the relaxation time of both spin S and I before acquiring the FID. Therefore the net magnetisation of the spin I reaches a steady-state value. The nOe difference spectrum is obtained by subtraction of the nOe enhancement spectrum (which contains the responses from the saturated resonance and from any nOe enhancements that exist) with the control 1D spectra obtained in absence of specific irradiation. This difference operation can generate artefacts. Indeed very small phase or frequency shifts between the two spectra will generate imperfect signal subtraction, along with artefacts arising from temperature instability, magnetic field drifts and short-term random instrumental instabilities. The accurate internuclear separation between two nuclei cannot be derived from the steady-state nOes measurement because they result from a balance between the influences of all the neighbouring spins. Only under suitable conditions, the growth rate of the nOes can be used to directly determine the distance between two spins.

The transient protocols 1D and 2D NOESY:

In the case of the transient protocol technique, the spin S is selectively irradiated by a very brief π pulse which leads to the inversion of population of this spin. The nOes are then allowed to develop in the absence of further external interference for a time τ_m or mixing time before the FID is acquired. During this mixing time two types of competing processes occur. To begin with, the cross-relaxation of the spins S and I creates the nOe enhancements then the spin autorelaxation tends to restore all intensities to their equilibrium values. Transient nOe experiments do not give as large nOe enhancements as steady-state experiments. Their advantage over the previously described technique

arises from the fact that transient nOes are not obtained by difference. The absence of subtraction means that much smaller nOes can be reliably interpreted. From a kinetic point of view, the nOe enhancements are seen to build up initially at a linear rate before ultimately fading away due to the spin autorelaxation process. This is in contrast to the steady-state where the spin S is continuously saturated, making the autorelaxation rate irrelevant. The domain called the initial rate approximation is defined when two cross-relaxing spins behaves as if they were an isolated spin pair and the transient nOes grow with a linear dependence on the mixing time. In this domain of validity, the nOe enhancements will depend on a single internuclear separation factor which makes the distance measurement accurate and possible. However the notion of single internuclear distance must be carefully interpreted. In reality the distance between two spins vary over time with the conformational mobility of the molecule. Depending on the exchange rate and the degree of flexibility of the substrate, it is likely that the internuclear separations calculated would represent an average distances weighted by the population percentage of each conformations. In general detailed structure calculations, based on quantitative distance measurements for flexible small molecules are rather rare. Yet if interpreted correctly under careful conditions, this experiment could be a powerful tool for structural and conformational elucidation.

3.3.2 Outline of the project:

Typically the conformation of small flexible cyclic molecules is governed by a balance of factors including stereoelectronic and steric effects. The introduction of a fluorine atom into conformationally flexible molecules such as pyrrolidines may impart a conformational bias whereby the "fluorine gauche effect" confers rigidity to the structure by establishing a gauche N-C-C-F arrangement as a result of hyperconjugative delocalization.[193] This stereoelectronic interaction, although comparatively weak (around 1 kcal.mol^{-1} [7]), strongly shifts the conformational equilibrium of the ring-pucker. For example, the influence of fluorine on the conformational preference of fluoroproline has shown a structural and thermal stability increase in collagen mimics as described in Chapter 1. In our study we wished to investigate the influence of fluorine as a conformation-directing element on the ring-puckering of a variety of 3-fluoro pyrrolidines and tetrahydrofurans

(Figure 3.8, the syntheses of which were described in the preceding chapter) in the solid-state, using single crystal X-ray analysis, and in the solution phase, using NMR spectroscopy supported by molecular modeling.

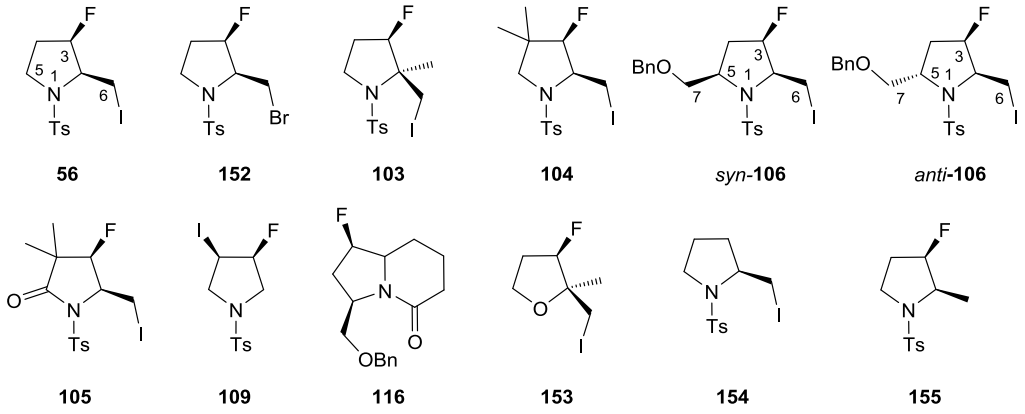

Figure 3.8: Structures of the fluorinated pyrrolidines and tetrahydrofuran considered in this study, illustrating the numbering scheme referred to in the text. For ring protons, the prime notation (H') is also used to indicate protons *cis* to the fluorine atom whilst for others this notation is used arbitrarily to differentiate diastereotopic geminal protons.

It is well known that the conformational analysis of saturated five-membered rings in solution is complicated by their inherent flexibility, and the interpretation of proton-proton scalar coupling constants (*J*) and nuclear Overhauser effects (nOes) is often challenging in such systems when attempting to define relative stereochemistry and/or conformation. The analyses described herein were conducted in collaboration with Dr. Tim Claridge, Dr. Barbara Odell and Phillip Clausen-Thue from the University of Oxford.[194] We wish to take advantage of the NMR active ^{19}F centre in the fluorinated compounds and gain additional conformational information derived from proton-fluorine coupling constants and heteronuclear nOes. We also describe 1D heteronuclear NOESY (1D-HOESY) sequences optimised for the observation of ^{19}F-^{1}H nOes in small molecules, which we find to be advantageous over traditional HOESY techniques. These techniques shall be described before discussing the conformations of the fluorinated compounds.

3.3.3. ^{19}F NMR HOESY methodology - Description of the new technique:

Our approach to the solution structural analysis of the fluorinated pyrrolidines described below was based on the typical use of scalar (*J*) coupling and nOe data with a particular focus on utilising the

fluorine atom as a reference in all compounds. We envisaged that the single ^{19}F centre in each structure could serve as a convenient and spectroscopically resolved target for probing internuclear separations through the observation of ^{19}F-^{1}H nOes. Such distances could be compared for those compounds for which crystal structures had been resolved and investigated in cases where the solid-state structures were unknown. Such information was augmented by analysis of ^{1}H-^{19}F and ^{1}H -^{1}H vicinal coupling constants through reference to appropriate Karplus-type dihedral angle relationships. In the case of heteronuclear fluorine couplings the equations of San Fabián *et al*[189] were employed and for homonuclear proton couplings those of Haasnoot-de Leeuw-Altona equation-expanded (chemical group) were utilised,[195] as implemented in the MestreJ graphical tool.[196]

Despite recent spectrometer hardware developments, many ^{19}F-^{1}H nOe experiments reported in the literature still utilise the traditional 2D HOESY experiment[197] to observe these interactions, although this is far from being the optimum approach in many cases. A classical experiment demands a long acquisition time to obtain a good quality well-resolved spectrum. The standard approach towards this type of experiment consists in choosing whether to detect ^{1}H or ^{19}F directly while the other nuclide will be indirectly detected. Since both nuclei have nearly the same sensitivity, the choice of direct detection will be determined by the level of resolution obtained. Direct ^{19}F detection is usually taken as the default choice since it has a much wider spectral width. We began our investigation by the direct detection of fluorine on the F2 (horizontal) axis and the indirect detection of proton on the F1 (vertical) axis of the 2D spectrum as documented for the classical 2D HOESY experiment.[197] Noteworthy the F2 axis has a higher digital resolution than the indirectly detected F1 axis. In this first attempt only the single proton decoupled ^{19}F resonance was observed, leading unfortunately to a poor ^{1}H resolution in the “indirect” dimension. Indeed on the 2D spectra four undefined contour plots could be distinguished, providing a relatively poor reading of the spatial interactions (Figure 3.9).

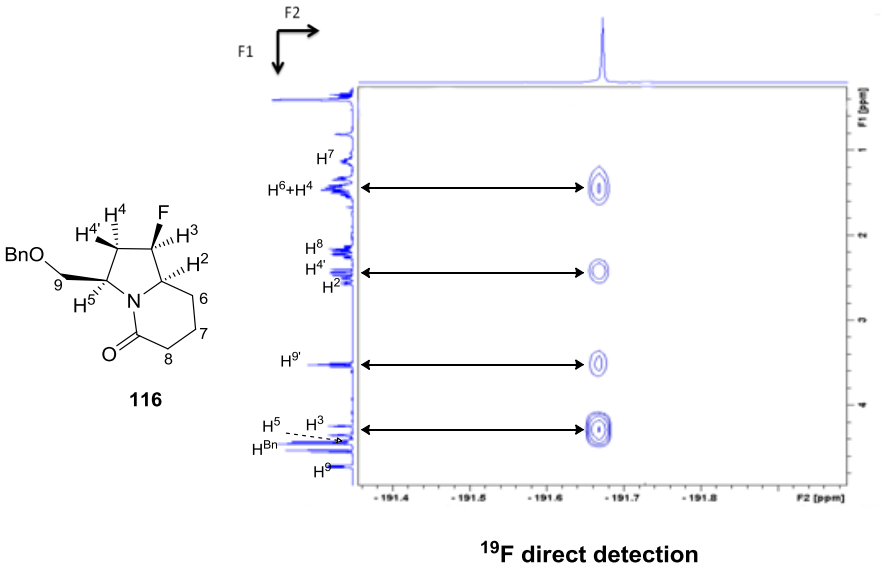

Figure 3.9: 2D HOESY spectrum with ^{19}F direct detection and ^{1}H direct detection. On the spectrum above, the average resolution allows the visualisation of four correlations.

With only a single ^{19}F centre in any compound under investigation, it is advantageous to invert the mode of detection so that a greater resolution is obtained for the ^{1}H spectrum. For the "inverse" 2D approach employing ^{1}H observation on the F2 axis, the resolution was significantly improved (Figure 3.10). The use of the coupled fluorine resonance on the F1 axis led to the refinement of the contour plots. Six interactions could then be observed, linking with great accuracy the protons resonances involved (Figure 3.10). In comparison to the Figure 3.9, the doublet corresponding to H^3 is resolved in Figure 3.10. In the same manner H^6 and H^4, which led to a single plot in Figure 3.9, were resolved separately in Figure 3.10.

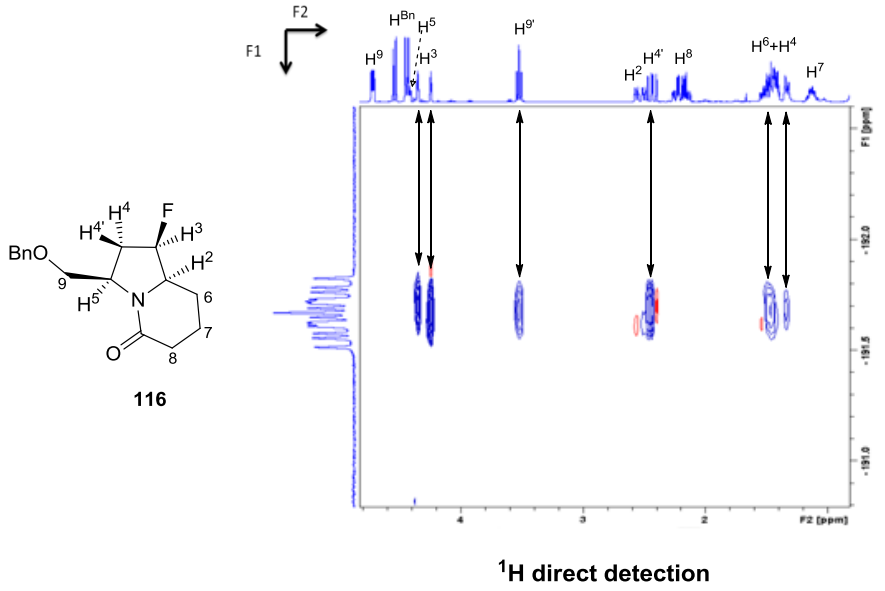

Figure 3.10: 2D HOESY spectra with ^{19}F indirect detection and ^{1}H direct detection. On the spectrum above, higher resolution allows for the visualisation of more correlations.

However in the present case, as the indirect frequency dimension contains only a single fluorine resonance, there would be no need to collect full 2D data sets. A optimum approach in such cases is to employ a ^{1}H observe heteronuclear one dimension (1D) nOe or NOESY experiment which is time efficient and provides high proton resolution. Moreover with the presence of only one well defined fluorine resonance, it might be worth considering the alternative use of a ^{19}F-selective 1D nOe experiment. For the present study we needed a robust and clean 1D HOESY experiment that would be suitable for the generation of nOe build-up curves from which quantitative distance estimates could be extracted. In fact, there exist very few nOe methods described specifically for ^{19}F since most heteronuclear nOe sequences have been tailored for low-abundance heteronuclides,[198] and are largely focused on 2D methodology which are overly elaborate for our needs. After some experimental investigation we derived what was found to be an optimal 1D gradient selected NOESY sequence that itself was derived from the work of Gerig,[199] whose investigations targeted the observation of ^{19}F nOes specifically in ^{19}F labelled biological macromolecules. The sequence used herein is shown in Figure 3.11 a), together with a selective variant suitable for use when multiple ^{19}F sites exist within the target molecule, or when a few fluorinated compounds exist in a mixture such that the full 2D HOESY is still deemed unnecessary.

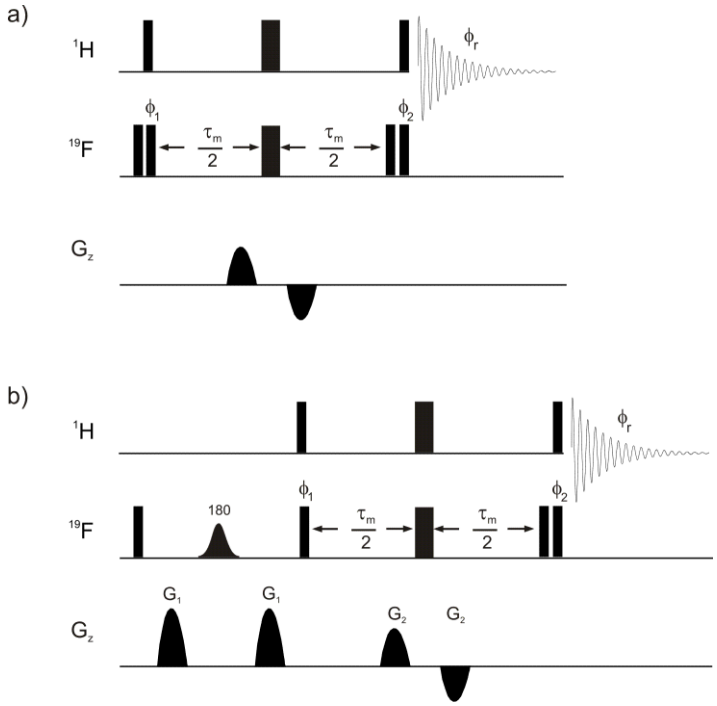

Figure 3.11: ^{19}F-^{1}H 1D HOESY sequences. **a**) Non-selective version and **b**) ^{19}F selective version. Narrow and wide bars represent 90^o and 180^o pulses respectively and G_z are shaped z-axis field gradient pulses. In (b) the shaped 180^o pulse is a selective inversion pulse applied to the target ^{1}H-coupled ^{19}F resonance. Phase cycling follows: Φ_1 = x, -x; Φ_2= x, x, -x, -x and Φ_r = x, -x, x, -x, with all other phases as x. Gradients are employed as a bipolar pair for purging during the mixing times (τ_m) and in (b) also as a gradient selective spin-echo where G_1:G_2 = 1.5:4. In practice, due to instrument limitations, it may not be possible to pulse simultaneously on both ^{1}H and ^{19}F channels, in which case it is possible to offset these pulses to operate sequentially, without detriment, to enable necessary changes in internal signal routing.

This gave clean 1D HOESY spectra exhibiting only nOes originating from the ^{19}F centre (Figure 3.12), so proved very effective at deriving nOe build-up profiles (Figure 3.13).

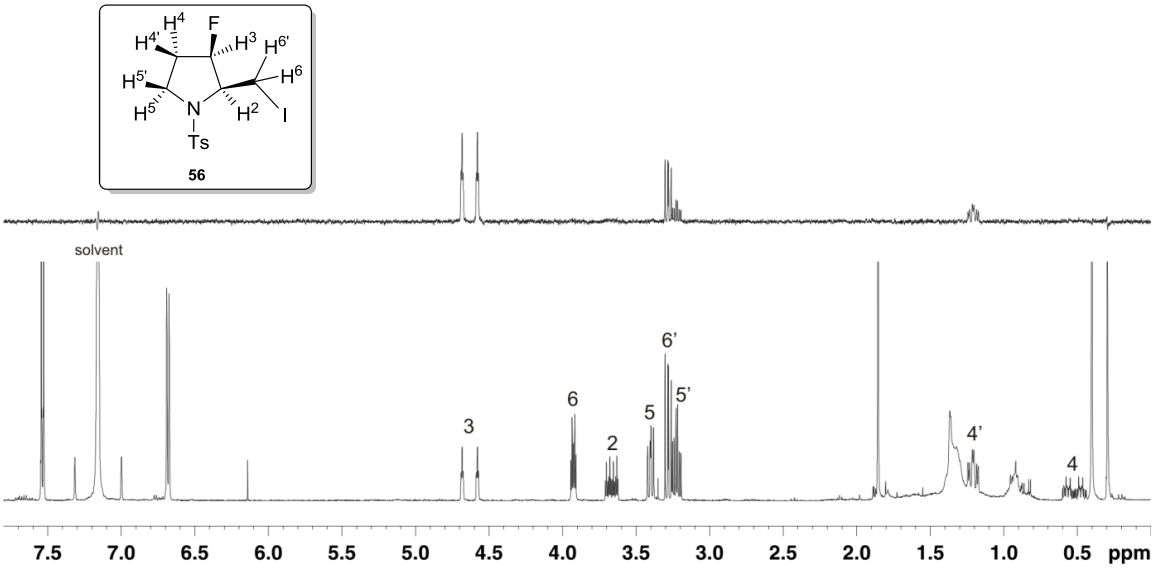

Figure 3.12: A 1D ^{19}F-^{1}H HOESY spectrum of compound **56** (Figure 3.8) in C_6D_6 recorded with the sequence of Figure 3.11 a) (mixing time, τ_m, 500 ms) shown above the reference 1D ^{1}H spectrum.

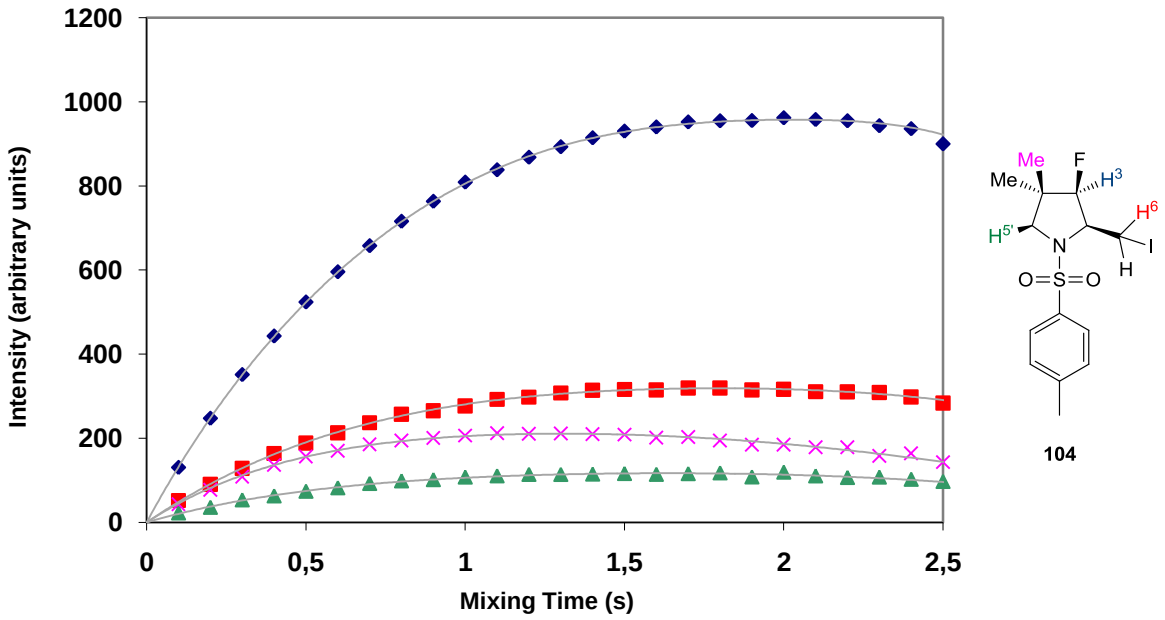

Figure 3.13: Example ^{19}F-^{1}H nOe build-up profile for compound **104** (*Grey lines provide a guide to the eye);* The fluorine centre serves as the source and nOes are observed onto neighbouring protons. Data were generated with the sequence of Figure 3.11a.

The basis of the sequence is the inversion of ^{19}F (through the combined action of the first two fluorine 90^{o} pulses) that allows the generation of the ^{19}F-^{1}H nOes through cross-relaxation during the mixing (nOe build-up) time τ_m, combined with purging of initial proton magnetisation through the ^{1}H (90^{o}) and bi-polar gradient combination. The 180^{o} pulses at the midpoint of the mixing time serve to maintain close to zero any longitudinal proton magnetisation generated through spin-relaxation during this period, as widely employed in proton 1D gradient NOESY sequences,[200] but allows the heteronuclear nOe to develop. This is subsequently observed with the final 90^{o} proton read pulse. The bipolar gradient pair also serves to purge any transverse magnetisation components arising from imperfect inversion pulses (note that as these gradients are not used for coherence selection there is no signal loss associated with molecular diffusion for this sequence). Any residual magnetisation generated from proton relaxation that is not completely nulled is cancelled on a second transient. Here, the phase of the first two 90^{o} fluorine pulses act such that no inversion of fluorine spins is present and thus no nOes develop. Subtraction of these two data sets leads to the desired cancellation of unwanted proton magnetisation and yields clean heteronuclear nOe spectra. We find that the use of additional gradient purge pulses during the mixing time does not improve the quality of nOe

spectra recorded. However, we do find that the use of a pair of additional fluorine purge pulses at the end of the mixing time leads to improvement in the authenticity of the multiplet structures through the removal of deleterious anti-phase contributions that can arise for ^{1}H-^{19}F coupled spins that also share an nOe, a relatively common occurrence in small fluorinated molecules. This pulse pair acts as ^{19}F inversion pulse applied on alternate transients (effectively $180^{o}_{\text{off-on}}$) and serves to alternately invert the sign of the anti-phase terms, leading to their cancellation through co-addition of data sets.[198b] Although this additional purging is optional, the minimal increase in phase-cycling required for this is not considered problematic since many transients are typically necessary to yield adequate signal-to-noise ratio for most samples of interest and will readily accommodate this extension. Hence, its use is recommended for small-molecule nOe measurements. In the ^{19}F-selective variant (Figure 3.11b) a single ^{19}F PFG spin-echo (90^{o}-G_1-180^{o}(sel)-G_1-) is employed to selectively excite the target fluorine resonance and to destroy all others, after which the sequence follows that of the non-selective variant. Here the fluorine inversion pulse acts on the *proton-coupled* resonance and the effective bandwidth must be set accordingly.

Estimates of ^{1}H-^{19}F internuclear separations were made through comparison of nOe relative intensities at short mixing time with those observed between proton-fluorine pairs of known internuclear distance using the isolated spin-pair (initial rate) approximation and assuming isotropic molecular tumbling occurs in solution (Figure 3.13). In all cases, the reference was taken as the geminal F-H distance of 1.97 Å, as determined from the available crystal structure data. Distances were then calculated as

$$r_{HF} = r_{HF(ref)} \left(\frac{I_{HF}}{I_{HF(ref)}} \right)^{-1/6}$$

r_{HF} : internuclear distance between the fluorine and the proton under consideration (Å)

$r_{HF(ref)}$: internuclear geminal F-H distance taken as reference (1.97 Å)

I_{HF}: experimental nOe intensity of the proton under consideration

$I_{HF(ref)}$: experimental nOe intensity of the geminal proton taken as reference

where r_{HF} is the distance to be determined, $r_{HF(ref)}$ the known geminal distance and I_{HF} and $I_{HF(ref)}$ the corresponding experimental nOe intensities. For all compounds studied, heteronuclear nOe build-up curves were recorded to identify the region in which the initial-rate approximation was valid. nOe intensities were then recorded from additional 1D HOESY spectra recorded with many transients for enhanced signal-to-noise ratio; for all compounds a mixing time of 500 ms was found to be within the linear build-up regime and produced significant nOe enhancements suitable for quantification. The application of this methodology is considered as part of the solution phase analysis together with the observation of the coupling constants. However, the analysis of the crystallographic data was firstly considered and is described below.

3.3.4 Solid-state crystallographic analysis:

Investigations into the structure and conformational preferences of the fluorinated pyrrolidines were first undertaken by consideration of their structures in the solid-state. This work was conducted in collaboration with Dr. Amber Thompson from the University of Oxford. The highly electronegative nature of the fluorine atom was anticipated to impart a substantial stereoelectronic influence on the conformations of these ring systems. For example, it has been widely reported that when proline is substituted with electronegative groups on the β or the γ position the pyrrolidine ring adopts, preferentially, two extreme conformations denoted C$^{\gamma}$-exo or C$^{\gamma}$-endo (Figure 3.14). The electronegativity of the substituent plays an important role in the distortion of the ring; the more electronegative the element, the more constrained the conformation.

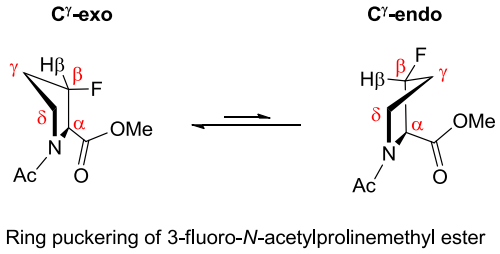

Figure 3.14: C$^{\gamma}$-exo/C$^{\gamma}$-endo conformational equilibrium of the 3-fluoro-N-acetylprolinemethyl ester ring puckering.

In the practical case of 3-fluoro-*N*-acetylprolinemethylester, the C$^{\gamma}$-exo conformation was enforced when the fluorine and the methylester substitutent were in *syn* relationship to each other.[201]

According to the thermodynamic parameters calculated at 25°C in D_2O and DFT studies, this conformation was found to be the most favored.[202]

As part of our study, compounds **56, 152, 103, 104**, *syn,syn*-**106**, **105** and **109** were available for single crystal X-ray analysis[203] (Figure 3.8; *syn,anti*-**106**, **116**, **153** and **155** could not be crystallized) and all demonstrated a C$^{\gamma}$-exo ring pucker conformation with the fluorine atom occupying a "pseudoaxial" position (Figure 3.15).

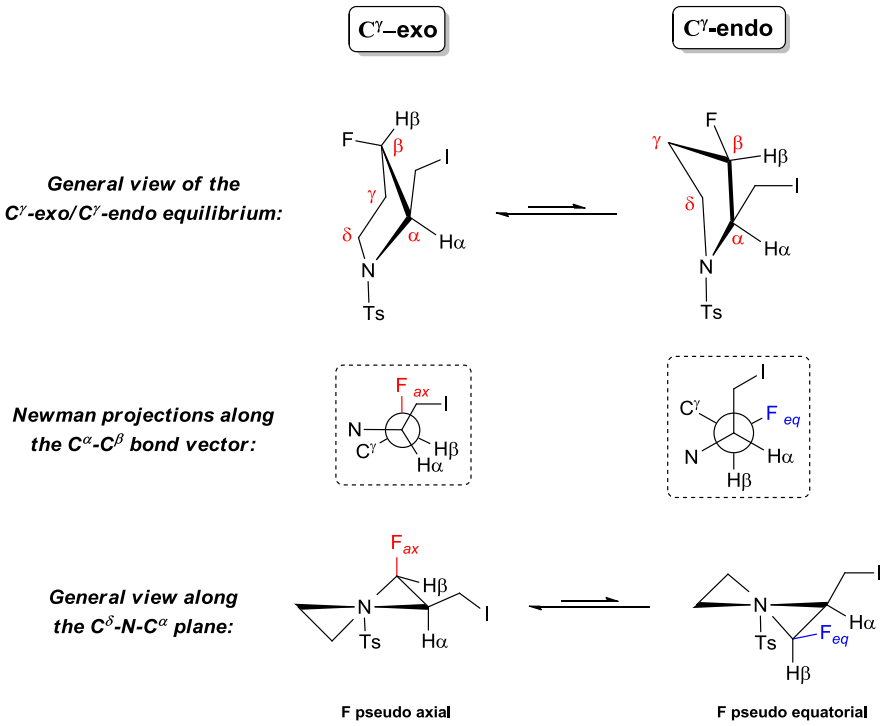

Figure 3.15: Schematic illustration of the C$^{\gamma}$-exo/ C$^{\gamma}$-endo equilibrium for the compound **56**.

The crystallographic structural data available for **56, 152, 103, 104,** *syn,syn*-**106** further indicate that in all cases there is a *trans* configuration between the *N*-tosyl and the iodomethyl substituent, thus avoiding steric clash of the two substituents. These key conformational features may be exemplified through consideration of compound **56** (Figure 3.16).

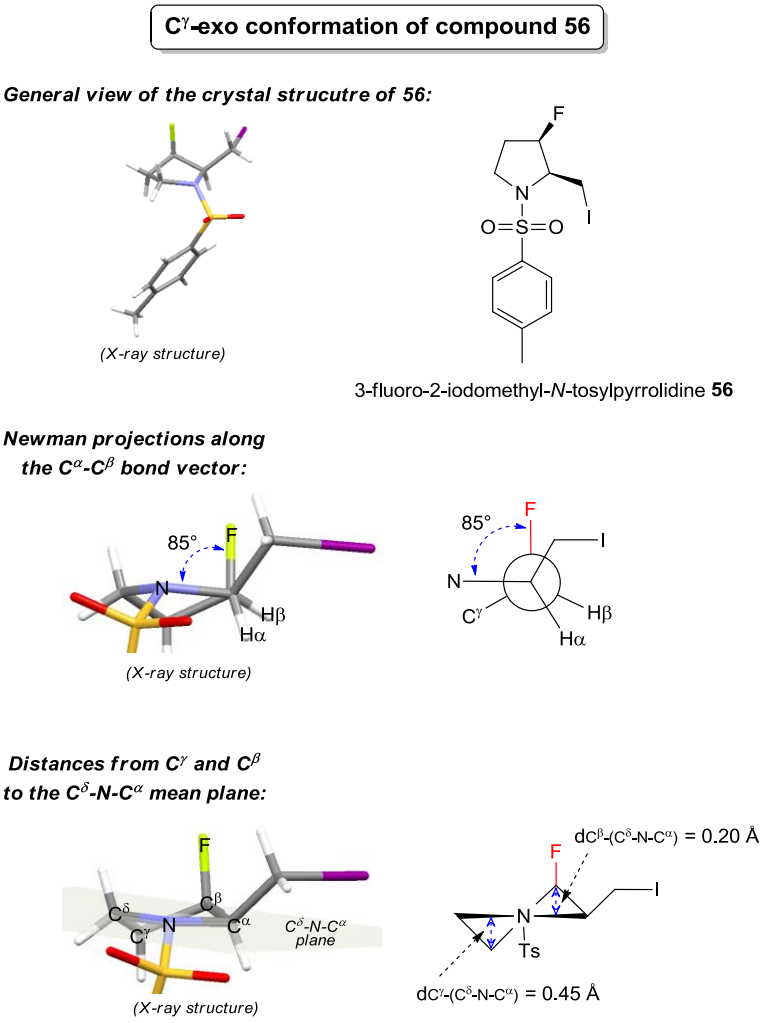

Figure 3.16: Single crystal X-ray structures of **56**; Measurement of the N-C$^{\alpha}$-C$^{\beta}$-F dihedral angle and distances from C$^{\beta}$ and C$^{\gamma}$ to the C$^{\delta}$-N-C$^{\alpha}$ mean plane.

Compound **56** shows a characteristic value for the dihedral angle N-C$^{\alpha}$-C$^{\beta}$-F of 85° indicating a gauche arrangement between the vicinal fluorine and the N-C$^{\alpha}$ bond arising from hyperconjugative delocalisation. As explained previously this "gauche effect" is caused by the donation of electron density from the bonding $\sigma_{C\alpha\text{-}H}$ molecular orbital to the low-lying electron-accepting $\sigma^*_{C\beta\text{-}F}$ molecular orbital through an antiperiplanar relationship that serves to maximize the stabilization of this geometry.[7,32] The extent of ring pucker in the pyrrolidines can be illustrated by calculating the distance of C$^{\beta}$ and C$^{\gamma}$ from the mean plane C$^{\delta}$-N-C$^{\alpha}$ and the corresponding data for compounds **56, 152, 103, 104,** *syn,syn*-**106** are presented in Table 3.2 (see Appendix for detailed crystallographic data). This data illustrates similar solid-state ring conformations for these compounds in the series that are dominated by the fluorine gauche effect, with only minor variations in the degree of pucker.

Likewise in 3-fluoroproline **156**[201] the displacement of C^{β} from the mean plane C^{δ}-N-C^{α} is relatively small and the N-C^{α}-C^{β}-F angle close to 90° (Figure 3.17).

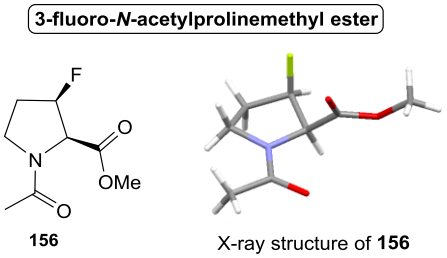

Figure 3.17: The single crystal structure of 3-fluoro-*N*-acetylprolinemethyl ester **156** exhibits similar characteristic as the crystal structure of compound **56**.

The small C^{β} displacement can be rationalized for the compounds reported herein by a steric clash between the fluorine and the bulky iodomethyl group in a "pseudoequatorial" position. The short non-bonding distance between the fluorine atom and the hydrogen of the iodomethyl substituent H^6 for example in **56** ($d_{F\text{-}H}$= 2.42 Å) is less than the sum of the corresponding van der Waals radii (2.67Å). For compound **56** the distance between F-$H^{5'}$ (2.64 Å) may also be considered a close contact comparable to weak van der Waals interactions in energy terms, although insufficient to account for the stabilisation of the observed ring conformation (Figure 3.18).[204]

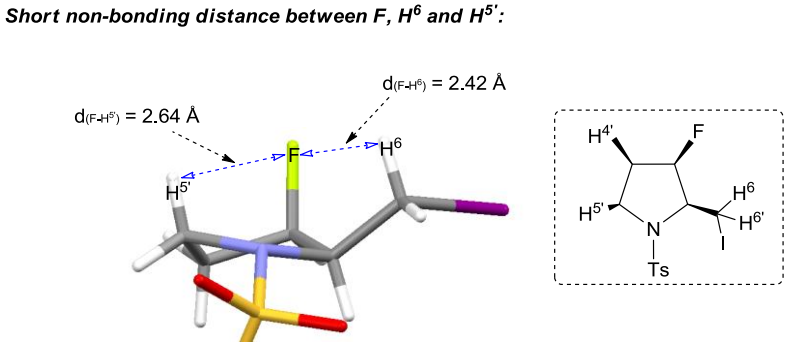

Figure 3.18: Short non-bonding distances between fluorine, H^6 and $H^{5'}$. Here the prime notation (H') is used to indicate proton *cis* to the fluorine.

Compound **109** is atypical in this series presenting a value for the dihedral angle N-C^{α}-C^{β}-F of 103°, indicative of a distorted envelope conformation rather than a gauche arrangement (Figure 3.19 and Table 3.2). Here, the iodine atom occupies an equatorial position, likely due to its bulkiness. In this peculiar conformation both C^{γ} and C^{β} atoms are placed below the mean plane of the pyrrolidine ring, while the fluorine remains in an axial position. It is also unusual in that the tosyl group is oriented on

the same side as the iodine and the fluorine atoms, presumably due to the lack of an adjacent iodomethyl substituent in **109**.

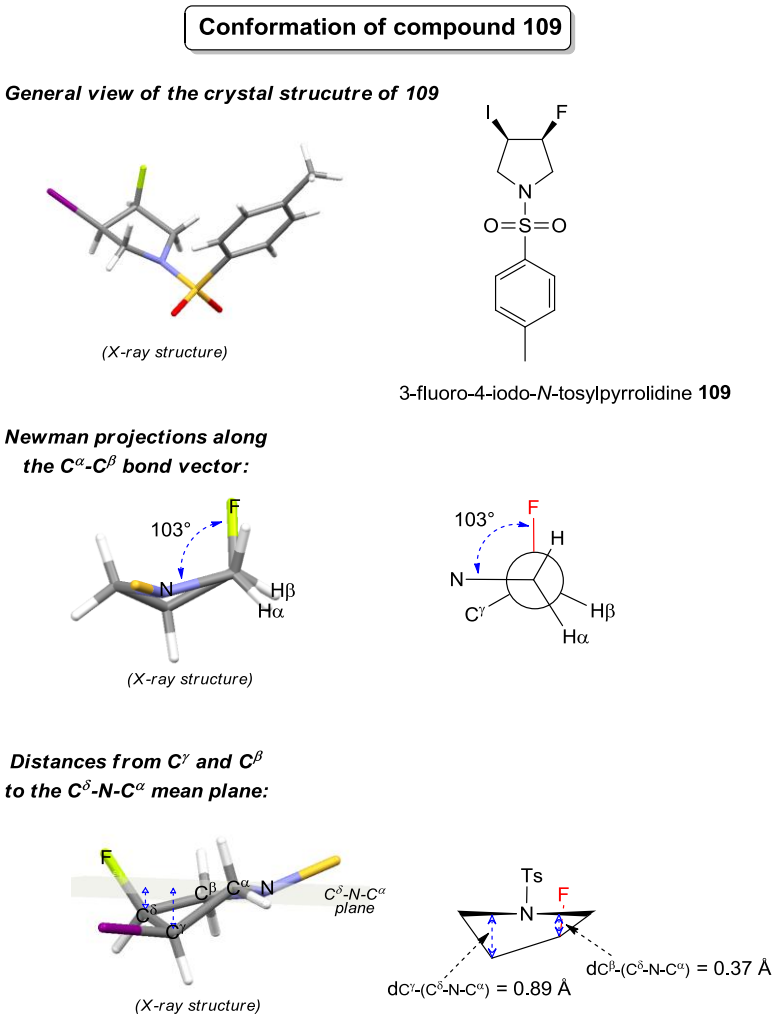

Figure 3.19: Single crystal X-ray structures of **109**; Measurement of the N-C$^{\alpha}$-C$^{\beta}$-F dihedral angle and distances from C$^{\beta}$ and C$^{\gamma}$ to the C$^{\delta}$-N-C$^{\alpha}$ mean plane. For clarity purposes, the tosyl group has been omitted in some representations of the crystal structure.

In contrast to structures **56, 152, 103, 104,** *syn*,*syn*-**106**, the non-fluorinated pyrrolidine **154** previously reported in the literature,[205] exhibits an "envelope" conformation in the solid state where four atoms of the ring (N-C$^{\alpha}$-C$^{\beta}$-C$^{\delta}$) belong to the same plane, highlighting further the influence of the fluorine gauche effect (Figure 3.20).

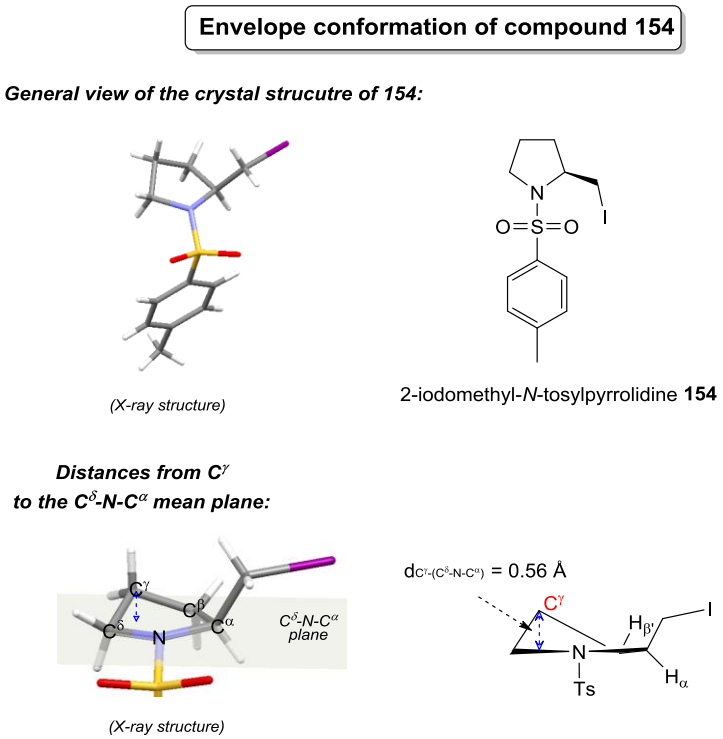

Figure 3.20: Single crystal X-ray structures of the non-fluorinated pyrrolidine **154**; Measurement of the distance from C^{γ} to the C^{δ}-N-C^{α} mean plane. Compound **154** adopts an evelope conformation where four atoms belong are contained inside the same plane.

Compound	56	151	103	104	*syn-syn*-**106**	109[a]	154[b; 205]	156[201]
N-C^{α}-C^{β}-F dihedral angle (°)	85	87	83	84	89	103	144	91
Distance from C^{β} to the mean plane C^{δ}-N-C^{α} (Å)	0.21	0.15	0.31	0.29	0.25	0.36	0	0.11
Distance from C^{γ} to the mean plane C^{δ}-N-C^{α} (Å)	0.44	0.47	0.33	0.34	0.30	0.8	0.56	0.460

Table 3.2: Characterization of the ring puckering observed in the solid state structures. [a] Compound **109** presents a conformation where C^{β} and C^{γ} reside on the same side of the mean plane C^{δ}-N-C^{α}; [b] Compound **154** adopts an "envelope" conformation, the dihedral angle refers to the N-C^{α}-C^{β}-$H^{3'}$ angle.

3.3.5 Solution phase NMR analysis:

An analysis of the solution phase conformations of the fluorinated pyrrolidines was undertaken to determine whether the conformational preferences observed in the solid state structures persisted in solution. These analyses focused principally on the scalar couplings and nOes observed for the series, as translated to torsion angles and internuclear distances respectively. Experiments were conducted at room temperature with sample concentrations ranging from 3 to 7 mg of compound per

tube (0.6 mL). The need for a high resolution spectrum and a solvent whose residual chemical shift would not interfere with the resonances of interest ($\delta(C_6H_6)$ = 7.16 in ^{1}H spectra), led us to consider the use of benzene-d_6. Indeed benzene has a relatively low viscosity which does not hinder the resolution and provides a sharp lock signal useful for accurate assignment of an internal reference. Moreover due to magnetic anisotropy exhibited by this aromatic solvent, the compound proton resonances are spread over a larger range of chemical shift. This effect leads to a better separation of the signals with improved multiplet resolution which is useful in 1D experiment such as nOe that uses selective excitation of a specific resonance. The deuterated solvent was not degassed prior to the experiments. Selected vicinal ^3J (^{1}H-^{1}H) and ^3J (^{19}F-^{1}H) coupling constants for compounds **56, 152, 103, 104,** *syn,syn*-**106,** *syn,anti*-**106, 105, 109, 116, 153, 154, 155** are summarised in Tables 3.3 and 3.4, together with the corresponding dihedral angles as determined from the relevant Karplus-type equations.[189,206] Across the series the data show considerable similarities, with the notable exceptions of *syn,anti*-**106** and **109** only, which are considered separately below. A description of **56** is again representative of the principle features observed across the series (Figure 3.21).

Thus, the predicted values for the F-C$^\beta$-C$^\gamma$-H^4 (*trans*) and F-C$^\beta$-C$^\gamma$-H$^{4'}$ (*cis*) torsion angles matched closely the angles seen in X-ray analysis and are consistent with the fluorine atom occupying a pseudoaxial position in a C$^\gamma$ exo conformation. Of note across the series (excepting *syn,anti*-**106** and **109**) are the unusually large values (in excess of 40 Hz) of the F-C$^\beta$-C$^\gamma$-H^4 (*trans*) coupling constants, themselves indicative of a predominantly *anti*- relationship between these atoms. Furthermore, dihedral angles deduced from the ^3J (^{1}H-^{1}H) coupling constants were in good agreement with the values observed in the solid state structures (Table 3.4), providing additional evidence for the fluorine gauche effect dictating the solution conformations.

Compound 56: Comparison between the dihedral angles deduced from NMR coupling constants and those extracted from the X-ray structure

^3J (F-H) coupling constants and corresponding dihedral angles:

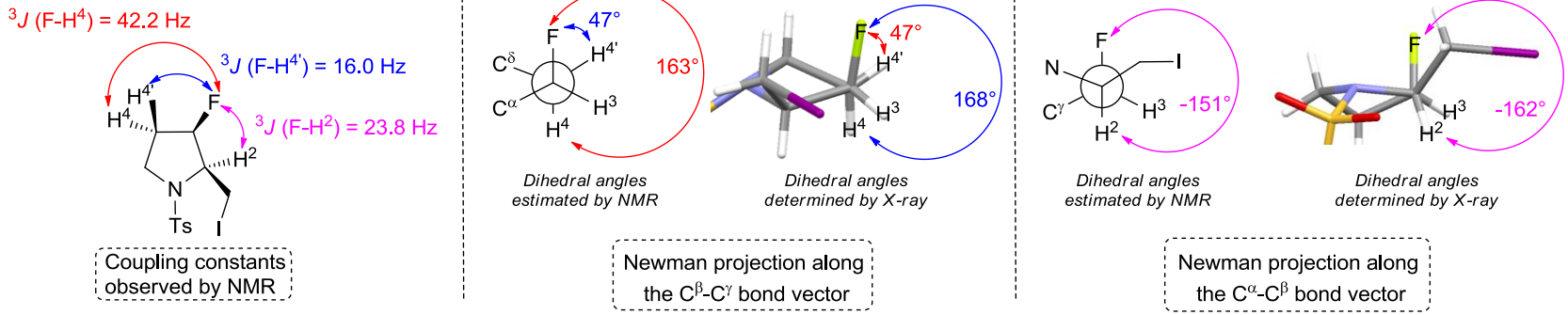

^3J (H^3-H) coupling constants and corresponding dihedral angles:

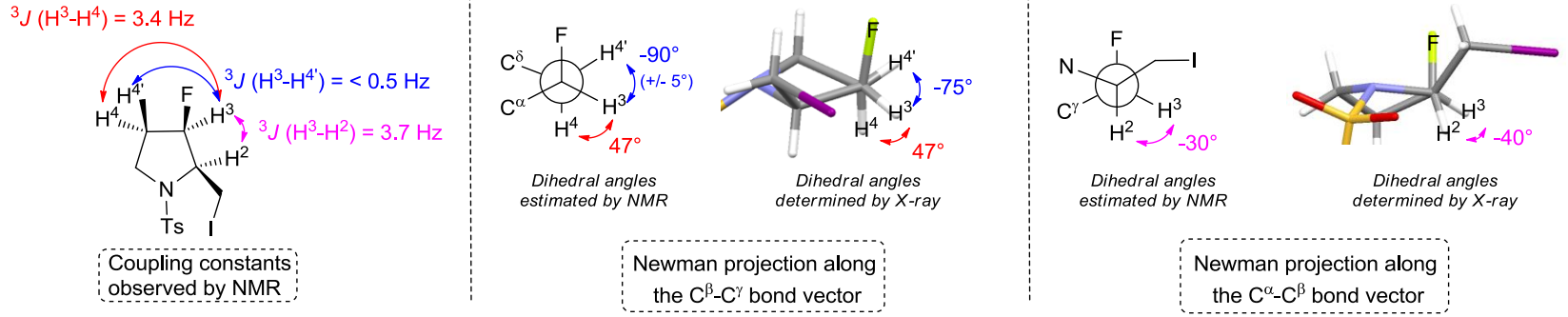

Figure 3.21: Comparison between the dihedral angles deduced from NMR coupling constants and those extracted from the X-ray strucutre.

Given the apparent consistency in structures between the solution and solid states it was also of interest to determine internuclear separations for the solution conformations for comparison with those in crystal structures (Figure 3.22). As described above, these were determined from heteronuclear nOe intensities, as summarized in Table 3.5. Once again, where crystal structures were available the solution distances were in good agreement. For example, in compounds **56, 152, 103** and **104** the F-H$^{5'}$ distances were ~ 2.7 Å, which are consistent only with the C$^{\gamma}$-exo ring conformations. This distance would average 4.4 Å for the corresponding C$^{\gamma}$-endo model obtained from molecular mechanics calculations.

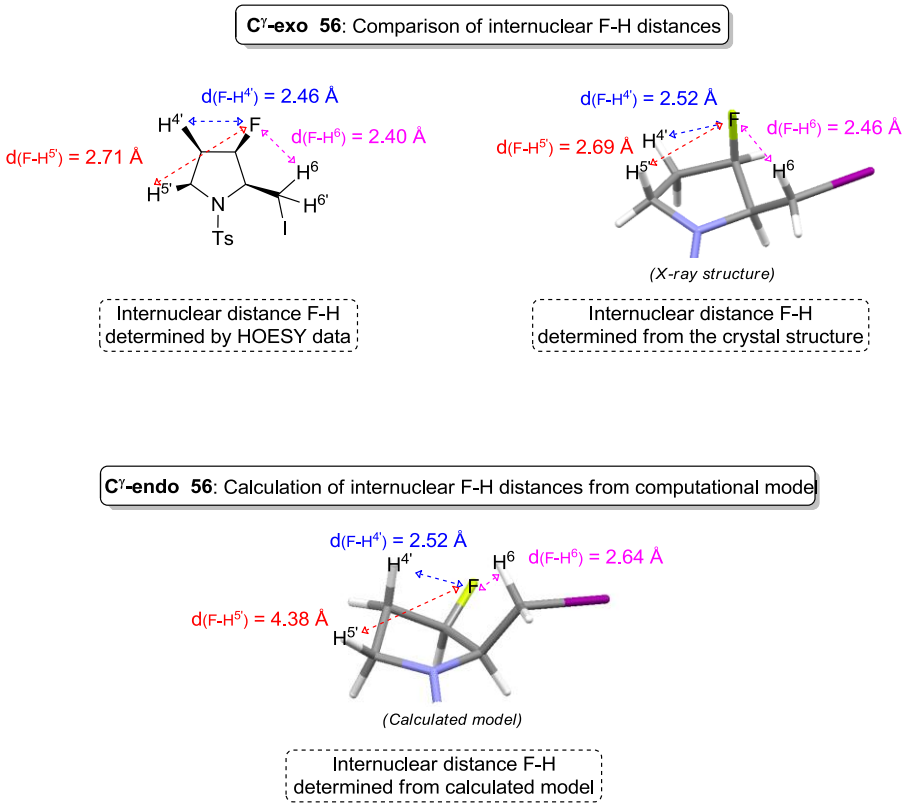

Figure 3.22: *C$^{\gamma}$-exo conformation of compound **56***: Comparison between the internuclear F-H distances determined from the crystal structure data and from HOESY data (H^6 refers to the proton closest in space from the fluorine); *C$^{\gamma}$-endo conformation of compound **56***: Internuclear distances extracted from calculated model.

Taken together, the NMR data indicate that compounds **56, 152, 103, 104,** *syn*,*syn*-**106, 105, 116, 153,** and **155** adopt in solution the C$^{\gamma}$-exo conformation observed in the available crystal structures. The dihedral angle and internuclear separation data for these structures is also suggestive of this ring conformation being persistent in solution with no evidence of conformational averaging of the ring pucker. It is also noteworthy that the nOe data for compounds **56, 152, 103, 104,** *syn*,*syn*-**106**

suggests that the orientation of the iodomethyl group to be conformationally fixed and similar to that observed in the corresponding crystal structures, where the bulky iodo group sits away from the pyrrolidine ring. Specifically, only one proton of the geminal pair H^6 and $H^{6'}$ received an nOe from the adjacent fluorine and in all cases the NMR derived F-H^6 distance matched closely that observed for the crystal (Table 3.5).

To further explore the observed C^{γ}-exo preference we undertook the conformational analysis of **56 (**as a representative example of the series) in collaboration with Dr. Mike King (UCB Pharma). Molecular dynamics computations were utilised, carried out using the Sybyl program,[207] with the Tripos implementation of the MMFF94 molecular mechanics force field.[208] Initial molecular models for each compound were energy minimised (convergence criterion: RMS energy gradient < 0.001 kcal/mol/Å), and used as starting points for *in vacuo* molecular dynamics simulations at an effective temperature of 2500 K. A total of 500 samples were extracted from each dynamics trajectory with a time interval of 1ps between samples. The sampled structures were then energy minimised, and structural duplicates removed (match criterion: heavy atom RMSD < 0.2 Å). The final set of unique minimum-energy conformers was then sorted according to calculated energy. For the compound **56**, these calculations generated a random array of 25 energetically distinct structures in the gas phase which could be broadly classified as the C^{γ}-exo/fluorine axial and C^{γ}-endo/fluorine equatorial conformations. According to moleculer mechanics, the conformer of lowest energy features a C^{γ}-exo conformation, which is in agreement with the experimental observations. Calculations confirm that this conformation is preferred by 3.3 kcal.mol^{-1} over the C^{γ}-endo/fluorine equatorial conformation. In comparison, *ab-initio* HF/3-21G(*) calculations (carried out using the Spartan '08 program[209]) gave a difference in energy of 1.8 kcal.mol^{-1} which is in closer agreement with the commonly accepted value of 0.5-0.9 kcal.mol^{-1} for fluorine gauche stabilisation (in 1,2-difluoroethane).[4,7] Thus, although calculations suggest a relatively small energy difference between C^{γ}-exo/C^{γ}-endo conformations for **56**, the NMR and solid state experimental data strongly favour the presence of one dominant conformation, namely C^{γ}-exo. This conformation is not only the lowest in energy but also the most populated. Indeed within a range of 5 kcal.mol^{-1}, 15 of the 25 conformers (58 %) generated by calculations have a C^{γ}-exo conformation. Likewise, experimental data for

compounds **56, 152, 103, 104,** *syn*,*syn*-**106, 105, 116, 153,** and **155** are consistent with the fluorine being constrained by a *gauche* interaction in relation to the *N*-tosyl group, thus stabilizing the C^{γ}-exo conformation.

Compound	$^3JF\text{-}H^2$ (Hz)	Φ (F-C^β-C^α-H2) (NMR)	Φ (F-C^β-C^α-H2) (X-Ray)	$^3JF\text{-}H^4$ (*trans*) (Hz)	Φ (F-C^β-C^γ-H^4) (NMR)	Φ (F-C^β-C^γ-H^4) (X-Ray)	$^3JF\text{-}H^{4'}$ (*cis*) (Hz)	Φ (F-C^β-C^γ-$H^{4'}$) (NMR)	Φ (F-C^β-C^γ-$H^{4'}$) (X-Ray)
56	23.8	-151	-162	42.2	163	168	16	47	47
152	23.2	-150	-155	42	162	167	14.9	49	45
103	NA[a]	NA	NA	43.2	167	166	18.4	41	46
104	25.1	-155	-156	NA	NA	NA	NA	NA	NA
syn,syn-**106**	22.8	-149	-154	45.1	177	160	18.8	41	40
syn,anti-**106**	15.4	-108	NX[b]	21.5	123	NX	23.6	30	NX
105	22.4	-148	NX	NA	NA	NA	NA	NA	NA
109	35.9	-150	-137	29.3	146	164	NA	NA	NA
116	29.5	-168	NX	44.1	173	NX	19.5	39	NX
153	NA	NA	NA	39	154	NX	234	30	NX
155	24.3	-153	NX	36.3	149	NX	19.9	38	NX

[a] NA = no proton present; [b] NX = no X-ray structure available.

Table 3.3: $^3J_{\text{F-H}}$ coupling constants and corresponding dihedral angles Φ (°) estimated from Karplus parameterization.[189,206]

Compound	$^3JH^3\text{-}H^2$ (Hz)	Φ (H^3-C^β-C^α-H^2) (NMR)	Φ (H^3-C^β-C^α-H^2) (X-Ray)	$^3JH^3\text{-}H^4$ (*cis*) (Hz)	Φ (H^3-C^β-C^γ-H^4) (NMR)	Φ (H^3-C^β-C^γ-H^4) (X-Ray)	$^3JH^3\text{-}H^{4'}$ (*trans*) (Hz)	Φ (H^3-C^β-C^γ-$H^{4'}$) (NMR)	Φ (H^3-C^β-C^γ-$H^{4'}$) (X-Ray)
56	3.7	-30	-40	3.4	47	47	<0.5	-90 ± 5	-75
152	3.7	-38	-34	3.4	47	45	<0.5	-90 ± 5	-77
103	NA	NA	NA	3.3	48	46	0.8	-76	-73
104	3.4	-41	-39	NA	NA	NA	NA	NA	NA
syn,syn-**106**	4	-36	-32	4.1	43	39	<0.5	-90 ± 5	-81
syn,anti-**106**	5.1	-27	NX	6	31	NX	5.2	-46	NX
105	3.8	-38	NX	NA	NA	NA	NA	NA	NA
109	3.7	-40	-15	3.2	47	41	NA	NA	NA
116	3	-44	NX	3	50	NX	<0.5	-90 ± 5	NX
153	NA	NA	NA	4.5	41	NX	1.1	-75	NX
155	4.4	-33	NX	2.5	60	NX	<0.5	-90 ± 5	NX

Table 3.4: Selected $^3J_{\text{H-H}}$ coupling constants and corresponding dihedral angles Φ (°) estimated from Karplus parameterization.[195,196]

Compound	d F-H^{2} (*trans*)		d F-H$^{2'}$ (*cis*)		d F-H^{4} (*trans*)		d F-H$^{4'}$ (*cis*)		d F-H$^{5'}$ (*cis*)		d F-H^{6} (*near*)		d F-H$^{6'}$ (*far*)		d F-H^{7} (*near*)	
	NMR	XRAY	NMR	XRAY	NMR	XRAY	NMR	XRAY	NMR	XRAY	NMR	XRAY	NMR	XRAY	NMR	XRAY
56	/[a]	3.25	NA	NA	/	3.22	2.46	2.52	2.71	2.64	2.40	2.42	/	3.70	/	/
152	/	3.17	NA	NA	/	3.17	2.46	2.48	2.72	2.70	2.42	2.43	/	3.66	/	/
103	NA[b]	NA	NA	NA	/	3.20	2.55	2.47	2.77	2.74	2.40	2.36	/	3.62	/	/
104	/	3.17	NA	NA	/	3.87[d]	2.42[e]	2.42[d]	2.74	2.77	2.34	2.32	/	3.66	/	/
syn,syn-**106**	/	3.15	NA	NA	/	3.18	2.57	2.46	NA	NA	2.45	2.36	/	3.62	2.55	2.52
syn,anti-**106**	3.20	NX[c]	NA	NA	2.48	NX	3.14	NX	3.26	NX	2.60	NX	2.94	NX	/	NX
105	/	NX	NA	NA	/	NX	2.41[e]	NX	NA	NA	2.33	NX	/	NX	/	NX
109	/	3.10	2.36	2.35	/	3.19	NA	NA	2.74	2.80	NA	NA	NA	NA	NA	NA
116	3.25	NX	NA	NA	2.41	NX	2.49	NX	NA	NA	2.97	NX	/	NX	2.54	NX
153	3.34[e]	NX	NA	NA	/	NX	2.30	NX	2.88	NX	2.40	NX	2.57	NX	/	NX
155	/	NX	NA	NA	/	NX	2.56	NX	2.85	NX	2.45[e]	NX	NA	NA	/	/

[a] NA = no proton present; [b] NX = no X-ray structure; [c] / = no nOe observed; [d] F-H distance to nearest methyl proton in crystal structure; [e] nOe averaged F-H distance for methyl group protons

Table 3.5: Internuclear ^{19}F-^{1}H distances (d/ Å) determined from crystal structure data (XRAY) or from heteronuclear nOe data (NMR).

In contrast to the data for compounds **56, 152, 103, 104,** *syn,syn*-**106, 105, 116, 153, 154** and **155** those for *syn,anti*-**106** and **109** indicate different conformational behaviour in solution and thus warrant further consideration (Tables 3.3-3.5). Due to the absence of X-ray data for *syn,anti*-**106** (the compound is an oil), much reliance was placed on the solution NMR data. Diastereoisomer *syn,anti*-**106** differed from *syn,syn*-**106** only by inversion at C^{δ}, and displayed very different *J* values (Figure 3.23); notably the $^{3}J_{\text{F-H2}}$ (15.4 Hz) and $^{3}J_{\text{F-H4}}$ (21.5 Hz) coupling constants of *syn,anti*-**106** were much lower than the value of its corresponding diastereoisomer *syn,syn*-**106** (22.8 Hz and 45.1 Hz respectively), whereas $^{3}J_{\text{F-H4'}}$ was slightly higher with a value of 23.6 Hz versus 18.8 Hz seen in *syn,syn*-**106**. Also noteworthy, *syn,anti*-**106** exhibited a value of 5.2 Hz for the $^{3}J_{\text{H3-H4'}}$ compared with ~0 Hz in most of the other compounds examined.

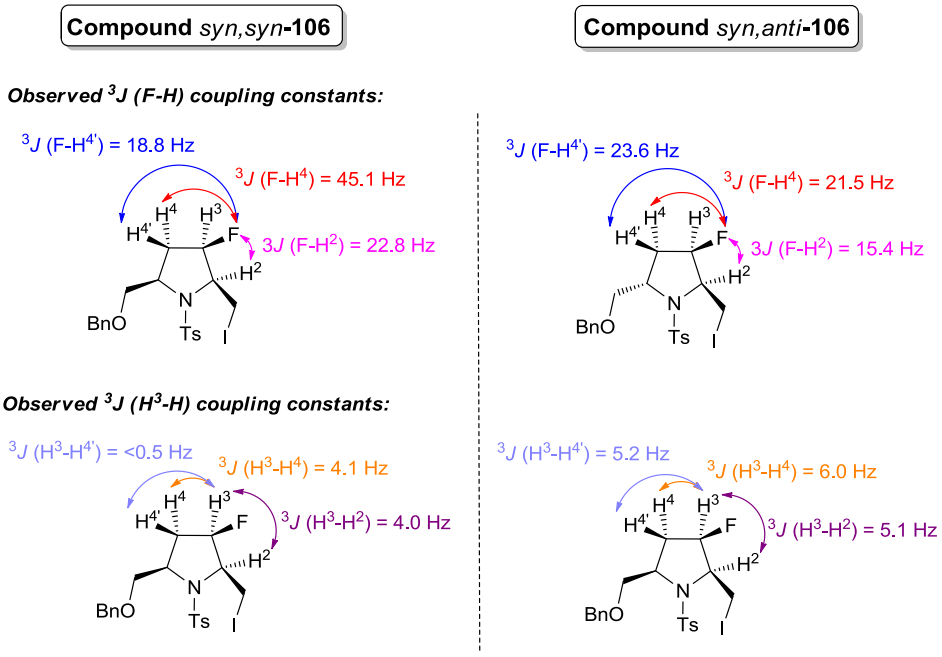

Figure 3.23: Comparison between the coupling constants observed in *syn,syn*-**106** (left) and *syn,anti*-**106** (right).

Likewise, the ^{19}F-^{1}H nOe derived distances were substantially different for *syn,anti*-**106**, as evidenced by the observation of significant F-H^2 and F-H^4 nOes and the greater F-$H^{5'}$ averaged distance. These combined observations suggested that the conformation of *syn,anti*-**106** was less rigid than that of *syn,syn*-**106** and was likely able to adopt the C^{γ}-endo conformation. This suggestion was initially investigated through molecular mechanics calculations which for *syn,syn*-**106** generated 143 conformers which clustered into the two distinct categories of C^{γ}-exo and C^{γ}-

endo. The structure of lowest energy, C^{γ}-exo/ fluorine axial, which represented half of the conformers obtained by calculation in a range of 10 kcal.mol^{-1}, corresponds closely to the conformation elucidated from crystallographic analysis (Figure 3.24). 2.8 kcal.mol^{-1} separates the two lowest energy conformers for each form.

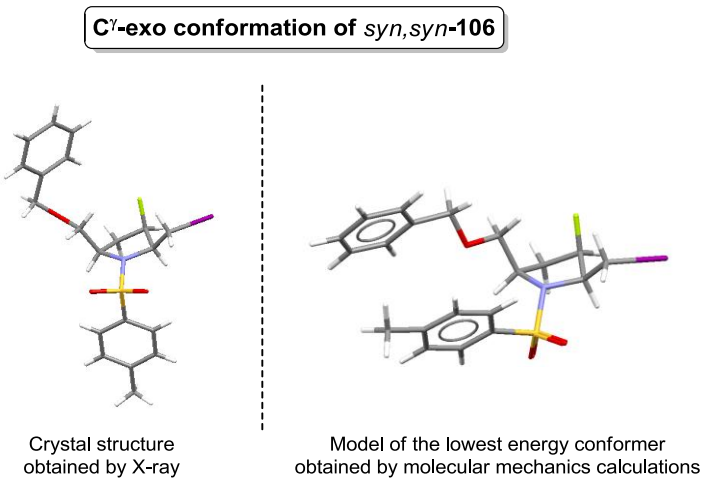

Figure 3.24: Single crystal X-ray structure of *syn,syn*-**106** (left) and lowest energy conformer model of *syn,syn*-**106** (right).

The same computational procedure applied to *syn,anti*-**106** yielded 182 different conformers which also were distributed in two main conformations C^{γ}-exo/ C^{γ}-endo. The C^{γ}-exo form representing 63% of the ensemble of conformers generated within a range of 10 kcal.mol^{-1}. However the difference in energy between the two lowest energy conformers of each type, was calculated to be negligible and within calculation errors (0.008 kcal/mol) (Figure 3.24). These observations suggest that interconversion between the two conformations might be readily achievable; a rapid conformational exchange would also be consistent with the observed NMR data (see below). The stacking between the two aromatic rings observed in the lowest energy conformation models is likely an artefact of the molecular mechanics calculations since gas phase structures *in vacuo* tend to optimise intramolecular interactions. In order to investigate experimentally the role of the possible π-π stacking in solution, compound *syn,anti*-**106** was examined in two different solvents CD_2Cl_2 and C_6D_6 and the *J* coupling constants of the pyrrolidine ring were compared. C_6D_6 used to compete with any π-π stacking that may change the ring conformation No evidence for such changes in coupling constants was found in function of the solvent π character.

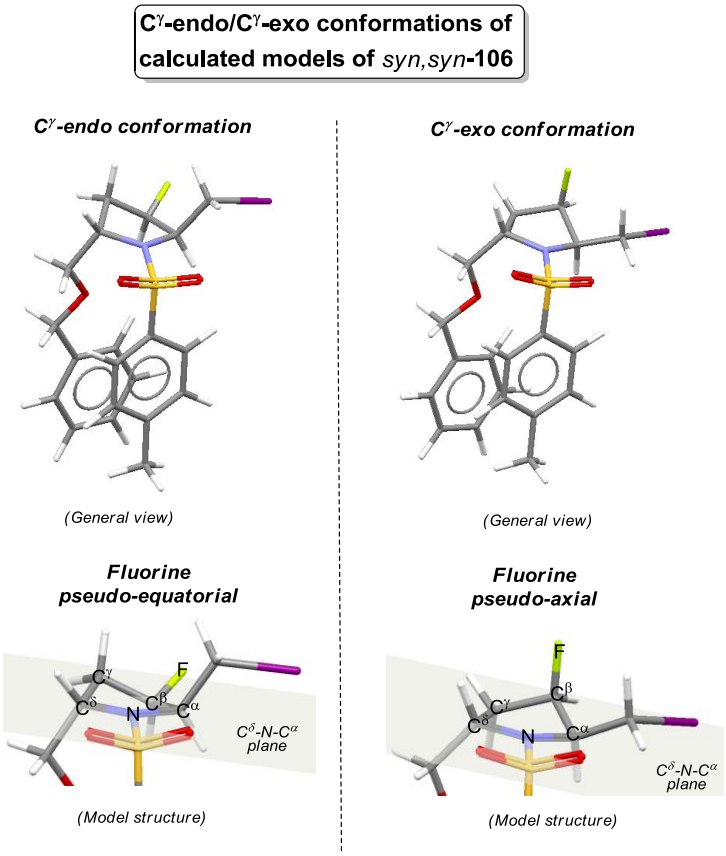

Figure 3.25: Calculated models of C$^{\gamma}$-endo/ fluorine equatorial of *syn,anti*-**106** (left) and C$^{\gamma}$-exo/ fluorine axial of *syn,anti*-**106** (right).

To explore the conformational equilibrium further, a series of low temperature NMR experiments of compound *syn,anti*-**106** were recorded over the range 298 to 183 K. For technical reasons, CD_2Cl_2 was chosen as solvent due to its lower melting point which allows conducting NMR experiments at very low temperature. In both ^{1}H and ^{19}F spectra resonance broadening was observed as temperature decreased, consistent with the onset of slower conformational exchange (Figure 3.26 and 3.27). Whilst it is clear the conformational behaviour of *syn,anti*-**106** varies across the temperature range reflecting the change in the Cγ-exo and Cγ-endo populations, the pattern observed for *syn,syn*-**106** (minor component) remains largely unaffected demonstrating the continued dominance of the Cγ-exo form.

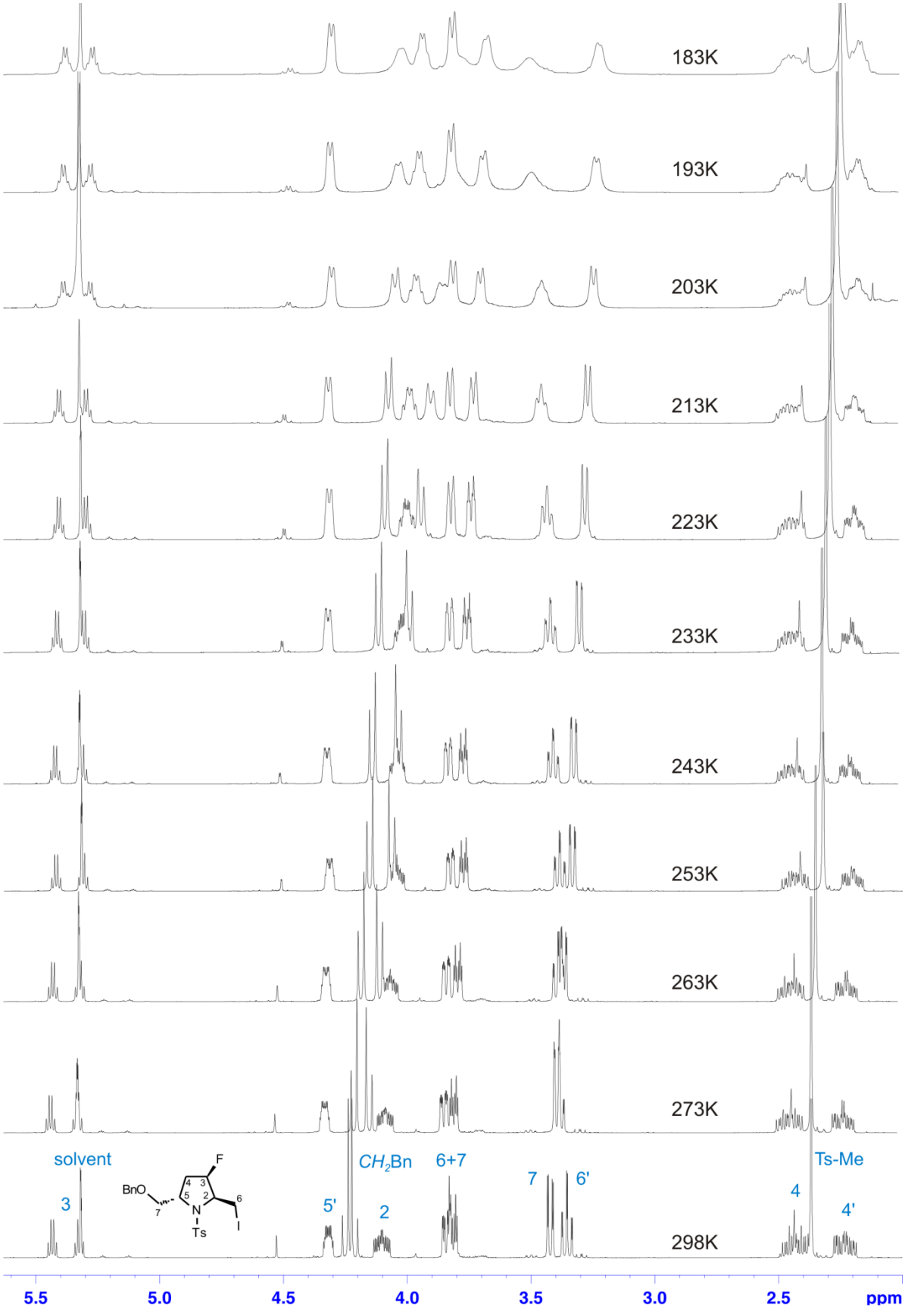

Figure 3.26: Variable temperature ^{1}H NMR spectra for compound *syn*,*anti*-**106** (500 MHz**).**

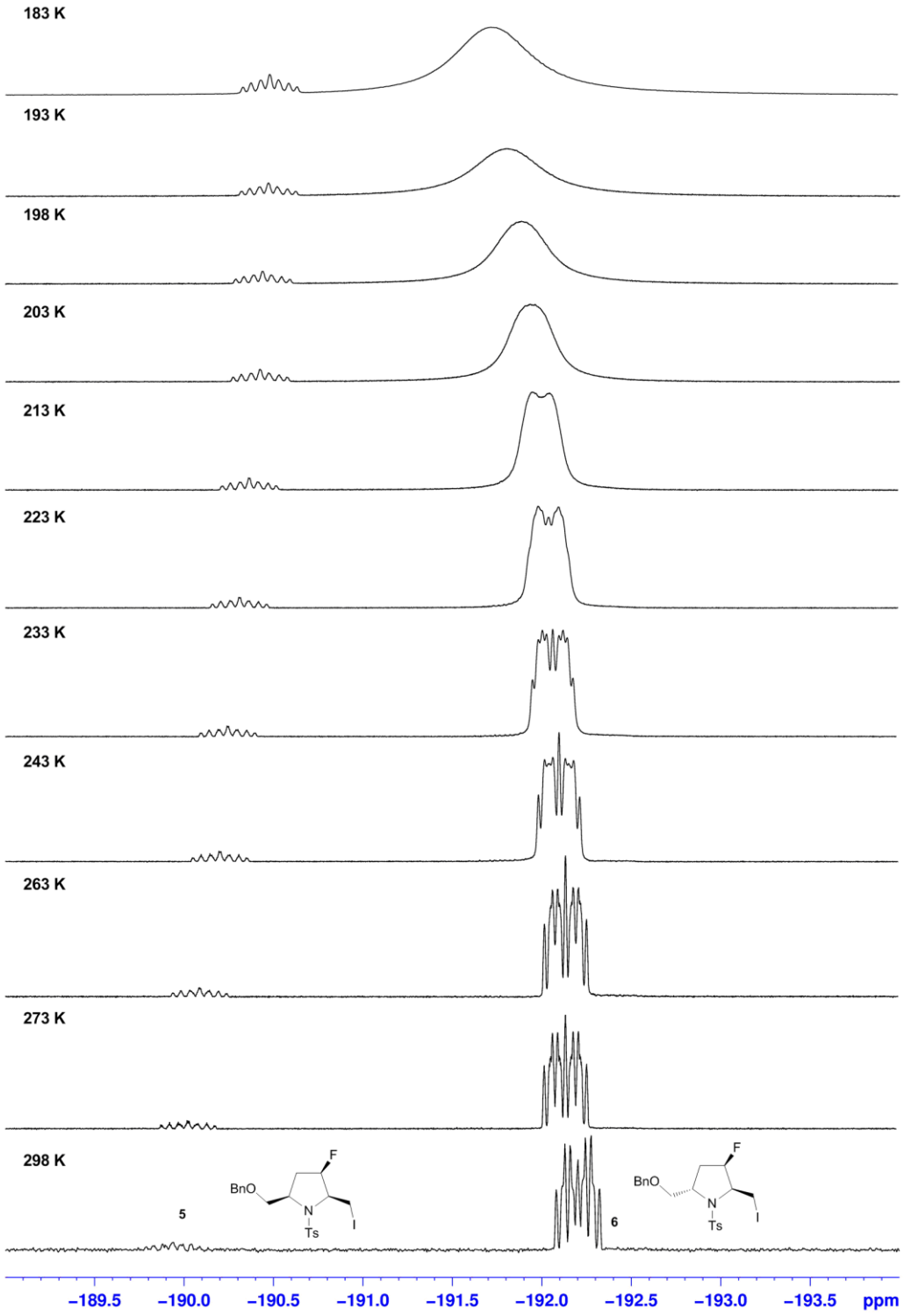

Figure 3.27: Variable temperature ^{19}F NMR spectra for compound *syn,anti*-**106.**

Significantly, changes in the values of $^{3}J_{FH}$ coupling constants demonstrated an increased preference for the C$^{\gamma}$-endo conformer at lower temperatures. Thus, the values of $^{3}J_{F\text{-}H4}$ and $^{3}J_{F\text{-}H2}$ demonstrated a linear decrease toward the values predicted for the C$^{\gamma}$-endo conformer (Figure 3.28; 6.9 and 11.7 Hz respectively) and away from the significantly larger values predicted for the C$^{\gamma}$-exo conformer (41.8 and 33.0 Hz respectively) based on the estimated dihedral torsion angles (Figure 3.28); even allowing for likely inaccuracies in the predicted coupling constants, the trend towards the C$^{\gamma}$-endo conformer remains clear. The invariant values of the $^{3}J_{F\text{-}H4'}$ coupling constant as a function of temperature are also consistent with such a change in conformational preference. The absolute magnitude of the F-H$^{4'}$ dihedral angle remains similar in both conformers (+40^{o} C$^{\gamma}$-exo *versus* -40^{o} in C$^{\gamma}$-endo) due to the F and H$^{4'}$ *syn* relationship, leading to similar values of predicted coupling constants in both cases (~ 19 Hz) and hence no change in the observed coupling as the conformer populations changed with temperature. Overall, these data demonstrate that *syn,anti*-**106** undergoes a rapid conformational exchange between C$^{\gamma}$-exo and C$^{\gamma}$-endo conformers and that there is a preference for the latter as sample temperature is decreased. As this preference is not observed for *syn,syn*-**106**, this behaviour is likely due to steric repulsion between the *N*-tosyl and benzyl groups competing with the stereoelectronic influence of fluorine, ultimately disfavouring the C$^{\gamma}$-exo form. When compound *syn,syn*-**106** was subjected to similar low-temperature NMR analysis, no changes in the corresponding coupling constants were observed, indicating the preference for the C$^{\gamma}$-exo conformer remains over the temperature range studied.

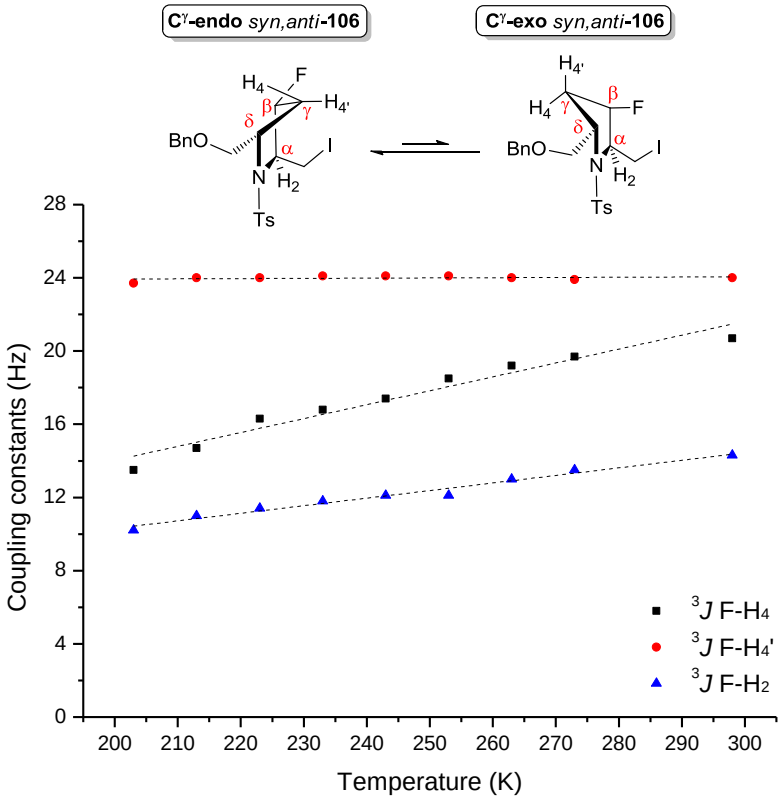

Figure 3.28: Influence of the temperature on the $^{3}J_{FH}$ coupling constants of compound *syn,anti*-**106.**

The NMR data for **109** were also markedly different from other compounds adopting the C$^{\gamma}$-exo conformation, displaying a unique set of F-H vicinal couplings that were also different to those of compound *syn,anti*-**106**. In the solid state **109** adopted an envelope conformation in which the fluorine and iodine atoms adopted a *pseudo* axial and *pseudo* equatorial orientation respectively. The large vicinal F-H^{2} coupling (35.9 Hz) suggests a largely *anti* relationship between these atoms consistent with an axial fluorine, with the close F-H$^{5'}$ distance (2.74 Å) also consistent with the iodine equatorial. A comparison of the NMR derived dihedral angles for the H^{2} proton *anti* to the fluorine with those observed in the crystal structure, suggests a greater F-H^{2} dihedral angle exists in the solution state conformation, possibly as a result of conformational mobility of the *N*-tosyl substituent (Figure 3.29).

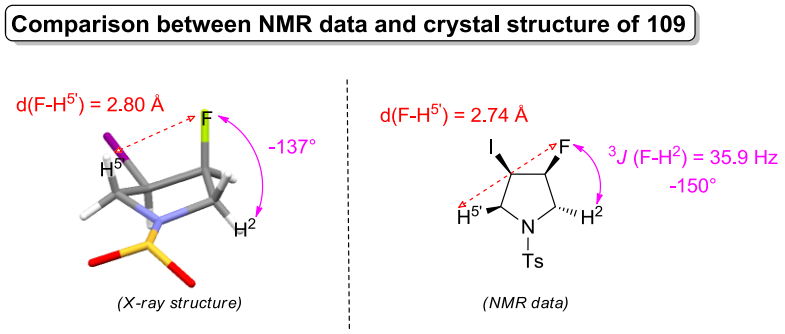

Figure 3.29: Comparison between NMR data and the crystal structure of **109**; For clarity purpose, the Tosyl group has been hidden in the representation of the crystal structure.

Variable temperature NMR analysis of **109** in CD_2Cl_2 revealed only minor changes in $^3J_{FH}$ values with temperature ($^3J_{H2\text{-}F}$ 36.4 to 39.9 Hz and $^3J_{H2'\text{-}F}$ 24.7 to 25.5 Hz at 298 and 193 K respectively) which argue against any significant conformational changes for **109** in solution.

3.4 Conclusion:

In summary we have developed ^{19}F-^{1}H 1D heteronuclear NOESY (HOESY) sequences optimised for small fluorinated molecules and used it along with the interpretation of fluorine-proton coupling constants to study the conformational analysis of fluorinated five-membered heterocycles. It has been shown that the internuclear distances calculated from the HOESY build-up curves obtained in solution were in good agreement with those observed in the solid state for conformationally constrained pyrrolidines. As suggested by the vicinal ^{1}H-^{1}H and ^{19}F-^{1}H coupling constants, the dihedral angles estimated from solution phase NMR data matched closely the torsion angles observed in the crystal structures of compounds **56, 152, 103, 104**, *syn,syn*-**106** and **105**. For those compounds where crystallographic analysis was not available (**116**, **153** and **155**), the study also showed that they adopted similar solution conformations. The combined NMR and crystallographic data, supported by theoretical calculations strongly suggest that fluorinated pyrrolidines substituted at the 3 position adopt preferentially a C$^\gamma$-exo conformation in both the crystalline and solution state. The fluorine acts as a conformation-directing element by the means of the weak stereoelectronic interaction known as the "fluorine *gauche* effect" which dictates the ring-pucker. However we were able to show the limitations of this interaction, which could be balanced by the steric hindrance acting in compound *syn,anti*-**106,** to an extent that varied with temperature.

Chapter 4:

EXPERIMENTAL SECTION

4.1 General information:

^{1}H NMR spectra were recorded in deuterated solvents using Bruker DPX200, DPX400, AV400 and AV500 spectrometers, calibrated using residual undeuterated solvent as an internal reference. ^{13}C NMR spectra were recorded in deuterated solvents using Bruker DPX200, DPX400, AV400 and AV500 spectrometers, calibrated using residual undeuterated solvent as an internal reference. ^{19}F spectra were recorded on an AV400 spectrometer, calibrated using fluorotrichloromethane ($CFCl_3$) as a reference. Chemical shifts (δ) are quoted in parts per million (ppm) and coupling constants (*J*) are measured in hertz (Hz). The following abbreviations are used to describe multiplicities s = singlet, d = doublet, t = triplet, q = quartet, br = broad, m = multiplet, app = apparent. NMR were processed in either MestRe-C or ACD/SpectManager. IUPAC names were obtained using the ACD/I-Lab service. High resolution mass spectra (HMRS, *m/z*) were recorded on Micromass GCT spectrometer using field ionisation (FI) or chemical ionisation (CI), or on Autospec-oa Tof and Bruker MicroTOF instruments for electrospray ionisation (ESI). Infrared spectra were recorded as thin films on NaCl plates in solution in CH_2Cl_2 or as solid on KBr disc on a Bruker Tensor 27 FT-IR spectrometer. Absorptions are measured in wavenumbers (cm^{-1}) and only peaks of interest are reported. Melting points of solids were measured on a Griffin apparatus and are uncorrected. All reactions requiring anhydrous conditions were conducted in dried apparatus under an inert atmosphere of argon. Solvents were dried on a column of alumina or purified before use according to standard procedures. All reactions were monitored by thin layer chromatography (TLC) using Merck Kiesegel 60 F_{254} plates. Visualisation of the reaction components was achieved using U.V. fluorescence (254 nm) and $KMnO_4$ stain. Silica gel chromatography was carried out over Merck silica gel C60 (40-60 μm) using eluent systems as described for each experiment.

4.2. General procedures:

General procedure A: Preparation of Organosilanes via Cross-Metathesis (CM)

To a solution of homoallylic amine (1 eq.) and allytrimethylsilane (3 eq.) in dry CH_2Cl_2 [0.3M] was added portion wise over 3 days Grubbs' 2nd generation catalyst (5 mol%) and 1,4-benzoquinone (0.5 eq.) at reflux. The reaction was maintained at reflux under an argon atmosphere until TLC showed complete consumption of the starting material (generally after 3 to 4 days), after which, the reaction was stopped and the solvent removed *in vacuo*. The resulting crude mixture was purified by flash column chromatography on silica gel.

General procedure B: Preparation of Allylic fluorides via Fluorodesilylation:

To a solution of organosilane (1 eq.) in dry CH_3CN [0.1M] was added Selectfluor (1.1 eq.) and $NaHCO_{3\ solid}$ (1.2 eq.). The reaction was stirred at r.t. until TLC showed complete consumption of the starting material (generally between 24 h and 48 h). The solvent was then removed *in vacuo* and the crude mixture was diluted in saturated $NaHCO_3$ aqueous solution. Then the aqueous phase was extracted four times with Et_2O. The combined organic phases were washed with H_2O, then brine, dried over $MgSO_4$, filtered and the solvent removed *in vacuo*. The crude compound was purified by flash column chromatography on silica gel (hexane/Et_2O 8:2) to give the corresponding allylic fluoride.

General procedure C: Preparation of Organosilanes via Mesylate formation and subsequent Tosylamine substitution

To a stirring solution of primary alcohol (1 eq.) and methane sulfonylchloride (1.2 eq.) in dry CH_2Cl_2 was added distilled NEt_3 (5 eq.) dropwise at 0 °C. The reaction was maintained stirring at ambient temperature under an atmosphere of argon until TLC showed consumption of the alcohol (generally 2 h). After which, the reaction mixture was quenched with H_2O and extracted three time with CH_2Cl_2. The combined organic phases were washed with H_2O, brine, dried over $MgSO_4$,

filtered and the solvent removed *in vacuo*. The resulting crude mixture was engaged without further purification to the next step.

Finely grounded potassium hydroxide (1.5 eq.) was dissolved in anhydrous DMF [0.5M] at 120 °C and tosylamine (1.5 eq.) added. The mixture was stirred for 30 minutes, after which a solution of mesylate (1 eq.) in anhydrous DMF [0.5M] was added. Once TLC showed complete consumption of the starting material (generally after 2-3 h), the reaction mixture was cooled, diluted with H_2O and extracted four times with EtOAc. The combined organic extracts were washed three times with H_2O then brine, dried over $MgSO_4$, filtered, and the solvent removed *in vacuo*. The crude product was purified by flash column chromatography on silica gel.

4.3 Synthesis of organotrimethylsilanes and allylic fluorides:

4.3.1 Synthesis of (±) *N*-(3-fluoropent-4-en-1-yl)-4-methylbenzenesulfonamide (55):

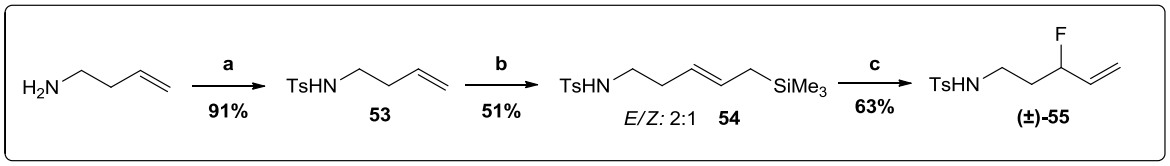

Scheme 4.1: Synthesis of (±) *N*-(3-fluoropent-4-en-1-yl)-4-methylbenzenesulfonamide (**55**). **a**) NEt_3, DMAP, TsCl, CH_2Cl_2, 3 h. **b**) allyltrimethylsilane, Grubbs 2nd (5 mol%), 1,4-benzoquinone, CH_2Cl_2, reflux, 3 days; **c**) Selectfluor, $NaHCO_3$, CH_3CN, 48 h.

_N_-but-3-en-1-yl-4-methylbenzenesulfonamide (53):[1]

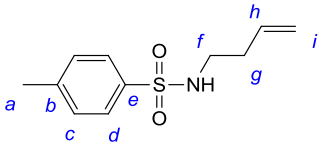

To a solution of **3-buten-1-amine** (2.57 mL, 28 mmol, 1 eq.), distilled NEt_3 (5.8 mL, 42 mmol, 1.5 eq.) and dimethylaminopyridine (1 g, 8.4 mmol, 0.3 eq.) in dry CH_2Cl_2 (60 mL) was added tosylchloride (6.4 g, 34 mmol, 1.2 eq). The reaction was stirred at r.t. for 3 h. The reaction was quenched by addition of H_2O and the aqueous layer was extracted three times with EtOAc, the combined organic phases were washed with brine, dried over $MgSO_4$, filtered and the solvent

[1] This substrate was synthesised according to the procedure described by T. Mizutani, Y. Ukaji, K. Inomata, *Bull. Chem. Soc. Jpn.* **2003**, *76*, 1251-1256. Analytical and spectroscopic data were in agreement with those previously reported by R. C. Larock, H. Yang, S. M. Weinreb, R. J. Herr, *J. Org. Chem.* **1994,** *59*, 4172-4178.

removed *in vacuo*. The crude mixture was purified by flash column chromatography on silica gel (hexane/EtOAc 4:1) to afford the corresponding tosylamine **53** as a colourless oil (5.8 g, 91%).

R_f = 0.4 (hexane/EtOAc 4:1); **^{1}H NMR (400 MHz, $CDCl_3$)** δ = 2.16 (apparent q, 2H, $^3J_{H\text{-}H}$ = 6.8 Hz, *g*), 2.37 (s, 3H, *a*), 2.91-2.98 (m, 2H, *f*), 4.93-5.00 (m, 2H, *i*), 5.25 (t, 1H, $^3J_{H\text{-}H}$ = 6.1 Hz, *NH*), 5.60 (ddt, 1H, $^3J_{H\text{-}H}$ = 17.9, 9.6, 6.8 Hz, *h*), 7.26 (d, 2H, $^3J_{H\text{-}H}$ = 8.2 Hz, *c/d*), 7.73 (d, 2H, $^3J_{H\text{-}H}$ = 8.2 Hz, *c/d*);

4-methyl-*N*-[5-(trimethylsilyl)pent-3-en-1-yl]benzenesulfonamide (54):

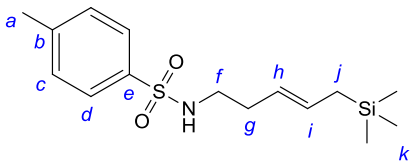

Following the general procedure A on 500 mg (2.22 mmol, 1 eq.) of ***N*-(but-3-en-1-yl)-*p*-toluenesulfonamide 53**, the reaction yielded 348 mg of a mixture diastereoisomers **54** obtained in 51% (*E:Z* = 2:1) as a yellow oil after flash column chromatography on silica gel (hexane/Et_2O 95:5 then 9:1).

Data for the major (E) isomer: **R_f** = 0.4 (hexane/Et_2O 6:4); **^{1}H NMR (400 MHz, $CDCl_3$)** δ = -0.03 (sbr, 9H, *k*), 1.39 (d, 2H, $^3J_{H\text{-}H}$ = 8.1 Hz, *j*), 2.09-2.18 (m, 2H, *g*), 2.43 (s, 3H, *a*), 2.91-2.99 (m, 2H, *f*), 4.52 (t, 1H, $^3J_{H\text{-}H}$ = 6.0 Hz, *NH*), 5.02 (dtt, 1H, $^3J_{H\text{-}H(trans)}$ = 15.0 Hz, $^3J_{H\text{-}H}$ = 7.1, $^4J_{H\text{-}H}$ = 1.3 Hz, *h*), 5.41 (dtt, 1H, $^3J_{H\text{-}H(trans)}$ = 15.0 Hz, $^3J_{H\text{-}H}$ = 8.1 Hz, $^4J_{H\text{-}H}$ = 1.3 Hz, *i*), 7.31 (d, 2H, $^3J_{H\text{-}H}$ = 8.2 Hz, *c/d*), 7.74 (d, 2H, $^3J_{H\text{-}H}$ = 8.2 Hz, *c/d*); **^{13}C NMR (101 MHz, $CDCl_3$)** δ = -2.0 (*k*), 21.5 (*a*), 22.9 (*j*), 32.6 (*g*), 42.8 (*f*), 123.6 (*h*), 127.1 (*c/d*), 129.6 (*c/d*), 130.7 (*i*), 136.9 (*b/e*), 143.3 (*b/e*); **IR (neat): ν =** 3285, 3061, 1673, 922, 772; **HRMS (CI^+):** *m/z* required for $C_{15}H_{26}NO_2SSi$ ($[M+H]^+$): 312.1454, found 312.1438, Δ = 5.0 ppm.

Identifiable data for the minor (Z) isomer: **^{1}H NMR (400 MHz, $CDCl_3$)** δ = -0.04 (sbr, 9H, *k*), 4.57 (t, 1H, $^3J_{H\text{-}H}$ = 6.1 Hz, *NH*), 5.06-5.11 (m, 1H, $^3J_{H\text{-}H(cis)}$ = 10.6 Hz, *h*), 5.48-5.59 (m, 1H, $^3J_{H\text{-}H(cis)}$ = 10.6 Hz, *i*); **^{13}C NMR (101 MHz, $CDCl_3$)** δ = -1.9 (*k*), 18.7 (*j*), 27.1 (*g*), 42.8 (*f*), 122.0 (*h*), 129.6 (*i*);

Note: *Separation of the desired homoallylic amine from the truncated side-product was not trivial and, in some cases, mixtures of the two were isolated and subjected to further reactions. Partial separation was achieved in most cases and the analytical data provided are of the pure homoallylic amine where possible.*

(±) *N*-(3-fluoropent-4-en-1-yl)-4-methylbenzenesulfonamide (55):

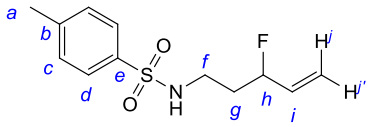

Following the general procedure B on 575 mg (1.85 mmol) of **4-methyl-*N*-[5-(trimethylsilyl)pent-3-en-1-yl]benzenesulfonamide 54**, the reaction yielded 300 mg of **55** (63%) as a white solid after flash column chromatography on silica gel (hexane/Et_2O 8:2).

R_f = 0.3 (hexane/Et_2O 6:4); **m.p.** = 73 °C; **^{1}H NMR (400 MHz, $CDCl_3$)** δ = 1.81-1.94 (m, 2H, $^3J_{H\text{-}F}$ = 21.2 Hz, *g*), 2.43 (sbr, 3H, *a*), 3.05-3.19 (m, 2H, *f*), 4.70 (t, 1H, $^3J_{H\text{-}H}$ = 5.7 Hz, *NH*), 4.97 (dddt, 1H, $^2J_{H\text{-}F}$ = 48.6 Hz, $^3J_{H\text{-}H}$ = 7.2, 5.8 Hz, $^4J_{H\text{-}H}$ = 1.3 Hz, *h*), 5.23 (dt, 1H, $^3J_{H\text{-}H(cis)}$ = 10.6 Hz, $^2J_{H\text{-}H}$ = 1.3 Hz, $^4J_{H\text{-}H}$ = 1.3 Hz, *j'*), 5.30 (ddt, 1H, $^3J_{H\text{-}H(trans)}$ = 17.2 Hz, $^4J_{H\text{-}F}$ = 3.3 Hz, $^2J_{H\text{-}H}$ = 1.3 Hz, $^4J_{H\text{-}H}$ = 1.3 Hz, *j*), 5.82 (dddd, 1H, $^3J_{H\text{-}F}$ = 14.9 Hz, $^3J_{H\text{-}H}$ = 17.2, 10.6, 5.8 Hz, *i*), 7.32 (d, 2H, $^3J_{H\text{-}H}$ = 8.1 Hz, *c/d*), 7.76 (d, 2H, $^3J_{H\text{-}H}$ = 8.1 Hz, *c/d*); **^{13}C NMR (101 MHz, $CDCl_3$)** δ = 21.5 (*a*), 35.0 (d, $^2J_{C\text{-}F}$ = 21.6 Hz, *g*), 39.3 (d, $^3J_{C\text{-}F}$ = 4.0 Hz, *f*), 91.5 (d, $^1J_{C\text{-}F}$ = 167.8 Hz, *h*), 117.6 (d, $^3J_{C\text{-}F}$ = 12.0 Hz, *j*), 127.1 (*c/d*), 129.8 (*c/d*), 135.4 (d, $^2J_{C\text{-}F}$ = 19.2 Hz, *i*), 136.7 (*b/e*), 143.6 (*b/e*); **^{19}F {^{1}H} NMR (377 MHz, $CDCl_3$)** δ = -180.3; **IR (neat): ν =** 3250, 3061, 2821, 1645, 1432; **HRMS (CI$^+$):** *m/z* required for $C_{12}H_{20}FN_2O_2S$ ($[M+NH_4]^+$): 275.1230, found 275.1243, Δ = 4.9 ppm.

4.3.2 Synthesis of (±) *tert*-butyl (3-fluoropent-4-en-1-yl)carbamate (61):

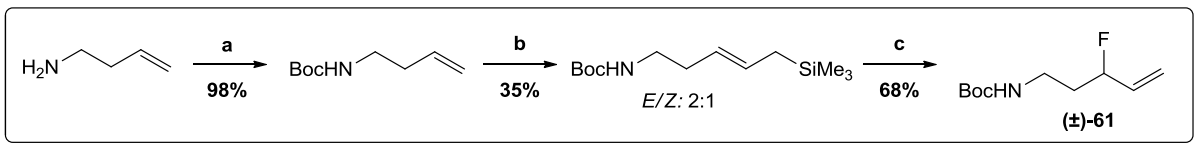

Scheme 4.2: Synthesis of (±) *tert*-butyl (3-fluoropent-4-en-1-yl)carbamate (**61**). **a**) NEt_3, di-*tert*-butylcarbamate, CH_2Cl_2, 15 h. **b**) allyltrimethylsilane, Grubbs 2nd (5 mol%), 1,4-benzoquinone, CH_2Cl_2, reflux, 3 days; **c**) Selectfluor, $NaHCO_3$, CH_3CN, 48 h.

***N-tert*-butyl but-3-en-1-ylcarbamate:**[2]

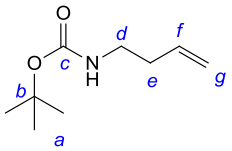

To a solution of **3-buten-1-amine** (1.0 g, 14 mmol, 1 eq.) in dry CH_2Cl_2 (70 mL) at r.t was added distilled NEt_3 (3.9 mL, 28 mmol, 2 eq.). The reaction was cooled to 0 °C and di-*tert*-butylcarbamate (3.2 g, 15.5 mmol, 1.1 eq.) was added portion wise. The reaction mixture was stirred overnight at r.t. The solvent was removed *in vacuo* and the crude mixture was purified by flash column chromatography on silica gel (petroleum spirit 30-40 °C/EtOAc 9:1) to give the corresponding ***N-tert*-butyl but-3-en-1-ylcarbamate** as a colourless oil (2.4 g, 98%).

R_f = 0.7 (hexane/EtOAc 7:3); **^{1}H NMR (400 MHz, $CDCl_3$)** δ = 1.43 (sbr, 9H, *a*), 2.23 (apparent q, 2H, $^3J_{H\text{-}H}$ = 6.8 Hz, *e*), 3.14-3.21 (m, 2H, *d*), 4.58 (sbr, 1H, *NH*), 5.06 (dd, 1H, $^3J_{H\text{-}H(cis)}$ =10.1 Hz, $^2J_{H\text{-}H}$ = 1.8 Hz, *g*), 5.08 (dd, 1H, $^3J_{H\text{-}H(trans)}$ = 16.9 Hz, $^2J_{H\text{-}H}$ = 1.8 Hz, *g'*), 5.75 (ddt, 1H, $^3J_{H\text{-}H(trans)}$ = 16.9 Hz, $^3J_{H\text{-}H(cis)}$ = 10.1 Hz, $^3J_{H\text{-}H}$ = 6.8 Hz, *f*);

***N-tert*-butyl[5-(trimethylsilyl)pent-3-en-1-yl]carbamate:**

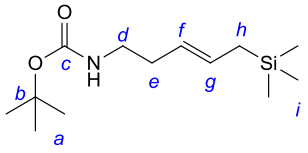

Following the general procedure A on 500 mg (2.92 mmol, 1 eq.) of ***N-tert*-butyl but-3-en-1-ylcarbamate** using Hoveyda-Grubbs 2nd generation catalyst (91 mg, 5 mol%), the reaction yielded 303 mg of a mixture containing ***N-tert*-butyl[5-(trimethylsilyl)pent-3-en-1-yl]carbamate** and the truncated side product ***N-tert*-butyl[5-(trimethylsilyl)but-2-en-1-yl]carbamate** obtained respectively in 35% (*E:Z* = 2:1) and 5% (corrected yield), as a yellow oil after flash column chromatography on silica gel (hexane/Et_2O 9:1).

Data for the major (E) isomer: **R_f** = 0.5 (hexane/Et_2O 7:3); **^{1}H NMR (400 MHz, $CDCl_3$)** δ = 0.00 (s, 9H, *i*), 1.43 (s, 9H, *a*), 1.48 (d, 2H, $^3J_{H\text{-}H}$ = 8.1 Hz, *h*), 2.12-2.22 (m, 2H, *e*), 3.08-3.18 (m, 2H, *d*), 4.53 (sbr, 1H, *NH*), 5.17 (dtt, 1H, $^3J_{H\text{-}H(trans)}$ = 15.1 Hz, $^3J_{H\text{-}H}$ = 7.1 Hz, $^4J_{H\text{-}H}$ = 1.2 Hz, *f*), 5.48 (dtt,

[2] Analytical and spectroscopic data were in agreement with those previously reported by C. Taillier, T. Hameury, V. Bellosta, J. Cossy, *Tetrahedron* **2007**, *63*, 4472-4490.

1H, $^{3}J_{H\text{-}H(trans)}$ = 15.1 Hz, $^{3}J_{H\text{-}H}$ = 8.1 Hz, $^{4}J_{H\text{-}H}$ = 1.3 Hz, *g*); **^{13}C NMR (101 MHz, $CDCl_3$)** δ = -2.0 (*i*), 22.8 (*h*), 28.4 (*a*), 33.1 (*e*), 40.3 (*d*), 78.9 (*b*), 124.9 (*f*), 129.3 (*g*), 155.9 (*c*); **IR (neat): ν =** 3356, 2955, 1698, 1515, 1365, 1174, 854; **HRMS (ESI$^+$):** *m/z* required for $C_{13}H_{27}NO_2SiNa^+$ ([M+Na]$^+$): 280.1698, found 280.1703, Δ = 1.2 ppm.

Identifiable data for the minor (Z) isomer: **^{1}H NMR (400 MHz, $CDCl_3$)** δ = 0.01 (s, 9H, *i*), 5.21-5.29 (m, 1H, $^{3}J_{H\text{-}H(cis)}$ = 10.9 Hz, *f*), 5.51-5.61 (m, 1H, $^{3}J_{H\text{-}H(cis)}$ = 10.9 Hz, *g*); **^{13}C NMR (101 MHz, $CDCl_3$)** δ = -1.8 (*i*), 18.6 (*h*), 27.4 (*e*), 124.5 (*f*), 128.4 (*g*);

(±) *N-tert*-butyl (3-fluoropent-4-en-1-yl)carbamate (61):

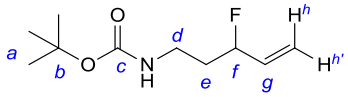

Following the general procedure B on 559 mg (2.2 mmol) of ***N-tert*-butyl[5-(trimethylsilyl)pent-3-en-1-yl]carbamate**, the reaction yielded 300 mg of **61** (68%) as a light orange oil after flash column chromatography on silica gel (hexane/Et_2O 9:1).

R_f = 0.4 (hexane/Et_2O 7:3); **^{1}H NMR (400 MHz, $CDCl_3$)** δ = 1.44 (sbr, 9H, *a*), 1.81-1.95 (m, 2H, $^{3}J_{H\text{-}F}$ = 25.7 Hz, *e*), 3.28 (d, 2H, $^{3}J_{H\text{-}H}$ = 6.3 Hz, *d*), 4.74 (sbr, 1H, *NH*), 4.98 (dddd, 1H, $^{2}J_{H\text{-}F}$ = 48.5 Hz, $^{3}J_{H\text{-}H}$ = 11.0, 5.8 Hz, $^{4}J_{H\text{-}H}$ = 1.3 Hz, *f*), 5.24 (dt, 1H, $^{3}J_{H\text{-}H(cis)}$ = 10.9, $^{2}J_{H\text{-}H}$ = 1.3 Hz, $^{4}J_{H\text{-}H}$ = 1.3 Hz, *h'*), 5.34 (ddt, 1H, $^{3}J_{H\text{-}H(trans)}$ = 17.2 Hz, $^{4}J_{H\text{-}F}$ = 3.3 Hz, $^{2}J_{H\text{-}H}$ = 1.3 Hz, $^{4}J_{H\text{-}H}$ = 1.3 Hz, *h*), 5.89 (dddd, 1H, $^{3}J_{H\text{-}H(trans)}$ = 17.2 Hz, $^{3}J_{H\text{-}F}$ = 14.9 Hz, $^{3}J_{H\text{-}H(cis)}$ = 10.9 Hz, $^{3}J_{H\text{-}H}$ = 5.8 Hz, *g*); **^{13}C NMR (101 MHz, $CDCl_3$)** δ = 28.3 (*a*), 35.3 (d, $^{2}J_{C\text{-}F}$ = 21.6 Hz, *e*), 36.7 (d, $^{3}J_{C\text{-}F}$ = 3.2 Hz, *d*), 79.2 (*b*), 91.5 (d, $^{1}J_{C\text{-}F}$ = 167.0 Hz, *f*), 117.1 (d, $^{3}J_{C\text{-}F}$ = 12.0 Hz, *h*), 135.9 (d, $^{2}J_{C\text{-}F}$ = 19.2 Hz, *g*), 155.9 (*c*); **^{19}F {^{1}H} NMR (377 MHz, $CDCl_3$)** δ = -179.90; **IR (neat): ν =** 3351, 2979, 1694, 1521, 1367, 1174, 989; **HRMS (ESI$^+$):** *m/z* required for $C_{10}H_{18}FNO_2Na^+$ ([M+Na]$^+$): 226.1214, found 226.1214, Δ = 0.2 ppm.

4.3.3 Synthesis of (±) *N*-(3-fluoro-3-methylpent-4-en-1-yl)-4-methylbenzenesulfonamide (62):

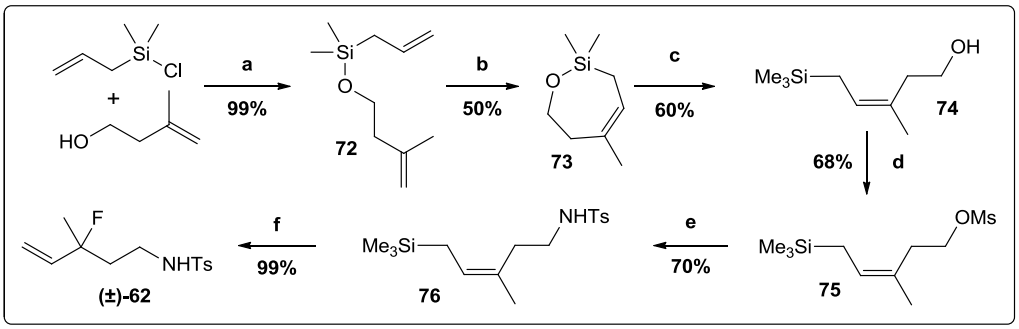

Scheme 4.3: Synthesis of (±) *N*-(3-fluoro-3-methylpent-4-en-1-yl)-4-methylbenzenesulfonamide (**62**). (**a**) NEt_3, CH_2Cl_2, 0 °C, 19 h; **b**) Hoveyda-Grubbs 2nd (2 mol%), CH_2Cl_2, reflux, 2 h; **c**) MeLi, THF, -78 °C, 3 h; **d**) MsCl, NEt_3, CH_2Cl_2, 0 °C, 2 h; **e**) NH_2Ts, KOH, DMF, 120 °C, 3 h (f) Selectfluor, CH_3CN, $NaHCO_3$, r.t., 24 h.

Allyl(dimethyl)[(3-methylbut-3-en-1-yl)oxy]silane (72):[3]

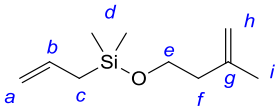

To a solution of **3-methyl-3-buten-1-ol** (1.5 mL, 15.0 mmol, 1 eq.), distilled NEt_3 (2.52 mL, 10 mmol, 1.2 eq.) in dry CH_2Cl_2 (15 mL) at 0 °C was added dropwise a solution of allylchlorodimethylsilane (2.6 mL, 18.0 mmol, 1.2 eq.) in CH_2Cl_2 (6 mL). The reaction mixture was stirred under inert atmosphere at r.t. for 16 h. After which, the reaction was quenched by addition of H_2O. The organic phase was washed with H_2O, brine then dried over $MgSO_4$, filtered and the solvent removed *in vacuo*. (**caution: volatile compound**). The crude product was purified by flash column chromatography on silica gel (petroleum ether 30-40 °C) to give the desired silane **72** as a colourless oil (2.8 g, 99 %).

R_f = 0.6 (hexane/Et_2O 95:5); **^{1}H NMR (400 MHz, $CDCl_3$) δ** = 0.13 (s, 6H, *d*), 1.64 (d, 2H, $^3J_{H\text{-}H}$ = 7.9 Hz, *c*), 1.74 (m, 3H, *i*), 2.26 (t, 2H, $^3J_{H\text{-}H}$ = 7.0 Hz, *f*), 3.72 (t, 2H, $^3J_{H\text{-}H}$ = 7.0 Hz, *e*), 4.71-4.78 (m, 2H, *a/h*), 4.86-4.96 (m, 2H, *a/h*), 5.70-5.92 (m, 1H, *b*).

[3] This compound was prepared according the procedure reported by M. Tredwell, J. A. R. Luft, M. Schuler, K. Tenza, K. N. Houk, V. Gouverneur, *Angew. Chem. Int. Ed.* **2008**, *47*, 357-360. Analytical and spectroscopic data were in agreement with those reported wherein.

2,2,5-trimethyl-2,3,6,7-tetrahydro-1,2-oxasilepine (73):[3]

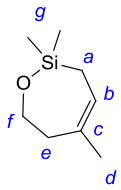

To a solution of **allyl(dimethyl)[(3-methylbut-3-en-1-yl)oxy]silane 72** (200 mg, 1.1 mmol, 1 eq.) in anhydrous CH_2Cl_2 (108 mL) at reflux was added Hoveyda-Grubbs 2nd generation catalyst (7 mg, 0.01 mmol, 1 mol%). The reaction was stirred at reflux for 6 h under an atmosphere of argon. After cooling to r.t. the solvent was removed *in vacuo* (**caution: volatile compound**) and the resulting residue was purified using a short flash column chromatography on silica gel (petroleum ether 30-40 °C) to afford the cyclic product **73** as a colourless oil (100 mg, 59%).

R_f = 0.5 (hexane/Et_2O 95:5); **^{1}H NMR (400 MHz, $CDCl_3$) δ** = 0.12 (s, 6H, *g*), 1.50 (d, 2H, $^3J_{H\text{-}H}$ = 7.4 Hz, *a*), 1.74 (s, 3H, *d*), 2.30-2.35 (m, 2H, *e*), 3.84-3.89 (m, 2H, *f*), 5.54 (t, 1H, $^3J_{H\text{-}H}$ = 7.4 Hz, *b*).

5-(trimethylsilyl)pent-3-en-1-ol (74):[3]

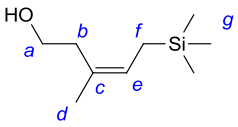

To a solution of **2,2,5-trimethyl-2,3,6,7-tetrahydro-1,2-oxasilepine 73** (100 mg, 0.6 mmol, 1 eq.) in anhydrous THF (3.3 mL) at -78 °C, was added MeLi (1.5 mL [1.6M] in hexanes, 2.4 mmol, 4 eq.) dropwise. The reaction was warmed to 0 °C and stirred at this temperature for 3 h. After which, the reaction was quenched by the addition of saturated $NH_4Cl_{(aq)}$ solution. The two layers were partitioned and the aqueous layer was extracted three times with Et_2O. The combined organic phases were washed with brine, dried over $MgSO_4$, filtered and the solvent removed *in vacuo* (**caution: volatile compound**). The resulting yellow crude mixture was purified by flash column chromatography on silica gel (petroleum ether 30-40 °C/Et_2O 9:1) to afford the corresponding alcohol **74** as a colourless oil (73 mg, 71 %).

R_f = 0.4 (hexane/Et_2O 7:3); **^{1}H NMR (400 MHz, $CDCl_3$) δ** = 0.00 (s, 9H, *g*) 1.46 (d, 2H, $^3J_{H\text{-}H}$ = 8.5 Hz, *f*), 1.73 (s, 3H, *d*), 2.30 (t, 2H, $^3J_{H\text{-}H}$ = 6.8 Hz, *b*), 3.68 (td, 2H, $^3J_{H\text{-}H}$ = 6.8 Hz, 2.1 Hz, *a*), 5.36 (t, 1H, $^3J_{H\text{-}H}$ = 8.5 Hz, *e*).

***N*-3-methyl-5-(trimethylsilyl)pent-3-en-1-yl methanesulfonate (75):**

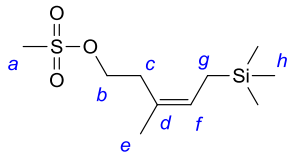

To a stirring solution of alcohol **5-(trimethylsilyl)pent-3-en-1-ol 74** (150 mg, 0.9 mmol, 1 eq.) and distilled NEt_3 (0.6 mL, 4.4 mmol, 5 eq.) in dry CH_2Cl_2 (5 mL) was added methanesulfonyl chloride (0.08 mL, 1.0 mmol, 1.2 eq.). The reaction was stirred at r.t for 2 h. The reaction was quenched by addition of H_2O and the aqueous layer was extracted three times with CH_2Cl_2, the combined organic phases were washed with brine, dried over $MgSO_4$, filtered and the solvent removed *in vacuo* (**caution : volatile compound**). The crude mixture was purified using flash column chromatography on silica gel (petroleum ether 30°-40 °C/ Et_2O 75:25) to afford the mesylate **75** as a colourless oil (160 mg, 71%).

R_f = 0.12 (hexane/Et_2O 8:2); **^{1}H NMR (400 MHz, $CO(CD_3)_2$)** δ = 0.04 (s, 9H, *h*), 1.52 (d, 2H, $^3J_{H\text{-}H}$ = 8.6 Hz, *g*), 1.79 (s, 3H, *a*), 2.51 (t, 2H, $^3J_{H\text{-}H}$ = 7.4 Hz, *c*), 3.11 (s, 3H, *e*), 4.28 (t, 2H, $^3J_{H\text{-}H}$ = 7.4 Hz, *b*), 5.40 (t, 1H, $^3J_{H\text{-}H}$ = 8.6 Hz, *f*); **^{13}C NMR (101 MHz, $CO(CD_3)_2$)** δ = 1.1 (*h*), 21.8 (*a*), 26.4 (*e*), 33.8 (*g*), 39.9 (*c*), 68.7 (*b*), 127.2 (*f*), 133.8 (*d*); **IR (neat): ν** = 1857, 1524, 1411, 900; **HRMS (CI$^+$):** *m/z* required for $C_{10}H_{23}O_3SSi$ ($[M+H]^+$): 251.1137, found 251.1144. Δ = 2.7 ppm.

***N*-4-methyl-*N*-[3-methyl-5-(trimethylsilyl)pent-3-en-1-yl]benzene sulphonamide (76):**

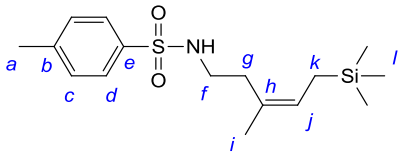

Finely ground potassium hydroxide (50 mg, 0.9 mmol, 1.5 eq.) was diluted in anhydrous DMF (0.9 mL) at 120 °C and tosylamine (153 mg, 0.89 mmol, 1.5 eq.) was added. The reaction was stirred at this temperature for 30 min until complete dissolution; after which a solution of **3-methyl-5-(trimethylsilyl)pent-3-en-1-yl methanesulfonate 75** (150 mg, 0.6 mmol, 1 eq.) in DMF (0.9 mL) was added. The reaction was heated at 120 °C for 3 h. After cooling to r.t. the mixture was diluted with H_2O. Then the aqueous phase was extracted four times with Et_2O. The combined organic layers were washed three times with H_2O then brine, dried over $MgSO_4$, filtered, and the solvent removed

in vacuo. The crude product was purified by flash column chromatography on silica gel (hexane/Et_2O 6:4) to yield a mixture of diastereomers of allylsilane **76** as a colourless oil as (154 mg, 79%, *E:Z*= 1:5).

Data for the major (Z) isomer: **R_f** = 0.3 (hexane/Et_2O 6:4); **^{1}H NMR (400 MHz, $CDCl_3$)** δ = -0.04 (sbr, 9H, *l*), 1.33 (d, 2H, $^3J_{H-H}$ = 8.8 Hz, *k*), 1.55 (d, 3H, $^4J_{H-H}$ = 1.0 Hz, *i*), 2.15 (t, 2H, $^3J_{H-H}$ = 6.9 Hz, *g*), 2.44 (sbr, 3H, *a*), 2.97-3.04 (m, 2H, *f*), 4.26 (t, 1H, $^3J_{H-H}$ = 5.8 Hz, *NH*), 5.30 (t, 1H, $^3J_{H-H}$ = 8.8 Hz, *j*), 7.32 (d, 2H, $^3J_{H-H}$ = 8.1 Hz, *c/d*), 7.75 (d, 2H, $^3J_{H-H}$ = 8.1 Hz, *c/d*); **^{13}C NMR (101 MHz, $CDCl_3$)** δ = -1.8 (*l*), 18.6 (*k*), 21.5 (*a*), 22.6 (*i*), 30.9 (*g*), 40.7 (*f*), 124.7 (*j*), 127.1 (*c/d*), 127.7 (*h*), 129.7 (*c/d*), 136.8 (*b/e*), 143.3 (*b/e*); **IR (neat) ν =** 3429, 3064, 1655, 992; **HRMS (CI^+):** *m/z* required for $C_{16}H_{28}NO_2SSi$ ($[M+H]^+$): 326.1610, found 326.1611, Δ = 0.3 ppm.

Identifiable data for the minor (E) isomer: **^{1}H NMR (400 MHz, $CDCl_3$)** δ = -0.00 (sbr, 9H, *l*), 1.46 (d, 2H, $^3J_{H-H}$ = 8.6 Hz, *k*), 1.73 (d, 3H, $^4J_{H-H}$ = 1.0 Hz, *i*), 2.31 (t, 2H, $^3J_{H-H}$ = 6.8 Hz, *g*), 3.65-3.71 (m, 2H, *f*), 5.36 (t, 1H, $^3J_{H-H}$ = 8.1 Hz, *j*); ^{13}C resonances for the (*E)* isomer could not be distinguished.

(±) *N*-(3-fluoro-3-methylpent-4-en-1-yl)-4-methylbenzene sulfonamide (62):

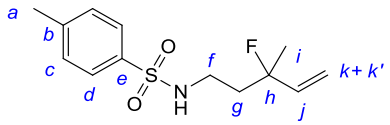

Following the general procedure B on 250 mg (0.76 mmol) of ***N*-4-methyl-*N*-[3-methyl-5-(trimethylsilyl)pent-3-en-1-yl]benzene sulphonamide 76**, the reaction yielded 213.9 mg of **62** (99%) as a colourless oil after flash column chromatography on silica gel (hexane/Et_2O 6:4).

R_f = 0.3 (hexane/Et_2O 6:4); **^{1}H NMR (500 MHz, $CO(CD_3)_2$)** δ = 1.36 (d, 3H, $^3J_{H-F}$ = 21.7 Hz, *i*), 1.83-1.96 (m, 2H, *g*), 2.42 (s, 3H, *a*), 2.94-2.09 (m, 2H, *f*), 5.09 (dt, 1H, $^3J_{H-H(cis)}$ = 11.0 Hz, $^2J_{H-H}$ = 1.3 Hz, $^4J_{H-F}$ = 1.3 Hz, *k'*), 5.20 (dt, 1H, $^3J_{H-H(trans)}$ = 17.3 Hz, $^2J_{H-H}$ = 1.3 Hz, $^4J_{H-F}$ = 1.3 Hz, *k*), 5.90 (ddd, 1H, $^3J_{H-F}$ = 18.6 Hz, $^3J_{H-H(trans)}$ = 17.3, $^3J_{H-H(cis)}$ = 11.0 Hz, *j*), 6.32 (t, 1H, $^3J_{H-H}$ = 5.3 Hz, *NH*), 7.40 (d, 2H, $^3J_{H-H}$ = 8.0 Hz, *c/d*), 7.72 (d, 2H, $^3J_{H-H}$ = 8.0 Hz, *c/d*); **^{13}C NMR (125 MHz, $CO(CD_3)_2$)** δ = 21.4 (*a*), 26.0 (d, $^2J_{C-F}$ = 24.8 Hz, *i*), 39.3 (d, $^3J_{C-F}$ = 4.7 Hz, *f*), 40.5 (d, $^2J_{C-F}$ = 22.9 Hz, *g*), 95.8 (d, $^1J_{C-F}$ = 169.7 Hz, *h*), 113.9 (d, $^3J_{C-F}$ = 11.4 Hz, *k*), 127.9 (*c/d*), 130.5 (*c/d*), 139.0 (*b/e*), 141.3 (d, $^2J_{C-F}$ = 22.9 Hz, *j*), 143.9 (*b/e*); **^{19}F {^{1}H} NMR (377 MHz, $CO(CD_3)_2$)** δ = -150.38; **IR (neat): ν =**

3283, 2926, 1598, 1333, 900; **HRMS (CI$^+$):** *m/z* required for $C_{13}H_{19}FNO_2S$ ($[M+H]^+$): 272.1121, found 272.1129, Δ = 3.1 ppm.

4.3.4 Synthesis of (±) *N*-(3-fluoro-4-methylpent-4-en-1-yl)-4-methylbenzenesulfonamide (63):

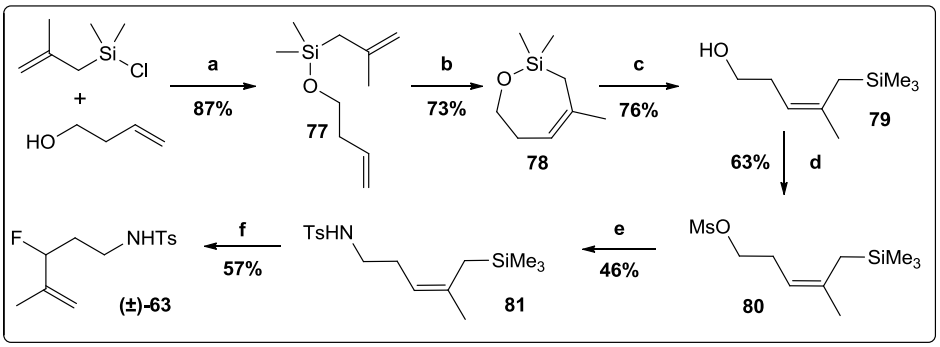

Scheme 4.4: Synthesis of (±) *N*-(3-fluoro-4-methylpent-4-en-1-yl)-4-methylbenzenesulfonamide (**63**); (**a**) NEt_3, CH_2Cl_2, 0 °C, 15 h (**b**) Hoveyda-Grubbs 2nd (2 mol%), CH_2Cl_2, reflux, 90 min (**c**) MeLi, THF, -78 °C, 4 h (**d**) MsCl, NEt_3, CH_2Cl_2, 0 °C, 2 h 30 min (**e**) NH_2Ts, KOH, DMF, 120 °C, 3 h (**f**) Selectfluor, CH_3CN, $NaHCO_3$, r.t, 24 h.

(But-3-enyloxy)dimethyl(2-methylallyl)silane (77):[3]

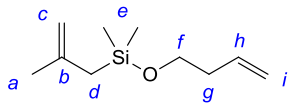

To a solution of **3-buten-1-ol** (0.8 mL, 8.8 mmol, 1 eq.), distilled NEt_3 (2.47 mL, 17.6 mmol, 2 eq.) and DMAP (540 mg, 4.4 mmol, 0.5 eq.) in CH_2Cl_2 (20 mL) was added a solution of chlorodimethyl(2-methylallyl)silane (1.6 g, 10.4 mmol, 1.2 eq.) in CH_2Cl_2 (7 mL) dropwise at 0 °C. The reaction was stirred overnight at r.t. The reaction was quenched by addition of a saturated solution of NH_4Cl(aq), and the different phases were separated. The aqueous phase was extracted with CH_2Cl_2. The combined organic phases were then washed with brine, dried over $MgSO_4$, filtered and the solvent removed *in vacuo* (**caution: volatile compound**). The crude mixture was purified by flash column chromatography on silica gel (petroleum ether 30-40 °C then petroleum ether 30-40 °C/Et_2O: 98/2) to yield the desired silane **77** as a colourless oil (1.6 g, 87%).

R_f = 0.6 (hexane/Et_2O 98:2); **^{1}H NMR (200 MHz, $CDCl_3$) δ** = 0.16 (s, 6H, *e*) 1.64 (d, 2H, $^4J_{H\text{-}H}$ = 0.8 Hz, *d*), 1.76 (m, 3H, *a*), 2.29 (qt, 2H, $^3J_{H\text{-}H}$ = 6.8 Hz, $^4J_{H\text{-}H}$ = 1.3 Hz, *g*), 3.66 (t, 2H, $^3J_{H\text{-}H}$ = 6.8 Hz, *f*), 4.51-4.56 (m, 1H, *c*), 4.61-4.65 (m, 1H, *c'*), 5.00-5.14 (m, 2H, *i*), 5.82 (ddt, 1H, $^3J_{H\text{-}H}$ = 17.1, 10.2, 6.8 Hz, *h*).

2,2,4-trimethyl-2,3,6,7-tetrahydro-1,2-oxasilepine (78):[3]

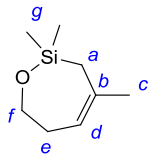

To a solution of **(but-3-enyloxy)dimethyl(2-methylallyl)silane 77** (115.6 mg, 0.6 mmol, 1 eq.) in CH_2Cl_2 (63 mL) at reflux was added Hoveyda-Grubbs 2nd generation catalyst (12 mg, 3 mol%), the reaction was stirred at reflux for 2 h. After cooling to r.t. the solvent was removed *in vacuo* (**caution: volatile compound**).The crude product was purified by column chromatography on a short pad of silica gel (petroleum ether 30-40 °C/Et_2O 95:5) to give the cyclic product **78** as a colourless oil (72 mg, 73%).

R_f = 0.5 (hexane/Et_2O 98:2); **^{1}H NMR (200 MHz, $CDCl_3$) δ** = 0.13 (s, 6H, *g*), 1.60 (s, 2H, *a*), 1.76 (s, 3H, *c*), 2.21-2.32 (m, 2H, *e*), 3.77-3.85 (m, 2H, *f*), 5.44 (td, 1H, $^3J_{H\text{-}H}$ = 7.4 Hz, *d*).

4-methyl-5-(trimethylsilyl)pent-3-en-1-ol (79):[3]

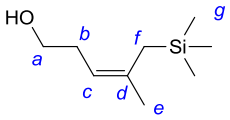

To a solution of **2,2,4-trimethyl-2,3,6,7-tetrahydro-1,2-oxasilepine 78** (426 mg, 2.7 mmol, 1 eq.) in anhydrous THF (14 mL) at -78 °C was added MeLi ([1.6M] in Et_2O, 6.8 mL, 10.9 mmol, 4 eq.) dropwise. The reaction was warmed to 0 °C and stirred at this temperature for 3 h. The reaction was quenched by the addition of a saturated solution of $NH_4Cl_{(aq)}$. The aqueous layer was extracted with Et_2O and the combined organic phases were washed with brine, dried over $MgSO_4$, filtered and the solvent removed *in vacuo* (**caution: volatile compound**). The crude compound was purified by flash column chromatography on silica gel (petroleum ether 30-40 °C/Et_2O 9:1) to give the corresponding alcohol **79** as a colourless oil (360 mg, 76%).

R_f = 0.2 (hexane/Et_2O 8:2); **^{1}H NMR (200 MHz, $(CD_3)_2CO$) δ** = 0.03 (s, 9H, ***g***), 1.56 (s, 2H, *f*), 1.67 (d, 3H, $^4J_{H\text{-}H}$ = 1.3 Hz, *e*), 2.15 (m, 2H, *b*), 3.43-3.53 (m, 3H, *a+OH*), 5.04 (t, 1H, $^3J_{H\text{-}H}$ = 7.0 Hz, *c*).

4-methyl-5-(trimethylsilyl)pent-3-en-1-yl methanesulfonate (80):

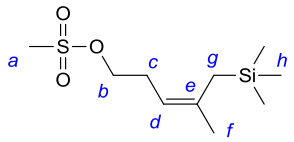

To a stirring solution of **79** (631 mg, 3.6 mmol, 1 eq.) and methanesulfonyl chloride (0.3 mL, 4.4 mmol, 1.2 eq.) in CH_2Cl_2 (19 mL) at 0 °C was added distilled NEt_3 (2.5 mL, 18.3 mmol, 5 eq.) dropwise. The reaction was warmed to r.t. and stirred at this temperature for 2 h 30 min. The reaction was quenched by addition of H_2O and the aqueous layer was extracted three times with CH_2Cl_2, the combined organic phases were washed with brine, dried over $MgSO_4$, filtered and the solvent removed *in vacuo* (**caution : volatile compound**) to give the corresponding mesylate **80** as a colourless oil (584 mg, 64%, *E:Z* = 1:7). The mixture was used for the next step without further purification.

Data for the major (Z) isomer: **R_f =** 0.6 **(**hexane/Et_2O 1:1); **^{1}H NMR (500 MHz, C_6D_6)** δ = -0.03 (s, 9H, *h*), 1.38 (s, 2H, *g*), 1.59 (s, 3H, *f*), 2.11-2.15 (m, 2H, *c*), 2.16 (s, 3H, *a*), 3.84-3.88 (m, 2H, *b*), 4.82 (t, 1H, $^3J_{H\text{-}H}$ = 6.9 Hz, *d*); **^{13}C NMR (125 MHz, C_6D_6)** δ = -0.4 (*h*), 23.8 (*g*), 26.7 (*f*), 29.3 (*c*), 37.1 (*b*), 69.3 (*a*), 116.3 (*d*), 137.4 (*e*).

Identifiable data for the minor (E) isomer: **^{1}H NMR (500 MHz, C_6D_6)** δ = 0.29 (s, 9H, *h*), 1.48 (s, 2H, *g*), 1.74-1.78 (m, 2H, *c*), 3.74-3.78 (m, 2H, *b*); **^{13}C NMR (125 MHz, C_6D6)** δ = -1.7 (*h*).

4-methyl-*N*-[4-methyl-5-(trimethylsilyl)pent-3-en-1-yl]benzene sulfonamide (81):

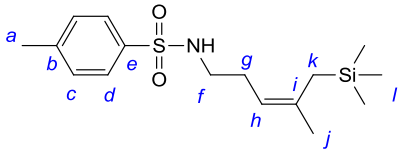

Finely ground potassium hydroxide (86 mg, 1.5 mmol, 1.5 eq) was diluted in anhydrous DMF (2 mL) at 120 °C and tosylamine (264 mg, 1.5 mmol, 1.5 eq) wasadded. The reaction was stirred at this temperature for 30 min until complete dissolution of KOH, after which a solution of **4-methyl-5-(trimethylsilyl)pent-3-en-1-yl methanesulfonate 80** (257 mg, 1.0 mmol) in DMF (2 mL) was added. The reaction was stirred at 120 °C for 3 h. After cooling to r.t. the mixture was diluted with H_2O. Then the aqueous phase was extracted four times with Et_2O. The combined organic phases

were washed three times with H_2O, then brine, dried over $MgSO_4$, filtered and the solvent removed *in vacuo*. The crude compound was purified by flash column chromatography on silica gel (hexane/Et_2O 9:1) to give the corresponding allylsilane **81** as a colourless oil (154 mg, 47%, *E:Z* = >1:20).

Data for the major (Z) isomer: **R_f =** 0.6 (hexane/Et_2O 1:1); **^{1}H NMR (400 MHz, $CDCl_3$)** δ = 0.01 (s, 9H, *l*), 1.44 (s, 2H, *k*), 1.65 (d, 3H, $^4J_{H\text{-}H}$ = 1.3 Hz, *j*), 2.05-2.09 (m, 2H, *g*), 2.44 (s, 3H, *a*), 2.91-2.97 (m, 2H, *f*), 4.38 (t, 1H, $^3J_{H\text{-}H}$ = 6.1 Hz, *NH*), 4.78 (tq, 1H, $^3J_{H\text{-}H}$ = 7.1 Hz, $^4J_{H\text{-}H}$ = 1.0 Hz, *h*), 7.31 (d, 2H, $^3J_{H\text{-}H}$ = 8.1 Hz, *c/d*), 7.75 (d, 2H, $^3J_{H\text{-}H}$ = 8.3 Hz, *c/d*); **^{13}C NMR (101 MHz, $CDCl_3$)** δ = 0.8 (*l*), 21.5 (*a*), 23.5 (*k*), 26.3 (*j*), 28.5 (*g*), 43.0 (*f*), 116.9 (*h*), 127.1 (*c/d*), 129.7 (*c/d*), 137.0 (*b/e*), 137.6 (*i*), 143.3 (*b/e*); **IR (in DCM): ν =** 3054, 1265, 737; **HRMS (CI^+):** *m/z* required for $C_{16}H_{28}NO_2SSi$ ($[M+H]^+$): 326.1610, found 326.1606, Δ = 1.4 ppm; *Identifiable data for the minor (E) isomer:* **^{1}H NMR (400 MHz, $CDCl_3$)** δ = 0.04 (s, 9H, *l*), 1.71-1.73 (m, 3H, *j*), 3.58-3.65 (m, 2H, *f*), 4.97-5.03 (m, 1H, *h*); ^{13}C resonances for the (*E)* isomer could not be distinguished.

(±) *N*-(3-fluoro-4-methylpent-4-en-1-yl)-4-methylbenzene sulfonamide (63):

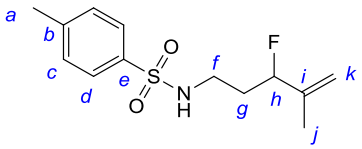

Following the general procedure B on 133 g (0.4 mmol) of **81**, the reaction yielded 64 mg of **63** (57%) as a light yellow oil after flash column chromatography on silica gel (hexane/Et_2O 8:2).

R_f = 0.2 (hexane/Et_2O 6:4); **^{1}H NMR (500 MHz, C_6D_6)** δ = 1.43 (s, 3H, *j*), 1.40-1.61 (m, 2H, *g*), 1.89 (s, 3H, *a*), 2.78-2.89 (m, 2H, *f*), 4.49-4.54 (m, 1H, *NH*), 4.57 (ddd, 1H, $^2J_{H\text{-}F}$ = 48.0 Hz, $^3J_{H\text{-}H}$ = 8.5, 3.8 Hz, *h*), 4.69 (d, 1H, $^2J_{H\text{-}H}$ = 1.6 Hz, *k*), 4.85 (s, 1H, *k'*), 6.79 (d, 2H, $^3J_{H\text{-}H}$ = 7.9 Hz, *c/d*), 7.78 (d, 2H, $^3J_{H\text{-}H}$ = 8.2 Hz, *c/d*); **^{13}C NMR (125 MHz, C_6D_6)** δ = 17.6 (d, $^3J_{C\text{-}F}$ = 3.8 Hz, *j*), 21.4 (*a*), 34.2 (d, $^2J_{C\text{-}F}$ = 21.9 Hz, *g*), 39.9 (d, $^3J_{C\text{-}F}$ = 3.8 Hz, *f*), 93.6 (d, $^1J_{C\text{-}F}$ = 170.7 Hz, *h*), 113.1 (d, $^3J_{C\text{-}F}$ = 9.5 Hz, *k*), 127.8 (*c/d*), 130.1 (*c/d*), 138.6 (*b/e*), 143.3 (d, $^2J_{C\text{-}F}$ = 17.2 Hz, *i*), 143.3 (*b/e*); **^{19}F {^{1}H} NMR (377 MHz, C_6D_6)** δ = -180.54; **IR (neat): ν =** 3441, 3054, 1641, 1422, 1265, 896, 737; **HRMS (CI^+):** *m/z* required for $C_{13}H_{19}FNO_2S$ ($[M+H^+]$): 272.1121, found 272.1133, Δ = 4.6 ppm.

4.3.5 Synthesis of (±) *N*-(3-fluoro-2,2-dimethylpent-4-en-1-yl)-4-methylbenzene sulfonamide (64):

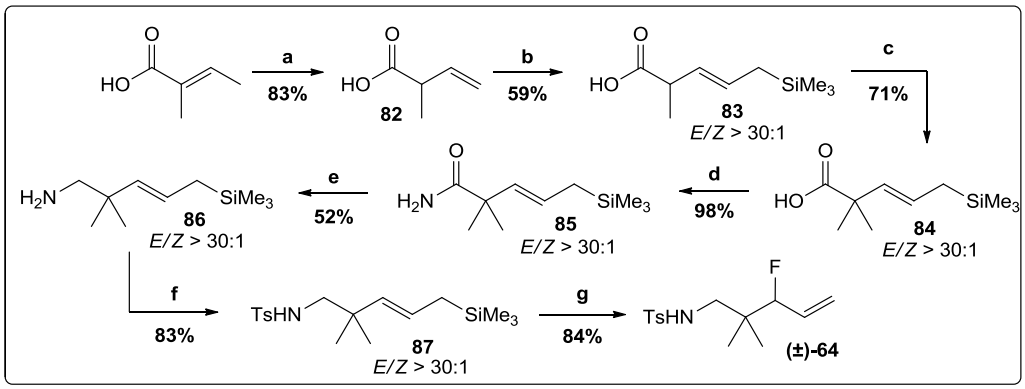

Scheme 4.5: Synthesis of (±) *N*-(3-fluoro-2,2-dimethylpent-4-en-1-yl)-4-methylbenzene sulfonamide (**64**); (**a**) LDA, THF, -78 °C, 1 h; (**b**) allyltrimethylsilane, Hoveyda-Grubbs 2nd (3 mol%), CH_2Cl_2, reflux, 24 h; (**c**) LDA, MeI, THF, -78 °C, 1 h; (**d**) 1,1'-CDI, NH_4OH, DMF, 80 °C, 1 h; (**e**) $LiAlH_4$, THF, r.t, 16 h; (**f**) TsCl, NEt_3, DMAP, CH_2Cl_2, r.t, 3 h; (**g**) Selectfluor, $NaHCO_3$, CH_3CN, r.t, 48 h.

(±) 2-methylbut-3-enoic acid (82):[3]

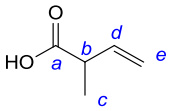

To a stirred solution of di*iso*propylamine (22.5 mL, 160 mmol, 2.25 eq.) in dry THF (75 mL) at -78 °C was added *n*-BuLi ([1.6M] in hexanes, 100 mL, 160 mmol, 2.25 eq.) dropwise. The mixture was stirred at this temperature for 30 min. **Tiglic acid** (7.1 g, 71 mmol, 1 eq.) in THF (45 mL) was then added dropwise to the solution. The mixture was warmed to r.t. and stirred for 1 h. The reaction was then quenched by pouring the crude mixture into a vigorously stirred solution of [3M] HCl at 0 °C. The aqueous layer was extracted with EtOAc. The combined organic phases were washed with brine, dried over $MgSO_4$, filtered and the solvent removed *in vacuo*. The crude product was purified byflash column chromatography on silica gel (hexane/EtOAc 8:2) to yield **82** as a colourless oil (5.9 g, 83%).

R_f = 0.3 (hexane/EtOAc 7:3); **^{1}H NMR (200 MHz, $CDCl_3$) δ** = 1.31 (d, 3H, $^3J_{H\text{-}H}$ = 7.1 Hz, *c*), 3.20 (pt, 1H, $^3J_{H\text{-}H}$ = 7.1 Hz, $^4J_{H\text{-}H}$ = 1.1 Hz, *b*), 5.16 (dt, 1H, $^3J_{H\text{-}H(cis)}$ = 10.2 Hz, $^4J_{H\text{-}H}$ = 1.1, *e*), 5.19 (dt, 1H, $^3J_{H\text{-}H(trans)}$ = 17.2 Hz, $^4J_{H\text{-}H}$ = 1.1 Hz, *e'*), 5.95 (ddd, 1H, $^3J_{H\text{-}H(trans)}$ = 17.2 Hz, $^3J_{H\text{-}H(cis)}$ = 10.2 Hz, $^3J_{H\text{-}H}$ = 7.1 Hz, *d*).

(±) 2-methyl-5-(trimethylsilyl)pent-3-enoic acid (83):[3]

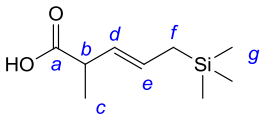

Following the general procedure A on 500 mg (5.0 mmol, 1 eq.) of **2-methylbut-3-enoic acid 82** using Hoveyda-Grubbs 2nd generation catalyst (92 mg, 3 mol%), the reaction yielded 552 mg of **2-methyl-5-(trimethylsilyl)pent-3-enoic acid 83** (59%, *E:Z* = > 30:1) as a yellow oil after flash column chromatography on silica gel (hexane/EtOAc 8:2).

R_f = 0.6 (hexane/EtOAc 6:4); **^{1}H NMR (400 MHz, $CDCl_3$) δ** = 0.00 (s, 9H, *g*) 1.27 (d, 3H, $^3J_{H\text{-}H}$ = 7.0 Hz, *c*), 1.47 (d, 2H, $^3J_{H\text{-}H}$ = 8.2 Hz, *f*), 3.09-3.17 (m, 1H, *b*), 5.33 (dd, 1H, $^3J_{H\text{-}H(trans)}$ = 15.3 Hz, $^3J_{H\text{-}H}$ = 8.0 Hz, *d*), 5.59 (dt, 1H, $^3J_{H\text{-}H(trans)}$ = 15.3 Hz, $^3J_{H\text{-}H}$ = 8.1, *e*).

2,2-dimethyl-5-(trimethylsilyl)pent-3-enoic acid (84):[3]

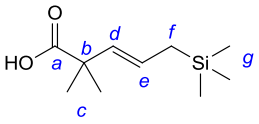

To a solution of di*iso*propylamine (1.2 mL, 8.6 mmol, 2.2 eq.) in THF (10 mL) at -78 °C was added *n*-BuLi ([2.0M] in hexanes, 4.4 mL, 2.2 eq.). The mixture was stirred at -78 °C for 30 min. **2-Methyl-5-(trimethylsilyl)pent-3-enoic acid 83** (738 mg, 3.8 mmol, 1 eq.) in THF (10 mL) was added dropwise to the mixture. The reaction was warmed to 0 °C and stirred at this temperature for 30 min; the reaction was then cooled to -78 °C. Methyl iodide (0.5 mL, 7.9 mmol, 2 eq.) was added and the reaction was stirred at -78 °C for 30 min followed by 1 h at r.t. The reaction was then quenched with saturated NH_4Cl solution, the aqueous layer was extracted with EtOAc. The combined organic phases were dried over $MgSO_4$, filtered and the solvent removed *in vacuo*. The crude product was purified by flash column chromatography on silica gel (hexane/Et_2O 8:2) to yield **84** as a brown oil (560 mg, 71%, *E:Z* = > 30:1).

R_f = 0.4 (hexane/Et_2O 7:3); **^{1}H NMR (400 MHz, $CDCl_3$) δ** = -0.01 (s, 9H, *g*), 1.29 (s, 6H, *c*), 1.46 (d, 2H, $^3J_{H\text{-}H}$ = 7.0 Hz, *f*), 5.45-5.58 (m, 2H, *d+e*).

2,2-dimethyl-5-(trimethylsilyl)pent-3-enamide (85):

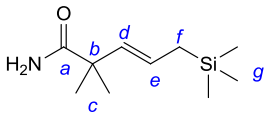

To a solution of **84** (300 mg, 1.5 mmol, 1 eq.) in dry DMF (5 mL) at r.t. was added 1,1'-carbonyldiimidazole (370 mg, 2.3 mmol, 1.5 eq.) portionwise. The solution was stirred at r.t. for 30 min, and heated at 40 ºC for 5 h. It was then treated with a concentrated NH_4OH solution (0.5 mL) in DMF (1 mL) and heated at 80 ºC for 30 min. The mixture was cooled at 0 ºC and quenched with [1M] HCl (11 mL) and extracted with CH_2Cl_2. The combined organic layers were washed with brine, dried over $MgSO_4$ and the solvent removed *in vacuo*. Purification of the resulting residue by flash column chromatography on silica gel (hexane/Et_2O 1:9) yielded **2,2-dimethyl-5-(trimethylsilyl)pent-3-enamide 85** as a white solid (320 mg, 98 % yield, *E:Z* = > 30:1).

Data for the major (E) isomer: **R_f** = 0.5 (Hexane/Et_2O 1:9); **m.p.** = 91 °C; **^{1}H NMR (400 MHz, $CDCl_3$)** δ = -0.01 (s, 9H, *g*), 1.25 (s, 6H, *c*), 1.48 (d, 2H, $^3J_{H\text{-}H}$ = 7.9 Hz, *f*), 5.44 (d, 1H, $^3J_{H\text{-}H(trans)}$ = 15.6 Hz, *d*), 5.61 (dt, 1H, $^3J_{H\text{-}H(trans)}$ = 15.6 Hz, $^3J_{H\text{-}H}$ = 7.9 Hz, *e*), 5.75 (sbr, 1H, *NH*), 6.14 (sbr, 1H, *NH*); **^{13}C NMR (101 MHz, $CDCl_3$)** δ = -2.0 (*g*), 22.9 (*f*), 25.5 (*c*), 44.4 (*b*), 126.6 (*d*), 133.3 (*e*), 180.3 (*a*); **IR (KBr): ν =** 3481, 3406, 2957, 1674, 1249, 910, 849, 734; **HRMS (CI^+):** *m/z* required for $C_{10}H_{22}NOSi$ ($[M+H]^+$): 200.1471, found 200.1472, Δ = 1.5 ppm.

2,2-dimethyl-5-(trimethylsilyl)pent-3-en-1-amine (86):

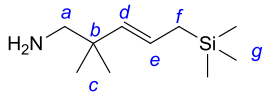

To a solution of **2,2-dimethyl-5-(trimethylsilyl)pent-3-enamide 85** (270 mg, 1.3 mmol, 1 eq.) in dry THF (15 mL) was added $LiAlH_4$ (100 mg, 2.7 mmol, 2 eq.), the mixture was stirred at r.t. overnight and then refluxed for 2 h. H_2O was added carefully to the mixture and extracted with Et_2O. The combined organic layers were washed with brine, dried over $MgSO_4$ and the solvent removed *in vacuo*. Purification of the resulting residue by flash column chromatography on deactivated silica gel (Et_2O/Et_3N 99:1) yielded **2,2-dimethyl-5-(trimethylsilyl)pent-3-en-1-amine 86** as a yellow oil (130 mg, 52 % yield, *E:Z* = > 30:1).

Data for the major (E) isomer: **R_f** = 0.4 (Et_2O/Et_3N 1%); **^{1}H NMR (500 MHz, $CDCl_3$)** δ = -0.10 (s, 9H, *g*), 0.86 (s, 6H, *c*), 1.36 (d, 2H, $^3J_{H\text{-}H}$ = 7.8 Hz, *f*), 2.35 (s, 2H, *a*), 5.05 (d, 1H, $^3J_{H\text{-}H(trans)}$ = 15.6 Hz, *d*), 5.26 (dt, 1H, $^3J_{H\text{-}H(trans)}$ = 15.6 Hz, $^3J_{H\text{-}H}$ = 7.8 Hz, *e*); **^{13}C NMR (125 MHz, $CDCl_3$)** δ = -2.2 (*g*), 22.7 (*f*), 24.9 (*c*), 37.8 (*b*), 53.4 (*a*), 124.1 (*d*), 136.1 (*e*); **IR (neat): ν =** 2956, 1470, 1248, 972, 853; **HRMS (CI^+):** *m/z* required for $C_{10}H_{24}NSi$ ($[M+H]^+$): 186.1678, found 186.1673, Δ = 0.5 ppm.

***N*-[2,2-dimethyl-5-(trimethylsilyl)pent-3-en-1-yl]-4-methylbenzene sulfonamide (87):**

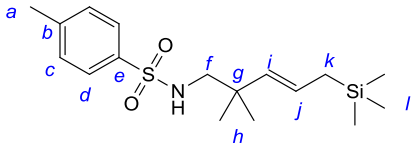

To a solution of **2,2-dimethyl-5-(trimethylsilyl)pent-3-en-1-amine 86** (130 mg, 0.7 mmol, 1 eq.), Et_3N (0.15 mL. 1.1 mmol, 1.5 eq.) and DMAP (20 mg, 0.2 mmol, 0.3 eq.) in dry CH_2Cl_2 (5 mL) was added tosylchloride (160 mg, 0.8 mmol, 1.2 eq.) and the mixture was stirred at r.t. for 3 h. Then the reaction was quenched with H_2O and extracted with AcOEt. The combined organic layers were washed with brine, dried over $MgSO_4$ and the solvent removed *in vacuo*. Purification of the resulting residue by flash column chromatography on silica gel (hexane/AcOEt 9:1) yielded **87** as a white solid (198 mg, 83 % yield, *E:Z* = > 30:1).

Data for the major (E) isomer: **R_f** = 0.3 (hexane/AcOEt 9:1); **m.p. =** 64 °C; **^{1}H NMR (400 MHz, $CDCl_3$)** δ = -0.03 (s, 9H, *l*), 0.95 (s, 6H, *h*), 1.39 (d, 2H, $^3J_{H\text{-}H}$ = 7.8 Hz, *k*), 2.42 (s, 3H, *a*), 2.68 (d, 2H, $^3J_{H\text{-}H}$ = 6.3 Hz, *f*), 4.40 (t, 1H, $^3J_{H\text{-}H}$ = 6.3 Hz, *NH*), 5.00 (d, 1H, $^3J_{H\text{-}H(trans)}$ = 15.7 Hz, *i*), 5.35 (dt, 1H, $^3J_{H\text{-}H(trans)}$ = 15.7, $^3J_{H\text{-}H}$ = 7.8 Hz, *j*), 7.30 (d, 2H, $^3J_{H\text{-}H}$ = 8.1 Hz, *c/d*), 7.72 (d, 2H, $^3J_{H\text{-}H}$ = 8.1 Hz, *c/d*); **^{13}C NMR (101 MHz, $CDCl_3$)** δ = -2.1 (*l*), 21.4 (*a*), 22.8 (*k*), 25.3 (*h*), 36.5 (*g*), 53.1 (*f*), 126.0 (*i*), 127.0 (*c/d*), 129.6 (*c/d*), 134.4 (*j*), 136.8 (*b/e*), 143.1 (*b/e*); **IR (KBr): ν** = 3386, 2957, 1329, 1248, 854; **HRMS (CI^+):** *m/z* required for $C_{17}H_{30}NO_2SSi$ ($[M+H]^+$): 340.1767, found 340.1760, Δ = 4.5 ppm.

(±) *N*-(3-fluoro-2,2-dimethylpent-4-en-1-yl)-4-methylbenzene sulfonamide (64):

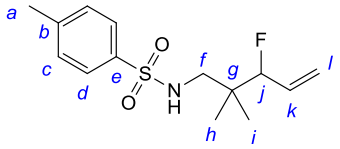

Following the general procedure B on 180 mg (0.5 mmol) of **87**, the reaction yielded 120 mg of **64** (84 %) as a white solid after flash column chromatography on silica gel (hexane/Et_2O 1:1).

R_f = 0.3 (hexane/Et_2O 6:4); **m.p. =** 81 °C; **^{1}H NMR (400 MHz, $CDCl_3$)** δ = 0.89 (d, 3H, $^4J_{H\text{-}F}$ = 0.8 Hz, *h/i*), 0.90 (d, 3H, $^4J_{H\text{-}F}$ = 1.3 Hz, *h/i*), 2.43 (s, 3H, *a*), 2.79 (dd, 1H, $^2J_{H\text{-}H}$ = 12.6 Hz, $^3J_{H\text{-}H}$ = 7.1 Hz, *f*), 2.88 (dd, 1H, $^2J_{H\text{-}H}$ = 12.6 Hz, $^3J_{H\text{-}H}$ = 6.6 Hz, *f'*), 4.62 (ddt, 1H, $^2J_{H\text{-}F}$ = 47.5 Hz, $^3J_{H\text{-}H}$ = 6.3 Hz, $^4J_{H\text{-}H}$ = 1.3 Hz, *j*), 4.93 (dd, 1H, $^3J_{H\text{-}H}$ = 7.1, 6.6 Hz, *NH*), 5.30 (dd, 1H, $^3J_{H\text{-}H(cis)}$ =10.9 Hz, $^2J_{H\text{-}H}$ = 1.5 Hz, *l*), 5.31 (dddd, 1H, $^3J_{H\text{-}H(trans)}$ = 17.2 Hz, $^4J_{H\text{-}F}$ = 3.1 Hz, $^2J_{H\text{-}H}$ = 1.5 Hz, $^4J_{H\text{-}H}$ = 1.3 Hz, *l'*), 5.83 (dddd, 1H, $^3J_{H\text{-}H(trans)}$ = 17.2 Hz, $^3J_{H\text{-}F}$ = 15.9 Hz, $^3J_{H\text{-}H(cis)}$ = 10.9 Hz, $^3J_{H\text{-}H}$ = 6.3 Hz, *k*), 7.31 (d, 2H, $^3J_{H\text{-}H}$ = 8.4 Hz, *c/d*), 7.75 (d, 2H, $^3J_{H\text{-}H}$ = 8.4 Hz, *c/d*); **^{13}C NMR (101 MHz, $CDCl_3$)** δ = 20.0 (d, $^3J_{C\text{-}F}$ = 3.2 Hz, *h/i*), 21.5 (*a*), 21.5 (d, $^3J_{C\text{-}F}$ = 6.4 Hz, *h/i*), 38.1 (d, $^2J_{C\text{-}F}$ = 19.2 Hz, *g*), 50.4 (d, $^3J_{C\text{-}F}$ = 3.2 Hz, *f*), 98.1 (d, $^1J_{C\text{-}F}$ = 174.2 Hz, *j*), 119.4 (d, $^3J_{C\text{-}F}$ = 12.8 Hz, *l*), 127.0 (*c/d*), 129.7 (*c/d*), 132.1 (d, $^2J_{C\text{-}F}$ = 19.2 Hz, *k*), 136.9 (*b/e*), 143.3 (*b/e*); **^{19}F {^{1}H} NMR (377 MHz, $CDCl_3$)** δ = -186.10; **IR (KBr): ν =** 3418, 2975, 1644, 1427, 1326, 1161, 664; **HRMS (CI^+):** *m/z* required for $C_{14}H_{24}N_2O_2FS$ ($[M+NH_4^+]$): 303.1543, found 303.1549, Δ = 3.5 ppm.

4.3.6 Synthesis of (±) 3-fluoro-2,2-dimethyl-*N*-tosylpent-4-enamide (66):

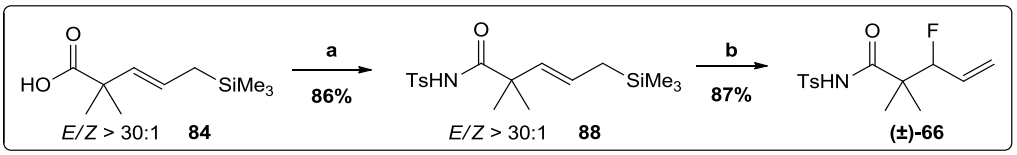

Scheme 4.6: Synthesis of (±) 3-fluoro-2,2-dimethyl-*N*-tosylpent-4-enamide (**66**); **a**) *p*-tosyl isocyanate, NEt_3, THF, 1 h; **b**) Selectfluor, $NaHCO_3$, CH_3CN, 48 h.

2,2-dimethyl-*N*-tosyl-5-(trimethylsilyl)pent-3-enamide (88):

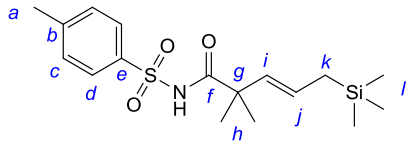

To a solution of acid **84** (502 mg, 2.5 mmol, 1 eq.) in dry THF (5 mL) under argon was added *p*-tosyl isocyanate (0.4 mL, 2.5 mmol, 1 eq.) from a freshly opened bottle. After stirring at r.t for 10 min, the inert atmosphere was disconnected and distilled NEt_3 (0.35 mL, 2.5 mmol, 1 eq.) was added dropwise to the open flask allowing the release of CO_2. The solution was left stirring at r.t for 1 h. The mixture was then diluted with an equal volume of EtOAc, washed twice with [2M] HCl and brine, dried over $MgSO_4$, filtered and the solvent removed *in vacuo*. The crude product was purified by flash chromatography on silica gel (hexane/Et_2O 9:1) to give **88** as a white solid (760 mg, 86%, *E:Z* = > 30:1).

Data for the major (E) isomer: **R_f** = 0.4 (hexane/Et_2O 6:4); **m.p. =** 81 °C; **^{1}H NMR (400 MHz, $CDCl_3$)** δ = 0.00 (s, 9H, *l*), 1.19 (s, 6H, *h*), 1.49 (d, 2H, $^3J_{H\text{-}H}$ = 8.2 Hz, *k*), 2.44 (s, 3H, *a*), 5.29 (d, 1H, $^3J_{H\text{-}H(trans)}$ = 15.7 Hz, *i*), 5.61 (dt, 1H, $^3J_{H\text{-}H(trans)}$ = 15.7 Hz, $^3J_{H\text{-}H}$ = 8.2 Hz, *j*), 7.33 (d, 2H, $^3J_{H\text{-}H}$ = 8.2 Hz, *c/d*), 7.92 (d, 2H, $^3J_{H\text{-}H}$ = 8.2 Hz, *c/d*), 8.30 (s, 1H, *NH*); **^{13}C NMR (101 MHz, $CDCl_3$)** δ = -2.0 (*l*), 21.6 (*a*), 23.2 (*k*), 24.8 (*h*), 45.7 (*g*), 128.3 (*c/d*), 129.5 (*c/d*), 129.6 (*j*), 130.9 (*i*), 135.4 (*b/e*), 144.9 (*b/e*), 174.5 (*f*); **IR (KBr): ν =** 3311, 2953, 1706, 1411, 1248, 1165, 974, 849, 660, 568; **HRMS (ESI^+):** *m/z* required for $C_{17}H_{28}NO_3SSi^+$ ($[M+H]^+$): 354.1550, found 354.1554, Δ = 1.5 ppm.

(±) 3-fluoro-2,2-dimethyl-*N*-tosylpent-4-enamide (66):

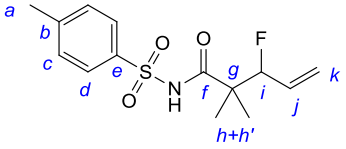

Following the general procedure B on 300 mg (0.85 mmol) of **88**, the reaction yielded 222 mg of **66** (87%) as a white solid after flash column chromatography on silica gel (hexane/Et_2O 8:2).

R_f = 0.4 (hexane/EtOAc 7:3); **m.p. =** 115 °C; **^{1}H NMR (400 MHz, $CDCl_3$)** δ = 1.11 (s, 3H, *h*), 1.21 (s, 3H, *h'*), 2.44 (s, 3H, *a*), 4.77 (ddt, 2H, $^2J_{H\text{-}F}$ = 47.5 Hz, $^3J_{H\text{-}H}$ = 6.6 Hz, $^4J_{H\text{-}H}$ = 1.0 Hz, *i*), 5.26 (dt, 1H, $^3J_{H\text{-}H(cis)}$ = 10.6, $^2J_{H\text{-}H}$ = 1.0 Hz, $^4J_{H\text{-}H}$ = 1.0 Hz, *k'*), 5.31 (ddt, 1H, $^3J_{H\text{-}H(trans)}$ = 17.2 Hz, $^4J_{H\text{-}F}$ = 3.0

Hz, $^{2}J_{H\text{-}H}$ = 1.0 Hz, $^{4}J_{H\text{-}H}$ = 1.0 Hz, *k*), 5.63 (dddd, 1H, $^{3}J_{H\text{-}H(trans)}$ = 17.2 Hz, $^{3}J_{H\text{-}F}$ = 15.1 Hz, $^{3}J_{H\text{-}H(cis)}$ = 10.6 Hz, $^{3}J_{H\text{-}H}$ = 6.6 Hz, *j*), 7.34 (d, 2H, $^{3}J_{H\text{-}H}$ = 8.0 Hz, *c/d*), 7.93 (d, 2H, $^{3}J_{H\text{-}H}$ = 8.0 Hz, *c/d*), 8.61 (sbr, 1H, *NH*); **^{13}C NMR (101 MHz, $CDCl_3$)** δ = 19.7 (d, $^{3}J_{C\text{-}F}$ = 4.8 Hz, *h*), 21.6 (d, $^{3}J_{C\text{-}F}$ = 5.6 Hz, *h'*), 21.6 (*a*), 47.3 (d, $^{2}J_{C\text{-}F}$ = 20.0 Hz, *g*), 97.1 (d, $^{1}J_{C\text{-}F}$ = 175.0 Hz, *i*), 121.0 (d, $^{3}J_{C\text{-}F}$ = 12.8 Hz, *k*), 128.4 (*c/d*), 129.5 (*c/d*), 130.5 (d, $^{2}J_{C\text{-}F}$ = 19.2 Hz, *j*), 135.3 (*b/e*), 145.0 (*b/e*), 172.3 (*f*); **^{19}F {^{1}H} NMR (377 MHz, $CDCl_3$)** δ = -180.20; **IR (KBr): ν =** 3285, 2989, 1714, 1409, 1168, 1087, 660, 545; **HRMS (ESI^+):** *m/z* required for $C_{14}H_{18}NO_3FSNa^+$ ($[M+Na]^+$): 322.0884, found 322.0883, Δ = 0.1 ppm.

4.3.7 Synthesis of (±) 3-fluoro-*N*-tosylpent-4-enamide (65):

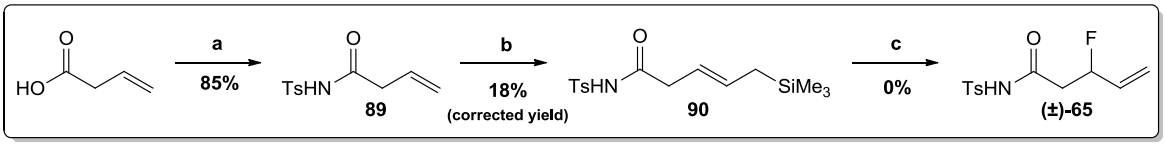

Scheme 4.7: Synthesis of (±) 3-fluoro-*N*-tosylpent-4-enamide (**65**); **a**) tosylisocyanate, NEt_3, THF, 1 h; **b**) allyltrimethylsilane, Grubbs 2nd (5 mol%), 1,4-benzoquinone, CH_2Cl_2, reflux, 4 days; **c**) Selectfluor, $NaHCO_3$, CH_3CN, r.t., 6 days.

***N*-tosylbut-3-enamide (89)**:

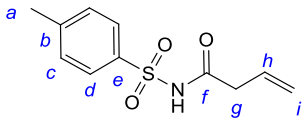

To a solution of acid **but-3-enoic acid** (1 g, 11.6 mmol, 1 eq.) in dry THF under argon was added *p*-tosyl isocyanate (1.8 mL, 11.6 mmol, 1 eq.) from a freshly opened bottle. After stirring at r.t for 10 min, the inert atmosphere was disconnected and distilled NEt_3 (1.6 mL, 2.5 mmol, 1 eq.) was added dropwise to the open flask allowing the release of CO_2. The solution was left stirring at r.t for 1 h. The mixture was then diluted with an equal volume of EtOAc, washed twice with [2M] HCl and brine, dried over $MgSO_4$, filtered and the solvent removed *in vacuo*. The crude product was purified by flash chromatography on silica gel (hexane/Et_2O 9:1) to give **89** as a white solid (2.3 g, 85%).

R_f = 0.1 (hexane/Et_2O 6:4); **^{1}H NMR (200 MHz, $CDCl_3$)** δ = 2.44 (s, 3H, *a*), 3.06 (d, 2H, $^{3}J_{H\text{-}H}$ = 6.9 Hz, *g*), 5.20 (dd, 1H, $^{3}J_{H\text{-}H(cis)}$ = 3.3 Hz, $^{2}J_{H\text{-}H}$ = 1.3 Hz, *i*), 5.19 (ddd, 1H, $^{3}J_{H\text{-}H(trans)}$ = 23.9 Hz, $^{4}J_{H\text{-}H}$ = 2.7 Hz, $^{2}J_{H\text{-}H}$ = 1.3 Hz, *i'*), 5.82 (ddd,1H, $^{3}J_{H\text{-}H(trans)}$ = 23.9 Hz, $^{3}J_{H\text{-}H}$ = 6.9 Hz, $^{3}J_{H\text{-}H(cis)}$ = 3.3 Hz, *h*), 7.34 (d, 2H, $^{3}J_{H\text{-}H}$ = 8.2 Hz, *c/d*), 7.95 (d, 2H, $^{3}J_{H\text{-}H}$ = 8.2 Hz, *c/d*), 9.06 (sbr, 1H, *NH*); **^{13}C NMR (50**

MHz, $CDCl_3$) δ = 21.6 (*a*), 41.0 (*g*), 120.8 (*i*+*i'*), 128.3 (*c/d*), 128.7 (*h*), 129.6 (*c/d*), 135.2 (*b/e*), 145.2 (*b/e*), 168.9 (*f*); **ν_{max}/cm^{-1} (neat):** 3110, 1691, 1454, 1332, 1137, 1088, 856, 811, 657; **HRMS (ESI^+):** *m/z* required for $C_{11}H_{13}NO_3SNa$ ($[M+Na]^+$): 262.0508, found 262.0512, Δ = 1.5 ppm.

***N*-tosyl-5-(trimethylsilyl)pent-3-enamide (90):**

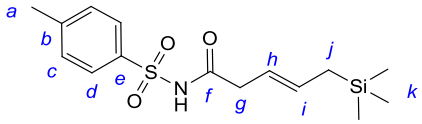

Following the general procedure A on 500 mg (2.1 mmol, 1 eq.) of ***N*-tosylbut-3-enamide 89**, the reaction yielded 334.9 mg of a mixture ***N*-tosyl-5-(trimethylsilyl)pent-3-enamide 90** (obtained in 18% yield after correction *E:Z* = 3:1) and the truncated product of isomerisation ***N*-tosyl-4-(trimethylsilyl)but-2-enamide** as a yellow oil after flash column chromatography on silica gel (hexane/Et_2O 95:5 then 9:1).

Data for the major (E) isomer: **R_f** = 0.2 (hexane/Et_2O 6:4); **^{1}H NMR (400 MHz, $CDCl_3$)** δ = -0.03 (s, 9H, *k*), 1.45 (d, 2H, $^3J_{H\text{-}H}$ = 8.3 Hz, *j*), 2.44 (s, 3H, *a*), 2.97 (d, 2H, $^3J_{H\text{-}H}$ = 7.1 Hz, *g*), 5.23 (dt, 1H, $^3J_{H\text{-}H(trans)}$ = 15.4 Hz, $^3J_{H\text{-}H}$ = 7.1 Hz, *h*), 5.59 (dt, 1H, $^3J_{H\text{-}H(trans)}$ = 15.4 Hz, $^3J_{H\text{-}H}$ = 8.3 Hz, *i*), 7.33 (d, 2H, $^3J_{H\text{-}H}$ = 8.2 Hz, *c/d*), 7.95 (d, 2H, $^3J_{H\text{-}H}$ = 8.2 Hz, *c/d*), 8.79 (sbr, 1H, *NH*); **^{13}C NMR (101 MHz, $CDCl_3$)** δ = -2.0 (*k*), 21.6 (*a*), 23.2 (*j*), 40.5 (*g*), 118.0 (*i*), 128.3 (*c/d*), 129.5 (*c/d*), 134.5 (*h*), 135.4 (*b/e*), 145.0 (*b/e*), 169.5 (*f*); **IR (in DCM): ν =** 3270, 1722, 1436, 1174, 1087, 853, 739; **HRMS (ESI^+):** *m/z* required for $C_{15}H_{23}NO_3SSiNa$ ($[M+Na]^+$): 348.1060, found 348.1065, Δ = 1.4 ppm.

Identifiable data for the minor (Z) isomer: **^{1}H NMR (400 MHz, $CDCl_3$)** δ = -0.04 (s, 9H, *k*), 1.43 (d, 2H, $^3J_{H\text{-}H}$ = 9.0 Hz, *j*), 3.01 (d, 2H, $^3J_{H\text{-}H}$ = 7.3 Hz, *g*), 5.35 (dt, 1H, $^3J_{H\text{-}H(cis)}$ = 10.6 Hz, $^3J_{H\text{-}H}$ = 7.3 Hz, *h*), 5.72 (dt, 1H, $^3J_{H\text{-}H(cis)}$ = 10.6 Hz, $^3J_{H\text{-}H}$ = 9.0 Hz, *i*); **^{13}C NMR (100 MHz, $CDCl_3$)** δ = -1.94 (*k*), 19.0 (*j*), 34.8 (*g*), 116.4 (*i*), 132.7 (*h*);

Identifiable data for the truncated side product N-tosyl-4-(trimethylsilyl)but-2-enamide:

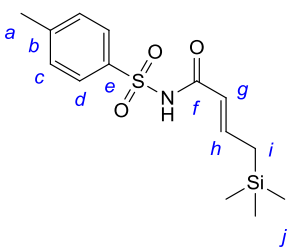

^{1}H NMR (400 MHz, $CDCl_3$) δ = -0.00 (s, 9H, *j*), 1.73 (dd, 2H, $^3J_{H\text{-}H}$ = 9.0 Hz, $^4J_{H\text{-}H}$ = 1.0 Hz, *i*), 5.69 (d, 1H, $^3J_{H\text{-}H}$ = 15.0 Hz, *g*), 7.09 (dt, 1H, $^3J_{H\text{-}H}$ =

15.0 Hz, $^{3}J_{H\text{-}H}$ = 9.0 Hz, *h*); **^{13}C NMR (101 MHz, CDCl$_3$)** δ = -1.90 (*j*), 25.6 (*i*), 118.5 (*h*), 128.3 (*c/d*), 128.4 (*c/d*), 135.8 (*b/e*), 144.9 (*b/e*), 150.3 (*g*), 163.3 (*f*);

4.3.8 Synthesis of (±) *N*-(1-(benzyloxy)-4-fluorohex-5-en-2-yl)-4-methylbenzene sulfonamide (*syn*-67) and (*anti*-67):

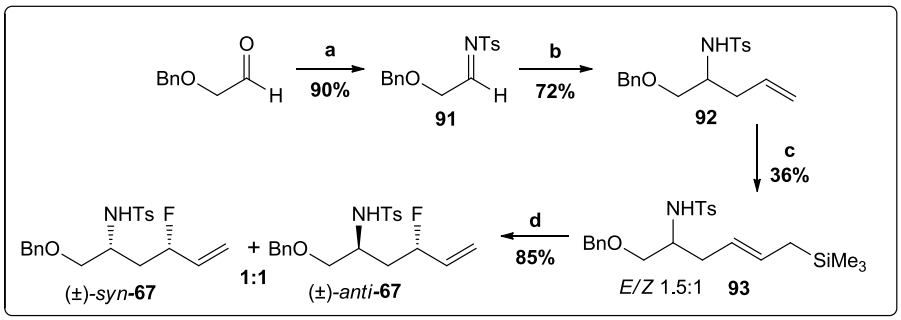

Scheme 4.8: Synthesis of (±) *N*-(1-(benzyloxy)-4-fluorohex-5-en-2-yl)-4-methylbenzene sulphonamide (*syn*- and *anti*-**67**); (**a**) tosyl amine, sodium toluene sulfimide, formic acid, H_2O, 24 h. (**b**) allylmagnesium bromide ([1M] in Et_2O), CH_2Cl_2, -78 °C, 5 h. (**c**) allyltrimethylsilane, Grubbs 2nd (5 mol%), 1,4-benzoquinone, CH_2Cl_2, reflux, 3 days; (**d**) Selectfluor, $NaHCO_3$, CH_3CN, 48 h.

N-(2-(benzyloxy)ethylidene)-4-methylbenzenesulfonamide (91):[4]

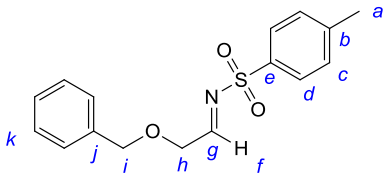

Benzyloxyacetaldehyde (962 mg, 6.4 mmol, 1 eq.) was added to tosyl amine (1.1 g, 6.4 mmol, 1 eq.), sodium *p*-tolenesulfinate (1.1 g, 6.4 mmol, 1 eq.) in formic acid (95%, 10 mL) and H_2O (10 mL) and the mixture was stirred for 24 h at r.t. The resulting white precipitate was collected by filtration, washed successively with H_2O and hexane, then dissolved in CH_2Cl_2 followed by addition of H_2O and a saturated solution of $NaHCO_{3(aq)}$. The solution was well stirred for 10 min at r.t. The organic phase was collected; the aqueous phase was extracted with CH_2Cl_2. The combined organic layers were dried over $MgSO_4$, concentrated *in vacuo* to yield the corresponding *N*-sulfonyl imine **91** as a colorless oil (1.75 g, 90%). This material was used without further purification.

[4] This compound was prepared according to the procedure reported by Y-Q. Wang, J. Song, R. Hong, H. Li, L. Deng, *J. Am. Chem. Soc.* **2006**, *128*, 8156-8157 and F. Chemla, V. Hebbe, J.-F. Normant, *Synthesis* **2000**, 75-77. Analytical and spectroscopic data were in agreement with those reported wherein.

^{1}H NMR (400 MHz, $CDCl_3$) δ = 2.45 (s, 3H, *a*), 4.35 (d, 2H, $^{3}J_{H\text{-}H}$ = 3.1 Hz, *h*), 4.60 (s, 2H, *i*), 7.28-7.39 (m, 7H, *c/d+k*), 7.82 (d, 2H, $^{3}J_{H\text{-}H}$ = 7.8 Hz, *c/d*), 8.56 (t, 1H, $^{3}J_{H\text{-}H}$ = 3.1 Hz, *f*).

(±) *N*-(1-(benzyloxy)pent-4-en-2-yl)-4-methylbenzenesulfonamide (92):

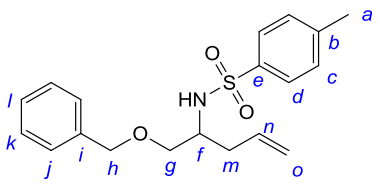

To a solution of ***N*-(2-(benzyloxy)ethylidene)-tosylamine 91** (1.7 g, 5.7 mmol, 1 eq.) in dry CH_2Cl_2 (30 mL) cooled at -78 °C was added dropwise allylmagnesium bromide ([1M] in Et_2O, 17 mL, 17.1 mmol, 3 eq.). The reaction was stirred at this temperature for 5 h and slowly warmed to r.t. A saturated solution of NH_4Cl (20 mL) was added and the resulting mixture was extracted three times with Et_2O. The combined organic phases were washed with brine, dried over Na_2SO_4, filtered and the solvent removed *in vacuo*. The crude product was purified by flash column chromatography on silica gel (hexane/EtOAc 9:1) to give the corresponding tosyl homoallylic amine **92** as a colourless oil (1.4 g, 72%).

R_f = 0.7 (hexane/EtOAc 7:3); **^{1}H NMR (400 MHz, $CDCl_3$)** δ = 2.23-2.29 (m, 2H, *m*), 2.39 (s, 3H, *a*), 3.21-3.26 (m, 1H, *f*), 3.34-3.42 (m, 2H, *g*), 4.35 (s, 2H, *h*), 4.89 (d, 1H, $^{3}J_{H\text{-}H}$ = 7.3 Hz, *NH*), 4.94-5.01 (m, 2H, *o*), 5.54 (ddt, 1H, $^{3}J_{H\text{-}H}$ = 20.7, 9.6, 7.3 Hz, *n*), 7.18-7.35 (m, 7H, *c/d+k+j+l*), 7.70 (d, 2H, $^{3}J_{H\text{-}H}$ = 8.3 Hz, *c/d*); **^{13}C NMR (101 MHz, $CDCl_3$)** δ = 21.5 (*a*), 36.6 (*m*), 52.8 (*f*), 70.5 (*g*), 73.1 (*h*), 118.4 (*o*), 127.0 (*c/d/j/k/l*), 127.5 (*c/d/j/k/l*), 127.7 (*c/d/j/k/l*), 128.3 (*c/d/j/k/l*), 129.5 (*c/d/j/k/l*), 135. 5 (*n*), 137.6 (*b/e/i*), 137.7 (*b/e/i*), 143.2 (*b/e/i*); **IR (neat): ν** = 3281, 2865, 1495, 1161, 1093, 996, 815, 666; **HRMS (ESI^+):** *m/z* required for $C_{19}H_{23}NO_3SNa^+$ ($[M+Na]^+$): 368.1295, found 368.1291, Δ = 1.2 ppm.

(±) *N*-(1-(benzyloxy)-6-(trimethylsilyl)hex-4-en-2-yl)-4-methylbenzene sulfonamide (93):

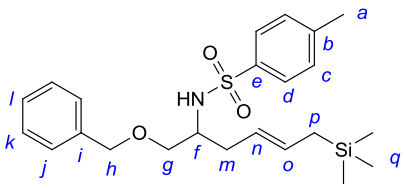

Following the general procedure A on 500 mg (1.45 mmol) of ***N*-(1-(benzyloxy)pent-4-en-2-yl)-4-methylbenzenesulfonamide 92**, the reaction yielded 225 mg of a mixture of isomers **93** (36%, *E:Z* = 1.5:1) as a colourless oil after flash column chromatography on silica gel (hexane/Et_2O 9:1 then 7:3).

Data for the major (E) isomer: **R_f** = 0.7 (hexane/EtOAc 7:3); **^{1}H NMR (400 MHz, $CDCl_3$)** δ = -0.03 (sbr, 9H, *q*), 1.35 (d, 2H, $^3J_{H\text{-}H}$ = 8.1 Hz, *p*), 2.18-2.24 (m, 2H, *m*), 2.42 (s, 3H, *a*), 3.25-3.31 (m, 1H, *g*), 3.31-3.39 (m, 1H, *f*), 3.39-3.45 (m, 1H, *g'*), 4.38 (sbr, 2H, *h*), 4.82 (d, 1H, $^3J_{H\text{-}H}$ = 7.3 Hz, *NH*), 4.98 (dt, 1H, $^3J_{H\text{-}H(trans)}$ = 15.2 Hz, $^3J_{H\text{-}H}$ = 7.3 Hz, *n*), 5.38 (dt, 1H, $^3J_{H\text{-}H(trans)}$ = 15.2, $^3J_{H\text{-}H}$ = 8.1 Hz, *o*), 7.22-7.38 (m, 7H, *c/d+k+j+l*), 7.73 (d, 2H, $^3J_{H\text{-}H}$ = 8.3 Hz, *c/d*); **^{13}C NMR (101 MHz, $CDCl_3$)** δ = -2.0 (*q*), 21.4 (*a*), 22.9 (*p*), 35.4 (*m*), 53.2 (*f*), 70.5 (*g*), 73.0 (*h*), 122.8 (*n*), 127.0 (*c/d*), 127.5 (*j/k/l*), 127.7 (*j/k/l*), 128.3 (*j/k/l*), 129.5 (*c/d*), 130.9 (*o*), 137.7 (*b/e/i*), 137.8 (*b/e/i*), 143.1 (*b/e/i*); **IR (neat): ν** = 3283, 2951, 1331, 1247, 1161, 1094, 854, 667; **HRMS (ESI^+):** *m/z* required for $C_{23}H_{33}NO_3SSiNa^+$ ($[M+Na]^+$): 454.1840, found 454.1843, Δ = 1.1 ppm.

Identifiable data for the minor (Z) isomer: **^{1}H NMR (400 MHz, $CDCl_3$)** δ = 4.89 (d, 1H, $^3J_{H\text{-}H}$ = 7.3 Hz, *NH*), 5.02-5.10 (m, 1H, $^3J_{H\text{-}H(cis)}$ = 10.6 Hz, *n*), 5.43-5.53 (m, 1H, $^3J_{H\text{-}H(cis)}$ = 10.6 Hz, *o*); **^{13}C NMR (101 MHz, $CDCl_3$)** δ = -1.9 (*q*), 18.6 (*p*), 29.6 (*m*), 53.4 (*f*), 70.5 (*g*), 73.1 (*h*), 121.4 (*n*), 129.3 (*o*);

(±) *N*-(1-(benzyloxy)-4-fluorohex-5-en-2-yl)-4-methylbenzene sulfonamide (*syn*-67) and (*anti*-67):

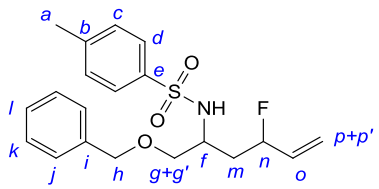

Following the general procedure B on 830 mg (1.92 mmol) of **93**, the reaction yielded 622 mg of a mixture of diastereoisomers **67** (85%, d.r. (*syn/anti*) 1:1) as a white solid after flash column

chromatography on silica gel (hexane/Et_2O 8:2). The two diastereoisomers could be separated during the purification.

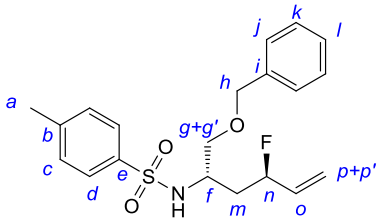

*Data for the anti-***67** *isomer:* **R_f** = 0.45 (hexane/EtOAc 7:3); **m.p.** = 48 °C; **^{1}H NMR (400 MHz, $CDCl_3$)** δ = 1.88-2.00 (m, 2H, *m*), 2.42 (s, 3H, *a*), 3.27 (dd, 1H, $^2J_{H\text{-}H}$ = 9.3 Hz, $^3J_{H\text{-}H}$ = 3.8 Hz, *g*), 3.41-3.53 (m, 2H, *f+g'*), 4.37 (sbr, 2H, *h*), 4.88 (ddd, 1H, $^2J_{H\text{-}F}$ = 48.5 Hz, $^3J_{H\text{-}H}$ = 12.6, 6.1 Hz, *n*), 5.02 (d, 1H, $^3J_{H\text{-}H}$ = 7.3 Hz, *NH*), 5.21 (d, 1H, $^3J_{H\text{-}H(cis)}$ = 10.8 Hz, *p*), 5.26 (d, 1H, $^3J_{H\text{-}H(trans)}$ = 17.3 Hz, *p'*), 5.80 (dddd, 1H, $^3J_{H\text{-}H(trans)}$ = 17.3 Hz, $^3J_{H\text{-}F}$ = 14.6 Hz, $^3J_{H\text{-}H(cis)}$ = 10.8, $^3J_{H\text{-}H}$ = 6.1 Hz, *o*), 7.19-7.38 (m, 7H, *c/d+k+j+l*), 7.72 (d, 2H, $^3J_{H\text{-}H}$ = 8.3 Hz, *c/d*); **^{13}C NMR (101 MHz, $CDCl_3$)** δ = 21.5 (*a*), 37.6 (d, $^2J_{C\text{-}F}$ = 22.4 Hz, *m*), 50.5 (d, $^3J_{C\text{-}F}$ = 4.0 Hz, *f*), 70.5 (d, $^4J_{C\text{-}F}$ = 2.4 Hz, *g*), 73.1 (*h*), 90.8 (d, $^1J_{C\text{-}F}$ = 167.0 Hz, *n*), 117.6 (d, $^3J_{C\text{-}F}$ = 12.0 Hz, *p*), 127.1 (*c/d/j/k/l*), 127.6 (c/d/*j*/*k*/*l*), 127.9 (c/d/*j*/*k*/*l*), 128.4 (c/d/*j*/*k*/*l*), 129.6 (*c/d/j/k/l*), 135.5 (d, $^2J_{C\text{-}F}$ = 19.2 Hz, *o*), 137.4 (*b/e/i*), 137.5 (*b/e/i*), 143.4 (*b/e/i*); **^{19}F {^{1}H} NMR (377 MHz, $CDCl_3$)** δ = -177.60; **IR (KBr): ν** = 3314, 2857, 1319, 1154, 1089, 816, 739, 668; **HRMS (ESI^+):** *m/z* required for $C_{20}H_{24}FNO_3SNa^+$ ($[M+Na]^+$): 400.1356, found 400.1353, Δ = 0.5 ppm.

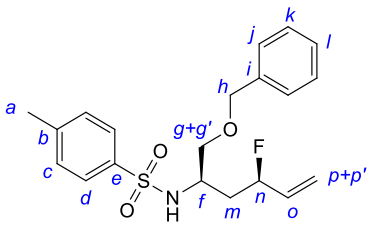

*Data for the syn-***67** *isomer:* **R_f** = 0.4 (hexane/EtOAc 7:3); **m.p.** = 54 °C; **^{1}H NMR (400 MHz, $CDCl_3$)** δ = 1.72-1.99 (m, 2H, *m*), 2.42 (s, 3H, *a*), 3.25 (dd, 1H, $^2J_{H\text{-}H}$ = 9.3 Hz, $^3J_{H\text{-}H}$ = 4.5 Hz, *g*), 3.32 (dd, 1H, $^2J_{H\text{-}H}$ = 9.3 Hz, $^3J_{H\text{-}H}$ = 3.3 Hz, *g'*), 3.63 (ddd, 1H, $^3J_{H\text{-}H}$ = 16.7, 8.6, 4.3 Hz, *f*), 4.34 (d, 1H, $^2J_{H\text{-}H}$ = 11.9 Hz, *h*), 4.39 (d, 1H, $^2J_{H\text{-}H}$ = 11.9 Hz, *h'*), 4.99 (d, 1H, $^2J_{H\text{-}F}$ = 49.0 Hz, *n*), 5.03 (d, 1H, $^3J_{H\text{-}H}$ = 8.6 Hz, *NH*), 5.18 (ddd, 1H, $^3J_{H\text{-}H(cis)}$ = 10.6 Hz, $^2J_{H\text{-}H}$ = 1.3 Hz, $^4J_{H\text{-}F}$ = 1.1 Hz, *p*), 5.27 (ddd, 1H, $^3J_{H\text{-}H(trans)}$ = 17.2 Hz, $^4J_{H\text{-}F}$ = 3.3 Hz, $^2J_{H\text{-}H}$ = 1.3 Hz, *p'*), 5.80 (dddd, 1H, $^3J_{H\text{-}H(trans)}$ = 17.2

Hz, $^{3}J_{H\text{-}F}$ = 14.4 Hz, $^{3}J_{H\text{-}H(cis)}$ = 10.6 Hz, $^{3}J_{H\text{-}H}$ = 5.8 Hz, *o*), 7.20-7.38 (m, 7H, *c/d+k+j+l*), 7.73 (d, 2H, $^{3}J_{H\text{-}H}$ = 8.1 Hz, *c/d*); **^{13}C NMR (101 MHz, $CDCl_3$)** δ = 21.5 (*a*), 38.7 (d, $^{2}J_{C\text{-}F}$ = 21.6 Hz, *m*), 50.3 (*f*), 71.4 (*g*), 73.2 (*h*), 90.4 (d, $^{1}J_{C\text{-}F}$ = 167.0 Hz, *n*), 117.1 (d, $^{3}J_{C\text{-}F}$ = 11.9 Hz, *p*), 127.0 (*c/d/j/k/l*), 127.7 (c/d/j/k/l), 127.9 (c/d/j/k/l), 128.4 (c/d/j/k/l), 129.6 (*c/d/j/k/l*), 135.8 (d, $^{2}J_{C\text{-}F}$ = 19.2 Hz, *o*), 137.4 (*b/e/i*), 137.7 (*b/e/i*), 143.4 (*b/e/i*); **^{19}F {^{1}H} NMR (377 MHz, $CDCl_3$)** δ = -179.47; **IR (DCM)**: **ν** = 2865, 1330, 1161, 1092, 815, 735, 666; **HRMS (ESI^{+}):** required for $C_{20}H_{24}NO_3SFNa^{+}$ ($[M+Na]^{+}$): 400.1341, found 400.1353, Δ = 3.5 ppm.

4.3.9 Synthesis of (±) *N*-(2-fluorobut-3-en-1-yl)-4-methylbenzenesulfonamide (68):

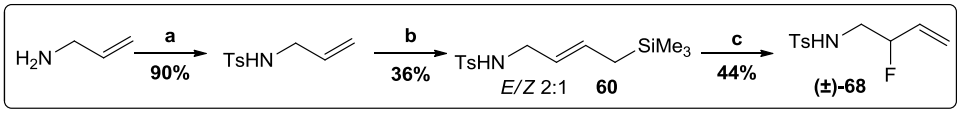

Scheme 4.9: Synthesis of (±) *N*-(2-fluorobut-3-en-1-yl)-4-methylbenzenesulfonamide (**68**); **a**) TsCl, NEt_3, CH_2Cl_2, 3 h; **b**) allyltrimethylsilane, Hoveyda-Grubbs 2nd (5 mol%), 1,4-benzoquinone, CH_2Cl_2, reflux, 3 days; **c**) Selectfluor, $NaHCO_3$, CH_3CN, 48 h.

***N*-allyl-4-methylbenzenesulfonamide:**[5]

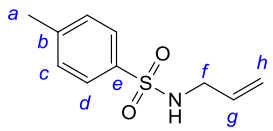

To a cold (0 °C) solution of tosylchloride (2.0 g, 10.5 mmol, 1 eq.) in anhydrous CH_2Cl_2 (50 mL), was added **allylamine** (4 mL, 53 mmol, 5 eq.) and distilled NEt_3 (1.5 mL, 10.5 mmol, 1 eq.) dropwise. The mixture was warmed to r.t. and stirred for 3 h. The solvent was then removed in *vacuo* and the crude residue dissolved in EtOAc (100 mL). This was subsequently washed with H_2O, brine, dried over $MgSO_4$, filtered and the solvent removed *in vacuo*. The crude mixture was purified by flash column chromatography on silica gel (hexane/Et_2O 8:2) to yield the ***N*-allyl-4-methylbenzenesulfonamide** as a white solid (2.0 g, 90%).

R_f = 0.3 (hexane/Et_2O 8:2); **m.p.** = 66 °C; **^{1}H NMR (400 MHz, $CDCl_3$)** δ = 2.40 (s, 3H, *a*), 3.60 (m, 2H, *f*), 4.30 (t, 1H, $^{3}J_{H\text{-}H}$ = 5.8 Hz, *NH*), 5.00 (dd, 1H, $^{3}J_{H\text{-}H(cis)}$ = 9.6 Hz, $^{2}J_{H\text{-}H}$ = 2.8 Hz, *h*), 5.10 (dd,

[5] The characterisation of this compound is in agreement with previous reports: for ^{1}H and ^{13}C NMR spectra, see L. De Luca, G. J. Giacomelli, *J. Org. Chem.* **2008**, *73*, 3967-3969; for (HRMS) Mass spectra, see V. K. Aggarwal, P. W. Davies, W. O. Moss, *Chem. Commun.* **2002**, 972-973.

1H, $^{3}J_{H\text{-}H(trans)}$ = 16.1 Hz, $^{2}J_{H\text{-}H}$ = 2.8 Hz, *h'*), 5.64 (m, 1H, *g*), 7.32 (d, 2H, $^{3}J_{H\text{-}H}$ = 8.6 Hz, *c/d*), 7.70 (d, 2H, $^{3}J_{H\text{-}H}$ = 8.6 Hz, *c/d*);

4-methyl-*N*-(4-(trimethylsilyl)but-2-enyl)benzenesulfonamide (60):

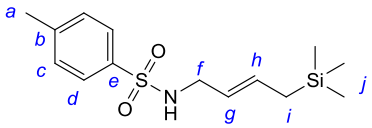

Following the general procedure A on 500 mg (2.4 mmol) of ***N*-allyl-4-methylbenzenesulfonamide** using Hoveyda-Grubbs 2nd generation catalyst (75 mg, 0.1 mmol, 5 mol%), the reaction yielded 250 mg of a mixture of isomers **60** (36%, *E:Z* = 2:1) as a colourless oil after flash column chromatography on silica gel (hexane).

Data for the major (E) isomer: **R_f** = 0.1 (hexane); **^{1}H NMR (400 MHz, $CDCl_3$)** δ = -0.04 (sbr, 9H, *j*), 1.40 (d, 2H, $^{3}J_{H\text{-}H}$ = 8.2 Hz, *i*), 2.44 (s, 3H, *a*), 3.51 (t, 2H, $^{3}J_{H\text{-}H}$ = 6.6 Hz, *f*), 4.21 (t, 1H, $^{3}J_{H\text{-}H}$ = 6.6 Hz, *NH*), 5.17 (dt, 1H, $^{3}J_{H\text{-}H(trans)}$ = 14.9 Hz, $^{3}J_{H\text{-}H}$ = 6.6 Hz, *g*), 5.56 (dt, 1H, $^{3}J_{H\text{-}H(trans)}$ = 14.9 Hz, $^{3}J_{H\text{-}H}$ = 8.2 Hz, *h*), 7.72 (d, 2H, $^{3}J_{H\text{-}H}$ = 8.2 Hz, *c/d*), 7.76 (d, 2H, *J* = 8.2 Hz, *c/d*); **^{13}C NMR (101 MHz, $CDCl_3$)** δ = -2.0 (*j*), 21.5 (*a*), 22.8 (*i*), 45.7 (*f*), 122.6 (*g*), 127.1 (*c/d*), 129.7 (*c/d*), 132.1 (*h*), 137.1 (*b/e*), 143.4 (*b/e*); **IR (DCM): ν =** 3111, 2928, 1685, 1183, 931; **HRMS (CI^{+}):** *m/z* required for $C_{14}H_{24}NO_2SSi$ ($[M+H]^{+}$): 298.1297, found 298.1311, Δ = 4.5 ppm.

Identifiable data for the minor (Z) isomer: **^{1}H NMR (400 MHz, $CDCl_3$)** δ = -0.04 (sbr, 9H, *j*), 3.56 (t, 2H, *J* = 5.4 Hz, *f*), 4.16 (t, 1H, *J* = 5.4 Hz, *NH*); **^{13}C NMR (101 MHz, $CDCl_3$)** δ = -1.9 (*j*), 29.7 (*i*), 39.9 (*f*), 120.9 (*g*), 131.3 (*h*);

(±) *N*-(2-fluorobut-3-en-1-yl)-4-methylbenzenesulfonamide (68):

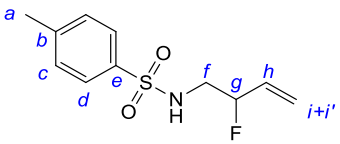

Following the general procedure B on 250 mg (0.8 mmol) of **60**, the reaction yielded 85 mg of **68** (44%) as a white solid after flash column chromatography on silica gel (hexane/Et_2O 8:2).

R_f = 0.3 (hexane/Et_2O 7:3); **m.p.** = 72 °C; **^{1}H NMR (400 MHz, $CDCl_3$)** δ = 2.44 (sbr, 3H, *a*), 3.10 (dddd, 1H, $^{2}J_{H\text{-}H}$ = 13.9 Hz, $^{3}J_{H\text{-}F}$ = 13.6 Hz, $^{3}J_{H\text{-}H}$ = 7.6, 4.8 Hz, *f*), 3.28 (dddd, 1H, $^{3}J_{H\text{-}F}$ = 27.3 Hz,

$^{2}J_{H\text{-}H}$ = 13.9 Hz, $^{3}J_{H\text{-}H}$ = 8.1, 3.3 Hz, *f'*), 4.82-4.88 (m, 1H, *NH*), 4.94 (dbr, 1H, $^{2}J_{H\text{-}F}$ = 48.5 Hz, *g*), 5.32 (d, 1H, $^{3}J_{H\text{-}H(cis)}$ = 10.6 Hz, *i*), 5.38 (dd, 1H, $^{3}J_{H\text{-}H(trans)}$ = 17.1 Hz, $^{4}J_{H\text{-}F}$ = 1.5 Hz, *i'*), 5.78 (dddd, 1H, $^{3}J_{H\text{-}H(trans)}$ = 17.1 Hz, $^{3}J_{H\text{-}F}$ = 15.2 Hz, $^{3}J_{H\text{-}H(cis)}$ = 10.6 Hz, $^{3}J_{H\text{-}H}$ = 5.8 Hz, *h*), 7.33 (d, 2H, $^{3}J_{H\text{-}H}$ = 8.3 Hz, *c/d*), 7.76 (d, 2H, $^{3}J_{H\text{-}H}$ = 8.3 Hz, *c/d*); **^{13}C NMR (101 MHz, $CDCl_3$)** δ = 21.5 (*a*), 46.8 (d, $^{2}J_{C\text{-}F}$ = 23.2 Hz, *f*), 91.5 (d, $^{1}J_{C\text{-}F}$ = 171.0 Hz, *g*), 119.5 (d, $^{3}J_{C\text{-}F}$ = 12.0 Hz, *i*), 127.0 (*c/d*), 129.8 (*c/d*), 132.4 (d, $^{2}J_{C\text{-}F}$ = 19.2 Hz, *h*), 136.7 (*b/e*), 143.7 (*b/e*); **^{19}F {^{1}H} NMR (377 MHz, $CDCl_3$)** δ = -184.75 ; **IR (KBr): ν =** 3025, 2927, 1651, 1588, 1592, 1377, 722; **HRMS (CI^{+}):** *m/z* required for $C_{11}H_{15}FNO_2S$ ($[M+H]^{+}$): 244.0808, found 244.0819, Δ = 4.5 ppm.

4.3.10 Synthesis of (±) *N*-(4-fluorohex-5-en-1-yl)-4-methylbenzenesulfonamide (63):

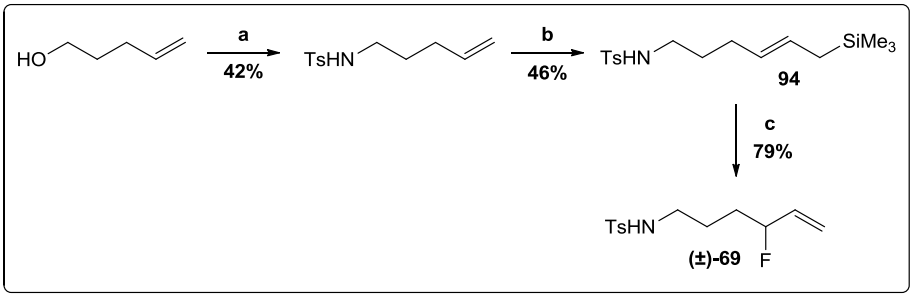

Scheme 4.10: Synthesis of (±) *N*-(4-fluorohex-5-en-1-yl)-4-methylbenzenesulfonamide (**69**); **a**) MsCl, NEt_3, CH_2Cl_2, 3 h, then KOH, TsCl, DMF, 5 h; **b**) allyltrimethylsilane, Hoveyda-Grubbs 2nd (5 mol%), 1,4-benzoquinone, CH_2Cl_2, reflux, 3 days; **c**) Selectfluor, $NaHCO_3$, CH_3CN, 6 days.

4-methyl-*N*-(pent-4-en-1-yl)benzenesulfonamide:[6]

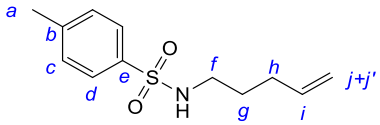

Following the general procedure C on 1 g (11.6 mmol, 1 eq.) of pent-4-en-1-ol, the reaction yielded 1.17 g of **4-methyl-*N*-(pent-4-en-1-yl)benzenesulfonamide** (42% over two steps) as a colourless oil after flash column chromatography on silica gel (hexane/EtOAc 95:1 then 9:1).

R_f = 0.3 (hexane/Et_2O 6:4); **^{1}H NMR (200 MHz, $CDCl_3$)** δ = 1.49-1.65 (m, 2H, *g*), 1.99-2.12 (m, 2H, *h*), 2.44 (s, 3H, *a*), 2.90-3.02 (m, 2H, *f*), 4.34-4.43 (m, 1H, *NH*), 4.92-4.95 (m, 1H, *j*), 4.97-5.04

[6] This compound was prepared according to the procedure described in M. C. Marcotullio, V. Campagna, S. Sternativo, F. Costantino, M. Curini, *Synthesis* **2006**, *16*, 2760-2766. Analytical and spectroscopic data were in agreement with those previously reported by R. C. Larock, H. Yang, S. M. Weinreb, R. J. Herr, *J. Org. Chem.* **1994,** *59*, 4172-4178.

(m, 1H, *j'*), 5.72 (ddt, 1H, $^{3}J_{H\text{-}H}$ = 17.4, 10.8, 6.7 Hz, *i*), 7.32 (d, 2H, $^{3}J_{H\text{-}H}$ = 8.1 Hz, *c/d*), 7.75 (d, 2H, $^{3}J_{H\text{-}H}$ = 8.1 Hz, *c/d*);

4-methyl-*N*-(6-(trimethylsilyl)hex-4-en-1-yl)benzenesulfonamide (94):

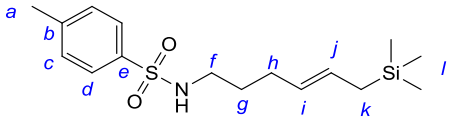

Following the general procedure A on 614 mg (2.3 mmol, 1 eq.) of **4-methyl-*N*-(pent-4-en-1-yl)benzenesulfonamide**, the reaction yielded 367 mg of **94** (46%, *E:Z* = 2:1) as a yellow oil after flash column chromatography on silica gel (hexane/Et_2O 95:5 to 7:3).

Data for the major (E) isomer: **R_f** = 0.3 (hexane/Et_2O 6:4); **^{1}H NMR (500 MHz, $CDCl_3$)** δ = -0.04 (s, 9H, *l*), 1.37 (dd, 2H, $^{3}J_{H\text{-}H}$ = 8.1 Hz, $^{4}J_{H\text{-}H}$ = 1.3 Hz, *k*), 1.51 (p, 2H, $^{3}J_{H\text{-}H}$ = 7.2 Hz, *g*), 1.94-2.00 (m, 2H, *h*), 2.44 (s, 3H, *a*), 2.92-2.97 (m, 2H, *f*), 4.27-4.36 (m, 1H, *NH*), 5.12 (dtt, 1H, $^{3}J_{H\text{-}H(trans)}$ = 15.0 Hz, $^{3}J_{H\text{-}H}$ = 6.6, $^{4}J_{H\text{-}H}$ = 1.3 Hz, *i*), 5.35 (dtt, 1H, $^{3}J_{H\text{-}H(trans)}$ = 15.0 Hz, $^{3}J_{H\text{-}H}$ = 8.1, $^{4}J_{H\text{-}H}$ = 1.3 Hz, *j*), 7.31 (d, 2H, $^{3}J_{H\text{-}H}$ = 8.1 Hz, *c/d*), 7.75 (d, 2H, $^{3}J_{H\text{-}H}$ = 8.1 Hz, *c/d*); **^{13}C NMR (125 MHz, $CDCl_3$)** δ = -2.0 (*l*), 21.4 (*a*), 22.6 (*k*), 29.7 (*g*), 29.7 (*h*), 42.7 (*f*), 126.9 (*i*), 127.1 (*c/d*), 127.7 (*j*), 129.7 (*c/d*), 137.0 (*b/e*), 143.3 (*b/e*); **IR (neat): ν =** 3282, 2953, 1324, 1247, 1157, 1094, 839, 813, 660; **HRMS (ESI$^+$):** *m/z* required for $C_{16}H_{27}NO_2SSiNa^+$ ($[M+Na]^+$): 348.1424, found 348.1425, Δ = 1.3 ppm.

Identifiable data for the minor (Z) isomer: **^{1}H NMR (500 MHz, $CDCl_3$)** δ = -0.01 (s, 9H, *l*), 1.41 (d, 2H, $^{3}J_{H\text{-}H}$ = 7.9 Hz, *k*), 2.14 (p, 2H, $^{3}J_{H\text{-}H}$ = 6.9 Hz, *g*), 2.95-2.98 (m, 2H, *f*), 5.12-5.18 (m, 1H, $^{3}J_{H\text{-}H(cis)}$ = 10.4 Hz, *i*), 5.41 (dt, 1H, $^{3}J_{H\text{-}H(cis)}$ = 10.4, $^{3}J_{H\text{-}H}$ = 9.1 Hz, *j*); **^{13}C NMR (125 MHz, $CDCl_3$)** δ = -1.8 (*l*), 18.5 (*k*), 24.1 (*h*), 29.5 (*g*), 43.0 (*f*), 122.6 (*i*), 125.6 (*j*);

(±) *N*-(4-fluorohex-5-en-1-yl)-4-methylbenzenesulfonamide (69):

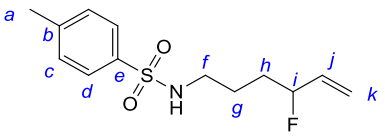

Following the general procedure B on 247 mg (0.76 mmol) of **94**, the reaction yielded 163 mg of **69** (79%) as a yellow oil after flash column chromatography on silica gel (hexane/EtOAc 9:1 to 7:3).

R_f = 0.5 (hexane/EtOAc 7:3); **^{1}H NMR (400 MHz, $CDCl_3$)** δ = 1.53-1.66 (m, 2H, *g*), 1.66-1.74 (m, 2H, *h*), 2.43 (s, 3H, *a*), 2.94-3.01 (m, 2H, *f*), 4.73-4.81 (m, 1H, *NH*), 4.83 (dddt, 1H, $^2J_{H\text{-}F}$ = 48.5 Hz, $^3J_{H\text{-}H}$ = 11.9, 5.8 Hz, $^4J_{H\text{-}H}$ = 1.3 Hz, *i*), 5.20 (dt, 1H, $^3J_{H\text{-}H(cis)}$ = 10.6 Hz, $^2J_{H\text{-}H}$ = 1.3 Hz, $^4J_{H\text{-}H}$ = 1.3 Hz, *k*), 5.27 (ddt, 1H, $^3J_{H\text{-}H(trans)}$ = 17.4 Hz, $^4J_{H\text{-}F}$ = 3.5 Hz, $^2J_{H\text{-}H}$ =1.3 Hz, $^4J_{H\text{-}H}$ = 1.3 Hz, *k'*), 5.80 (dddd, 1H, $^3J_{H\text{-}H(trans)}$ = 17.4 Hz, $^3J_{H\text{-}F}$ = 14.4 Hz, $^3J_{H\text{-}H(cis)}$ = 10.6 Hz, $^3J_{H\text{-}H}$ = 5.8 Hz, *j*), 7.32 (d, 2H, $^3J_{H\text{-}H}$ = 8.1 Hz, *c/d*), 7.75 (d, 2H, $^3J_{H\text{-}H}$ = 8.1 Hz, *c/d*); **^{13}C NMR (101 MHz, $CDCl_3$)** δ = 21.5 (*a*), 24.9 (d, $^3J_{C\text{-}F}$ = 4.8 Hz, *g*), 32.0 (d, $^2J_{C\text{-}F}$ = 22.4 Hz, *h*), 42.8 (*f*), 92.9 (d, $^1J_{C\text{-}F}$ = 167.8 Hz, *i*), 117.1 (d, $^3J_{C\text{-}F}$ = 12.8 Hz, *k*), 127.0 (*c/d*), 129.7 (*c/d*), 136.0 (d, $^2J_{C\text{-}F}$ = 20.8 Hz, *j*), 136.7 (*b/e*), 143.4 (*b/e*); **^{19}F {^{1}H} NMR (377 {^{1}H} MHz, $CDCl_3$)** δ = -178.18; **IR (neat): ν** = 2923, 1337, 1155, 1089, 1000, 817, 664; **HRMS (ESI^+):** *m/z* required for $C_{13}H_{18}FNO_2SNa^+$ ($[M+Na]^+$): 294.0934, found 294.0938, Δ = 1.1 ppm.

4.3.11 Synthesis of (±)-2,6-bis(benzyloxy)-5-fluoro-*N*-tosylhex-3-enamide (70):

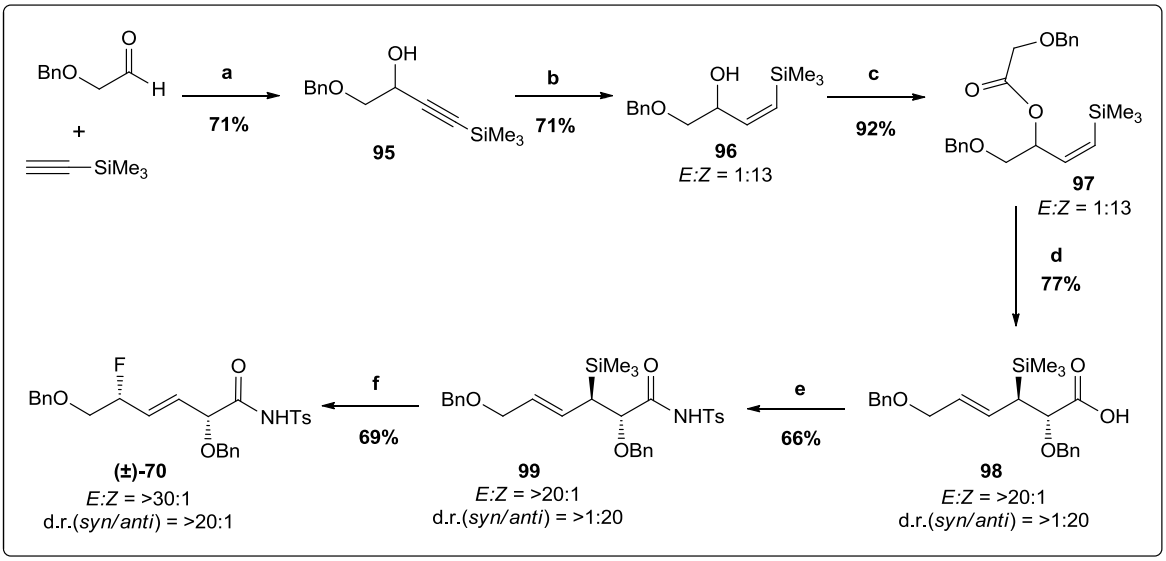

Scheme 4.11: Synthesis of (±)-2,6-bis(benzyloxy)-5-fluoro-*N*-tosylhex-3-enamide (X); (**a**) *n*-BuLi, THF, 78 °C, 35 min then 0 °C 2 h; (**b**) BH_3, THF, cyclohexene, 15 h; (**c**) 2-benzyloxy acetic acid, DMAP, DCC, DCM, 0 °C, 15 h; (d) LiHMDS, THF, -78 °C, 1 h then r.t. 13 h; (**e**) TsCl, DMAP, DCC, DCM, 0 °C to r.t. 15 h; (**f**) Selectfluor, $NaHCO_3$, CH_3CN, 48 h.

(±) 1-(benzyloxy)-4-(trimethylsilyl)but-3-yn-2-ol (95):[7]

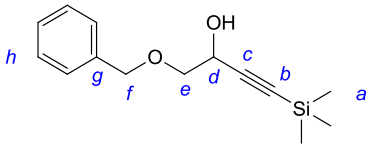

To a solution of trimethylsilylacetylene (5.5 mL, 39.0 mmol, 1.2 eq.) in dry THF (65 mL), was added a solution of *n*-BuLi [1M] in hexane (15.6 mL, 39.0 mmol, 1.2 eq.) at -78 °C, and the reaction mixture was stirred at this temperature for 30 min. A solution of **2-(benzyloxy) acetaldehyde** (5.0 g, 33.0 mmol, 1 eq.) in THF (14 mL) was added dropwise and the reaction mixture was stirred at -78 °C for 5 min, then at 0 °C for 2 h. The reaction was then quenched by addition of water at 0 °C and the mixture was extracted with Et_2O. The combined organic layers were washed with brine, dried over $MgSO_4$ and the solvent was removed *in vacuo*. Purification by flash column chromatography on silica gel (petrol ether 40-60°/Et_2O 6:4) yielded the racemic propargylic alcohol (±)-**95** as a colourless oil (5.8 g, 71% yield).

R_f = 0.4 (hexane/Et_2O 6:4); **^{1}H (400 MHz, $CDCl_3$) δ** = 0.18 (s, 9H, *a*), 2.47 (d, 1H, $^3J_{H\text{-}H}$ = 4.5 Hz, *OH*), 3.57 (dd, 1H, $^2J_{H\text{-}H}$ = 9.7 Hz, $^3J_{H\text{-}H}$ = 7.6 Hz, *e*), 3.67 (dd, 1H, $^2J_{H\text{-}H}$ = 9.7 Hz, $^3J_{H\text{-}H}$ = 3.5 Hz, *e'*), 4.58 (ddd, 1H, $^3J_{H\text{-}H}$ = 7.6, 4.5, 3.5 Hz, *d*), 4.63 (2H, d, $^2J_{H\text{-}H}$ = 1.8 Hz, *f*), 7.29-7.38 (m, 5H, *h*).

(±) 1-(benzyloxy)-4-(trimethylsilyl)but-3-en-2-ol (96):[7]

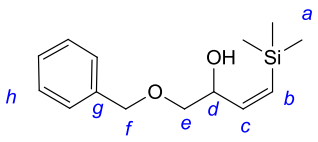

Freshly distilled cyclohexene (6.5 mL, 64.0 mmol) was added dropwise over 5 min to a solution of BH_3 ([1M] in THF, 32.0 mL, 32.0 mmol) under argon at 0 °C. The reaction mixture was stirred for 1 h at 0 °C before the dropwise (15 min) addition of a solution of the propargylic alcohol **95** (4.0 g, 16.0 mmol) in THF (16 mL). The reaction mixture was stirred at 0 °C until everything is dissolved then warmed to r.t. After 1 h acetic acid (1.8 mL, 32.0 mmol) was added and the mixture stirred overnight. The reaction was quenched by addition of Et_2O and water and the aqueous phase was

[7] This compound was prepared according to the procedure reported by G. T. Giuffredi, S. Purser, M. Sawicki, A. L. Thompson, V. Gouverneur, *Tetrahedron: Asymmetry*, **2009**, *20*, 910-920. Analytical and spectroscopic data were in agreement with those reported wherein.

extracted with Et_2O. Combined organic layers were washed with brine, dried over $MgSO_4$, filtered and the solvent removed *in vacuo*. Purification by flash column chromatography on silica gel (hexane/Et_2O 8:2) furnished the vinylsilane **96** as a colourless oil (2.86 g, 71% yield, *E:Z* = 1:13).

Data for the major (Z) isomer: **R_f** = 0.4 (hexane/Et_2O 7:3); **^{1}H (400 MHz, $CDCl_3$) δ** = 0.13 (s, 9H, *a*), 2.43 (d, 1H, $^3J_{H\text{-}H}$ = 2.4 Hz, *OH*), 3.40 (dd, 1H, $^2J_{H\text{-}H}$ = 9.6 Hz, $^3J_{H\text{-}H}$ = 8.5 Hz, *e*), 3.49 (dd, 1H, $^2J_{H\text{-}H}$ = 9.6 Hz, $^3J_{H\text{-}H}$ = 3.3 Hz, *e'*), 4.49 (app td, 1H, $^3J_{H\text{-}H}$ = 8.5, 2.4 Hz, *d*), 4.59 (d, 2H, $^2J_{H\text{-}H}$ = 2.1 Hz, *f*), 5.77 (dd, 1H, $^3J_{H\text{-}H(cis)}$ = 14.3 Hz, $^4J_{H\text{-}H}$ = 0.8 Hz, *b*), 6.22 (dd, 1H, $^3J_{H\text{-}H(cis)}$ = 14.3 Hz, $^3J_{H\text{-}H}$ = 8.5 Hz, *c*), 7.28-7.38 (m, 5H, *h*); *Identifiable data for the minor (E) isomer:* **^{1}H (400 MHz, $CDCl_3$) δ** = 0.18 (s, 9H, *a*), 2.47 (d, 1H, $^3J_{H\text{-}H}$ = 4.8 Hz, *OH*), 3.57 (dd, 1H, $^2J_{H\text{-}H}$ = 9.9 Hz, $^3J_{H\text{-}H}$ = 7.8 Hz, *e*), 3.66 (dd, 1H, $^2J_{H\text{-}H}$ = 9.9 Hz, $^3J_{H\text{-}H}$ = 3.4 Hz, *e'*), 4.63 (d, 2H, $^2J_{H\text{-}H}$ = 2.7 Hz, *f*).

(±) 1-(Benzyloxy)-4-(trimethylsilyl)but-3-en-2-yl (benzyloxy)acetate (97):[7]

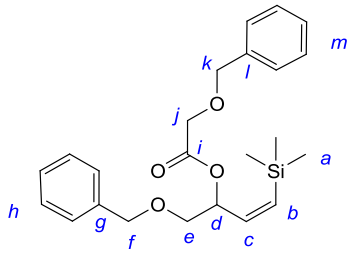

To a solution of vinylsilane **96** (2.86 g, 12.0 mmol, 1 eq.) in dry CH_2Cl_2 (24 mL) at 0 °C, was added 2-benzyloxy acetic acid (2.0 mL, 14.0 mmol, 1.2 eq.) and DMAP (147.0 mg, 1.2 mmol, 0.1 eq.). A solution of DCC (2.48 g, 12.0 mmol, 1.2 eq.) in DCM (15 mL) was then added dropwise at 0 °C and the reaction was left to warm to r.t. over 15 h without removal of the cooling bath. The reaction mixture was diluted with Et_2O then filtered through a short pad of Celite. After purification by flash column chromatography on silica gel (hexane/Et_2O 8:2), the desired product **97** was obtained as a yellow oil (4.26 g, 92%, *E:Z* = 1:13).

Data for the major (Z) isomer: **R_f** = 0.6 (hexane/Et_2O, 7:3); **^{1}H (400 MHz, $CDCl_3$) δ** = 0.18 (s, 9H, *a*), 3.52 (dd, 1H, $^2J_{H\text{-}H}$ = 10.9 Hz, $^3J_{H\text{-}H}$ = 3.8 Hz, *e*), 3.60 (dd, 1H, $^2J_{H\text{-}H}$ = 10.8 Hz, $^3J_{H\text{-}H}$ = 7.3 Hz, *e'*), 4.13 (d, 2H, $^2J_{H\text{-}H}$ = 0.5 Hz, *k*), 4.53 (d, 1H, $^2J_{H\text{-}H}$ = 12.1 Hz, *j*), 4.59 (d, 1H, $^2J_{H\text{-}H}$ = 12.1 Hz, *j'*), 4.63 (s, 2H, *f*), 5.77 (dddd, 1H, $^3J_{H\text{-}H}$ = 9.1, 7.4, 3.8, $^4J_{H\text{-}H}$ = 0.7 Hz, *d*), 5.85 (dd, 1H, $^3J_{H\text{-}H(cis)}$ = 14.4

Hz, $^{4}J_{H\text{-}H}$ = 0.5 Hz, *b*), 6.19 (dd, 1H, $^{3}J_{H\text{-}H(cis)}$ = 14.4 Hz, $^{3}J_{H\text{-}H}$ = 9.1 Hz, *c*), 7.27-7.38 (m, 10H, *h+m*); *Characteristic data for the minor (E) isomer could not be distinguished.*

(±) *anti*-2,6-Bis(benzyloxy)-3-(trimethylsilyl)hex-4-enoic acid (98):[7]

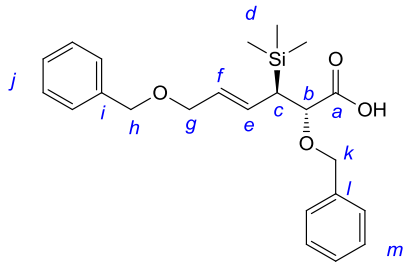

To a solution of **1-(Benzyloxy)-4-(trimethylsilyl)but-3-en-2-yl (benzyloxy)acetate 97** (4.19 g, 11.0 mmol, 1 eq.) in dry THF (92 mL) at -78 °C, was added dropwise LiHMDS [1M] in THF (19.8 mL, 19.8 mmol, 1.8 eq.) and the reaction mixture was stirred for 1 h at -78 °C. Chlorotrimethyl silane (4.2 mL, 33.0 mmol, 3 eq.) was added dropwise and the reaction was left to warm to r. t. over 16 h without removing the cooling bath. Then 10% HCl was added at 0 °C and the mixture was extracted with EtOAc. The combined organic layers were washed with brine, dried over $MgSO_4$ and the solvent was removed *in vacuo*. Purification by flash column chromatography on silica gel (DCM/MeOH, 9:1) furnished the acid **98** as a yellow oil (3.37 g, 77% yield, *E:Z* = > 20:1, d.r. (*syn:anti*) > 1:20).

Data for the major anti-(E) isomer: **R_f** = 0.9 (DCM/MeOH 9:1); **^{1}H (400 MHz, $CDCl_3$) δ** = 0.01 (s, 9H, *d*), 2.08 (dd, 1H, $^{3}J_{H\text{-}H}$ = 10.6, 2.8 Hz, *c*), 3.98 (dd, 1H, $^{3}J_{H\text{-}H}$ = 6.3 Hz, $^{4}J_{H\text{-}H}$ = 1.3 Hz, *g*), 3.99 (dd, 1H, $^{3}J_{H\text{-}H}$ = 6.3 Hz, $^{4}J_{H\text{-}H}$ = 1.3 Hz, *g'*), 4.18 (d, 1H, $^{3}J_{H\text{-}H}$ = 2.8 Hz, *b*), 4.35 (d, 1H, $^{2}J_{H\text{-}H}$ = 11.0 Hz, *k*), 4.46 (s, 2H, *h*), 4.69 (d, 1H, $^{2}J_{H\text{-}H}$ = 11.0 Hz, *k'*), 5.52 (dt, 1H, $^{3}J_{H\text{-}H(trans)}$ = 15.5 Hz, $^{3}J_{H\text{-}H}$ = 6.3 Hz, *f*), 5.83 (ddt, 1H, $^{3}J_{H\text{-}H(trans)}$ = 15.5 Hz, $^{3}J_{H\text{-}H}$ = 10.6 Hz, $^{4}J_{H\text{-}H}$ = 1.3 Hz, *e*), 7.28-7.39 (m, 10H, *h+m*); *Characteristic data for the minor syn-(E) isomer could not be distinguished.*

(±) *anti*-2,6-bis(benzyloxy)-*N*-tosyl-3-(trimethylsilyl)hex-4-enamide (99):

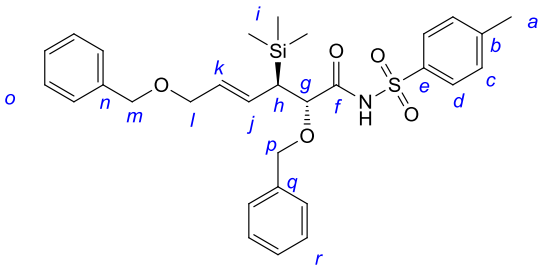

To a solution of **2,6-Bis(benzyloxy)-3-(trimethylsilyl)hex-4-enoic acid 98** (150 mg, 0.37 mmol, 1 eq.) in anhydrous DCM (1.5 mL), was added at 0 °C tosylamine (77.4 mg, 0.45, 1.2 eq.) and DMAP (5 mg, 0.04 mmol, 0.1 eq.). A solution of DCC (93.3 mg, 0.45 mmol, 1.2 eq.) in CH_2Cl_2 (1mL) was then added dropwise. The mixture was slowly warmed to room temperature and stirred overnight then diluted with water and extracted three times with CH_2Cl_2. The combined organic phases were washed with brine, dried over $MgSO_4$, filtered and the solvent removed under reduced pressure. The crude mixture was purified using flash column chromatography on silica gel (hexane/EtOAc 8:2 up to 7:3) to produce **99** as a brown oil (135 mg, 66 %, *E:Z* = > 20:1, d.r. (*syn:anti*) > 1:20).

Data for the major anti-(E) diastereomer: **R_f** = 0.4 (hexane/EtOAc 7:3); **^{1}H NMR (400 MHz, $CDCl_3$)** δ = -0.08 (s, 9H, *i*), 1.82 (dd, 1H, $^3J_{H\text{-}H}$ = 10.9, 2.3 Hz, *h*), 2.31 (s, 3H, *a*), 3.68-3.80 (m, 2H, *l*), 3.93 (d, 1H, $^3J_{H\text{-}H}$ = 2.3 Hz, *g*), 4.33-4.49 (m, 4H, *m+p*), 5.20 (dt, 1H, $^3J_{H\text{-}H(trans)}$ = 15.4 Hz, $^3J_{H\text{-}H}$ = 6.1 Hz, *k*), 5.58 (dd, 1H, $^3J_{H\text{-}H(trans)}$ = 15.4 Hz, $^3J_{H\text{-}H}$ = 10.9 Hz, *j*), 7.16 (d, 2H, $^3J_{H\text{-}H}$ = 8.2 Hz, *c/d*), 7.19-7.36 (m, 10H, *o+r*), 7.82 (d, 2H, $^3J_{H\text{-}H}$ = 8.2 Hz, *c/d*), 8.69 (s, 1H, *NH*); **^{13}C NMR (101 MHz, $CDCl_3$)** δ = -2.5 (*i*), 21.6 (*a*), 38.0 (*h*), 70.3 (*l*), 71.6 (*m/p*), 73.8 (*m/p*), 80.9 (*g*), 127.5 (*j*), 127.7 (*c/d/o/r*), 127.8 (*c/d/o/r*), 128.3 (*c/d/o/r*), 128.4 (*c/d/o/r*), 128.6 (*c/d/o/r*), 128.7 (*k*), 128.8 (*c/d/o/r*), 129.4 (*c/d/o/r*), 135.5 (*n/q*), 135.6 (*n/q*), 138.3 (*b/e*), 144.9 (*b/e*), 171.2 (*f*); **IR (in DCM): ν =** 2955, 1728, 1409, 1349, 1088, 839, 699; **HRMS (ESI$^+$):** *m/z* required for $C_{30}H_{37}NO_5SSiNa^+$ ($[M+Na]^+$): 574.2054, found 574.2054, Δ = 0.9 ppm; *Characteristic data for minor syn-(E) diastereoisomer could not be observed.*

(±) *syn*-2,6-bis(benzyloxy)-5-fluoro-*N*-tosylhex-3-enamide (70):

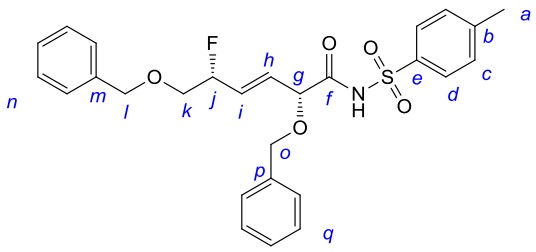

Following general procedure B on 150 mg (0.27 mmol, 1 eq.) of **99**, the reaction yielded 93 mg of *syn*-**70** (69%, *E:Z* = > 30:1, d.r. (*syn:anti*) > 20:1) as a colourless oil after flash column chromatography on silica gel (hexane/Et_2O 8:2).

Data for the major syn-(E) diastereoisomer: **R_f** = 0.2 (hexane/EtOAc 7:3); **^{1}H NMR (400 MHz, $CDCl_3$)** δ = 2.42 (s, 3H, *a*), 3.55 (d, 1H, $^3J_{H\text{-}H}$ = 4.5 Hz, *k*), 3.61 (d, 1H, $^3J_{H\text{-}H}$ = 4.5 Hz, *k'*), 4.32 (d, 1H, $^3J_{H\text{-}H}$ = 6.2 Hz, *g*), 4.46 (d, 1H, $^2J_{H\text{-}H}$ = 11.6 Hz, *o*), 4.58 (s, 2H, *l*), 4.60 (d, 1H, $^2J_{H\text{-}H}$ =11.6 Hz, *o'*), 5.08 (ddt, 1H, $^2J_{H\text{-}F}$ = 48.5 Hz, $^3J_{H\text{-}H}$ = 5.1, 4.5 Hz, *j*), 5.74 (dd, 1H, $^3J_{H\text{-}H(trans)}$ = 15.7 Hz, $^3J_{H\text{-}H}$ = 6.2 Hz, *h*), 5.90 (td, 1H, $^3J_{H\text{-}H(trans)}$ = 15.7, $^3J_{H\text{-}F}$ = 15.7 Hz, $^3J_{H\text{-}H}$ = 5.1 Hz, *i*), 7.24-7.40 (m, 12H, *c/d+n+q*), 7.94 (d, 2H, $^3J_{H\text{-}H}$ = 8.1 Hz, *c/d*), 9.19 (s, 1H, *NH*); **^{13}C NMR (101 MHz, $CDCl_3$)** δ = 21.5 (*a*), 71.4 (d, $^2J_{C\text{-}F}$ = 22.4 Hz, *k*), 71.7 (*o*), 73.3 (*l*), 78.7 (*g*), 90.8 (d, $^1J_{C\text{-}F}$ = 174.2 Hz, *j*), 126.8 (d, $^3J_{C\text{-}F}$ = 11.2 Hz, *h*), 127.6 (*c/d/n/q*), 127.7 (*c/d/n/q*), 128.1 (*c/d/n/q*), 128.2 (*c/d/n/q*), 128.3 (*c/d/n/q*), 128.4 (*c/d/n/q*), 128.6 (*c/d/n/q*), 129.4 (*c/d/n/q*), 131.0 (d, $^2J_{C\text{-}F}$ = 19.2 Hz, *i*), 135.1 (*b/e/m/p*), 135.6 (*b/e/m/p*), 137.4 (*b/e/m/p*), 145.1 (*b/e/m/p*), 167.7 (*f*); **^{19}F {^{1}H} NMR (377 MHz, $CDCl_3$)** δ = -184.97; **IR (in DCM)**: **ν =** 3055, 2380, 1422, 1265, 896, 739; **HRMS (ESI$^+$):** *m/z* required for $C_{27}H_{28}FNO_2SNa^+$ ([M+Na]$^+$): 520.1564, found 520.1568, Δ = 1.5ppm; *Identifiable data for the minor anti-(E) diastereoisomer:* **^{19}F {^{1}H} NMR (377 MHz, $CDCl_3$)** δ = -179.09.

The (*E)* nature of this isomer has been confirmed by NOESY experiments.

4.4 Synthesis of 3-fluoro-2-iodomethylpyrrolidines and 4-fluoro-5-iodomethylpyrrolidin-2-ones

4.4.1 General procedures:

General procedure for condition A:

To a solution of allylic fluoride (1 eq.) in dry CH_3CN [0.2 M] in a darkened vessel, was added iodine (2.2 eq.). The reaction mixture was then stirred overnight before being quenched by addition of saturated $NaS_2O_{3(aq.)}$ solution/saturated $NaHCO_{3(aq.)}$ solution (1:1). The aqueous layer was extracted three times with Et_2O, the combined organic phases were washed with brine, dried over $MgSO_4$, filtered and the solvent removed *in vacuo*. The crude product was purified by flash column chromatography on silica gel (hexane/Et_2O 8:2).

General procedure for condition B:

To a solution of allylic fluoride (1 eq.) in saturated $NaHCO_{3\ (aq.)}$ solution/CH_2Cl_2 (1:1, [0.13 M]) in a darkened vessel, was added iodine (2.2 eq). The reaction mixture was then stirred overnight before being quenched by addition of saturated $NaS_2O_{3(aq.)}$ solution/saturated $NaHCO_{3(aq.)}$ solution (1:1). The aqueous layer was extracted three times with Et_2O, the combined organic phases were washed with brine, dried over $MgSO_4$, filtered and the solvent removed *in vacuo*. The crude product was purified by flash column chromatography on silica gel (hexane/Et_2O 8:2).

4.4.2 Synthesis of 3-fluoro-2-iodomethylpyrrolidines and 4-fluoro-5- iodomethyl pyrrolidin-2ones:

(±) 3-fluoro-2-(iodomethyl)-1-[(4methylphenyl)sulfonyl] pyrrolidine (56):

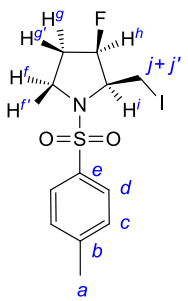

Following the general procedure for the iodocyclisation using Condition **A** on 100 mg (0.39 mmol) of **(±)-55**, the reaction yielded 75 mg of **56** (51%, d.r. (*syn:anti*) 10:1) as a white solid.

Following the general procedure for the iodocyclisation using Condition **B** on 100 mg (0.39 mmol) of **(±)-55**, the reaction yielded 131 mg of **56** (88%, d.r. (*syn:anti*) 14:1) .

Following the general procedure for the iodocyclisation using Condition **A** with NIS (2.2 eq.) on 100 mg (0.39 mmol) of **(±)-55**, the reaction yielded 85 mg of **56** (56 %, d.r. (*syn:anti*) 11:1).

Following the general procedure for the iodocyclisation using Condition **B** with NIS (2.2 eq.) on 50 mg (0.195 mmol) on **(±)-55**, the reaction yielded 62 mg of **56** (82%, d.r. (*syn:anti*) 12:1).

Data for the major syn diastereoisomer: **R_f** = 0.4 (hexane/EtOAc 7:3); **m.p.** = 72 °C; **^{1}H NMR (500 MHz, C_6D_6)** δ = 0.52 (ddddd, 1H, $^3J_{H-F}$ = 42.2 Hz, $^2J_{H-H}$ = 14.0 Hz, $^3J_{H-H}$ =12.2, 8.7, 3.4 Hz, *g*), 1.21 (ddd, 1H, $^3J_{H-F}$ = 16.0 Hz, $^2J_{H-H}$ = 14.0 Hz, $^3J_{H-H}$ = 5.4 Hz, *g'*), 1.86 (s, 3H, *a*), 3.22 (ddd, 1H, $^2J_{H-H}$ = 11.7 Hz, $^3J_{H-H}$ = 12.2 Hz, 5.4 Hz, *f''*), 3.28 (dd, 1H, $^3J_{H-H}$ = 11.6 Hz, $^2J_{H-H}$ = 9.3 Hz, *j'*), 3.40 (dd, 1H, $^2J_{H-H}$ = 11.7 Hz, $^3J_{H-H}$ = 8.7 Hz, *f*), 3.67 (dddd, 1H, $^3J_{H-F}$ = 23.8 Hz, $^3J_{H-H}$ = 11.6, 3.9, 3.7 Hz, *i*), 3.93 (ddd, 1H, $^2J_{H-H}$ = 9.3 Hz, $^4J_{H-F}$ = 3.9 Hz, $^3J_{H-H}$ = 3.9 Hz, *j*), 4.63 (ddd, 1H, $^2J_{H-F}$ = 52.2 Hz, $^3J_{H-H}$ = 3.7, 3.4 Hz, *h*), 6.68 (d, 2H, $^3J_{H-H}$ = 7.9 Hz, *c/d*), 7.54 (d, 2H, $^3J_{H-H}$ = 8.5 Hz, *c/d*); **^{13}C NMR (101 MHz, $CDCl_3$)** δ = 1.1 (d, $^3J_{C-F}$ = 12.8 Hz, *j*), 21.6 (*a*), 31.5 (d, $^2J_{C-F}$ = 21.6 Hz, *g*), 48.6 (*f*), 65.9 (d, $^2J_{C-F}$ = 19.2 Hz, *i*), 93.5 (d, $^1J_{C-F}$ = 184.5 Hz, *h*), 127.4 (*c/d*), 130.1 (*c/d*), 133.9 (*b/e*), 144.3 (*b/e*); **^{19}F {^{1}H} NMR (377 MHz, C_6D_6)** δ = -196.48; **IR (KBr)**: **ν =** 1685, 1330, 1160, 982, 772; **HRMS (CI^+):** *m/z* required for $C_{12}H_{16}FINO_2S$ ($[M+H]^+$): 383.9931, found 383.9947, Δ = 4.3 ppm. *Identifiable data for the minor anti diastereoisomer:* **^{19}F {^{1}H} NMR (377 MHz, $CDCl_3$)** δ = -176.26;

The structure was unambiguously confirmed by X-ray crystallography and NOESY/HOESY experiments. Crystallographic data are deposited at the Cambridge Crystallographic Data Centre (CCDC-896055).

(±) 2-(bromomethyl)-3-fluoro-1-[(4-methylphenyl)sulfonyl] pyrrolidine (152):

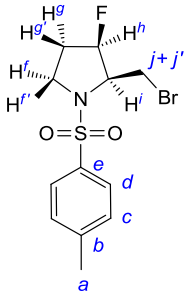

Following the general procedure for the iodocyclisation using Condition **A** on 100 mg (0.39 mmol) of **(±)-55**, the reaction yielded 80 mg of **152** (61%, d.r. (*syn:anti*) 11:1) as a white solid.

Following the general procedure for the iodocyclisation using Condition **B** on 100 mg (0.39 mmol) of **(±)-55**, the reaction gave 71% conversion of **152** (d.r. (*syn:anti*) 8:1). The product was not isolated using this method.

Data for the major syn diastereoisomer: **R_f** = 0.25 (hexane/Et_2O 6:4); **m.p.** = 105 °C; **^{1}H NMR (500 MHz, C_6D_6)** δ = 0.51 (ddddd, 1H, $^3J_{H-F}$ = 42.0 Hz, $^2J_{H-H}$ = 14.0 Hz, $^3J_{H-H}$ = 12.2, 8.7, 3.4 Hz, *g*), 1.22 (ddd, 1H, $^3J_{H-F}$ = 14.9 Hz, $^2J_{H-H}$ = 14.0 Hz, $^3J_{H-H}$ = 5.4 Hz, *g'*), 1.86 (s, 3H, *a*), 3.21 (ddd, 1H, $^2J_{H-H}$ = 11.6 Hz, $^3J_{H-H}$ = 12.2, 5.4 Hz, *f'*), 3.33 (dd, 1H, $^2J_{H-H}$ = 11.6 Hz, $^3J_{H-H}$ = 8.7 Hz, *f*), 3.53 (dd, 1H, $^3J_{H-H}$ = 11.3 Hz, $^2J_{H-H}$ = 9.4 Hz, *j'*), 3.65 (dddd, 1H, $^3J_{H-F}$ = 23.2 Hz, $^3J_{H-H}$ = 11.3, 4.0, 3.5 Hz, *i*), 4.12 (ddd, 1H, $^2J_{H-H}$ = 9.4 Hz, $^3J_{H-H}$ = 4.0 Hz, $^4J_{H-F}$ = 3.5 Hz, *j*), 4.60 (ddd, 1H, $^2J_{H-F}$ = 52.2 Hz, $^3J_{H-H}$ = 3.4, 3.0 Hz, *h*), 6.69 (d, 2H, $^3J_{H-H}$ = 7.9 Hz, *c/d*), 7.53 (d, 2H, $^3J_{H-H}$ = 8.2 Hz, *c/d*); **^{13}C NMR (101 MHz, $CDCl_3$)** δ = 21.6 (*a*), 28.3 (d, $^3J_{C-F}$ = 13.6 Hz, *j*), 31.5 (d, $^2J_{C-F}$ = 20.7 Hz, *g*), 48.2 (*f*), 65.3 (d, $^2J_{C-F}$ = 19.2 Hz, *i*), 92.8 (d, $^1J_{C-F}$ = 185.3 Hz, *h*), 127.5 (*c/d*), 130.1 (*c/d*), 133.7 (*b/e*), 144.3 (*b/e*); **^{19}F {^{1}H} NMR (377 MHz, C_6D_6)** δ = -196.21; **IR (KBr)**: **ν =** 2907, 1598, 1342, 1158, 1104, 659, 544; **HRMS (CI^+):** *m/z* required for $C_{12}H_{16}FBrNO_2S$ ($[M+H]^+$): 338.0049, found 338.0040; *Identifiable data for the minor anti diastereoisomer:* **^{19}F {^{1}H} NMR (377 MHz, $CDCl_3$)** δ = -177.11;

The structure was unambiguously confirmed by X-ray crystallography and NOESY/HOESY experiments. Crystallographic data are deposited at the Cambridge Crystallographic Data Centre (CCDC-896056).

(±) *tert*-butyl [3-fluoro-2-(iodomethyl) pyrrolidin-1-yl]acetate (101):

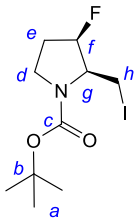

Following the general procedure for the iodocyclisation using Condition **B** on 100 mg (0.39 mmol) of **(±)-61**, the reaction yielded 68 mg of **101** (42%, d.r. (*syn:anti*) 4:1) as a white solid. *Note: this compound is very unstable and must be stored at -20 °C in absence of light. NMR analysis at higher temperature did not give a better resolution of the rotamers but lead instead to the decomposition of the product.*

Data for the major syn diastereoisomer: **R_f** = 0.5 (hexane/Et_2O 7:3); **m.p.** = 65 °C; **^{1}H NMR (500 MHz, $(CD_3)_2CO$)** δ = 1.45 (sbr, 9H, *a*), 2.06-2.16 (m, 2H, *e*), 3.09-3.28 (m, 1H, *h*), 3.29-3.45 (m, 1H, *d*), 3.79-3.87 (m, 2H, *h'+d'*), 4.04-4.15 (m, 1H, *g*), 5.38 (d, 1H, $^2J_{H\text{-}F}$ = 52.6 Hz, *f*); **^{13}C NMR (125 MHz, $(CD_3)_2CO$)** δ = 1.7 (*h*), 29.0 (*a*), 32.1 (d, $^2J_{C\text{-}F}$ = 18.1 Hz, *e*), 46.6 (*d rotamer 101(a)*), 47.3 (*d rotamer 101(b)*), 64.2 (d, $^2J_{C\text{-}F}$ = 18.1 Hz, *g*), 80.8 (*b*), 95.2 (d, $^1J_{C\text{-}F}$ = 178.3 Hz, *f rotamer 101(a)*), 95.5 (d, $^1J_{C\text{-}F}$ = 181.2 Hz, *f rotamer 101(b)*), 155.1 (*c rotamer 101(a)*), 155.8 (*c rotamer 101(b)*); **^{19}F {^{1}H} NMR (377 MHz, $CDCl_3$)** δ = -197.68; **IR (KBr): ν =** 2975, 2360, 1677, 1407, 1167, 573; **HRMS (ESI^+):** *m/z* required for $C_{10}H_{17}FINO_2Na^+$ ($[M+Na]^+$): 352.0182, found 352.0180, Δ = 0.41 ppm. *Identifiable data for the minor anti diastereoisomer:* **^{19}F {^{1}H} NMR (377 MHz, $CDCl_3$)** δ = -175.84;

(±) 3-fluoro-2-(iodomethyl)-3-methyl-1-[(4-methylphenyl)sulfonyl]pyrrolidine (102):

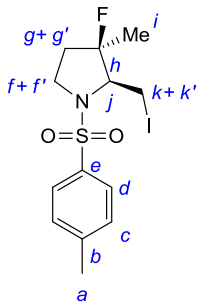

Following the general procedure for the iodocyclisation using Condition **A** on 106 mg (0.39 mmol) of **(±)-62**, the reaction yielded 69 mg of **102** (45%, d.r. (*syn:anti*) 4:1) as a white solid.

Following the general procedure for the iodocyclisation using Condition **B** on 60 mg (0.21 mmol) of **(±)-62**, the reaction yielded 73 mg of **102** (86%, d.r. (*syn:anti*) 8:1).

Data for the major syn diastereoisomer: **R_f** = 0.5 (hexane/Et_2O 7:3); **m.p.** = 68 °C; **^{1}H NMR (400 MHz, $CDCl_3$)** δ = 1.27-1.41 (m, 1H, *g*), 1.44 (d, 3H, $^3J_{H-F}$ = 21.2 Hz, *i*), 2.00-2.11 (m, 1H, *g'*), 2.46 (s, 3H, *a*), 3.34-3.42 (m, 1H, *f*), 3.43-3.53 (m, 2H, *f'+k*), 3.62 (dt, 1H, $^2J_{H-H}$ = 10.1 Hz, $^3J_{H-H}$ = 3.3 Hz, *k'*), 3.65-3.75 (m, 1H, *j*), 7.36 (d, 2H, $^3J_{H-H}$ = 8.4 Hz, *c/d*), 7.74 (d, 2H, $^3J_{H-H}$ = 8.4 Hz, *c/d*); **^{13}C NMR (101 MHz, $CDCl_3$)** δ = 0.7 (d, $^3J_{C-F}$ = 11.2 Hz, *k*), 21.6 (*a*), 24.9 (d, $^2J_{C-F}$ = 25.5 Hz, *i*), 38.4 (d, $^2J_{C-F}$ = 24.0 Hz, *g*), 46.0 (*f*), 67.1 (d, $^2J_{C-F}$ = 20.7 Hz, *j*), 100.8 (d, $^1J_{C-F}$ = 186.9 Hz, *h*), 127.4 (*c/d*), 130.0 (*c/d*), 134.1 (*b/e*), 144.2 (*b/e*); **^{19}F NMR {^{1}H} (377 MHz, $CDCl_3$)** δ = -156.62; **IR (KBr)**: **ν** = 1699, 1232, 1122, 922; **HRMS (CI^+):** *m/z* required for $C_{13}H_{18}FINO_2S$ ($[M+H]^+$): 398.0087, found 398.0100, Δ = 3.3 ppm. *Identifiable data for the minor anti diastereoisomer:* **^{19}F {^{1}H} NMR (377 MHz, $CDCl_3$)** δ = -159.29;

The structure was unambiguously confirmed by X-ray crystallography and NOESY/HOESY experiments. Crystallographic data are deposited at the Cambridge Crystallographic Data Centre (CCDC-896062).

(±) 3-fluoro-2-(iodomethyl)-2-methyl-1-[(4-methylphenyl)sulfonyl]pyrrolidine (103):

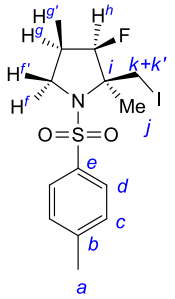

Following the general procedure for the iodocyclisation using Condition **A** on 51 mg (0.19 mmol) of **(±)-63**, the reaction yielded 49 mg of **103** (65%, d.r. (*syn:anti*) 10:1) as a white solid.

Data for the major syn diastereoisomer: **R_f** = 0.4 (hexane/Et_2O 1:1); **m.p.** = 52 °C; **^{1}H NMR (500 MHz, C_6D_6)** δ = 1.19 (ddddd, 1H, $^3J_{H-F}$ = 43.2 Hz, $^2J_{H-H}$ = 14.2 Hz, $^3J_{H-H}$ = 10.9, 9.2, 3.3 Hz, *g*), 1.29 (ddddd, 1H, $^3J_{H-F}$ = 18.4 Hz, $^2J_{H-H}$ = 14.2 Hz, $^3J_{H-H}$ = 6.7, 1.6, 0.8 Hz, *g'*), 1.41 (dd, 3H, $^4J_{H-F}$ = 1.8 Hz, $^4J_{H-H}$ = 0.9 Hz, *j*), 1.86 (s, 3H, *a*), 3.18 (ddd, 1H, $^2J_{H-H}$ = 9.4, $^3J_{H-H}$ = 10.9, 6.7 Hz, *f'*), 3.49 (ddd,

1H, $^{2}J_{H\text{-}H}$ = 9.4 Hz, $^{3}J_{H\text{-}H}$ = 9.2, 1.6 Hz, *f*), 3.51 (ddq, 1H, $^{2}J_{H\text{-}H}$ = 9.2 Hz, $^{4}J_{H\text{-}H}$ = 0.9 Hz, $^{4}J_{H\text{-}F}$ = 0.9 Hz, *k'*), 4.22 (dd, 1H, $^{2}J_{H\text{-}H}$ = 9.2 Hz, $^{4}J_{H\text{-}F}$ = 5.1 Hz, *k*), 4.34 (ddd, 1H, $^{2}J_{H\text{-}F}$ = 51.2 Hz, $^{3}J_{H\text{-}H}$ = 3.3, 0.8 Hz, *h*), 6.71 (d, 2H, $^{3}J_{H\text{-}H}$ = 7.8 Hz, *c/d*), 7.61 (d, 2H, $^{3}J_{H\text{-}H}$ = 8.2 Hz, *c/d*); **^{13}C NMR (125 MHz, C_6D_6)** δ = 8.4 (d, $^{3}J_{C\text{-}F}$ = 12.4 Hz, *k*), 21.4 (*a*), 23.7 (d, $^{3}J_{C\text{-}F}$ = 3.8 Hz, *j*), 28.4 (d, $^{2}J_{C\text{-}F}$ = 21.9 Hz, *g*), 48.4 (*f*), 70.3 (d, $^{2}J_{C\text{-}F}$ = 17.2 Hz, *i*), 99.8 (d, $^{1}J_{C\text{-}F}$ = 187.9 Hz, *h*), 127.6 (*c/d*), 130.0 (*c/d*), 139.4 (*b/e*), 143.3 (*b/e*); **^{19}F {^{1}H} NMR (377 MHz, C_6D_6)** δ = -185.38; **IR (KBr): ν =** 2979, 2361, 1597, 1339, 1158, 1094, 547; **HRMS (CI^{+}):** *m/z* required for $C_{13}H_{21}FIN_2O_2S$ ($[M+NH_4]^{+}$): 415.0353, found 415.0332, Δ = 5 ppm. *Identifiable data for the minor anti diastereoisomer:* **^{19}F {^{1}H} NMR (377 MHz, C_6D_6)** δ = -186.36;

The structure was unambiguously confirmed by X-ray crystallography and NOESY/HOESY experiments. Crystallographic data are deposited at the Cambridge Crystallographic Data Centre (CCDC-896057).

(±) 3-fluoro-2-(iodomethyl)-4,4-dimethyl-1-[(4-methylphenyl)sulfonyl]pyrrolidine (104):

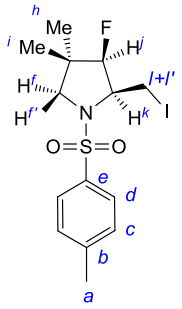

Following the general procedure for the iodocyclisation using Condition **B** on 100 mg (0.35 mmol) of **(±)-64**, the reaction yielded 139 mg of **104** (97%, d.r. (*syn:anti*) > 20:1) as a white solid.

R_f = 0.5 (hexane/Et_2O 6:4); **m.p.** = 149 °C; **^{1}H NMR (500 MHz, C_6D_6)** δ = -0.06 (d, 3H, $^{4}J_{H\text{-}F}$ = 1.8 Hz, *h*), 0.62 (d, 3H, $^{4}J_{H\text{-}F}$ = 2.2 Hz, *i*), 1.96 (s, 3H, *a*), 3.14 (d, 1H, $^{2}J_{H\text{-}H}$ = 11.0 Hz, *f'*), 3.21 (dd, 1H, $^{2}J_{H\text{-}H}$ = 11.0 Hz, $^{4}J_{H\text{-}F}$ = 0.9 Hz, *f*), 3.35 (dd, 1H, $^{3}J_{H\text{-}H}$ = 11.6 Hz, $^{2}J_{H\text{-}H}$ = 9.1 Hz, *l*), 4.03 (dddd, 1H, $^{3}J_{H\text{-}F}$ = 25.1 Hz, $^{3}J_{H\text{-}H}$ = 11.5, 4.0, 3.6 Hz, *k*), 4.11 (ddd, 1H, $^{2}J_{H\text{-}H}$ = 9.1 Hz, $^{4}J_{H\text{-}F}$ = 4.6 Hz, $^{3}J_{H\text{-}H}$ = 4.0 Hz, *l'*), 4.32 (dd, 1H, $^{2}J_{H\text{-}F}$ = 51.8 Hz, $^{3}J_{H\text{-}H}$ = 3.4 Hz, *j*), 6.69 (d, 2H, $^{3}J_{H\text{-}H}$ = 7.6 Hz, *c/d*), 7.58 (d, 2H, $^{3}J_{H\text{-}H}$ = 8.2 Hz, *c/d*); **^{13}C NMR (125 MHz, C_6D_6)** δ = 1.8 (d, $^{3}J_{C\text{-}F}$ = 15.3 Hz, *l*), 19.4 (d, $^{3}J_{C\text{-}F}$ = 8.6 Hz, *h*), 21.4 (*a*), 22.6 (d, $^{3}J_{C\text{-}F}$ = 6.7 Hz, *i*), 41.5 (d, $^{2}J_{C\text{-}F}$ = 18.1 Hz, *g*), 60.1 (*f*), 65.6 (d, $^{2}J_{C\text{-}F}$ = 20.0

Hz, *k*), 99.8 (d, $^{1}J_{C\text{-}F}$ = 190.7 Hz, *j*), 128.0 (*c/d*), 130.2 (*c/d*), 136.4 (*b/e*), 143.8 (*b/e*); **^{19}F {^{1}H} NMR (377 MHz, C_6D_6)** δ = -199.93; **IR (neat): ν =** 1445, 1181, 1088, 671; **HRMS (CI^{+}):** *m/z* required for $C_{14}H_{20}NO_2FSI$ ([M+H]$^{+}$): 412.0244, found: 412.0249, Δ = 1.3 ppm.

The structure was unambiguously confirmed by X-ray crystallography and NOESY/HOESY experiments. Crystallographic data are deposited at the Cambridge Crystallographic Data Centre (CCDC-896058).

(±) 4-fluoro-5-(iodomethyl)-3,3-dimethyl-1-1tosylpyrrolidin-2-one (105):

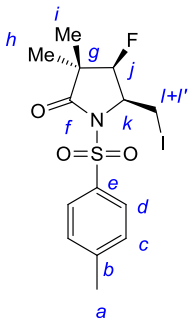

Following the general procedure for the iodocyclisation using Condition **B** on 50 mg (0.17 mmol) of **(±)-66**, the reaction yielded 44 mg of **105** (62%, d.r. (*syn:anti*) > 20:1) and 17 mg of **107** (24%, d.r. (*syn:anti*) > 20:1) as two separable white solids.

*Data for the major product syn-***105** *diastereoisomer:* **R_f** = 0.6 (hexane/EtOAc 7:3); **m.p.** = 168 °C; **^{1}H NMR (500 MHz, C_6D_6)** δ = 0.32 (d, 3H, $^{4}J_{H\text{-}F}$ = 1.6 Hz, *h*), 0.91 (d, 3H, $^{4}J_{H\text{-}F}$ = 2.7 Hz, *i*), 1.78 (s, 3H, *a*), 3.19 (dd, 1H, $^{3}J_{H\text{-}H}$ = 11.4 Hz, $^{2}J_{H\text{-}H}$ = 8.9 Hz, *l*), 4.25 (dddd, 1H, $^{3}J_{H\text{-}F}$ = 22.4 Hz, $^{3}J_{H\text{-}H}$ = 11.4, 3.8, 3.8 Hz, *k*), 4.31 (dd, 1H, $^{2}J_{H\text{-}F}$ = 52.0 Hz, $^{3}J_{H\text{-}H}$ = 3.8 Hz, *j*), 4.35 (ddd, 1H, $^{2}J_{H\text{-}H}$ = 8.9 Hz, $^{4}J_{H\text{-}F}$ = 5.3 Hz, $^{3}J_{H\text{-}H}$ = 3.8 Hz, *l'*), 6.66 (d, 2H, $^{3}J_{H\text{-}H}$ = 7.8 Hz, *c/d*), 7.84 (d, 2H, $^{3}J_{H\text{-}H}$ = 8.2 Hz, *c/d*); **^{13}C NMR (125 MHz, C_6D_6)** δ = -0.2 (d, $^{3}J_{C\text{-}F}$ = 14.3 Hz, *l*), 16.6 (d, $^{3}J_{C\text{-}F}$ = 10.5 Hz, *i*), 21.2 (d, $^{3}J_{C\text{-}F}$ = 5.7 Hz, *h*), 21.5 (*a*), 46.2 (d, $^{2}J_{C\text{-}F}$ = 20.0 Hz, *g*), 61.9 (d, $^{2}J_{C\text{-}F}$ = 20.0 Hz, *k*), 93.5 (d, $^{1}J_{C\text{-}F}$ = 193.6 Hz, *j*), 128.9 (*c/d*), 130.0 (*c/d*), 136.5 (*b/e*), 145.3 (*b/e*), 177.3 (*f*); **^{19}F {^{1}H} NMR (377 MHz, C_6D_6)** δ = -200.03; **IR (KBr)**: **ν =** 2977, 1738, 1363, 1177, 1077, 663, 573; **HRMS (ESI^{+}):** *m/z* required for $C_{14}H_{18}FINO_3S^{+}$ ([M+H]$^{+}$): 426.0031, found 426.0029, Δ = 0.5 ppm;

The structure was unambiguously confirmed by X-ray crystallography and NOESY/HOESY experiments. Crystallographic data are deposited at the Cambridge Crystallographic Data Centre (CCDC-896060).

(±) *N*-(4-fluoro-5-(iodomethyl)-3,3-dimethyldihydrofuran-2-(3*H*)-ylidene)-4-methylbenzene sulfonamide (107):

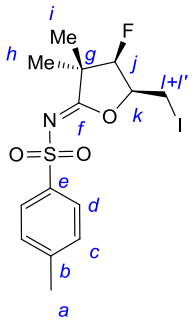

Data for the minor product syn-**107***:* **R_f** = 0.2 (hexane/EtOAc 7:3); **m.p.** = 135 °C; **^{1}H NMR (500 MHz, C_6D_6)** δ = 0.44 (d, 3H, $^4J_{H\text{-}F}$ = 1.6 Hz, *h*), 0.95 (d, 3H, $^4J_{H\text{-}F}$ = 2.8 Hz, *i*), 1.85 (s, 3H, *a*), 2.72 (ddd, 1H, $^2J_{H\text{-}H}$ = 9.8 Hz, $^3J_{H\text{-}H}$ = 5.7 Hz, $^4J_{H\text{-}F}$ = 3.5 Hz, *l*), 2.78 (dd, 1H, $^2J_{H\text{-}H}$ = 9.8 Hz, $^3J_{H\text{-}H}$ = 9.5 Hz, *l'*), 3.91 (dddd, 1H, $^3J_{H\text{-}F}$ = 24.6 Hz, $^3J_{H\text{-}H}$ = 9.8, 5.7, 2.8 Hz, *k*), 3.91 (dd, 1H, $^2J_{H\text{-}F}$ = 53.0, $^3J_{H\text{-}H}$ = 2.8 Hz, *j*), 6.77 (d, 2H, $^3J_{H\text{-}H}$ = 8.2 Hz, *c/d*), 8.08 (d, 2H, $^3J_{H\text{-}H}$ = 8.5 Hz, *c/d*); **^{13}C NMR (125 MHz, C_6D_6)** δ = -4.6 (d, $^3J_{C\text{-}F}$ = 13.3 Hz, *l*), 18.2 (d, $^3J_{C\text{-}F}$ = 10.5 Hz, *i*), 21.4 (*a*), 22.7 (d, $^3J_{C\text{-}F}$ = 4.8 Hz, *h*), 48.8 (d, $^2J_{C\text{-}F}$ = 20.0 Hz, *g*), 85.2 (d, $^2J_{C\text{-}F}$ = 21.0 Hz, *k*), 94.9 (d, $^1J_{C\text{-}F}$ = 194.5 Hz, *j*), 128.7 (*c/d*), 129.7 (*c/d*), 140.3 (*b/e*), 143.4 (*b/e*), 175.5 (*f*); **^{19}F {^{1}H} NMR (377 MHz, C_6D_6)** δ = -202.49; **ν_{max}/cm^{-1} (DCM)**: 3055, 1650, 1265, 738, 705; **HRMS (ESI$^+$):** *m/z* required for $C_{14}H_{18}FINO_3SNa^+$ ($[M+Na]^+$): 447.9850, found 447.9834, Δ = 3.8 ppm;

The structure was unambiguously confirmed by X-ray crystallography. Crystallographic data are deposited at the Cambridge Crystallographic Data Centre (CCDC-896063).

(±) (*syn,anti*)-5-(benzyloxymethyl)-3-fluoro-2-(iodomethyl)-1-tosylpyrrolidine (*syn,anti*-106):

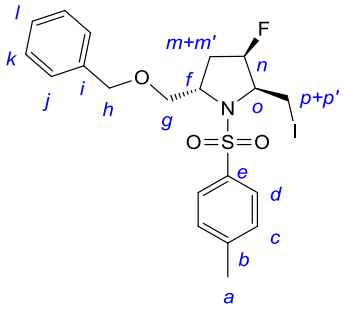

Following the general procedure of the iodocyclisation using Condition **B** on 82 mg (0.22 mmol) of *syn*-**67**, the reaction yielded 86 mg of *syn,anti*-**106** (78%, d.r. (*syn:anti*) 17:1) as a colourless oil.

Data for the major syn,anti-**106** *diastereoisomer:* $\mathbf{R_f}$ = 0.5 (hexane/Et_2O 6:4); **^{1}H NMR (500 MHz, C_6D_6)** δ = 1.70 (dddd, 1H, $^3J_{H-F}$ = 21.1 Hz, $^2J_{H-H}$ = 13.9 Hz, $^3J_{H-H}$ = 6.0, 4.4 Hz, *m*), 1.84 (s, 3H, *a*), 2.05 (dddd, 1H, $^3J_{H-F}$ = 23.6 Hz, $^2J_{H-H}$ = 13.9 Hz, $^3J_{H-H}$ = 8.8, 5.4 Hz, *m'*), 3.07 (dd, 1H, $^2J_{H-H}$ = 9.7 Hz, $^3J_{H-H}$ = 2.1 Hz, *g*), 3.36 (ddd, 1H, $^2J_{H-H}$ = 9.7 Hz, $^3J_{H-H}$ = 9.8 Hz, $^4J_{H-F}$ = 1.6 Hz, *p*), 3.70 (ddd, 1H, $^2J_{H-H}$ = 9.7 Hz, $^3J_{H-H}$ = 4.1 Hz, $^5J_{H-F}$ = 1.3 Hz, *g'*), 3.92 (ddd, 1H, $^2J_{H-H}$ = 9.8 Hz, $^4J_{H-F}$ = 3.2 Hz, $^3J_{H-H}$ = 2.8 Hz, *p'*), 3.94 (d, 1H, $^2J_{H-H}$ = 11.7 Hz, *h*), 3.98 (dddd, 1H, $^3J_{H-F}$ = 15.1 Hz, $^3J_{H-H}$ = 9.7, 5.1, 2.7 Hz, *o*), 3.99 (d, 1H, $^2J_{H-H}$ = 11.7 Hz, *h'*), 4.08 (dddd, 1H, $^3J_{H-H}$ = 8.5, 4.4, 4.1, 2.2 Hz, *f*), 5.07 (ddd, 1H, $^2J_{H-H}$ = 54.2 Hz, $^3J_{H-H}$ = 5.6, 5.3 Hz, *n*), 6.70 (d, 2H, $^3J_{H-H}$ = 8.2 Hz, *c/d*), 6.99 (d, 1H, $^3J_{H-H}$ = 6.6 Hz, *l*), 7.07 (t, 2H, $^3J_{H-H}$ = 7.2 Hz, *k/j*), 7.10-7.15 (m, 2H, *j/k*), 7.64 (d, 2H, $^3J_{H-H}$ = 8.2 Hz, *c/d*); **^{13}C NMR (125 MHz, C_6D_6)** δ = 1.6 (d, $^3J_{C-F}$ = 11.4 Hz, *p*), 21.4 (*a*), 34.2 (d, $^2J_{C-F}$ = 21.0 Hz, *m*), 60.5 (d, $^3J_{C-F}$ = 3.8 Hz, *f*), 64.3 (d, $^2J_{C-F}$ = 20.0 Hz, *o*), 71.5 (*g*), 73.4 (*h*), 92.5 (d, $^1J_{C-F}$ = 187.9 Hz, *n*), 127.5 (*j/k/l*), 128.0 (*c/d*), 128.7 (*j/k/l*), 128.90 (*j/k/l*), 130.0 (*c/d*), 138.7 (*b/e*), 140.0 (*i*), 143.3 (*b/e*); **^{19}F {^{1}H} NMR (377 MHz, C_6D_6)** δ = -191.77; **IR (DCM)**: **ν =** 2924, 1345, 1261, 1104, 750; **HRMS (ESI$^+$):** *m/z* required for $C_{20}H_{23}FINO_3SNa^+$ ($[M+Na]^+$): 526.0320, found 326.0312, Δ = 1.5 ppm.

Identifiable data for the minor anti,syn-**106** *diastereoisomer:* **^{19}F {^{1}H} NMR (377 MHz, C_6D_6)** δ = -174.75;

The structure was unambiguously confirmed by NOESY/HOESY experiments.

(±) (*syn,syn*)-5-(benzyloxymethyl)-3-fluoro-2-(iodomethyl)-1-tosylpyrrolidine (*syn,syn*-106):

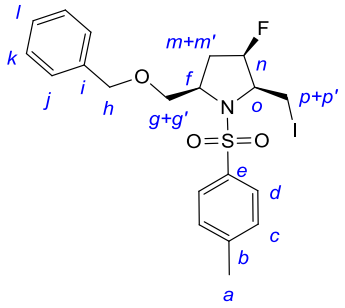

Following the general procedure for the iodocyclisation using Condition **B** on 50 mg (0.132 mmol) of *anti*-**67**, the reaction yielded 63 mg of *syn,syn*-**106** (95%, d.r. (*syn:anti*) 13:1) as a white solid.

Data for the major syn,syn-**106** *diastereoisomer:* **R_f =** 0.8 (hexane/Et_2O 6:4); **m.p.** = 132 °C; **^{1}H NMR (500 MHz, C_6D_6)** δ = 0.80 (dddd, 1H, $^3J_{H-F}$ = 45.1 Hz, $^2J_{H-H}$ = 14.9 Hz, $^3J_{H-H}$ = 8.8, 4.1 Hz, *m*), 1.87 (s, 3H, *a*), 2.02 (dd, 1H, $^3J_{H-F}$ = 18.8 Hz, $^2J_{H-H}$ = 14.9 Hz, *m'*), 3.25 (dd, 1H, $^3J_{H-H}$ = 11.6 Hz, $^2J_{H-H}$ = 9.4 Hz, *p*), 3.49 (ddd, 1H, $^3J_{H-H}$ = 10.4 Hz, $^2J_{H-H}$ = 8.8 Hz, $^5J_{H-F}$ = 2.2 Hz, *g*), 3.64 (dddd, 1H, $^3J_{H-F}$ = 22.8 Hz, $^3J_{H-H}$ = 11.6, 4.0, 3.8 Hz, *o*), 3.85 (ddd, 1H, $^2J_{H-H}$ = 8.8 Hz, $^3J_{H-H}$ = 5.1 Hz, $^5J_{H-F}$ = 2.2 Hz, *g'*), 4.03 (ddd, 1H, $^2J_{H-H}$ = 9.4 Hz, $^4J_{H-F}$ = 4.0 Hz, $^3J_{H-H}$ = 3.8 Hz, *p'*), 4.16 (ddd, 1H, $^3J_{H-H}$ = 10.4, 8.8, 5.1 Hz, *f*), 4.26 (d, 1H, $^2J_{H-H}$ = 11.9 Hz, *h*), 4.30 (d, 1H, $^2J_{H-H}$ = 11.9, *h'*), 4.62 (ddd, 1H, $^2J_{H-F}$ = 51.8 Hz, $^3J_{H-H}$ = 4.1, 4.0 Hz, *n*), 6.68 (d, 2H, $^3J_{H-H}$ = 7.9 Hz, *c/d*), 6.98-7.24 (m, 5H, *j+k+l*), 7.54 (d, 2H, $^3J_{H-H}$ = 8.2 Hz, *c/d*); **^{13}C NMR (101 MHz, C_6D_6)** δ = 1.8 (d, $^3J_{C-F}$ = 12.8 Hz, *p*), 21.4 (*a*), 33.2 (d, $^2J_{C-F}$ = 20.8 Hz, *m*), 62.0 (*f*), 65.6 (d, $^2J_{C-F}$ = 20.0 Hz, *o*), 73.7 (*g*), 73.8 (*h*), 94.4 (d, $^1J_{C-F}$ = 186.1 Hz, *n*), 128.1 (*c/d*), 128.2 (*j/k/l*), 128.3 (*j/k/l*), 128.9 (*j/k/l*), 130.3 (*c/d*), 134.3 (*i*), 139.0 (*b/e*), 144.2 (*b/e*); **^{19}F {^{1}H} NMR (377 MHz, C_6D_6)** δ = -189.49; **IR (KBr)**: **ν =** 2924, 1344, 1163, 1108, 741, 669, 555, 541; **HRMS (ESI$^+$):** *m/z* required for $C_{20}H_{23}FINO_3SNa^+$ ([M+Na]$^+$): 526.0319, found 326.0319;

Identifiable data for the minor anti,anti-**106** *diastereoisomer:* **^{19}F {^{1}H} NMR (377 MHz, C_6D_6)** δ = -171.16;

The structure was unambiguously confirmed by X-ray crystallography and NOESY/HOESY experiments. Crystallographic data are deposited at the Cambridge Crystallographic Data Centre (CCDC-896059).

(±) 1-(3-fluoro-4-iodocyclopentylsulfonyl)-4-methylbenzene (109):

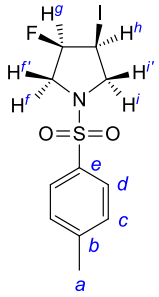

General procedure for the iodocyclisation using Condition **C**: To a solution of **(±)-68** (100 mg, 0.4 mmol, 1 eq.) in CH_3CN (1.4 mL) in a darkened vessel, was added iodine (312 mg, 1.2 mmol, 3 eq). The reaction mixture was then stirred at 75 °C for 15 h before being quenched by addition of saturated NaS_2O_3 solution/saturated $NaHCO_3$ solution (1:1, 7 mL). The aqueous layer was extracted three times with Et_2O, the combined organic phases were washed with brine, dried over $MgSO_4$, filtered and the solvent removed *in vacuo*. The crude product was purified by flash column chromatography on silica gel (hexane/Et_2O 8:2) to afford the two diastereomeric pyrrolidines (32 mg, 29%, d.r. (*syn:anti*) 10:1) as separable isomers each of them under the form of a white solid.

*Data for the major syn-***109** *diastereoisomer:* **R_f =** 0.3 (hexane/Et_2O 6:4); **m.p.** = 52 °C; **^{1}H NMR (500 MHz, C_6D_6)** δ = 1.83 (s, 3H, *a*), 2.91 (dddd, 1H, $^3J_{H\text{-}F}$ = 29.3 Hz, $^3J_{H\text{-}H}$ = 11.1, 7.6, 3.2 Hz, *h*), 3.02 (ddd, 1H, $^3J_{H\text{-}F}$ = 35.9 Hz, $^2J_{H\text{-}H}$ = 12.5 Hz, $^3J_{H\text{-}H}$ = 3.7 Hz, *f*), 3.19 (dd, 1H, $^3J_{H\text{-}F}$ = 24.4 Hz, $^2J_{H\text{-}H}$ =12.5 Hz, *f'*), 3.22 (dd, 1H, $^3J_{H\text{-}H}$ = 11.1, $^2J_{H\text{-}H}$ = 9.8 Hz, *i'*), 3.64 (dd, 1H, $^2J_{H\text{-}H}$ = 9.8 Hz, $^3J_{H\text{-}H}$ = 7.6 Hz, *i*), 3.81 (ddd, 1H, $^2J_{H\text{-}F}$ = 52.5 Hz, $^3J_{H\text{-}H}$ = 3.7, 3.2 Hz, *g*), 6.72 (d, 2H, $^3J_{H\text{-}H}$ = 7.9 Hz, *c/d*), 7.59 (d, 2H, $^3J_{H\text{-}H}$ = 8.2 Hz, *c/d*); **^{13}C NMR (125 MHz, C_6D_6)** δ = 17.1 (d, $^2J_{C\text{-}F}$ = 20.0 Hz, *h*), 21.4 (*a*), 52.2 (d, $^2J_{C\text{-}F}$ = 24.8 Hz, *f*), 55.2 (d, $^3J_{C\text{-}F}$ = 31.5 Hz, *i*), 92.2 (d, $^1J_{C\text{-}F}$ = 186.9 Hz, *g*), 125.8 (*c/d*), 130.2 (*c/d*), 134.9 (*b/e*), 143.8 (*b/e*); **^{19}F {^{1}H} NMR (377 MHz, C_6D_6)** δ = -173.92; **IR (KBr)**: **ν =** 2922, 1333, 1163, 813, 667, 548; **HRMS (CI^+):** *m/z* required for $C_{11}H_{17}FIN_2O_2S$ ($[M+NH_4]^+$): 387.0040, found 387.0028, Δ = 3.5 ppm.

The structure was unambiguously confirmed by X-ray crystallography and NOESY/HOESY experiments. Crystallographic data are deposited at the Cambridge Crystallographic Data Centre (CCDC-896061).

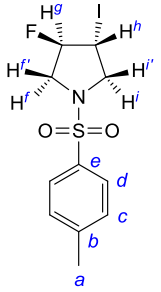

*Data for the minor anti-***109** *diastereoisomer:* **R_f** = 0.5 (hexane/Et_2O 6:4); **m.p.** = 121 °C; **^{1}H NMR (500 MHz, $CDCl_3$)** δ = 2.44 (s, 3H, *a*), 3.68 (dd, 1H, $^3J_{H\text{-}F}$ = 25.8 Hz, $^2J_{H\text{-}H}$ = 12.6 Hz, *f*), 3.81 (d, 1H, $^2J_{H\text{-}H}$ = 12.0 Hz, *i*), 4.00 (ddd, 1H, $^3J_{H\text{-}F}$ = 38.1 Hz, $^2J_{H\text{-}H}$ = 12.6 Hz, $^3J_{H\text{-}H}$ = 3.5 Hz, *f'*), 4.02 (dd, 1H, $^2J_{H\text{-}H}$ = 12.0 Hz, $^3J_{H\text{-}H}$ = 5.0 Hz, *i'*), 4.28 (dd, 1H, $^3J_{H\text{-}F}$ = 14.2 Hz, $^3J_{H\text{-}H}$ = 5.0 Hz, *h*), 5.21 (dd, 1H, $^2J_{H\text{-}F}$ = 52.0 Hz, $^3J_{H\text{-}H}$ = 3.5 Hz, *g*), 7.35 (d, 2H, $^3J_{H\text{-}H}$ = 8.2 Hz, *c/d*), 7.74 (d, 2H, $^3J_{H\text{-}H}$ = 8.2 Hz, *c/d*); **^{13}C NMR (125 MHz, $CDCl_3$)** δ = 19.6 (d, $^2J_{C\text{-}F}$ = 22.9 Hz, *h*), 21.6 (*a*), 51.4 (d, $^2J_{C\text{-}F}$ = 22.9 Hz, *f*), 55.8 (*i*), 97.7 (d, $^1J_{C\text{-}F}$ = 188.8 Hz, *g*), 127.5 (*c/d*), 129.8 (*c/d*), 133.7 (*b/e*), 144.0 (*b/e*); **^{19}F {^{1}H} NMR (377 MHz, $CDCl_3$)** δ = -157.47; **IR (DCM)**: **ν =** 2927, 1345, 1160, 1092, 808, 667, 552; **HRMS (ESI^+):** *m/z* required for $C_{11}H_{13}FINO_2SNa^+$ ($[M+Na]^+$): 391.9588, found 391.9584, Δ = 0.8 ppm.

The structure was confirmed by NOESY/HOESY experiments.

(±) (2,3,4-*syn*)-3-(benzyloxy)-5-[2-(benzyloxy)-1-fluoroethyl]-4-iodo-1-[(4-methylphenyl) sulfonyl]pyrrolidin-2-one (111):

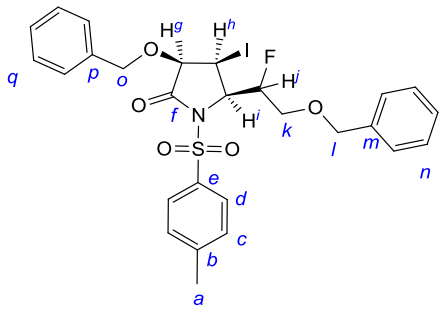

Following the general procedure of the iodocyclisation using <u>Condition **B**</u> on 85 mg (0.17 mmol) of *syn*-**70**, the reaction yielded 52 mg of *syn,syn*-**111** (49%, d.r. (*syn:anti*) > 20:1) as a yellow oil.

Data for the major syn,syn diastereoisomer: **R_f =** 0.5 (hexane/Et_2O 7:3); **^{1}H NMR (500 MHz, C_6D_6)** δ = 1.77 (s, 3H, *a*), 3.66 (d, 1H, $^3J_{H\text{-}H}$ = 4.7 Hz, *k*), 3.70 (d, 1H, $^3J_{H\text{-}H}$ = 4.7 Hz, *k*), 4.00 (d, 1H, $^3J_{H\text{-}H}$ = 3.2 Hz, *g*), 4.28 (d, 1H, $^2J_{H\text{-}H}$ = 11.8 Hz, *l*), 4.33 (d, 1H, $^2J_{H\text{-}H}$ = 11.8 Hz, *l'*), 4.35 (d, 1H, $^2J_{H\text{-}H}$ = 11.6

Hz, *o*), 4.39 (t, 1H, $^{3}J_{H\text{-}H}$ = 3.2 Hz, *h*), 4.54 (d, 1H, $^{2}J_{H\text{-}H}$ = 11.6 Hz, *o'*), 4.87 (ddd, 1H, $^{3}J_{H\text{-}F}$ = 16.4 Hz, $^{3}J_{H\text{-}H}$ = 4.7, 3.2 Hz, *i*), 5.40 (dq, 1H, $^{2}J_{H\text{-}F}$ = 47.9 Hz, $^{3}J_{H\text{-}H}$ = 4.7 Hz, *j*), 6.70 (d, 2H, $^{3}J_{H\text{-}H}$ = 8.3 Hz, *c/d*), 7.00-7.19 (m, 8H, *n/q*), 7.29 (d, 2H, $^{3}J_{H\text{-}H}$ = 7.2 Hz, *n/q*), 8.10 (d, 2H, $^{3}J_{H\text{-}H}$ = 8.3 Hz, *c/d*); **^{13}C NMR (125 MHz, C_6D_6)** δ = 15.0 (d, $^{3}J_{C\text{-}F}$ = 4.7 Hz, *h*), 21.5 (*a*), 69.4 (d, $^{2}J_{C\text{-}F}$ = 21.9 Hz, *k*), 69.6 (d, $^{2}J_{C\text{-}F}$ = 23.8 Hz, *i*), 73.4 (*o*), 74.0 (*l*), 84.6 (*g*), 92.3 (d, $^{1}J_{C\text{-}F}$ = 182.2 Hz, *j*), 128.3 (*c/d/n/q*), 128.5 (*c/d/n/q*), 128.7 (*c/d/n/q*), 128.8 (*c/d/n/q*), 129.0 (*c/d/n/q*), 129.1 (*c/d/n/q*), 129.8 (*c/d/n/q*), 129.9 (*c/d/n/q*), 135.6 (*b/e/p/m*), 137.2 (*b/e/p/m*), 138.5 (*b/e/p/m*), 145.8 (*b/e/p/m*), 169.4 (*f*); **^{19}F {^{1}H} NMR (377 MHz, C_6D_6)** δ = -196.83; **IR (in DCM)**: **ν =** 1741, 1421, 1265, 896, 739; **HRMS (ESI^{+}):** *m/z* required for $C_{27}H_{27}FINNaO_5S^{+}$ ($[M+Na]^{+}$): 646.0531, found 646.0536, Δ = 1.9 ppm; *Identifiable data for the minor anti diastereoisomer:* **^{19}F {^{1}H} NMR (377 MHz, C_6D_6)** δ = -202.55;

The structure was confirmed by NOESY/HOESY experiments.

(±) 3-fluoro-2-(methyl)-1-[(4methylphenyl)sulfonyl] pyrrolidine (155):

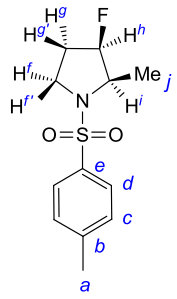

To a solution of 3-fluoro-2-iodomethyl pyrrolidine **56** (235 mg, 0.6 mmol, 1 eq.) in benzene (60 mL), was added Bu_3SnH (1.6 mL, 6.1 mmol, 10 eq.) and AIBN (272 mg, 1.6 mmol, 2.7 eq.). The solution was heated at reflux overnight, concentrated *in vacuo* and purified by flash column chromatography on silica gel containing approximatively 10% of NaF (hexane/Et_2O 8:2) to produce **155** as a white solid (130 mg, 82%, d.r. 12:1).

Data for the major syn diastereoisomer: **R_f** = 0.3 (hexane/Et_2O: 6/4); **m.p.** = 72 °C; **^{1}H NMR (500 MHz, C_6D_6)** δ = 0.82 (ddddd, 1H, $^{3}J_{H\text{-}F}$ = 36.3 Hz, $^{2}J_{H\text{-}H}$ = 13.7 Hz, $^{3}J_{H\text{-}H}$ = 12.2, 8.7, 3.4 Hz, *g*), 1.31-1.40 (m, 1H, *g'*), 1.44 (dd, 3H, $^{3}J_{H\text{-}H}$ = 6.6 Hz, $^{4}J_{H\text{-}F}$ = 2.8 Hz, *j*), 1.89 (s, 3H, *a*), 3.26-3.29 (m, 2H, *f+f'*), 3.41 (dqd, 1H, $^{3}J_{H\text{-}F}$ = 24.3 Hz, $^{3}J_{H\text{-}H}$ = 6.6, 4.4 Hz, *i*), 4.10 (dtd, 1H, $^{2}J_{H\text{-}F}$ = 53.3 Hz, $^{3}J_{H\text{-}H}$ = 4.4, 2.5 Hz, *h*), 6.76 (d, 2H, $^{3}J_{H\text{-}H}$ = 7.9 Hz, *c/d*), 7.66 (d, 2H, $^{3}J_{H\text{-}H}$ = 8.5 Hz, *c/d*); **^{13}C NMR (101**

MHz, $CDCl_3$) δ = 1.1 (d, $^3J_{C-F}$ = 12.8 Hz, *j*), 21.6 (*a*), 31.5 (d, $^2J_{C-F}$ = 21.6 Hz, *g*), 48.6 (*f*), 65.9 (d, $^2J_{C-F}$ = 19.2 Hz, *i*), 93.5 (d, $^1J_{C-F}$ = 184.5 Hz, *h*), 127.4 (*c/d*), 130.1 (*c/d*), 133.9 (*b/e*), 144.3 (*b/e*); **^{19}F {^{1}H} NMR (377 MHz, $CDCl_3$)** δ = -193.04; **IR (DCM): ν =** 1592, 1347, 1163, 949, 659, 549; **HRMS (ESI^+):** *m/z* required for $C_{12}H_{16}FNO_2SNa$ ($[M+Na]^+$): 280.0778, found: 280.0781, Δ = 1.2 ppm. *Identifiable data for the minor anti diastereoisomer:* **^{19}F {^{1}H} NMR (377 MHz, $CDCl_3$)** δ = -173.82;

4.5 Synthesis of indolizidines:

(±) 3-fluoro-1-tosylpyrrolidin-2-yl)butanoate (113):

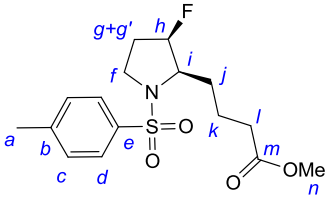

To a suspension of ultrapure CuI (749 mg, 3.9 mmol, 3.4 eq.) and Zn dust (609 mg, 9.3 mmol, 8 eq.) in degassed H_2O/EtOH (3:7, 26.3 mL), was added methyl acrylate (2.6 mL, 29.2 mmol, 25.1 eq.). The suspension was sonnicated for 10 min in the presence of light before adding the **(2*S*, 3*R*)-3-fluoro-2-(iodomethyl)-1-[(4methylphenyl)sulfonyl] pyrrolidine (±)56** (446 mg, 1.2 mmol, 1 eq.). The reaction mixture was sonnicated for 45 min at r.t then diluted with H_2O, washed with brine, dried over $MgSO_4$ and the solvent removed *in vacuo*. The crude product was purified by flash column chromatography on silica gel (hexane/Et_2O 9:1 then 8:2) to give the desired compound **113** as a thick white oil (248 mg, 62%, d.r. (*syn/anti*) = 14:1).

Data for the major syn diastereoisomer: **R_f =** 0.3 (hexane/Et_2O 7:3); **^{1}H NMR (500 MHz, $CDCl_3$)** δ = 1.27-1.43 (m, 1H, *g*), 1.68-1.80 (m, 2H, *k*), 1.81-1.90 (m, 1H, *g'*), 1.91-2.06 (m, 2H, *j*), 2.39 (t, 2H, $^3J_{H-H}$ = 7.6 Hz, *l*), 2.44 (s, 3H, *a*), 3.45-3.52 (td, 1H, $^3J_{H-H}$ = 11.3 Hz, $^3J_{H-F}$ = 5.6 Hz, *i*), 3.52-3.64 (m, 2H, *f*), 3.69 (s, 3H, *n*), 4.99 (d, 1H, $^2J_{H-F}$ = 52.6 Hz, *h*), 7.33 (d, 2H, $^3J_{H-H}$ = 8.2 Hz, *c/d*), 7.72 (d, 2H, $^3J_{H-H}$ = 8.2 Hz, *c/d*); **^{13}C NMR (125 MHz, $CDCl_3$)** δ = 21.5 (*k*), 21.5 (*a*), 29.3 (d, $^3J_{C-F}$ = 10.5 Hz, *j*), 31.6 (d, $^2J_{C-F}$ = 21.9 Hz, *g*), 33.9 (*l*), 46.8 (*f*), 51.5 (*n*), 64.1 (d, $^2J_{C-F}$ = 20.4 Hz, *i*), 92.0 (d, $^1J_{C-F}$ = 183.11 Hz, *h*), 127.4 (*c/d*), 129.8 (*c/d*), 134.8 (*b/e*), 143.7 (*b/e*), 173.4 (*m*); **^{19}F {^{1}H} NMR (377**

MHz, $CDCl_3$) δ = -194.34; **IR (neat)**: **ν =** 2955, 1734, 1598, 1438, 1337, 1157, 851; **HRMS (ESI^+):** *m/z* required for $C_{16}H_{22}FNO_4SNa^+$ ($[M+Na]^+$): 366.1144, found 366.1146. *Identifiable data for the minor anti diastereoisomer:* **^{19}F {^1H} NMR (377 MHz, $CDCl_3$)** δ = -174.59;

(±) methyl-4-{(*syn,syn*)-5-[(benzyloxy)methyl]-3-fluoro-1-[(4-methylphenyl)sulfonyl]pyrrolidin-2-yl}butanoate (*syn,syn*-115):

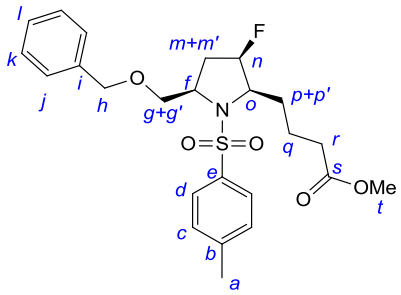

To a suspension of ultrapure CuI (98 mg, 0.5 mmol, 3.4 eq.) and Zn dust (79.5 mg, 1.2 mmol, 8 eq.) in degassed H_2O/EtOH (3:7, 3.5 mL), was added methyl acrylate (0.3 mL, 3.8 mmol, 25.1 eq.). The suspension was sonnicated for 10 min in presence of light before adding *syn,syn*-**106** (77 mg, 0.2 mmol, 1 eq.). The reaction mixture was sonnicated for 45 min at r.t then diluted with H*2*O, washed with brine, dried over $MgSO_4$ and the solvent removed *in vacuo*. The crude product was purified by flash column chromatography (hexane/Et_2O 9:1 then 8:2) to give 34 mg of a mixture of diastereoisomers **115** (48%, d.r. (*syn:anti*) > 20:1) as a colourless oil along 13 mg of the allylic fluoride *anti*-**67** (23%).

Data for the major syn,syn-**115** *diastereoisomer:* **R_f =** 0.2 (hexane/Et_2O 6:4); **^1H NMR (500 MHz, $CDCl_3$)** δ = 1.50 (dddd, 1H, $^3J_{H-F}$ = 38.2 Hz, $^2J_{H-H}$ = 13.8 Hz, $^3J_{H-H}$ = 8.5, 4.7 Hz, *m'*), 1.68-1.77 (m, 2H, *q*), 1.78-1.87 (m, 1H, *p*), 2.00-2.09 (m, 1H, *p'*), 2.20-2.29 (m, 1H, *m*), 2.37 (t, 2H, $^3J_{H-H}$ = 7.6 Hz, *r*), 2.43 (s, 3H, *a*), 3.45-3.54 (m, 2H, *o*+*g'*), 3.69 (s, 3H, *t*), 3.75 (ddd, 1H, $^2J_{H-H}$ = 8.9 Hz, $^3J_{H-H}$ = 4.7 Hz, $^5J_{H-F}$ = 0.9 Hz, *g*), 3.97 (dddd, 1H, $3J_{H-H}$ = 10.0, 8.6, 4.9, 1.9 Hz, *f*), 4.54 (s, 2H, *h*), 4.86 (dtd, 1H, $^2J_{H-F}$ = 52.6 Hz, $^3J_{H-H}$ = 4.7, 2.2 Hz, *n*), 7.29-7.38 (m, 7H, *c/d/j/k/l*), 7.70 (d, 2H, $^3J_{H-H}$ = 8.2 Hz, *c/d/j/k/l*); **^{13}C NMR (125 MHz, $CDCl_3$)** δ = 21.4 (*q*), 21.5 (*a*), 30.0 (d, $^3J_{C-F}$ = 8.6 Hz, *p*), 33.1 (d, $^2J_{C-F}$ = 20.9 Hz, *m*), 33.9 (*r*), 51.6 (*t*), 59.1 (*f*), 64.8 (d, $^2J_{C-F}$ = 21.0 Hz, *o*), 72.9 (d, $^4J_{C-F}$ = 2.8 Hz, *g*), 73.4 (*h*), 92.9 (d, $^1J_{C-F}$ = 185.0 Hz, *n*), 127.6 (*l/k/j/c/d*), 127.7 (*l/k/j/c/d*), 127.8 (*l/k/j/c/d*), 128.4 (*l/k/j/c/d*), 129.8 (*l/k/j/c/d*), 133.8 (*i/b/e*), 138.0 (*i/b/e*), 143.9 (*i/b/e*), 173.7 (*s*); **^{19}F {^1H} NMR (377 MHz,**

$CDCl_3$) δ = -189.04; **IR (neat)**: **ν =** 3055, 1733, 1421, 1265, 1165, 896, 748; **HRMS (ESI^+):** *m/z* required for $C_{26}H_{37}FN_3O_5S^+$ ($[M+CH_3CN+NH_4]^+$): 522.2432, found 522.2448, Δ = 2.9 ppm; *Identifiable data for the minor anti,anti-***115** *diastereoisomer:* **^{19}F {^1H} NMR (377 MHz, $CDCl_3$)** δ = -169.72;

(±) 1-fluorohexahydroindolizin-5-(1*H*)-one (114):

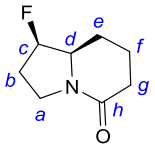

To a solution of **(±) 3-fluoro-1-tosylpyrrolidin-2-yl)butanoate 113** (42 mg, 0.12 mmol, 1eq.) in MeOH (0.4 mL), was added Na_2HPO_4 (174 mg, 1.2 mmol, 10 eq.) followed by NaHg (5% in Na, 16.9 mg, 0.73 mmol, 6 eq. of Na; being equivalent to 337.5 mg of amalgam). The resulting slurry was stirred at r.t for 3 h. The reaction mixture was then diluted with Et_2O and H_2O, filtered, and the aqueous layer extracted three times with Et_2O. The combined organic phases were washed with H_2O, brine, dried over $MgSO_4$, filtered and the solvent removed under reduced pressure. A conversion of 92% was determined by ^{19}F NMR of the crude mixture.

The following characterisation was obtained by ^1H and ^{19}F NMR of the crude mixture.

Data for the major syn diastereoisomer: Identifiable peaks in **^1H NMR (400 MHz, $CDCl_3$)** δ = 3.47-3.59 (m, 2H, *a*), 3.82 (m, 1H, *d*), 5.05 (dt, 1H, $^2J_{H\text{-}F}$ = 52.8 Hz, $^3J_{H\text{-}H}$ = 2.8 Hz, *c*); **^{19}F {^1H} NMR (377 MHz, $CDCl_3$)** δ = -194.11; **MS (ESI^+):** 158.1 ($[M+H]^+$); *Identifiable data for the minor anti diastereoisomer* **^{19}F {^1H} NMR (377 MHz, $CDCl_3$)** δ = -185.04;

(±) (1,3,8a*syn,syn*)-3-[(benzyloxy)methyl]-1-fluorohexahydroindolizin-5(1*H*)-one (*syn,syn*-116):

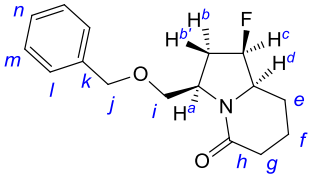

To a solution of *syn,syn*-**115** (34 mg, 0.07 mmol, 1eq.) in MeOH (0.25 mL) was added Na_2HPO_4 (104 mg, 0.73 mmol, 10 eq.) followed by NaHg (5% in Na, 10.1 mg, 0.44 mmol, 6 eq. of Na; being equivalent to 202 mg of amalgam). The resulting slurry was stirred at r.t for 3 h. The reaction

mixture was then diluted with Et_2O and H_2O, filtered, and the aqueous layer extracted three times with Et_2O. The combined organic phases were washed with H_2O, brine, dried over $MgSO_4$, filtered and the solvent removed *in vacuo*. The crude product was purified by flash column chromatography on silica gel (hexane/MeOH 9:1) to give 10.5 mg of a mixture of diastereoisomers **116** (53%, d.r. (*syn:anti*) > 12:1) as a yellow oil.

*Data for the major syn,syn-***116** *diastereoisomer:* **R_f =** 0.1 (hexane/Et_2O 4:6); **^{1}H NMR (500 MHz, C_6D_6)** δ = 0.94-1.05 (m, 1H, *f'*), 1.18-1.40 (m, 3H, *e+f*), 1.38 (dddd, 1H, $^3J_{H-F}$ = 44.1 Hz, $^2J_{H-H}$ = 15.0 Hz, $^3J_{H-H}$ = 9.4, 3.7 Hz, *b*), 2.04 (ddd, 1H, $^2J_{H-H}$ = 17.7 Hz, $^3J_{H-H}$ = 11.1, 6.9 Hz, *g*), 2.13 (ddd, 1H, $^2J_{H-H}$ = 17.7 Hz, $^3J_{H-H}$ = 6.4, 1.8 Hz, *g'*), 2.32 (dd, 1H, $^3J_{H-F}$ = 19.5 Hz, $^2J_{H-H}$ = 15.1 Hz, *b'*), 2.39 (ddt, 1H, $^3J_{H-F}$ = 29.6 Hz, $^3J_{H-H}$ = 11.3, 2.9 Hz, *d*), 3.41 (ddd, 1H, $^3J_{H-H}$ = 9.9 Hz, $^2J_{H-H}$ = 8.2 Hz, $^5J_{H-F}$ = 1.9 Hz, *i'*), 4.17 (dt, 1H, $^2J_{H-F}$ = 53.3 Hz, $^3J_{H-H}$ = 3.0 Hz, *c*), 4.32 (d, 1H, $^2J_{H-H}$ = 11.9 Hz, *j'*), 4.33 (td, 1H, $^3J_{H-H}$ = 9.5, 4.0 Hz, *a*), 4.43 (d, 1H, $^2J_{H-H}$ = 11.9 Hz, *j*), 4.62 (dd, 1H, $^2J_{H-H}$ = 8.2 Hz, $^3J_{H-H}$ = 4.0 Hz, *i*), 7.08 (dd, 1H, $^3J_{H-H}$ = 7.6, 7.3 Hz, *n*), 7.13-7.18 (m, 2H, *m/l*), 7.28 (d, 2H, $^3J_{H-H}$ = 7.2 Hz, *m/l*); **^{13}C NMR (125 MHz, C_6D_6)** δ = 21.4 (*f*), 23.3 (d, $^3J_{C-F}$ = 6.4 Hz, *e*), 32.0 (*g*), 33.4 (d, $^2J_{C-F}$ = 20.0 Hz, *b*), 56.1 (*a*), 63.6 (d, $^2J_{C-F}$ = 20.0 Hz, *d*), 70.8 (d, $^4J_{C-F}$ = 2.4 Hz, *i*), 73.7 (*j*), 94.0 (d, $^1J_{C-F}$ = 182.2 Hz, *c*), 127.9 (*l/m/n*), 128.3 (*l/m/n*), 128.8 (*l/m/n*), 139.6 (*k*), 169.2 (*h*); **^{19}F {^{1}H} NMR (377 MHz, C_6D_6)** δ = -191.66; **IR (in DCM)**: **ν =** 3055, 1721, 1642, 1266, 896, 739, 437; **HRMS (ESI$^+$):** *m/z* required for $C_{16}H_{20}FNO_2Na^+$ ($[M+Na]^+$): 300.1370, found 300.1368, Δ = 1.3 ppm. *Identifiable data for the minor anti,anti-***116** *diastereoisomer* **^{19}F {^{1}H} NMR (377 MHz, $CDCl_3$)** δ = -185.05;

The structure was confirmed by NOESY/HOESY experiments.

4.6 Synthesis of organosilanes:

4.6.1 Synthesis of allylsilanes:

Allyldimethylphenylsilane,[8] allylbenzhydryldimethylsilane,[9] allyl(diisopropyl)(4-methylphenyl) silane,[10] were synthesised according to literature procedures. Allyltriisopropylsilane and allyltriphenylsilane were commercially available and used without further purification.

4.6.2 Synthesis of organosilanes:

(*E*)-4-methyl-*N*-(5-(triisopropylsilyl)pent-3-en-1-yl)benzenesulfonamide (117):

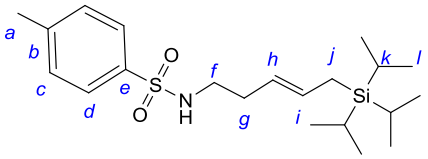

Following the general procedure A on 500 mg (2.2 mmol, 1 eq.) of ***N*-but-3-en-1-yl-4-methylbenzenesulfonamide 53**, the reaction yielded 782 mg of **117** (89%, *E:Z* = 5:1) as a colourless oil after flash column chromatography on silica gel (hexane/Et_2O 8:2 to 7:3).

Data for the major (E) isomer: **R_f** = 0.4 (hexane/Et_2O 6:4); **^{1}H NMR (400 MHz, $CDCl_3$)** δ = 0.94-1.04 (m, 21H, *l+k*), 1.49 (d, 2H, $^3J_{H\text{-}H}$ = 8.1 Hz, *j*), 2.08 (q, 2H, $^3J_{H\text{-}H}$ = 6.9 Hz, *g*), 2.40 (s, 3H, *a*), 2.88-2.94 (m, 2H, *f*), 4.88 (t, 1H, $^3J_{H\text{-}H}$ = 5.8 Hz, *NH*), 5.07 (1H, dtt, $^3J_{H\text{-}H(trans)}$ = 15.0 Hz, $^3J_{H\text{-}H}$ = 6.9 Hz, $^4J_{H\text{-}H}$ = 1.4 Hz, *h*), 5.45 (dtt, 1H, $^3J_{H\text{-}H(trans)}$ = 15.0 Hz, $^3J_{H\text{-}H}$ = 8.1 Hz, $^4J_{H\text{-}H}$ = 1.4 Hz, *i*), 7.28 (d, 2H, $^3J_{H\text{-}H}$ = 7.8 Hz, *c/d*), 7.73 (d, 2H, $^3J_{H\text{-}H}$ = 8.3 Hz, *c/d*); **^{13}C NMR (101 MHz, CDCl3)** δ = 10.8 (*k*), 15.3 (*j*), 18.5 (*l*), 21.5 (*a*), 32.6 (*g*), 42.8 (*f*), 123.5 (*h*), 127.0 (*c/d*), 129.5 (*c/d*), 131.1 (*i*), 136.9 (*b/e*), 143.1 (*b/e*); **IR (CH_2Cl_2): ν =** 2948, 2000, 1699, 1130, 1047, 988, 883; **HRMS (CI^+):** *m/z* required for $C_{21}H_{38}NO_2SSi$ ($[M+H]^+$): 396.2393, found 396.2400, Δ = 1.9 ppm.

[8] J. A. Soderquist, A. Hassner, *J. Org. Chem.* **1983**, *48*, 1801-1810.
[9] Z.-H. Peng, K. A. Woerpel, *Org. Lett.* **2000**, *2*, 1379-1381.
[10] S. C. Wilkinson, O. Lozano, M. Schuler, M. C. Pacheco, R. Salmon, V. Gouverneur, *Angew. Chem. Int. Ed.* **2009**, *48*, 7083-7086.

(*E*)-4-methyl-*N*-(5-(triphenylsilyl)pent-3-en-1-yl)benzenesulfonamide (118):

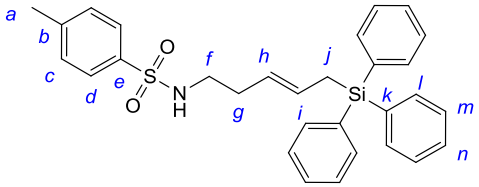

Following the general procedure A on 200 mg (0.9 mmol, 1 eq.) of ***N*-but-3-en-1-yl-4-methylbenzenesulfonamide 53**, the reaction gave 343 mg of a mixture containing 64% of **118** (*E:Z* = 3:1) and 15% of the correspondind truncated side product, as a white solid after flash column chromatography on silica gel (hexane/Et_2O 8:2 then 7:3).

Data for the major (E) isomer: **R_f** = 0.2 (hexane/Et_2O 7:3); **m.p.** = 119 °C; **^{1}H NMR (400 MHz, $CDCl_3$)** δ = 1.98-2.06 (m, 2H, *g*), 2.31 (d, 2H, $^3J_{H\text{-}H}$ = 7.8 Hz, *j*), 2.44 (s, 3H, *a*), 2.80-2.87 (m, 2H, *f*), 4.16 (t, 1H, $^3J_{H\text{-}H}$ = 6.1 Hz, *NH*), 5.08 (dtt, 1H, $^3J_{H\text{-}H(trans)}$ = 15.1 Hz, $^3J_{H\text{-}H}$ = 7.1 Hz, $^4J_{H\text{-}H}$ = 1.4 Hz, *h*), 5.52 (dtt, 1H, $^3J_{H\text{-}H(trans)}$ = 15.1 Hz, $^3J_{H\text{-}H}$ = 7.8 Hz, $^4J_{H\text{-}H}$ = 1.1 Hz, *i*), 7.27 (d, 2H, $^3J_{H\text{-}H}$ = 8.3 Hz, *c/d*), 7.35-7.55 (m, 15H, *l+m+n*), 7.66 (d, 2H, $^3J_{H\text{-}H}$ = 8.3 Hz, *c/d*); **^{13}C NMR (101 MHz, $CDCl_3$)** δ = 19.5 (*j*), 21.5 (*a*), 32.8 (*g*), 42.7 (*f*), 126.2 (*h*), 127.0 (*c/d*), 127.9 (*l/m/n*), 129.0 (*i*), 129.6 (*c/d*), 129.6 (*l/m/n*), 134.3 (*k*), 135.6 (*l/m/n*), 137.2 (*b/e*), 143.2 (*b/e*); **IR (CH_2Cl_2): ν =** 3282, 3068, 1428, 1327, 1161, 702; **HRMS (ESI$^+$):** *m/z* required for $C_{30}H_{31}NO_2SSiNa^+$ ($[M+Na]^+$): 520.1737, found 520.1731, Δ = 1.9 ppm.

Identifiable data for the minor (Z) isomer: **^{1}H NMR (400 MHz, $CDCl_3$)** δ = 1.87-1.94 (m, 2H, *g*), 2.28 (d, 2H, $^3J_{H\text{-}H}$ = 7.6 Hz, *j*), 2.41 (s, 3H, *a*), 2.73-2.79 (m, 2H, *f*), 4.22 (t, 1H, $^3J_{H\text{-}H}$ = 6.1 Hz, *NH*), 5.12-5.24 (m, 1H, *h*), 5.58-5.75 (m, 1H, *i*); **^{13}C NMR (101 MHz, $CDCl_3$)** δ = 15.4 (*j*), 27.1 (*g*), 42.5 (*f*), 124.6 (*h*), 128.0 (*i*);

Identifiable data for the truncated side product: **^{1}H NMR (400 MHz, $CDCl_3$)** δ = 3.38-3.43 (m, 2H, *f*), 4.01-4.06 (m, 1H, *NH*); **^{13}C NMR (101 MHz, $CDCl_3$)** δ = 45.5 (*f*);

(*E*)-*N*-(5-(dimethyl(phenyl)silyl)pent-3-en-1-yl)-4-methylbenzenesulfonamide (119):

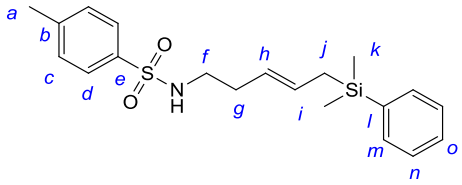

Following the general procedure A on 100 mg (0.4 mmol, 1 eq.) of ***N*-but-3-en-1-yl-4-methylbenzenesulfonamide 53**, the reaction yielded 90 mg of **119** (54%, *E:Z* = 2:1) as a colourless oil after flash column chromatography on silica gel (hexane/Et_2O 8:2 then 7:3).

Data for the major (E) isomer: **R_f** = 0.2 (hexane/Et_2O 7:3); **^{1}H NMR (400 MHz, $CDCl_3$)** δ = 0.28 (s, 6H, *k*), 1.66 (d, 2H, $^3J_{H\text{-}H}$ = 7.8 Hz, *j*), 2.06-2.12 (m, 2H, *g*), 2.44 (s, 3H, *a*), 2.88-2.94 (m, 2H, *f*), 4.56 (t, 1H, $^3J_{H\text{-}H}$ = 6.1 Hz, *NH*), 5.04 (dtt, 1H, $^3J_{H\text{-}H(trans)}$ = 15.2 Hz, $^3J_{H\text{-}H}$ = 6.8 Hz, $^4J_{H\text{-}H}$ = 1.2 Hz, *h*), 5.40 (dtt, 1H, $^3J_{H\text{-}H(trans)}$ = 15.2 Hz, $^3J_{H\text{-}H}$ = 7.8 Hz, $^4J_{H\text{-}H}$ = 1.2 Hz, *i*), 7.30 (d, 2H, $^3J_{H\text{-}H}$ = 8.1 Hz, *c/d*), 7.34-7.40 (m, 3H, *m/n/o*), 7.47-7.51 (m, 2H, *m/n/o*), 7.74 (d, 2H, $^3J_{H\text{-}H}$ = 8.1 Hz, *c/d*); **^{13}C NMR (101 MHz, $CDCl_3$)** δ = -3.5 (*k*), 21.4 (*a*), 21.9 (*j*), 32.6 (*g*), 42.8 (*f*), 124.5 (*h*), 127.0 (*c/d*), 127.7 (*m/n/o*), 129.0 (*i*), 129.6 (*m/n/o*), 129.6 (*c/d*), 133.5 (*m/n/o*), 137.0 (*b/e*), 138.3 (*l*), 143.2 (*b/e*); **IR (CH_2Cl_2):** **ν** = 3283, 2956, 1426, 1327, 1161, 836; **HRMS (ESI^+):** *m/z* required for $C_{20}H_{27}NO_2SSiNa^+$ ($[M+Na]^+$): 396.1424, found 396.1416, Δ = 2.0 ppm.

Identifiable data for the minor (Z) isomer: **^{1}H NMR (400 MHz, $CDCl_3$)** δ = 0.27 (s, 6H, *k*), 1.65 (d, 2H, $^3J_{H\text{-}H}$ = 8.6 Hz, *j*), 2.01-2.07 (m, 2H, *g*), 2.42 (s, 3H, *a*), 2.84-2.90 (m, 2H, *f*), 4.62 (t, 1H, $^3J_{H\text{-}H}$ = 6.1 Hz, *NH*), 5.14 (dtt, 1H, $^3J_{H\text{-}H(cis)}$ = 10.6 Hz, $^3J_{H\text{-}H}$ = 7.1 Hz, $^4J_{H\text{-}H}$ = 1.3 Hz, *h*), 5.51 (dtt, 1H, $^3J_{H\text{-}H(cis)}$ = 10.6 Hz, $^3J_{H\text{-}H}$ = 8.6 Hz, $^4J_{H\text{-}H}$ = 1.5 Hz, *i*); **^{13}C NMR (101 MHz, $CDCl_3$)** δ = -3.4 (*k*), 17.9 (*j*), 27.1 (*g*), 42.7 (*f*), 122.9 (*h*), 128.5 (*i*).

(*E*)-*N*-(5-(benzhydryldimethylsilyl)pent-3-en-1-yl)-4-methylbenzene sulfonamide (120):

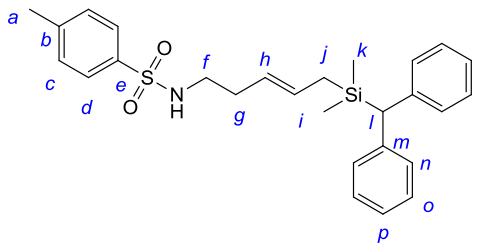

Following the general procedure A on 150 mg (0.6 mmol) of ***N*-but-3-en-1-yl-4-methylbenzenesulfonamide 53**, the reaction gave 178 mg of **120** (58%, *E:Z* = 4:1) as a colourless oil after flash column chromatography on silica gel (hexane/Et_2O 8:2 then 7:3).

Data for the major (E) isomer: **R_f** = 0.2 (hexane/Et_2O 7:3); **^{1}H NMR (400 MHz, $CDCl_3$)** δ = 0.06 (s, 6H, *k*), 1.42-1.49 (m, 2H, *j*), 2.06-2.14 (m, 2H, *g*), 2.42 (s, 3H, *a*), 2.86-2.95 (m, 2H, *f*), 3.58 (s, 1H, *l*), 4.85 (t, 1H, $^3J_{H\text{-}H}$ = 6.1 Hz, *NH*), 4.96 (dt, 1H, $^3J_{H\text{-}H(trans)}$ = 15.1 Hz, $^3J_{H\text{-}H}$ = 6.8 Hz, *h*), 5.28 (dt, 1H, $^3J_{H\text{-}H(trans)}$ = 15.1 Hz, $^3J_{H\text{-}H}$ = 7.7 Hz, *i*), 7.12-7.19 (m, 2H, *c/d*), 7.23-7.34 (m, 10H, *n+o+p*), 7.79 (d, 2H, $^3J_{H\text{-}H}$ = 8.1 Hz, *c/d*), 7.74 (d, 2H, $^3J_{H\text{-}H}$ = 8.1 Hz, *c/d*); **^{13}C NMR (101 MHz, $CDCl_3$)** δ = -3.8 (*k*), 20.7 (*j*), 21.3 (*a*), 32.5 (*g*), 42.8 (*f*), 44.6 (*l*), 125.1 (*h*), 126.9 (*c/d*), 128.2 (*n/o*), 128.2 (*p*), 128.6 (*n/o*), 129.2 (*i*), 129.5 (*c/d*), 136.8 (*b/e*), 142.2 (*m*), 143.1 (*b/e*); **IR (CH_2Cl_2): ν =** 3280, 3090, 1597, 1447; **HRMS (CI^+):** *m/z* required for $C_{27}H_{34}NO_2SSi$ ($[M+H]^+$): 464.2080, found 464.2063, Δ = 3.6 ppm.

Identifiable data for the minor (Z) isomer: **^{1}H NMR (400 MHz, $CDCl_3$)** δ = 0.05 (s, 6H, *k*), 1.98-2.06 (m, 2H, *g*), 4.89 (t, 1H, $^3J_{H\text{-}H}$ = 6.1 Hz, *NH*), 5.09 (dt, 1H, $^3J_{H\text{-}H(cis)}$ = 10.1 Hz, $^3J_{H\text{-}H}$ = 7.3 Hz, *h*), 5.40 (dt, 1H, $^3J_{H\text{-}H(cis)}$ = 10.1 Hz, $^3J_{H\text{-}H}$ = 8.8 Hz, *i*); **^{13}C NMR (101 MHz, $CDCl_3$)** δ = -3.7 (*k*), 16.4 (*j*), 26.9 (*g*), 42.7 (*f*), 44.6 (*l*), 124.4 (*h*).

(*E*)-*tert*-butyl (5-(triisopropylsilyl)pent-3-en-1-yl)carbamate (121):

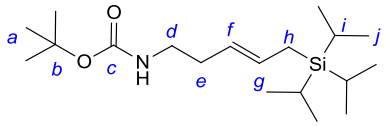

Following the general procedure A on 500 mg (2.9 mmol, 1 eq.) of ***tert*-butyl but-3-en-1-ylcarbamate**, the reaction yielded 887 mg of **121** (89%, *E:Z* = 5:1) as a yellow oil after flash column chromatography on silica gel (hexane/Et_2O 9:1).

Data for the major (E) isomer: **R_f** = 0.7 (hexane/Et_2O 9:1); **^{1}H NMR (400 MHz, $CDCl_3$)** δ = 1.04 (s, 21H, *i+j*), 1.43 (s, 9H, *a*), 1.56 (d, 2H, $^3J_{H\text{-}H}$ = 8.0 Hz, *h*), 2.13-2.17 (m, 2H, *e*), 3.11 (m, 2H, *d*), 5.22 (d, 1H, $^3J_{H\text{-}H(trans)}$ = 14.8 Hz, *f*), 5.55 (d, 1H, $^3J_{H\text{-}H(trans)}$ = 14.8 Hz, *g*); **^{13}C NMR (101 MHz, $CDCl_3$)** δ = 10.9 (*i*), 15.4 (*h*), 18.7 (*j*), 28.4 (*a*), 33.1 (*e*), 40.2 (*d*), 78.0 (*b*), 124.9 (*f*), 130.2 (*g*), 155.9 (*c*); **IR (CH_2Cl_2): ν =** 3044, 2322, 1761, 1543; **HRMS (CI^+):** *m/z* required for $C_{19}H_{40}NO_2Si$ ($[M+H]^+$): 342.2828, found 342.2845, Δ = 4.9 ppm. *Data for the minor (Z) isomer could not be identified.*

Synthesis of (*E*)-*N*-(5-(diisopropyl(*p*-tolyl)silyl)pent-3-en-1-yl)-4-methylbenzenesulfonamide (123):

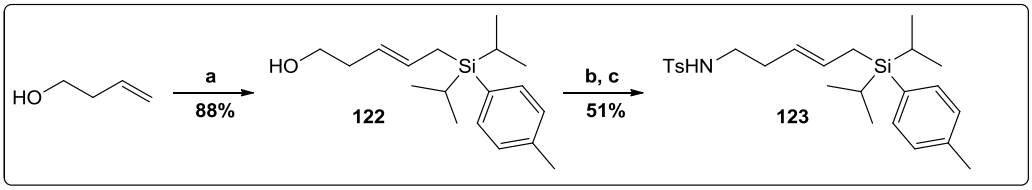

Scheme 4.12: Synthesis of (*E*)-*N*-(5-(diisopropyl(*p*-tolyl)silyl)pent-3-en-1-yl)-4-methylbenzenesulfonamide (**123**); **a**) allyl(diisopropyl)(4-methylphenyl)silane, Grubbs 2nd (5 mol%), 1,4-benzoquinone, CH_2Cl_2, reflux, 3 days; **b**) MsCl, NEt_3, CH_2Cl_2, 3 h; **c**) KOH, TsCl, DMF, 5 h;

5-(diisopropyl(*p*-tolyl)silyl)pent-3-en-1-ol (122):[11]

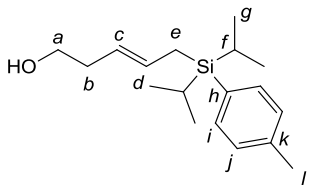

Following the general procedure A on 107.5 mg (1.22 mmol, 1 eq.) of **but-3-en-1-ol**, the reaction yielded 311.5 mg (88% *E:Z* = 2:1) of **5-(diisopropyl(*p*-tolyl)silyl)pent-3-en-1-ol 122** as a colourless oil after flash column chromatography on silica gel (hexane/Et_2O 8:2).

Data for the major (E) isomer: **R_f** = 0.2 (hexane/Et_2O 8:2); **^{1}H NMR (400 MHz, $CDCl_3$)** δ = 1.00-1.06 (m, 12H, *g*), 1.22-1.29 (m, 2H, *f*), 1.89 (d, 2H, $^3J_{H\text{-}H}$ = 8.1 Hz, *e*), 2.21-2.25 (m, 2H, *b*), 2.36 (s, 3H, *l*), 3.56 (t, 2H, $^3J_{H\text{-}H}$ = 6.5 Hz, *a*), 5.24-5.34 (m,1H, *c*), 5.60-5.77 (m, 1H, *d*), 7.19 (d, 2H, $^3J_{H\text{-}H}$ = 7.3 Hz, *i/j*), 7.35 (d, 2H, $^3J_{H\text{-}H}$ = 7.8 Hz, *i/j*);

***(E)*-*N*-(5-(diisopropyl(*p*-tolyl)silyl)pent-3-en-1-yl)-4-methylbenzenesulfonamide (*E*-123):**

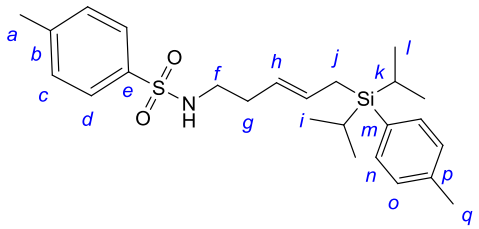

Following the general procedure C on 311.5 mg (1.12 mmol, 1 eq.) of **5-(diisopropyl(*p*-tolyl)silyl)pent-3-en-1-ol 122,** the reaction yielded 255.2 mg (51% over two steps, *E:Z* = 2:1) of ***(E)*-*N*-(5-(diisopropyl(*p*-tolyl)silyl)pent-3-en-1-yl)-4-methylbenzene sulfonamide 123** as a colourless oil after flash column chromatography on silica gel (hexane/Et_2O 9:1 to 8:2). Note: the synthesis of this product by direct cross-metathesis of the homoallylic tosyl-amine with allyl(diisopropyltolyl)silane gave a mixture of the desired product along up to 50% of the truncated side-product despite the addition of 1,4-benzoquinone.

[11] This compound was prepared according the procedure reported by S. C. Wilkinson, O. Lozano, M. Schuler, M. C. Pacheco, R. Salmon, V. Gouverneur, *Angew. Chem. Int. Ed.* **2009**, *48*, 7083-7086. Analytical and spectroscopic data were in agreement with those reported wherein.

Data for the major (E) isomer: **R_f** = 0.2 (hexane/Et_2O 7:3); **^{1}H NMR (400 MHz, $CDCl_3$)** δ = 0.96-1.05 (m, 12H, *l*), 1.18-1.30 (m, 2H, *k*), 1.82 (d, 2H, $^3J_{H\text{-}H}$ = 7.8 Hz, *j*), 2.05-2.12 (m, 2H, *g*), 2.36 (s, 3H, *a*), 2.43 (s, 3H, *q*), 2.90-2.96 (m, 2H, *f*), 4.35-4.42 (m, 1H, *NH*), 5.13 (dt,1H, $^3J_{H\text{-}H(trans)}$ = 15.1 Hz, $^3J_{H\text{-}H}$ = 7.1 Hz, *h*), 5.51 (dtt, 1H, $^3J_{H\text{-}H(trans)}$ = 15.1 Hz, $^3J_{H\text{-}H}$ = 7.8 Hz, $^4J_{H\text{-}H}$ = 1.3 Hz, *i*), 7.19 (d, 2H, $^3J_{H\text{-}H}$ = 7.3 Hz, *n/o*), 7.30 (d, 2H, $^3J_{H\text{-}H}$ = 8.3 Hz, *c/d*), 7.37 (d, 2H, $^3J_{H\text{-}H}$ = 7.8 Hz, *n/o*), 7.72 (d, 2H, $^3J_{H\text{-}H}$ = 8.3 Hz, *c/d*); **^{13}C NMR (101 MHz, $CDCl_3$)** δ = 10.9 (*k*), 15.6 (*j*), 18.0 (*l*), 21.4 (*a*), 21.5 (*q*), 32.6 (*g*), 42.7 (*f*), 124.3 (*h*), 127.0 (*c/d*), 128.4 (*i*), 128.5 (*n/o*), 129.6 (*c/d*), 130.8 (*m/p*), 134.8 (*n/o*), 137.0 (*m/p*), 138.7 (*b/e*), 143.2 (*b/e*); **IR (CH_2Cl_2): ν =** 2942, 2864, 1599, 1328, 1100, 882, 814; **HRMS (ESI^+):** *m/z* required for $C_{25}H_{37}NO_2SSiNa^+$ ($[M+Na]^+$): 466.2206, found 466.2209, Δ = 0.6 ppm.

Synthesis of (*Z*)-4-methyl-*N*-(5-(triisopropylsilyl)pent-3-en-1-yl)benzenesulfonamide (117):

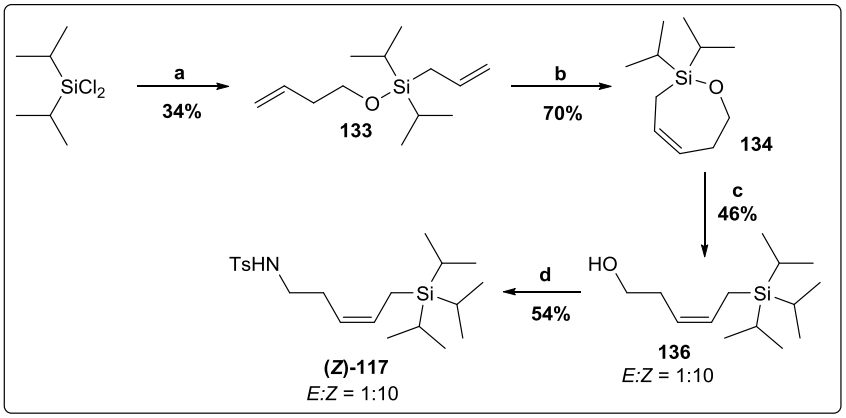

Scheme 4.13: Synthesis of (*Z*)-4-methyl-*N*-(5-(triisopropylsilyl)pent-3-en-1-yl)benzenesulfonamide (*Z*)-**117**. **a**) Allylmagnesium chloride, THF, r.t., 2 h, then NEt_3, 3-buten-1-ol, DMAP, THF, r.t., 13 h, yield over two steps; **b**) Grubbs' 2nd (3 mol%), DCM, reflux, 1 h; **c**) isopropyllithium, Et_2O, -78 °C-r.t., overnight; **d**) $MeSO_2Cl$, NEt_3, DCM, r.t., 2 h, then KOH, $TsNH_2$, DMF, 120 °C, 3 h, yield over two steps.

Allyl(but-3-en-yloxy)diisopropylsilane (133):[11]

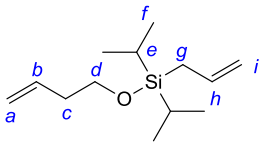

A solution of dichloro(di*iso*propyl)silane (1 mL, 5.5 mmol, 1 eq), in dry THF (5 mL) was cooled to 0 °C and allylmagnesium chloride (2M in THF, 2.8 mL, 5.6 mmol, 1 eq) was added. The reaction mixture was stirred for 2 hours at room temperature. A solution of **3-buten-1-ol** (0.53 mL, 6.05

mmol, 1.1 eq), distilled triethylamine (0.85 mL, 6.05 mmol, 1.1eq) and 4-dimethylaminopyridine (67 mg, 0.55 mmol, 0.1 eq) in dry THF (5 mL) was then added and the reaction mixture was stirred at room temperature overnight. After 13 hours the reaction was quenched with sat. $NH_4Cl_{(aq)}$ and extracted 3 times with dichloromethane. The combined organic layers were dried over $MgSO_4$, filtered and the solvent removed under reduced pressure. The reaction yielded 423.4 mg (34%) of **allyl(but-3-en-yloxy)diiso propylsilane 133** as a colourless oil after flash column chromatography on silica gel (hexane 100%).

R_f = 0.3 (hexane); **^{1}H NMR (400 MHz, $CDCl_3$)** δ = 1.04-1.06 (m, 14H, *e+f*), 1.71 (dt, 2H, $^3J_{H-H}$ = 8.0 Hz, $^4J_{H-H}$ = 1.2 Hz, *g*), 2.27-2.32 (m, 2H, *c*), 3.72 (m, 2H, *d*), 4.81-5.10 (m, 4H, *a+i*), 5,78-5.92 (m, 2H, *b+h*).

2,2-diisopropyl-2,3,6,7-tetrahydro-1,2-oxasilepine (134):

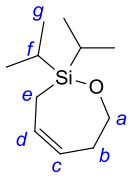

A [0.2 M] solution of **allyl(but-3-en-yloxy)diisopropylsilane 133** (233 mg, 1 mmol, 1 eq) in dichloromethane (52 mL) was heated to reflux. Grubbs' Second Generation catalyst (44 mg, 0.05 mmol, 5 mol %) was subsequently added as a solid and the reaction was allowed to reflux for 3 hours. The solvent was then removed *in vacuo*. The reaction yielded 152 mg (74%) of **2,2-diisopropyl-2,3,6,7-tetrahydro-1,2-oxasilepine 134** as a brown oil after flash column chromatography on silica gel (hexane/Et_2O 98:2).

R_f = 0.3 (hexane/Et_2O 98:2); **^{1}H NMR (400 MHz, $CDCl_3$)** δ = 1.01 (m, 14H, *f+g*), 1.62 (m, 2H, *e*), 2.32-2.41 (m, 2H, *b*), 3.92 (m, 2H, *a*), 5.47-5.59 (m, 1H, *c/d*), 5.77-5.90 (m, 1H, *c/d*).

(*Z*)-5-(triisopropylsilyl)pent-3-en-1-ol (136):[11]

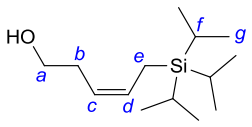

To a solution of **2,2-diisopropyl-2,3,6,7-tetrahydro-1,2-oxasilepine 134** (150 mg, 0.75 mmol, 1 eq.) in dry THF (4.2 mL) at -78 °C was added isopropyllithium (5.6 mL, [0.4M] in pentane, 2.25 mmol, 3 eq.) dropwise. The reaction flask was warmed to 0 °C and allowed to stir at this temperature for four hours. After which time, $NH_4Cl_{(aq.\ sat.)}$ was added and the reaction mixture extracted three times using diethyl ether. The combined organic extracts were washed with brine, dried over $MgSO_4$, filtered and the solvent removed under reduced pressure. The reaction yielded 85 mg (46 %, *E:Z* = 1:10) of **5-(triisopropylsilyl)pent-3-en-1-ol 136** as a colourless oil after flash column chromatography on silica gel (hexane 100%).

Data for the major (Z) isomer: **R_f** = 0.3 (hexane/Et_2O 9:1); **^{1}H NMR (500 MHz, $CDCl_3$)** δ = 1.04 (s, 21H, *f+g*), 1.60 (d, 2H, $^3J_{H\text{-}H}$ = 8.6 Hz, *e*), 2.32-2.38 (m, 2H, *b*), 3.67 (m, 2H, *a*), 5.21-5.26 (d, 1H, $^3J_{H\text{-}H(cis)}$ = 10.9 Hz, *c*), 5.65-5.74 (d, 1H, $^3J_{H\text{-}H(cis)}$ = 10.9 Hz, *d*).

(*Z*)-4-methyl-*N*-(5-(triisopropylsilyl)pent-3-en-1-yl)benzenesulfonamide (117):

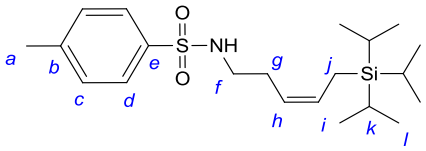

Following the general procedure C on 164.5 mg (0.68 mmol, 1 eq.) of **(*Z*)-5-(triisopropylsilyl)pent-3-en-1-ol (136),** the reaction yielded 145.4 mg (54% over two steps, *E:Z* = 1:10) of **117** as a colourless oil after flash column chromatography on silica gel (hexane/Et_2O 9:1 to 7:3).

Data for the major (Z) isomer: **R_f** = 0.5 (hexane/Et_2O 6:4); **^{1}H NMR (400 MHz, $CDCl_3$)** δ = 0.95-1.05 (m, 21H, *l+k*), 1.45 (d, 2H, $^3J_{H\text{-}H}$ = 8.6 Hz, *j*), 2.16-2.23 (m, 2H, *g*), 2.40 (s, 3H, *a*), 2.92-2.99 (m, 2H, *f*), 4.86-4.96 (m, 1H, *NH*), 5.02 (dtt, 1H, $^3J_{H\text{-}H(cis)}$ = 10.5 Hz, $^3J_{H\text{-}H}$ = 7.3 Hz, $^4J_{H\text{-}H}$ = 1.5 Hz, *h*), 5.57 (dt, 1H, $^3J_{H\text{-}H(cis)}$ = 10.5 Hz, $^3J_{H\text{-}H}$ = 8.8 Hz, *i*), 7.28 (d, 2H, $^3J_{H\text{-}H}$ = 8.3 Hz, *c/d*), 7.76 (d, 2H, $^3J_{H\text{-}H}$ = 8.3 Hz, *c/d*); **^{13}C NMR (101 MHz, $CDCl_3$)** δ = 10.8 (*j*), 10.9 (*k*), 18.5 (*l*), 21.4 (*a*), 27.1 (*g*),

42.8 (*f*), 122.0 (*h*), 127.0 (*c/d*), 129.5 (*c/d*), 130.0 (*i*), 136.9 (*b/e*), 143.1 (*b/e*); **IR (CH_2Cl_2): ν =** 2942, 2865, 1463, 1328, 1161, 883, 663; **HRMS (ESI^+):** *m/z* required for $C_{21}H_{37}NO_2SSiNa^+$ ($[M+Na]^+$): 418.2206, found 418.2206, Δ = 1 ppm.

Synthesis of (*Z*)-*N*-(5-(diisopropyl(*p*-tolyl)silyl)pent-3-en-1-yl)-4-methylbenzenesulfon amide (123):

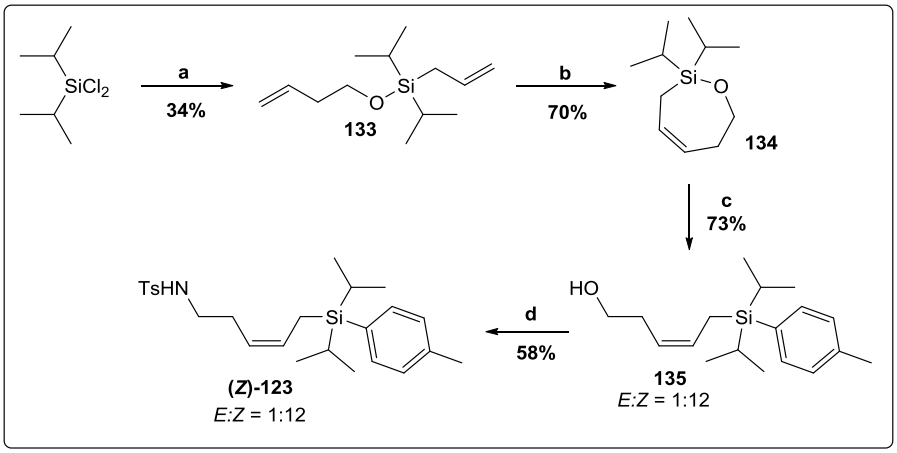

Scheme 4.14: Synthesis of *Z* allylsilanes **(*Z*)-123**. **a**) Allylmagnesium chloride, THF, r.t., 2 h, then NEt_3, 3-buten-1-ol, DMAP, THF, r.t., 13 h, yield over two steps; **b**) Grubbs' 2nd (3 mol%), DCM, reflux, 1 h; **c**) tolyllithium Et_2O, -78 °C-r.t., overnight; **d**) $MeSO_2Cl$, NEt_3, DCM, r.t., 2 h, then KOH, $TsNH_2$, DMF, 120 °C, 3 h, yield over two steps.

(*Z*)-5-[diisopropyl(4-methylphenyl)silyl]pent-3-en-1-ol (135):[11]

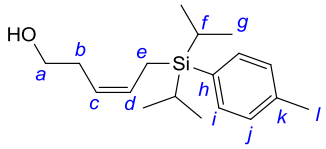

To a solution of 4-iodotoluene (1.31 g, 6.03 mmol, 3 eq.) in anhydrous toluene (5 mL) at 0 °C under argon, was added nBuLi ([2.5 M] in hexanes, 2.5 mL, 6.33 mmol, 3.05 eq.). The resulting white suspension was stirred for 1 h at 0 °C. A solution of **2,2-diisopropyl-2,3,6,7- tetrahydro-1,2-oxasilepine 134** (400 mg, 2.01 mmol, 1 eq.) in anhydrous THF (2 mL) was then added to this freshly prepared solution of tolyllithium. After 20 min at 0 °C, the reaction mixture was warmed at room temperature and stirred for 2.5 h under argon. Saturated aqueous solution of ammonium chloride was added and the mixture was extracted 3 times with diethyl ether. The combined organic layers were washed with brine, dried over $MgSO_4$, filtered and the solvents evaporated *in vacuo*. The

reaction yielded 428 mg of **135** (73%, *E:Z* = 1:12) as a yellow oil after flash column chromatography on silica gel (hexane/Et_2O 9:1 to 8:2).

Data for the major (Z) isomer: **R_f** = 0.3 (hexane/Et_2O 9:1); **^{1}H NMR (400 MHz, $CDCl_3$)** δ = 1.00 (s, 12H, *g*), 1.24-1.35 (m, 2H, *f*), 1.91 (d, 2H, $^3J_{H\text{-}H}$ = 8.3 Hz, *e*), 2.37 (s, 3H, *l*), 2.36-2.39 (m, 2H, *b*), 3.65 (m, 2H, *a*), 5.24-5.31 (d, 1H, $^3J_{H\text{-}H(cis)}$ = 9.6 Hz, *c*), 5.70-5.77 (d, 1H, $^3J_{H\text{-}H(cis)}$ = 9.6 Hz, *d*), 7.19 (d, 2H, $^3J_{H\text{-}H}$ = 8.1 Hz, *i/j*), 7.41 (d, 2H, $^3J_{H\text{-}H(cis)}$ = 8.1 Hz, *i/j*).

(*Z*)-*N*-(5-(diisopropyl(*p*-tolyl)silyl)pent-3-en-1-yl)-4-methylbenzenesulfon amide (123):

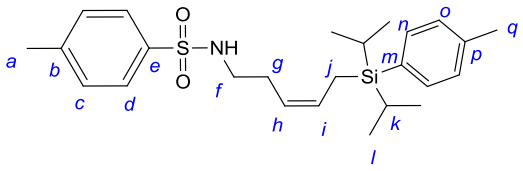

Following the general procedure C on 300 mg (1.1 mmol, 1 eq.) of **(*Z*)-5-[diisopropyl(4-methylphenyl)silyl]pent-3-en-1-ol (135),** the reaction yielded 277 mg of **123** (58% over two steps, *E:Z* = 1:12) as a colourless oil after flash column chromatography on silica gel (hexane/Et_2O 9:1 to 8:2).

Data for the major (Z) isomer: **R_f** = 0.2 (hexane/Et_2O 7:3); **^{1}H NMR (400 MHz, $CDCl_3$)** δ = 0.96-1.03 (m, 12H, *l*), 1.19-1.29 (m, 2H, *k*), 1.77 (d, 2H, $^3J_{H\text{-}H}$ = 8.3 Hz, *j*), 2.15-2.23 (m, 2H, *g*), 2.37 (s, 3H, *a*), 2.41 (s, 3H, *q*), 2.94-2.99 (m, 2H, *f*), 4.60-4.73 (m, 1H, *NH*), 5.07 (dt, 1H, $^3J_{H\text{-}H(cis)}$ = 10.1 Hz, $^3J_{H\text{-}H}$ = 7.3 Hz, *h*), 5.65 (dt, 1H, $^3J_{H\text{-}H(cis)}$ = 10.1 Hz, $^3J_{H\text{-}H}$ = 8.7 Hz, *i*), 7.18 (d, 2H, $^3J_{H\text{-}H}$ = 7.6 Hz, *n/o*), 7.30 (d, 2H, $^3J_{H\text{-}H}$ = 8.1 Hz, *c/d*), 7.37 (d, 2H, $^3J_{H\text{-}H}$ = 7.8 Hz, *n/o*), 7.77 (d, 2H, $^3J_{H\text{-}H}$ = 8.3 Hz, *c/d*); **^{13}C NMR (101 MHz, $CDCl_3$)** δ = 10.9 (*k*), 11.2 (*j*), 17.9 (*l*), 21.4 (*a*), 21.4 (*q*), 27.2 (*g*), 42.7 (*f*), 122.7 (*h*), 127.0 (*c/d*), 128.4 (*n/o*), 129.5 (*i*), 129.6 (*c/d*), 130.8 (*m/p*), 134.8 (*n/o*), 137.0 (*m/p*), 138.7 (*b/e*), 143.2 (*b/e*); **IR (CH_2Cl_2): ν =** 2958, 1717, 1630, 1427, 949 ; **HRMS (CI^+):** *m/z* required for $C_{25}H_{38}NO_2SSi$ ($[M+H]^+$): 444.2393, found 444.2401, Δ = 1.9 ppm.

Synthesis of (*Z*)-4-methyl-*N*-(4-methyl-5-(triisopropylsilyl)pent-3-en-1-yl)benzenesulfonamide (130):

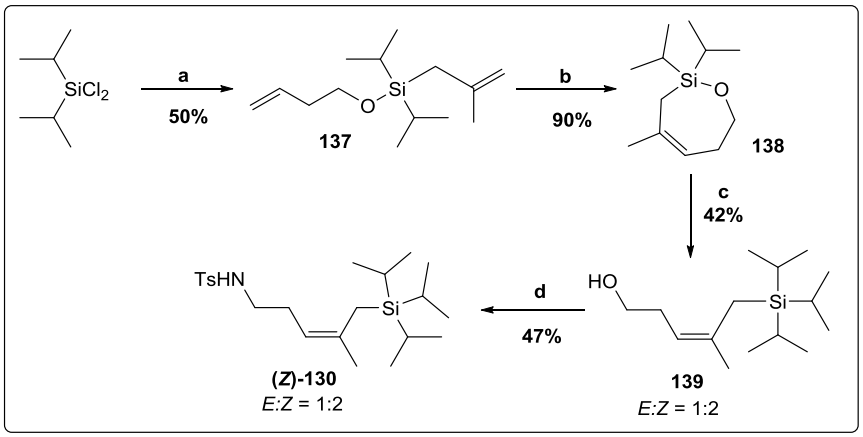

Scheme 4.15: Synthesis of trisubstitued allylsilane **(*Z*)-130**; **a**) 3-buten-1-ol, NEt_3, DCM, reflux, 48 h, then 2-methylallylmagnesium chloride, THF, r.t., 16 h, yield over two steps; **b**) Hoveya-Grubbs 2nd (2 mol%), DCM, reflux, 2 h; **c**) Isopropyllithium, THF, r.t., 23 h; **d**) $MeSO_2Cl$, NEt_3, DCM, r.t., 2 h, then KOH, $TsNH_2$, DMF, 120 °C, 3 h, yield over two steps.

(But-3-enyloxy)(diisopropyl)(2-methylprop-2-en-1-yl)silane (137):[11]

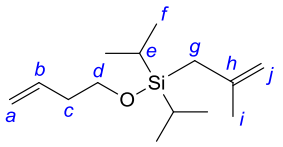

To a solution of **(3-butenoxy)diisopropylsilyl chloride** (1 g, 4.5 mmol, 1 eq.) in dry THF (5 mL) at 0 °C, was added 2-methylallylmagnesium chloride ([0.5M] in THF, 18 mL, 9 mmol, 2 eq.) dropwise. The reaction mixture was then stirred at room temperature under argon. After 16 hours, the reaction was quenched with sat. $NH_4Cl_{(aq)}$ and extracted 3 times with Et_2O. The combined organic layers were dried over $MgSO_4$, filtered and the solvent removed under reduced pressure. The reaction yielded 865.6 mg of **137** (80%) as a colourless oil after flash column chromatography on silica gel (hexane).

R_f = 0.3 (hexane); **^{1}H NMR (400 MHz, $CDCl_3$)** δ = 1.05 (sbr, 14H, *e+f*), 1.67 (s, 2H, *g*), 1.80 (s, 3H, *i*), 2.27-2.34 (m, 2H, *c*), 3.73 (m, 2H, *d*), 4.59-4.64 (m, 2H, *j*), 4.99-5.11 (m, 2H, *a*), 5.78-5.90 (m, 2H, *b*).

2,2-diisopropyl-4-methyl-2,3,6,7-tetrahydro-1,2-oxasilepine (138):[11]

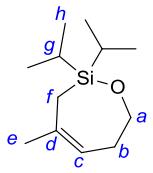

A [0.01 M] solution of **(but-3-enyloxy)(di*iso*propyl)(2-methylprop-2-en-1-yl)silane 137** (215 mg, 0.89 mmol, 1 eq) in dichloromethane (83 mL) was heated to reflux. Hoveyda-Grubbs' Second Generation catalyst (11 mg, 0.018 mmol, 2 mol %) was subsequently added as a solid and the reaction was allowed to reflux for 2 hours. The solvent was then removed *in vacuo* to give brown oil. The crude mixture was purified by flash column chromatography on silica gel (petroleum ether 30-40 °C/Et_2O 9:1) to give 181 mg of the corresponding product **138** (96%) as a colourless oil.

R_f = 0.4 (hexane/Et_2O 9:1); **^{1}H NMR (400 MHz, $CDCl_3$)** δ = 0.99-1.05 (m, 14H, *g+h*), 1.61 (s, 2H, *f*), 1.81 (s, 3H, *e*), 2.26-2.30 (m, 2H, *b*), 3.85-3.88 (m, 2H, *a*), 5.34-5.37 (m, 1H, *c*).

(*Z*)-5-(triisopropylsilyl)-4-methylpent-3-en-1-ol (139):

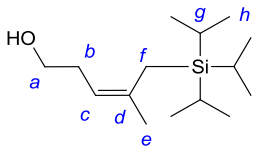

To a solution of **2,2-diisopropyl-4-methyl-2,3,6,7-tetrahydro-1,2-oxasilepine 138** (791 mg, 3.7 mmol, 1 eq.) in anhydrous THF at -78 °C under argon, was added dropwise a solution of *s*BuLi ([0.7 M] in pentane, 16 mL, 11.2 mmol, 3 eq.). The reaction mixture was then stirred at 0 °C for 4 h. It was quenched with a saturated $NH_4Cl_{(aq)}$ solution and the aqueous phase was extracted 3 times with Et_2O. The combined organic phases were washed with brine, dried over $MgSO_4$, filtered and the solvent removed *in vacuo*. The crude mixture was purified by flash column chromatography on silica gel (hexane/Et_2O 9:1 to 7:3) to give 405 mg of the corresponding alcohol **139** (42%, *E:Z* = 1:2) as a colourless oil.

Data for the major (Z) isomer: **R_f** = 0.3 (hexane/Et_2O 7:3); **^{1}H NMR (400 MHz, $CDCl_3$)** δ = 0.85-0.90 (m, 3H, *g*), 0.99-1.10 (m, 17 H, *h*), 1.48-1.52 (m, 1H, *OH*), 1.58 (s, 2H, *f*), 1.76 (s, 3H, *e*), 2.24-2.33 (m, 2H, *b*), 3.63 (t, 2H, $^3J_{H\text{-}H}$ = 6.5 Hz, *a*), 4.96 (t, 1H, $^3J_{H\text{-}H}$ = 7.1 Hz, *c*); **^{13}C NMR (101 MHz,**

$CDCl_3$) δ = 11.9 (*g*), 16.2 (*f*), 18.7 (*h*), 26.6 (*e*), 33.0 (*b*), 62.6 (*a*), 117.7 (*c*), 137.3 (*d*); **IR (neat): ν** = 3329, 2943, 2867, 1465, 1167, 1049, 918; **HRMS (FI^+):** *m/z* required for $C_{15}H_{32}OSi$ ($[M]^+$): 256.2223, found 256.2228, Δ = 2.2 ppm.

Identifiable data for the minor (E) isomer: **^{1}H NMR (400 MHz, $CDCl_3$)** δ = 1.62 (s, 2H, *f*), 1.79 (s, 3H, *e*); **^{13}C NMR (101 MHz, $CDCl_3$)** δ = 11.9 (*g*), 15.3 (*f*), 18.3 (*h*), 26.7 (*e*), 118.1 (*c*), 137.5 (*d*);

(*Z*)-4-methyl-*N*-(4-methyl-5-(triisopropylsilyl)pent-3-en-1-yl)benzenesulfonamide (130):

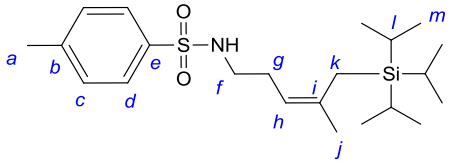

Following the general procedure C on 405 mg (1.6 mmol, 1 eq.) of **(*Z*)-5-(triisopropylsilyl)-4-methylpent-3-en-1-ol 139** the reaction yielded 306 mg of **130** (47% over two steps, *E:Z* = 1:2) as a yellow oil after flash column chromatography on silica gel (hexane/Et_2O 9:1 to 7:3).

Data for the major (Z) isomer: **R_f** = 0.6 (hexane/Et_2O 6:4); **^{1}H NMR (400 MHz, $CDCl_3$)** δ = 0.83-0.86 (m, 3H, *l*), 0.91-0.97 (m, 18H, *m*), 1.41 (s, 2H, *k*), 1.64 (s, 3H, *j*), 2.06-2.16 (m, 2H, *g*), 2.38 (s, 3H, *a*), 2.86-2.96 (m, 2H, *f*), 4.73 (t, 1H, $^3J_{H\text{-}H}$ = 6.8 Hz, *h*), 4.98-5.20 (m, 1H, *NH*), 7.25 (d, 2H, $^3J_{H\text{-}H}$ = 7.8 Hz, *c/d*), 7.75 (d, 2H, $^3J_{H\text{-}H}$ = 8.1 Hz, *c/d*); **^{13}C NMR (101 MHz, $CDCl_3$)** δ = 11.7 (*l*), 16.0 (*k*), 18.5 (*m*), 21.3 (*a*), 26.3 (*j*), 28.5 (*g*), 42.9 (*f*), 117.5 (*h*), 127.0 (*c/d*), 129.4 (*c/d*), 137.0 (*b/e*), 137.3 (*i*), 142.9 (*b/e*); **IR (CH_2Cl_2): ν** = 2944, 2866, 1464, 1328, 1161, 883; **HRMS (ESI^-):** *m/z* required for $C_{22}H_{38}NO_2SSi$ ($[M\text{-}H]^-$): 408.2398, found 408.2392, Δ = 1.4 ppm.

Identifiable data for the minor (E) isomer: **^{1}H NMR (400 MHz, $CDCl_3$)** δ = 0.80-0.83 (m, 3H, *l*), 0.97-1.02 (m, 18H, *m*), 1.44 (s, 2H, *k*), 1.66 (s, 2H, *j*); **^{13}C NMR (101 MHz, $CDCl_3$)** δ = 11.6 (*l*), 15.1 (*k*), 18.0 (*m*), 26.4 (*j*), 28.5 (*g*), 117.8 (*h*).

Synthesis of (*E*)-2,2-dimethyl-*N*-tosyl-5-(triisopropylsilyl)pent-3-enamide (132):

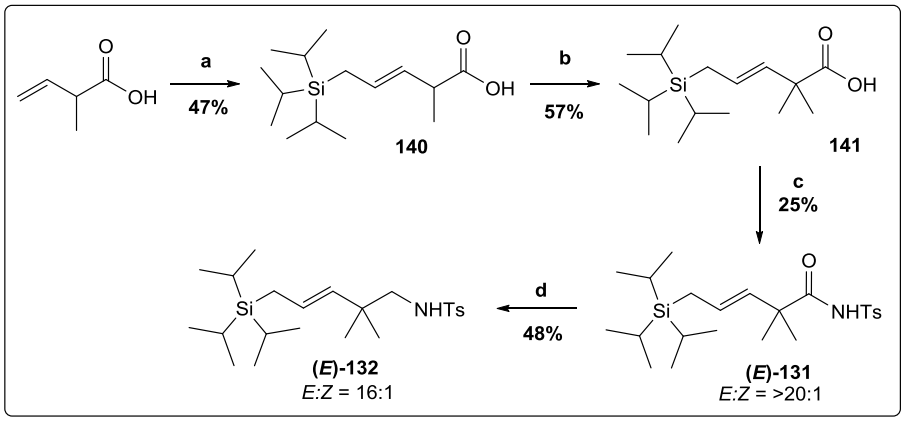

Scheme 4.16: Synthesis of gem-dimethyl substituted allylsilanes **(*E*)-131** and **(*E*)-132**; **a**) allyltriisopropylsilane, Hoveyda-Grubbs' 2nd (5 mol %) DCM, reflux, 3 days; **b**) LDA, MeI, THF, -78 °C, 1 h; **c**) tosylisocyanate, NEt_3, THF, r.t., overnight; **d**) $LiAlH_4$, THF, r.t, 16 h;

2-methyl-5-(triisopropylsilyl)pent-3-enoic acid (140):[11]

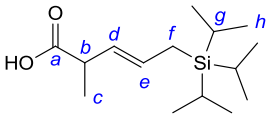

To a solution of **2-methylbut-3-enoic acid** (500 mg, 5 mmol, 1eq.) and allyltriisopropylsilane (3.6 mL, 15 mmol, 3 eq.) in dichloromethane (15 mL) was added Hoveyda-Grubbs' second generation catalyst (156 mg, 5 mol %) and the reaction was heated to reflux for 3 days.

The reaction mixture was then concentrated *in vacuo* to give a brown oil. The crude mixture was purified by flash column chromatography on silica gel (hexane/Et_2O 9:1 to 8:2) to give 630 mg (47%) of **140** as a colourless oil.

R_f = 0.6 (hexane/Et_2O 6:4); **^{1}H NMR (400 MHz, $CDCl_3$)** δ = 1.04-1.06 (m, 21H, *g+h*), 1.24 (d, 3H $^3J_{H\text{-}H}$ = 7.0 Hz, *c*), 1.59 (dd, 2H, $^3J_{H\text{-}H}$ = 8.2 Hz, $^4J_{H\text{-}H}$ = 0.8 Hz, *f*), 3.07-3.14 (m, 1H, *b*), 5.38 (dd, 1H $^3J_{H\text{-}H(trans)}$ = 15.2 Hz, $^3J_{H\text{-}H}$ = 7.9 Hz, *d*), 5.61-5.69 (m, 1H, *e*).

2,2-dimethyl-5-(triisopropylsilyl)pent-3-enoic acid (141):[11]

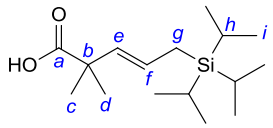

To a solution of diisopropylamine (0.33 mL, 2.4 mmol, 2.2 eq) in THF (8 mL) at -78 °C was added *n*-BuLi ([1.0 M], 2.4 mL, 2.4 mmol, 2.2 eq). The mixture was allowed to stir at -78 °C for 30 minutes. **2-Methyl-5-(triisopropylsilyl)pent-3-enoic acid** (290 mg, 1.1 mmol, 1 eq) in THF (2 mL) was added dropwise to the mixture. The reaction was allowed to warm to 0 °C and stirred at this temperature for 30 minutes, the reaction was then cooled to -78 °C. Methyl iodide (0.2 mL, 3.3 mmol, 3 eq) was added and the reaction allowed to stir at -78 °C for 30 minutes followed by 1 hour at room temperature. The reaction was then quenched with saturated NH_4Cl solution, the aqueous layer was extracted with ethyl acetate. The combined organic phases were dried ($MgSO_4$), filtered and the solvent removed *in vacuo.* The crude product was purified by flash column chromatography on silica gel (hexane/Et_2O 8:2) to yield 180 mg of the corresponding acid **141** (57%) as a colourless oil.

R_f = 0.3 (hexane/Et_2O 8:2); **^{1}H NMR (400 MHz, $CDCl_3$)** δ = 1.03 (s, 21H, *h+i*), 1.28 (s, 6H, *c+d*), 1.59 (dd, 2H, $^3J_{H\text{-}H}$ = 7.9 Hz, $^4J_{H\text{-}H}$ = 0.9 Hz, *g*), 5.49 (d, 1H, $^3J_{H\text{-}H(trans)}$ = 15.4 Hz, *e*), 5.57-5.65 (m, 1H, *f*).

(*E*)-2,2-dimethyl-*N*-tosyl-5-(triisopropylsilyl)pent-3-enamide (131):

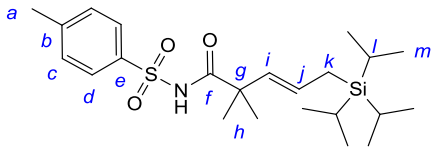

To a solution of **(*E*)-2,2-dimethyl-5-(triisopropylsilyl)pent-3-enoic acid 141** (824 mg, 2,9 mmol, 1 eq.) in THF (6 mL) under argon was added tosyl isocyannate (0.45 mL, 2.9 mmol, 1 eq.). After stirring at ambient temperature for 10 minutes, the inert atmosphere was disconnected and distilled triethylamine (0.40 mL, 2.9 mmol, 1 eq.) was added dropwise to the open flask allowing the release of CO_2. The reaction was stirred overnight. The mixture was then diluted with an equal volume of EtOAc, washed twice with 2M HCl and brine, dried over $MgSO_4$, filtered and the solvent removed

in vacuo. The crude product was purified by flash column chromatography on silica gel (hexane/Et_2O 9:1 to 7:3) to yield 322 mg of the corresponding tosyl amide **131** (25%, E:Z = >20:1) as a colourless oil.

Data for the major (E) isomer: **R_f** = 0.3 (hexane/Et_2O 7:3); **^{1}H NMR (400 MHz, $CDCl_3$)** δ = 1.03-1.06 (m, 21H, *l+m*), 1.19 (s, 6H, *h*), 1.63 (d, 2H, $^3J_{H-H}$ = 8.3 Hz, *k*), 2.44 (s, 3H, *a*), 5.34 (d, 1H, $^3J_{H-H(trans)}$ = 15.6 Hz, *i*), 5.70 (dt, 1H, $^3J_{H-H(trans)}$ = 15.6 Hz, $^3J_{H-H}$ = 8.3 Hz, *j*), 7.33 (d, 2H, $^3J_{H-H}$ = 8.1 Hz, *c/d*), 7.92 (d, 2H, $^3J_{H-H}$ = 8.3 Hz, *c/d*), 8.15-8.19 (m, 1H, *NH*); **^{13}C NMR (101 MHz, $CDCl_3$)** δ = 11.0 (*l*), 16.1 (*k*), 18.6 (*m*), 21.7 (*a*), 24.6 (*h*), 45.8 (*g*), 128.4 (*c/d*), 129.5 (*c/d*), 130.4 (*i*), 130.5 (*j*), 135.4 (*b/e*), 144.9 (*b/e*), 174.4 (*f*); **IR (CH_2Cl_2): ν =** 2949, 1699, 1423, 1239, 1165, 964, 853; **HRMS (ESI$^+$):** *m/z* required for $C_{23}H_{39}NO_3SSiNa^+$ ($[M+Na]^+$): 460.2312, found 460.2293, Δ = 4 ppm.

(*E*)-*N*-(2,2-dimethyl-5-(triisopropylsilyl)pent-3-en-1-yl)-4-methylbenzenesulfonamide (132):

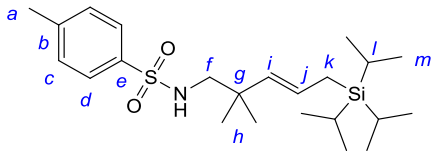

In a flask charged with $LiAlH_4$ (83 mg, 2.2 mmol, 5 eq.) in dry Et_2O (9 mL) at 0 °C under argon, was added dropwise a solution of **(*E*)-2,2-dimethyl-*N*-tosyl-5-(triisopropylsilyl)pent-3-enamide 131** (193 mg, 0.4 mmol, 1 eq.) in 1 mL of Et_2O. The reaction mixture stirred at 0 °C for 1 h then at room temperature overnight. H_2O was added carefully to the mixture which was filtered through Celite and then extracted with Et_2O. The combined organic layers were washed with brine, dried over $MgSO_4$ and the solvent removed *in vacuo*. Purification of the resulting residue by flash column chromatography on silica gel (hexane/Et_2O 8:2) yielded 90.3 mg of the product **132** (48%, E:Z = 16:1) as a colourless oil.

Data for the major (E) isomer: **R_f** = 0.5 (hexane/Et_2O 6:4); **^{1}H NMR (400 MHz, $CDCl_3$)** δ = 0.95 (s, 6H, *h*), 0.99-1.04 (m, 21H, *l+m*), 1.52 (d, 2H, $^3J_{H-H}$ = 7.9 Hz, *k*), 2.42 (s, 3H, *a*), 2.68 (d, 2H, $^3J_{H-H}$ = 6.3 Hz, *f*), 4.39-4.46 (m, 1H, *NH*), 5.05 (d, 1H, $^3J_{H-H(trans)}$ = 15.6 Hz, *i*), 5.42 (dt, 1H, $^3J_{H-H(trans)}$ = 15.6 Hz, $^3J_{H-H}$ = 7.9 Hz, *j*), 7.30 (d, 2H, $^3J_{H-H}$ = 7.8 Hz, *c/d*), 7.72 (d, 2H, $^3J_{H-H}$ = 8.1 Hz, *c/d*); **^{13}C**

NMR (101 MHz, $CDCl_3$) δ = 10.9 (*l*), 15.6 (*k*), 18.6 (*m*), 21.4 (*a*), 25.1 (*h*), 36.5 (*g*), 53.2 (*f*), 126.8 (*j*), 127.0 (*c/d*), 129.6 (*c/d*), 134.1 (*i*), 136.9 (*b/e*), 143.1 (*b/e*); **IR (neat): ν =** 1265, 1162, 739, 705; **HRMS (ESI^-):** *m/z* required for $C_{23}H_{40}NO_2SSi$ ($[M-H]^-$): 422.2555, found 422.2548, Δ = 1.5 ppm.

Identifiable data for the minor (Z) isomer: **^{1}H NMR (400 MHz, $CDCl_3$)** δ = 1.45 (d, 2H, $^3J_{H-H}$ = 8.3 Hz, *k*), 2.84 (d, 2H, $^3J_{H-H}$ = 6.6 Hz, *f*), 4.95 (d, 1H, $^3J_{H-H(cis)}$ = 11.9 Hz, *i*), 5.47-5.56 (m, 1H, *j*).

4.7 Fluorocyclisation of organosilanes:

General procedure D:

To a solution of allylsilane (1 eq.) in dry CH_3CN [0.1 M] was added $NaHCO_3$ (1.1 eq.). The mixture was treated with Selectfluor (1.1 eq) and the reaction was stirred for 48 hours at r.t. The solvent was removed *in vacuo* and the reaction mixture was treated with a saturated solution of $NaHCO_3$ and extracted three times with Et_2O. The combined organic phases were washed with H_2O, brine, dried over $MgSO_4$, filtered and the solvent removed *in vacuo*. The crude product was purified by flash column chromatography on silica gel (hexane/Et_2O 8:2).

***syn*-3-fluoro-1-tosyl-2-((triisopropylsilyl)methyl)pyrrolidine (*syn*-124):**

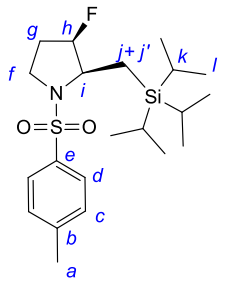

Following the general procedure D on 100 mg (0.25 mmol, 1 eq.) of *(E)*-**117**, the reaction yielded 62 mg of *syn*-**124** (58%, d.r. *(syn:anti)* 9:1) as a white solid, with 22 mg of the corresponding allylic fluoride **55** (34%).

Data for the major syn diastereoisomer: **R_f** = 0.5 (hexane/Et_2O 6:4); **m.p.** = 73 °C; **^{1}H NMR (400 MHz, $CDCl_3$)** δ = 1.06-1.13 (m, 21H, *k+l*), 1.23-1.47 (m, 2H, *g'+j'*), 1.53 (ddd, 1H, $^2J_{H-H}$ = 14.5 Hz, $^3J_{H-F}$ = 4.3 Hz, $^3J_{H-H}$ = 3.4 Hz, *j*), 1.95 (td, 1H, *J* = 14.9, 5.3 Hz, *g*), 2.43 (s, 3H, *a*), 3.45-3.55 (m, 1H, *f'*), 3.68 (dd, 1H, $^2J_{H-H}$ = 11.4 Hz, $^3J_{H-H}$ = 8.3 Hz, *f*), 3.88 (ddt, 1H, $^3J_{H-F}$ = 25.3 Hz, $^3J_{H-H}$ =

12.7, 3.4 Hz, *i*), 4.89 (dt, 1H, $^{2}J_{H\text{-}F}$ = 52.3 Hz, $^{3}J_{H\text{-}H}$ = 3.1 Hz, *h*), 7.31 (d, 2 H, $^{3}J_{H\text{-}H}$ = 8.1 Hz, *c/d*), 7.73 (d, 2H, $^{3}J_{H\text{-}H}$ = 8.3 Hz, *c/d*); **^{13}C NMR (101 MHz, $CDCl_3$)** δ = 11.3 (*k'*), 11.4 (*j*), 11.5 (*k*), 18.5 (*l'*), 18.8 (*l*), 21.5 (*a*), 32.1 (d, $^{2}J_{C\text{-}F}$ = 22.4 Hz, *g*), 46.4 (*f*), 63.3 (d, $^{2}J_{C\text{-}F}$ = 20.8 Hz, *i*), 94.1 (d, $^{1}J_{C\text{-}F}$ = 182.9 Hz, *h*), 127.2 (*c/d*), 129.7 (*c/d*), 135.6 (*b/e*), 143.5 (*b/e*); **^{19}F {^{1}H} NMR (377 MHz, $CDCl_3$)** δ = -188.59; **IR (CH_2Cl_2)**: **ν** = 3029, 1900, 1400, 902, 760; **HRMS (CI^+):** *m/z* required for $C_{21}H_{37}FNO_2SSi$ ($[M+H]^+$): 414.2298, found 414.2300, Δ = 4.8 ppm.

The structure was unambiguously confirmed by X-ray crystallography and NOESY/HOESY experiments.

***anti*-3-fluoro-1-tosyl-2-((triisopropylsilyl)methyl)pyrrolidine (*anti*-124):**

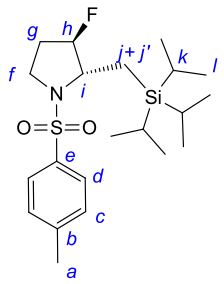

Following the general procedure D on 145 mg (0.37 mmol, 1 eq.) of *(Z)*-**117**, the reaction yielded 52 mg of *anti*-**124** (34%, d.r. *(syn:anti)* 1:21) as a white solid, with 36 mg (38%) of the corresponding allylic fluoride **55**.

Data for the major anti diastereoisomer: **R_f** = 0.5 (hexane/Et_2O 6:4); **m.p.** = 70 °C; **^{1}H NMR (400 MHz, C_6D_6)** δ = 0.62 (ddd, 1H, $^{2}J_{H\text{-}H}$ = 15.1 Hz, $^{3}J_{H\text{-}H}$ = 13.4 Hz, $^{4}J_{H\text{-}F}$ = 1.5 Hz, *j'*), 0.91-1.02 (m, 3H, *k*), 1.02-1.10 (m, 18H, *l*), 1.41-1.56 (m, 2H, *g*), 1.66 (ddd, 1H, $^{2}J_{H\text{-}H}$ = 15.1 Hz, $^{4}J_{H\text{-}F}$ = 4.8 Hz, $^{3}J_{H\text{-}H}$ = 2.8 Hz, *j*), 1.85 (s, 3H, *a*), 3.11 (ddd, 1H, $^{3}J_{H\text{-}H}$ = 10.6 Hz, $^{2}J_{H\text{-}H}$ = 9.3 Hz, $^{3}J_{H\text{-}H}$ = 7.6 Hz, *f*), 3.45 (ddd, 1H, $^{2}J_{H\text{-}H}$ = 9.3 Hz, $^{3}J_{H\text{-}H}$ = 7.6, 2.1 Hz, *f'*), 4.21 (ddd, 1H, $^{3}J_{H\text{-}F}$ = 25.3 Hz, $^{3}J_{H\text{-}H}$ = 13.1, 2.3 Hz, *i*), 4.52 (d, 1H, $^{2}J_{H\text{-}F}$ = 53.1 Hz, *h*), 6.84 (d, 2H, $^{3}J_{H\text{-}H}$ = 8.1 Hz, *c/d*), 7.88 (d, 2H, $^{3}J_{H\text{-}H}$ = 8.3 Hz, *c/d*); **^{13}C NMR (100 MHz, C_6D_6)** δ = 11.9 (*k*), 18.4 (d, $^{3}J_{C\text{-}F}$ = 11.2 Hz, *j*), 19.2 (*l*), 21.5 (*a*), 30.5 (d, $^{2}J_{C\text{-}F}$ = 21.6 Hz, *g*), 46.4 (*f*), 65.2 (d, $^{2}J_{C\text{-}F}$ = 22.4 Hz, *i*), 97.1 (d, $^{1}J_{C\text{-}F}$ = 179.7 Hz, *h*), 128.0 (*c/d*), 130.0 (*c/d*), 135.7 (*b/e*), 143.4 (*b/e*); **^{19}F {^{1}H} NMR (377 MHz, C_6D_6)** δ = -173.33; **IR (CH_2Cl_2)**: **ν**

= 3002, 1923, 1355, 991; **HRMS (CI$^+$):** *m/z* required for $C_{21}H_{37}FNO_2SSi$ ([M+H]$^+$): 414.2298, found 414.2310, Δ = 4.5 ppm.

The structure was unambiguously confirmed NOESY/HOESY experiments.

***Syn*-2-((diisopropyl(*p*-tolyl)silyl)methyl)-3-fluoro-1-tosylpyrrolidine (*syn*-125):**

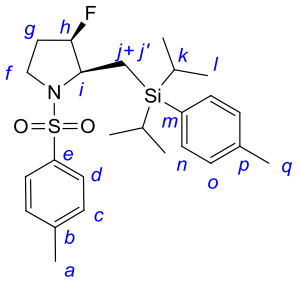

Following the general procedure D on 100 mg (0.22 mmol, 1 eq.) of *(E)*-**123**, the reaction yielded 24 mg of *syn*-**125** (23%, d.r. *(syn:anti)* 5:1) as a colourless oil, with 29 mg (50%) of the corresponding allylic fluoride **55**.

Data for the major syn diastereoisomer: **R$_f$** = 0.4 (hexane/Et$_2$O 7:3); **^{1}H NMR (500 MHz, CDCl$_3$)** δ = 1.08-1.13 (m, 12H, *l*), 1.13-1.18 (m, 1H, *g'*), 1.29-1.35 (m, 2H, *k*), 1.56-1.61 (m, 1H, *j*), 1.79-1.89 (m, 2H, *g+j'*), 2.39 (s, 3H, *q*), 2.42 (s, 3H, *a*), 3.46-3.54 (m, 1H, *f'*), 3.61 (dd, 1H, $^2J_{H-H}$ = 12.0 Hz, $^3J_{H-H}$ = 8.2 Hz, *f*), 3.69 (ddd, 1H, $^3J_{H-F}$ = 25.8 Hz, $^3J_{H-H}$ = 12.6, 3.3 Hz, *i*), 4.59 (ddd, 1H, $^2J_{H-F}$ = 52.0 Hz, $^3J_{H-H}$ = 3.5, 2.8 Hz, *h*), 7.21 (d, 2H, $^3J_{H-H}$ = 7.2 Hz, *n/o*), 7.25 (d, 2H, $^3J_{H-H}$ = 7.9 Hz, *c/d*), 7.47 (*d*, 2H, $^3J_{H-H}$ = 7.9 Hz, *n/o*), 7.61 (d, 2H, $^3J_{H-H}$ = 8.2 Hz, *c/d*); **^{13}C NMR (125 MHz, CDCl$_3$)** δ = 11.5 (*k*), 11.6 (*k'*), 12.1 (d, $^3J_{C-F}$ = 10.5 Hz, *j*), 18.2 (*l'*), 18.3 (*l*), 21.5 (*q*), 21.5 (*a*), 31.9 (d, $^2J_{C-F}$ = 21.9 Hz, *g*), 46.6 (*f*), 63.2 (d, $^2J_{C-F}$ = 21.0 Hz, *i*), 93.7 (d, $^1J_{C-F}$ = 183.1 Hz, *h*), 127.3 (*c/d*), 128.6 (*n/o*), 129.6 (*c/d*), 130.9 (*m/p*), 135.1 (*b/e*), 135.2 (*n/o*), 138.7 (*m/p*), 143.4 (*b/e*); **^{19}F {^{1}H} NMR (377 MHz, CDCl$_3$)** δ = -188.77; **IR (CH$_2$Cl$_2$)**: **ν =** 2944, 2866, 1599, 1349, 1161, 1099, 817, 737; **HRMS (ESI$^+$):** *m/z* required for $C_{25}H_{36}FNO_2SSiNa^+$ ([M+Na]$^+$): 484.2112, found 484.2096, Δ = 3.2 ppm.

The structure was unambiguously confirmed NOESY/HOESY experiments.

***Anti*-2-((diisopropyl(*p*-tolyl)silyl)methyl)-3-fluoro-1-tosylpyrrolidine (*anti*-125):**

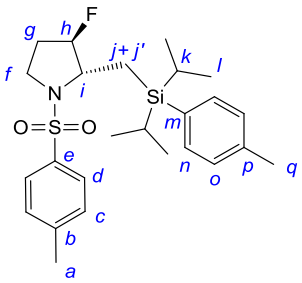

Following the general procedure D on 100 mg (0.22 mmol, 1 eq.) of *(Z)*-**123**, the reaction yielded 15 mg of *anti*-**125** (14%, d.r. *(syn:anti)* > 1:20) as a colourless oil, with 39 mg (57%) of the corresponding allylic fluoride **55**.

Data for the major anti diastereoisomer: **R_f** = 0.5 (hexane/Et_2O 7:3); **^{1}H NMR (500 MHz, $CDCl_3$)** δ = 1.04 (dd, 6H, $^3J_{H-H}$ = 10.4, 7.6 Hz, *l*), 1.05 (m, 1H, *j*), 1.15 (dd, 6H, $^3J_{H-H}$ = 10.7, 7.6 Hz, *l*), 1.26 (p, 1H, $^3J_{H-H}$ = 7.6 Hz, *k*), 1.41 (p, 1H, $^3J_{H-H}$ = 7.6 Hz, *k'*), 1.74 (ddd, 1H, $^2J_{H-H}$ = 15.1 Hz, $^4J_{H-F}$ = 4.4 Hz, $^3J_{H-H}$ = 3.1 Hz, *j'*), 1.92-2.14 (m, 2H, *g*), 2.37 (s, 3H, *q*), 2.42 (s, 3H, *a*), 3.11 (ddd, 1H, $^3J_{H-H}$ = 11.4 Hz, $^2J_{H-H}$ = 9.5 Hz, $^3J_{H-H}$ = 6.2 Hz, *f''*), 3.62 (dd, 1H, $^2J_{H-H}$ = 9.5 Hz, $^3J_{H-H}$ = 1.0 Hz, *f*), 3.97 (dddd, 1H, $^3J_{H-F}$ = 25.2 Hz, $^3J_{H-H}$ = 13.2, 3.1, 1.1 Hz, *i*), 4.56 (dd, 1H, $^2J_{H-F}$ = 51.7 Hz, $^3J_{H-H}$ = 2.5 Hz, *h*), 7.21 (d, 2H, $^3J_{H-H}$ = 7.6 Hz, *n/o*), 7.28 (d, 2H, $^3J_{H-H}$ = 8.2 Hz, *c/d*), 7.40 (*d*, 2H, $^3J_{H-H}$ = 7.8 Hz, *n/o*), 7.65 (d, 2H, $^3J_{H-H}$ = 8.2 Hz, *c/d*); **^{13}C NMR (125 MHz, $CDCl_3$)** δ = 10.8 (*k*), 11.5 (*k'*), 18.0 (*l*), 18.2 (*l'*), 18.4 (d, $^3J_{C-F}$ = 11.4 Hz, *j*), 21.5 (*q*), 21.5 (*a*), 30.1 (d, $^2J_{C-F}$ = 21.0 Hz, *g*), 45.7 (*f*), 64.6 (d, $^2J_{C-F}$ = 21.9 Hz, *i*), 96.1 (d, $^1J_{C-F}$ = 179.3 Hz, *h*), 127.6 (*c/d*), 128.8 (*n/o*), 129.5 (*c/d*), 130.5 (*m/p*), 133.8 (*b/e*), 134.8 (*n/o*), 139.0 (*m/p*), 143.3 (*b/e*); **^{19}F {^{1}H} NMR (377 MHz, $CDCl_3$)** δ = -174.06; **IR (CH_2Cl_2)**: **ν** = 2945, 2866, 1599, 1345, 1161, 1099, 739; **HRMS (CI^+):** *m/z* required for $C_{25}H_{37}FNO_2SSi$ ($[M+H]^+$): 462.2298, found 462.2311, Δ = 2.7 ppm.

The structure was unambiguously confirmed NOESY/HOESY experiments.

***Anti*-3-fluoro-2-methyl-1-tosyl-2-((triisopropylsilyl)methyl)pyrrolidine (142):**

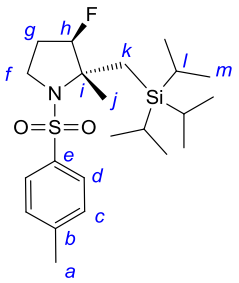

Following the general procedure D on 163 mg (0.39 mmol, 1 eq.) of *(Z)*-**130**, the reaction yielded 102 mg of *anti*-**142** (61%, d.r. *(syn:anti)* 1:1) as a yellow oil, with 29 mg (27%) of the corresponding allylic fluoride **63**.

Data for the major anti diastereoisomer: **R_f** = 0.6 (hexane/Et_2O 6:4); **^{1}H NMR (500 MHz, C_6D_6)** δ = 0.78-0.87 (m, 1H, *k*), 0.89-1.09 (m, 21H, *l+m*), 1.55-1.80 (m, 2H, *g*), 1.72 (d, 3H, $^3J_{H-H}$ = 4.7 Hz, *j*), 1.93 (s, 3H, *a*), 2.12 (dd, 1H, $^2J_{H-H}$ = 15.1 Hz, $^4J_{H-F}$ = 6.3 Hz, *k'*), 3.34 (ddd, 1H, $^2J_{H-H}$ = 16.8 Hz, $^3J_{H-H}$ = 9.7, 7.3 Hz, *f*), 3.56 (ddd, 1H, $^2J_{H-H}$ = 16.8 Hz, $^3J_{H-H}$ = 9.1, 2.5 Hz, *f'*), 4.59 (ddd, 1H, $^2J_{H-F}$ = 53.0 Hz, $^3J_{H-H}$ = 3.8, 1.9 Hz, *h*), 6.83 (d, 2H, $^3J_{H-H}$ = 8.5 Hz, *c/d*), 7.80 (d, 2H, $^3J_{H-H}$ = 8.2 Hz, *c/d*); **^{13}C NMR (125 MHz, C_6D_6)** δ = 12.7 (*l*), 19.5 (*m*), 21.5 (*a*), 22.4 (d, $^3J_{C-F}$ = 12.4 Hz, *j*), 24.4 (d, $^3J_{C-F}$ = 5.7 Hz, *k*), 29.3 (d, $^2J_{C-F}$ = 22.9 Hz, *g*), 46.4 (*f*), 72.0 (d, $^2J_{C-F}$ = 19.1 Hz, *i*), 99.7 (d, $^1J_{C-F}$ = 186.0 Hz, *h*), 127.7 (*c/d*), 129.9 (*c/d*), 140.3 (*b/e*), 142.8 (*b/e*); **^{19}F {^{1}H} NMR (377 MHz, $CDCl_3$)** δ = -181.97; **IR (CH_2Cl_2)**: **ν =** 2952, 1464, 1341, 1158, 1011, 814, 711; **HRMS (ESI^+):** *m/z* required for $C_{22}H_{38}FNO_2SSiNa^+$ ($[M+Na]^+$): 450.2269, found 450.2261, Δ = 1.4 ppm.

Identifiable data for minor syn diastereoisomer: **^{1}H NMR (500 MHz, C_6D_6)** δ = 1.74 (d, 3H, $^3J_{H-H}$ = 5.3 Hz, *j*), 2.20 (dd, 1H, $^2J_{H-H}$ = 15.4 Hz, $^4J_{H-F}$ = 6.9 Hz, *k'*), 4.62 (ddd, 1H, $^2J_{H-F}$ = 53.0 Hz, $^3J_{H-H}$ = 3.5, 1.3 Hz, *h*); **^{13}C NMR (125 MHz, C_6D_6)** δ = 12.6 (*l*), 19.4 (*m*), 22.3 (d, $^3J_{C-F}$ = 12.4 Hz, *j*), 24.3 (d, $^3J_{C-F}$ = 5.7 Hz, *k*), 29.4 (d, $^2J_{C-F}$ = 21.9 Hz, *g*), 46.4 (*f*), 72.3 (d, $^2J_{C-F}$ = 18.1 Hz, *i*), 99.7 (d, $^1J_{C-F}$ = 186.0 Hz, *h*); **^{19}F {^{1}H} NMR (377 MHz, $CDCl_3$)** δ = -181.75;

The structure was unambiguously confirmed NOESY/HOESY experiments.

***Syn*-3-fluoro-4,4-dimethyl-1-tosyl-2-((triisopropylsilyl)methyl)pyrrolidine (143):**

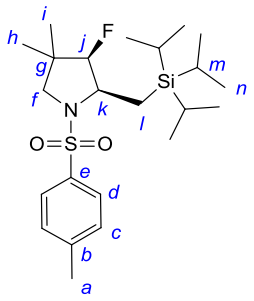

Following the general procedure D on 90 mg (0.22 mmol, 1 eq.) of *(E)*-**132**, the reaction yielded 35 mg of *syn*-**143** (36%, d.r. *(syn:anti)* 6:1) as a yellow oil, with 28 mg (45%) of the corresponding allylic fluoride **64**.

Data for the major syn diastereoisomer: **R_f** = 0.6 (hexane/Et_2O 6:4); **^{1}H NMR (500 MHz, C_6D_6)** δ = 0.43 (d, 3H, $^4J_{H\text{-}F}$ = 1.7 Hz, *h*), 0.80 (d, 3H, $^4J_{H\text{-}F}$ = 1.9 Hz, *i*), 1.01-1.03 (m, 3H, *m*), 1.10 (d, 9H, $^3J_{H\text{-}H}$ = 6.9 Hz, *n*), 1.15 (d, 9H, $^3J_{H\text{-}H}$ = 7.2 Hz, *n'*), 1.41 (dd, 1H, $^2J_{H\text{-}H}$ = 13.2 Hz, $^3J_{H\text{-}H}$ = 12.9 Hz, *l*), 1.85 (s, 3H, *a*), 1.86-1.92 (m, 1H, *l'*), 3.22 (d, 1H, $^2J_{H\text{-}H}$ = 10.7 Hz, *f*), 3.41 (d, 1H, $^2J_{H\text{-}H}$ = 10.4 Hz, *f'*), 4.19 (dd, 1H, $^2J_{H\text{-}F}$ = 52.6 Hz, $^3J_{H\text{-}H}$ = 3.5 Hz, *j*), 4.36 (ddt, 1H, $^3J_{H\text{-}F}$ = 27.4, $^3J_{H\text{-}H}$ = 16.6, 3.1 Hz, *k*), 6.81 (d, 2H, $^3J_{H\text{-}H}$ = 7.9 Hz, *c/d*), 7.84 (d, 2H, $^3J_{H\text{-}H}$ = 8.2 Hz, *c/d*); **^{13}C NMR (125 MHz, C_6D_6)** δ = 11.9 (*d*, $^3J_{C\text{-}F}$ = 12.4 Hz, *l*), 12.3 (*m*), 19.2 (*n*), 19.4 (*n'*), 19.7 (d, $^3J_{C\text{-}F}$ = 7.6 Hz, *h*), 21.4 (*a*), 23.3 (d, $^3J_{C\text{-}F}$ = 6.7 Hz, *i*), 42.1 (d, $^2J_{C\text{-}F}$ = 19.1 Hz, *g*), 58.0 (*f*), 63.6 (d, $^2J_{C\text{-}F}$ = 21.9 Hz, *k*), 101.1 (d, $^1J_{C\text{-}F}$ = 189.8 Hz, *j*), 127.9 (*c/d*), 130.0 (*c/d*), 139.2 (*b/e*), 143.1 (*b/e*); **^{19}F {^{1}H} NMR (377 MHz, C_6D_6)** δ = -192.61; **IR (CH_2Cl_2)**: **ν =** 2945, 2868, 1470, 1265, 1156, 739; **HRMS (ESI$^+$):** *m/z* required for $C_{23}H_{40}FNO_2SSiNa^+$ ($[M+Na]^+$): 464.2425, found 464.2413, Δ = 2.7 ppm. *Identifiable data for minor anti diastereoisomer:* **^{19}F {^{1}H} NMR (377 MHz, $CDCl_3$)** δ = -197.73.

The structure was unambiguously confirmed NOESY/HOESY experiments.

***Syn*-4-fluoro-3,3-dimethyl-1-tosyl-5-((triisopropylsilyl)methyl)pyrrolidin-2-one (144):**

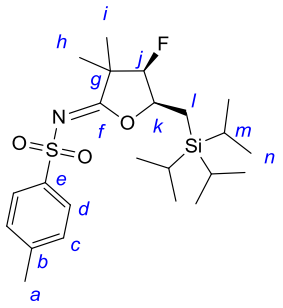

Following the general procedure D on 100 mg (0.23 mmol, 1 eq.) of *(E)*-**131**, the reaction yielded 32 mg of *syn*-**144** (31%, d.r. *(syn:anti)* 7:1) as a white solid.

Data for the major syn diastereoisomer: **R_f** = 0.1 (hexane/Et_2O 7:3); **m.p. =** 73 °C; **^{1}H NMR (400 MHz, $CDCl_3$)** δ = 1.04-1.09 (m, 21H, *m+n*), 1.13-1.20 (m, 1H, *l*), 1.27 (s, 3H, *h*), 1.28 (d, 3H, $^4J_{H\text{-}F}$ = 2.8 Hz, *i*), 1.29-1.36 (m, 1H, *l'*), 2.41 (s, 3H, *a*), 4.53 (dd, 1H, $^2J_{H\text{-}F}$ = 52.5 Hz, $^3J_{H\text{-}H}$ = 2.5 Hz, *j*), 4.97 (dddd, 1H, $^3J_{H\text{-}F}$ = 25.5 Hz, $^3J_{H\text{-}H}$ = 8.8, 5.8, 2.5 Hz, *k*), 7.27 (d, 2H, $^3J_{H\text{-}H}$ = 8.1 Hz, *c/d*), 7.84 (d, 2H, $^3J_{H\text{-}H}$ = 8.1 Hz, *c/d*); **^{13}C NMR (100 MHz, $CDCl_3$)** δ = 8.96 (d, $^3J_{C\text{-}F}$ = 8.0 Hz, *l*), 11.2 (*m*), 18.2 (d, $^3J_{C\text{-}F}$ = 10.4 Hz, *i*), 18.5 (*n*), 18.7 (*n'*), 21.4 (*a*), 23.3 (d, $^3J_{C\text{-}F}$ = 5.6 Hz, *h*), 49.4 (d, $^2J_{C\text{-}F}$ = 20.0 Hz, *g*), 86.2 (d, $^2J_{C\text{-}F}$ = 23.2 Hz, *k*), 96.0 (d, $^1J_{C\text{-}F}$ = 194.1 Hz, *j*), 127.2 (*c/d*), 129.1 (*c/d*), 138.6 (*b/e*), 143.1 (*b/e*), 176.7 (*f*); **^{19}F {^{1}H} NMR (377 MHz, $CDCl_3$)** δ = -197.27; **IR (KBr)**: **ν =** 2944, 2866, 1632, 1313, 1155, 827, 660; **HRMS (ESI^+):** *m/z* required for $C_{23}H_{38}FNO_3SSiNa^+$ ($[M+Na]^+$): 478.2209, found 478.2218, Δ = 1.8 ppm. *Identifiable data for the minor anti diastereoisomer:* **^{19}F {^{1}H} NMR (377 MHz, $CDCl_3$)** δ = -179.12;

The structure was unambiguously confirmed NOESY/HOESY experiments.

***Syn-tert*-butyl-3-fluoro-2-((triisopropylsilyl)methyl)pyrrolidine-1-carboxylate (129):**

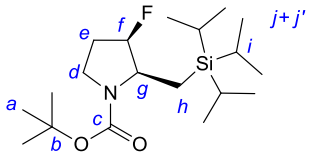

Following the general procedure D on 100 mg (0.29 mmol) of *(E)*-**121**, the reaction yielded after purification by flash column chromatography on silica gel, 56 mg of *syn*-**129** (54%, d.r. (*syn:anti*) 5:1) as a colourless oil, with 27 mg (43%) of the corresponding allylic fluoride **61**.

Data for the major syn diastereoisomer: **R_f** =0.6 (hexane/Et_2O: 9/1); **^{1}H NMR (500 MHz, $CDCl_3$)** δ = 1.08 (m, 23H, *h+i+j*), 1.48 (s, 9H, *a*), 1.88 (ddddd, 1H, $^3J_{H-F}$ = 39.1 Hz, $^3J_{H-H}$ = 11.3, 11.0, 8.5, 3.8 Hz, *e*), 2.09, (m, 1H, *e'*), 3.40 (ddd, 1H, $^2J_{H-H}$ = 17.0 Hz, $^3J_{H-H}$ = 11.1, 6.0 Hz, *d*), 3.71 (m, 1H, *d'*), 4.01 (m, 1H, *g*), 5.04 (ddt, 1H, $^2J_{H-F}$ = 52.9 Hz, $^3J_{H-H}$ = 6.9, 3.7 Hz, *f*); **^{13}C NMR (125 MHz, $CDCl_3$)** δ = 11.6 (*i*), 18.7 (*j/h*), 18.9 (*i/j*), 28.6 (*a*), 31.3 (d, $^2J_{C-F}$ = 21.0 Hz, *e*), 44.0 (*d*), 59.4 (d, $^2J_{C-F}$ = 20 Hz, *g*), 79.7 (*b*), 94.2 (d, $^1J_{C-F}$ = 173.7 Hz, *f*), 154.5 (*c*); **^{19}F {^{1}H} NMR (377 MHz, $CDCl_3$)** δ = -188.0; **IR (DCM)**: **ν =** 2800, 1715, 1352; **HRMS (CI^+):** *m/z* required for $C_{21}H_{37}FNO_2SSi$ ($[M+H]^+$): 360.2730, found: 360.2734, Δ = 1.1 ppm. *Identifiable data for the minor anti diastereoisomer:* **^{19}F {^{1}H} NMR (371 MHz, $CDCl_3$)** δ = -172.7.

The structure was unambiguously confirmed NOESY/HOESY experiments.

References CHAPTER 1

[1] a) R. D. Chambers, *Fluorine in Organic Chemistry*, G. Olah, 2nd ed., Blackwell Publishing Ltd., Oxford, **2004**; b) R. E. Banks, *Preparation, Properties and Industrial Applications of Organofluorine Compounds*, Ellis Horwood Ltd, John Wiley and Sons, **1982**; c) R. E. Banks, D. W. A. Sharp, J. C. Tatlow, *Fluorine – The First Hundred Years (1886-1986)*, Elsevier Sequoia, New York, **1986**; d) G. A. Olah, R. D. Chambers, G. K. Surya Prakash, *Synthetic Fluorine Chemistry*, Wiley, New York, **1992**; e) P. Kirsch, *Modern Fluoroorganic Chemistry: Synthesis, Reactivity, Applications*, WILEY-VCH, Weinheim, **2004**; f) I. Ojima, *Fluorine in Medicinal Chemistry and Chemical Biology*, Wiley-Blackwell Publishing, **2009**; g) T. Hiyama, *Organofluorine Compounds: Chemistry and Applications*, Springer, Berlin, **2000**; h) Special edition on organofluorine chemistry: *Chem. Rev.* **1996**, *96*, 1557–1823; i) J.-P. Bégué, D. Bonnet-Delpon, *Bioorganic and Medicinal Chemistry of Fluorine*, John Wiley & Sons, **2008**; j) K. Uneyama, *Organofluorine Chemistry*, Blackwell Publising Ltd, Oxford, **2006**.

[2] a) D. O'Hagan, D. B. Harper *J. Fluorine Chem.* **1999**, *100*, 127-133; b) D. B. Harper, D. O'Hagan, *Nat. Prod. Rep.* **1994**, *11*, 123-133.

[3] a) H. Moissan, *C. R. Acad. Sci.* **1886**, *102*, 1534; b) H. Moissan, *C. R. Acad. Sci.* **1886**, *103*, 202; c) H. Moissan, *C. R. Acad. Sci.* **1886**, *103*, 256.

[4] L. Hunter, *Beilstein J. Org. Chem.* **2010**, *6*, No. 38.

[5] W. R. Dolbier Jr., *Guide to Fluorine NMR for Organic Chemists*, John Wiley & Sons, **2009**,

[6] S. E. Snyder, M. R. Kilbourn, Chemistry of fluorine-18 radiopharmaceuticals, in *Handbook of Radiopharmaceuticals*, John Wiley & Sons, **2003**.

[7] D. O'Hagan, *Chem. Soc. Rev.* **2008**, *37*, 308-319.

[8] L. Pauling, *The Nature of the Chemical Bond and the Structure of Molecules and Crystals: An Introduction to Modern Structural Chemistry*, Cornell University Press, Ithaca, NY, **1939**; D. R. Lide, *Handbook of Chemistry and Physics*, 86th edn., CRC Press, NY, **2005**.

[9] a) B. E. Smart, *J. Fluorine Chem.* **2001**, *109*, 3-11; b) D. R. Linde, *Handbook of Chemistry and Physics*, 86th edn., CRC Press, New York, **2005**.

[10] A. Bondi, *J. Phys. Chem.* **1968**, *68*, 441-451.

[11] a) K. B. Wiberg, P. R. Rablen, *J. Am. Chem. Soc.* **1993**, *115*, 614-625; K. Wiberg, *Acc. Chem. Res.* **1996**, *29*, 229-234.

[12] A) B. E. Smart, in *Properties of Fluorinated Organic Compounds*, ACS Monograph 187, ACS, Washington DC, **1995**, *Vol. 1*, 979; b) J. A. Dean, Lange's Handbook of Chemistry, 15th edn., McGraw-Hill, New York, 1999; c) B. E. Smart, in *Molecular Structure and Energetics*, J. F. Liebman and A. Greenberg Eds., VCH Publishers, Deerfield Beach, FL, **1986**, *Vol. 3*, Chap. 4.

[13] a) J. C. Biffinger, H. W. Kim, S. G. DiMagno, *ChemBioChem*, **2004**, *5*, 622-627; S. G. DiMagno, H. Sun, *Curr. Top. Med. Chem.* **2006**, *6*, 1473-1482.

[14] a) I. A. Koppel, R. W. Taft, F. Anvia, S. Z. Zhu, L. Q. Hu, K. S. Sung, D. D. DesMarteaux, L. M. Yagupolskii, Y. L. Yagupolskii, V. M. Vlasov, R. Notario, P. C. Maria, *J. Am. Chem. Soc.* **1994**, *116*, 3047; b) H. J. Castejon, K. B. Wiberg, *J. Org. Chem.* **1998**, *63*, 3937; c) M. H. Abraham, P. L. Grellier, D. V. Prior, J. J. Morris, P. J. Taylor, *J. Chem. Soc. Perkin Trans.* **1990**, 521.

[15] a) A. D. Williams, P. R. Le Breton, J. L. Beauchamp, *J. Am. Chem. Soc.* **1976**, *98*, 2705; b) A. D. Allen, T. T. Tidwell, in *Advances in Carbocation Chemistry*, X. Creary, Ed., JAI Press, Greenwich, CT, **1989**, Chap. 1.

[16] X. Creary, *Chem. Rev.* **1991**, *91*, 1625.

[17] W. R. Dolbier, *Chem. Rev.* **1996**, *96*, 1558.

[18] S. A. Harrell, D. H. McDaniel, *J. Am. Chem. Soc.* **1964**, *86*, 4497.

[19] J. A. K. Howard, V. J. Hoy, D. O'Hagan, G. T. Smith, *Tetrahedron*, **1996**, *52*, 12613-12622.

[20] N. E. J. Gooseman, D. O'Hagan, M. J. G. Peach, A. M. Z. Slawin, D. J. Tozer, R. J. Young, *Angew. Chem. Int. Ed.* **2007**, *46*, 5904-5908.

[21] J. D. Dunitz, R. Taylor, *Chem-Eur. J.* **1997**, *3*, 89-98.

[22] W. Caminati, S. Melandri, A. O. Maris, P. Ottaviani, *Angew. Chem. Int. Ed.* **2006**, *46*, 2438.

[23] E. Carosati, S. Sciabola, G. Cruciani, *J. Med. Chem.* **2004**, *47*, 5114-5125.

[24] J. W. Banks, A. S. Batsanov, J. A. K. Howard, D. O'Hagan, H. S. Rzeppa, S. Martin-Santamaria, *J. Chem. Soc., Perkin Trans. 2*, **1999**, 2409-2051.

[25] a) B. J. van der Veken, S. Truyen, W. A. Herrebout, G. Watkins, *J. Mol. Struct.* **1993**, *293*, 55-58; b) R. J. Abraham, A. D. Jones, M. A. Warne, R. Rittner, C. F. Tormena, *J. Chem. Soc., Perkin Trans 2*, **1996**, 533-539; c) H. V. Phan, J. R. Durig, *THEOCHEM*, **1990**, *209*, 333-347.

[26] A. M. Sum, D. C. Lankin, K. Hardcastle, J. P. Snyder, *Chem-Eur. J.* **2005**, *11*, 1579-1591.

[27] C. R. S. Briggs, M. J. Allen, D. O'Hagan, D. J. Tozer, A. M. Z. Slawin, A. E. Goeta, J. A. K. Howard, *Org. Biomol. Chem.* **2004**, *2*, 732-740.

[28] N. E. J. Gooseman, D. O'Hagan, A. M. Z. Slawin, A. M. Teale, D. J. Tozer, R. J. Young, *Chem. Commun.* **2006**, 3190-3192.

[29] D. Majumdar, S. Guha, *J. Mol. Struct. THEOCHEM*, **1988**, *180*, 125-140.

[30] a) G. Deniau, A. M. Z. Slawin, T. Lebl, F. Chorki, J. P. Issberner, T. van Mourik, J. M. Heygate, J. J. Lambert, L.-A. Etherington, K. T. Sillar, D. O'Hagan, *ChemBioChem* **2007**, *8*, 2265-2274 ; b) M. D. Clift, H. Ji, G. P. Deniau, D. O'Hagan, R. B. Silverman, *Biochemistry* **2007,** *46*, 13819-13828.

[31] M. L. Trapp, J. K. Watts, N. Weinberg, B. M. Pinto, *Can. J. Chem.* **2006**, *84*, 692-701.

[32] I. V. Alabugin, K. M. Gilmore, P.W. Peterson, *WIREs Comput. Mol. Sci*. **2011**, *1*, 109-141.

[33] P. Klaboe, J. R. Nielsen, *J. Chem. Phys*. **1960**, *33*, 1764-1774.

[34] T. Hirano, S. Nonoyama, T. Miyajima, Y. Kurita, T. Kawamura, H. Sato, *J. Chem. Soc., Chem. Commun*. **1986**, 606-607.

[35] L. Fernholt, K. Kveseth, *J. Am. Chem. Soc.* **1980**, *102*, 3987-3994.

[36] a) D. A. Dixon, N. Matsuzawa, S. C. Walker, *J. Phys. Chem.* **1992**, *96*, 10740-10746; b) K. B. Wiberg, T. A. Keith, M. J. Frisch, M. Murcko, *J. Phys. Chem.* **1995**, *99*, 9072-9079.

[37] a) K. Hagen, K. Hedberg, *J. Am. Chem. Soc.* **1973**, *95*, 8263-8266; b) J.-F. Huang, K. Hedberg, *J. Am. Chem. Soc*. **1989**, *111*, 6909-6913; c) S. M. Chitale, C. I. Jose, *J. Chem. Soc., Faraday Trans. 1*, **1986**, *82*, 663-679.

[38] a) J. M. Bakke, L. H. Bjerkeseth, T. E. C. L. Rønnow, K. Steinsvoll, *J. Mol. Struct.* **1994**, *321*, 205-214; b) Y. Hoppilliard, D. Solgadi, *Tetrahedron*, **1980**, *36*, 377-380.

[39] P. R. Rablen, R. W. Hoffmann, D. A. Hrovat, W. T. Borden, *J. Chem. Soc., Perkin Trans. 2*, **1999**, 1719-1726.

[40] C. R. Briggs, D. O'Hagan,H. S. Rzepa, A. M. Z. Slawin, *J. Fluorine Chem.* **2004**, *125*, 19-25.

[41] D. O'Hagan, C. Bilton, J. A. K. Howard, L. Knight, D. J. Tozer, *J. Chem. Soc., Perkin Trans. 2*, **2000**, *125*, 605-607.

[42] K. B. Wiberg, M. A. Murcko, K. E. Laidig, P. J. MacDougall, *J. Phys. Chem.* **1990**, *94*, 6956-6969.

[43] L. Goodman, H. Gu, V. Pophristic, *J. Phys. Chem. A*, **2005**, *109*, 1223-1229.

[44] D. Wu, A. Tian, H. Sun, *J. Phys. Chem. A*, **1998**, *102*, 9901-9905.

[45] L. Hunter, D. O'Hagan, *Org. Biomol. Chem.* **2008**, *6*, 2843-2848.

[46] L. Hunter, P. Kirsch, A. M. Z. Slawin, D. O'Hagan, *Angew. Chem. Int. Ed.* **2009**, *48*, 5457-5460.

[47] M. E. Nimni, *Collagen*, CRC Press: Boca Raton, FL, **1988**, Vols. 1-4; G. N. Ramachandran, A. H. Reddi, *Biochemistry of Collagen*, Plenum Press: New York, **1976**.

[48] B. Brodsky, N. K. Shah, *FASEB*, **1995**, *J. 9*, 1537-1546.

[49] E. Suzuki, R. D. B. Fraser, T. P. MacRae, *Int. J. Biol. Macromol.* **1980**, *2*, 54-56.

[50] S. K. Holmgren, K. M. Taylor, L. E. Bretscher, R. T. Raines, *Nature*, **1998**, *392*, 666-667.

[51] E. S. Eberhardt, N. Panasik Jr., R. T. Raines, *J. Am. Chem. Soc*, **1996**, *118*, 2261; S. K. Holmgren, L. E. Bretscher, K. M. Taylor, R. T. Raines, *Chem. Biol*. **1999**, *6*, 63; L. E. Bretscher, C. L. Jenkins, K. M. Taylor, M. L. DeRider, R. T. Raines, *J. Am. Chem. Soc*. **2001**, *123*, 777; N. Panasik Jr., E. S. Eberhardt, A. S. Edison, D. R. Powell, R. T. Raines, *Int. J. Pept. Protein Res.* **1994**, *44*, 262-269.

[52] G. Némethy, K. D. Gibson, K. A. Palmer, C. N. Yoon, G. Paterlini, A. Zagari, S. Rumsey, H. A. Scheraga, *J. Phys. Chem.* **1992**, *96*, 6472.

[53] M. L. DeRider, S. J. Wilkens, M. J. Waddell, L. E. Bretscher, F. Weinhold, R. T. Raines, *J. Am. Chem. Soc.* **2002**, *124*, 2497-2505; R. Importa, C. Benzi, V. Barone, *J. Am. Chem. Soc*. **2001**, *123*, 12568-12577.

[54] P. H. Maccallum, R. Poet, E. J. Milner-White, *J. Mol. Biol.* **1995**, *248*, 374-384.

[55] M. D. Shoulders, R.T. Raines, *J. Biol. Chem*. **2011**, *286*, 22905–22912.

[56] K. L. Kirk, *Fluorinated Five-Membered Nitrogen-Containing Heterocycles*, in *Fluorinated Heterocyclic Compounds: Synthesis, Chemistry, and Applications*, V. A. Petrov, John Wiley and Sons, **2009**.

[57] L. E. Zimmer, C. Sparr, R. Gilmour, *Angew. Chem. Int. Ed.* **2011**, *50*, 11860-11871.

[58] D. W. C. MacMillan, *Nature*, **2008**, *455*, 304-308.

[59] C. Sparr, E. Salamanova, W. B. Schweizer, H. M. Senn, R. Gilmour, *Chem. Eur. J*. **2011**, *17*, 8850-8857.

[60] C. Sparr, W. B. Schweizer, H. M. Senn, R. Gilmour, *Angew. Chem. Int. Ed.* **2009**, *48*, 3065-3068.

[61] F. Goosens, G. VanHoof, I. De Meester, K. Augustyns, M. Borloo, D. Tourwe, A. Haemers, S. Scharpé, *Eur. J. Biochem*. **1997**, *250*, 177-183.

[62] B. D. Green, P. R. Flatt, C. J. Bailey, *Diabetes Vasc. Dis. Res.* **2006**, *3*, 159-165; E. Sebokova, A. D Christ, M. Boehringer, J. Mizrahi, *Curr. Top. Med. Chem.* **2007**, *7*, 547-555.

[63] T. W. von Geldern, J. M. Trevillyan, *Drug Dev. Res.* **2006**, *67*, 627-642.

[64] S. D. Edmondson, A. Mastracchio, R. J. Mathvink, J. He, B. Harper, Y.-J. Park, M. Beconi, J. Di Salvo, G. J. Eiermann, H. He, B. Leiting, J. F. Leone, D. A. Levorse, K. Lyons, R. A. Patel, S. B. Patel, A. Petrov, G. Scapin, J. Shang, R. S. Roy, A. Smith, J. K. Wu, S. Xu, B. Zhu, N. A. Thornberry, A. E. Weber, *J. Med. Chem.* **2006**, *49*, 3614-3627.

[65] J. Xu, L. Wei, R. J. Mathvink, S. D. Edmondson, G. J. Eiermann, H. He, J. F. Leone, B. Leiting, K. A. Lyons, F. Marsilio, R. A. Patel, S. B. Patel, A. Petrov, G. Scapin, J. K. Wu, N. A. Thornberry, A. E. Weber, *Bioorg, Med. Chem. Lett.* **2006**, *16*, 5373-5377.

[66] C. G. Caldwell, P. Chen, J. He, E. R. Parmee, B. Leiting, F. Marsilio, R. A. Patel, J. K. Wu, G. J. Eiermann, A. Petrov, H. He, K. A. Lyons, N. A. Thornberry, A. E. Weber, *Bioorg. Med. Chem. Lett.* **2004**, *14*, 1265-1268.

[67] B. Hulin, S. Cabral, M. G. Lopaze, M. A. Van Volkenburg, K. M. Andrews, J. C. Parker, *Bioorg. Med. Chem. Lett.* **2005**, *15*, 4770-4773.

[68] C. D. Haffner, D. L. McDougald, S. M. Reister, B. D. Thompson, C. Conlee, J. Fang, J. Bass, J. M. Lenhard, D. Croom, M. B. Secosky-Chang, T. Tomaszek, D. McConn, K. Wells-Knecht, P. R. Johnson, *Bioorg. Med. Chem. Lett.* **2005**, *15*, 5257-5261.

[69] D. E. Patterson, J. D. Powers, M. LeBlanc, T. Sharkey, E. Boehler, E. Irdam, M. H. Osterhout, *Org. Process Res. Dev*. **2009**, *13*, 900–906.

[70] G. Giardina, G. Dondio, M. Grugni, *Synlett*, **1995**, 55-57.

[71] R. P. Singh, J. M. Shreeve, *J. Fluorine Chem.* **2002**, *116*, 23-26.

[72] A. G. Avent, A. N. Bowler, P. M. Doyle, C. M. Marchand, D. W. Young, *Tetrahedron Lett.* **1992**, *33*, 1509-1512.

[73] R. P. Singh, J. M. Shreeve, *Acc. Chem. Res.* **2004,** *37*, 31-44

[74] L. Demange, A. Ménez, C. Dugave, *Tetrahedron Lett.* **1998**, *39*, 1169-1172.

[75] T. Ayad, Y. Génisson, S. Broussy, M. Baltas, L. Gorrichon, *Eur. J. Org. Chem.* **2003**, 2903-2910.

[76] O. Schwardt, U. Veith, C. Gaspard, V. Jäger, *Synthesis* **1999**,1473-1490 and references cited therein.

[77] a) S. Bruns, G. Haufe, *J. Fluorine Chem.* **2000**, *104*, 247-254; b) G. Haufe, S. Bruns, M. Runge, *J. Fluorine Chem.* **2001**, *112*, 55-61; c) G. Haufe, S. Bruns, *Adv. Synth. Catal.* **2002**, *344*, 165-171.

[78] J. A. Kalow, A. G. Doyle, *J. Am. Chem. Soc.* **2010**, *132*, 3268-3269.

[79] B. Drouillat, F. Couty, O. David, G. Evano, J. Marrot, Synlett, 2008, 9, 1345-1348.

[80] I. Déchamps, D. Gomez Pardo, J. Cossy, *Synlett*, **2007**, *2*, 263-267 ; I. Déchamps, D. Gomez Pardo, J. Cossy, *Eur. J. Org. Chem.* **2007**, 4224-4234.

[81] B. F. Bonini, F. Boschi, M. C. Franchini, M. Fochi, F. Fini, A. Mazzanti, A. Ricci, *Synlett*, **2006**, *4*, 543-546.

[82] H. Inagaki, S. Miyauchi, R. N. Miyauchi, H. C. Kawato, H. Ohki, N. Matsuhashi, K. Kawakami, H. Takahashi, M. Takemura, *J. Med. Chem.* **2003**, *46*, 1005-1015.

References CHAPTER 2

[83] F. A. Carey, R. J. Sunberg, *Polar Addition and Elimination Reaction*, in *Advanced Organic Chemistry – Part A: Structure and Mechanism*, 5th ed. Springer, **2007**.

[84] S. Fukuzumi, J. K. Kochi, *J. Am. Chem. Soc.* **1982**, *104*, 7599; G. Belluci, R. Bianchi, R. Ambrosetti, *J. Am. Chem. Soc.* **1985**, *107*, 2464.

[85] M.-F. Ruasse, A. Argile, J. E. Dubois, *J. Am. Chem. Soc.* **1978**, *100*, 7645.

[86] For bromonium ion : G. A. Olah, P. Schilling, P. W. Westerman, H. C. Lin, *J. Am. Chem. Soc.* **1974**, *96*, 3581; R. S. Brown, *Acc. Chem. Rev.* **1997**, *30*, 131; G. Belluci, R. Bianichini, C. Chiappe, F. Marioni, R. Ambrosetti, R. S. Brown, H. Slebocka-Tilk, *J. Am. Chem. Soc.* **1989**, *111*, 2640; G. Belluci, C. Chiappe, R. Bianchini, D. Lenoir, R. Herges, *J. Am. Chem. Soc.***1995**, *117*, 12001; H. Slebocka-Tilk, R. G. Ball, R. S. Brown, *J. Am. Chem. Soc.***1985**, *107*, 4504; For iodonium and chloronium ions: R. S. Brown, R. W. Nagorski, A. J. Bennet, R. E. D. McClung, G.H. M. Aarts, M. Klobukowski, R. McDonald, B. D. Santarisiero, *J. Am. Chem. Soc.***1994**, *116*, 2448.

[87] J. R. Chretien, J.-D. Coudert, M.-F. Ruasse, J. Org. Chem. 1993, 58, 1917.

[88] J. H. Rolston, K. Yates, *J. Am. Chem. Soc.* **1969**, *91*, 1469-1476; J. H. Rolston, K. Yates, *J. Am. Chem. Soc.* **1969**, *91*, 1477-1483.

[89] K. Yates, H. W. Leung, *J. Org. Chem.* **1980**, *45*, 1401.

[90] R. Damrauer, M. D. Leavell, C. M. Hadad, *J. Org. Chem.* **1998**, *63*, 9476.

[91] W. J. Hehre, P. C. Hiberty, *J. Am. Chem. Soc.* **1974**, *96*, 2665; T. Iwaoka, C. Kaneko, A. Shigihara, H. Ichikawa, *J. Phys. Org. Chem.* **1993**, *6*, 195.

[92] S. Rozen, M. Brand, *J. Org. Chem.* **1986**, *51*, 3607; S. Rozen, *Acc. Chem. Res.* **1996**, *29*, 243.

[93] S. Rozen, O. Lerman, M. Kol, D. Hebel, *J. Org. Chem.* **1985**, *50*, 4753.

[94] S. G. Lal, G. P. Pez, R. G. Syvret, *Chem. Rev.* **1996**, *96*, 1737-1755; S. D. Taylor, C. C. Kotoris, G. Hum, *Tetrahedron*, **1999**, *55*, 12431-12477; R. P . Singh, J. M. Shreeve, *Acc. Chem. Rev.* **2004**, *37*, 31-44.

[95] G. S. Lal, *J. Org. Chem.* **1993**, *58*, 2791.

[96] D. D. DesMarteau, Z. Xu, M. Witz, *J. Org. Chem.* **1992**, *57*, 629.

[97] T. Umemoto, S. Fukami, G. Tomizawa, K. Harasawa, K. Kawada, K. Tomita, *J. Am. Chem. Soc.* **1990**, *112*, 8563-8575.

[98] S. Stavber, T. Sotler, M. Zupan, *Tetrahedron Lett.* **1994**, *35*, 1105.

[99] S. Stavber, T. Sotler Pecăn, M.Papež, M. Zupan, *Chem. Commun.* **1996**, 2247.

[100] S. Stavber, T. S. Pecan, M. Zupan, *Bull. Chem. Soc. Jpn.* **1996**, 169.

[101] I. Fleming, A. Barbero, D. Walter, *Chem. Rev.* **1997**, *97*, 2063-2192; C. E. Masse, J. S. Panek, *Chem. Rev.* **1995**, *95*, 1293-1316; L. Chabaud, P. James, Y. Landais, *Eur. J. Org. Chem.* **2004**, 3173-3199.

[102] J. B. Lambert, Y. Zhao, R. W. Emblidge, L. A. Salvador, X. Liu, J-H. So, E. C. Chelius, *Acc. Chem. Res.* **1999**, *32*, 183-190; J. B. Lambert, *Tetrahedron*, **1990**, *46*, 2677-2689.

[103] S. D. Kahn, C. F. Pau, A. R. Chamberlin, W. J. Hehre, *J. Am. Chem. Soc.* **1987**, *109*, 650; H. Mayr, G. Hagen, *J. Chem. Soc., Chem. Commun.* **1989**, 91-92.

[104] H. Mayr, R. Pock, *Tetrahedron*, **1986**, *42*, 4211-4214.

[105] Y. Apeloig, M. Karni, A. Stangar, H. Schwarz, T. Drewello, G. Czukay, *J. Chem. Soc., Chem. Commun.* **1987**, 989-990.

[106] S. E. Wierschke, J. Chandrasekhar, W. L. Jorgensen, *J. Am. Chem. Soc.* **1985**, *107*, 1496-1500.

[107] S. Thibaudeau, V. Gouverneur**,** *Org. Lett.* **2003,** *5*,4891-4893.

[108] M. Tredwell, K.Tenza, M. C. Pacheco, V. Gouverneur, *Org. Lett.* **2005,** *7*, 4495-4497.

[109] M. Sawicki, A. Kwok, M. Tredwell, V. Gouverneur, *Beil. J. Org. Chem.* **2007**, *3*, 34-38.

[110] G. T. Giuffredi, S. Purser, M. Sawicki, A. L. Thompson, V. Gouverneur, *Tetrahedron: Asymmetry* **2009**, *20*, 910-920.

[111] S. Purser, C. Wilson, P. R. Moore, V. Gouverneur, *Synlett* **2007**, *7*, 1166-1168.

[112] S. Purser, B. Odell, T. D. W. Claridge, P. R. Moore, V. Gouverneur, *Chem. Eur. J.* **2006**, *12*, 9176-9185.

[113] Y.-h. Lam, C. Bobbio, I. R. Cooper, V. Gouverneur, *Angew. Chem. Int. Ed.* **2007**, *46*, 5106-5110.

[114] Y.-h. Lam, M. N. Hopkinson, S. J. Stanway, V. Gouverneur, *Synlett* **2007**, *19*, 3022-3027.

[115] B. Greedy, J.-M. Paris, T. Vidal, V. Gouverneur, *Angew. Chem. Int. Ed.* **2003**, *42*, 3291-3294.

[116] T. Ishimaru, N. Shibata, T. Horikawa, N.Yasuda, S. Nakamura,T. Toru, M. Shiro, *Angew. Chem. Int. Ed.* **2008**, *47*, 4157-4161.

[117] H. Teare, F. Huguet, M. Tredwell, S. Thibaudeau, S. Luthra, V. Gouverneur, *Arkivoc*, **2007**, 232-244.

[118] G. Giuffredi, C. Bobbio, V. Gouverneur, *J. Org. Chem.* **2006**, *71*, 5361-5364.

[119] A. N. French, S. Bissmire, T. Wirth, *Chem. Soc. Rev*. **2004**, *33*, 354-362.

[120] J. E. Baldwin, *J. Chem. Soc.*, *Chem. Commun.* **1976**, 734; J. E. Baldwin, *J. Chem. Soc.*, *Chem. Commun.*, **1976**, 738; J. E. Baldwin, J. Cutting, W. Dupont, L. Kruse, L. Silberman, R. C. Thomas, *J. Chem. Soc.*, *Chem. Commun.*, **1976**, 736.

[121] R. G. Bernett, J. T. Doi and W. K. Musker, *J. Org. Chem.*, **1985**, *50*, 2048-2050.

[122] P. A. Bartlett, J. Myerson, *J. Am. Chem. Soc*. **1978**, *100*, 3950-3952

[123] G. Cardillo, M. Orena, *Tetrahedron*, **1990**, *46*, 3321-3408.

[124] Y. Tamaru, M. Hojo, S. Kawamura, S. Sawada, Z. Yoshida, *J. Org. Chem.* **1987**, *52*, 4062-4072.

[125] Y. Tamaru, S. Kawamura, T. Bando, K. Tanaka, M. Hojo, Z. Yoshida, *J. Org. Chem.* **1988**, *53*, 5491-501.

[126] A. R. Chambedin, R. L. Mulholland, Jr., S. D. Kahn, W. J. Hehre, *J. Am. Chem. Soc.* **1987**, *109*, 672-677.

[127] M. Labelle, Y. Guindon, *J. Am. Chem. Soc.* **1989**, *111*, 2204-2210.

[128] M. Tredwell, J. A. R. Luft, M. Schuler, K. Tenza, K. N. Houk, V. Gouverneur, *Angew. Chem. Int. Ed.* **2008**, *47*, 357-360.

[129] D. Bourgeois, A. Pancrazi, S. P. Nolan, J. Prunet, *J. Organomet. Chem.* **2002**, *643-644*, 247-252.

[130] S. H. Hong, D. P. Sanders, C. W. Lee, R. H. Grubbs, *J. Am. Chem. Soc.* **2005**, *127*, 17160-17161.

[131] A. K. Chatterjee, R. H. Grubbs, *Org. Lett.* **1999**, *1*, 1751-1753.

[132] M. Tredwell, *DPhil Thesis, University of Oxford*, **2007**.

[133] A. Fürstner, K. Langemann, *J. Am. Chem. Soc.* **1997**, *119*, 9130-9136; A. K. Ghosh, J. Cappiello, D. Shin, *Tetrahedron Lett.* **1998**, *39*, 4651-4654; A. Fürstner, O. R. Thiel, C. W. Lehmann, *Organometallics*, **2001**, *21*, 331-335.

[134] A. J. Biloski, R. D. Wood and B. Ganem, *J. Am. Chem. Soc.*, **1982**, *104*, 3233-3225.

[135] M. Morgenthaler, E. Schweizer, A. Hoffmann-Roder, F. Benini, R. E. Martin, G. Jaeschke, B. Wagner, H. Fischer, S. Bendels, D. Zimmerli, J. Schneider, F. Diederich, M. Kansy, K. Muller, *ChemMedChem* **2007**, *2*, 1100-1115.

[136] S. Knapp, A. T. Levorse, *J. Org. Chem.* **1988**, *53*, 4006-4014; S. Knapp, F. S. Gibson, *Org. Synth.* **1992**, *70*, 101; A. Bongini, G. Cardillo, M. Orena, S. Sandri, C. Tomasini, *J. Org. Chem.*, **1986**, *51*, 4905; A. Bongini, G. Cardillo, M. Orena, S. Sandri, C. Tomasini, *J. Chem. Soc., Perkin Trans. 1*, **1986**, 1339; M. J. Kurth, S. H. Bloom, *J. Org. Chem.*, **1989**, *54*, 411.

[137] M. Fujita, O. Kitagawa, T. Suzuki, T. Taguchi, *J. Org. Chem.* **1997**, *62*, 7330-7335.

[138] H. Takahata, T. Takamatsu, T. Yamazaki, *J. Org. Chem.* **1989**, *54*, 4812-4822; H. Takahata, T. Takamatsu, M. Mozumi, Y.-S. Chen, T. Yamazaki, K. Aoe, *J. Chem. Soc., Chem. Commun.* **1987**, 1627; H. Takahata, T. Suzuki, M. Maruyama, K. Moriyama, M. Mozumi, T. Takamatsu, T. Yamazaki, *Tetrahedron*, **1988**, *44*, 4777; S. Kano, T. Yokomatsu, H. Iwasawa, S. Shibuya, *Heterocycles*, **1987**, *26*, 359.

[139] A. D. Jones, D.W. Knight, A. L. Redfern, J. Gilmore, *Tetrahedron Lett.* **1999**, *40*, 3267-3270.

[140] A. D. Jones, D. W. Knight, D. E. Hibbs, *J. Chem. Soc., Perkin Trans. 1*, **2001**, 1182-1203; A. D. Jones, David W. Knight, *Chem. Commun.*, **1996,** 915-916; M. C. Marcotullio, V. Campagna, S. Sternativo, F. Costantino, M. Curini, *Synthesis*, **2006**, *16*, 2760–2766.

[141] W. S. Lee, K. C. Jang, J. H. Kim, K. H. Park, *Chem. Commun.* **1999**, 251-252.

[142] S. P. Bew, J. M. Barks, D. W. Knight, R. J. Middleton, *Tetrahedron Lett.* **2000**, *41*, 4447-4451.

[143] a) Donohoe, T. J.; Bataille, C. J. R.; Churchill, G. H. *Annu. Rep. Prog. Chem. Sect. B* **2006**, *102*, 98-122; b) Liddell, J. R. *Nat. Prod. Rep*. **2002**, *19*, 773-781; c) Enders, D.; Thiebes, T. *Pure Appl. Chem*. **2001**, *73*, 573-578; d) O'Hagan, D. *Nat. Prod. Rep*. **2000**, *17*, 435-446; e) Michael, J. P. *Nat. Prod. Rep*. **2000**, *17*, 579-602; f) Saxton, J. E. *Nat. Prod. Rep*. **1997**, *14*, 559-590.

[144] Giese, B. *Angew. Chem. Int. Ed*. **1985**, *97*, 553-65.

[145] a) Suarez, R. M.; Sestelo, J. P.; Sarandeses, L. A. *Synlett* **2002**, 1435-1438; b) Luche, J. L.; Allavena, C.; Petrier, C.; Dupuy, C. *Tetrahedron Lett*. **1988**, *29*, 5373-4; c) Luche, J. L.; Allavena, C.; Petrier, C.; Dupuy, C. *Tetrahedron Lett*. **1988**, *29*, 5373-4.

[146] For a comprehensive compilation of Bordwell pKa data see:

http://www.chem.wisc.edu/areas/reich/pkatable/index.htm

[147] a) C. Cox, T. Lectka, *J. Org. Chem.* **1998**, *63*, 2426-2427; b) M. J. Deetz, C. C. Forbes, M. Jonas, J. P. Malerich, B. D. Smith, O. Wiest, *J. Org. Chem.* **2002**, *67*, 3949-3952; c) M. Avalos, R. Babiano, J. L. Barneto, J. L. Bravo, P. Cintas, J. L. Jiménez, J. C. Palacios, *J. Org. Chem.* **2001**, *66*, 7275-7282 d) P. V. Bharatam, A. A. Gupta, D. Kaur, *Tetrahedron* **2002**, *58*, 1759-1764; e) J. Elguero, P. Goya, I. Rozas, J. Catalán, J. L. G. De Paz, *J. Mol. Struct. THEOCHEM*, **1989**, *184*, 115-129; f) R. D. Bindal, J. T. Golab, J. A. Katzenellenbogen, *J. Am. Chem. Soc.* **1990,** *112*, 7861-7868.

[148] D. Grée, L. Vallerie, R. Grée, L. Toupet, I. Washington, J.-P. Pelicier, M. Villacampa, J. M. Pérez, K. N. Houk, *J. Org. Chem.* **2001**, *66*, 2374-2381.

[149] R. S. Brown, R. W. Nagorski, A. J. Bennet, R. E. D. McClung, G. H. M. Aarts, M. Klobukowski, R. McDonald, B. D. Santarsiero, *J. Am. Chem. Soc.* **1994**, *116*, 2448.

[150] A. R. Chamberlin, M. Dezube, P. Dussault, *Tetrahedron Lett.* **1981**, *22*, 4611-4614 ; A. R. Chamberlin, M. Dezube, P. Dussault, M. C. McMills, *J. Am. Chem. Soc.* **1983**, *105*, 5819-5825.

[151] K. N. Houk, S. R. Moses, Y-D. Wu, N. G. Rondan, V. Jäger, R. Schohe, F. R. Fronczek, *J. Am. Chem. Soc.* **1984**, *106*, 3880-3882.

[152] S. C. Wilkinson, R. Salmon, V. Gouverneur, *Future Med. Chem.* **2009**, *1*, 847-863.

[153] P. C. Ting, P. A. Bartlett, *J. Am. Chem. Soc.* **1984,** *106*, 2668-2671.

[154] G. Adiwidjaja, H. Flörke, A. Kirshning, E. Schaumann, *Liebigs Ann.* **1995**, 501-507.

[155] A. Hosomi, H. Sakurai, *Tetrahedron Lett.* **1976**, *16*, 1295-1298.

[156] H.-J. Knölker, N. Foitzik, H. Goesmann, R. Graf, *Angew. Chem. Int. Ed.* **1993**, *32*, 1081-1083; M. D. Groaning, G. P. Brengel, A. I. Meyers, *J. Org. Chem.* **1998,** *63*, 5517-5522; Z.-H. Peng, K. A. Woerpel, *Org. Lett.* **2000**, *2*, 1379-1381.

[157] S. C. Wilkinson, O. Lozano, M. Schuler, M. Pacheco, R. Salmon, V. Gouverneur, *Angew. Chem. Int. Ed.* **2009**, *48*, 7083-7086.

[158] a) K. Tamao, *Adv. Silicon Chem.* **1996**, *3*, 1-62; b) G. R. Jones, Y. Landais, *Tetrahedron* **1996**, *52*, 7599-7662; c) I. Fleming, R. Henning, D. C. Parker, H. E. Plaut, P. E. J. Sanderson, *J. Chem. Soc. Perkin Trans. 1* **1995**, 317-337; d) T. Akiyama, E. Hoshi, S. Fujiyoshi, *J. Chem. Soc. Perkin Trans. 1* **1998**, 2121-2122; e) I. Fleming, S. K. Ghosh, *J. Chem. Soc., Chem. Commun.* **1992**, 1775-1777.

[159] R. P. Singh, J. M. Shreeve, *Chem. Commun.* **2001**, 1196-1197.

[160] S. C. Wilkinson, *DPhil Thesis, University of Oxford*, **2009**.

[161] H. E. Blackwell, D. J. O'Leary, A. K. Chatterjee, R. A. Washenfelder, D. A. Bussmann, R. H. Grubbs, *J. Am. Chem. Soc.* **2000**, *122*, 58-71; F. C. Engelhardt, M. J. Schmitt, R. E. Taylor, *Org. Lett.* **2001**, *3*, 2209-2212.

[162] S. D. Kahn, C. F. Pau, W. J. Hehre, *J. Am. Chem. Soc.* **1986**, *108*, 7396-7398.

[163] R. W. Hoffmann, *Chem. Rev.* **1989**, *89*, 1841.

[164] A. D. Jones, D. W. Knight, D. E. Hibbs, *J. Chem. Soc., Perkin Trans. 1*, **2001**, 1182-1203; F. A. Davis, M. Song, A. Augustine, *J. Org. Chem.* **2006**, *71*, 2779-2786.

[165] M. J. C. Buckle, I. Fleming and S. Gil, *Tetrahedron Lett.*, **1992**, *33*, 4479-4482; M. J. C. Buckle, I. Fleming, S. Gil, K. L. C. Pang, *Org. Biomol. Chem.* **2004**, *2*, 749-769.

References CHAPTER 3

[166] W. R. Dolbier, Jr, *Guide to Fluorine NMR for Organic Chemists*, John Wiley & Sons, **2009**.

[167] Data taken from R. K. Harris, *NMR Spectroscopy: A Physicochemical View*, Pitman, London, **1983**.

[168] M. L. Martin, J.-J. Delpuech, G. J. Martin, *Practical NMR Spectroscopy*, Heyden, London, **1980**.

[169] J. W. Akitt, *NMR and Chemistry: An Introduction to the Fourier Transform-multinuclear era 2nd ed*. Chapman and Hall, London, **1983**.

[170] a) P. L. Rinaldi, *J. Am. Chem. Soc.* **1983**, *105*, 5167-5168; b) C. Yu, G. C. Levy, *J. Am. Chem. Soc.* **1984**, *106*, 6533-6537.

[171] J. Battiste, R. A. Newmark, *Prog. Nucl. Magn. Reson. Spectrosc.* **2006**, *48*, 1-23.

[172] P. Espinet, A. C. Albéniz, J. A. Casares, J. M. Martinez-Ilarduya, *Coord. Chem. Rev.* **2008**, *252*, 2180-2208.

[173] P. S. Pregosin, P. G. A. Kumar, I. Fernandez, *Chem. Rev.* **2005**, *105*, 2977-2998.

[174] M. Pellecchia, I. Bertini, D. Cowburn, C. Dalvit, E. Giralt, W. Jahnke, T. L. James, S. W. Homans, H. Kessler, C. Luchinat, B. Meyer, H. Oschkinat, J. Peng, H. Schwalbe, G. Siegal, *Nature Rev. Drug Discov.* **2008**, *7*, 738-745.

[175] Y. G. Gakh, A. A. Gakh, A. M. Gronenborn, *Magn. Reson. Chem.* **2000**, *38*, 551-558; S. L. Cobb, C. D. Murphy, *J. Fluorine Chem.* **2009**, *130*, 132-143; J. T. Gerig, *Prog. Nucl. Magn. Reson. Spectrosc.* **1994** , *26* , 293-370.

[176] C. Dalvit, A. Vulpetti, *ChemMedChem.* **2011**, *6*, 104-114.

[177] C. Dalvit, *Prog. Nucl. Magn. Reson. Spectrosc.* **2007**, *51*, 243-271.

[178] J. Ruiz-Cabello, B. P. Barnett, P. A. Bottomley, J. W.M. Bulte, *NMR Biomed.* **2011**, *24*, 114-129.

[179] M. Malet-Martino, V. Gilard, F. Desmoulin, R. Martino, *Clin. Chim. Acta*, **2006**, *366*, 61-73; W. Wolf, C. A. Presant, V. Waluch, *Adv. Drug Deliv. Rev.* **2000**, *41*, 55-74.

[180] M. L. DeRider, S. J. Wilkens, M. J. Waddell, L. E. Bretscher, F. Weinhold, R. T. Raines, *J. Am. Chem. Soc.* **2002**, *124*, 2497-2505.

[181] S. Arnott, R. Chandrasekaran, R. P. Millane, H.-S. Park, J. Mol. Biol. 1986, 188, 631-640.

[182] a) C. Altona, M. Sundaralingam, *J. Am. Chem. Soc.* **1973**, *95*, 2333-2344; b) IUPAC-IUB Joint Commission on Biochemical Nomenclature (JCBN) Conformational nomenclature for five and six-membered ring forms of monosaccharides and their derivatives, Recommendations 1980, *Arch. Biochem. Biophys.* **1981**, *207*, 469-472; *Eur. J. Biochem.* **1980**, *111*, 295-298; *Pure Appl. Chem.* **1981**, *53*, 1901-1905.

[183] J. T. Gerig, R. S. McLeod, *J. Am. Chem. Soc.* **1973**, *95*, 5725-5729.

[184] J. Donohue, K. N. Trueblood, Acta Crystallographica, 1952, 5, 419-431.

[185] a) M. Karplus, *J. Chem. Phys.* **1959**, *30*, 11; b) M. Karplus, *J. Am. Chem. Soc.* **1963**, *85,* 2870; c) K. L. Williamson, Y.-F. Li Hsu, F. H. Hall, **S.** Swager, M. S. Coulter, *J. Am. Chem. Soc.* **1968**, *90*, 6717; d) K. L. Williamson, S. Moser, and D. E. Stedman, *J. Am. Chem. Soc.* **1971**, *93*,7208.

[186] M. Blandin, T.-D. Son, J. C. Catlin, W. Guschlbauer, *Biochim. Biophys. Acta*, **1974**, *361*, 249-256.

[187] D. Suck, W. Saeger, P. Main, G. Germain, J. P. Leclercq, Biochim. Biophys. Acat, 1974, 361, 257-265.

[188] J. J. Barchi, Jr., L.-S. Jeong, M. A. Siddiqui, V. E. Marquez, J. Biochem. Biophys. Methods, 1997, 34, 11-29.

[189] J. San Fabián, J. Guilleme, E. Diez, *J. Magn. Reson.* **1998**, *133*, 255-265.

[190] C. Thibaudeau, J. Plavec, J. Chattopadhyaya, *J. Org. Chem.* **1998,** *63*, 4967-4984.

[191] J. J. Barchi, Jr., R. G. Karki, M. C. Nicklaus, M. A. Siddiqui, C. George, I. A. Mikhailopulo, V. E. Marquez, *J. Am. Chem. Soc.* **2008**, *130*, 9048-9057.

[192] D. Neuhaus, M. P. Williamson, The *Nuclear Overhauser Effect in Structural and Conformational Analysis* (2nd Edn), John Wiley & Sons, **2000**; T. D. W. Claridge, *High-Resolution NMR Techniques in Organic Chemistry* (2nd Edn), Elsevier, **2009**.

[193] I. V. Alabugin, K. M. Gilmore, P. W. Peterson, *Wiley Interdiscip. Rev. Comput. Mol. Sci*. **2011**, *1*, 109-141.

[194] P. Clausen-Thue, Master Thesis, University of Oxford, **2009**.

[195] C. Altona, in *Encyclopedia of NMR*, (Eds.: D. M. Grant, R. Morris), Wiley, New York, NY, **1996**, 4909-4923.

[196] A. Navarro-Vázquez, J. C. Cobas, F. J. Sardina, J. Casanueva, E. Díez, *J. Chem. Inf. Comput. Sci.* **2004,** *44*, 1680-1685.

[197] a) P. L. Rinaldi, *J. Am. Chem. Soc.* **1983**, *105*, 5167-5168; (b) C. Yu, G. C. Levy, *J. Am. Chem. Soc.* **1984**, *106*, 6533-6537.

[198] a) W. Bauer, *Magn. Reson. Chem.* **1996**, *34*, 532-537; (b) K. Stott, J. Keeler, *Magn. Reson. Chem.* **1996**, *34*, 554-558; (c) T. M. Alam, D. M. Pedrotty, T. J. Boyle, *Magn. Reson. Chem.* **2002**, *40*, 361-365; (d) O. Walker, P. Mutzenhardt, D. Canet, *Magn. Reson. Chem.* **2003,** *41*, 776-781.

[199] J. T. Gerig, *Magn. Reson. Chem.* **1999**, *37*, 647-652.

[200] K. Stott, J. Keeler, Q. N. Van, A. J. Shaka, *J. Magn. Reson.* **1997**, *125*, 302-324.

[201] W. Kim, K. I. Hardcastle, V. P. Conticello, *Angew. Chem. Int. Ed.* **2006**, *45*, 8141-8145.

[202] J. A. Hodges, R. T. Raines, *J. Am. Chem. Soc*. **2005**, *127*, 15923-15932

[203] See the appendix for a table summarizing X-rays characteristics.

[204] J. A. K. Howard, V. J. Hoy, D. O'Hagan, G. T. Smith, *Tetrahedron*, **1996**, *52*, 12613-12622.

[205] Y-W. Wang, Y. Peng, *Acta Crystallogr., Sect. E: Struct. Rep. Online*. **2008**, E64, o56.

[206] http://joule.qfa.uam.es/3jhf/index.php; J. San Fabian, J. Guilleme, *Chem. Phys.* **1996**, *206*, 325-337.

[207] SYBYL-X 1.0, Tripos International, 1699 South Hamley Rd, St Louis, Missouri, 63144, USA.

[208] MMFF94: Maximally Diagonal Force Constants in Dependent Angle-Binding Coordinates. 2. Implications for the design of empirical force fields. T. Halgren, *J. Am. Chem. Soc.*, **1990**, 112, 4710-4723.

[209] Spartan'08, Wavefunction Inc., Irvine, CA.

Appendix:

CRYSTALLOGAPHIC DATA

Data collection:

Crystals of suitable compounds were recrystallised from diethyl ether by slow diffusion of hexane. A typical single crystal of the compound under investigation was mounted on a loop using perfluoropolyether oil and cooled rapidly to 150 K in a stream of cold N_2 using an Oxford Cryosystems CRYOSTREAM unit.[1] Diffraction data were measured using an Enraf-Nonius KappaCCD diffractometer (graphite-monochromated MoK_α radiation, $\lambda = 0.71073$ Å). Intensity data were processed using DENZO-SMN/SCALEPACK including unit cell refinement and inter-frame scaling.[2] The structures were solved using direct-methods with the program SIR92,[3] which located all non-hydrogen atoms. Subsequent full-matrix least-squares refinement was carried out using the CRYSTALS[4] suite including refinement of the Flack x parameter where appropriate[5] and using a Chebychev polynomial weighting scheme.[6] Hydrogen atoms were refined independently with soft restraints prior to inclusion in the final refinement using a riding model.[7] Distances to and angles to planes were calculated using PLATON[8] and F···H distances were calculated using the full variance-

[1] J. Cosier, A. M. Glazer, *J. Appl. Cryst.* **1986**, *19*, 105-107.
[2] Z. Otwinowski, W. Minor, *Processing of X-ray Diffraction Data Collected in Oscillation Mode, Methods Enzymol.* (Eds.: C. W. Carter, R. M. Sweet), Academic Press, **1997**, 276.
[3] A. Altomare, G. Cascarano, C. Giacovazzo, A. Guagliardi, M. C. Burla, G. Polidori, M. Camalli, *J. Appl. Cryst.* **1994**, *27*, 435.
[4] P. W. Betteridge, J. R. Carruthers, R. I. Cooper, K. Prout, D. J. Watkin, *J. Appl. Cryst.* **2003**, *36*, 1487.
[5] a) H. D. Flack, *Acta Cryst.* **1983**, A39, 876-881; b) H. D. Flack, G. Bernardinelli, *J. Appl. Cryst.* **2000**, *33*, 1143-1148; c) A. L. Thompson, D. J. Watkin, *Tetrahedron Asymm.* **2009**, *20*, 712-717; d) A. L. Thompson, D. J. Watkin, *J. Appl. Cryst.* **2011**, *44*, 1017-1022.
[6] E. Prince, *Mathematical Techniques in Crystallography and Materials Science*, Springer-Verlag, New York, **1982**; J. R. Carruthers, D. J. Watkin, *Acta Crystallogr., Sect. A: Found.* **1979**, A35, 698-699; D. J. Watkin, *Acta Crystallogr., Sect. A: Found.* **1994**, A50, 411-437.
[7] R. I. Cooper, A. L. Thompson, D. J. Watkin, *J. Appl. Cryst.* **2010**, *43*, 1100-1107.
[8] A. L. Spek, *PLATON, A Multipurpose Crystallographic Tool*, Utrecht, the Netherlands, **1998**; A. Spek, *J. Appl. Cryst.* **2003**, *36*, 7-13.

covariance matrix. Plots were produced using Mercury.[9] Full crystallographic data for the following structures have been deposited with the Cambridge Crystallographic Data Centre (CCDC). Copies of these data can be obtained free of charge from The Cambridge Crystallographic Data Centre via www.ccdc.cam.ac.uk/data_request/cif.

(±) 3-fluoro-2-(iodomethyl)-3-methyl-1-[(4-methylphenyl)sulfonyl]pyrrolidine (102): (CCDC-896062)

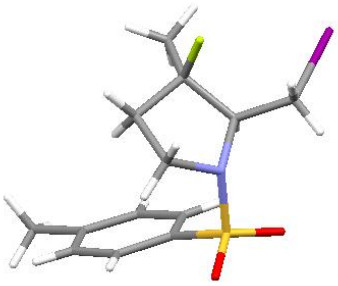

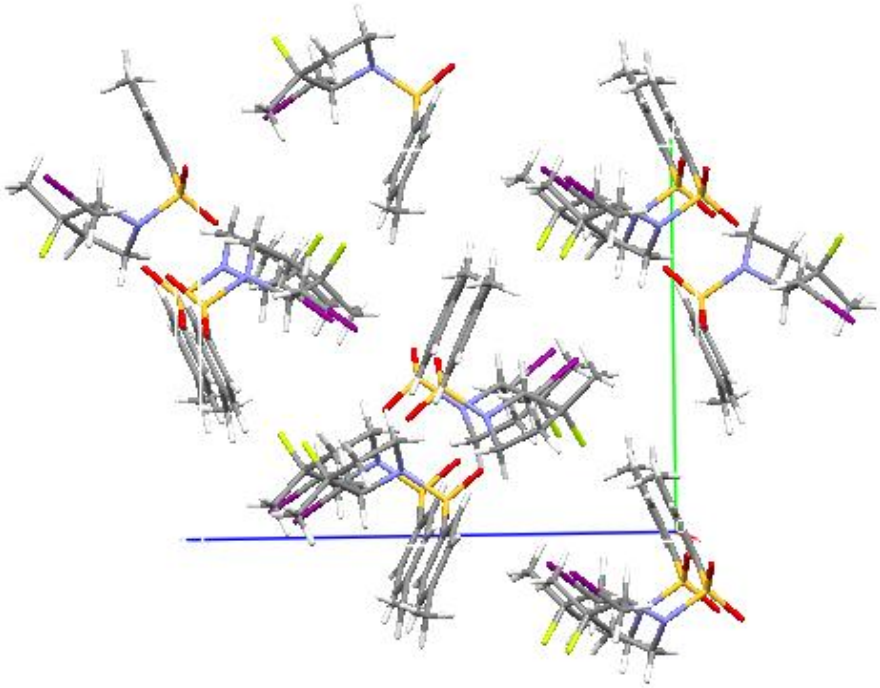

[9] C. F. Macrae, I. J. Bruno, J. A. Chisholm, P. R. Edgington, P. McCabe, E. Pidcock, L. Rodriguez-Monge, R. Taylor, J. van de Streek, P. A. Wood, *J. Appl. Cryst.* **2008**, *41*, 466-470.

Crystal data

$C_{13}H_{17}FINO_2S$	D_x = 1.708 Mg m^{-3}
M_r = 397.25	Melting point: not measured K
Orthorhombic, $P2_12_12_1$	Mo $K\alpha$ radiation, λ = 0.71073 Å
Hall symbol: P 2ac 2ab	Cell parameters from 2030 reflections
a = 8.2204 (3) Å	θ = 5–28°
b = 12.1941 (5) Å	μ = 2.22 mm^{-1}
c = 15.4065 (7) Å	T = 150 K
V = 1544.35 (11) Å^3	Plate, Clear_pale_colourless
Z = 4	0.34 × 0.06 × 0.04 mm
F(000) = 784	

Data collection

Nonius KappaCCD diffractometer	3131 reflections with $I > 3.0\sigma(I)$
Graphite monochromator	R_{int} = 0.054
ω scans	θ_{max} = 27.9°, θ_{min} = 5.1°
Absorption correction: Multi-scan *DENZO*/*SCALEPACK* (Otwinowski & Minor, 1997)	h = −10→10
T_{min} = 0.74, T_{max} = 0.92	k = −15→16
8845 measured reflections	l = −20→20
3624 independent reflections	

Refinement

Refinement on F	Hydrogen site location: Inferred from neighbouring sites
Least-squares matrix: Full	H-atom parameters constrained
$R[F^2 > 2\sigma(F^2)]$ = 0.044	Method, part 1, Chebychev polynomial, (Watkin, 1994, *P*rince, 1982) [*w*eight] = 1.0/[A_0*T_0(x) + A_1*T_1(x) ⋯ + A_{n-1}]*T_{n-1}(x)] where A_i are the Chebychev coefficients listed below and x = F /Fmax Method = Robust Weighting (*P*rince, 1982) W = [*w*eight] * [1-(delta$F$/6*sigma$F$)^2]^2 A_i are: 1.62 0.741 1.74 0.323 0.490
$wR(F^2)$ = 0.040	$(\Delta/\sigma)_{max}$ = 0.0003
S = 1.04	$\Delta\rho_{max}$ = 1.69 e Å^{-3}
3131 reflections	$\Delta\rho_{min}$ = −1.89 e Å^{-3}
173 parameters	Absolute structure: Flack (1983), 0 Friedel-pairs
0 restraints	Flack parameter: 0.52 (3)
Primary atom site location: Structure-invariant direct methods	

Fractional atomic coordinates and isotropic or equivalent isotropic displacement parameters (Å^2)

	x	*y*	*z*	U_{iso}*/U_{eq}
S1	0.51341 (13)	0.38621 (10)	0.49052 (7)	0.0282
N2	0.4945 (5)	0.3107 (3)	0.4029 (2)	0.0286
C3	0.4469 (6)	0.3684 (4)	0.3212 (3)	0.0298
C4	0.5690 (6)	0.3271 (5)	0.2519 (3)	0.0375
C5	0.7103 (6)	0.2815 (4)	0.3042 (4)	0.0383
C6	0.6291 (5)	0.2323 (4)	0.3835 (3)	0.0315
F7	0.4942 (4)	0.2383 (3)	0.2087 (2)	0.0561
C8	0.6165 (8)	0.4139 (7)	0.1857 (4)	0.0640
C9	0.2677 (6)	0.3444 (4)	0.3066 (4)	0.0367
I10	0.16271 (5)	0.44183 (3)	0.20376 (2)	0.0453
C11	0.6844 (6)	0.4718 (3)	0.4750 (3)	0.0260
C12	0.8384 (6)	0.4303 (4)	0.4945 (3)	0.0293
C13	0.9729 (6)	0.4933 (4)	0.4746 (3)	0.0329
C14	0.9571 (6)	0.5968 (4)	0.4370 (3)	0.0324
C15	0.8020 (6)	0.6369 (4)	0.4200 (4)	0.0384
C16	0.6646 (6)	0.5743 (4)	0.4373 (3)	0.0338
C17	1.1075 (7)	0.6647 (5)	0.4188 (4)	0.0475
O18	0.3716 (3)	0.4543 (3)	0.4931 (2)	0.0348
O19	0.5469 (4)	0.3116 (3)	0.5601 (2)	0.0372
H31	0.4618	0.4477	0.3286	0.0345*
H51	0.7840	0.3413	0.3222	0.0460*
H52	0.7715	0.2283	0.2708	0.0462*
H61	0.7036	0.2254	0.4327	0.0381*
H62	0.5848	0.1600	0.3697	0.0377*
H81	0.7187	0.3940	0.1592	0.1011*
H82	0.6231	0.4846	0.2138	0.1006*
H83	0.5319	0.4147	0.1422	0.1011*
H91	0.2568	0.2677	0.2916	0.0430*
H92	0.2086	0.3569	0.3601	0.0430*
H121	0.8514	0.3610	0.5197	0.0349*
H131	1.0757	0.4666	0.4856	0.0380*
H151	0.7910	0.7073	0.3973	0.0457*
H161	0.5626	0.6004	0.4229	0.0420*
H171	1.0779	0.7393	0.4096	0.0696*
H172	1.1771	0.6603	0.4673	0.0701*
H173	1.1645	0.6362	0.3683	0.0698*

Atomic displacement parameters (Å^2)

	U^{11}	U^{22}	U^{33}	U^{12}	U^{13}	U^{23}
S1	0.0217 (5)	0.0361 (6)	0.0267 (5)	−0.0016 (4)	0.0006 (4)	0.0010 (4)

N2	0.0236 (18)	0.0347 (19)	0.0276 (18)	0.0012 (16)	−0.0037 (15)	0.0026 (15)
C3	0.032 (2)	0.031 (2)	0.026 (2)	0.0024 (18)	−0.0026 (17)	0.0040 (17)
C4	0.037 (3)	0.047 (3)	0.029 (2)	0.004 (2)	0.004 (2)	−0.001 (2)
C5	0.035 (2)	0.045 (3)	0.035 (2)	0.0037 (19)	0.007 (2)	0.002 (2)
C6	0.025 (2)	0.033 (2)	0.037 (2)	0.0068 (17)	0.0053 (18)	0.0001 (19)
F7	0.0528 (19)	0.072 (2)	0.0436 (17)	0.0059 (17)	−0.0092 (18)	−0.0276 (18)
C8	0.052 (4)	0.093 (6)	0.046 (3)	0.013 (3)	0.015 (3)	0.028 (3)
C9	0.031 (2)	0.043 (3)	0.036 (3)	−0.0007 (19)	−0.003 (2)	0.004 (2)
I10	0.04529 (18)	0.04026 (16)	0.05042 (19)	0.00087 (17)	−0.02020 (16)	0.00502 (17)
C11	0.023 (2)	0.030 (2)	0.0260 (19)	−0.0014 (17)	−0.0024 (16)	−0.0035 (15)
C12	0.0303 (19)	0.027 (2)	0.0309 (19)	0.002 (2)	−0.0028 (19)	0.0033 (18)
C13	0.025 (2)	0.038 (3)	0.035 (3)	−0.0026 (19)	−0.0023 (18)	0.003 (2)
C14	0.025 (2)	0.034 (2)	0.038 (3)	−0.0047 (17)	0.0046 (19)	−0.0012 (19)
C15	0.040 (3)	0.031 (2)	0.044 (3)	−0.001 (2)	−0.002 (2)	0.003 (2)
C16	0.025 (2)	0.037 (3)	0.039 (2)	0.001 (2)	−0.003 (2)	−0.0026 (19)
C17	0.036 (3)	0.049 (3)	0.057 (4)	−0.017 (2)	0.007 (2)	0.004 (3)
O18	0.0168 (15)	0.049 (2)	0.0389 (17)	0.0015 (14)	0.0035 (11)	−0.0059 (16)
O19	0.0326 (18)	0.049 (2)	0.0295 (17)	−0.0075 (15)	−0.0006 (13)	0.0095 (15)

Geometric parameters (Å, º)

S1—N2	1.641 (4)	C8—H83	0.965
S1—C11	1.767 (5)	C9—I10	2.161 (5)
S1—O18	1.431 (3)	C9—H91	0.968
S1—O19	1.432 (4)	C9—H92	0.969
N2—C3	1.494 (6)	C11—C12	1.396 (7)
N2—C6	1.493 (6)	C11—C16	1.388 (6)
C3—C4	1.551 (7)	C12—C13	1.382 (7)
C3—C9	1.518 (7)	C12—H121	0.935
C3—H31	0.981	C13—C14	1.394 (7)
C4—C5	1.519 (7)	C13—H131	0.922
C4—F7	1.412 (7)	C14—C15	1.391 (7)
C4—C8	1.521 (8)	C14—C17	1.514 (7)
C5—C6	1.516 (7)	C15—C16	1.389 (7)
C5—H51	0.988	C15—H151	0.932
C5—H52	0.969	C16—H161	0.924
C6—H61	0.977	C17—H171	0.952
C6—H62	0.978	C17—H172	0.943
C8—H81	0.964	C17—H173	0.973
C8—H82	0.967		
N2—S1—C11	107.2 (2)	H81—C8—H82	111.4
N2—S1—O18	105.7 (2)	C4—C8—H83	106.7
C11—S1—O18	108.0 (2)	H81—C8—H83	109.7
N2—S1—O19	106.1 (2)	H82—C8—H83	110.1

C11—S1—O19	108.9 (2)	C3—C9—I10	113.0 (3)
O18—S1—O19	120.3 (2)	C3—C9—H91	108.2
S1—N2—C3	116.9 (3)	I10—C9—H91	108.6
S1—N2—C6	117.0 (3)	C3—C9—H92	109.3
C3—N2—C6	109.1 (3)	I10—C9—H92	109.6
N2—C3—C4	104.9 (4)	H91—C9—H92	108.0
N2—C3—C9	106.7 (4)	S1—C11—C12	118.5 (3)
C4—C3—C9	117.6 (4)	S1—C11—C16	119.7 (4)
N2—C3—H31	109.5	C12—C11—C16	121.6 (4)
C4—C3—H31	108.6	C11—C12—C13	118.4 (4)
C9—C3—H31	109.2	C11—C12—H121	121.3
C3—C4—C5	104.4 (4)	C13—C12—H121	120.2
C3—C4—F7	107.0 (4)	C12—C13—C14	121.4 (5)
C5—C4—F7	107.6 (4)	C12—C13—H131	119.7
C3—C4—C8	113.7 (5)	C14—C13—H131	118.8
C5—C4—C8	114.5 (5)	C13—C14—C15	118.8 (5)
F7—C4—C8	109.2 (5)	C13—C14—C17	119.7 (5)
C4—C5—C6	103.7 (4)	C15—C14—C17	121.4 (5)
C4—C5—H51	110.3	C14—C15—C16	121.1 (5)
C6—C5—H51	109.6	C14—C15—H151	118.9
C4—C5—H52	111.2	C16—C15—H151	120.0
C6—C5—H52	113.1	C15—C16—C11	118.7 (5)
H51—C5—H52	108.9	C15—C16—H161	120.1
C5—C6—N2	103.6 (4)	C11—C16—H161	121.2
C5—C6—H61	112.5	C14—C17—H171	110.0
N2—C6—H61	111.3	C14—C17—H172	108.5
C5—C6—H62	110.2	H171—C17—H172	109.2
N2—C6—H62	110.2	C14—C17—H173	110.2
H61—C6—H62	108.9	H171—C17—H173	110.2
C4—C8—H81	109.4	H172—C17—H173	108.7
C4—C8—H82	109.5		

(±) *N*-(4-fluoro-5-(iodomethyl)-3,3-dimethyldihydrofuran-2-(*3H*)-ylidene)-4-methyl benzenesulfonamide (107):
(CCDC-896063)

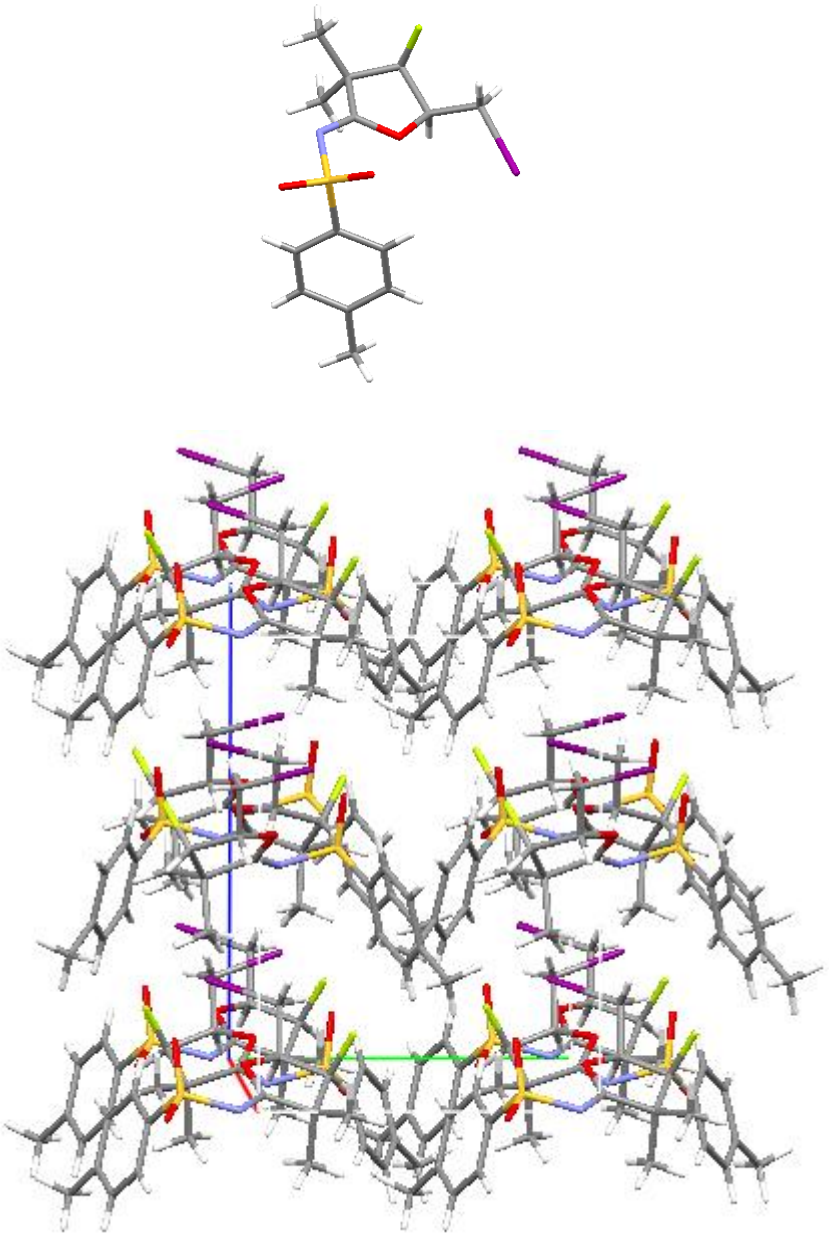

Crystal data

$C_{14}H_{17}FINO_3S$
M_r = 425.26
Orthorhombic, $Pca2_1$
Hall symbol: P 2c -2ac
a = 13.6271 (4) Å
b = 9.2546 (2) Å
c = 12.9252 (3) Å
V = 1630.04 (7) Å^3

D_x = 1.733 Mg m^{-3}
Melting point: not measured K
Mo $K\alpha$ radiation, λ = 0.71073 Å
Cell parameters from 2058 reflections
θ = 5–27°
μ = 2.11 mm^{-1}
T = 150 K
Block, Clear_intense_red

$Z = 4$
$F(000) = 840$
0.20 × 0.20 × 0.20 mm

Data collection

Nonius KappaCCD diffractometer
Graphite monochromator
ω scans
Absorption correction: Multi-scan *DENZO*/*SCALEPACK* (Otwinowski & Minor, 1997)
$T_{min} = 0.58$, $T_{max} = 0.66$
13300 measured reflections
3490 independent reflections
3191 reflections with $I > 2.0\sigma(I)$
$R_{int} = 0.041$
$\theta_{max} = 27.5°$, $\theta_{min} = 5.2°$
$h = -17 \rightarrow 17$
$k = -11 \rightarrow 12$
$l = -16 \rightarrow 16$

Refinement

Refinement on F^2
Least-squares matrix: Full
$R[F^2 > 2\sigma(F^2)] = 0.026$
$wR(F^2) = 0.063$
$S = 1.00$
3490 reflections
191 parameters
1 restraint
Primary atom site location: Structure-invariant direct methods
Hydrogen site location: Difference Fourier map
H-atom parameters constrained
Method, part 1, Chebychev polynomial, (Watkin, 1994, *P*rince, 1982) [*w*eight] = 1.0/[A_0*T_0(x) + A_1*T_1(x) ⋯ + A_{n-1}]*T_{n-1}(x)] where A_i are the Chebychev coefficients listed below and x = *F* /*F*max Method = Robust Weighting (*P*rince, 1982) W = [*w*eight] * [1-(delta*F*/6*sigma*F*)^2]^2 A_i are: 24.1 38.0 22.9 9.90 2.53
$(\Delta/\sigma)_{max} = 0.002$
$\Delta\rho_{max} = 0.41$ e Å^{-3}
$\Delta\rho_{min} = -0.77$ e Å^{-3}
Absolute structure: Flack (1983), 1559 Friedel-pairs
Flack parameter: 0.57 (2)

Fractional atomic coordinates and isotropic or equivalent isotropic displacement parameters (Å^2)

	x	*y*	*z*	U_{iso}*/U_{eq}
I1	0.761664 (14)	0.87391 (2)	0.75010 (7)	0.0321
C2	0.6971 (3)	1.0765 (4)	0.7058 (3)	0.0254
C3	0.6561 (2)	1.0743 (4)	0.5988 (3)	0.0215
O4	0.57881 (17)	0.9644 (2)	0.5913 (2)	0.0218
C5	0.5037 (2)	1.0136 (3)	0.5352 (3)	0.0193
N6	0.4274 (2)	0.9379 (3)	0.5114 (3)	0.0218
S7	0.42086 (6)	0.76607 (9)	0.54669 (9)	0.0215

O8	0.32867 (19)	0.7177 (3)	0.5051 (2)	0.0320
O9	0.4367 (2)	0.7482 (3)	0.6558 (2)	0.0312
C10	0.5160 (3)	0.6787 (4)	0.4775 (2)	0.0194
C11	0.6035 (2)	0.6429 (4)	0.5258 (3)	0.0242
C12	0.6763 (3)	0.5750 (4)	0.4689 (3)	0.0244
C13	0.6625 (2)	0.5420 (4)	0.3646 (3)	0.0234
C14	0.5736 (2)	0.5792 (4)	0.3181 (3)	0.0226
C15	0.5005 (2)	0.6474 (4)	0.3741 (3)	0.0221
C16	0.7417 (3)	0.4676 (4)	0.3024 (3)	0.0316
C17	0.5207 (3)	1.1662 (4)	0.4972 (3)	0.0211
C18	0.6054 (3)	1.2150 (4)	0.5657 (3)	0.0229
F19	0.56751 (17)	1.2830 (2)	0.65487 (18)	0.0315
C20	0.4293 (3)	1.2605 (4)	0.5027 (4)	0.0309
C21	0.5570 (4)	1.1548 (5)	0.3855 (3)	0.0365
H21	0.6457	1.0978	0.7548	0.0304*
H22	0.7464	1.1509	0.7107	0.0302*
H31	0.7069	1.0487	0.5492	0.0259*
H111	0.6131	0.6651	0.5952	0.0296*
H121	0.7356	0.5489	0.5003	0.0287*
H141	0.5640	0.5549	0.2491	0.0270*
H151	0.4414	0.6722	0.3428	0.0253*
H161	0.7203	0.4481	0.2329	0.0476*
H162	0.7993	0.5273	0.3003	0.0474*
H163	0.7577	0.3776	0.3340	0.0469*
H181	0.6505	1.2800	0.5277	0.0268*
H201	0.4452	1.3577	0.4814	0.0459*
H202	0.3788	1.2222	0.4587	0.0460*
H203	0.4059	1.2615	0.5727	0.0457*
H211	0.5737	1.2491	0.3591	0.0546*
H212	0.5069	1.1138	0.3419	0.0548*
H213	0.6136	1.0922	0.3823	0.0551*

Atomic displacement parameters (Å^2)

	U^{11}	U^{22}	U^{33}	U^{12}	U^{13}	U^{23}
I1	0.03507 (11)	0.02394 (10)	0.03733 (12)	0.00155 (8)	−0.00802 (19)	0.00167 (15)
C2	0.0311 (18)	0.0131 (15)	0.0320 (18)	−0.0012 (13)	−0.0060 (15)	0.0005 (14)
C3	0.0192 (15)	0.0176 (15)	0.0278 (18)	−0.0022 (12)	0.0010 (13)	0.0002 (13)
O4	0.0231 (11)	0.0150 (11)	0.0273 (12)	−0.0041 (9)	−0.0038 (9)	0.0039 (10)
C5	0.0216 (15)	0.0180 (15)	0.0183 (14)	0.0018 (11)	0.0013 (12)	−0.0033 (13)
N6	0.0206 (14)	0.0185 (13)	0.0263 (16)	−0.0009 (11)	−0.0016 (12)	−0.0012 (12)
S7	0.0200 (4)	0.0203 (4)	0.0242 (4)	−0.0044 (3)	0.0044 (3)	−0.0035 (3)
O8	0.0181 (12)	0.0333 (13)	0.0445 (15)	−0.0073 (10)	0.0038 (11)	−0.0133 (13)
O9	0.0435 (16)	0.0283 (14)	0.0217 (13)	−0.0081 (12)	0.0065 (11)	0.0016 (11)

C10	0.0222 (17)	0.0153 (14)	0.0208 (17)	−0.0024 (13)	0.0003 (12)	0.0017 (11)
C11	0.0247 (16)	0.0211 (16)	0.027 (2)	0.0006 (13)	−0.0052 (13)	−0.0006 (13)
C12	0.0238 (18)	0.0191 (16)	0.0303 (18)	0.0017 (13)	−0.0077 (14)	0.0025 (14)
C13	0.0224 (16)	0.0151 (15)	0.0327 (19)	0.0022 (12)	0.0002 (14)	0.0018 (14)
C14	0.0217 (16)	0.0260 (17)	0.0202 (15)	0.0016 (13)	0.0002 (12)	0.0012 (14)
C15	0.0182 (15)	0.0239 (18)	0.0242 (17)	−0.0001 (12)	−0.0029 (12)	0.0024 (13)
C16	0.0281 (19)	0.0280 (19)	0.039 (2)	0.0065 (15)	0.0036 (15)	−0.0040 (17)
C17	0.0293 (18)	0.0157 (14)	0.0183 (14)	0.0010 (13)	0.0027 (13)	−0.0005 (13)
C18	0.0218 (16)	0.0163 (15)	0.030 (2)	0.0018 (12)	0.0058 (14)	−0.0053 (13)
F19	0.0409 (13)	0.0265 (11)	0.0270 (11)	0.0079 (9)	−0.0019 (9)	−0.0096 (9)
C20	0.029 (2)	0.0250 (17)	0.039 (2)	0.0052 (16)	−0.0033 (16)	0.0036 (18)
C21	0.053 (3)	0.034 (2)	0.0228 (19)	−0.0064 (17)	0.0083 (17)	0.0020 (16)

Geometric parameters (Å, º)

I1—C2	2.149 (3)	C13—C14	1.395 (5)
C2—C3	1.492 (5)	C13—C16	1.511 (5)
C2—H21	0.965	C14—C15	1.383 (5)
C2—H22	0.964	C14—H141	0.929
C3—O4	1.467 (4)	C15—H151	0.930
C3—C18	1.535 (5)	C16—H161	0.962
C3—H31	0.973	C16—H162	0.961
O4—C5	1.334 (4)	C16—H163	0.954
C5—N6	1.291 (4)	C17—C18	1.522 (5)
C5—C17	1.513 (4)	C17—C20	1.523 (5)
N6—S7	1.657 (3)	C17—C21	1.530 (5)
S7—O8	1.438 (3)	C18—F19	1.411 (4)
S7—O9	1.436 (3)	C18—H181	0.991
S7—C10	1.770 (4)	C20—H201	0.966
C10—C11	1.386 (5)	C20—H202	0.961
C10—C15	1.384 (5)	C20—H203	0.959
C11—C12	1.386 (5)	C21—H211	0.965
C11—H111	0.930	C21—H212	0.962
C12—C13	1.395 (5)	C21—H213	0.965
C12—H121	0.936		
I1—C2—C3	112.9 (2)	C13—C14—H141	118.4
I1—C2—H21	107.5	C15—C14—H141	120.8
C3—C2—H21	109.8	C10—C15—C14	119.4 (3)
I1—C2—H22	108.7	C10—C15—H151	120.0
C3—C2—H22	109.4	C14—C15—H151	120.6
H21—C2—H22	108.5	C13—C16—H161	111.5
C2—C3—O4	109.9 (3)	C13—C16—H162	109.7
C2—C3—C18	114.5 (3)	H161—C16—H162	109.2
O4—C3—C18	104.3 (3)	C13—C16—H163	109.5

C2—C3—H31	110.3	H161—C16—H163	107.8
O4—C3—H31	107.4	H162—C16—H163	109.1
C18—C3—H31	110.1	C5—C17—C18	101.8 (3)
C3—O4—C5	110.5 (2)	C5—C17—C20	113.2 (3)
O4—C5—N6	124.2 (3)	C18—C17—C20	115.0 (3)
O4—C5—C17	112.2 (3)	C5—C17—C21	106.9 (3)
N6—C5—C17	123.6 (3)	C18—C17—C21	109.0 (3)
C5—N6—S7	119.9 (3)	C20—C17—C21	110.3 (3)
N6—S7—O8	104.08 (16)	C3—C18—C17	104.6 (3)
N6—S7—O9	111.86 (16)	C3—C18—F19	108.4 (3)
O8—S7—O9	117.53 (18)	C17—C18—F19	109.3 (3)
N6—S7—C10	105.06 (15)	C3—C18—H181	111.9
O8—S7—C10	107.98 (17)	C17—C18—H181	111.2
O9—S7—C10	109.50 (17)	F19—C18—H181	111.2
S7—C10—C11	120.7 (3)	C17—C20—H201	109.7
S7—C10—C15	118.2 (3)	C17—C20—H202	110.3
C11—C10—C15	121.1 (3)	H201—C20—H202	109.6
C10—C11—C12	119.0 (3)	C17—C20—H203	108.8
C10—C11—H111	120.2	H201—C20—H203	109.5
C12—C11—H111	120.7	H202—C20—H203	108.9
C11—C12—C13	121.0 (3)	C17—C21—H211	110.4
C11—C12—H121	120.3	C17—C21—H212	110.5
C13—C12—H121	118.7	H211—C21—H212	108.5
C12—C13—C14	118.7 (3)	C17—C21—H213	109.8
C12—C13—C16	121.1 (3)	H211—C21—H213	109.8
C14—C13—C16	120.2 (3)	H212—C21—H213	107.8
C13—C14—C15	120.8 (3)		

Hydrogen-bond geometry (Å, º)

D—H···*A*	*D*—H	H···*A*	*D*···*A*	*D*—H···*A*
C16—H163···O8^{i}	0.95	2.57	3.349 (5)	139
C18—H181···O8^{ii}	0.99	2.44	3.203 (5)	133

Symmetry codes: (i) *x*+1/2, −*y*+1, *z*; (ii) *x*+1/2, −*y*+2, *z*.

(±) 3-fluoro-2-(iodomethyl)-1-[(4-methylphenyl)sulfonyl]pyrrolidine (56): (CCDC-896055)

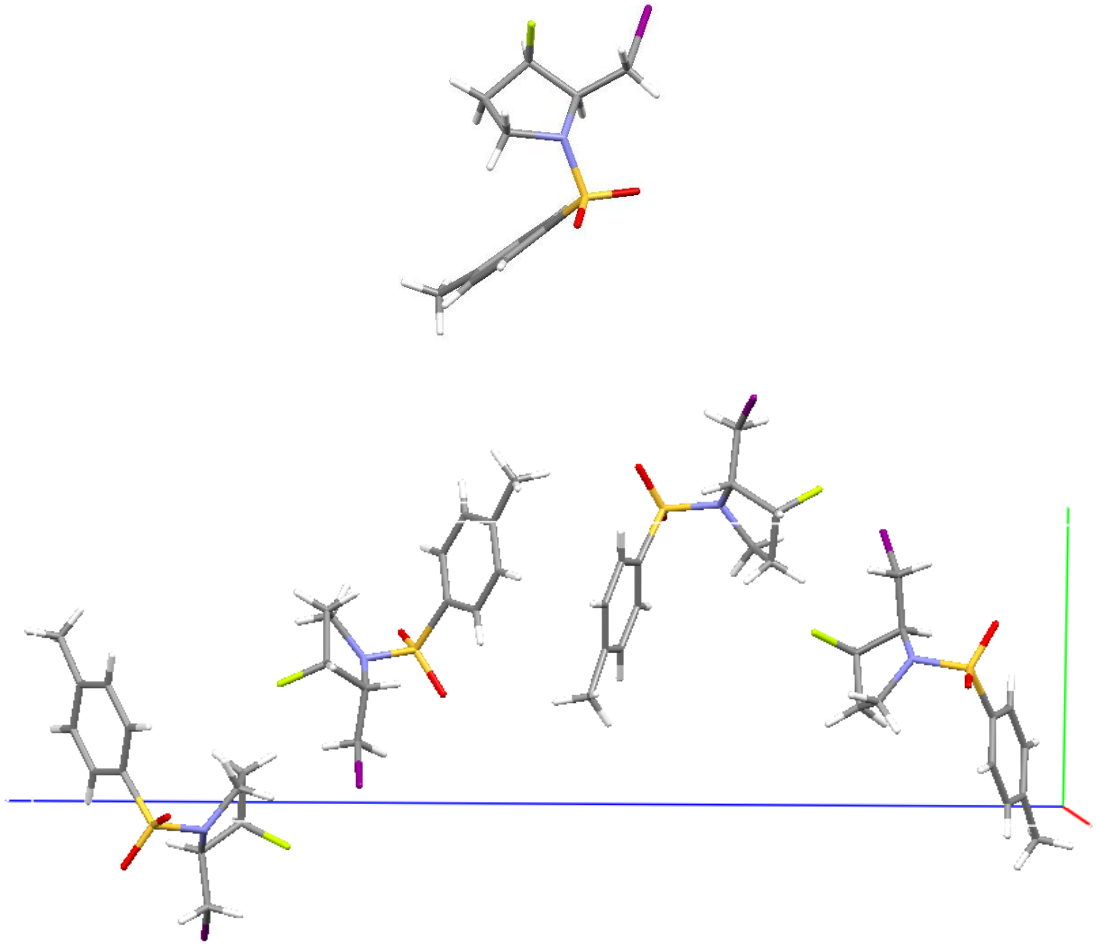

Crystal data

$C_{12}H_{15}FINO_2S$
M_r = 383.22
Orthorhombic, $P2_12_12_1$
Hall symbol: P 2ac 2ab
a = 5.9511 (1) Å
b = 8.2067 (1) Å
c = 29.0461 (5) Å
V = 1418.58 (4) Å^3
Z = 4
F(000) = 752

D_x = 1.794 Mg m^{-3}
Melting point: not measured K
Mo $K\alpha$ radiation, λ = 0.71073 Å
Cell parameters from 1901 reflections
θ = 5–27°
μ = 2.41 mm^{-1}
T = 150 K
Plate, Clear_pale_colourless
0.40 × 0.12 × 0.04 mm

Data collection

Nonius KappaCCD diffractometer

2658 reflections with $I > 2.0\sigma(I)$

Graphite monochromator	R_{int} = 0.056
ω scans	θ_{max} = 27.5°, θ_{min} = 5.2°
Absorption correction: Multi-scan *DENZO*/*SCALEPACK* (Otwinowski & Minor, 1997)	h = −7→7
T_{min} = 0.83, T_{max} = 0.91	k = −10→10
23032 measured reflections	l = −37→37
3247 independent reflections	

Refinement

Refinement on F^2	Hydrogen site location: Difference Fourier map
Least-squares matrix: Full	H-atom parameters constrained
$R[F^2 > 2\sigma(F^2)]$ = 0.031	Method, part 1, Chebychev polynomial, (Watkin, 1994, *P*rince, 1982) [*w*eight] = 1.0/[A_0*T_0(x) + A_1*T_1(x) ⋯ + A_{n-1}]*T_{n-1}(x)] where A_i are the Chebychev coefficients listed below and x = *F* /*F*max Method = Robust Weighting (*P*rince, 1982) W = [*w*eight] * [1-(delta*F*/6*sigma*F*)^2]^2 A_i are: 10.9 16.8 11.1 5.49 1.65
$wR(F^2)$ = 0.062	$(\Delta/\sigma)_{max}$ = 0.002
S = 1.00	$\Delta\rho_{max}$ = 0.83 e Å^{-3}
3226 reflections	$\Delta\rho_{min}$ = −1.12 e Å^{-3}
164 parameters	Absolute structure: Flack (1983), 1352 Friedel-pairs
0 restraints	Flack parameter: 0.47 (2)
Primary atom site location: Structure-invariant direct methods	

Fractional atomic coordinates and isotropic or equivalent isotropic displacement parameters (Å^2)

	x	*y*	*z*	U_{iso}*/U_{eq}
N1	0.4233 (7)	1.0259 (4)	0.33964 (10)	0.0261
C2	0.6480 (6)	1.1090 (5)	0.33574 (13)	0.0238
C3	0.7576 (8)	1.0213 (5)	0.29563 (15)	0.0307
C4	0.6622 (9)	0.8509 (6)	0.29750 (17)	0.0368
C5	0.4174 (9)	0.8828 (5)	0.30795 (14)	0.0333
C6	0.6115 (6)	1.2920 (4)	0.32966 (16)	0.0271
I7	0.93099 (5)	1.41377 (3)	0.323835 (12)	0.0398
F8	0.6862 (4)	1.0944 (4)	0.25397 (8)	0.0377
S9	0.31403 (17)	1.00258 (13)	0.39084 (4)	0.0253
O10	0.3727 (5)	1.1454 (4)	0.41618 (11)	0.0333
O11	0.0837 (5)	0.9603 (3)	0.38375 (11)	0.0365
C12	0.4425 (8)	0.8326 (5)	0.41699 (13)	0.0238
C13	0.6503 (7)	0.8491 (5)	0.43853 (15)	0.0257

C14	0.7546 (7)	0.7117 (5)	0.45625 (14)	0.0275
C15	0.6564 (8)	0.5573 (5)	0.45246 (14)	0.0286
C16	0.4446 (9)	0.5450 (4)	0.43228 (15)	0.0307
C17	0.3395 (8)	0.6809 (5)	0.41425 (16)	0.0285
C18	0.7761 (9)	0.4071 (7)	0.46948 (16)	0.0442
H21	0.7386	1.0892	0.3633	0.0288*
H31	0.9230	1.0244	0.2969	0.0360*
H42	0.7332	0.7897	0.3224	0.0439*
H41	0.6826	0.7915	0.2684	0.0434*
H52	0.3467	0.7922	0.3240	0.0400*
H51	0.3354	0.9098	0.2800	0.0403*
H61	0.5333	1.3357	0.3564	0.0326*
H62	0.5270	1.3132	0.3016	0.0329*
H131	0.7163	0.9498	0.4415	0.0314*
H141	0.8935	0.7223	0.4709	0.0333*
H161	0.3732	0.4436	0.4307	0.0367*
H171	0.1973	0.6697	0.4001	0.0340*
H182	0.7401	0.3157	0.4510	0.0662*
H181	0.7330	0.3858	0.5003	0.0665*
H183	0.9344	0.4248	0.4683	0.0668*

Atomic displacement parameters (Å^2)

	U^{11}	U^{22}	U^{33}	U^{12}	U^{13}	U^{23}
N1	0.0250 (15)	0.0274 (14)	0.0259 (16)	0.0021 (16)	−0.0015 (16)	−0.0003 (12)
C2	0.0212 (16)	0.024 (2)	0.026 (2)	0.0031 (14)	0.0020 (13)	0.0010 (16)
C3	0.033 (2)	0.033 (2)	0.026 (2)	0.0110 (19)	0.0039 (18)	0.0037 (18)
C4	0.051 (3)	0.028 (2)	0.031 (3)	0.008 (2)	−0.002 (2)	−0.0058 (19)
C5	0.037 (2)	0.037 (2)	0.0257 (19)	−0.002 (2)	−0.005 (2)	−0.0047 (16)
C6	0.025 (2)	0.0267 (17)	0.030 (2)	0.0012 (14)	0.0042 (18)	0.0038 (17)
I7	0.03492 (13)	0.03238 (12)	0.05202 (17)	−0.00569 (14)	0.00351 (17)	0.00508 (16)
F8	0.0487 (14)	0.0402 (13)	0.0243 (12)	0.0135 (15)	0.0053 (11)	0.0053 (13)
S9	0.0231 (5)	0.0254 (5)	0.0275 (5)	0.0020 (4)	0.0018 (4)	0.0015 (4)
O10	0.043 (2)	0.0277 (15)	0.0295 (16)	0.0042 (12)	0.0051 (14)	−0.0009 (12)
O11	0.0187 (12)	0.0409 (17)	0.0500 (17)	0.0032 (13)	0.0010 (15)	0.0103 (13)
C12	0.0236 (18)	0.0264 (18)	0.0214 (19)	0.0003 (19)	0.003 (2)	−0.0007 (15)
C13	0.0236 (19)	0.0257 (18)	0.028 (2)	−0.0055 (15)	0.0025 (17)	0.0003 (17)
C14	0.025 (2)	0.036 (2)	0.022 (2)	0.0039 (17)	−0.0013 (17)	0.0029 (18)
C15	0.037 (2)	0.028 (2)	0.0209 (19)	0.0070 (17)	−0.0011 (17)	0.0012 (17)
C16	0.034 (2)	0.024 (2)	0.034 (2)	−0.0002 (19)	0.002 (2)	−0.0050 (15)
C17	0.029 (2)	0.027 (2)	0.029 (2)	−0.0023 (18)	0.0015 (19)	−0.0024 (19)
C18	0.056 (3)	0.037 (2)	0.039 (3)	0.016 (3)	−0.009 (2)	0.004 (3)

Geometric parameters (Å, º)

N1—C2	1.505 (5)	S9—O10	1.427 (3)
N1—C5	1.493 (5)	S9—O11	1.429 (3)
N1—S9	1.634 (4)	S9—C12	1.763 (4)
C2—C3	1.517 (6)	C12—C13	1.392 (6)
C2—C6	1.528 (5)	C12—C17	1.390 (6)
C2—H21	0.978	C13—C14	1.386 (6)
C3—C4	1.510 (7)	C13—H131	0.919
C3—F8	1.416 (5)	C14—C15	1.399 (6)
C3—H31	0.985	C14—H141	0.935
C4—C5	1.511 (7)	C15—C16	1.394 (6)
C4—H42	0.976	C15—C18	1.508 (6)
C4—H41	0.983	C16—C17	1.381 (6)
C5—H52	0.973	C16—H161	0.935
C5—H51	0.972	C17—H171	0.945
C6—I7	2.154 (4)	C18—H182	0.947
C6—H61	0.975	C18—H181	0.949
C6—H62	0.973	C18—H183	0.954
C2—N1—C5	109.3 (3)	H61—C6—H62	110.8
C2—N1—S9	118.4 (3)	N1—S9—O10	106.00 (18)
C5—N1—S9	117.3 (3)	N1—S9—O11	106.20 (19)
N1—C2—C3	103.0 (3)	O10—S9—O11	120.55 (19)
N1—C2—C6	109.1 (3)	N1—S9—C12	108.20 (18)
C3—C2—C6	116.0 (3)	O10—S9—C12	108.75 (18)
N1—C2—H21	110.7	O11—S9—C12	106.62 (19)
C3—C2—H21	108.2	S9—C12—C13	120.1 (3)
C6—C2—H21	109.6	S9—C12—C17	119.5 (3)
C2—C3—C4	104.5 (3)	C13—C12—C17	120.3 (4)
C2—C3—F8	109.0 (3)	C12—C13—C14	119.0 (4)
C4—C3—F8	108.1 (4)	C12—C13—H131	120.7
C2—C3—H31	112.9	C14—C13—H131	120.3
C4—C3—H31	113.5	C13—C14—C15	121.4 (4)
F8—C3—H31	108.7	C13—C14—H141	119.3
C3—C4—C5	102.1 (4)	C15—C14—H141	119.3
C3—C4—H42	109.9	C14—C15—C16	118.4 (4)
C5—C4—H42	111.0	C14—C15—C18	121.2 (4)
C3—C4—H41	112.5	C16—C15—C18	120.4 (4)
C5—C4—H41	112.2	C15—C16—C17	120.7 (4)
H42—C4—H41	109.1	C15—C16—H161	119.7
C4—C5—N1	103.7 (4)	C17—C16—H161	119.6
C4—C5—H52	112.4	C12—C17—C16	120.1 (4)
N1—C5—H52	108.5	C12—C17—H171	120.4
C4—C5—H51	110.9	C16—C17—H171	119.5
N1—C5—H51	110.3	C15—C18—H182	110.8
H52—C5—H51	110.9	C15—C18—H181	109.4

C2—C6—I7	109.9 (2)	H182—C18—H181	109.3
C2—C6—H61	109.7	C15—C18—H183	109.3
I7—C6—H61	108.3	H182—C18—H183	108.9
C2—C6—H62	110.2	H181—C18—H183	109.2
I7—C6—H62	107.9		

Hydrogen-bond geometry (Å, º)

D—H···*A*	*D*—H	H···*A*	*D*···*A*	*D*—H···*A*
C2—H21···O11^{i}	0.98	2.39	3.187 (6)	139
C6—H61···O10	0.98	2.52	3.128 (6)	120
C16—H161···O10^{ii}	0.94	2.48	3.341 (6)	152
C18—H181···O10^{iii}	0.95	2.58	3.398 (6)	145

Symmetry codes: (i) *x*+1, *y*, *z*; (ii) *x*, *y*−1, *z*; (iii) *x*+1/2, −*y*+3/2, −*z*+1.

(±) 2-(bromomethyl)-3-fluoro-1-[(4-methylphenyl)sulfonyl]pyrrolidine (152): (CCDC-896056)

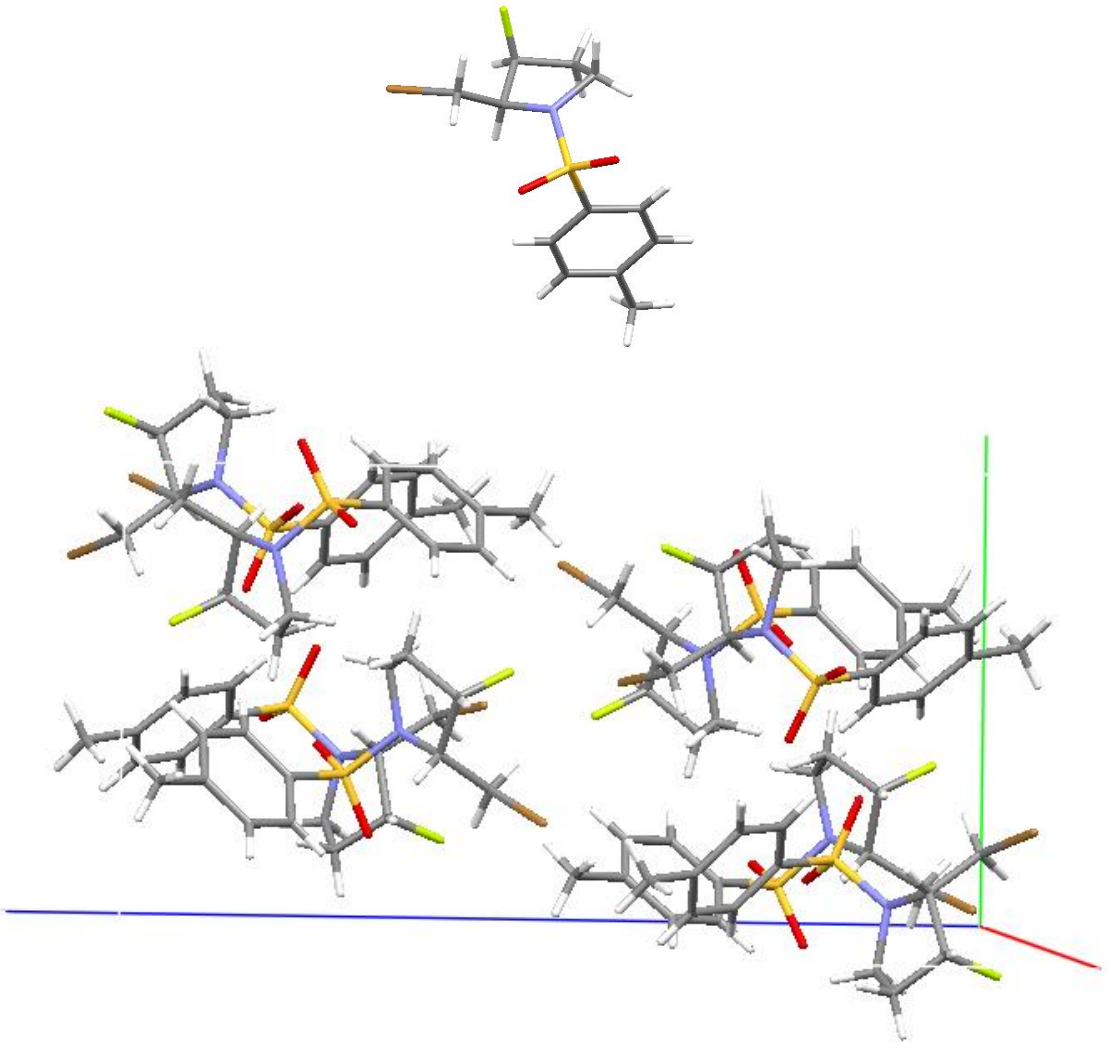

Crystal data

$C_{12}H_{15}BrFNO_2S$	$F(000)$ = 1360
M_r = 336.22	D_x = 1.618 Mg m^{-3}
Monoclinic, $P2_1/c$	Melting point: not measured K
Hall symbol: -P 2ybc	Mo $K\alpha$ radiation, λ = 0.71073 Å
a = 12.0292 (2) Å	Cell parameters from 6020 reflections
b = 10.9162 (2) Å	θ = 5–27°
c = 21.7503 (4) Å	μ = 3.13 mm^{-1}
β = 104.8554 (7)°	T = 150 K
V = 2760.64 (9) Å^3	Plate, Clear_pale_colourless
Z = 8	0.30 × 0.20 × 0.10 mm

Data collection

Nonius KappaCCD diffractometer	4581 reflections with $I > 2.0\sigma(I)$
Graphite monochromator	R_{int} = 0.028
ω scans	θ_{max} = 27.5°, θ_{min} = 5.1°
Absorption correction: Multi-scan *DENZO*/*SCALEPACK* (Otwinowski & Minor, 1997)	h = −15→15
T_{min} = 0.54, T_{max} = 0.73	k = −14→14
26734 measured reflections	l = −28→28
6237 independent reflections	

Refinement

Refinement on F^2	Primary atom site location: Structure-invariant direct methods
Least-squares matrix: Full	Hydrogen site location: Difference Fourier map
$R[F^2 > 2\sigma(F^2)]$ = 0.038	H-atom parameters constrained
$wR(F^2)$ = 0.086	Method, part 1, Chebychev polynomial, (Watkin, 1994, *P*rince, 1982) [*w*eight] = 1.0/[A_0*T_0(x) + A_1*T_1(x) ⋯ + A_{n-1}]*T_{n-1}(x)] where A_i are the Chebychev coefficients listed below and x = F /Fmax Method = Robust Weighting (*P*rince, 1982) W = [*w*eight] * [1-(delta*F*/6*sigma*F*)^2]^2 A_i are: 44.6 69.0 40.9 16.6 3.83
S = 1.00	$(\Delta/\sigma)_{max}$ = 0.001
6237 reflections	$\Delta\rho_{max}$ = 0.71 e Å^{-3}
325 parameters	$\Delta\rho_{min}$ = −0.93 e Å^{-3}
0 restraints	

Fractional atomic coordinates and isotropic or equivalent isotropic displacement parameters (Å^2)

	x	*y*	*z*	U_{iso}*/U_{eq}
N1	0.48591 (19)	0.5807 (2)	0.34279 (10)	0.0256
C2	0.3925 (2)	0.6176 (3)	0.37234 (12)	0.0231
C3	0.3388 (3)	0.4964 (3)	0.38405 (14)	0.0327
C4	0.3594 (3)	0.4139 (3)	0.33288 (16)	0.0446
C5	0.4811 (3)	0.4468 (3)	0.33066 (15)	0.0376
C6	0.4445 (3)	0.6924 (3)	0.43120 (14)	0.0340
Br7	0.32443 (4)	0.74825 (4)	0.47013 (2)	0.0586
F8	0.39909 (16)	0.44886 (18)	0.44337 (8)	0.0428
S9	0.51823 (6)	0.67100 (7)	0.29050 (3)	0.0282
O10	0.5230 (2)	0.7923 (2)	0.31639 (11)	0.0400
O11	0.61736 (17)	0.6201 (3)	0.27537 (11)	0.0454
C12	0.4041 (2)	0.6683 (3)	0.22076 (13)	0.0245
C13	0.3166 (3)	0.7533 (3)	0.21285 (14)	0.0323
C14	0.2266 (3)	0.7501 (3)	0.15875 (16)	0.0386
C15	0.2217 (2)	0.6619 (3)	0.11239 (14)	0.0371
C16	0.3102 (3)	0.5763 (3)	0.12118 (14)	0.0361
C17	0.4020 (3)	0.5795 (3)	0.17492 (13)	0.0301
C18	0.1215 (3)	0.6565 (4)	0.05405 (17)	0.0575
N51	0.98736 (19)	0.8254 (2)	0.84409 (11)	0.0260
C52	0.8857 (2)	0.8460 (3)	0.87017 (12)	0.0252
C53	0.8406 (3)	0.7166 (3)	0.87566 (14)	0.0336
C54	0.8777 (3)	0.6445 (3)	0.82557 (16)	0.0409
C55	0.9977 (3)	0.6930 (3)	0.83000 (16)	0.0368
C56	0.9228 (2)	0.9161 (3)	0.93172 (14)	0.0321
Br57	0.79113 (3)	0.95035 (4)	0.965780 (17)	0.0505
F58	0.89517 (17)	0.66767 (18)	0.93595 (8)	0.0431
S59	1.01369 (6)	0.92488 (6)	0.79362 (3)	0.0270
O60	0.99967 (19)	1.04312 (19)	0.81959 (10)	0.0359
O61	1.12125 (17)	0.8913 (2)	0.78210 (10)	0.0396
C62	0.9077 (2)	0.9106 (2)	0.72098 (13)	0.0245
C63	0.8090 (2)	0.9811 (3)	0.71009 (14)	0.0304
C64	0.7271 (3)	0.9704 (3)	0.65268 (15)	0.0375
C65	0.7413 (3)	0.8908 (3)	0.60586 (15)	0.0368
C66	0.8408 (3)	0.8209 (3)	0.61791 (16)	0.0425
C67	0.9243 (3)	0.8301 (3)	0.67468 (14)	0.0339
C68	0.6513 (4)	0.8793 (4)	0.54353 (18)	0.0586
H21	0.3341	0.6653	0.3427	0.0270*
H31	0.2575	0.5049	0.3827	0.0387*
H42	0.3524	0.3292	0.3428	0.0543*
H41	0.3058	0.4325	0.2925	0.0540*
H52	0.5369	0.4057	0.3644	0.0452*
H51	0.4955	0.4292	0.2897	0.0449*
H61	0.4803	0.7652	0.4200	0.0410*

H62	0.5005	0.6446	0.4620	0.0412*
H131	0.3195	0.8135	0.2438	0.0391*
H141	0.1677	0.8090	0.1529	0.0464*
H161	0.3082	0.5173	0.0903	0.0432*
H171	0.4612	0.5237	0.1794	0.0365*
H182	0.1336	0.5934	0.0256	0.0860*
H181	0.1160	0.7329	0.0321	0.0862*
H183	0.0514	0.6404	0.0652	0.0861*
H521	0.8289	0.8931	0.8399	0.0295*
H531	0.7584	0.7167	0.8706	0.0397*
H542	0.8775	0.5575	0.8323	0.0489*
H541	0.8281	0.6645	0.7841	0.0489*
H552	1.0543	0.6532	0.8642	0.0439*
H551	1.0182	0.6828	0.7903	0.0443*
H561	0.9790	0.8695	0.9628	0.0391*
H562	0.9550	0.9936	0.9237	0.0391*
H631	0.8003	1.0363	0.7414	0.0358*
H641	0.6603	1.0180	0.6451	0.0453*
H661	0.8514	0.7664	0.5869	0.0512*
H671	0.9912	0.7826	0.6819	0.0414*
H682	0.6813	0.8215	0.5191	0.0876*
H681	0.6373	0.9562	0.5228	0.0880*
H683	0.5826	0.8482	0.5512	0.0880*

Atomic displacement parameters (Å^2)

	U^{11}	U^{22}	U^{33}	U^{12}	U^{13}	U^{23}
N1	0.0250 (11)	0.0256 (12)	0.0249 (11)	0.0023 (9)	0.0041 (9)	−0.0013 (9)
C2	0.0209 (12)	0.0254 (13)	0.0220 (12)	0.0016 (11)	0.0036 (10)	0.0027 (10)
C3	0.0285 (15)	0.0350 (16)	0.0305 (15)	−0.0044 (13)	0.0002 (11)	0.0121 (13)
C4	0.060 (2)	0.0272 (16)	0.0379 (17)	−0.0107 (15)	−0.0029 (15)	0.0005 (13)
C5	0.0529 (19)	0.0241 (15)	0.0350 (16)	0.0095 (14)	0.0098 (14)	0.0003 (13)
C6	0.0396 (16)	0.0349 (17)	0.0277 (14)	−0.0003 (14)	0.0091 (12)	−0.0026 (12)
Br7	0.0811 (3)	0.0529 (2)	0.0569 (2)	0.0018 (2)	0.0452 (2)	−0.00943 (19)
F8	0.0479 (11)	0.0452 (11)	0.0312 (9)	−0.0006 (9)	0.0027 (8)	0.0170 (8)
S9	0.0222 (3)	0.0341 (4)	0.0291 (3)	−0.0050 (3)	0.0084 (3)	−0.0026 (3)
O10	0.0498 (13)	0.0321 (12)	0.0397 (12)	−0.0192 (10)	0.0141 (10)	−0.0053 (10)
O11	0.0219 (10)	0.0766 (18)	0.0386 (12)	0.0024 (11)	0.0095 (9)	−0.0017 (12)
C12	0.0239 (13)	0.0255 (14)	0.0262 (13)	0.0019 (11)	0.0100 (10)	0.0051 (11)
C13	0.0347 (15)	0.0281 (14)	0.0382 (16)	0.0070 (13)	0.0169 (13)	0.0056 (13)
C14	0.0281 (15)	0.0423 (18)	0.0477 (18)	0.0095 (14)	0.0140 (13)	0.0181 (16)
C15	0.0265 (15)	0.051 (2)	0.0323 (15)	−0.0057 (14)	0.0042 (12)	0.0186 (15)
C16	0.0418 (17)	0.0392 (18)	0.0266 (14)	−0.0021 (14)	0.0074 (12)	0.0018 (13)
C17	0.0318 (15)	0.0282 (15)	0.0306 (14)	0.0033 (12)	0.0086 (12)	0.0014 (12)

C18	0.0397 (19)	0.082 (3)	0.043 (2)	−0.007 (2)	−0.0035 (15)	0.022 (2)
N51	0.0243 (11)	0.0245 (12)	0.0284 (12)	0.0013 (9)	0.0051 (9)	−0.0003 (9)
C52	0.0239 (13)	0.0243 (14)	0.0252 (13)	0.0002 (11)	0.0023 (10)	0.0000 (11)
C53	0.0308 (15)	0.0342 (16)	0.0323 (15)	−0.0053 (13)	0.0018 (12)	0.0051 (12)
C54	0.058 (2)	0.0222 (15)	0.0389 (17)	−0.0092 (14)	0.0065 (15)	−0.0050 (13)
C55	0.0474 (18)	0.0240 (15)	0.0397 (17)	0.0059 (14)	0.0127 (14)	0.0022 (13)
C56	0.0302 (15)	0.0357 (17)	0.0285 (14)	0.0003 (13)	0.0042 (11)	−0.0065 (12)
Br57	0.0481 (2)	0.0682 (3)	0.03976 (18)	0.00801 (18)	0.01961 (15)	−0.00880 (18)
F58	0.0532 (11)	0.0384 (11)	0.0341 (9)	0.0000 (9)	0.0049 (8)	0.0102 (8)
S59	0.0229 (3)	0.0266 (3)	0.0311 (3)	−0.0038 (3)	0.0061 (3)	−0.0025 (3)
O60	0.0453 (12)	0.0228 (10)	0.0388 (11)	−0.0078 (9)	0.0090 (9)	−0.0051 (9)
O61	0.0220 (10)	0.0538 (14)	0.0429 (12)	−0.0033 (10)	0.0081 (9)	−0.0026 (11)
C62	0.0225 (13)	0.0248 (14)	0.0265 (13)	−0.0013 (11)	0.0070 (10)	0.0036 (11)
C63	0.0294 (14)	0.0331 (16)	0.0306 (15)	0.0050 (12)	0.0113 (11)	0.0017 (12)
C64	0.0269 (15)	0.0433 (19)	0.0419 (17)	0.0050 (13)	0.0080 (13)	0.0134 (14)
C65	0.0350 (16)	0.0379 (17)	0.0337 (16)	−0.0099 (14)	0.0018 (13)	0.0081 (13)
C66	0.053 (2)	0.0348 (18)	0.0369 (17)	−0.0009 (16)	0.0069 (15)	−0.0073 (14)
C67	0.0332 (16)	0.0317 (16)	0.0368 (16)	0.0048 (13)	0.0091 (12)	−0.0033 (13)
C68	0.061 (2)	0.057 (2)	0.043 (2)	−0.018 (2)	−0.0132 (17)	0.0093 (18)

Geometric parameters (Å, º)

N1—C2	1.486 (3)	N51—C52	1.491 (3)
N1—C5	1.484 (4)	N51—C55	1.489 (4)
N1—S9	1.626 (2)	N51—S59	1.632 (2)
C2—C3	1.522 (4)	C52—C53	1.528 (4)
C2—C6	1.512 (4)	C52—C56	1.507 (4)
C2—H21	0.974	C52—H521	0.966
C3—C4	1.501 (5)	C53—C54	1.502 (4)
C3—F8	1.407 (3)	C53—F58	1.413 (3)
C3—H31	0.976	C53—H531	0.966
C4—C5	1.519 (5)	C54—C55	1.518 (5)
C4—H42	0.958	C54—H542	0.961
C4—H41	0.968	C54—H541	0.971
C5—H52	0.969	C55—H552	0.973
C5—H51	0.970	C55—H551	0.964
C6—Br7	1.950 (3)	C56—Br57	1.949 (3)
C6—H61	0.964	C56—H561	0.968
C6—H62	0.972	C56—H562	0.964
S9—O10	1.435 (2)	S59—O60	1.436 (2)
S9—O11	1.428 (2)	S59—O61	1.427 (2)
S9—C12	1.766 (3)	S59—C62	1.765 (3)
C12—C13	1.380 (4)	C62—C63	1.383 (4)
C12—C17	1.387 (4)	C62—C67	1.390 (4)

C13—C14	1.380 (4)	C63—C64	1.383 (4)
C13—H131	0.934	C63—H631	0.935
C14—C15	1.385 (5)	C64—C65	1.382 (5)
C14—H141	0.941	C64—H641	0.935
C15—C16	1.392 (5)	C65—C66	1.388 (5)
C15—C18	1.511 (4)	C65—C68	1.508 (4)
C16—C17	1.388 (4)	C66—C67	1.381 (4)
C16—H161	0.925	C66—H661	0.932
C17—H171	0.923	C67—H671	0.936
C18—H182	0.961	C68—H682	0.953
C18—H181	0.955	C68—H681	0.947
C18—H183	0.952	C68—H683	0.947
C2—N1—C5	110.1 (2)	C52—N51—C55	110.1 (2)
C2—N1—S9	118.79 (18)	C52—N51—S59	118.38 (18)
C5—N1—S9	118.56 (19)	C55—N51—S59	117.80 (19)
N1—C2—C3	103.7 (2)	N51—C52—C53	103.5 (2)
N1—C2—C6	108.5 (2)	N51—C52—C56	109.2 (2)
C3—C2—C6	115.4 (2)	C53—C52—C56	115.5 (2)
N1—C2—H21	110.8	N51—C52—H521	109.1
C3—C2—H21	108.1	C53—C52—H521	110.0
C6—C2—H21	110.1	C56—C52—H521	109.3
C2—C3—C4	103.9 (2)	C52—C53—C54	104.5 (2)
C2—C3—F8	109.5 (2)	C52—C53—F58	109.4 (2)
C4—C3—F8	108.3 (3)	C54—C53—F58	108.7 (3)
C2—C3—H31	112.2	C52—C53—H531	111.3
C4—C3—H31	112.9	C54—C53—H531	113.8
F8—C3—H31	109.9	F58—C53—H531	108.9
C3—C4—C5	103.0 (3)	C53—C54—C55	103.0 (2)
C3—C4—H42	111.7	C53—C54—H542	113.3
C5—C4—H42	112.1	C55—C54—H542	112.0
C3—C4—H41	110.4	C53—C54—H541	109.3
C5—C4—H41	110.2	C55—C54—H541	109.2
H42—C4—H41	109.3	H542—C54—H541	109.8
C4—C5—N1	102.8 (2)	C54—C55—N51	102.9 (2)
C4—C5—H52	110.7	C54—C55—H552	111.1
N1—C5—H52	109.5	N51—C55—H552	110.8
C4—C5—H51	112.5	C54—C55—H551	111.1
N1—C5—H51	110.6	N51—C55—H551	110.5
H52—C5—H51	110.5	H552—C55—H551	110.2
C2—C6—Br7	110.2 (2)	C52—C56—Br57	110.50 (19)
C2—C6—H61	110.2	C52—C56—H561	110.4
Br7—C6—H61	106.3	Br57—C56—H561	108.9
C2—C6—H62	110.9	C52—C56—H562	109.0
Br7—C6—H62	109.2	Br57—C56—H562	107.7

H61—C6—H62	110.0	H561—C56—H562	110.2
N1—S9—O10	106.12 (12)	N51—S59—O60	105.71 (12)
N1—S9—O11	106.81 (14)	N51—S59—O61	106.75 (13)
O10—S9—O11	119.82 (15)	O60—S59—O61	120.19 (14)
N1—S9—C12	108.56 (12)	N51—S59—C62	108.86 (12)
O10—S9—C12	107.25 (14)	O60—S59—C62	107.49 (13)
O11—S9—C12	107.88 (13)	O61—S59—C62	107.46 (13)
S9—C12—C13	119.7 (2)	S59—C62—C63	119.7 (2)
S9—C12—C17	119.7 (2)	S59—C62—C67	119.9 (2)
C13—C12—C17	120.5 (3)	C63—C62—C67	120.3 (3)
C12—C13—C14	119.7 (3)	C62—C63—C64	119.3 (3)
C12—C13—H131	119.8	C62—C63—H631	119.0
C14—C13—H131	120.5	C64—C63—H631	121.7
C13—C14—C15	121.0 (3)	C63—C64—C65	121.6 (3)
C13—C14—H141	119.8	C63—C64—H641	119.5
C15—C14—H141	119.1	C65—C64—H641	118.9
C14—C15—C16	118.6 (3)	C64—C65—C66	118.1 (3)
C14—C15—C18	121.0 (3)	C64—C65—C68	121.3 (3)
C16—C15—C18	120.4 (3)	C66—C65—C68	120.7 (3)
C15—C16—C17	120.9 (3)	C65—C66—C67	121.6 (3)
C15—C16—H161	119.4	C65—C66—H661	119.1
C17—C16—H161	119.7	C67—C66—H661	119.4
C16—C17—C12	119.1 (3)	C62—C67—C66	119.1 (3)
C16—C17—H171	119.9	C62—C67—H671	120.4
C12—C17—H171	120.9	C66—C67—H671	120.4
C15—C18—H182	110.4	C65—C68—H682	105.6
C15—C18—H181	108.9	C65—C68—H681	110.6
H182—C18—H181	107.9	H682—C68—H681	111.6
C15—C18—H183	111.2	C65—C68—H683	109.2
H182—C18—H183	108.8	H682—C68—H683	109.5
H181—C18—H183	109.7	H681—C68—H683	110.2

Hydrogen-bond geometry (Å, º)

D—H···*A*	*D*—H	H···*A*	*D*···*A*	*D*—H···*A*
C6—H61···O10	0.96	2.45	3.087 (5)	123
C17—H171···O10^{i}	0.92	2.53	3.254 (5)	135.)
C52—H521···O11^{ii}	0.97	2.58	3.376 (5)	140
C56—H562···O60	0.96	2.52	3.143 (5)	123

Symmetry codes: (i) −*x*+1, *y*−1/2, −*z*+1/2; (ii) *x*, −*y*+3/2, *z*+1/2.

(±) 3-fluoro-2-(iodomethyl)-2-methyl-1-[(4-methylphenyl)sulfonyl]pyrrolidine (103): (CCDC-896057)

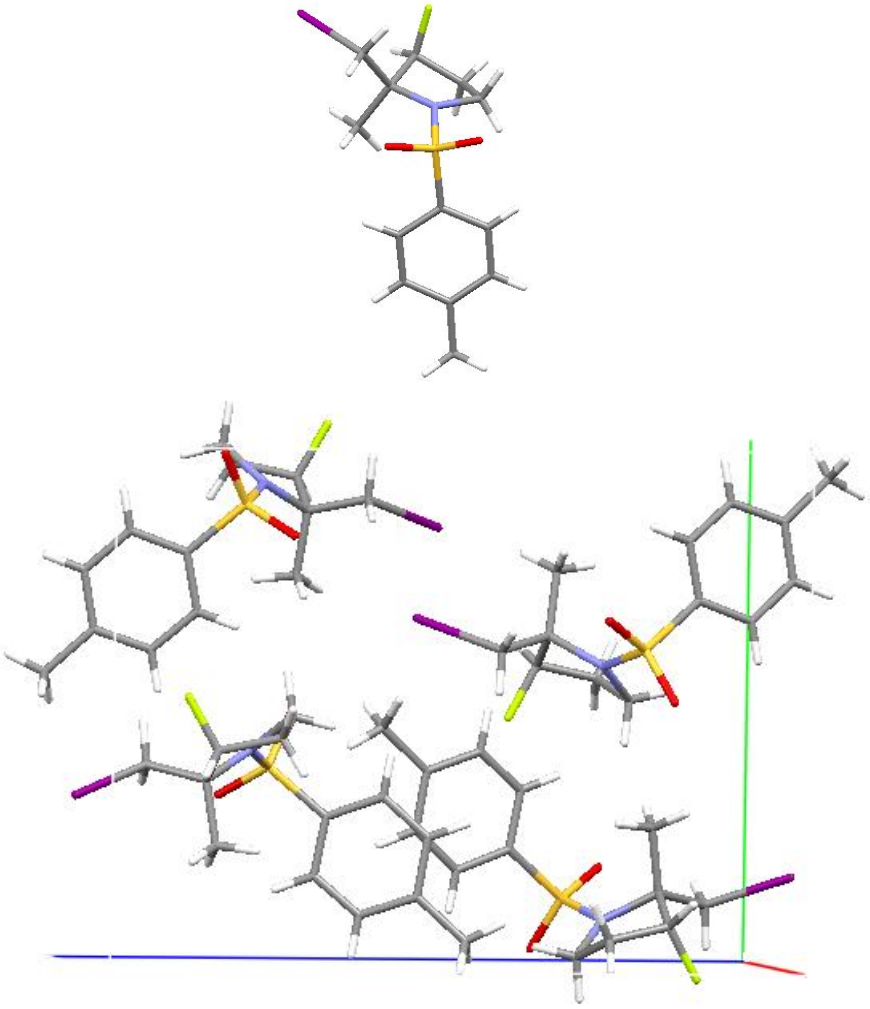

Crystal data

$C_{13}H_{17}FINO_2S$
M_r = 397.25
Orthorhombic, $P2_12_12_1$
Hall symbol: P 2ac 2ab
a = 7.5704 (1) Å
b = 12.0552 (1) Å
c = 16.3755 (2) Å
V = 1494.47 (3) Å^3
Z = 4
F(000) = 784

D_x = 1.765 Mg m^{-3}
Melting point: not measured K
Mo $K\alpha$ radiation, λ = 0.71073 Å
Cell parameters from 1965 reflections
θ = 5–27°
μ = 2.29 mm^{-1}
T = 150 K
Plate, Clear_pale_colorles
0.45 × 0.30 × 0.25 mm

Data collection

Nonius KappaCCD

3373 reflections with $I > 2.0\sigma(I)$

diffractometer

Graphite monochromator

ω scans

Absorption correction: Multi-scan *DENZO*/*SCALEPACK* (Otwinowski & Minor, 1997)

T_{min} = 0.50, T_{max} = 0.56

26115 measured reflections

3417 independent reflections

R_{int} = 0.028

θ_{max} = 27.5°, θ_{min} = 5.2°

h = −9→9

k = −15→15

l = −21→21

Refinement

Refinement on F^2

Least-squares matrix: Full

$R[F^2 > 2\sigma(F^2)]$ = 0.020

$wR(F^2)$ = 0.049

S = 1.00

3396 reflections

173 parameters

0 restraints

Primary atom site location: Structure-invariant direct methods

Hydrogen site location: Difference Fourier map

H-atom parameters constrained

Method, part 1, Chebychev polynomial, (Watkin, 1994, *P*rince, 1982) [*w*eight] = 1.0/[A_0*T_0(x) + A_1*T_1(x) ⋯ + A_{n-1}]*T_{n-1}(x)] where A_i are the Chebychev coefficients listed below and x = *F* /*F*max Method = Robust Weighting (*P*rince, 1982) W = [*w*eight] * [1-(delta*F*/6*sigma*F*)^2]^2 A_i are: 39.6 65.5 42.3 20.3 6.58

$(\Delta/\sigma)_{max}$ = 0.006

$\Delta\rho_{max}$ = 0.59 e Å^{-3}

$\Delta\rho_{min}$ = −0.70 e Å^{-3}

Absolute structure: Flack (1983), 1465 Friedel-pairs

Flack parameter: 0.499 (13)

Fractional atomic coordinates and isotropic or equivalent isotropic displacement parameters (Å^2)

	x	*y*	*z*	U_{iso}*/U_{eq}
N1	0.7236 (2)	0.41717 (16)	0.77752 (12)	0.0219
C2	0.8131 (3)	0.36148 (17)	0.84865 (13)	0.0211
C3	0.9922 (3)	0.4217 (2)	0.84822 (15)	0.0275
C4	1.0289 (3)	0.4479 (3)	0.75984 (17)	0.0340
C5	0.8486 (3)	0.4846 (2)	0.72857 (16)	0.0328
C6	0.7048 (3)	0.38731 (19)	0.92476 (13)	0.0233
I7	0.823304 (19)	0.330460 (12)	1.036945 (8)	0.0269
C8	0.8393 (4)	0.23672 (19)	0.83590 (15)	0.0283
F9	0.9762 (2)	0.52316 (13)	0.89014 (11)	0.0388
S10	0.53865 (7)	0.38052 (4)	0.73495 (3)	0.0196
O11	0.4372 (2)	0.32336 (15)	0.79606 (10)	0.0257
O12	0.4691 (2)	0.47902 (14)	0.69761 (10)	0.0256

C13	0.5819 (3)	0.28651 (19)	0.65473 (14)	0.0209
C14	0.5786 (3)	0.1728 (2)	0.67071 (13)	0.0230
C15	0.6132 (3)	0.09907 (18)	0.60819 (15)	0.0240
C16	0.6481 (3)	0.13588 (19)	0.52865 (14)	0.0258
C17	0.6496 (4)	0.2496 (2)	0.51408 (14)	0.0305
C18	0.6171 (3)	0.3261 (2)	0.57651 (15)	0.0274
C19	0.6805 (4)	0.0527 (2)	0.46171 (17)	0.0369
H31	1.0865	0.3770	0.8740	0.0323*
H41	1.1199	0.5037	0.7542	0.0402*
H42	1.0692	0.3804	0.7325	0.0401*
H51	0.8331	0.5657	0.7359	0.0390*
H52	0.8390	0.4661	0.6720	0.0393*
H61	0.6911	0.4665	0.9295	0.0282*
H62	0.5880	0.3520	0.9205	0.0275*
H81	0.9182	0.2076	0.8763	0.0429*
H82	0.8928	0.2281	0.7828	0.0433*
H83	0.7280	0.2005	0.8365	0.0427*
H141	0.5504	0.1463	0.7235	0.0290*
H151	0.6130	0.0230	0.6184	0.0289*
H171	0.6668	0.2769	0.4606	0.0361*
H181	0.6173	0.4021	0.5662	0.0327*
H191	0.7198	0.0865	0.4126	0.0558*
H192	0.7675	−0.0016	0.4767	0.0560*
H193	0.5733	0.0148	0.4481	0.0559*

Atomic displacement parameters (Å^2)

	U^{11}	U^{22}	U^{33}	U^{12}	U^{13}	U^{23}
N1	0.0208 (9)	0.0243 (9)	0.0205 (9)	−0.0025 (7)	−0.0026 (7)	0.0063 (7)
C2	0.0206 (9)	0.0258 (9)	0.0170 (9)	0.0003 (8)	−0.0040 (8)	0.0021 (7)
C3	0.0217 (11)	0.0332 (12)	0.0275 (11)	−0.0030 (9)	−0.0013 (9)	0.0031 (9)
C4	0.0240 (11)	0.0479 (15)	0.0301 (13)	−0.0047 (11)	0.0000 (10)	0.0095 (11)
C5	0.0291 (13)	0.0412 (13)	0.0282 (12)	−0.0083 (11)	−0.0023 (9)	0.0111 (10)
C6	0.0236 (11)	0.0280 (10)	0.0184 (9)	0.0025 (8)	−0.0032 (9)	0.0024 (8)
I7	0.02899 (8)	0.03356 (8)	0.01806 (7)	0.00229 (6)	−0.00308 (6)	0.00042 (5)
C8	0.0327 (12)	0.0272 (10)	0.0252 (10)	0.0061 (10)	−0.0038 (10)	−0.0011 (8)
F9	0.0393 (8)	0.0361 (8)	0.0409 (9)	−0.0141 (7)	−0.0038 (7)	−0.0065 (7)
S10	0.0194 (2)	0.0222 (2)	0.0172 (2)	0.00126 (19)	−0.00125 (18)	−0.00092 (18)
O11	0.0213 (7)	0.0354 (8)	0.0204 (7)	−0.0028 (7)	0.0021 (6)	−0.0005 (7)
O12	0.0293 (8)	0.0256 (8)	0.0219 (8)	0.0087 (7)	−0.0065 (7)	−0.0018 (6)
C13	0.0215 (10)	0.0217 (9)	0.0196 (10)	0.0012 (8)	−0.0007 (8)	−0.0002 (8)
C14	0.0245 (10)	0.0244 (10)	0.0200 (10)	−0.0014 (9)	−0.0006 (7)	0.0016 (9)
C15	0.0273 (10)	0.0213 (9)	0.0235 (10)	−0.0033 (8)	−0.0036 (9)	−0.0027 (9)
C16	0.0228 (10)	0.0316 (10)	0.0231 (11)	−0.0002 (8)	0.0020 (9)	−0.0052 (9)

C17	0.0393 (14)	0.0339 (11)	0.0182 (10)	−0.0001 (10)	0.0049 (9)	0.0013 (8)
C18	0.0366 (11)	0.0240 (10)	0.0216 (10)	−0.0007 (10)	0.0021 (9)	0.0026 (9)
C19	0.0399 (13)	0.0416 (13)	0.0291 (12)	0.0004 (12)	0.0024 (15)	−0.0143 (10)

Geometric parameters (Å, º)

N1—C2	1.506 (3)	C8—H83	0.949
N1—C5	1.483 (3)	S10—O11	1.4373 (17)
N1—S10	1.6251 (19)	S10—O12	1.4356 (16)
C2—C3	1.538 (3)	S10—C13	1.766 (2)
C2—C6	1.524 (3)	C13—C14	1.395 (3)
C2—C8	1.531 (3)	C13—C18	1.393 (3)
C3—C4	1.507 (3)	C14—C15	1.381 (3)
C3—F9	1.407 (3)	C14—H141	0.945
C3—H31	0.989	C15—C16	1.401 (3)
C4—C5	1.524 (4)	C15—H151	0.932
C4—H41	0.968	C16—C17	1.391 (4)
C4—H42	0.977	C16—C19	1.506 (3)
C5—H51	0.992	C17—C18	1.399 (3)
C5—H52	0.955	C17—H171	0.944
C6—I7	2.156 (2)	C18—H181	0.932
C6—H61	0.963	C19—H191	0.950
C6—H62	0.984	C19—H192	0.960
C8—H81	0.958	C19—H193	0.957
C8—H82	0.965		
C2—N1—C5	112.03 (17)	H81—C8—H82	108.8
C2—N1—S10	126.76 (15)	C2—C8—H83	109.6
C5—N1—S10	117.84 (15)	H81—C8—H83	112.2
N1—C2—C3	100.53 (17)	H82—C8—H83	109.4
N1—C2—C6	107.42 (17)	N1—S10—O11	106.98 (9)
C3—C2—C6	112.42 (18)	N1—S10—O12	105.87 (10)
N1—C2—C8	113.00 (17)	O11—S10—O12	119.82 (11)
C3—C2—C8	110.5 (2)	N1—S10—C13	109.51 (10)
C6—C2—C8	112.44 (18)	O11—S10—C13	108.02 (11)
C2—C3—C4	105.41 (19)	O12—S10—C13	106.38 (10)
C2—C3—F9	109.40 (19)	S10—C13—C14	119.17 (17)
C4—C3—F9	107.6 (2)	S10—C13—C18	120.00 (18)
C2—C3—H31	112.1	C14—C13—C18	120.8 (2)
C4—C3—H31	113.0	C13—C14—C15	119.3 (2)
F9—C3—H31	109.1	C13—C14—H141	120.5
C3—C4—C5	102.6 (2)	C15—C14—H141	120.2
C3—C4—H41	111.6	C14—C15—C16	121.4 (2)
C5—C4—H41	113.8	C14—C15—H151	120.0
C3—C4—H42	108.9	C16—C15—H151	118.6

C5—C4—H42	111.5	C15—C16—C17	118.2 (2)
H41—C4—H42	108.3	C15—C16—C19	119.8 (2)
C4—C5—N1	103.35 (18)	C17—C16—C19	122.0 (2)
C4—C5—H51	110.6	C16—C17—C18	121.5 (2)
N1—C5—H51	113.5	C16—C17—H171	120.2
C4—C5—H52	109.0	C18—C17—H171	118.2
N1—C5—H52	110.4	C17—C18—C13	118.7 (2)
H51—C5—H52	109.8	C17—C18—H181	121.0
C2—C6—I7	114.09 (14)	C13—C18—H181	120.3
C2—C6—H61	109.1	C16—C19—H191	112.4
I7—C6—H61	106.9	C16—C19—H192	112.3
C2—C6—H62	109.7	H191—C19—H192	107.1
I7—C6—H62	107.3	C16—C19—H193	110.4
H61—C6—H62	109.7	H191—C19—H193	105.9
C2—C8—H81	110.3	H192—C19—H193	108.5
C2—C8—H82	106.4		

Hydrogen-bond geometry (Å, º)

D—H···*A*	*D*—H	H···*A*	*D*···*A*	*D*—H···*A*
C6—H62···O11	0.98	2.36	3.023 (3)	124
C14—H141···O12^{i}	0.95	2.40	3.200 (3)	142

Symmetry code: (i) −*x*+1, *y*−1/2, −*z*+3/2.

(±) 3-fluoro-2-(iodomethyl)-4,4-dimethyl-1-[(4-methylphenyl)sulfonyl]pyrrolidine (104): (CCDC-896058)

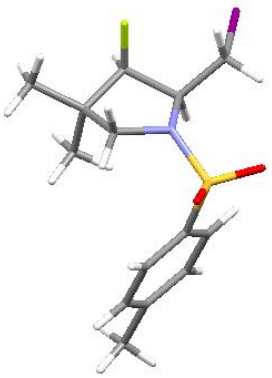

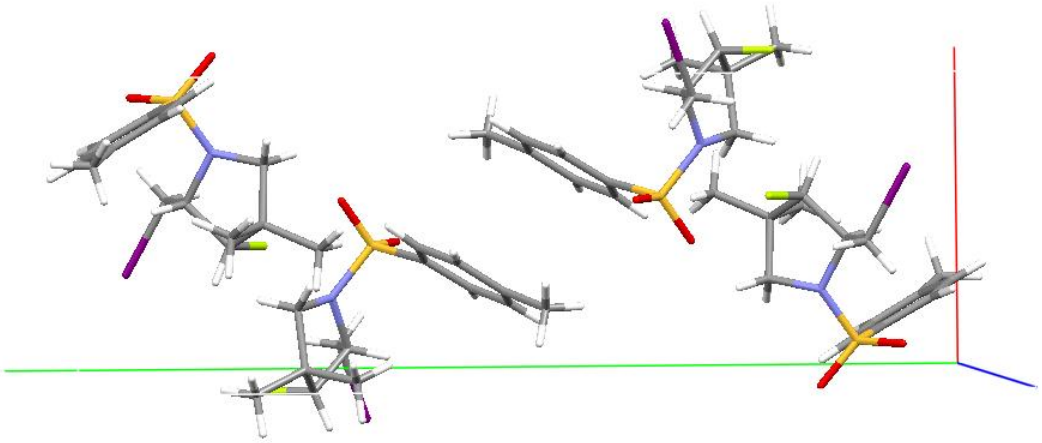

Crystal data

$C_{14}H_{19}FINO_2S$	$F(000)$ = 816
M_r = 411.28	D_x = 1.694 Mg m^{-3}
Monoclinic, $P2_1/n$	Melting point: not measured K
Hall symbol: -P 2yn	Mo $K\alpha$ radiation, λ = 0.71073 Å
a = 7.8150 (1) Å	Cell parameters from 4624 reflections
b = 24.2745 (3) Å	θ = 1–30°
c = 8.5288 (1) Å	μ = 2.13 mm^{-1}
β = 94.7816 (6)°	T = 150 K
V = 1612.33 (3) Å^3	Plate, Clear_pale_colorless
Z = 4	0.40 × 0.33 × 0.31 mm

Data collection

Nonius KappaCCD diffractometer	4025 reflections with $I > 2.0\sigma(I)$
Graphite monochromator	R_{int} = 0.015
ω scans	θ_{max} = 30.0°, θ_{min} = 1.7°
Absorption correction: Multi-scan *DENZO*/*SCALEPACK* (Otwinowski & Minor, 1997)	h = −10→11
T_{min} = 0.45, T_{max} = 0.52	k = −34→33
21748 measured reflections	l = −12→12
4669 independent reflections	

Refinement

Refinement on F^2	Primary atom site location: Structure-invariant direct methods
Least-squares matrix: Full	Hydrogen site location: Difference Fourier map
$R[F^2 > 2\sigma(F^2)]$ = 0.024	H-atom parameters constrained
$wR(F^2)$ = 0.066	Method, part 1, Chebychev polynomial, (Watkin, 1994, *P*rince, 1982) [*w*eight] = 1.0/[A_0*T_0(x) +

$A_1*T_1(x) \cdots + A_{n-1}]*T_{n-1}(x)]$
where A_i are the Chebychev coefficients listed below and x = *F* /*F*max Method = Robust Weighting (*P*rince, 1982) W = [*w*eight] * [1-(delta*F*/6*sigma*F*)^2]^2 A_i are: 41.6 68.4 42.5 19.1 4.92

S = 1.00
4648 reflections
181 parameters
0 restraints

$(\Delta/\sigma)_{max}$ = 0.005
$\Delta\rho_{max}$ = 0.51 e Å^{-3}
$\Delta\rho_{min}$ = −0.96 e Å^{-3}

Fractional atomic coordinates and isotropic or equivalent isotropic displacement parameters (Å^2)

	x	*y*	*z*	U_{iso}*/U_{eq}
N1	0.23814 (17)	0.66792 (6)	0.18511 (16)	0.0208
C2	0.07096 (19)	0.64511 (7)	0.11775 (18)	0.0194
C3	−0.0574 (2)	0.68691 (8)	0.1731 (2)	0.0257
C4	0.0220 (2)	0.70807 (8)	0.3308 (2)	0.0287
C5	0.2118 (2)	0.71258 (7)	0.2989 (2)	0.0286
C6	0.0682 (2)	0.63999 (9)	−0.0600 (2)	0.0278
I7	−0.171544 (16)	0.604683 (5)	−0.152943 (14)	0.0325
F8	−0.0672 (2)	0.73073 (6)	0.06536 (16)	0.0456
C9	−0.0529 (4)	0.76327 (11)	0.3777 (3)	0.0538
C10	−0.0055 (3)	0.66486 (10)	0.4574 (2)	0.0363
S11	0.40408 (5)	0.627510 (19)	0.21756 (5)	0.0245
O12	0.40402 (19)	0.59141 (7)	0.08459 (16)	0.0355
O13	0.54811 (17)	0.66259 (7)	0.25942 (17)	0.0371
C14	0.3695 (2)	0.58705 (8)	0.3835 (2)	0.0234
C15	0.2801 (3)	0.53757 (7)	0.3631 (2)	0.0284
C16	0.2416 (3)	0.50775 (8)	0.4947 (2)	0.0309
C17	0.2912 (2)	0.52636 (8)	0.6462 (2)	0.0283
C18	0.3840 (2)	0.57539 (8)	0.6641 (2)	0.0270
C19	0.4235 (2)	0.60599 (7)	0.5341 (2)	0.0248
C20	0.2467 (3)	0.49380 (9)	0.7871 (3)	0.0383
H21	0.0493	0.6093	0.1629	0.0224*
H31	−0.1715	0.6710	0.1777	0.0306*
H51	0.2363	0.7475	0.2519	0.0344*
H52	0.2854	0.7077	0.3937	0.0344*
H61	0.0820	0.6753	−0.1078	0.0331*
H62	0.1579	0.6158	−0.0868	0.0339*
H92	0.0076	0.7762	0.4748	0.0804*
H93	−0.0442	0.7904	0.2959	0.0809*
H91	−0.1740	0.7581	0.3939	0.0804*
H101	0.0510	0.6766	0.5568	0.0536*
H103	−0.1264	0.6607	0.4696	0.0538*

H102	0.0412	0.6295	0.4313	0.0536*
H151	0.2477	0.5243	0.2617	0.0342*
H161	0.1818	0.4746	0.4792	0.0374*
H181	0.4222	0.5879	0.7642	0.0322*
H191	0.4894	0.6377	0.5488	0.0300*
H202	0.3255	0.5011	0.8747	0.0585*
H201	0.1371	0.5031	0.8157	0.0588*
H203	0.2497	0.4556	0.7641	0.0588*

Atomic displacement parameters (Å^2)

	U^{11}	U^{22}	U^{33}	U^{12}	U^{13}	U^{23}
N1	0.0155 (5)	0.0266 (6)	0.0201 (6)	−0.0033 (5)	−0.0003 (4)	−0.0009 (5)
C2	0.0149 (6)	0.0259 (7)	0.0173 (6)	−0.0027 (5)	−0.0001 (5)	0.0011 (5)
C3	0.0220 (7)	0.0331 (8)	0.0218 (7)	0.0067 (6)	−0.0002 (6)	0.0026 (6)
C4	0.0308 (8)	0.0313 (8)	0.0238 (7)	0.0083 (7)	0.0013 (6)	−0.0038 (6)
C5	0.0312 (8)	0.0258 (8)	0.0280 (8)	−0.0025 (6)	−0.0028 (7)	−0.0059 (6)
C6	0.0204 (7)	0.0447 (10)	0.0182 (7)	−0.0079 (7)	0.0004 (6)	−0.0035 (6)
I7	0.02845 (7)	0.04005 (8)	0.02730 (7)	−0.00950 (5)	−0.00754 (5)	−0.00278 (5)
F8	0.0600 (8)	0.0407 (7)	0.0342 (6)	0.0199 (6)	−0.0075 (6)	0.0108 (5)
C9	0.0628 (16)	0.0460 (13)	0.0520 (14)	0.0261 (12)	0.0016 (12)	−0.0157 (11)
C10	0.0357 (10)	0.0530 (12)	0.0210 (8)	0.0082 (9)	0.0085 (7)	0.0032 (8)
S11	0.01478 (16)	0.0388 (2)	0.01999 (17)	0.00136 (14)	0.00163 (13)	0.00053 (15)
O12	0.0306 (7)	0.0525 (8)	0.0239 (6)	0.0130 (6)	0.0049 (5)	−0.0050 (6)
O13	0.0163 (5)	0.0624 (10)	0.0323 (7)	−0.0096 (6)	−0.0002 (5)	0.0074 (7)
C14	0.0195 (7)	0.0286 (7)	0.0216 (7)	0.0051 (6)	−0.0002 (5)	−0.0013 (6)
C15	0.0319 (8)	0.0263 (8)	0.0262 (8)	0.0037 (6)	−0.0019 (6)	−0.0040 (6)
C16	0.0351 (9)	0.0231 (7)	0.0341 (9)	0.0027 (7)	0.0011 (7)	0.0002 (7)
C17	0.0256 (8)	0.0296 (8)	0.0298 (8)	0.0079 (6)	0.0034 (6)	0.0051 (7)
C18	0.0241 (7)	0.0354 (9)	0.0209 (7)	0.0034 (6)	−0.0013 (6)	0.0000 (6)
C19	0.0206 (7)	0.0318 (8)	0.0213 (7)	−0.0006 (6)	−0.0022 (6)	−0.0017 (6)
C20	0.0423 (11)	0.0364 (10)	0.0371 (10)	0.0055 (8)	0.0078 (8)	0.0109 (8)

Geometric parameters (Å, º)

N1—C2	1.490 (2)	C10—H101	0.966
N1—C5	1.481 (2)	C10—H103	0.965
N1—S11	1.6311 (15)	C10—H102	0.967
C2—C3	1.529 (2)	S11—O12	1.4332 (15)
C2—C6	1.519 (2)	S11—O13	1.4326 (14)
C2—H21	0.972	S11—C14	1.7620 (18)
C3—C4	1.523 (2)	C14—C15	1.393 (3)
C3—F8	1.404 (2)	C14—C19	1.396 (2)
C3—H31	0.976	C15—C16	1.389 (3)
C4—C5	1.534 (3)	C15—H151	0.939

C4—C9	1.529 (3)	C16—C17	1.393 (3)
C4—C10	1.533 (3)	C16—H161	0.935
C5—H51	0.963	C17—C18	1.395 (3)
C5—H52	0.959	C17—C20	1.503 (3)
C6—I7	2.1506 (17)	C18—C19	1.391 (2)
C6—H61	0.959	C18—H181	0.932
C6—H62	0.957	C19—H191	0.928
C9—H92	0.971	C20—H202	0.945
C9—H93	0.966	C20—H201	0.938
C9—H91	0.976	C20—H203	0.947
C2—N1—C5	111.08 (13)	H93—C9—H91	108.5
C2—N1—S11	120.08 (11)	C4—C10—H101	109.5
C5—N1—S11	118.75 (11)	C4—C10—H103	110.1
N1—C2—C3	102.18 (13)	H101—C10—H103	108.5
N1—C2—C6	110.76 (12)	C4—C10—H102	111.6
C3—C2—C6	114.02 (14)	H101—C10—H102	108.1
N1—C2—H21	110.9	H103—C10—H102	108.9
C3—C2—H21	109.4	N1—S11—O12	106.60 (8)
C6—C2—H21	109.5	N1—S11—O13	106.37 (9)
C2—C3—C4	105.50 (13)	O12—S11—O13	120.60 (9)
C2—C3—F8	107.60 (14)	N1—S11—C14	107.37 (7)
C4—C3—F8	108.58 (16)	O12—S11—C14	107.75 (9)
C2—C3—H31	112.0	O13—S11—C14	107.52 (8)
C4—C3—H31	113.9	S11—C14—C15	119.30 (13)
F8—C3—H31	109.0	S11—C14—C19	120.04 (14)
C3—C4—C5	101.33 (14)	C15—C14—C19	120.58 (16)
C3—C4—C9	112.97 (17)	C14—C15—C16	119.26 (16)
C5—C4—C9	112.37 (19)	C14—C15—H151	120.4
C3—C4—C10	108.70 (16)	C16—C15—H151	120.4
C5—C4—C10	111.60 (16)	C15—C16—C17	121.19 (18)
C9—C4—C10	109.63 (18)	C15—C16—H161	118.3
C4—C5—N1	104.66 (14)	C17—C16—H161	120.5
C4—C5—H51	111.4	C16—C17—C18	118.70 (17)
N1—C5—H51	109.1	C16—C17—C20	120.39 (19)
C4—C5—H52	111.3	C18—C17—C20	120.91 (18)
N1—C5—H52	110.9	C17—C18—C19	121.08 (16)
H51—C5—H52	109.5	C17—C18—H181	120.2
C2—C6—I7	109.88 (11)	C19—C18—H181	118.7
C2—C6—H61	111.0	C14—C19—C18	119.17 (17)
I7—C6—H61	109.0	C14—C19—H191	121.3
C2—C6—H62	109.8	C18—C19—H191	119.5
I7—C6—H62	107.5	C17—C20—H202	110.7
H61—C6—H62	109.6	C17—C20—H201	111.0
C4—C9—H92	109.8	H202—C20—H201	107.3

C4—C9—H93	110.9	C17—C20—H203	109.7
H92—C9—H93	109.7	H202—C20—H203	108.8
C4—C9—H91	108.7	H201—C20—H203	109.1
H92—C9—H91	109.3		

Hydrogen-bond geometry (Å, º)

D—H···*A*	*D*—H	H···*A*	*D*···*A*	*D*—H···*A*
C3—H31···O13^{i}	0.98	2.36	3.283 (3)	157
C6—H62···O12	0.96	2.39	3.043 (3)	125

Symmetry code: (i) *x*−1, *y*, *z*.

(±) (*syn,syn*)-5-(benzyloxymethyl)-3-fluoro-2-(iodomethyl)-1-tosylpyrrolidine (*syn,syn*-106):
(CCDC-896059)

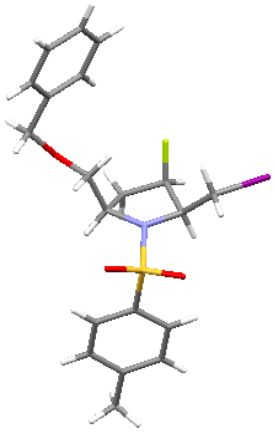

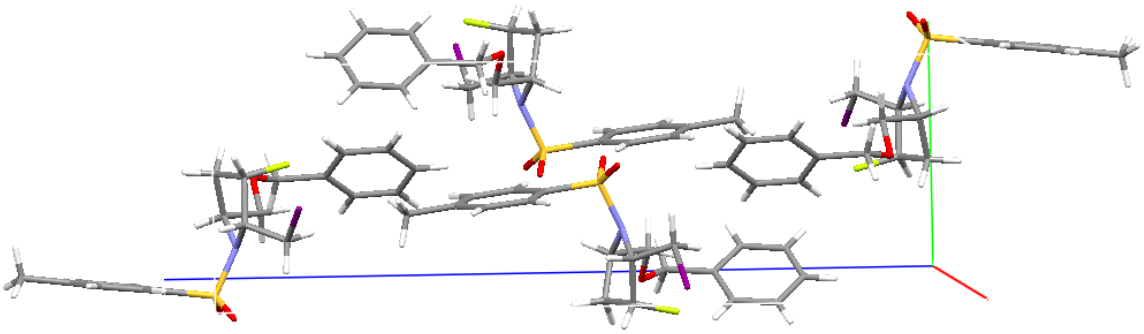

Crystal data

$C_{20}H_{23}FINO_3S$
M_r = 503.38

$F(000)$ = 1008
D_x = 1.615 Mg m^{-3}

Monoclinic, $P2_1/c$
Hall symbol: -P 2ybc
a = 11.6035 (2) Å
b = 7.6096 (2) Å
c = 23.8340 (6) Å
β = 100.2762 (8)°
V = 2070.74 (8) Å^3
Z = 4

Melting point: not measured K
Mo $K\alpha$ radiation, λ = 0.71073 Å
Cell parameters from 4689 reflections
θ = 5–28°
μ = 1.68 mm^{-1}
T = 150 K
Plate, Clear_pale_colourless
0.26 × 0.17 × 0.06 mm

Data collection

Nonius KappaCCD diffractometer
Graphite monochromator
ω scans
Absorption correction: Multi-scan *DENZO*/*SCALEPACK* (Otwinowski & Minor, 1997)
T_{min} = 0.77, T_{max} = 0.90
22389 measured reflections
4876 independent reflections

3566 reflections with $I > 2.0\sigma(I)$
R_{int} = 0.033
θ_{max} = 27.9°, θ_{min} = 5.1°
h = −15→15
k = −9→9
l = −31→31

Refinement

Refinement on F^2
Least-squares matrix: Full
$R[F^2 > 2\sigma(F^2)]$ = 0.059
$wR(F^2)$ = 0.106
S = 1.00
4874 reflections
244 parameters
0 restraints

Primary atom site location: Structure-invariant direct methods
Hydrogen site location: Difference Fourier map
H-atom parameters constrained
Method, part 1, Chebychev polynomial, (Watkin, 1994, *P*rince, 1982) [*w*eight] = 1.0/[A_0*T_0(x) + A_1*T_1(x) ⋯ + A_{n-1}]*T_{n-1}(x)] where A_i are the Chebychev coefficients listed below and x = F /Fmax Method = Robust Weighting (*P*rince, 1982) W = [*w*eight] * [1-(delta$F$/6*sigma$F$)^2]^2 A_i are: 11.7 15.0 6.80 1.51
$(\Delta/\sigma)_{max}$ = 0.001
$\Delta\rho_{max}$ = 1.40 e Å^{-3}
$\Delta\rho_{min}$ = −2.00 e Å^{-3}

Fractional atomic coordinates and isotropic or equivalent isotropic displacement parameters (Å^2)

	x	*y*	*z*	U_{iso}*/U_{eq}
N1	0.7213 (3)	0.2730 (5)	0.45136 (14)	0.0273
C2	0.8274 (4)	0.1666 (7)	0.44729 (19)	0.0338
C3	0.7821 (4)	−0.0215 (7)	0.44347 (19)	0.0378

C4	0.6788 (4)	−0.0212 (7)	0.4734 (2)	0.0360
C5	0.6213 (4)	0.1590 (6)	0.45982 (18)	0.0302
C6	0.8802 (4)	0.2263 (8)	0.39657 (19)	0.0408
I7	1.03362 (3)	0.07811 (8)	0.391134 (16)	0.0668
F8	0.7417 (3)	−0.0628 (5)	0.38550 (12)	0.0527
C9	0.5311 (4)	0.1630 (6)	0.40537 (18)	0.0316
O10	0.4464 (3)	0.0289 (4)	0.40919 (13)	0.0338
C11	0.3399 (4)	0.0539 (7)	0.37019 (18)	0.0350
C12	0.3508 (4)	0.0419 (7)	0.30789 (18)	0.0324
C13	0.2735 (4)	0.1341 (7)	0.2673 (2)	0.0410
C14	0.2805 (5)	0.1214 (8)	0.2098 (2)	0.0506
C15	0.3650 (5)	0.0168 (8)	0.1932 (2)	0.0510
C16	0.4428 (5)	−0.0749 (9)	0.2331 (2)	0.0515
C17	0.4352 (4)	−0.0636 (8)	0.29050 (19)	0.0402
S18	0.73434 (10)	0.46706 (16)	0.48123 (5)	0.0321
O19	0.8349 (3)	0.5470 (5)	0.46461 (14)	0.0452
O20	0.6215 (3)	0.5469 (5)	0.46726 (14)	0.0396
C21	0.7652 (4)	0.4369 (6)	0.55593 (18)	0.0318
C22	0.8795 (4)	0.4161 (8)	0.5832 (2)	0.0465
C23	0.9020 (5)	0.3960 (9)	0.6426 (2)	0.0560
C24	0.8130 (5)	0.3924 (7)	0.6735 (2)	0.0478
C25	0.6989 (5)	0.4113 (8)	0.6450 (2)	0.0474
C26	0.6739 (4)	0.4339 (7)	0.58603 (19)	0.0378
C27	0.8376 (7)	0.3664 (9)	0.7377 (2)	0.0726
H21	0.8853	0.1786	0.4817	0.0408*
H31	0.8435	−0.1045	0.4605	0.0450*
H41	0.7064	−0.0328	0.5149	0.0432*
H42	0.6247	−0.1166	0.4603	0.0432*
H51	0.5875	0.2014	0.4918	0.0359*
H61	0.9002	0.3500	0.4001	0.0492*
H62	0.8246	0.2059	0.3615	0.0487*
H91	0.4927	0.2776	0.4018	0.0382*
H92	0.5698	0.1422	0.3730	0.0379*
H111	0.3071	0.1678	0.3773	0.0418*
H112	0.2870	−0.0389	0.3779	0.0420*
H131	0.2169	0.2055	0.2787	0.0492*
H141	0.2287	0.1839	0.1829	0.0609*
H151	0.3700	0.0086	0.1545	0.0609*
H161	0.5010	−0.1443	0.2217	0.0620*
H171	0.4870	−0.1264	0.3172	0.0479*
H221	0.9401	0.4161	0.5623	0.0563*
H231	0.9789	0.3844	0.6613	0.0670*
H251	0.6379	0.4080	0.6660	0.0570*
H261	0.5975	0.4459	0.5672	0.0451*

H271	0.7734	0.4122	0.7540	0.1093*
H272	0.9083	0.4267	0.7537	0.1090*
H273	0.8464	0.2434	0.7461	0.1092*

Atomic displacement parameters (Å^2)

	U^{11}	U^{22}	U^{33}	U^{12}	U^{13}	U^{23}
N1	0.0295 (17)	0.025 (2)	0.0276 (17)	0.0002 (15)	0.0056 (14)	−0.0038 (15)
C2	0.030 (2)	0.042 (3)	0.029 (2)	0.006 (2)	0.0048 (17)	0.003 (2)
C3	0.045 (3)	0.038 (3)	0.028 (2)	0.011 (2)	0.0005 (19)	−0.002 (2)
C4	0.043 (3)	0.027 (3)	0.037 (2)	0.001 (2)	0.003 (2)	0.004 (2)
C5	0.030 (2)	0.037 (3)	0.025 (2)	−0.0064 (19)	0.0061 (16)	−0.0029 (19)
C6	0.034 (2)	0.060 (4)	0.030 (2)	0.010 (2)	0.0096 (19)	0.008 (2)
I7	0.04275 (19)	0.1146 (4)	0.0457 (2)	0.0342 (2)	0.01484 (14)	0.0124 (2)
F8	0.0644 (19)	0.054 (2)	0.0386 (15)	0.0066 (17)	0.0076 (14)	−0.0142 (15)
C9	0.030 (2)	0.030 (3)	0.034 (2)	−0.0045 (19)	0.0025 (18)	−0.0001 (19)
O10	0.0298 (15)	0.0383 (19)	0.0329 (16)	−0.0063 (14)	0.0049 (12)	−0.0012 (15)
C11	0.030 (2)	0.044 (3)	0.031 (2)	−0.002 (2)	0.0051 (17)	−0.004 (2)
C12	0.032 (2)	0.034 (3)	0.030 (2)	−0.0053 (19)	0.0020 (17)	−0.005 (2)
C13	0.037 (2)	0.042 (3)	0.041 (3)	−0.002 (2)	−0.001 (2)	0.004 (2)
C14	0.053 (3)	0.053 (4)	0.040 (3)	−0.011 (3)	−0.008 (2)	0.012 (3)
C15	0.062 (3)	0.064 (4)	0.027 (2)	−0.017 (3)	0.007 (2)	−0.008 (3)
C16	0.054 (3)	0.060 (4)	0.043 (3)	−0.008 (3)	0.017 (2)	−0.016 (3)
C17	0.036 (2)	0.053 (3)	0.032 (2)	0.000 (2)	0.0048 (18)	−0.006 (2)
S18	0.0374 (6)	0.0272 (6)	0.0312 (5)	−0.0036 (5)	0.0052 (4)	−0.0004 (5)
O19	0.050 (2)	0.043 (2)	0.0456 (19)	−0.0171 (17)	0.0151 (16)	−0.0011 (17)
O20	0.0447 (18)	0.032 (2)	0.0402 (18)	0.0076 (15)	0.0012 (14)	0.0045 (15)
C21	0.038 (2)	0.028 (3)	0.028 (2)	−0.004 (2)	0.0011 (17)	−0.0026 (19)
C22	0.038 (2)	0.055 (4)	0.044 (3)	−0.006 (3)	−0.001 (2)	−0.006 (3)
C23	0.052 (3)	0.062 (4)	0.045 (3)	−0.004 (3)	−0.014 (2)	−0.005 (3)
C24	0.076 (4)	0.031 (3)	0.032 (2)	−0.005 (3)	−0.002 (2)	−0.002 (2)
C25	0.064 (3)	0.041 (3)	0.039 (3)	−0.002 (3)	0.013 (2)	−0.004 (3)
C26	0.043 (2)	0.036 (3)	0.036 (2)	0.005 (2)	0.0097 (19)	−0.005 (2)
C27	0.112 (6)	0.059 (4)	0.037 (3)	−0.012 (4)	−0.013 (3)	0.001 (3)

Geometric parameters (Å, º)

N1—C2	1.491 (5)	C13—C14	1.389 (7)
N1—C5	1.491 (5)	C13—H131	0.930
N1—S18	1.634 (4)	C14—C15	1.376 (8)
C2—C3	1.522 (7)	C14—H141	0.928
C2—C6	1.519 (6)	C15—C16	1.379 (8)
C2—H21	0.967	C15—H151	0.936
C3—C4	1.501 (7)	C16—C17	1.388 (6)
C3—F8	1.413 (5)	C16—H161	0.935

C3—H31	0.983	C17—H171	0.925
C4—C5	1.534 (7)	S18—O19	1.433 (3)
C4—H41	0.987	S18—O20	1.428 (3)
C4—H42	0.974	S18—C21	1.767 (4)
C5—C9	1.515 (6)	C21—C22	1.377 (6)
C5—H51	0.973	C21—C26	1.382 (6)
C6—I7	2.131 (5)	C22—C23	1.401 (7)
C6—H61	0.969	C22—H221	0.932
C6—H62	0.973	C23—C24	1.372 (8)
C9—O10	1.430 (5)	C23—H231	0.927
C9—H91	0.976	C24—C25	1.384 (8)
C9—H92	0.973	C24—C27	1.519 (7)
O10—C11	1.420 (5)	C25—C26	1.394 (7)
C11—C12	1.515 (6)	C25—H251	0.937
C11—H111	0.974	C26—H261	0.924
C11—H112	0.975	C27—H271	0.965
C12—C13	1.387 (6)	C27—H272	0.957
C12—C17	1.386 (6)	C27—H273	0.958
C2—N1—C5	111.3 (4)	C11—C12—C17	121.0 (4)
C2—N1—S18	120.4 (3)	C13—C12—C17	119.2 (4)
C5—N1—S18	118.7 (3)	C12—C13—C14	120.5 (5)
N1—C2—C3	103.6 (4)	C12—C13—H131	119.6
N1—C2—C6	110.1 (4)	C14—C13—H131	119.9
C3—C2—C6	114.7 (4)	C13—C14—C15	119.7 (5)
N1—C2—H21	110.5	C13—C14—H141	120.1
C3—C2—H21	108.6	C15—C14—H141	120.3
C6—C2—H21	109.2	C14—C15—C16	120.4 (5)
C2—C3—C4	105.5 (4)	C14—C15—H151	119.7
C2—C3—F8	108.6 (4)	C16—C15—H151	119.9
C4—C3—F8	108.1 (4)	C15—C16—C17	120.0 (5)
C2—C3—H31	111.2	C15—C16—H161	120.2
C4—C3—H31	112.7	C17—C16—H161	119.8
F8—C3—H31	110.5	C16—C17—C12	120.2 (5)
C3—C4—C5	104.8 (4)	C16—C17—H171	119.8
C3—C4—H41	109.4	C12—C17—H171	120.0
C5—C4—H41	110.0	N1—S18—O19	106.2 (2)
C3—C4—H42	111.8	N1—S18—O20	105.8 (2)
C5—C4—H42	111.6	O19—S18—O20	120.9 (2)
H41—C4—H42	109.2	N1—S18—C21	107.9 (2)
C4—C5—N1	103.3 (3)	O19—S18—C21	107.7 (2)
C4—C5—C9	114.0 (4)	O20—S18—C21	107.6 (2)
N1—C5—C9	107.9 (3)	S18—C21—C22	119.7 (4)
C4—C5—H51	110.6	S18—C21—C26	119.3 (3)
N1—C5—H51	110.2	C22—C21—C26	121.1 (4)

C9—C5—H51	110.6	C21—C22—C23	118.7 (5)
C2—C6—I7	110.5 (3)	C21—C22—H221	120.2
C2—C6—H61	110.2	C23—C22—H221	121.2
I7—C6—H61	109.2	C22—C23—C24	121.5 (5)
C2—C6—H62	109.6	C22—C23—H231	119.1
I7—C6—H62	107.3	C24—C23—H231	119.4
H61—C6—H62	110.0	C23—C24—C25	118.7 (5)
C5—C9—O10	108.0 (4)	C23—C24—C27	121.3 (6)
C5—C9—H91	109.1	C25—C24—C27	119.9 (6)
O10—C9—H91	109.6	C24—C25—C26	121.1 (5)
C5—C9—H92	109.3	C24—C25—H251	118.8
O10—C9—H92	110.7	C26—C25—H251	120.1
H91—C9—H92	110.1	C25—C26—C21	119.0 (5)
C9—O10—C11	113.0 (4)	C25—C26—H261	120.7
O10—C11—C12	114.7 (3)	C21—C26—H261	120.3
O10—C11—H111	109.1	C24—C27—H271	109.8
C12—C11—H111	109.1	C24—C27—H272	109.4
O10—C11—H112	106.4	H271—C27—H272	109.5
C12—C11—H112	107.9	C24—C27—H273	109.3
H111—C11—H112	109.5	H271—C27—H273	109.3
C11—C12—C13	119.7 (4)	H272—C27—H273	109.5

Hydrogen-bond geometry (Å, º)

D—H···*A*	*D*—H	H···*A*	*D*···*A*	*D*—H···*A*
C4—H42···O20^{i}	0.97	2.57	3.351 (7)	138
C6—H61···O19	0.97	2.37	3.027 (7)	125
C26—H261···O20^{ii}	0.92	2.53	3.439 (7)	169

Symmetry codes: (i) *x*, *y*−1, *z*; (ii) −*x*+1, −*y*+1, −*z*+1.

(±) 4-fluoro-5-(iodomethyl)-3,3-dimethyl-1-tosylpyrrolidin-2-one (105): (CCDC-896061)

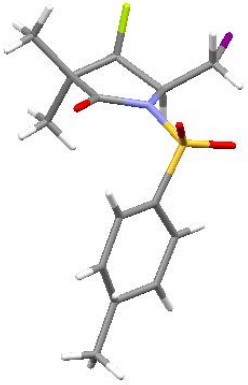

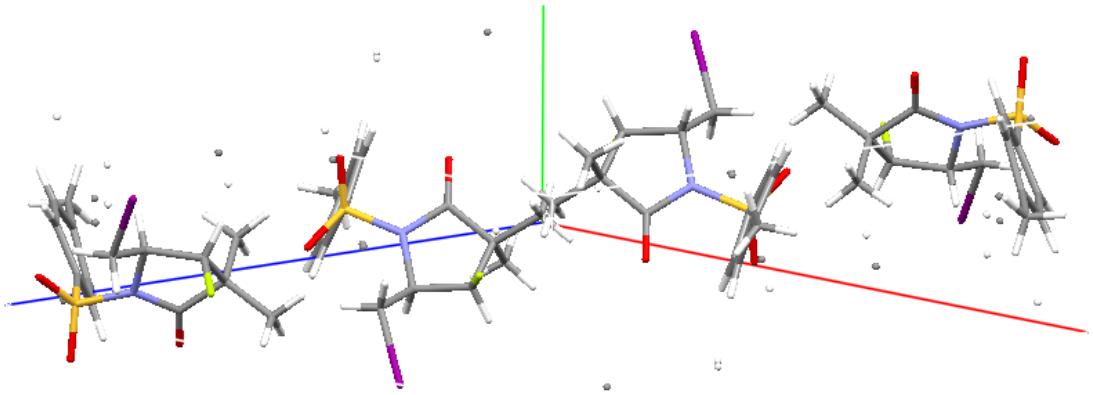

Crystal data

$C_{14}H_{17}FINO_3S$
M_r = 425.26
Monoclinic, $P2_1/c$
Hall symbol: -P 2ybc
a = 17.7254 (8) Å
b = 5.7868 (2) Å
c = 16.3001 (7) Å
β = 109.991 (5)°
V = 1571.21 (12) Å^3
Z = 4

$F(000)$ = 840
D_x = 1.798 Mg m^{-3}
Melting point: not measured K
Cu $K\alpha$ radiation, λ = 1.54180 Å
Cell parameters from 16637 reflections
θ = 3–76°
μ = 17.45 mm^{-1}
T = 150 K
Lath, Clear_pale_colourless
0.49 × 0.04 × 0.01 mm

Data collection

Oxford Diffraction SuperNova diffractometer
Graphite monochromator
ω scans
Absorption correction: Multi-scan CrysAlis, (Oxford Diffraction, 2002)
T_{min} = 0.15, T_{max} = 0.84
3296 measured reflections
3296 independent reflections

2206 reflections with $I > 2.0\sigma(I)$
R_{int} = 0.126
θ_{max} = 76.5°, θ_{min} = 5.3°
h = −22→21
k = 0→7
l = 0→20

Refinement

Refinement on F^2
Least-squares matrix: Full
$R[F^2 > 2\sigma(F^2)]$ = 0.047
$wR(F^2)$ = 0.124
S = 1.00

Primary atom site location: Structure-invariant direct methods
Hydrogen site location: Difference Fourier map
H-atom parameters constrained
Method = Modified Sheldrick $w = 1/[\sigma^2(F^2) + (0.05P)^2 + 16.4P]$, where $P = (\max(F_o^2,0) + 2F_c^2)/3$
$(\Delta/\sigma)_{max}$ = 0.001

2384 reflections
227 parameters
0 restraints

$\Delta\rho_{max}$ = 1.39 e Å^{-3}
$\Delta\rho_{min}$ = −0.91 e Å^{-3}

Fractional atomic coordinates and isotropic or equivalent isotropic displacement parameters (Å^2)

	x	*y*	*z*	U_{iso}*/U_{eq}	Occ. (<1)
N1	0.2695 (4)	0.2901 (10)	0.5351 (4)	0.0329	
C2	0.3135 (4)	0.0660 (13)	0.5598 (5)	0.0344	
C3	0.3757 (4)	0.0901 (15)	0.5130 (5)	0.0398	
C4	0.3376 (5)	0.2439 (13)	0.4345 (5)	0.0361	
C5	0.2824 (4)	0.3964 (13)	0.4636 (5)	0.0338	
C6	0.3503 (5)	0.0376 (13)	0.6582 (5)	0.0375	
I7	0.42126 (3)	−0.27088 (8)	0.69230 (3)	0.0356	
F8	0.4444 (3)	0.1965 (9)	0.5692 (3)	0.0498	
C9	0.3971 (6)	0.3881 (19)	0.4070 (7)	0.0625	
C10	0.2827 (6)	0.0997 (16)	0.3573 (6)	0.0590	
O11	0.2513 (3)	0.5762 (9)	0.4307 (4)	0.0452	
S12	0.19218 (11)	0.3733 (3)	0.56482 (12)	0.0334	
O13	0.1928 (3)	0.2235 (9)	0.6337 (3)	0.0410	
O14	0.1980 (3)	0.6174 (9)	0.5793 (4)	0.0440	
C15	0.1059 (4)	0.3166 (13)	0.4739 (5)	0.0355	
C16	0.0684 (11)	0.107 (3)	0.4752 (12)	0.0375	0.50 (2)
C17	−0.0029 (11)	0.064 (3)	0.4078 (12)	0.0420	0.50 (2)
C18	−0.0367 (5)	0.2246 (14)	0.3373 (5)	0.0409	
C19	0.0018 (16)	0.440 (4)	0.3493 (17)	0.0410	0.50 (2)
C20	0.0747 (14)	0.487 (4)	0.4156 (15)	0.0397	0.50 (2)
C21	−0.1154 (5)	0.1756 (18)	0.2670 (6)	0.0554	
C161	0.0957 (11)	0.100 (3)	0.4307 (13)	0.0421	0.50 (2)
C171	0.0245 (10)	0.051 (3)	0.3598 (12)	0.0384	0.50 (2)
C191	−0.0224 (16)	0.431 (4)	0.3731 (16)	0.0378	0.50 (2)
C201	0.0471 (14)	0.477 (3)	0.4392 (14)	0.0347	0.50 (2)
H21	0.2767	−0.0624	0.5348	0.0411*	
H31	0.3893	−0.0616	0.4954	0.0482*	
H61	0.3078	0.0294	0.6825	0.0452*	
H62	0.3835	0.1713	0.6833	0.0452*	
H91	0.3688	0.4938	0.3608	0.0940*	
H92	0.4298	0.2868	0.3863	0.0941*	
H93	0.4308	0.4749	0.4568	0.0940*	
H102	0.2538	0.2007	0.3103	0.0891*	
H103	0.2446	0.0155	0.3764	0.0890*	
H101	0.3146	−0.0076	0.3370	0.0890*	
H161	0.0902	0.0012	0.5195	0.0449*	0.50 (2)
H171	−0.0298	−0.0729	0.4078	0.0510*	0.50 (2)

H191	−0.0225	0.5585	0.3106	0.0500*	0.50 (2)
H201	0.1003	0.6290	0.4194	0.0481*	0.50 (2)
H211	−0.1230	0.2800	0.2195	0.0831*	
H212	−0.1580	0.1957	0.2903	0.0830*	
H213	−0.1165	0.0196	0.2460	0.0832*	
H1611	0.1361	−0.0105	0.4487	0.0510*	0.50 (2)
H1711	0.0179	−0.0878	0.3294	0.0460*	0.50 (2)
H1911	−0.0604	0.5475	0.3526	0.0460*	0.50 (2)
H2011	0.0550	0.6242	0.4622	0.0421*	0.50 (2)

Atomic displacement parameters (Å^2)

	U^{11}	U^{22}	U^{33}	U^{12}	U^{13}	U^{23}
N1	0.031 (3)	0.028 (3)	0.036 (3)	0.000 (3)	0.005 (3)	0.002 (3)
C2	0.031 (4)	0.028 (4)	0.040 (4)	−0.001 (3)	0.007 (3)	−0.006 (3)
C3	0.035 (4)	0.042 (4)	0.041 (4)	0.004 (3)	0.011 (3)	−0.003 (4)
C4	0.038 (4)	0.031 (4)	0.041 (4)	−0.004 (3)	0.016 (3)	−0.002 (3)
C5	0.030 (4)	0.029 (4)	0.036 (4)	−0.006 (3)	0.003 (3)	0.002 (3)
C6	0.041 (4)	0.029 (4)	0.040 (4)	0.008 (3)	0.011 (3)	0.004 (3)
I7	0.0301 (3)	0.0254 (3)	0.0437 (3)	0.00321 (19)	0.0030 (2)	0.0042 (2)
F8	0.033 (2)	0.058 (3)	0.050 (3)	−0.007 (2)	0.004 (2)	0.008 (2)
C9	0.057 (6)	0.068 (7)	0.068 (6)	0.000 (5)	0.030 (5)	0.013 (5)
C10	0.085 (7)	0.043 (5)	0.041 (5)	0.004 (5)	0.010 (5)	−0.002 (4)
O11	0.051 (3)	0.032 (3)	0.050 (3)	0.003 (3)	0.015 (3)	0.012 (3)
S12	0.0305 (9)	0.0296 (9)	0.0372 (9)	0.0021 (7)	0.0077 (8)	0.0009 (8)
O13	0.036 (3)	0.045 (3)	0.042 (3)	0.008 (2)	0.013 (2)	0.006 (2)
O14	0.040 (3)	0.031 (3)	0.055 (3)	0.002 (2)	0.009 (3)	−0.010 (3)
C15	0.029 (4)	0.030 (4)	0.045 (4)	0.002 (3)	0.010 (3)	0.002 (3)
C16	0.044 (10)	0.036 (9)	0.033 (9)	0.003 (7)	0.014 (8)	0.012 (7)
C17	0.054 (11)	0.032 (9)	0.041 (10)	−0.012 (7)	0.018 (9)	−0.013 (7)
C18	0.030 (4)	0.045 (5)	0.045 (4)	0.001 (3)	0.009 (3)	0.006 (4)
C19	0.050 (15)	0.038 (10)	0.034 (12)	0.015 (10)	0.014 (9)	0.006 (9)
C20	0.038 (12)	0.036 (10)	0.048 (12)	−0.008 (9)	0.020 (9)	0.001 (9)
C21	0.039 (5)	0.066 (6)	0.053 (5)	−0.007 (4)	0.005 (4)	0.015 (5)
C161	0.033 (9)	0.033 (9)	0.046 (11)	0.008 (7)	−0.005 (8)	0.019 (8)
C171	0.044 (10)	0.028 (8)	0.034 (10)	−0.011 (7)	0.001 (8)	−0.004 (7)
C191	0.043 (14)	0.031 (10)	0.039 (13)	0.012 (9)	0.014 (9)	−0.002 (9)
C201	0.039 (12)	0.023 (8)	0.041 (11)	0.002 (8)	0.013 (9)	−0.002 (7)

Geometric parameters (Å, º)

N1—C2	1.495 (9)	C15—C16	1.384 (19)
N1—C5	1.405 (10)	C15—C20	1.35 (2)
N1—S12	1.673 (6)	C15—C161	1.42 (2)
C2—C3	1.546 (11)	C15—C201	1.36 (2)

C2—C6	1.520 (10)	C16—C17	1.39 (2)
C2—H21	0.980	C16—H161	0.926
C3—C4	1.515 (11)	C17—C18	1.44 (2)
C3—F8	1.393 (9)	C17—H171	0.926
C3—H31	0.979	C18—C19	1.40 (3)
C4—C5	1.509 (11)	C18—C21	1.498 (11)
C4—C9	1.528 (12)	C18—C21	1.498 (11)
C4—C10	1.546 (11)	C18—C171	1.432 (19)
C5—O11	1.214 (9)	C18—C191	1.32 (3)
C6—I7	2.144 (7)	C19—C20	1.40 (3)
C6—H61	0.965	C19—H191	0.933
C6—H62	0.973	C20—H201	0.929
C9—H91	0.966	C21—H211	0.954
C9—H92	0.963	C21—H212	0.961
C9—H93	0.968	C21—H213	0.963
C10—H102	0.961	C161—C171	1.42 (2)
C10—H103	0.966	C161—H1611	0.930
C10—H101	0.971	C171—H1711	0.930
S12—O13	1.416 (6)	C191—C201	1.36 (3)
S12—O14	1.430 (6)	C191—H1911	0.929
S12—C15	1.759 (8)	C201—H2011	0.925
C2—N1—C5	112.6 (6)	N1—S12—C15	105.4 (3)
C2—N1—S12	125.1 (5)	O13—S12—C15	108.8 (4)
C5—N1—S12	119.8 (5)	O14—S12—C15	108.5 (3)
N1—C2—C3	100.5 (6)	S12—C15—C16	115.7 (8)
N1—C2—C6	112.0 (6)	S12—C15—C20	119.0 (10)
C3—C2—C6	114.1 (6)	C16—C15—C20	124.5 (13)
N1—C2—H21	109.5	S12—C15—C161	120.6 (8)
C3—C2—H21	110.3	S12—C15—C201	123.0 (10)
C6—C2—H21	109.9	C161—C15—C201	116.4 (11)
C2—C3—C4	106.5 (6)	C15—C16—C17	117.3 (14)
C2—C3—F8	109.1 (6)	C15—C16—H161	121.2
C4—C3—F8	109.4 (6)	C17—C16—H161	121.5
C2—C3—H31	110.6	C16—C17—C18	122.4 (14)
C4—C3—H31	111.2	C16—C17—H171	119.0
F8—C3—H31	109.9	C18—C17—H171	118.6
C3—C4—C5	103.1 (6)	C17—C18—C19	114.3 (13)
C3—C4—C9	114.6 (7)	C17—C18—C21	120.9 (9)
C5—C4—C9	111.1 (7)	C19—C18—C21	123.8 (12)
C3—C4—C10	110.2 (7)	C21—C18—C171	119.3 (9)
C5—C4—C10	106.0 (7)	C21—C18—C191	119.9 (13)
C9—C4—C10	111.3 (7)	C171—C18—C191	120.6 (14)
C4—C5—N1	108.2 (6)	C18—C19—C20	124 (2)
C4—C5—O11	127.5 (7)	C18—C19—H191	118.0

N1—C5—O11	124.3 (7)	C20—C19—H191	118.0
C2—C6—I7	111.5 (5)	C19—C20—C15	116.6 (18)
C2—C6—H61	108.9	C19—C20—H201	121.7
I7—C6—H61	108.9	C15—C20—H201	121.7
C2—C6—H62	109.7	C18—C21—H211	109.7
I7—C6—H62	109.6	C18—C21—H212	109.1
H61—C6—H62	108.1	H211—C21—H212	109.3
C4—C9—H91	110.2	C18—C21—H213	110.5
C4—C9—H92	109.2	H211—C21—H213	109.0
H91—C9—H92	109.2	H212—C21—H213	109.3
C4—C9—H93	109.1	C15—C161—C171	120.5 (13)
H91—C9—H93	109.4	C15—C161—H1611	119.9
H92—C9—H93	109.7	C171—C161—H1611	119.6
C4—C10—H102	109.6	C18—C171—C161	117.0 (14)
C4—C10—H103	109.0	C18—C171—H1711	121.6
H102—C10—H103	108.9	C161—C171—H1711	121.4
C4—C10—H101	110.1	C18—C191—C201	121 (2)
H102—C10—H101	109.3	C18—C191—H1911	119.5
H103—C10—H101	109.9	C201—C191—H1911	119.6
N1—S12—O13	105.6 (3)	C15—C201—C191	123.8 (18)
N1—S12—O14	108.2 (3)	C15—C201—H2011	118.1
O13—S12—O14	119.6 (4)	C191—C201—H2011	118.1

Hydrogen-bond geometry (Å, º)

D—H···*A*	*D*—H	H···*A*	*D*···*A*	*D*—H···*A*
C2—H21···O14^{i}	0.98	2.57	3.39 (2)	141
C6—H61···O13	0.97	2.22	2.89 (2)	125

Symmetry code: (i) *x*, *y*−1, *z*.

(±) 1-(3-fluoro-4-iodocyclopentylsulfonyl)-4-methylbenzene (*syn*-109): (CCDC-896061)

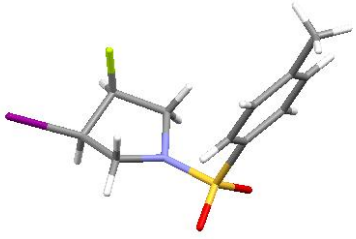

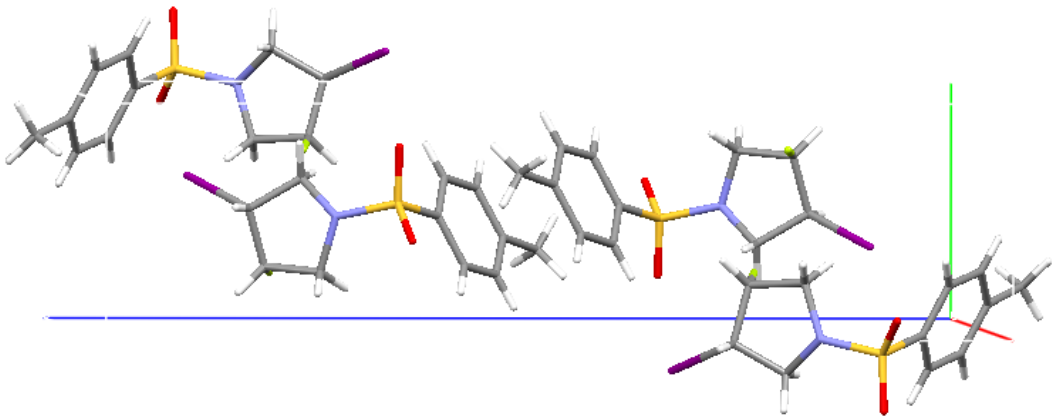

Crystal data

$C_{11}H_{13}FINO_2S$
M_r = 369.20
Monoclinic, $P2_1/n$
Hall symbol: -P 2yn
a = 9.6806 (4) Å
b = 5.9001 (2) Å
c = 22.6427 (9) Å
β = 98.1913 (16)°
V = 1280.08 (9) Å^3
Z = 4

$F(000)$ = 720
D_x = 1.916 Mg m^{-3}
Melting point: not measured K
Mo $K\alpha$ radiation, λ = 0.71073 Å
Cell parameters from 2733 reflections
θ = 5–27°
μ = 2.67 mm^{-1}
T = 150 K
Needle, Clear_pale_colourless
0.24 × 0.05 × 0.04 mm

Data collection

Nonius KappaCCD diffractometer
Graphite monochromator
ω scans
Absorption correction: Multi-scan *DENZO*/*SCALEPACK* (Otwinowski & Minor, 1997)
T_{min} = 0.83, T_{max} = 0.90
13530 measured reflections
2903 independent reflections

1704 reflections with $I > 2.0\sigma(I)$
R_{int} = 0.074
θ_{max} = 27.5°, θ_{min} = 5.3°
$h = -12 \rightarrow 12$
$k = 0 \rightarrow 7$
$l = 0 \rightarrow 29$

Refinement

Refinement on F^2
Least-squares matrix: Full
$R[F^2 > 2\sigma(F^2)]$ = 0.047
$wR(F^2)$ = 0.126

Primary atom site location: Structure-invariant direct methods
Hydrogen site location: Difference Fourier map
H-atom parameters constrained
Method, part 1, Chebychev polynomial, (Watkin, 1994, *P*rince, 1982) [*w*eight] = 1.0/[A_0*T_0(x) +

$A_1*T_1(x) \cdots + A_{n-1}]*T_{n-1}(x)]$
where A_i are the Chebychev coefficients listed below and x = *F* /*F*max Method = Robust Weighting (*P*rince, 1982) W = [*w*eight] * [1-(delta*F*/6*sigma*F*)^2]^2 A_i are: 10.1 13.3 6.59 1.84

S = 1.00
2376 reflections
154 parameters
0 restraints

$(\Delta/\sigma)_{max}$ = 0.001
$\Delta\rho_{max}$ = 1.65 e Å^{-3}
$\Delta\rho_{min}$ = −1.43 e Å^{-3}

Fractional atomic coordinates and isotropic or equivalent isotropic displacement parameters (Å^2)

	x	*y*	*z*	U_{iso}*/U_{eq}
N1	0.5873 (7)	0.4851 (11)	0.7182 (3)	0.0250
C2	0.5619 (9)	0.2484 (13)	0.7342 (4)	0.0267
C3	0.4916 (8)	0.2655 (14)	0.7907 (4)	0.0257
C4	0.5176 (8)	0.5111 (14)	0.8098 (3)	0.0251
C5	0.5062 (8)	0.6392 (16)	0.7511 (3)	0.0279
F6	0.3504 (5)	0.2266 (10)	0.7756 (2)	0.0437
I7	0.38147 (6)	0.63939 (11)	0.86816 (3)	0.0355
S8	0.6298 (2)	0.5439 (3)	0.65326 (9)	0.0238
O9	0.7424 (5)	0.3955 (10)	0.6448 (2)	0.0290
O10	0.6506 (6)	0.7843 (10)	0.6528 (2)	0.0291
C11	0.4881 (8)	0.4774 (14)	0.5990 (3)	0.0235
C12	0.4840 (9)	0.2678 (15)	0.5696 (4)	0.0293
C13	0.3711 (9)	0.2191 (16)	0.5270 (4)	0.0316
C14	0.2631 (8)	0.3672 (16)	0.5118 (3)	0.0283
C15	0.2669 (8)	0.5752 (15)	0.5416 (4)	0.0311
C16	0.3784 (8)	0.6288 (15)	0.5848 (4)	0.0297
C17	0.1409 (10)	0.3041 (19)	0.4665 (4)	0.0415
H21	0.6488	0.1661	0.7423	0.0319*
H22	0.5007	0.1743	0.7025	0.0320*
H31	0.5328	0.1607	0.8218	0.0309*
H41	0.6128	0.5246	0.8303	0.0298*
H51	0.5482	0.7882	0.7561	0.0331*
H52	0.4106	0.6533	0.7325	0.0329*
H121	0.5564	0.1640	0.5785	0.0350*
H131	0.3687	0.0825	0.5073	0.0379*
H151	0.1943	0.6771	0.5324	0.0372*
H161	0.3800	0.7671	0.6046	0.0362*
H171	0.1693	0.1959	0.4392	0.0620*
H172	0.1058	0.4356	0.4448	0.0621*
H173	0.0686	0.2392	0.4860	0.0620*

Atomic displacement parameters (Å^2)

	U^{11}	U^{22}	U^{33}	U^{12}	U^{13}	U^{23}
N1	0.031 (4)	0.017 (3)	0.028 (4)	0.003 (3)	0.010 (3)	0.002 (3)
C2	0.036 (5)	0.011 (4)	0.033 (4)	0.001 (4)	0.006 (4)	0.005 (3)
C3	0.028 (4)	0.020 (4)	0.029 (4)	−0.004 (3)	0.004 (3)	0.002 (3)
C4	0.025 (4)	0.026 (4)	0.024 (4)	−0.002 (3)	0.001 (3)	−0.009 (3)
C5	0.028 (4)	0.021 (4)	0.035 (4)	0.001 (4)	0.007 (3)	−0.003 (4)
F6	0.033 (3)	0.047 (3)	0.053 (3)	−0.015 (3)	0.012 (2)	−0.008 (3)
I7	0.0393 (3)	0.0356 (3)	0.0340 (3)	0.0058 (3)	0.0137 (2)	0.0000 (3)
S8	0.0221 (9)	0.0210 (9)	0.0284 (10)	−0.0016 (8)	0.0041 (8)	0.0008 (8)
O9	0.021 (3)	0.030 (3)	0.037 (3)	0.007 (2)	0.007 (2)	−0.001 (3)
O10	0.036 (3)	0.023 (3)	0.029 (3)	−0.005 (2)	0.007 (2)	0.002 (2)
C11	0.026 (4)	0.023 (4)	0.022 (4)	−0.003 (3)	0.007 (3)	0.006 (3)
C12	0.031 (4)	0.026 (4)	0.032 (4)	0.006 (4)	0.009 (4)	0.005 (4)
C13	0.040 (5)	0.030 (5)	0.025 (4)	−0.003 (4)	0.006 (4)	−0.009 (4)
C14	0.026 (4)	0.031 (4)	0.028 (4)	−0.006 (4)	0.008 (3)	0.006 (4)
C15	0.020 (4)	0.031 (5)	0.041 (5)	0.006 (3)	−0.001 (3)	0.009 (4)
C16	0.029 (4)	0.020 (4)	0.040 (4)	0.008 (4)	0.003 (3)	0.002 (4)
C17	0.035 (5)	0.058 (7)	0.032 (5)	−0.005 (5)	0.007 (4)	−0.001 (4)

Geometric parameters (Å, º)

N1—C2	1.472 (9)	S8—C11	1.751 (8)
N1—C5	1.472 (10)	C11—C12	1.402 (12)
N1—S8	1.620 (7)	C11—C16	1.390 (11)
C2—C3	1.536 (11)	C12—C13	1.381 (12)
C2—H21	0.966	C12—H121	0.931
C2—H22	0.968	C13—C14	1.369 (12)
C3—C4	1.522 (11)	C13—H131	0.919
C3—F6	1.381 (9)	C14—C15	1.399 (13)
C3—H31	0.978	C14—C17	1.498 (12)
C4—C5	1.519 (11)	C15—C16	1.386 (12)
C4—I7	2.133 (8)	C15—H151	0.926
C4—H41	0.975	C16—H161	0.930
C5—H51	0.968	C17—H171	0.957
C5—H52	0.965	C17—H172	0.955
S8—O9	1.432 (6)	C17—H173	0.958
S8—O10	1.433 (6)		
C2—N1—C5	109.9 (6)	O9—S8—O10	119.6 (4)
C2—N1—S8	120.0 (5)	N1—S8—C11	108.3 (4)
C5—N1—S8	123.4 (6)	O9—S8—C11	107.7 (4)
N1—C2—C3	104.6 (6)	O10—S8—C11	108.3 (4)
N1—C2—H21	110.6	S8—C11—C12	119.8 (6)
C3—C2—H21	110.6	S8—C11—C16	121.0 (7)
N1—C2—H22	110.6	C12—C11—C16	119.2 (7)

C3—C2—H22	110.6	C11—C12—C13	118.8 (8)
H21—C2—H22	109.8	C11—C12—H121	120.6
C2—C3—C4	103.0 (6)	C13—C12—H121	120.6
C2—C3—F6	108.8 (7)	C12—C13—C14	122.9 (8)
C4—C3—F6	110.3 (7)	C12—C13—H131	119.0
C2—C3—H31	112.0	C14—C13—H131	118.1
C4—C3—H31	111.3	C13—C14—C15	118.2 (7)
F6—C3—H31	111.2	C13—C14—C17	121.0 (8)
C3—C4—C5	103.7 (6)	C15—C14—C17	120.8 (8)
C3—C4—I7	115.0 (5)	C14—C15—C16	120.4 (8)
C5—C4—I7	113.0 (5)	C14—C15—H151	119.6
C3—C4—H41	108.7	C16—C15—H151	120.1
C5—C4—H41	108.8	C11—C16—C15	120.6 (8)
I7—C4—H41	107.6	C11—C16—H161	119.5
C4—C5—N1	99.1 (7)	C15—C16—H161	119.9
C4—C5—H51	112.0	C14—C17—H171	109.6
N1—C5—H51	112.0	C14—C17—H172	109.8
C4—C5—H52	111.8	H171—C17—H172	108.8
N1—C5—H52	112.3	C14—C17—H173	110.1
H51—C5—H52	109.5	H171—C17—H173	109.1
N1—S8—O9	106.7 (3)	H172—C17—H173	109.4
N1—S8—O10	105.8 (4)		

(±) 3-fluoro-1-tosyl-2-((tri*iso*propylsilyl)methyl)pyrrolidine (*syn*-124):

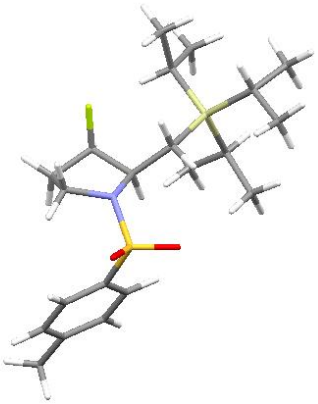

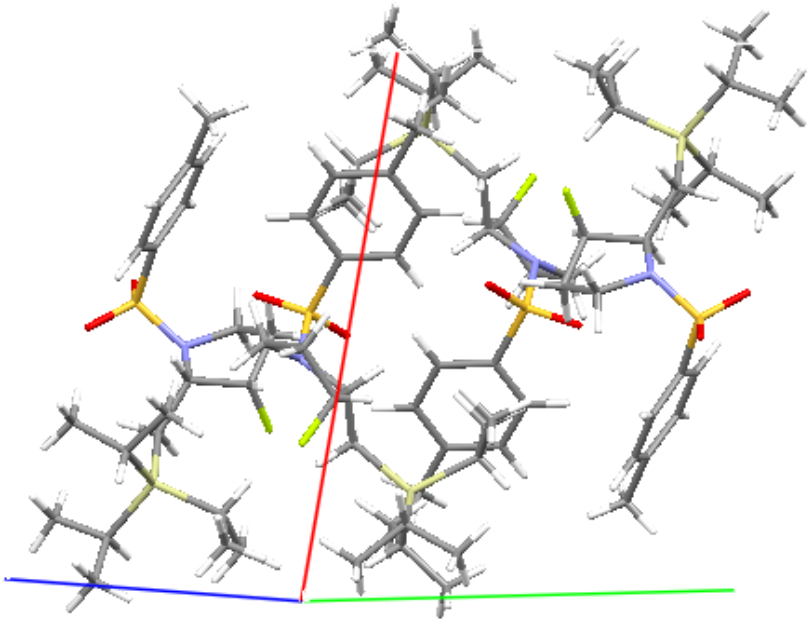

Crystal data

$C_{21}H_{36}FNO_2SSi$	$F(000)$ = 896
M_r = 413.67	D_x = 1.197 Mg m^{-3}
Monoclinic, $P2_1/c$	? radiation, λ = ? Å
Hall symbol: -P 2ybc	Cell parameters from 22732 reflections
a = 14.3170 (4) Å	θ = 5–28°
b = 13.3153 (3) Å	μ = 0.22 mm^{-1}
c = 12.4990 (3) Å	T = 150 K
β = 105.5482 (9)°	Block, Colourless
V = 2295.55 (10) Å^3	0.40 × 0.32 × 0.28 mm
Z = 4	

Data collection

ω scans	R_{int} = 0.056
Absorption correction: Multi-scan *DENZO*/*SCALEPACK* (Otwinowski & Minor, 1997)	θ$_{max}$ = 27.5°, θ$_{min}$ = 5.1°
T_{min} = 0.92, T_{max} = 0.94	h = −18→18
22732 measured reflections	k = −17→17
5223 independent reflections	l = −16→16
3331 reflections with I > 3.00u(I)	

Refinement

$R[F^2 > 2\sigma(F^2)]$ = 0.037	0 restraints
$wR(F^2)$ = 0.041	Method, part 1, Chebychev polynomial, (Watkin,

	1994, *P*rince, 1982) [*w*eight] = 1.0/[A_0*T_0(x) + A_1*T_1(x) ⋯ + A_{n-1}]*T_{n-1}(x)] where A_i are the Chebychev coefficients listed belo*w* and x = *F* /*F*max Method = Robust Weighting (*P*rince, 1982) W = [*w*eight] * [1-(delta*F*/6*sigma*F*)^2]^2 A_i are: 0.381 0.136 0.133
S = 1.11	$(\Delta/\sigma)_{max}$ = 0.002
3331 reflections	$\Delta\rho_{max}$ = 0.31 e Å^{-3}
244 parameters	$\Delta\rho_{min}$ = −0.30 e Å^{-3}

Fractional atomic coordinates and isotropic or equivalent isotropic displacement parameters (Å^2)

	x	*y*	*z*	U_{iso}*/U_{eq}
N1	0.41963 (11)	0.21190 (12)	0.45167 (13)	0.0221
C1	0.36386 (13)	0.26086 (14)	0.34517 (15)	0.0206
C2	0.35740 (14)	0.17719 (16)	0.26001 (17)	0.0279
C3	0.44658 (14)	0.11392 (16)	0.30550 (17)	0.0290
C4	0.45162 (14)	0.10997 (14)	0.42865 (17)	0.0261
S1	0.49817 (3)	0.27927 (4)	0.54249 (4)	0.0242
O1	0.45452 (10)	0.37606 (11)	0.54448 (12)	0.0301
O2	0.52709 (11)	0.21996 (12)	0.64194 (11)	0.0335
C5	0.60087 (14)	0.29432 (15)	0.49158 (15)	0.0246
C6	0.67573 (14)	0.22416 (16)	0.51930 (18)	0.0306
C7	0.75340 (15)	0.23250 (18)	0.4734 (2)	0.0367
C8	0.75771 (15)	0.31036 (19)	0.40040 (19)	0.0367
C9	0.68396 (16)	0.38132 (18)	0.37673 (19)	0.0367
C10	0.60544 (15)	0.37451 (16)	0.42188 (17)	0.0305
C11	0.84121 (19)	0.3178 (3)	0.3488 (2)	0.0571
C12	0.26807 (13)	0.30343 (15)	0.35606 (15)	0.0239
Si1	0.18285 (4)	0.37591 (4)	0.23880 (4)	0.0204
C13	0.08167 (14)	0.41861 (15)	0.30026 (17)	0.0281
C14	0.00715 (18)	0.4853 (2)	0.2213 (2)	0.0456
C15	0.11382 (18)	0.4684 (2)	0.4147 (2)	0.0454
C16	0.13009 (14)	0.29117 (15)	0.11542 (17)	0.0280
C17	0.08087 (17)	0.34552 (18)	0.00627 (18)	0.0378
C18	0.06120 (17)	0.21253 (18)	0.1420 (2)	0.0411
C19	0.24543 (14)	0.48566 (15)	0.19106 (16)	0.0248
C20	0.31697 (16)	0.45377 (16)	0.12512 (18)	0.0318
C21	0.29693 (18)	0.55588 (18)	0.2858 (2)	0.0394
F1	0.27510 (9)	0.11683 (9)	0.25631 (12)	0.0387
H11	0.4036	0.3170	0.3274	0.0250*
H21	0.3556	0.2049	0.1851	0.0339*
H31	0.5056	0.1465	0.2927	0.0352*
H32	0.4387	0.0453	0.2718	0.0352*
H41	0.5193	0.0963	0.4742	0.0320*

H42	0.4071	0.0573	0.4440	0.0320*
H61	0.6734	0.1682	0.5719	0.0355*
H71	0.8070	0.1820	0.4929	0.0432*
H91	0.6874	0.4385	0.3261	0.0433*
H101	0.5531	0.4264	0.4045	0.0357*
H111	0.8945	0.3582	0.3982	0.0700*
H112	0.8656	0.2489	0.3393	0.0700*
H113	0.8189	0.3513	0.2747	0.0700*
H121	0.2846	0.3497	0.4215	0.0294*
H122	0.2301	0.2451	0.3724	0.0294*
H131	0.0461	0.3563	0.3106	0.0352*
H141	−0.0442	0.5055	0.2578	0.0554*
H142	0.0400	0.5467	0.2030	0.0554*
H143	−0.0231	0.4474	0.1516	0.0554*
H151	0.0554	0.4879	0.4393	0.0571*
H152	0.1530	0.5296	0.4102	0.0571*
H153	0.1541	0.4201	0.4693	0.0571*
H161	0.1859	0.2531	0.1014	0.0330*
H171	0.0555	0.2948	−0.0535	0.0432*
H172	0.1291	0.3898	−0.0155	0.0432*
H173	0.0260	0.3873	0.0169	0.0432*
H181	0.0348	0.1693	0.0753	0.0480*
H182	0.0065	0.2472	0.1625	0.0480*
H183	0.0974	0.1698	0.2054	0.0480*
H191	0.1937	0.5262	0.1395	0.0302*
H201	0.3475	0.5148	0.1024	0.0406*
H202	0.3684	0.4101	0.1726	0.0406*
H203	0.2815	0.4157	0.0575	0.0406*
H211	0.3284	0.6120	0.2552	0.0484*
H212	0.2485	0.5840	0.3224	0.0484*
H213	0.3474	0.5174	0.3415	0.0484*

Atomic displacement parameters (Å^2)

	U^{11}	U^{22}	U^{33}	U^{12}	U^{13}	U^{23}
N1	0.0252 (8)	0.0196 (8)	0.0222 (8)	0.0036 (6)	0.0074 (6)	0.0041 (6)
C1	0.0221 (8)	0.0212 (9)	0.0191 (8)	0.0028 (7)	0.0064 (7)	0.0039 (7)
C2	0.0243 (9)	0.0327 (11)	0.0276 (10)	0.0007 (8)	0.0087 (8)	−0.0050 (9)
C3	0.0289 (10)	0.0303 (11)	0.0288 (10)	0.0060 (8)	0.0094 (8)	−0.0028 (8)
C4	0.0287 (9)	0.0177 (9)	0.0336 (10)	0.0048 (7)	0.0114 (8)	0.0038 (8)
S1	0.0282 (2)	0.0255 (2)	0.0193 (2)	0.00491 (19)	0.00681 (17)	0.00123 (19)
O1	0.0348 (7)	0.0265 (7)	0.0287 (7)	0.0060 (6)	0.0079 (6)	−0.0053 (6)
O2	0.0388 (8)	0.0404 (9)	0.0207 (7)	0.0070 (7)	0.0069 (6)	0.0072 (6)
C5	0.0250 (9)	0.0257 (10)	0.0213 (9)	−0.0010 (7)	0.0032 (7)	−0.0033 (8)

C6	0.0278 (10)	0.0280 (10)	0.0329 (11)	0.0036 (8)	0.0030 (8)	0.0000 (9)
C7	0.0258 (10)	0.0383 (12)	0.0438 (13)	0.0032 (9)	0.0055 (9)	−0.0072 (10)
C8	0.0256 (10)	0.0505 (14)	0.0332 (11)	−0.0063 (9)	0.0066 (8)	−0.0065 (10)
C9	0.0305 (11)	0.0432 (13)	0.0345 (11)	−0.0056 (10)	0.0056 (9)	0.0066 (10)
C10	0.0284 (10)	0.0298 (10)	0.0310 (10)	−0.0008 (8)	0.0042 (8)	0.0025 (9)
C11	0.0325 (12)	0.086 (2)	0.0569 (16)	−0.0040 (13)	0.0186 (12)	0.0003 (15)
C12	0.0250 (9)	0.0259 (10)	0.0226 (9)	0.0060 (7)	0.0096 (7)	0.0019 (8)
Si1	0.0207 (2)	0.0187 (2)	0.0228 (2)	0.00155 (19)	0.00751 (19)	0.0017 (2)
C13	0.0265 (9)	0.0266 (10)	0.0349 (11)	0.0051 (8)	0.0147 (8)	0.0055 (8)
C14	0.0427 (13)	0.0515 (15)	0.0443 (13)	0.0265 (12)	0.0144 (11)	0.0070 (12)
C15	0.0424 (13)	0.0619 (16)	0.0386 (13)	0.0125 (12)	0.0223 (11)	−0.0029 (12)
C16	0.0271 (9)	0.0257 (10)	0.0296 (10)	−0.0019 (8)	0.0048 (8)	−0.0005 (8)
C17	0.0402 (12)	0.0397 (13)	0.0282 (11)	0.0009 (10)	−0.0001 (9)	−0.0019 (9)
C18	0.0404 (12)	0.0325 (12)	0.0472 (14)	−0.0109 (10)	0.0063 (10)	−0.0025 (10)
C19	0.0263 (9)	0.0227 (9)	0.0264 (9)	−0.0007 (7)	0.0091 (8)	0.0009 (8)
C20	0.0357 (11)	0.0306 (11)	0.0353 (11)	−0.0025 (9)	0.0201 (9)	0.0034 (9)
C21	0.0470 (13)	0.0341 (12)	0.0400 (12)	−0.0169 (10)	0.0164 (10)	−0.0093 (10)
F1	0.0273 (6)	0.0318 (7)	0.0549 (8)	−0.0019 (5)	0.0074 (6)	−0.0134 (6)

Geometric parameters (Å, º)

N1—C1	1.505 (2)	C12—H121	1.000
N1—C4	1.485 (2)	C12—H122	1.000
N1—S1	1.6351 (16)	Si1—C13	1.8996 (19)
C1—C2	1.526 (3)	Si1—C16	1.897 (2)
C1—C12	1.523 (2)	Si1—C19	1.892 (2)
C1—H11	1.000	C13—C14	1.529 (3)
C2—C3	1.508 (3)	C13—C15	1.531 (3)
C2—F1	1.417 (2)	C13—H131	1.000
C2—H21	1.000	C14—H141	1.000
C3—C4	1.522 (3)	C14—H142	1.000
C3—H31	1.000	C14—H143	1.000
C3—H32	1.000	C15—H151	1.000
C4—H41	1.000	C15—H152	1.000
C4—H42	1.000	C15—H153	1.000
S1—O1	1.4354 (15)	C16—C17	1.538 (3)
S1—O2	1.4368 (14)	C16—C18	1.535 (3)
S1—C5	1.763 (2)	C16—H161	1.000
C5—C6	1.394 (3)	C17—H171	1.000
C5—C10	1.391 (3)	C17—H172	1.000
C6—C7	1.386 (3)	C17—H173	1.000
C6—H61	1.000	C18—H181	1.000
C7—C8	1.393 (3)	C18—H182	1.000
C7—H71	1.000	C18—H183	1.000

C8—C9	1.388 (3)	C19—C20	1.537 (3)
C8—C11	1.506 (3)	C19—C21	1.533 (3)
C9—C10	1.389 (3)	C19—H191	1.000
C9—H91	1.000	C20—H201	1.000
C10—H101	1.000	C20—H202	1.000
C11—H111	1.000	C20—H203	1.000
C11—H112	1.000	C21—H211	1.000
C11—H113	1.000	C21—H212	1.000
C12—Si1	1.8999 (19)	C21—H213	1.000
C1—N1—C4	110.04 (14)	H121—C12—H122	109.467
C1—N1—S1	118.65 (12)	C12—Si1—C13	103.99 (9)
C4—N1—S1	116.46 (12)	C12—Si1—C16	111.01 (9)
N1—C1—C2	102.66 (14)	C13—Si1—C16	109.04 (9)
N1—C1—C12	111.05 (14)	C12—Si1—C19	112.03 (9)
C2—C1—C12	116.50 (16)	C13—Si1—C19	111.92 (9)
N1—C1—H11	108.772	C16—Si1—C19	108.79 (9)
C2—C1—H11	108.772	Si1—C13—C14	112.88 (15)
C12—C1—H11	108.772	Si1—C13—C15	115.88 (15)
C1—C2—C3	104.95 (16)	C14—C13—C15	109.54 (18)
C1—C2—F1	109.35 (15)	Si1—C13—H131	105.914
C3—C2—F1	107.94 (17)	C14—C13—H131	105.914
C1—C2—H21	111.447	C15—C13—H131	105.914
C3—C2—H21	111.447	C13—C14—H141	109.466
F1—C2—H21	111.447	C13—C14—H142	109.467
C2—C3—C4	101.91 (15)	H141—C14—H142	109.476
C2—C3—H31	111.329	C13—C14—H143	109.466
C4—C3—H31	111.329	H141—C14—H143	109.476
C2—C3—H32	111.329	H142—C14—H143	109.476
C4—C3—H32	111.329	C13—C15—H151	109.466
H31—C3—H32	109.467	C13—C15—H152	109.467
C3—C4—N1	103.34 (15)	H151—C15—H152	109.476
C3—C4—H41	110.982	C13—C15—H153	109.466
N1—C4—H41	110.982	H151—C15—H153	109.475
C3—C4—H42	110.982	H152—C15—H153	109.476
N1—C4—H42	110.982	Si1—C16—C17	115.41 (14)
H41—C4—H42	109.467	Si1—C16—C18	111.66 (15)
N1—S1—O1	106.44 (8)	C17—C16—C18	110.16 (17)
N1—S1—O2	106.50 (9)	Si1—C16—H161	106.330
O1—S1—O2	120.29 (9)	C17—C16—H161	106.330
N1—S1—C5	107.26 (8)	C18—C16—H161	106.331
O1—S1—C5	108.26 (9)	C16—C17—H171	109.467
O2—S1—C5	107.45 (9)	C16—C17—H172	109.467
S1—C5—C6	119.62 (16)	H171—C17—H172	109.476
S1—C5—C10	119.81 (15)	C16—C17—H173	109.467

C6—C5—C10	120.55 (19)	H171—C17—H173	109.476
C5—C6—C7	119.5 (2)	H172—C17—H173	109.476
C5—C6—H61	120.251	C16—C18—H181	109.466
C7—C6—H61	120.251	C16—C18—H182	109.467
C6—C7—C8	120.8 (2)	H181—C18—H182	109.476
C6—C7—H71	119.601	C16—C18—H183	109.467
C8—C7—H71	119.601	H181—C18—H183	109.476
C7—C8—C9	118.8 (2)	H182—C18—H183	109.476
C7—C8—C11	120.6 (2)	Si1—C19—C20	113.31 (14)
C9—C8—C11	120.6 (2)	Si1—C19—C21	113.44 (14)
C8—C9—C10	121.4 (2)	C20—C19—C21	109.33 (17)
C8—C9—H91	119.302	Si1—C19—H191	106.769
C10—C9—H91	119.302	C20—C19—H191	106.769
C5—C10—C9	118.92 (19)	C21—C19—H191	106.769
C5—C10—H101	120.542	C19—C20—H201	109.467
C9—C10—H101	120.542	C19—C20—H202	109.467
C8—C11—H111	109.466	H201—C20—H202	109.476
C8—C11—H112	109.466	C19—C20—H203	109.467
H111—C11—H112	109.476	H201—C20—H203	109.476
C8—C11—H113	109.467	H202—C20—H203	109.476
H111—C11—H113	109.476	C19—C21—H211	109.467
H112—C11—H113	109.476	C19—C21—H212	109.467
C1—C12—Si1	121.84 (13)	H211—C21—H212	109.475
C1—C12—H121	106.299	C19—C21—H213	109.467
Si1—C12—H121	106.299	H211—C21—H213	109.476
C1—C12—H122	106.299	H212—C21—H213	109.476
Si1—C12—H122	106.299		